**Helena Isabel Caseiro Rego Gomes**

Licenciada em Engenharia do Ambiente (Ramo Ambiente),
Mestre em Ciência e Sistemas de Informação Geográfica

# Coupling electrokinetics and iron nanoparticles for the remediation of contaminated soils

Dissertação para obtenção do Grau de Doutor em
Ambiente

Orientador: Professora Doutora Alexandra de Jesus Branco Ribeiro,
Professora Associada com Agregação, Faculdade de Ciências e Tecnologia da Universidade Nova de Lisboa

Co-orientador: Doutora Célia Maria Dias Ferreira, Investigadora do Centro de Estudos de Recursos Naturais, Ambiente e Sociedade, Escola Superior Agrária de Coimbra

Júri:
Presidente: Prof. Doutor Fernando José Pires Santana
Arguentes: Prof. Doutor Knud Henrik Hansen
Prof. Doutor Marco Diogo Richter Gomes da Silva

Vogais: Prof. Doutor José Miguel Rodriguez Maroto
Prof. Doutora Alexandra de Jesus Branco Ribeiro
Prof. Doutora Maria Margarida Cruz Godinho Ribau Teixeira

FACULDADE DE CIÊNCIAS E TECNOLOGIA
UNIVERSIDADE NOVA DE LISBOA

**Setembro. 2014**

**Coupling electrokinetics and iron nanoparticles for the remediation of contaminated soils**

*“All my life through, the new sights of nature made me rejoice like a child.”*

*— Marie Curie*

*To my mother*

*who always told me to*
*be strong and never, never, give up*

# Preface

This dissertation is submitted as partial fulfillment of the requirements for the Doctoral Degree in Environment and includes the results of my Ph.D. study carried out from September 2011 to June 2014 in the Faculty of Sciences and Technology from the New University of Lisbon, with stays abroad as visiting researcher in the Department of Civil and Environmental Engineering, Lehigh University, Bethlehem, PA, USA (September 2011-August 2012); in the Department of Civil Engineering, Technical University of Denmark (DTU), Lyngby, Denmark (September-December 2013), and in the Department of Chemical Engineering, Málaga University, Málaga, Spain (January-March 2014).

The dissertation is organized as follows:

**Part I** – provides all the summarized information regarding the problem statement, motivation and the objectives of the work, compiles the major findings of the experimental work and examines some limitations, outlines the main conclusions and identifies future areas of research.

**Part II** – includes all the publications in international peer reviewed journals done for this Ph.D. study, as an integral component of the dissertation:

- Gomes, H. I., Dias-Ferreira, C., & A. B. Ribeiro (2012). Electrokinetic remediation of organochlorines in soil: Enhancement techniques and integration with other remediation technologies. *Chemosphere*, **87**: 1077-1090.

- Gomes, H. I.; Ferreira, C.D., Ribeiro, A. B. & S. Pamukcu (2012). Electrokinetic enhanced transport of zero valent iron nanoparticles for chromium (VI) reduction in soils. *Chemical Engineering Transactions*, **28**: 139-144.

- Gomes, H. I., Dias-Ferreira, C., & A. B. Ribeiro (2013). Overview of *in situ* and *ex situ* remediation technologies for PCB-contaminated soils and sediments and obstacles for full-scale application. *Science of the Total Environment*, **445-446**: 237-260.

- Gomes, H. I.; Ferreira, C. D., Ribeiro, A. B. & S. Pamukcu (2013). Enhanced transport and transformation of zerovalent nanoiron in clay using direct electric current, *Water, Air, & Soil Pollution*, **224**: 1-12.

- Gomes, H. I.; Dias-Ferreira, C.; Ribeiro, A. B. & S. Pamukcu (2014). Influence of electrolyte and voltage on the direct current enhanced transport of iron nanoparticles in clay. *Chemosphere*, **99**: 171-179.

- Gomes, H. I.; Fan, G. P.; Mateus, E. P.; Dias-Ferreira, C. & A. B. Ribeiro (2014). Assessment of combined electro-nanoremediation of molinate contaminated soil. *Science of the Total Environment*, **493**: 178-184.

- Gomes, H. I.; Dias-Ferreira, C.; Ottosen, L. M. & A. B. Ribeiro (2014). Electroremediation of PCB contaminated soil with iron nanoparticles: performance of a new electrodialytic setup. Submitted.

- Gomes, H. I., Dias-Ferreira, C., Ottosen, L. M., & Ribeiro, A. B. (2014). Electrodialytic remediation of polychlorinated biphenyls contaminated soil with iron nanoparticles and two different surfactants. *Journal of Colloid and Interface Science*, **433**, 189-195.

- Gomes, H. I.; Dias-Ferreira, C.; Ottosen, L. M. & A. B. Ribeiro (2014). Enhanced electrokinetic techniques for remediation of different PCB polluted soils. Submitted.

- Gomes, H. I.; Maroto, J. M. R.; Dias-Ferreira, C.; Ribeiro, A. B. & S. Pamukcu (2014). Numerical prediction of diffusion and electric field-induced iron nanoparticle transport. Submitted.

I hereby declare that, as the first author of the above mentioned manuscripts, I provided the major contribution to the research and experimental work developed, to the results interpretation and the preparation of these publications submitted during the Ph.D. project. The copyright of the publications was transferred to the editors, and these articles are reproduced with permission of the original publishers and subject to copy restrictions imposed by them.

# Acknowledgments

*"Let us be grateful to the people who make us happy;*
*they are the charming gardeners who make our souls blossom."*
*— Marcel Proust*

First of all, I would like to express my gratitude and my friendship to my advisers, Alexandra Ribeiro and Célia Ferreira, for believing in me and include me in their research projects, as well as for their continuous support, lending me objective and helpful advice. Thank you so much! A special word of thanks to Alexandra Ribeiro – that accompanied me in different periods of my career path – for her friendship and for being such a kind mentor.

I had the opportunity to work with top research groups around the world and I would like to thank:

- Sibel Pamukcu, Reena Amatya Shrestha, Alla Miroshnik, Rebekah Brosky, Ehsan Ghazanfari and Yi Don, from the Department of Civil and Environmental Engineering – Lehigh University, USA;
- Lisbeth M. Ottosen, Gunvor Kirkelund, Ebba Schnell, Louise Gammeltoft, Tian Ran Sun, Wan Chen, Sabrina Madsen and Louise Birkemose from the Department of Civil Engineering – Technical University of Denmark (DTU), Denmark;
- José Miguel Rodríguez-Maroto, Francisco García Herruzo, César Goméz-Lahoz, Carlos Vereda Alonso, María Villen, Ana García Rubio, Gema Amaya Santos, Irene Sanchéz-Trujillo, Ana Belén Muñoz and Brahim Arhoun from the Department of Chemical Engineering – Málaga University, Spain;

for being so welcoming and friendly, for providing me good conditions to carry my work and for sharing their experience and knowledge. I want to express my sincere appreciation for their help and availability. It was my pleasure to meet you and work with you all!

I am grateful for the help from Fan Guangping from the Institute of Soil Science, Chinese Academy of Sciences that during her exchange program in Portugal worked with me in the experiments with molinate contaminated soil.

I would like to thank Eduardo Mateus for his help in setting up the GC/MS and all the support on the analytical determinations, as well as the lively discussions of methods and results. Many thanks to Paula Guedes and Nazaré Couto for being always there – I knew I could count on you girls!

Thank you so much Helena Silva (NanoDC project) for all the help in the PCB analytical work! I would also like to thank Emílio Rosales for the brainstorming/discussion on the nanoparticles reactions and transport, for helping me in the setup of some experiments, as well as for all the support during my stay in Coimbra. Jorge Varejão and Sandra Santos from ESAC are also acknowledged for providing work conditions and support in the lab at Coimbra.

I would like to thank Thomas Hougaard for the indication of the site for sampling PCB contaminated soil near Copenhagen, as well as for the discussion on field scale projects using electrokinetics.

I have no words to thank Júlio for being my close companion and for all the support in these last years that have been so hard for him. I would also like to thank all my friends, for being by my side and accompany me in this journey. And, last but not least, I would like to thank to my parents and sister for being a constant source of encouragement.

The Department of Civil and Environmental Engineering at Lehigh University is acknowledged for the funding of equipment development, testing and analysis in the study of the enhanced transport of the iron nanoparticles. Also the Department of Civil Engineering from the Technical University of Denmark (DTU) and the Department of Chemical Engineering from Málaga University are acknowledged for receiving me and providing all the conditions needed for my research.

This work has been funded by the European Regional Development Fund (ERDF) through COMPETE – Operational Programme for Competitiveness Factors (OPCF), by Portuguese National funds through the “FCT - Fundação para a Ciência e a Tecnologia” under project «PTDC/AGR-AAM/101643/2008 NanoDC», by the research grant SFRH/BD/76070/2011, and by FP7-PEOPLE-IRSES-2010-269289-ELECTROACROSS.

# Abstract

Contaminated soils and sediments are a serious environmental problem worldwide. Different contaminants, such as heavy metals, pesticides and other persistent organic pollutants are challenging, and there is an urgent need to develop cost-effective and sustainable remediation technologies. Zero valent iron nanoparticles (nZVI) were considered promising for the remediation of contaminated soils and groundwaters, targeting a wide range of contaminants, and especially organochlorines such as polychlorinated biphenyls (PCB). However, critical issues related to their limited mobility remain unsolved. A direct current can be used to enhancing the nanoparticles transport, based on the same principles of electrokinetic remediation (EK). Integrating both technologies, the role of direct electric current would be to get nZVI into the soil for *in-situ* transformation and subsequent destruction of the contaminants, instead of aiming at the contaminants transport for removal.

In this dissertation, the direct current assisted transport of iron nanoparticles was studied in model soils: kaolin as representative of low permeability soils, and mixtures of kaolin and glass beads to represent different porosity media. Also, different electrolytes of varying ionic strengths and initial pH and high nZVI concentrations (typical of field applications) were used. Other experimental phases tested the combined use of electrokinetics and nZVI in spiked soils with inorganic and organic contaminants (Cr and the herbicide molinate), and PCB historically contaminated soils. The PCB works include the comparison between the traditional three-compartment electrokinetic setup and the new two-compartment electrodialytic setup developed at the Technical University of Denmark, and also the comparison between two different surfactants (saponin and Tween 80) and two different soils. A generalized physicochemical and numerical model was developed to describe the nZVI transport through different porous media under electric fields.

The results show that the aggregation and settling of the iron nanoparticles remain a problem, although a direct current enhances the transport through different porosity media. The soil characteristics are fundamental, and affect both the reaction between nZVI and the target contaminant, and the transport of the nZVI and the contaminant. In some cases, it is counterproductive to use both methods simultaneously and better results (higher removal rates) are obtained just with the iron nanoparticles or just with electrokinetics. A case-by-case selection is recommended. The two-compartment setup shows numerous advantages when compared with the three-compartment setup, but further testing and scale up will be necessary.

**Keywords:** Electroremediation, Zero Valent Iron Nanoparticles (nZVI), Contaminated Soil, Electrokinetics (EK), Electrodialytic remediation (EDR)

# Resumo

A contaminação de solos e sedimentos representa um problema ambiental grave à escala mundial. Diferentes contaminantes – metais pesados, pesticidas e poluentes orgânicos persistentes – constituem um desafio e é necessário desenvolver urgentemente tecnologias de remediação sustentáveis e com uma boa relação custo-eficácia. As nanopartículas de ferro zero valente (nZVI) foram consideradas promissoras para a remediação de solos e águas subterrâneas, abrangendo uma vasta gama de contaminantes, especialmente compostos organoclorados como os bifenis policlorados (PCB). Contudo, a sua reduzida mobilidade em solos é limitante. A corrente contínua pode ser utilizada para potenciar o transporte das nanopartículas com base nos mesmos princípios do método electrocinético (EK). Integrando as duas tecnologias, o papel da corrente eléctrica seria transportar as nanopartículas no solo para transformação *in situ* e posterior destruição dos contaminantes, em vez da sua remoção.

Nesta tese foi estudado o transporte das nanopartículas sob ação da corrente contínua em solos modelo: caulinite como representante de solos com baixa permeabilidade e misturas de caulinite e esferas de vido para materiais com diferentes porosidades. Foram usados diferentes electrólitos, com distintas forças iónicas e pH inicial, a par de nZVI com concentrações típicas de aplicação no terreno. Outras fases experimentais testaram o uso combinado dos dois métodos em solos contaminados intencionalmente com crómio e com o herbicida molinato e em contaminações antigas de solos com PCB. Nestes últimos foram comparadas a configuração tradicional da célula electrocinética (três compartimentos) com uma célula electrodialítica de dois compartimentos, desenvolvida na Universidade Técnica da Dinamarca (DTU). Foram também comparados dois solos diferentes e dois surfactantes (saponina e Tween 80). Um modelo numérico e físicoquímico foi desenvolvido para descrever o transporte das nZVI nos meios de diferentes porosidades.

Os resultados mostram que a agregação e a sedimentação das nZVI permanece um problema, embora a corrente contínua melhore o seu transporte nos meios de diferentes porosidades. As características do solo são fundamentais e afetam, tanto a reação entre nZVI e o contaminante alvo, como o transporte das nZVI e de contaminantes. Em alguns casos, não há vantagem em usar ambos os métodos simultaneamente, dado que são obtidos melhores resultados (maiores taxas de remoção) apenas com as nZVI ou com o método electrocinético. É recomendável uma seleção caso-a-caso. A configuração de dois compartimentos mostra inúmeras vantagens relativamente à configuração tradicional, mas é necessário realizar mais testes a maior escala.

**Palavras-chave:** Electrorremediação, Nanopartículas de Ferro Zero Valente, Solo Contaminado, Método Electrocinético, Remediação Electrodialítica

# Acronyms, Abbreviations and Notations

| | |
|---|---|
| AAS | Atomic absorption spectroscopy |
| ANOVA | Analysis of variance |
| BZ | Ballschmiter and Zell |
| CAT | Cation exchange membrane |
| CMC | Carboxymethyl cellulose |
| CTAB | Cetyltrimethylammonium bromide |
| DC | Direct current |
| DCE | Dichloroethene |
| DTU | Technical University of Denmark |
| ED | Electrodialytic |
| EK | Electrokinetic |
| EOF | Electroosmotic flow |
| EP | Electrophoretic cell |
| EU | European Union |
| GC | Gas chromatography |
| GC/MS | Gas chromatography/mass spectrometry |
| HCB | Hexachlorobenzene |
| ICP | Inductively coupled plasma-atomic emission spectrometry |
| IUPAC | International Union of Pure and Applied Chemistry |
| nZVI | Zero valent iron nanoparticles |
| ORP | Oxidation reduction potential |
| PAA | Polyacrilyc acid |
| PAH | Polycyclic aromatic hydrocarbons |
| PAP | Sodium polyaspartate |
| PBDE | Polybrominated diphenyl ethers |
| PCB | Polychlorinated biphenyls |
| PCE | Perchloroethylene |
| PCP | Pentachlorophenol |
| POP | Persistent organic pollutant |
| PRB | Permeable reactive barriers |

| | |
|---|---|
| PV3A | Polyvinyl alcohol-co-vinyl acetate-co-itaconic acid |
| SDS | Sodium dodecyl sulfonate |
| SPE | Solid phase extraction |
| TCE | Trichloroethene |
| TEF | Toxic equivalency factor |
| TNT | Trinitrotoluene |
| UN | United Nations |
| USA | United States of America |
| USEPA | United States Environmental Protection Agency |
| VC | Vinyl chloride |
| VOC | Volatile organic compounds |
| WHO | World Health Organization |
| ZVI | Zero valent iron |

## Model notations

| | |
|---|---|
| A | cross-sectional area ($cm^2$) |
| $c$ | concentration (mol $cm^{-3}$) |
| $D^*$ | effective diffusion coefficient |
| E | redox potential (V) |
| $E^0$ | standard redox potential (V) |
| $F$ | Faraday constant |
| $I$ | current intensity |
| $k_e$ | electroosmotic permeability coefficient |
| $N$ | mass flux (mol $cm^2$ $s^{-1}$) |
| Q | reaction quotient |
| $R$ | ideal gas constant |
| $R$ | reaction rate |
| $T$ | temperature (K), assuming a constant room temperature of 25ºC |
| $t$ | time |
| U* | effective electrophoretic mobility |
| $V$ | volume ($cm^3$) |
| $z$ | ionic charge |

**Greek letters**

| | |
|---|---|
| $\phi$ | electrical potential |
| $\eta$ | Faradaic efficiency |

# Contents

**Part II**

# List of Figures

# List of Tables

# Part I

1

# 1. Introduction

## 1.1 Problem Statement

### 1.1.1 Soil contamination

Soil contamination is a major environmental issue worldwide, with more than three million potentially contaminated sites [1]. According to the latest data from the European Commission, an estimation points to 2.5 million potentially contaminated sites in Europe of which about 14% (340,000 sites) are probably contaminated and need remediation [2]. In the United States of America (USA), there are now 1,739 Superfund sites [3] and more than 450,000 brownfields [4] . Developing countries like China and India have also to deal with this environmental problem, due to rapid industrialization and economic growth [5-10].

In North America and Europe, many countries have a legal framework to classify and deal with contaminated soils [11, 12]. However, in most countries, the scale of the problem is difficult to assess as “contaminated land” or “site contamination” are often subjectively or poorly defined [13]. In Portugal, a specific regulatory framework for contaminated land management is still in development. References to soil protection can be found scattered throughout the European Union (EU) regulatory structure, establishing instruments and measures that have a direct or indirect impact on soil quality [12], and also addressing prevention and control of polluting activities in waste management, chemicals and industrial emissions [14]. The EU Thematic Strategy for Soil Protection identifies erosion, organic matter decline, salinization, compaction, landslides, contamination, sealing and biodiversity loss as the major threats to soils [15]. Still, the long-awaited binding EU Soil Directive has been pending for eight years, without effective results. In 2013, the withdrawal of the Soil Framework Directive proposal was proposed (MEMO/13/833, from 02/10/2013), thus opening the way for another initiative in the next mandate of the European Commission.

Water and air quality are of immediate concern for most people because we all breathe and drink several times a day, but the importance of soil is more difficult to grasp for an average citizen or politician. Nevertheless, soil is a non-renewable natural resource at a human life span with many important functions and services such as: (i) biomass production, including agriculture and forestry; (ii) storing, filtering and transforming nutrients, substances and water; (iii) biodiversity pool for habitats, species and genes; (iv) physical and cultural environment for humans and human activities; (v) source of raw materials; (vi) carbon pool; (vii) archive of geological and archeological heritage [16]. Soil is "*the biogeochemical engine of Earth's life support system*", providing us food, forage, fiber and fuel [17]. The importance of soil as a sink of $CO_2$ and consequently slowing climate change was highlighted in a recent study published on Nature [18].

Soil contamination is a result of anthropogenic activities, especially after the Industrial Revolution, and can be caused by both diffuse and local sources. It is usually defined by increased concentrations of acidifying contaminants (e.g. $SO_2$, $NO_x$), metals (e.g. cadmium, chromium, copper, lead, mercury), metalloids such as arsenic, and organic compounds, such as pesticides, herbicides, polycyclic aromatic hydrocarbons (PAH), and polychlorinated biphenyls (PCB). The main sources of soil contaminants are mining and smelting; fossil fuel combustion; sewage sludge; process and manufacturing industries (specifically metallurgical, electronics and chemical); waste disposal; the land spreading of fertilizers, fungicides and other agricultural materials; atmospheric deposition from traffic and waste incineration; the spillage of liquids such as solvents or oil; and practices of irrigation with contaminated waters [19]. Contaminated soils can be simultaneously source and sink for pollution as, once introduced, pollutants may accumulate for a long time. Although soil contamination has been recognized since the 1960s, less than a tenth of potentially contaminated sites globally have been remediated, due to the complex and challenging nature of both surface and subsurface contamination, as well as the cost and technical difficulty of dealing with contaminant mixtures, recalcitrant and persistent pollutants [13].

#### *1.1.1.1 Heavy metals*

Heavy metals, a wide concept that includes any metal or metalloid of environmental concern, occur naturally at trace levels in the soil environment, as a result from the pedogenetic processes of weathering of rock materials. Due to anthropogenic influence, most soils may accumulate one or more of the heavy metals above defined background values, high enough to cause risks to human health, plants, animals and ecosystems, or other media, such as water and air. In Europe, heavy metals are the predominant contaminants, both in soil and groundwater (Figure 1.1).

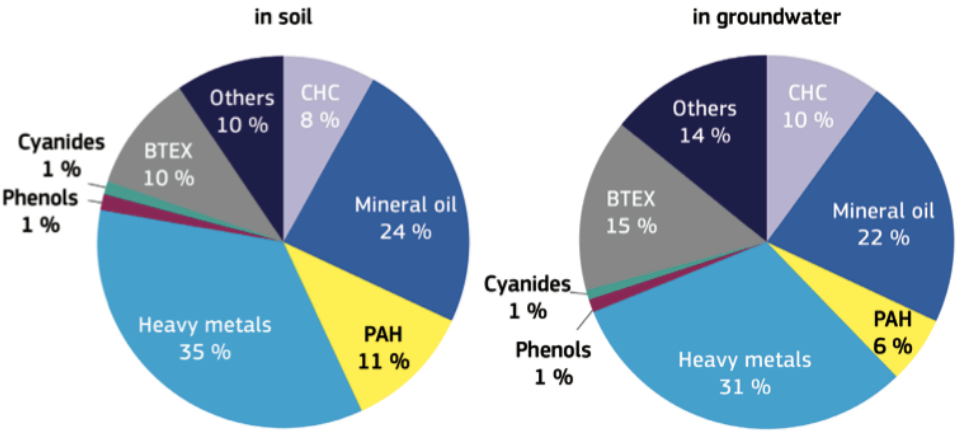


**Figure 1.1** Overview of contaminants affecting soil and groundwater in Europe as reported in 2011 [2].

Large quantities of chromium have been discharged into the environment, mainly to soils and groundwater, due to improper disposal and leakage in industrial activities (ore refining, production of steel and alloys, metal plating, tannery, wood preservation and pigmentation). Chromium is one of the most frequent metal soil contaminants and is one of the top 20 contaminants on the Superfund priority list of hazardous substances for the past 15 years [20].

Oxidation states of Cr range from -4 to +6, but only the +3 (III) and +6 (VI) states are stable under most natural environments. These two oxidation states are different in charge, physicochemical properties, as well as chemical and biochemical reactivity [21]. Cr(VI) is extremely mobile in the environment and is toxic to humans, animals, plants, and microorganisms. Because of its significant mobility in the subsurface environment, the potential risk of groundwater contamination is high. Cr(III), on the other hand, is less toxic, immobile, and readily precipitates as $Cr(OH)_3$ [22]. Cr(III) is also considered to be a trace element essential for the proper functioning of living organisms [23].

#### *1.1.1.2 Pesticides*

Pesticides are substances used to protect plants from pests, such as weeds, plant diseases or insects. Target pests can be insects, plant pathogens, weeds, mollusks, birds, mammals, fish, nematodes, and microorganisms. A pesticide is usually a chemical or biological agent that deters, incapacitates, kills, or otherwise discourages pests. Despite the benefits in the crop protection, the extensive use of pesticides and their characteristics can lead to potential toxicity to humans and damage in the ecosystems. According to the Stockholm Convention on persistent organic pollutants (POP), 14 of the persistent organic chemicals are pesticides [24].

The widespread use of pesticides in intensive agriculture leads to soil and groundwater contamination. One of the pesticides that causes environmental concern is molinate (S-ethyl N,N-hexamethylene-1-carbamate), often applied annually to flooded fields during rice seeding to control the overgrowth of weeds [25]. In 2013, there were 165.5 million hectares of rice paddies worldwide [26]. Molinate can be found in natural surface and ground waters and also in wastewaters [27] due to its high water solubility, as well as in soils and sediments near rice paddies [25, 28, 29].

#### *1.1.1.3 Persistent organic pollutants and polychlorinated biphenyls*

Soil contamination with persistent organic pollutants is particularly alarming. The classification as POP arises from the United Nations (UN) Stockholm Convention in 2001, due to accumulated evidence of the potential toxicity of these chemicals based on *in vitro* or *in vivo* assays [17]. These pollutants are synthetic organic compounds resistant to environmental degradation through chemical, biological, and photolytic processes, which make them persist in the environment, transport through long-range distances and reach remote areas where they have never been used, bioaccumulate in human and animal tissue, and biomagnificate in food chains [30-32]. Soil plays an important role in the global fate and distribution of POP, as an effective sink for these chemicals due to its large retention capacity for hydrophobic compounds [33].

Polychlorinated biphenyls (PCB) are a group of synthetic aromatic compounds that comprise two benzene rings connected at the C-1 carbon, with the general formula $C_{12}H_{10-x}Cl_x$. Each ring can have up to 5 chlorines in the *ortho*, *meta*, or *para* positions (Figure 1.2), ranging from mono- to decachlorobiphenyl (Table 1.1), totalizing 209 structural arrangements (congeners) differing in chlorine number and position and exhibiting unique chemical properties. Ballschmiter and Zell (BZ), in 1980, introduced a system in which congeners were arranged in ascending numerical order based on the number of chlorine atoms and their position on the biphenyl structure. The BZ system was recognized by the International Union of Pure and Applied Chemistry (IUPAC) and is the generally accepted notation [34].

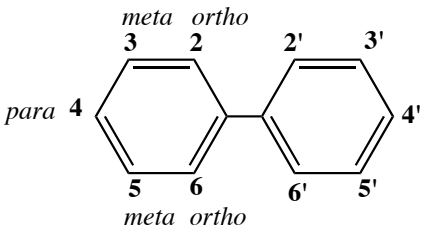


**Figure 1.2.** Chemical structure of PCB. The possible positions of chlorine atoms on the benzene rings are denoted by numbers assigned to the carbon atoms.

**Table 1.1.** Molecular formula, name, number of isomers, IUPAC number, molecular mass, percentage of chlorine and number of isomers identified [35].

| Molecular Formula | Name: Chlorobiphenyl | No. of Isomers | Ballschmiter and Zell (BZ) No. | Molecular Mass | % of Chlorine | No. of Isomers identified |
|---|---|---|---|---|---|---|
| $C_{12}H_9Cl$ | Mono | 3 | 1-3 | 188.65 | 18.79 | 3 |
| $C_{12}H_8Cl_2$ | Di | 12 | 4-15 | 233.10 | 31.77 | 12 |
| $C_{12}H_7Cl_3$ | Tri | 24 | 16-39 | 257.54 | 41.30 | 23 |
| $C_{12}H_6Cl_4$ | Tetra | 42 | 40-81 | 291.99 | 48.65 | 41 |
| $C_{12}H_5Cl_5$ | Penta | 46 | 82-127 | 326.43 | 54.30 | 39 |
| $C_{12}H_4Cl_6$ | Hexa | 42 | 128-169 | 360.88 | 58.93 | 31 |
| $C_{12}H_3Cl_7$ | Hepta | 24 | 170-193 | 395.32 | 62.77 | 18 |
| $C_{12}H_2Cl_8$ | Octa | 12 | 194-205 | 429.77 | 65.98 | 11 |
| $C_{12}HCl_9$ | Nona | 3 | 206-208 | 464.21 | 68.73 | 3 |
| $C_{12}Cl_{10}$ | Deca | 1 | 209 | 498.66 | 71.10 | 1 |

Manufactured by subjecting biphenyl to chlorine, commercial PCB typically came in a mixture of many congeners, classified by the amount of chlorine by weight present. For instance, Aroclor 1260, marketed by Monsanto from 1930 to 1977, contained 60% wt. of chlorine [36]. Other commercial mixtures of different congeners were Clophen (Bayer, Germany), Kanechlor (Kanegafuchi, Japan), Santotherm (Mitsubishi, Japan), Phenoclor and Pyralene (Prodolec, France) [37, 38]. PCB were used for industrial application in closed systems: lubricants (industrial oils), dielectric fluids in electrical equipment such as transformers, capacitors, heat transfer and hydraulic systems [39-42]. They were also employed in open uses, such as pesticide extenders, sealants, carbonless copy paper, lubricants, paints, adhesives, plastics, flame retardants and dedusting agents on roads [43-46]. Other uses, in partially open systems, include: heat transfer fluids; hydraulic fluid in lifting equipment, trucks and high-pressure pumps; vacuum pumps; voltage regulators; liquid filled electrical cables and liquid filled circuit breakers [40, 43, 47, 48]. Recently, PCB congeners (namely PCB11 or 3,3'-dichlorobiphenyl) were detected in azo and phthalocyanine pigments, commonly used in paint and also in inks, textiles, paper, cosmetics, leather, plastics, food and other materials [49, 50], as by-products (inadvertently produced) of industrial synthetic process of paint pigments [49].

PCB pose a real human health threat through numerous exposure pathways [51]. Of the 209 different types of PCBs, 13 exhibit a dioxin-like toxicity [24]. The Toxic Equivalency Factor (TEF) defined by the World Health Organization (WHO) for PCB varies between $10^{-5}$ for 2,3',4,4',5,5'-hexachlorobiphenyl and 0.1 for 3,3',4,4',5-pentachlorobiphenyl. The non-dioxin-like PCB and their metabolites do not interact substantially with the aryl hydrocarbon receptor and may act through

different pathways than the dioxin-like chemicals, so their effects are not accounted for in TEF [52]. Adverse effects associated to the exposure of PCB comprise damage to the immune system, liver, skin irritation (acne), reproductive system, gastrointestinal tract and thyroid gland [53-55]. Research has also shown that PCB can cause severe neurological problems in children, including impairment of cognitive and motor abilities and can be transmitted from mother to child during breastfeeding [54]. PCB are listed as probable human carcinogens [24]. Occurrences of PCB toxic effects in invertebrates, fish, birds and other animals are also well documented [47, 56].

In the 1970s, several countries limited PCB use due to the concerns on human toxicity and later, in 1985, the European Community heavily restricted the use and marketing of PCB. Nevertheless, PCB production was estimated around 1.2 and 2 million t, with some of the most detailed data indicating a total global production of approximately 1.3 million t between 1929 and 1993 [57]. Of this cumulative global production, previsions point to 440 to 92,000 t emitted into the environment [57, 58]. According to Ockenden et al. [59], most of the PCB manufactured/used (perhaps > 70%) have not yet entered the environmental pool because they are still associated with diffusive source materials. Around 10% of the total produced PCB [60] is accumulated in the geosphere because of their low volatility, low solubility in water and high affinity for particulates, both biotic and abiotic [36, 60, 61].

Under the UN Stockholm Convention, the parties (currently 179) have to eliminate the use of PCB in equipment (e.g. transformers and capacitors) by 2025 and to ensure the environmentally sound management of PCB waste (including contaminated soils) by 2028 [24].

### 1.1.2 Technologies for PCB contaminated soils and sediments

The extent of PCB contamination in soils and sediments worldwide is unknown. In the USA, 25% of the Superfund Sites (total number of 433 sites) have PCB contaminated soils or sediments [62], whereas in Canada there are 338 sites according to the Federal Contaminated Sites Inventory [63]. In European countries, an estimate points towards 272,000 contaminated sites with chlorinated hydrocarbons but a total quantification of PCB contaminated sites is missing [2]. Additionally to the local contamination near industrial sites, an inventory on atmospheric deposition in background surface soil estimates a PCB global soil burden of 21,000 t [64].

For this Ph.D. dissertation, the state of the art of the technologies for *in situ* and *ex situ* remediation of PCB-contaminated soils and sediments was reviewed (Section II.1), including laboratory, pilot and full-scale case studies [65]. The main emergent remediation technologies were described and their

current status was evaluated, assessing major advantages and also potential obstacles to their full-scale application (Table 6, Section II.1). Although there are promising results in bench-scale studies, most technologies are still in the initial stage of development. Further research and scale up are needed for the progress of cost-effective and sustainable alternatives for PCB remediation. After this review, recent studies include the electrokinetically enhanced persulfate oxidation of PCB in contaminated soils with [66] and without surfactant [67]; the phytoremediation by alfalfa, tall fescue, single, and mixed plants cultivation [68]; and the use of biosurfactant on combined chemical-biological treatment [69]. In none of those studies was clearly demonstrated the method efficiency for full-scale implementation. There is a critical need for a cost-effective and sustainable technology for the remediation of PCB contaminated soils and sediments, as the most common solutions are "dig and dump" and "dig and incinerate".

### 1.1.3 Zero valent iron nanoparticles (nZVI)

Permeable reactive barriers (PRB) filled with granular zero valent iron (ZVI) have been successfully used for groundwater remediation for twenty years [70], targeting both organic (methanes, ethanes, ethenes, propanes, aromatics) and inorganic (trace metals and anions) contaminants. In 1996, Lehigh University researchers developed a method to synthesize zero valent iron nanoparticles (nZVI) using sodium borohydride as reductant [71, 72]. Since then, in a growing number of studies and publications, nZVI were used (both as reductant and as oxidant), with several modifications, focusing in different organic and inorganic contaminants, in different matrices (Table 1.2).

**Table 1.2.** Studies on the use of several types of zero valent iron nanoparticles for remediation, targeting different contaminants in different matrices.

| Target Contaminant | Type of nZVI | Matrix | Ref. |
|---|---|---|---|
| 1-(2-chlorobenzoyl)-3-(4-chlorophenyl) | Bare | Water/Methanol solution | [73] |
| Amoxicillin and ampicillin | Bare | Aqueous solutions | [74] |
| As (III) | Bare | Aqueous solutions | [75] |
| Atrazine | Bare and bimetallic nanoparticles Fe/Pd | Aqueous solutions and soil slurry | [76] |
| $Cd^{2+}$ | Bare | Aqueous solutions | [77] |
| Chloramphenicol | Bimetallic Fe/Ag nanoparticles | Aqueous solutions | [78] |
| Chlorinated ethanes | Bare | Water/Methanol solution | [79] |
| Chlorinated ethenes and heavy metals | Bimetallic Fe/Ni | Simulated groundwater | [80] |
| Cr(VI) and Pb(II) | Bare and supported Ferragel nanoparticles | Aqueous solutions | [81] |
| Cr(VI), Pb(II), TcO4- | Polymer resin supported nZVI | Aqueous solutions | [82] |
| γ -hexachlorocyclohexane (γ-HCH) | CMC stabilized Fe/Pd bimetallic nanoparticles | Spiked soil slurry | [83] |
| Hexachlorobenzene | Bare and bimetallic Fe/Pd | Aqueous solutions | [84] |
| Hexachlorobenzene | Bare | Aqueous solutions | [85] |
| Hexachlorocyclohexanes | Bare | Contaminated groundwater | [86] |
| Hexahydro-1,3,5-trinitro-1,3,5-triazine | Bare and CMC and PAA stabilized nZVI | Aqueous solutions | [87] |
| Ibuprofen | "Green" nanoparticles[a] | Aqueous solutions and sandy soil | [88] |

| Target Contaminant | Type of nZVI | Matrix | Ref. |
|---|---|---|---|
| Lindane | Bare | Aqueous solutions | [89] |
| Lindane | Bare and CMC, PAP and PAA coated nZVI | Water/Methanol solution | [90] |
| Malathion | Bare | Spiked soil slurry | [91] |
| Methylene blue and methyl orange dyes | "Green" nanoparticles[b] | Aqueous solutions | [92] |
| Metronidazole | Polyvinylpyrrolidone stabilized nanoparticle | Aqueous solutions | [93] |
| Molinate | Bare | Aqueous solutions | [94] |
| Nitrates | Bare | Aqueous solutions | [95] |
| PCB | Bare | Water/Methanol solution | [96] |
| PCB | Bare | Soil | [97] |
| PCE, TCE, *cis*-DCE and VC and several chlorinated aromatic compounds | Bimetallic nanoparticles (Pd/Fe, Pd/Zn, Pt/Fe, Ni/Fe) | Aqueous solutions | [72] |
| Pentachlorophenol | Lactate-modified nZVI | Spiked soils | [98] |
| Polybrominated diphenyl ethers (PBDEs) | Bare | Aqueous solutions | [99] |
| Pyrene | Bare | Spiked soil | [100] |
| TCE | Bare | Aqueous solutions | [101] |
| TCE | Sodium carboxymethyl cellulose (CMC) stabilized bimetallic Fe/Pd | Water/Methanol solution | [102] |
| TCE and PCB | Bare and Bimetallic Fe/Pd | Aqueous and water/methanol solution | [71] |
| TCE and PCB | Starch-stabilized bimetallic Fe/Pd | Aqueous solutions | [103] |
| Trichloroethene and other chlorinated hydrocarbons | Bimetallic Fe/Pd | Groundwater (field application) | [104] |
| Trichloroethylene | CMC stabilized Fe/Pd bimetallic nanoparticles | Aqueous solutions and 2 different soils slurries | [105] |
| Trinitrotoluene (TNT) | Bare | Aqueous solutions and soils slurries | [106] |
| Uranium | Bare | Liquid waste effluent | [107] |
| VOC | Bare | Groundwater (field application) | [108] |

[a] Green nZVI were produced using natural extracts (black tea, grapes, and vine leaves).
[b] Green nZVI were produced using extracts of green tea leaves.

Iron nanoparticles have some specific advantages, such as high reactivity for a wide range of contaminants, lower degradation times when compared to the granular ZVI, generation of less toxic intermediate products, and also the possibility of injection in the form of aqueous slurries to treat contaminated soils and groundwaters (Figure 1.3). The growing use of these nanomaterials in pilot and full-scale applications in the last decade is expressive. According to the United States Environmental Protection Agency (USEPA), in November 2011, there were 36 projects at pilot and full-scale (11 were Superfund sites), including private, state and federal cleanup projects [109]. There were 15 pilot tests in Europe [110] and full scale applications in Italy, Germany, Czech Republic and Slovakia [111]. Most of them target soil and groundwater contamination with volatile organic compounds (perchloroethylene – PCE, trichloroethylene – TCE and corresponding daughter products); perchlorate; PCB and other organochlorines, as well as diesel products in sandy or silty sandy soils. There are also applications in glacial till soils and unconsolidated sediments [109].

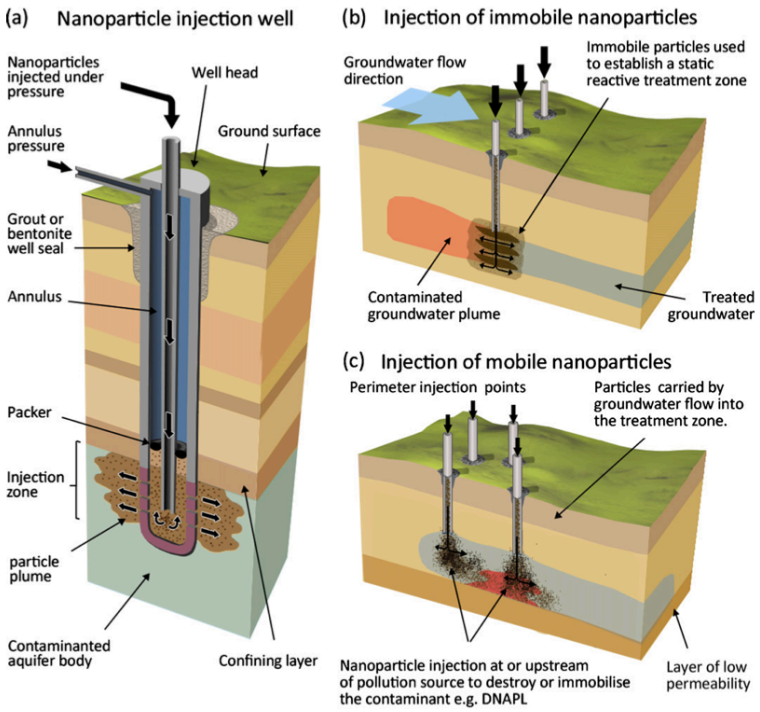


**Figure 1.3.** Different technologies for nZVI injection: (a) layout of a typical nanoparticle injection well; (b) injection targeting mobile contaminants, and (c) targeting immobile contaminants [112].

The mobility of nZVI in the subsurface is normally less than a few meters, as several field applications show [104, 108, 113-115], ranging from 1 m [116] to 6-10 m [114]. This is due to Brownian motion, the density of iron, long-range magnetic attractive forces and ionic strength in groundwater, which increase the aggregation of nZVI [117]. One strategy that has been used to tackle this limitation is coating the nanoparticles with different polymers (polyelectrolytes) or surfactants (Table 1.2), such as starch [103], sodium carboxymethyl cellulose (CMC) [102, 117], polyvinyl alcohol-co-vinyl acetate-co-itaconic acid (PV3A) [118], guar gum [119, 120], polyacrylic acid (PAA) [121-123], and olefin maleic acid copolymer [124, 125]. This coating allows electrosteric (combination of electrostatic and steric) repulsions that minimize magnetic and van der Waals attractions, responsible for agglomeration and limited mobility of the nZVI. There are a large number of studies on the transport of iron nanoparticles, mostly in column tests with sand [123, 126-129], glass beads [121, 127, 129, 130] and model soils [102, 131, 132]. Studies using high concentrations representative of field applications show that, although stabilized nanoparticles are more mobile than bare nZVI [121, 123, 127, 133], aggregation remains an important process, and can be affected by the particle size distribution and $Fe^0$ content of nZVI, as well as by groundwater ionic strength and composition [129, 130]. The affinity with soil minerals, resulting in nZVI deposition onto the porous matrix [134], also limits their

mobility. The main factors that influence nZVI adsorption onto soil and aquifer materials are: i) surface chemistry of soil and the nanoparticles; ii) groundwater chemistry (ionic strength, pH, organic matter content); iii) hydrodynamic conditions (pore size, porosity, flow velocity, and degree of mixing and turbulence) [135].

Another nZVI limitation is the shorter lifetime compared to granular zero valent iron, due to high consumption via undesired reactions, i.e. corrosion in aqueous media, with $Fe^0$ being oxidized to $Fe^{2+}$ (fast process) and $Fe^{3+}$ (slower process) [134]. Rapid corrosion occurs in the presence of dissolved oxygen [eq. (1.1)], and then $Fe^{2+}$ could be further oxidated by $H^+$ [eq. (1.2)] with the precipitation of the less soluble ferric $Fe^{3+}$ hydroxides (rust). Besides, corrosion can also occur under anaerobic conditions with water as the oxidant [eq. (1.3)], generating molecular hydrogen [136]:

$$2Fe^0_{(s)} + 4H^+_{(aq)} + O_{2\,(aq)} \rightarrow 2Fe^{2+}_{(aq)} + 2H_2O_{(l)} \quad (1.1)$$

$$4Fe^{2+}_{(aq)} + 4H^+_{(aq)} + O_{2(aq)} \rightarrow 4Fe^{3+}_{(aq)} + 2H_2O_{(l)} \quad (1.2)$$

$$Fe^0_{(s)} + 2H_2O_{(l)} \rightarrow Fe^{2+}_{(aq)} + H_{2(g)} + 2OH^-_{(aq)} \quad (1.3)$$

The reaction of nZVI with inorganic contaminants is controlled by the redox potential of the inorganic species [137]: if it is significantly higher than the redox potential of $Fe^0$, the compound is removed by reduction, and subsequent precipitation or co-precipitation; if it is significantly lower, then the reduction is not possible, and the compound can be eliminated only via adsorption on the iron particles; if the redox potential is moderately higher, a concurrence of reduction and (co)precipitation could be observed. A comprehensive review on nZVI reactivity was published in O'Carroll et al. [137] and by Yan et al. [138]. O'Carroll et al. [137] classified the predominant nZVI removal mechanism for the most common inorganic contaminants into the following categories:

I. Reduction: Cr, As, Cu, U, Pb, Ni, Se, Co, Pd, Pt, Hg, Ag;
II. Adsorption: Cr, As, U, Pb, Ni, Se, Co, Cd, Zn, Ba;
III. Oxidation/reoxidation: As, U, Se, Pb;
IV. Co-precipitation: Cr, As, Ni, Se;
V. Precipitation: Cu, Pb, Cd, Co, Zn.

Zero valent iron nanoparticles were considered a promising alternative for PCB degradation in aqueous solutions [71, 96, 139] because they can promote reductive dechlorination (Figure 1.4), with a multi-step removal of chlorine atoms in different pathways, which can occur in parallel or sequentially. However, a 95% dechlorination in historically contaminated soils was only achieved at

high temperatures (300 °C) [97]. Another recent study reported 81.5% and 53.4% PCB removal from soils from an e-waste recycling area in batch tests with 12 days duration, using the Fe/Pd bimetallic nanoparticles, compared with 67.4% and 48.3% using bare nZVI [140]. Until now, the efficiency of PCB dechlorination in soils and soil slurries is limited when compared with aqueous solutions, due to competing reactions occurring and also to the strong PCB adsorption to soil organic matter.

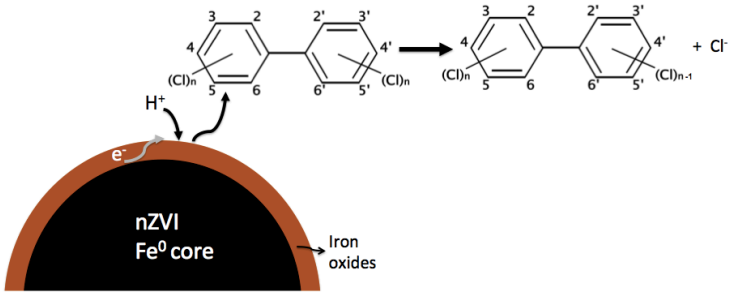


**Figure 1.4.** Dechlorination of PCB by zero valent iron nanoparticles (adapted from Wang and Zhang [71] and Yan et al. [138]).

Most of the benefits of using nZVI are based on short-term considerations, and there are large data and knowledge gaps within almost all aspects of environmental exposure and effect assessment (i.e. potential for persistency, bioaccumulation, toxicity) in which further research is needed [141]. The potential risks and environmental impacts associated with the use of nZVI have been studied, but contradictory results can be found in the literature [142-147]. Besides that most toxicity studies are limited, due to the use of a relatively high dose of nZVI, and to the absence of an environmental background matrix [138]. According to Grieger et al. [141], the current and traditional environmental risk assessment approaches are not applicable and there is an urgent need to develop analytical methods to identify and quantify nanomaterials in environmental samples and complex matrices [148, 149], despite the recent developments using techniques like field-flow fractionation, ultrafiltration and nanofiltration, size-exclusion chromatography, capillary electrophoresis, hydrodynamic chromatography, isoelectric focusing, and inductively coupled plasma-mass spectroscopy [150-152].

### 1.1.4 Electrokinetic remediation

Electrokinetic (EK) remediation, also called electrokinetics, electroremediation or electroreclamation, is a solid technology that has been successfully used since the late 1980s to treat contaminated soils, specially low permeability soils [153-157]. Electrokinetics can be defined as the application or induction of a low-level direct current on the order of mA $cm^{-1}$ of cross-sectional area between the electrodes or an electric potential difference about few V $cm^{-1}$ across a soil mass containing fluid or a high fluid content slurry/suspension, causing or caused by the motion of electricity, charged soil and/or fluid particles [158]. In this method, the current act as the "cleaning agent", generating transport processes (as electroosmosis, electromigration and electrophoresis) and electrochemical reactions (electrolysis and electrodeposition) [155] as showed in Figure 1.5.

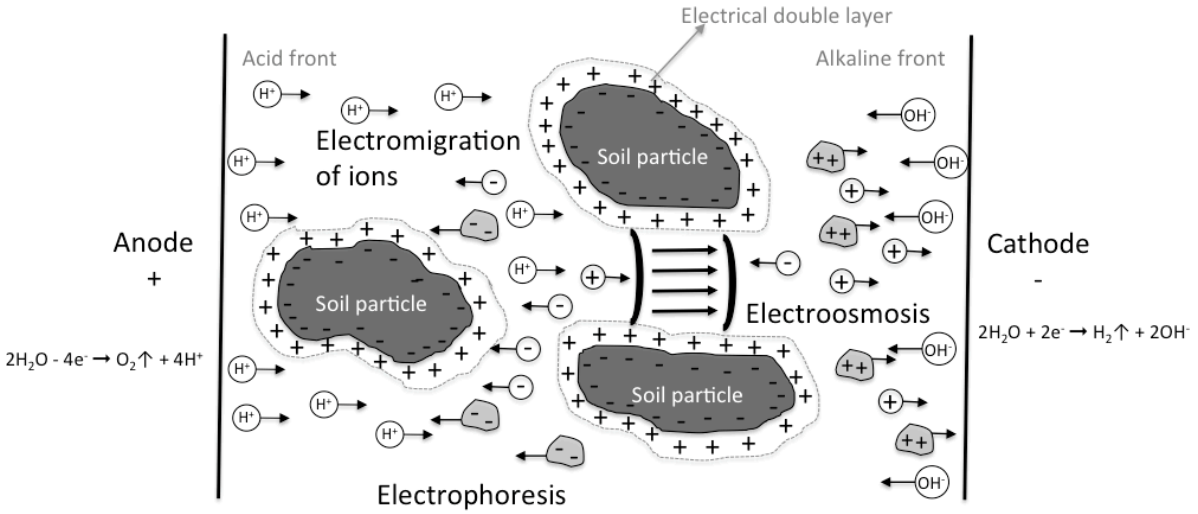


**Figure 1.5.** Schematic representation of the main phenomena occurring in electrokinetics.

Early EK models assumed that *electroosmosis* (field-induced convection of fluid through a porous medium towards the positive or negative electrode depending on the overall surface charge of the porous material) was the only significant transport process [159]. This approach was inadequate for explaining the movement of ionic species (ions and ionic complexes) in the aqueous pore solution, which mainly depends on *electromigration* (field-induced transport of ions in an electrolyte towards the electrode of opposite charge). The electromigration flux is determined by the ionic mobility, tortuosity, porosity of the material, and charge of the ions [155]. In the case of colloidal suspended charged particles (colloids, clay particles, and organic particles), electrophoresis is the prime transport process. *Diffusion* is the movement of the ionic species in soil solution caused by

concentration gradients formed by the electrically induced mass transport. Diffusion is often ignored when studying EK as the ionic mobility of a species is much higher than its diffusion coefficient [155].

Electrochemical reactions are also important in electroremediation. Electrolysis reactions prevail at the electrodes, due to the oxidation occurring at the anode and the reduction at the cathode, resulting in water electrolysis, generating an acid front from the anode, whereas reduction at the cathode produces an alkaline front:

$2H_2O - 4e^- \rightarrow O_2\uparrow + 4H^+$ $E_0 = -1.229$ V (anode) (1.4)

$2H_2O + 2e^- \rightarrow H_2\uparrow + 2OH^-$ $E_0 = -0.828$ V (cathode) (1.5)

Secondary reactions may occur depending on the concentration of available species, like metals $M_e$, for example [155]:

$H^+ + e^- \rightarrow \frac{1}{2} H_2\uparrow$ (1.6)

$M_e^{n+} + ne^- \rightarrow M_e$ (1.7)

$Me(OH)_{n(s)} + ne^- \rightarrow M_e + nOH^-$ (1.8)

Electrodialytic soil remediation (EDR) is a remediation method developed for removing heavy metals from polluted soil, based on the combination of the electrokinetic movement of ions in soil with the principle of electrodialysis [160]. Electrodialytic remediation of solid waste products started in 1992 at the Technical University of Denmark (DTU) and was patented in 1995 (PCT/DK95/00209). EDR was originally applied to moist and consolidated soil for *in situ* treatment. Later, a faster and continuous process was developed [161-163]: the soil is suspended in a solution (most often water) and stirred, primarily to use *ex situ*. This method was used successfully for the remediation of heavy metals contaminated soils, both in soil mass containing fluid [157] or a high fluid content slurry/suspension [161-163], for the cleanup of different contaminated matrices like mine tailings, different types of fly ashes, sewage sludge, freshwater sediments and harbor sediments [164-170]. Recently, a new development in EDR is the two-compartment electrodialytic setup also developed [171] at DTU, in which the anode is placed directly in the compartment in which the soil or the contaminated matrix is suspended and stirred simultaneously.

The removal of heavy metals from soils is one of the most studied processes in electroremediation [172]. Despite the success at bench scale, there are limited full-scale applications for soil remediation (Figure 1.6). In the last years, numerous research teams developed methods to increase electrokinetics removal efficiency, such as pH control [173, 174], enhancement solutions [175], desorbing agents [176], surfactants [177], pulse [178, 179] and alternating [180] current.

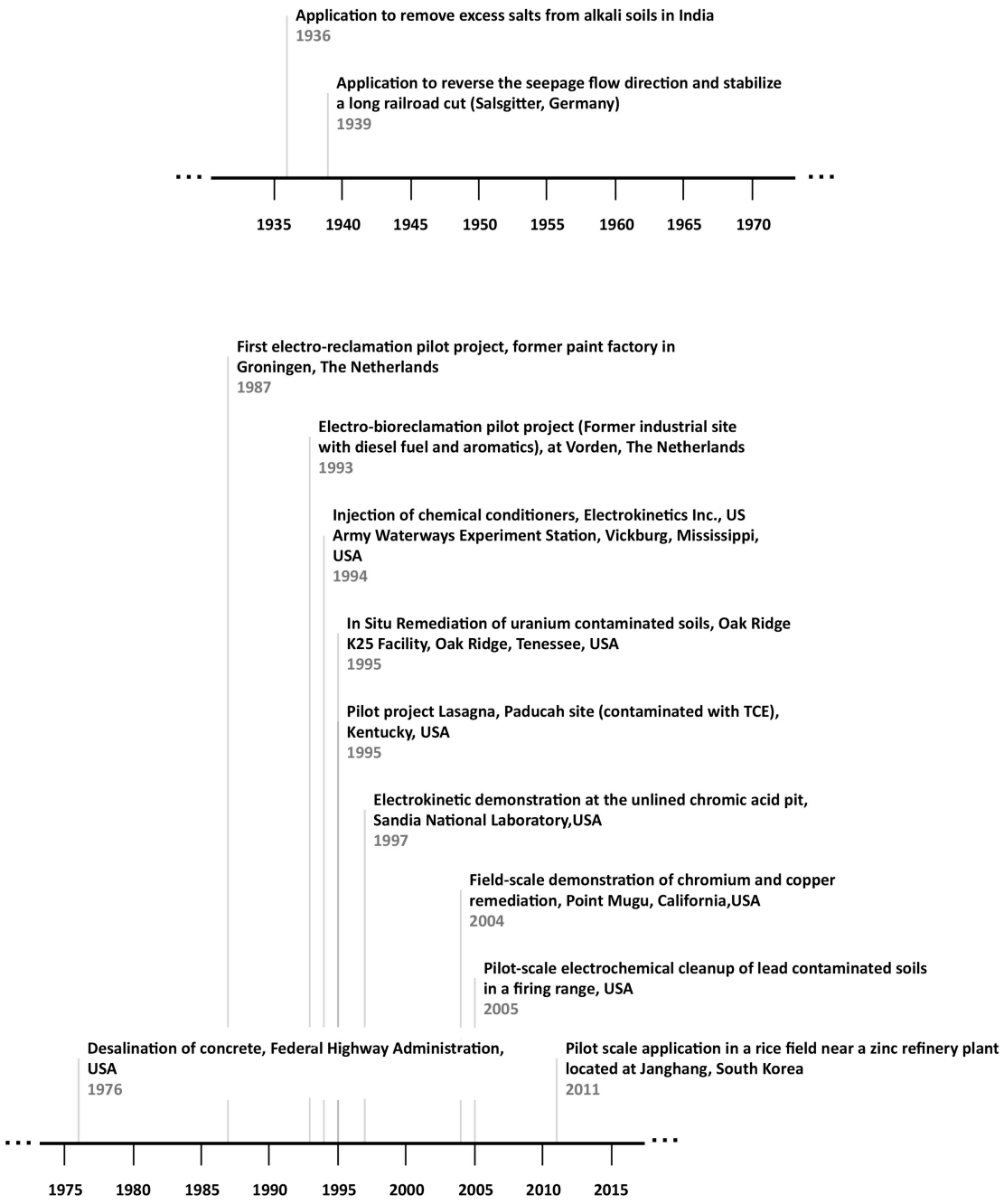


**Figure 1.6.** Timeline of the main pilot and full-scale applications of electrokinetics [159, 172, 181-185].

For this Ph.D. study, Gomes et al. [186] made a literature review of the experimental work carried out to improve organochlorines electroremediation from contaminated soils, both with enhancement solutions or using other remediation technologies simultaneously (Section II.2). The main conclusions indicate that it is not possible to clearly state which technique is the best, as experimental approaches and contaminants are different. Also, removal efficiencies in spiked kaolinite are much higher than in real contaminated soils, showing the influence of the

organochlorines chemical properties, especially their low water solubility and sorption to soil particles, as well as other factors like aging of the contamination [186].

When the referred review was made, EK had never been used to extract PCB from soils. Since then, a study on spiked soils reported an 87% removal efficiency for PCB just with EK [187]. Still this paper fails to explain this removal, because no quantification of PCB in the anolyte and the catholyte was made, nor degradation processes were identified or proposed. Recently, two studies tested the electrokinetically enhanced persulfate oxidation of PCB in spiked soils [67] and in contaminated soils using also a surfactant [66]. In the first study, the highest level of PCB oxidation, 78%, was achieved in spiked kaolin with temperature activated persulfate in 7 days [67]. These results could not be replicated in the glacial till soil (with only 14% oxidation), probably due to the high buffering capacity, non-homogeneous mineral content and high organic content [67]. In the second study, the surfactant used was Igepal CA720 and zero valent iron (added in the cathode reservoir) was the persulfate activator [66]. The highest PCB degradation rate was 38% in the treatment without activator. The authors found that the use of iron as persulfate activator was ineffective as it consumed most of persulfate and inhibited its transport into the cell.

### 1.1.5 Coupling EK and nZVI

The primary goal of soil remediation is achieving the required risk reduction for regulatory compliance or liability reduction at minimal cost [188]. According to Rao et al. [188], the use of treatment trains or integration of remediation technologies that, when coupled together work in a synergistic manner, minimizes the cost of achieving risk-based endpoints. The general principle of treatment trains is the use of a combination of techniques, simultaneously or in succession, to enhance treatment performance in a quicker, more efficient, and cost effective way. In some cases, a combination of two technologies might result in more efficient risk reduction, e.g. coupling abiotic and biotic transformations. In other cases, a sequential application of successively less aggressive technologies might be the best approach, e.g. thermal treatment, followed by less aggressive engineered bioremediation, then monitored natural attenuation [188].

Some case studies include combining hydraulic flushing and the electrokinetic treatment for the simultaneous removal of PAH and heavy metals [189], electrokinetic-enhanced bioaugmentation for remediation of clays contaminated with chlorinated solvents [190], hydraulic pressure injection of electrolyte to enhance electrokinetics for the remediation of pentachlorophenol (PCP) contaminated soil [191], electrochemical Fenton oxidation for the remediation of hexachlorobenzene (HCB)

contaminated soil [192-195], coupling surfactants/cosolvents with oxidants for enhanced dense non-aqueous phase liquid removal [196].

Electrokinetic remediation and zero valent iron nanoparticles were used in conjunction, both to enhance the transport of iron nanoparticles in low permeability fine-grain soils, and to degrade organic contaminants (Table 1.3). The simultaneous use of both remediation techniques (EK and nZVI) allows the contaminant removal from soil (traditional outcome in EK) and also its degradation by nZVI, whose transport is enhanced by the direct current, both by electrophoresis and electroosmosis.

**Table 1.3.** Coupling of electrokinetic remediation and zero valent iron nanoparticles in bench-scale experiments (modified from [186]).

| Matrix | Target contaminant | Duration of test(s) | Electrolyte | Voltage gradient ($V\ cm^{-1}$) | % contaminant removal best results | Ref. |
|---|---|---|---|---|---|---|
| White Georgia kaolin clay | - | 46 h | 0.2 M NaCl | 0.25 | - | [197] |
| Loamy sand | - | 6 d | Simulated groundwater | 1.0 | - | [132] |
| Spiked soil | $KNO_3$ | 6 d | Simulated groundwater | 1.0 | 99 | [198] |
| Spiked kaolin | PCP | 427 h; 960 h | Deionized water | 1.0 | 55 | [199] |
| Spiked silica sand | PCE | 100 h | 0.01 M $Na_2CO_3$ | 1.0 | 76 | [200] |
| 40/60 or 100/200 sands | - | 10 d | 0.007 or 0.02 M NaCl | 0.55; 1.30 | - | [201] |
| Spiked sandy soil | TCE | 10 d | Simulated groundwater | 1.0 | 70 | [202] |
| Coarse and fine sand | - | 48 h | Simulated groundwater | 0.25; 0.5 | - | [203] |
| Spiked turf | PCP | 8 d; 14 d | 0.025 M $Na_2SO_4$ and 0.025 M $Na_2CO_3$ | 6.0 | 70 | [204] |
| Contaminated soil | PCB | 14 d | 0.01 M $NaNO_3$ | 1.0 ⟶ 2.0 | 20 | [205] |
| Boom clay | - | 160 h; 360 h | 0.01 M NaCl | 4.0 | - | [206] |

Fan et al. [205] were the first to combine EK and nZVI for remediation of PCB historically contaminated soil. Brij35-xanthan gum stabilized Fe/Pd bimetallic nanoparticles obtained the highest PCB removal efficiency, both in batch experiments and EK tests, with removal rates of about 50% and 20%, respectively. This limited removal is due to the strong adsorption of PCB to soils. The other surfactants tested (sodium dodecyl benzene sulfonate – SDBS and rhamnolipid) showed even lower PCB removal in the EK experiments.

## 1.2 Motivation and Objectives

There is an important need to develop new solutions for the remediation of persistent organic pollutants in contaminated soils and sediments, both due to their ecotoxicity and the regulatory obligations to soundly dispose or eliminate these contaminants. The common solutions of "dig and dump" and "dig and incinerate" are expensive and need to be replaced by sustainable alternatives.

The main research objective of this Ph.D. study was to find out if coupling electrokinetics and zero valent iron nanoparticles could be an efficient method for treating contaminated soils (with inorganic and organic contaminants), and which enhancement methods could be more useful and cost-effective. Chromium and two types of organic contaminants – the herbicide molinate and PCB – were considered for the experimental phase, at bench scale. Another important goal was to develop a deeper understanding of the mechanisms underlying the coupling of these two remediation techniques, namely the assisted direct current transport of iron nanoparticles, both through experiments and modeling.

Other objectives were:

- Development and testing a methodological and analytical approach for determining the fate of iron nanoparticles in the soil;
- Analysis of the mobility, reactivity and functional life-time of zero valent iron nanoparticles in the soil;
- Identification of the dechlorination pathways of PCB congeners by nZVI.

## 1.3 Original contribution

This dissertation presents several contributions targeting the aforementioned objectives and including some existing knowledge gaps. Regarding the direct current assisted transport of iron nanoparticles, it specifically considered the following:

- The assisted transport was tested here with high concentrations, typical of field applications, which represent more realistic experimental conditions than with diluted concentrations [197]. At high particle concentration (1-6 g $L^{-1}$) there is a higher agglomeration [128], so it is important to assess if a direct current can also enhance the nZVI transport in these conditions.

- Previous studies have only considered the nZVI transport in sand and clay [197, 201, 203]. Different porosity media (with mixtures of glass beads and kaolin clay) were tested as model soils and as an approach to more complex matrices.

- The influence of different electrolytes and the ionic strength in the assisted direct current transport was studied for the first time. Both factors also contribute to nZVI agglomeration and settling, hindering the transport of these nanoparticles.

- The modeling of the assisted transport only included the electrophoretic transport [201, 203]. The model now developed, and validated with the experimental data, includes all the transport processes – diffusion, electromigration of ions, electrophoresis and electroosmosis.

For the simultaneous use of electrokinetics and zero valent iron nanoparticles several innovations were also implemented:

- The conjunction of EK and nZVI was tested, for the first time, for chromium (VI) and molinate contaminated soils.

- In the experiments with EK and nZVI, diffusion experiments were always performed as control, to measure the effective improvement when using both methods. In previous studies [198-200, 202, 204-205], this issue was overlooked, only considering the effectiveness of both methods together.

- The suspended electrodialytic remediation of PCB contaminated soils was tested for the first time. Regarding organic contaminants, it was only tested before for polycyclic aromatic hydrocarbons (PAH) [207].

- The two-compartment electrodialytic setup developed at DTU [171] together with the addition of iron nanoparticles was tested and compared with the traditional three-compartment electrokinetic setup.

- Enhancement methods, like the use of surfactants, were also tested for the first time, when using the two-compartment electrodialytic setup. Two different surfactants (saponin and Tween 80) were assessed as enhancement methods.

## 1.4 Dissertation outline and content

After this introductory chapter, Section 2 presents a synthesis of the experimental approaches implemented to reach the objectives. Section 3 shows the major findings from the experimental work presented in detail in the Part II of the dissertation, namely II.3 to II.10, focusing on the direct current assisted nZVI transport in different porous media and with different electrolytes, the electroremediation with nZVI of Cr (VI), molinate and PCB contaminated soils. The main findings of the numeric modeling of nZVI direct current assisted transport are also presented in this Section. The discussion and limitations of the experimental work done is presented in Section 4. Finally, Section 5 summarizes the overall conclusions and identifies areas for future research.

Part II of the dissertation includes all the publications in peer-reviewed journals (published and submitted) that were developed during the Ph.D. study. As Part I is a summary of the publications presented in Part II, some overlap and repetition are inevitable.

2

# 2. Research methodology

The general methodology followed in this Ph.D. study is illustrated in Figure 2.1. The works started with a comprehensive state of the art review (phase 1, Figure 2.1) on the enhancement methods and technologies used in conjunction with electrokinetics for the remediation of organochlorines in soil (Section II.1), and on the technologies for *in situ* and *ex situ* remediation of PCB contaminated soils and sediments (Section II.2). The experimental work comprises phase 2 and 3, detailed in Figure 2.2 and 2.3, respectively, and also in Table 2.1. Finally, phase 4 is the numerical modeling of the nZVI transport under electric fields.

The direct current assisted transport of iron nanoparticles (phase 2) was tested in model soils – kaolin clay, as a low permeability medium, and different percentages of kaolin and glass beads for different porosity media – in a modified electrophoretic cell (Figure 2.4). Various electrolytes with different ionic strengths were used in the experiments. The applied voltage gradient was another variable considered in this phase and two different values were tested.

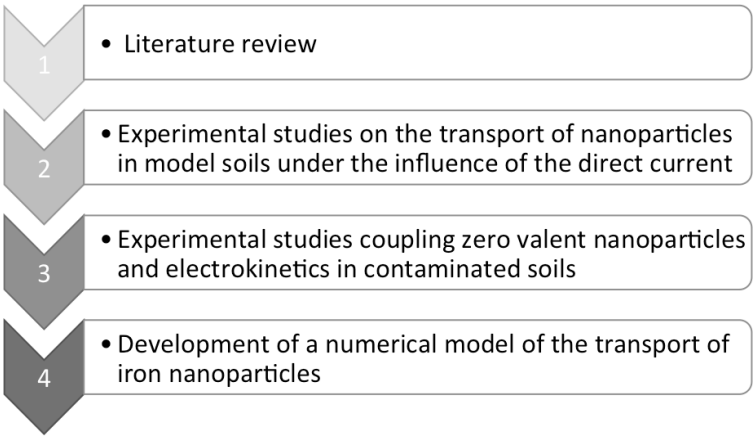


**Figure 2.1.** Identification of the four main phases in the methodology used.

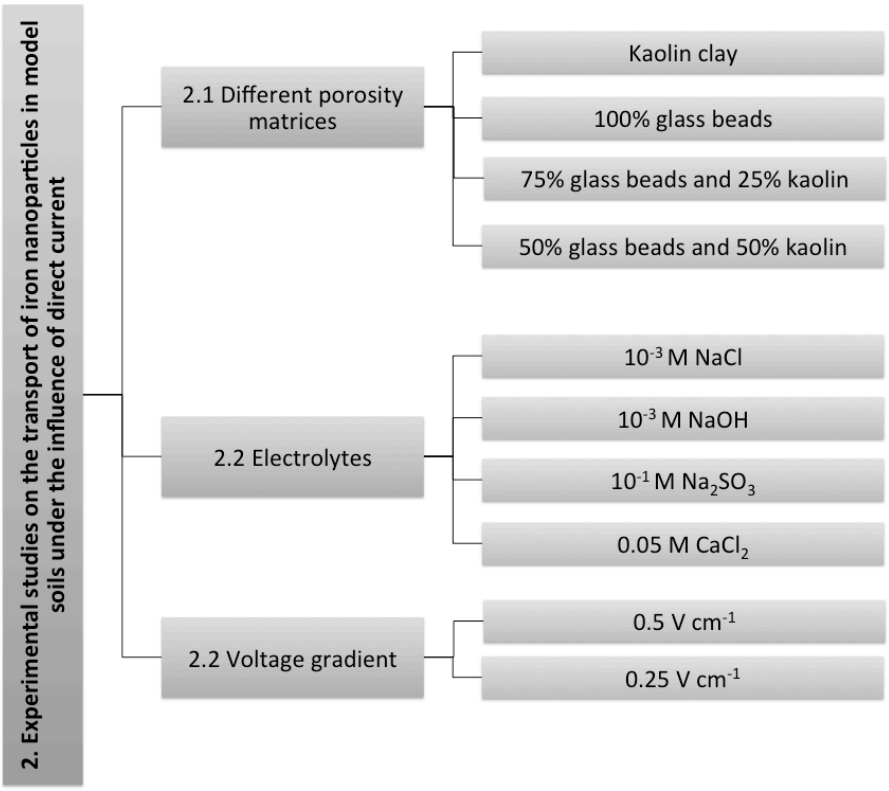


**Figure 2.2.** Different variables and conditions considered in the experiments for the study of iron nanoparticles transport in model soils, under the influence of the direct current.

In phase 3 (Figure 2.3), the simultaneous use of electrokinetics and zero valent iron nanoparticles was tested with inorganic and organic contaminants. The starting point was the heavy metal – Cr(VI), as previous works have demonstrated the EK effectiveness for its removal [208]. Kaolin clay spiked with Cr(VI) was used in the modified EP cell to assess the EK plus nZVI efficacy. The next step was the test with an organic contaminant also previously tested with EK [209]. Two different soils were spiked with molinate (S-ethyl N,N-hexamethylene-1-carbamate), an herbicide traditionally used in rice paddies worldwide. Molinate degradation with nZVI in soils was tested for the first time. The experiments were designed to test two different soils, the importance of pH control in the anolyte (minimizing the acid front), and also the influence of a direct current in the nZVI transport and molinate degradation in the conjunction of the two techniques. The electrokinetic cell was modified in the New University of Lisbon to include an injection reservoir (separated with a 1 mm nylon mesh) for the daily injection of a commercial suspension of iron nanoparticles (Figure 2.5 and Section II.6).

The most recalcitrant contaminants – PCB – were the last to be tested. The experiments also tested two different contaminated soils (Figure 2.3 and Table 2.1). Soil 1 was provided by a hazardous waste operator in Portugal and is a mixture of contaminated soils from industrial sites with transformers oils spills. Soil 2 was sampled in a decommissioned school, in Hovedstaden (Capital Region of Denmark), and the PCB resulted from the weathering of the windows joint sealants. In these experiments, two different setups were tested: the traditional three-compartment electrokinetic setup (Figure 2.6) and the two-compartment electrodialytic setup (Figure 2.7) developed at the Technical University of Denmark [171]. The enhancing/desorption effects of two different surfactants (Tween 80 and saponin) when using electro-nano remediation were also assessed.

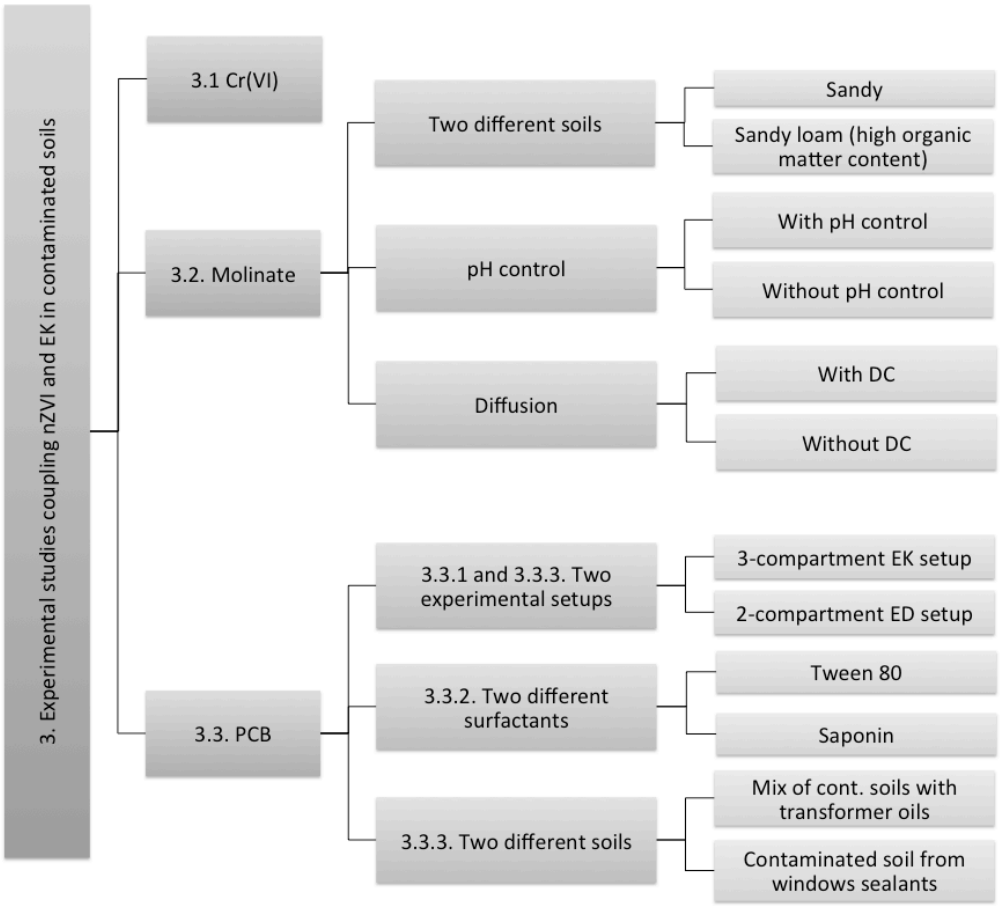


**Figure 2.3**. Different variables and conditions considered in the experiments coupling electrokinetics and zero valent iron nanoparticles in contaminated soils.

The modeling of the iron nanoparticles transport (phase 4) is the combination of two strongly coupled modules: one for the transport process and the other for chemical equilibrium calculations. The model consists in the Nernst–Planck coupled system of equations, which accounts for the mass

balance equation of ionic species in a fluid medium, when diffusion and electromigration are considered in the ions transport process. In the case of nZVI (with negative charge), diffusion and electrophoretic terms have been considered. In both cases, also the electroosmotic flow was included in the equation. Regarding the chemical equilibrium, only the water chemical equilibrium and the electrochemical reactions at the electrodes were considered.

The transport processes of nZVI take place in a domain that consists of the modified electrophoretic cell (Figure 2.4) with a square tray (20 cm x 20 cm) containing a layer of solid (kaolin and/or glass beads) saturated with electrolyte, and the anode and cathode compartments filled with the same electrolyte solutions. The model operates in two steps, first simulating the process kinetic by integrating forward in time one-dimensional transport equations, including electrochemical reactions in the electrodes, and, after that, reestablishing the chemical equilibriums before the next step of integration.

**Table 2.1.** Summary of the experimental conditions.

| Phase | Number of experiments | Matrix | Duration (d) | Electrolyte (anolyte and catholyte) | pH control (in the electrolytes) | Voltage gradient (V $cm^{-1}$) | PAA-nZVI added (g) | Control experiments | Experimental cell | Section |
|---|---|---|---|---|---|---|---|---|---|---|
| 2.1 | 10 | Kaolin clay<br>100 % glass beads<br>75 % glass beads and 25 % kaolin<br>50 % glass beads and 50 % kaolin | 2 | $10^{-3}$ M NaCl | None | 0.25 | 0.008 | Diffusion (no current)<br>Current without nZVI | Modified electrophoretic cell | II.3 |
| 2.2 | 14 | Kaolin clay | 2 | $10^{-3}$ M NaCl<br>$10^{-3}$ M NaOH<br>$10^{-1}$ M $Na_2SO_3$<br>0.05 M $CaCl_2$ | None | 0.25 and 0.5 | 0.008 | Diffusion (no current)<br>Current without nZVI | Modified electrophoretic cell | II.4 |
| 3.1 | 3 | Kaolin clay | 1 | $10^{-3}$ M NaCl | None | 0.25 | | Diffusion (no current)<br>Current without nZVI | Modified electrophoretic cell | II.5 |
| 3.2 | 5 | Spiked soils (sandy and loamy sand) | 6 | $10^{-2}$ M $NaNO_3$ | 2 experiments with NaOH 1M added to anolyte | ~ 5* | 1.150 | Diffusion (no current)<br>pH control | Modified cylindrical cell with injection reservoir near to anode | II.6 |
| 3.3.1 | 6 | PCB historically contaminated soil (loamy sand) | 5, 10, 20 and 45 | $10^{-2}$ M NaCl | HCl 5M added to the catholyte in the ED setup | 2 | 2.990; 2.300 and 4.6000 | Diffusion (no current)<br>Setup | Cylindrical cell<br>Three-compartment cell and Two-compartment cell | II.7 |
| 3.3.2 | 6 | PCB historically contaminated soil (loamy sand) | 5 | $10^{-2}$ M NaCl | HCl 5M added to the catholyte in the ED setup | 1 | 2.300 | Diffusion (no current)<br>Current without nZVI<br>Type of surfactant | Two-compartment cell | II.8 |
| 3.3.3 | 15 | PCB historically contaminated soils (loamy sand and silt loam) | 5 | $10^{-2}$ M NaCl | HCl 5M added to the catholyte in some experiments | 2 (EK)<br>1 (ED) | 2.990 and 2.300 | Diffusion (no current)<br>Current without nZVI<br>Setup | Cylindrical cell<br>Three-compartment cell and Two-compartment cell | II.9 |

* Experiments with constant current density of 2.5 mA $cm^{-1}$.

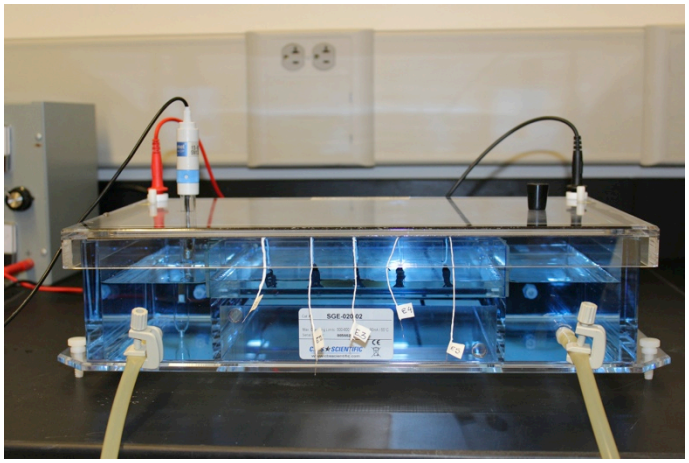

**Figure 2.4.** Electrophoretic cell used in the nZVI transport and the Cr(VI) experiments.

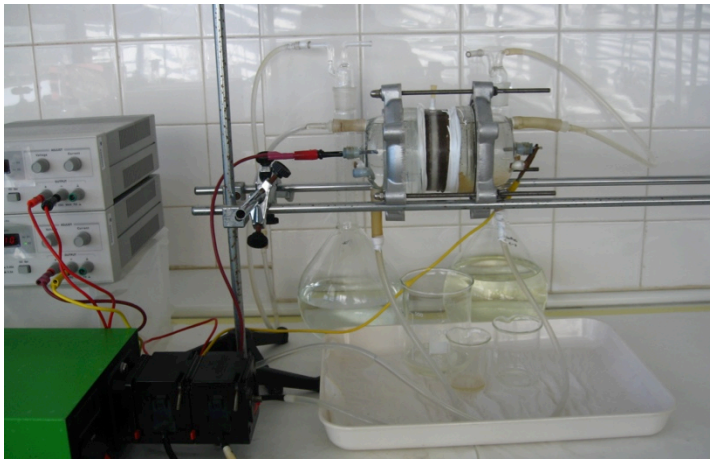

**Figure 2.5.** Modified EK cell for the molinate experiments with nZVI injection reservoir.

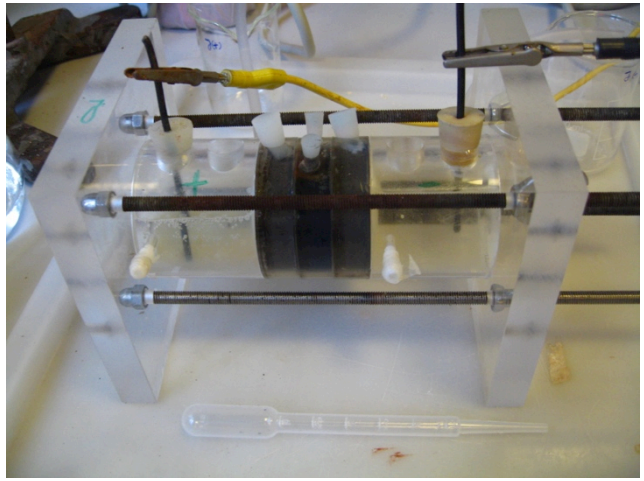

**Figure 2.6.** Three compartment EK setup used with PCB contaminated soil.

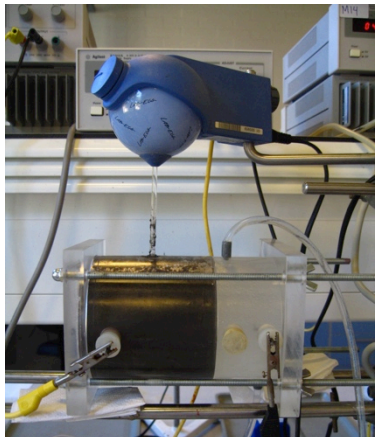

**Figure 2.7.** Two compartment ED setup used with PCB contaminated soil.

3

# 3. Major findings from the experimental work

## 3.1 Expeditious methods for nZVI detection

A methodological and analytical approach for determining the fate of nZVI in the soil was developed and tested (Section II.3) before starting the nZVI direct current assisted transport experiments. The approach was based in the measurement of parameters such as pH, electrical conductivity, and oxidation-reduction potential (ORP). The selection of these parameters was related with field observations in groundwaters after nZVI injection, in which ORP values decreased from about −100 to −400 mV [210], and pH and conductivity increased [211]. The measurements were made in suspensions of different concentrations of PAA-nZVI, prepared with deionized water, 0.1 M and 0.001 M NaCl solutions, at fixed times. The data obtained was used to generate calibration curves of relative nZVI concentration.

In the tested suspensions, there was no clear fit for the pH calibration curves, as the pH values measured at different concentrations of PAA-nZVI were identical, and did not show meaningful changes in time (Figure 3, Section II.3). The PAA-nZVI concentrations in deionized water showed good fits to the linear regression analysis for conductivity, except for the measurements made at 12 h. However, when NaCl is added, the salt conductivity completely masked the nZVI presence and there was no change in conductivity with increasing concentrations of PAA-nZVI. Hence, the conductivity could not be used as an expedite method to evaluate the distribution trends of the iron nanoparticles in the enhanced transport experiments.

As ORP measurements have been widely used as an indirect method to assess the results of injection of nZVI for groundwater remediation [104, 108, 212], it was expected that these values could be used as a reliable indicator of nZVI concentration in the transport experiments. It was challenging to

obtain stable values of the ORP for the suspensions tested, with some readings taking more than 30 min. The results showed that ORP decreased with increasing concentration of nZVI. The relationships between these variables were highly nonlinear, suggesting a complex response function that cannot be reliably used as a calibration curve (Figure 3.1).

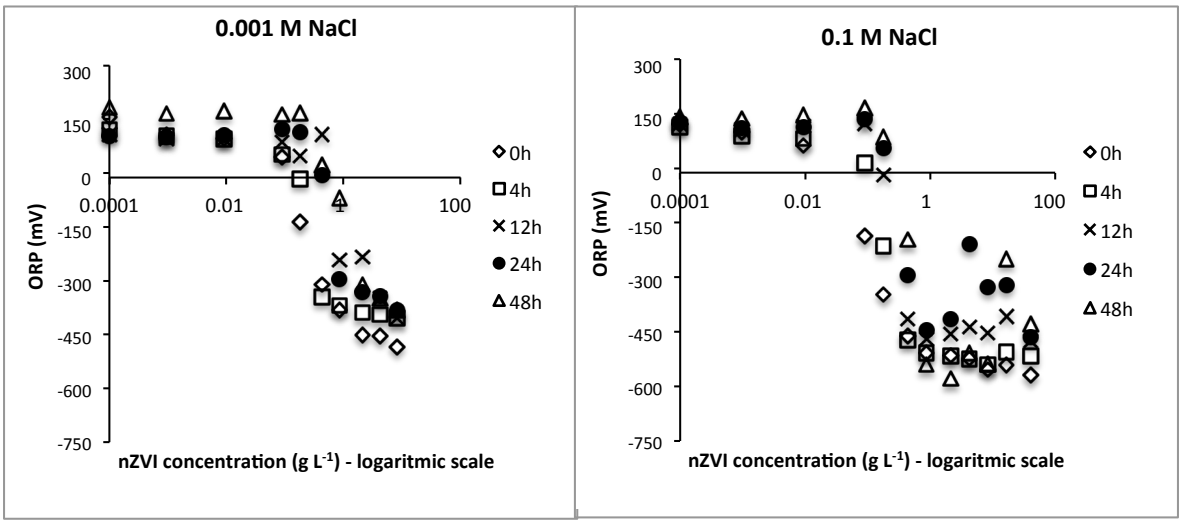


**Figure 3.1.** ORP values measured in the PAA-nZVI suspensions with 0.001 M and 0.1 M NaCl.

Although for nZVI concentrations lower than 0.1 g $L^{-1}$ there is an approximately linear relationship (with $R^2 > 0.90$), at higher concentrations, the ORP becomes relatively independent of the nZVI concentration. Both observations are consistent with the results of Shi et al. [213] that used rotating disk electrodes in nZVI suspensions to assess the effects of nanoparticles on ORP. These researchers found that the response of ORP electrodes to suspensions of nZVI is not a simple function of iron nanoparticles concentration. At high concentrations of nZVI, ORP is dominated by direct interaction between the electrode and the nanoparticles, but this response is nonlinear and saturates with increased coverage of the electrode surface with adsorbed particles [213]. At low nZVI concentrations, in aqueous suspensions, the measured ORP is a mixture of contributions that includes adsorbed nZVI and the dissolved $H_2$ and the Fe(II) species that arise from corrosion of nZVI [213]. Therefore, the changes in ORP at low concentrations of nZVI (< 0.1 g $L^{-1}$) may be a viable method to track the relative spatial and temporal distribution of nZVI in controlled experiments.

## 3.2 Direct current assisted transport of zero valent iron nanoparticles

### 3.2.1 Different porosity matrices

The direct current assisted transport of zero valent iron nanoparticles in different porosity media was investigated in Section II.3 and compared with diffusion. In general, higher concentrations of iron across the test bed (in samples over the auxiliary electrodes E1-E5) were measured when a direct current was applied (Figure 3.2), indicating that the nZVI transport was enhanced.

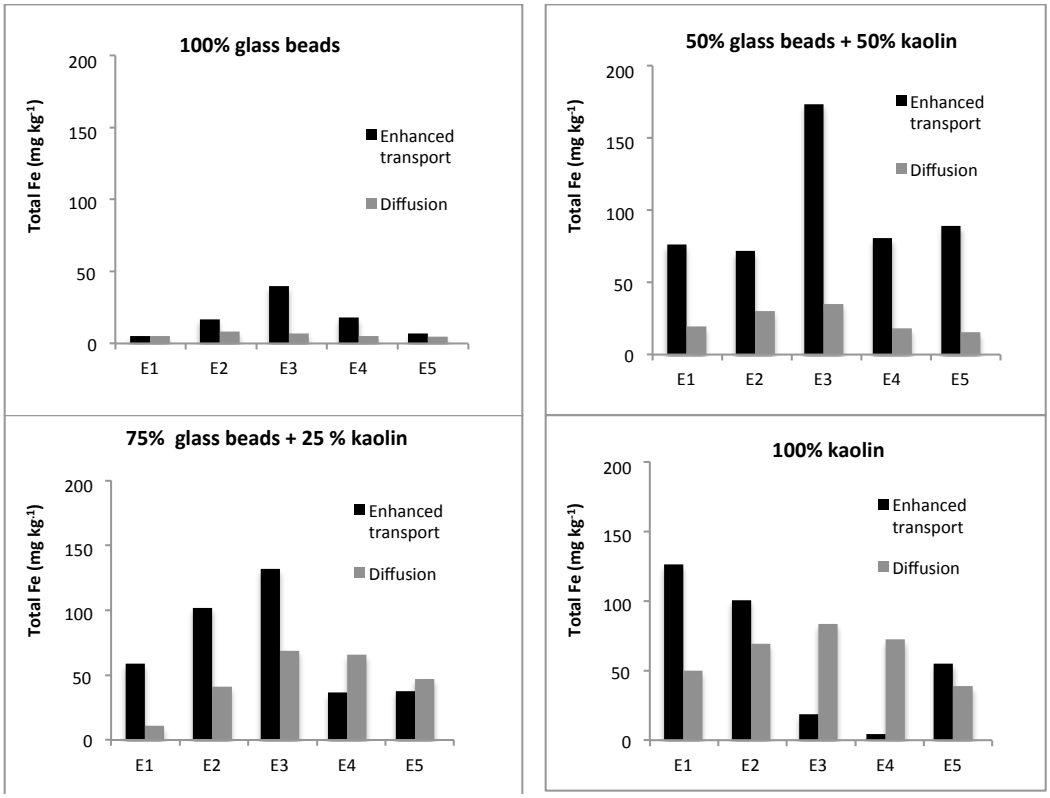


**Figure 3.2.** Additional total iron (mg $kg^{-1}$) in soil sections compared with the initial soil concentration using different porous media in the enhanced transport and diffusion experiments.

In all the experiments with glass beads there was a well-defined peak of concentration at E3 (i.e., practically the injection point). This was probably due to the nZVI aggregation, or to the fast corrosion of the iron nanoparticles, or to both phenomena. It has been previously shown that at high particle concentrations (1-6 g $L^{-1}$) nZVI have a higher tendency for agglomeration [128]. When nZVI aggregate and form clusters larger than the soil pores, their transport becomes restricted [214]. Changes to the nZVI mobility can be due to volumetric expansion with corrosion (eq. 1.1 and 1.3).

The volume of corrosion products (Fe hydroxide or oxide) is larger than that of the original metal ($Fe^0$) and these products are likely to contribute to porosity loss, promoting simultaneously particle agglomeration [135].

PAA-nZVI did not move into the aqueous phase in the electrode chambers, except for the cathode chamber in the enhanced transport tests with 100% kaolin (final concentration of 0.43 mg $L^{-1}$) and 100% glass beads (0.74 mg $L^{-1}$ in the anode compartment and 0.09 mg $L^{-1}$ in the cathode). This indicates that the electroosmotic flow (EOF) was possibly dominant in transporting nZVI in pure clay, whereas electrophoresis was the main mechanism to transport nZVI in surface neutral glass beads. In mixed samples, it appears that the EOF and electrophoresis compete, resulting in the prolonged presence of iron in the pores and potential capture on the clay surfaces. Other experimental results showed that there was greater deposition of nZVI onto clay minerals compared to similar sized silica fines due to charge heterogeneity on clay mineral surfaces [215].

The pH and ORP conditions measured during the experiments were favorable to the nZVI oxidation. Also, the initial conditions were not advantageous to the mobility of PAA-nZVI, because low pH (such as the kaolin pH = 4.97) increases deposition of nZVI in clay, as well as nZVI aggregation [215]. The typical profile in electrokinetic treatments of a pH front increasing from the anode to the cathode was not observed in the media in the experiments, which can be attributed to the low values of current density applied, or to the absence of the physical conditions for fast transport of $H^+$ and $OH^-$ from the electrode compartments into the media. Only in the experimental setups with 100% glass beads was noticed the effect on pH from the injection of the PAA-nZVI, particularly in E2, E3 and E4, in which pH values higher than 8 were measured.

The use of Pourbaix (Eh-pH) diagrams, as an indication of the dominance of particular Fe species at the recorded Eh and pH measurements, allowed observing that all data from diffusion tests form a cluster that corresponds to the formation of $Fe_2O_3$ under oxidizing conditions (passivity region) (Figure 3.3). Regarding the experiments with direct current enhanced transport of PAA-nZVI, the values measured above E1 and E2 electrodes (i.e., nearest to the anode), during the first 6-7 h of the experiments match the $Fe^{2+}$ area (corrosion region). There is a distinct cluster of values measured in the glass beads bed, in which pH values were much higher than in other experiments. Predictions from these stability diagrams are only accurate when the system approaches thermodynamic equilibrium in aqueous solutions, however, the results are consistent with the visual observations of the iron injected in the cell, since only after one hour it was clearly visible that the iron nanoparticles had started to present an orange color, typical of its oxidation.

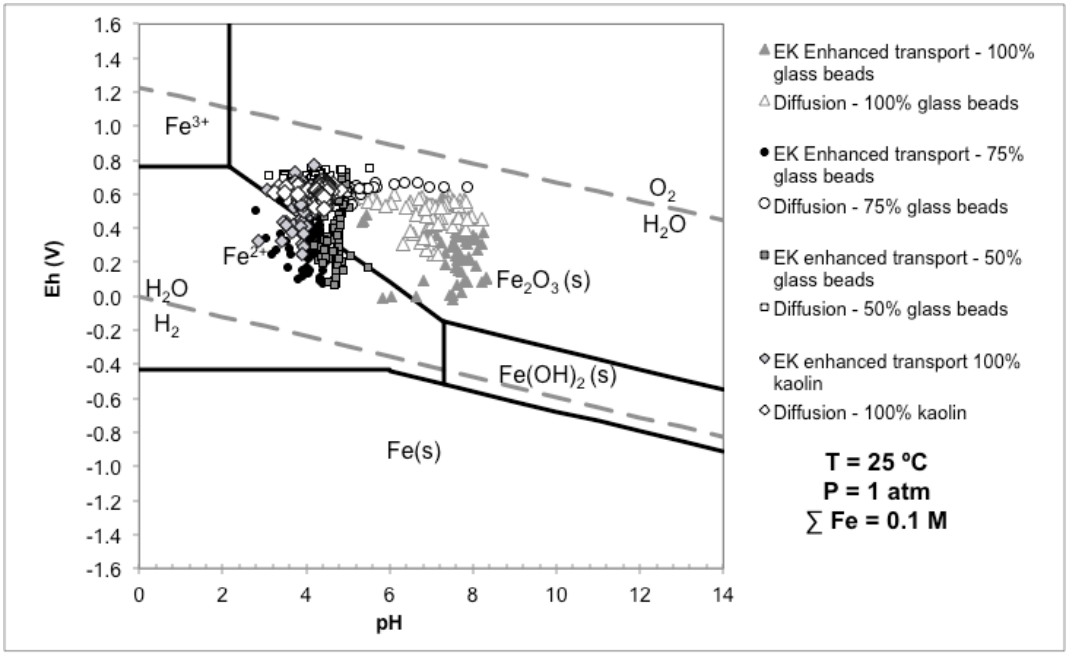


**Figure 3.3.** Pourbaix diagram with the values measured during 48 h in the electrodes embedded in the electrophoretic cell.

### 3.2.2 Different ionic strength electrolytes

The main objective of this study was to assess if low direct current can enhance the nZVI transport at concentrations typical of field applications, in clay rich soils, varying the electrolyte ionic strength and voltage (Section II.4). As in the previous experiments, kaolin clay represented a low permeability medium. The experimental setup adopted allowed monitoring the oxidation-reduction potential and pH values variation in the kaolin, during short-term experiments, estimating the temporal and spatial distribution of the iron oxidation states, and hence the reactivity of the nanoparticles.

Similarly to the previous experiments (Section 3.2.1), higher iron concentrations were measured when a direct current was applied (Figure 3.4), indicating an enhancement of nZVI transport over diffusion in kaolin clay. A 25% increase in the average concentration was observed. The Fe concentrations obtained in the enhanced transport tests were statistically different from the diffusion tests at a 0.05 level of significance [one-way ANOVA, $F(1,38) = 5.04$, $p = 0.03$]. Simultaneously, statistic models with variables pH, ORP, electrode location and voltage did not return any of these variables to be significant to explain this variance. No significant differences were found in the diffusion experiments for the tested electrolytes [one-way ANOVA, $F(3,16) = 0.60$, $p = 0.62$].

The electrolyte 1 mM NaOH presented the highest differences in the experiments with and without direct current, as well as higher iron concentrations near the cathode in relation with the other electrolytes (Figure 3.5). The experiments using $Na_2SO_3$ and $CaCl_2$ showed limited enhancement in PAA-nZVI transport when compared with diffusion. The higher ionic strength of these electrolytes may have contributed to lower nanoparticles stability, increasing their agglomeration and limiting the transport. Recent studies in columns showed that the addition of salts (more than 0.5 mM $L^{-1}$ $CaCl_2$), can decrease nZVI mobility, and changes in pH to values below six can inhibit mobility at all [216]. Also, the higher ionic strength and the divalent cation $Ca^{2+}$ can have affected the kaolin by reducing the diffuse double layer of the clay particles, and consequently the electroosmotic transport.

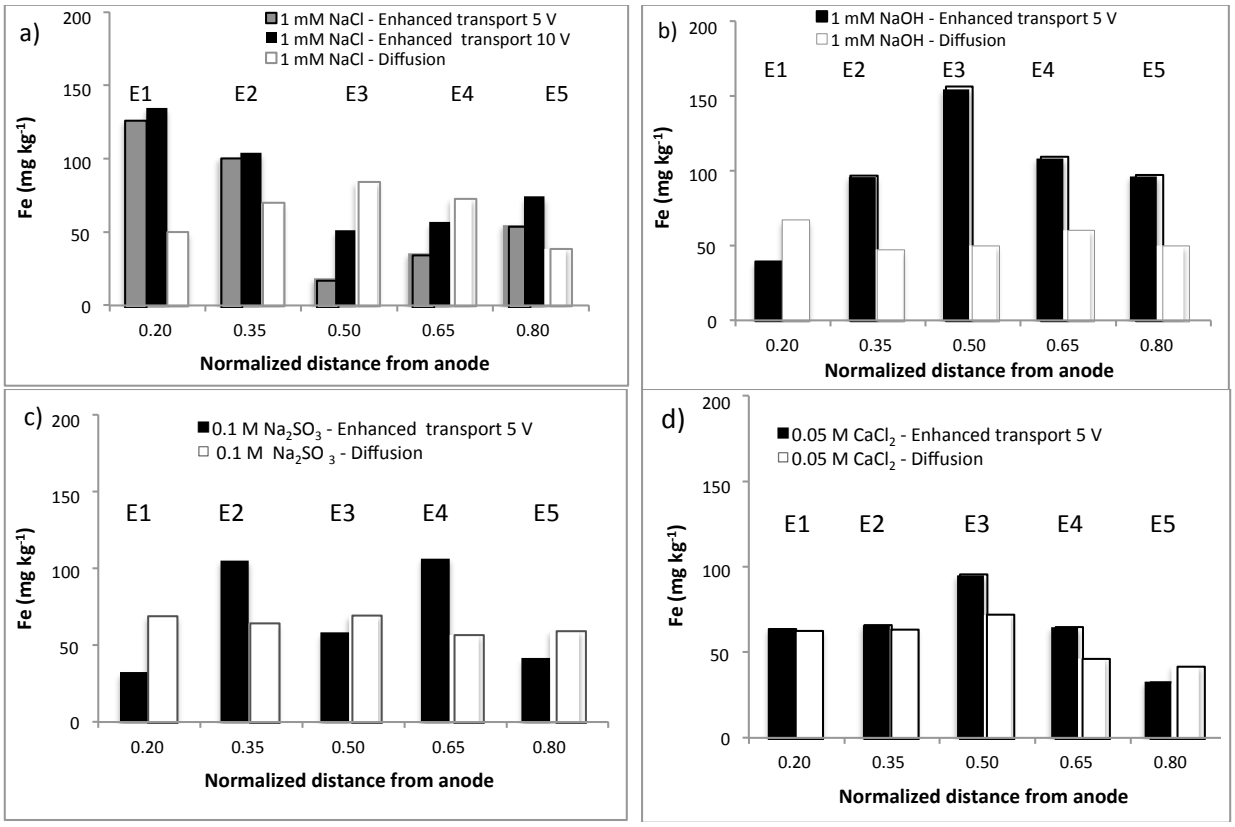


**Figure 3.4.** Additional total iron (mg $kg^{-1}$) in soil sections compared with the initial soil concentration using different electrolytes and voltages in the enhanced transport and diffusion experiments: a) Results using 1 mM NaCl with 0, 5 and 10 V; b) 1 mM NaOH using 0 and 5 V; c) 0.1 M $Na_2SO_3$ using 0 and 5 V and d) 0.05 M $CaCl_2$ using 0 and 5 V.

The increase in the applied voltage resulted in an increase in the transport of nZVI towards the cathode side locations (E4 and E5) for the NaCl electrolyte clay sample, as well as in an even larger

increase in transport towards the anode. This transport is mainly due to electrophoresis, due to the negative charge of the nZVI polymer coating, whereas the movement towards the cathode is due to electroosmosis. The concentrations of total Fe measured in the 10 V test in E4 and E5 are around 1.5 times higher than in the 5 V test, possibly due to an increase in the electroosmotic advection with voltage. Yang et al. [198] considered electroosmosis as the most relevant mechanism for Pd/Fe bimetallic nanoparticles transport under direct electric current. Electroosmotic flow measurements were not made in these experiments, but the results show the need for additional research to assess the electroosmotic advection of iron nanoparticles in clays. Other researchers observed that the enhancement in transport of nZVI from the cathode to the anode, compared to diffusion, was proportional to the applied current [201, 203]. In those studies, electrophoresis was the predominant transport mechanism, because the tested soils were fine-grained sands. In clay systems, apparently, electroosmotic advection may be strong enough to counteract electrophoresis, reducing the overall migration rate of nZVI toward the anolyte. However, if the pH is low, the polarity of the surface charge may become inverted and electroosmosis towards the anode will occur. Potentially electroosmosis towards the anode could have happened in the experiments with $CaCl_2$, with pH values close and below the $pH_{iep}$ 2.5 for the clay.

In all the experiments, and similarly to the results of the experiments with different porosity materials, PAA-nZVI accumulation was visible around the injection location. First of all, this is due to the generally slow dispersion from an injection point in this kind of porous media. Second, the accumulation was also attributed to the aggregation of the iron nanoparticles or to their corrosion, or to both, as mentioned in 3.2.1.

The ORP values measured in the clay during the experiments are well above typical values associated with nZVI in groundwater in field applications (- 100 mV) [104, 108, 139, 217], and those needed for reductive dechlorination, but are consistent with other studies on nZVI enhanced transport in clay [197, 214]. The nZVI effect on clay ORP is minor when compared with groundwater. The temporal and spatial evolution of ORP from the tests with 0.05 M $CaCl_2$ in the pore fluid is plotted in Figure 3.5. For this electrolyte (with the higher ionic strength), the influence of nZVI in ORP is less important than with NaCl (Figure 3, Section II.4), and the evolution shows the general trend of oxidizing to reducing conditions from the anode toward the cathode (E1 to E5). This trend is due to the oxidation occurring in the anode and the reduction in the cathode, resulting in water electrolysis according to the equations 1.4 and 1.5 (see Section 1.1.4).

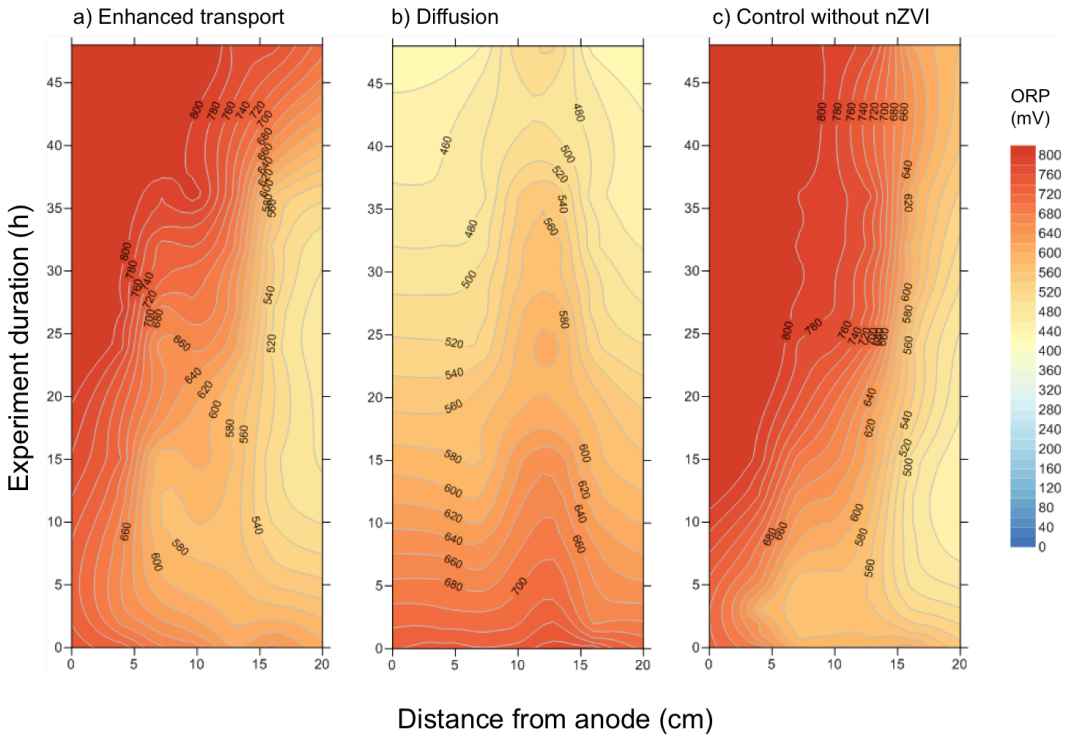


**Figure 3.5.** Variation of ORP in the kaolin medium in the a) enhanced transport, b) diffusion and c) control experiments using 0.05 M $CaCl_2$ as electrolyte and 5 V. The plots were obtained by interpolation (kriging) of the ORP values measured in each electrode (E1-E5) over time.

In general, higher voltages corresponded to lower ORP values (with or without nanoparticles), with exception of the experiments with NaOH, in which the inverse occurred. Higher ORP values were obtained with $CaCl_2$. The statistical analysis carried out in Section II.4 showed that only the factors "Voltage", "Electrolyte" and "nZVI" were significant and showed an interaction that could explain most of the ORP variability ($\omega^2 = 0.62$). Independently, the factor more significant was "Electrolyte" ($\omega^2 = 0.12$). These results show the importance of the electrolyte and the respective ionic strength in the variation of the oxidation-reduction potential and how to interpret it for effectiveness of nZVI transport.

Also in these experiments, initial pH measured in the clay was favorable for nZVI oxidation, varying from 4.23±0.13 to 4.77±0.28, except for the electrolytes $Na_2SO_3$ (6.66±0.28) and $CaCl_2$ (3.73±0.28) that presented the highest and lowest pH values. Slight acidification of the kaolin at E1 and E2 (near the anode) after 24 h and 30 h, respectively, was noted in all the EK tests. The electrolyte that showed the most variation in the pH values was $Na_2SO_3$, especially near the injection point of PAA-nZVI (E2 and E3), between 6 h and 32 h. A similar trend was observed in the diffusion tests with $Na_2SO_3$. This was attributed to the oxidation of $SO_3^{2-}$ to $SO_4^{2-}$ generating acid. The statistical analysis of pH data presented in Section II.4 showed that also for pH, the type of electrolyte could explain

most of the pH variability ($\omega^2$ = 0.64). Thus, the electrolyte (and its ionic strength) is the most important factor in the pH variation during the experiments.

The Pourbaix (Eh-pH) diagrams for the Fe oxidation states in these experiments (Figure 3.6) are similar to the ones obtained in the different porous media (Figure 3.3), with the most oxidizing conditions occurring with $CaCl_2$ and the most reducing conditions with NaOH. In the diffusion experiments, there is a cluster that corresponds to the formation of $Fe_2O_3$ under oxidizing conditions (passivity region), with small differences between the electrolytes tested. Comparing the diagrams a) and b) (Figure 3.6), the effect of the direct current in the kaolin pH and redox conditions is discernible, as well as its influence on the distribution of the iron oxidation states.

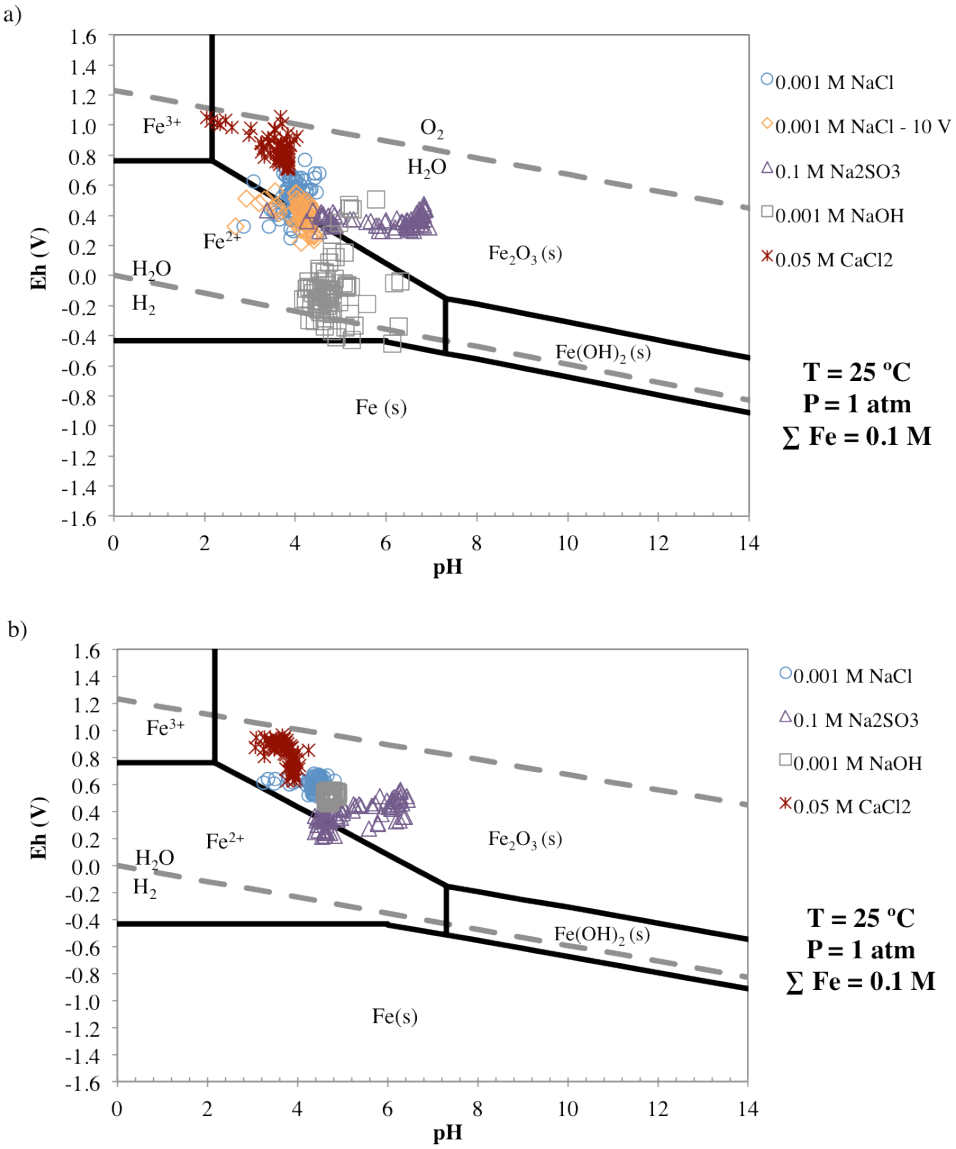


**Figure 3.6.** Pourbaix diagram with the values measured at 48 h in the electrodes embedded in the electrophoretic cell: a) assisted current enhanced transport and b) diffusion tests.

## 3.3 Electroremediation of contaminated soils with nZVI

### 3.3.1 Chromium (VI)

Short duration experiments with $K_2Cr_2O_7$ spiked kaolin were performed in the modified electrophoretic cell used for the assisted current transport experiments (Section II.5). At the end of 24 h treatment, no iron or chromium was detected in either the anolyte or the catholyte in all the experiments. The Fe/Cr ratio distribution in soil remained relatively uniform (Figure 3.7) in the electrodes E1 to E5, throughout the cell as observed by Pamukcu et al. [208]. This is attributed to retarded chromium transport and uniform distribution of the excess iron across the thin cross-section of the kaolin during treatment.

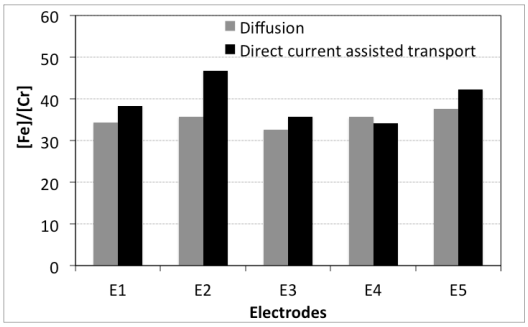


**Figure 3.7.** Post-treatment average distribution of total iron to total chromium ratio in the clay.

Comparing the ratio between Cr(VI) and total chromium concentrations along the electrodes, it is apparent that less chromium is on this oxidation state, when direct current is used. In this case, across the soil, at the end of 24 h, an average of 62 % of chromium is transformed into the less toxic and less mobile oxidation state Cr(III). Results also show that PAA-nZVI transport is enhanced with direct current, as more $Fe^{2+}$ was found compared with diffusion. The high value in E3 is consistent with the visual observation of nZVI transport as well.

### 3.3.2 Molinate

Molinate degradation with nZVI in spiked soils was tested for the first time, both in degradation tests and also combining electrokinetics with nZVI (Section II.6). In aqueous solutions, molinate degradation occurs via an oxidative pathway that requires oxygen and the formation of hydrogen peroxide and hydroxyl radical [94]. After the degradation tests, comparing the molinate final amount in the experiments with and without nanoparticles (one-way analysis of variance – ANOVA), we

found a significant difference for the concentrations of molinate in soils ($p < 0.01$). This supports the hypothesis that the iron nanoparticles degraded the molinate added to the tested soils.

Regarding the nZVI transport, the aqueous solution in the anode compartment always presented higher Fe concentrations than in the cathode compartment. This is related with the cell configuration, as the injection reservoir is near the anode. The highest iron concentration was found in the anode compartment in the diffusion experiments. Comparing the two different soils tested, more iron was found in the anolyte with soil S1 (sandy soil) when compared with soil S2 (loamy soil with high organic matter content). The sandy soil S1 allowed a faster transport of the iron nanoparticles, due to its high pore volume [218]. Adsorption phenomena [105] in soil particles and humic acid accumulation on the nZVI surface [219] most likely hinder iron transport, and this can also contribute to the lower iron concentrations in the anolyte in experiments with soil S2, when compared to those with soil S1 under similar conditions.

In the experiments with direct current, lower amounts of Fe were measured in the anolyte than in the diffusion experiments. Even though nanoparticles have a negative surface charge due to the polymer (PAA) coating, and thus would be potentially transported towards the anode by electrophoresis, electroosmotic flow generally occurs in the opposite direction (towards the cathode), and may hinder transport towards the anode, explaining the low concentrations found in the anolyte when a direct current was applied. In the experiment with pH control in the anolyte (soil S2), in average, ten times more iron was found in the anolyte than in experiment without pH control (soil S2), possibly because in the later the advance of the acid front ($H^+$) oxidizes nanoparticles ($Fe^0 \longrightarrow Fe^{2+}$), and the resulting positively charged iron ion is transported towards the cathode. Still only small amounts of iron were measured in the catholyte in all experiments, probably because there was not enough time to reach the cathode compartment. The statistical analysis showed that the observed variance can be explained, at a 0.05 level, by the type of soil (S1 and S2) and the electric current (0 and 10 mA). The pH control was not significant.

In addition to iron in the electrolyte, its presence in the soil was also analyzed and compared to the initial content. Iron enrichment in the different soil sections is shown in Figure 3.8. The highest iron concentration in the soil in experiment A may be explained by the change of the soil charge with the advance of the acid front from the anode end due to the absence of pH control. In these conditions, ions of $H^+$ may adsorb to soil particles and increase the zeta-potential, resulting in an augmented adsorption of the PAA-coated iron nanoparticles. Most of the iron was always in the sections immediately after the injection reservoir. The section near the cathode (Section 5) presented the lowest amounts of additional iron (Figure 3.8), what is consistent with the concentrations found in

the catholyte. This means that the iron accumulates in the nearest sections to the injection point. Nevertheless, no major differences existed in the three samples in the middle section (top, central and bottom) in experiments B, C and D, with relative standard deviation (RSD) of 9%, 6% and 5%, respectively; whereas in experiments A and E was higher (22% and 37%). There was no iron accumulation or deposition in the bottom part of this section (section 3), when compared to the central and top samples.

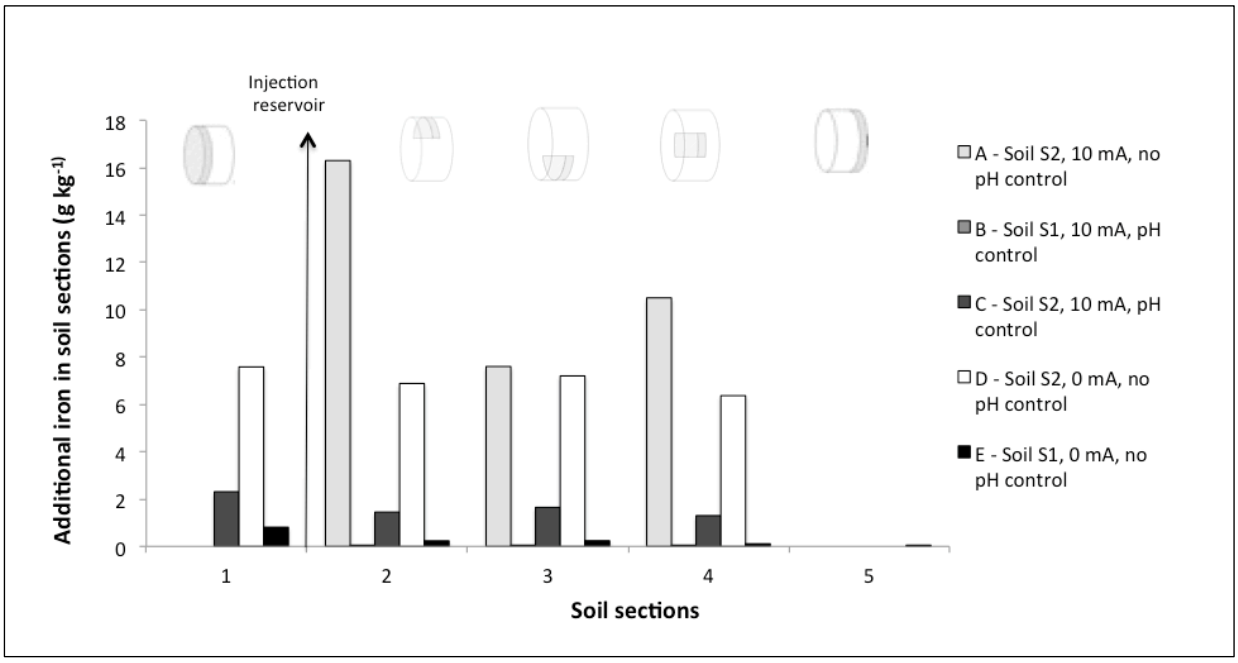


**Figure 3.8.** Iron enrichment (g $kg^{-1}$) in soil sections (compared with initial soil concentration: 18 g $kg^{-1}$ in Soil S1 and 0.9 g $kg^{-1}$ in Soil S2) in experiments A-E. Section 1: between the anode compartment and the injection reservoir; Section 2: central soil section after the injection reservoir, top; Section 3: central soil section after the injection reservoir, bottom; Section 4: central soil section after the injection reservoir, center; Section 5: between the central soil section and the cathode compartment.

The mass balance of the iron shows that most of it stays in the injection reservoir of the cell, followed by the sum found in the soil and the passive membranes (Figure 3.9). This balance indicates a low mobility of the iron nanoparticles inside the experimental electrokinetic cell, most likely due to aggregation and sedimentation as also showed in other experimental setups with columns [128, 129, 220].

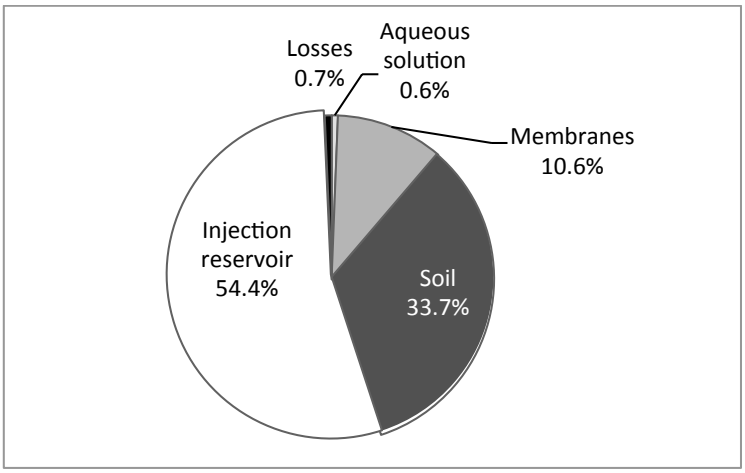


**Figure 3.9.** Average mass balance of iron after the experiments. Average recovery of iron was 86%.

The results confirm the transport of molinate towards the cathode with EK, as the experimental data and modeling by Ribeiro et al. [209] demonstrated. However, in the diffusion experiments, with both soils, more molinate was found in the anode side and in the compartment, than in the cathode, due to direct contact between molinate-spiked soil and the anode compartment. At the cathode side, the placement of a non-contaminated soil layer hinders the diffusive transport of molinate to the cathode compartment (see Figure 1, Section II.6). Another important factor is the strong adsorption of molinate in soils with high organic matter content [221] and this explains the 10-fold decrease in molinate in the anolyte of experiment D (soil S2, sandy-loam, 12.8% organic matter) when compared with experiment E (soil S1, sandy, 0.4% organic matter).

The soil type was statistically significant to explain the molinate variance in the electrolyte. Comparing the data of all experiments, the direct current and pH control were not statistically significant ($p$ = 0.05) to explain molinate concentrations in the aqueous phase. When a direct current was applied (experiments A, B and C), the amount of molinate in the anolyte decreases, and molinate appears in soil section 5 (initially clean) near the cathode. This shows the electrokinetic transport of molinate towards the cathode. Once again, the higher amount of molinate in soil S2 (experiment C) compared with soil S1 (experiment B) can be explained by adsorption to soil organic matter, resulting in lower molinate removal efficiencies in these experiments (around 70% in B vs. almost 90% in C).

The cumulative amounts of molinate found in the electrolytes (anolyte and catholyte) were less than 6% the initial amount in the soil. In previous studies with EK but without nanoparticles [222], around 60% of the molinate was found in the catholyte, less than 2% in the anolyte and a maximum of 9% was found in soil. These differences support the hypothesis that there was molinate degradation by

nZVI in the experiments as, in identical conditions, fewer molinate was found in the electrolytes (catholyte).

The results now obtained show no enhancement in molinate degradation when both EK and nZVI are used, contrary to what was found for nitrates [198], dinitrotoluene [214] and PCP [204]. Although in those studies no diffusion tests were made (to assess the degradation only with nZVI), the degradation of those contaminants is dependent on reduction reactions, whereas molinate is degraded by nano $Fe^0$ *via* an oxidative pathway with hydroxyl radicals [94]. This requires desorption of molinate and higher contact times than the common reductive pathway. In our experiments, the diffusion tests were more effective for soil S2, most likely because EK, by transporting the molinate out of the system faster, reduced the contact times with iron nanoparticles.

## 3.3.3 PCB

### *3.3.3.1 Comparison between two different experimental setups*

The combined electro-nano remediation of PCB contaminated soils was tested in two different experimental setups – both developed at the Technical University of Denmark (DTU). In the electrodialytic (ED) two-compartment cell, the soil is suspended and stirred simultaneously with the addition of nZVI vs. a conventional three-compartment electrokinetic (EK) cell (Section II.7).

The two-compartment ED setup shows PCB removal percentages of 83% with and 29% without direct current (Figure 3.10). These results are higher than in previous studies with EK [205] and batch tests without current [140]. The suspension and stirring of the soil can enhance the PCB dechlorination by nZVI, due to an increase in desorption from soil or to a higher contact and reaction between nZVI and PCB, or to both. In the traditional three-compartment EK setup, the iron has to be transported across the compacted saturated soil to reach the contaminants. Previous studies show that even a low proportion of carbonate minerals may cause an increase in the deposition of PAA-nZVI particles and aggregates, due to the lower negative surface charge [223]. As the soil used in the experiments has high carbonate content (18%), the limited dechlorination (12-58%) observed is probably related to the iron precipitation with the carbonates (Figure 3.10).

In both setups, there are chemical reactions that deplete the $Fe^0$ reductant power (eq. 1.1 – 1.3) and the presence of transformer oil was found to adversely affect the PCB degradation [224]. A higher PCB removal is obtained in the ED setup compared with the traditional electrokinetic setup, despite the introduction of $H^+$ (resultant of hydrolysis in the anode) and the atmospheric $O_2$ dissolved by the slurry stirring that oxidize $Fe^0$.

In other remediation techniques [68, 225-227] lower chlorinated congeners (tri and tetrachlorobiphenyls) were the ones with highest removal rates. In this study, there was degradation of lower chlorinated congeners, namely PCB28, PCB52 and PCB65 (particularly in the EK setup), but also of higher chlorinated congeners. In some experiments, PCB65 increased due to dechlorination of higher chlorinated congeners, such as PCB204. In the EK setup, removal rates for each congener are lower than in the ED setup.

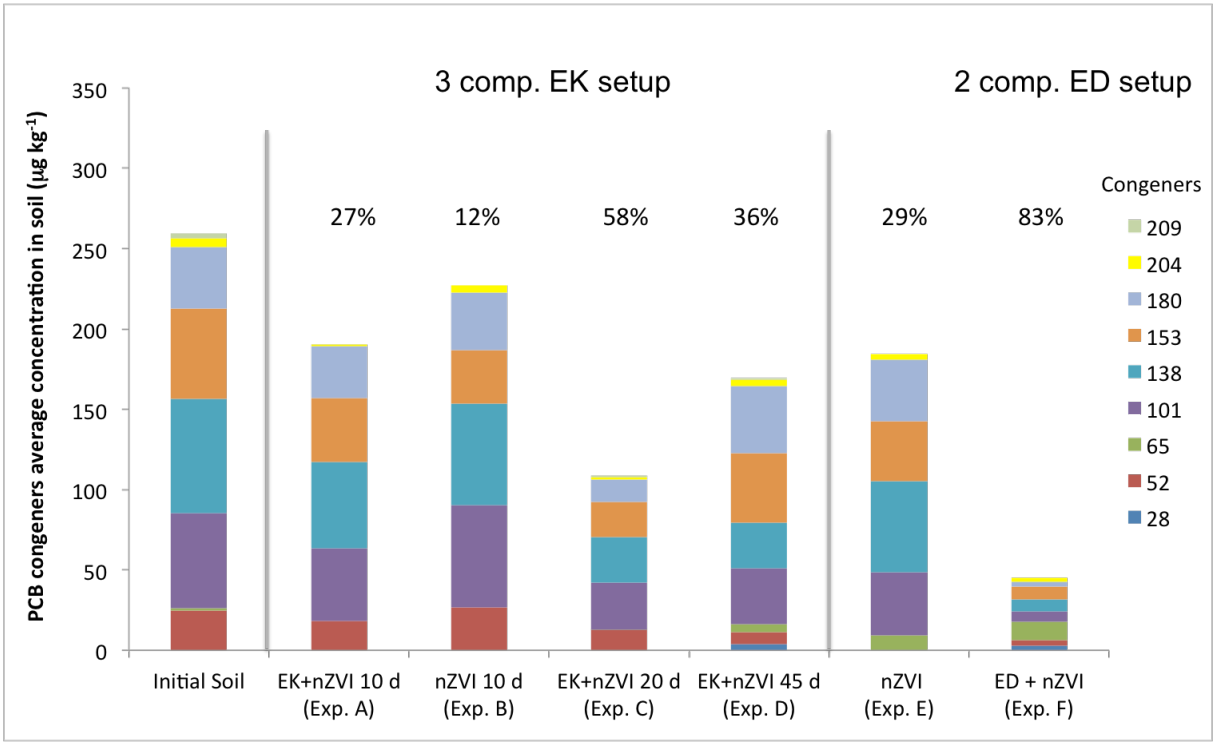


**Figure 3.10.** Average concentration of PCB congeners (PCB28, 52, 65, 101, 138, 153, 180, 204 and 209) in soil before and after the experiments, using the three-compartment cell and the two-compartment cell. Percentages on the top of each column represent PCB removal regarding the sum of congeners analyzed in the initial soil.

The experiments with the EK setup had different durations to assess if longer times would increase the PCB dechlorination. Comparing the 10 d experiment (A) with the 45 d experiment (D), the PCB removal has a small increase (27% vs. 36%) (Figure 3.10). Although the removal percentages are higher than in previous studies with 14 d experiments [205], their values are not encouraging for a scale up of the process (pilot and full scale) for the remediation of PCB contaminated soils and sediments. The congeners concentrations obtained in the soil are not statistically different in the three experiments (A, C and D) at a 0.05 level of significance [one-way ANOVA, $F(2,20) = 2.14$, $p = 0.14$].

Direct current can be used to enhance nZVI transport in different porous matrices or model soils [218, 228] but, in the ED setup, the contact between the nanoparticles and the contaminated soil is ensured by the stirring, so the current may not be needed for the PCB dechlorination. However, results show that the experiment with direct current (Exp. F) had a higher PCB removal rate (83%) than the experiment just with the iron nanoparticles (Exp. E) (29%), due to the high pH and buffer capacity of the soil tested (Figure 3.11). In the experiment without current (Exp. E), the soil suspension with nZVI kept a constant alkaline pH, which promotes the passivation of the iron nanoparticles. In the experiment with current (Exp. F), water electrolysis produces $H^+$ in the anode, thus lowering the pH. A slightly acidic pH (4.90–5.10) increases the dechlorination rate of PCB by nZVI and nZVI/Pd [229].

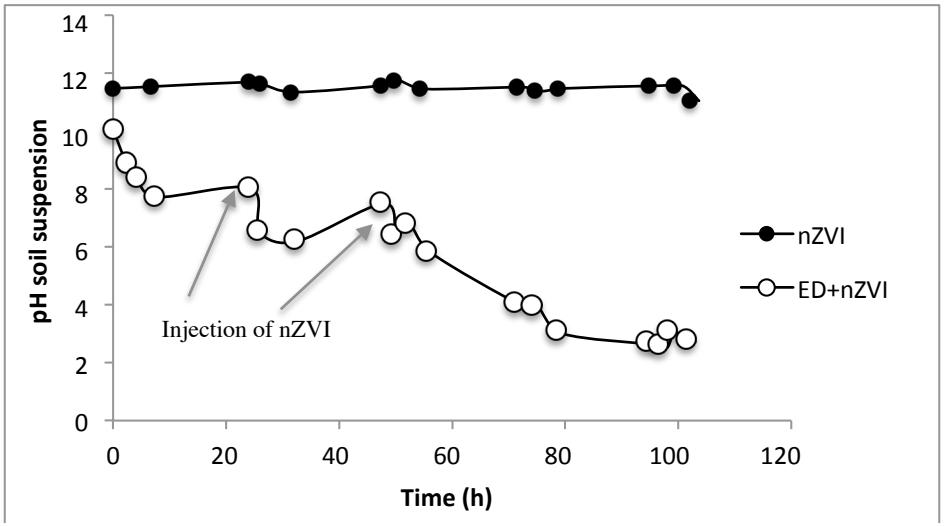


**Figure 3.11.** Evolution of pH in the soil suspension during the experiments using the two-compartment ED setup.

### *3.3.3.2 Comparison between two surfactants*

In Section II.8, two different surfactants (saponin and Tween 80) were tested to enhance PCB desorption and removal efficiency from a contaminated soil. A two-compartment ED setup in which the soil was stirred in a slurry with 1% surfactant, 10 mL of nZVI commercial suspension, and a voltage gradient of 1 V $cm^{-1}$.

The results show that, in the tested conditions, saponin allowed to obtain higher PCB removal from soil (Figure 3.12) when compared with Tween 80. The most efficient removal (76%) was obtained with 1% saponin, 10 mL nZVI and a voltage gradient of 1 V $cm^{-1}$ (Exp. A). The lowest removal was obtained with 1% Tween 80 and nZVI (8% removal), without application of a direct current. This removal is consistent with previous studies that showed that Tween 80 was one of the surfactants

with the least efficient degradation of 1-(2-chloro-benzoyl)-3-(4-chlorophenyl) urea by nZVI, when compared with Triton X-100, Tween 20, sodium dodecyl sulfonate (SDS), and cetyltrimethylammonium bromide (CTAB), probably due to the effect of the hydrophobic chain length [230].

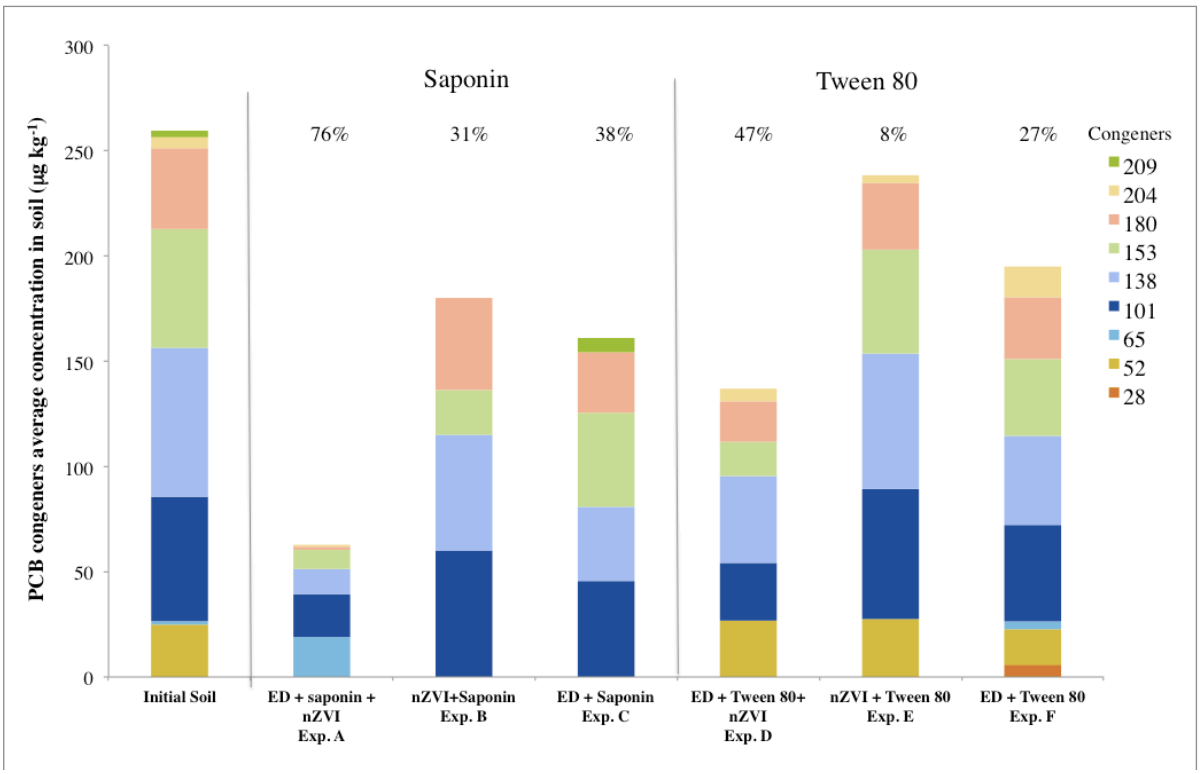


**Figure 3.12.** Average concentration of PCB congeners (PCB28, 52, 65, 101, 138, 153, 180, 204 and 209) in soil before and after the electrodialytic experiments using saponin and Tween 80. Percentages on the top of each column represent PCB removal regarding the sum of congeners analyzed in the initial soil.

Surfactants increase the rates of desorption of hydrophobic compounds from soil and transfer the target contaminants into aqueous micelles through solubilization. However, surfactants have also affinity for PCB and nZVI surface sites and can influence their interactions, namely they can affect the degradation of PCB through various mechanisms, such as enhanced solubilization, enhanced sorption, competitive sorption, and electron transfer mediation [230]. PCB dechlorination by nZVI, like other reductive reactions, is a surface-mediated reaction [231], heterogeneous in nature, involving adsorption of the contaminants at the iron surface before breaking of carbon–chlorine bonds [138]. The adsorbed polyelectrolyte used to stabilize nZVI suspensions decreased dechlorination activity of nZVI, by either blocking available reactive surface sites or else, by a combination of site blocking and inhibited mass transfer of chlorinated organic compounds in bulk solution to the nanoparticle surface [133, 232]. Cationic and non-ionic surfactants were also found to inhibit the trichloroethylene degradation by CMC stabilized nZVI [105].

Usually lower chlorinated congeners (tri and tetrachlorobiphenyls) are the ones with highest removal rates from contaminated soils [68, 225-227]. In this work, beside lower chlorinated congeners, also higher chlorinated congeners (penta, hexa, hepta and octachlorobiphenyl) showed removal percentages between 9 and 96% (average value 44%). The results also present an increase in the concentration of PCB52 (Exp. D and E), PCB65 (Exp. A and F) and PCB101 (Exp. B and E), due to dechlorination of higher chlorinated congeners. The congeners with higher removal rates were PCB138 (Exp. C and F), PCB153 (Exp. A, B and D), and PCB180 (Exp. A). Previously, Chen et al. [140] identified the PCB153 dechlorination pathways by nZVI. Figures 3.13 and 3.14 show the proposed dechlorination pathways for PCB138 and PCB180, considering that nZVI reactivity decreases according to the chlorine position in the following order: *ortho* < *para* < *meta* [225, 233].

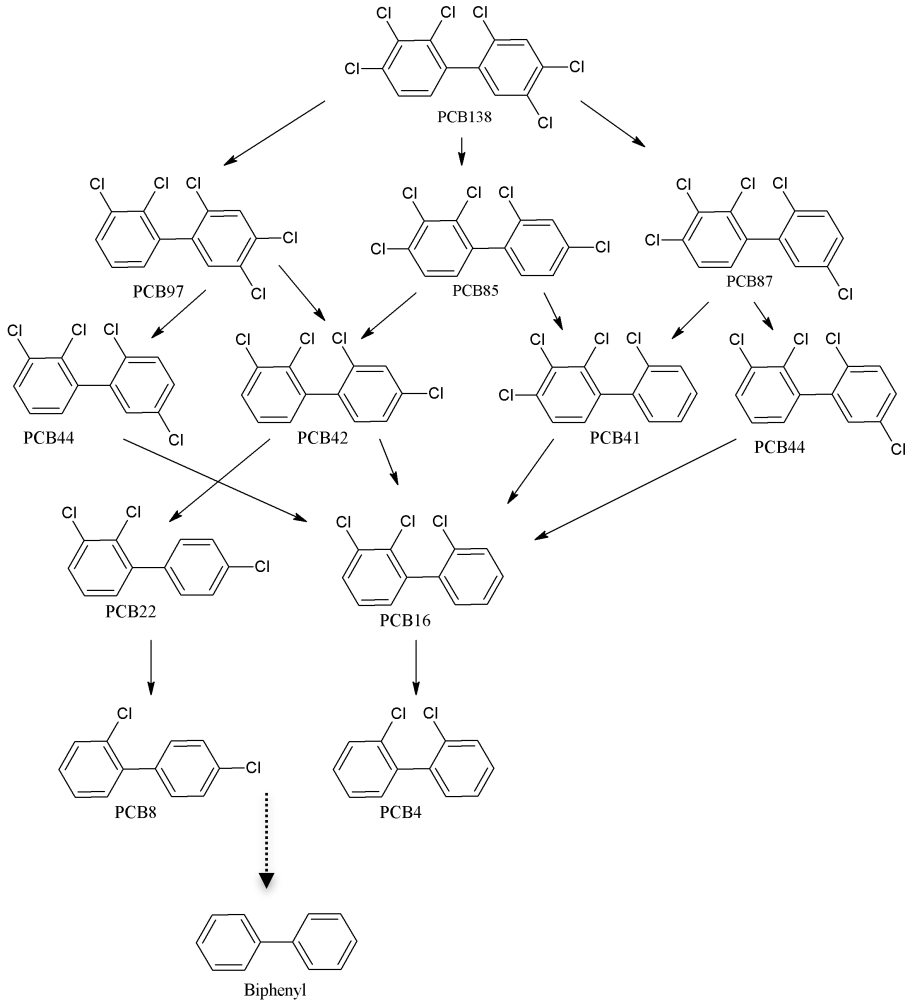


**Figure 3.13.** Possible dechlorination pathways proposed for PCB138.

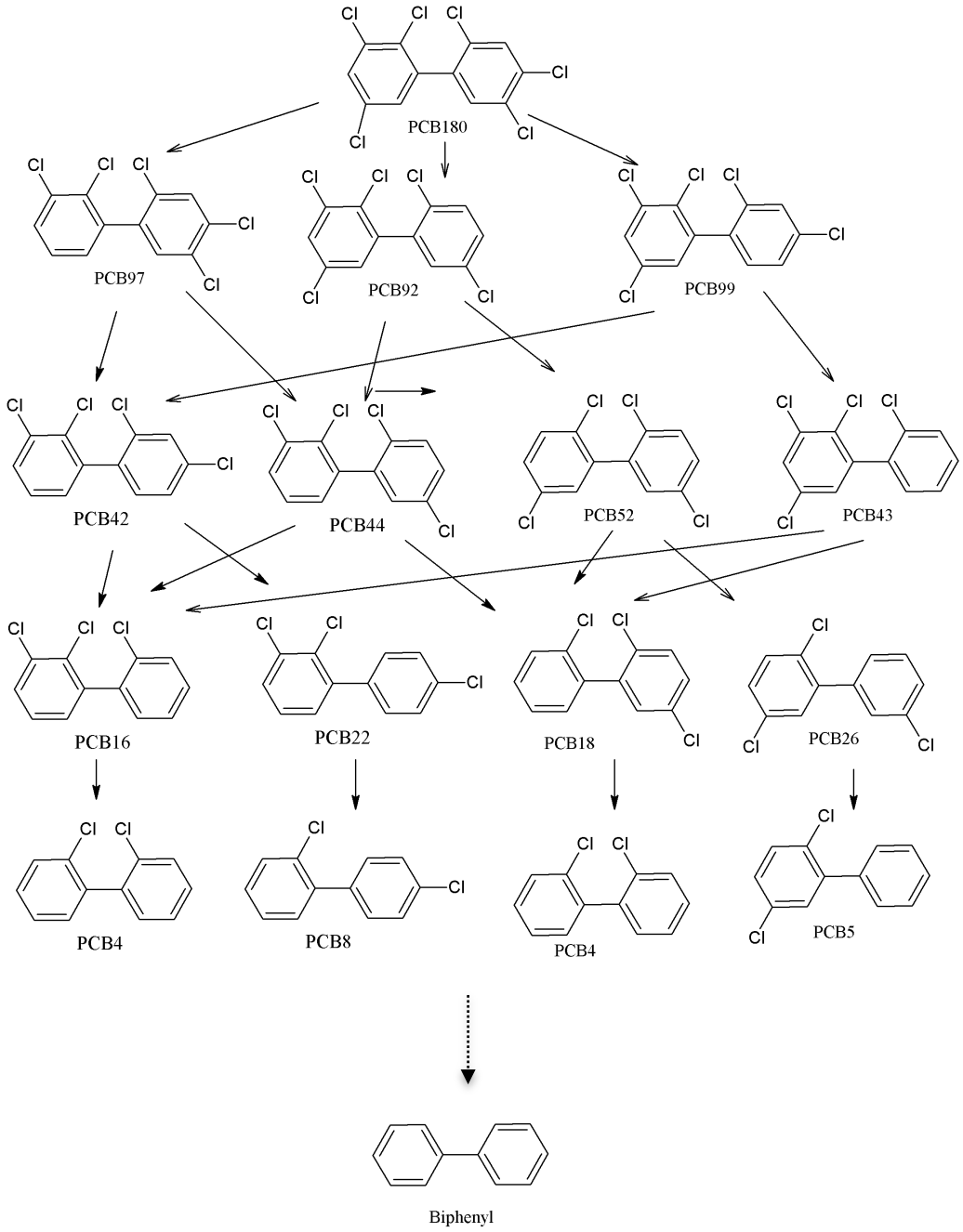


**Figure 3.14.** Possible dechlorination pathways proposed for PCB180.

In the aqueous samples (soil filtrate and catholyte), most of the PCB congeners were below the detection limit. PCB have low water solubility (0.0027-0.42 ng $L^{-1}$) and are hydrophobic [234]. In the soil filtrate, we could measure PCB only in two samples. Experiment B had 0.08 ng $L^{-1}$ of PCB153 and Experiment D presented 3.81 ng $L^{-1}$ of PCB101. These concentrations, higher than the typical solubility range, are due to the surfactants. In the catholyte samples, some congeners were also found, mostly lower chlorinated congeners (PCB28), but also penta, hexa and heptachlorobiphenyls.

These congeners are identified only in the experiments with current, probably due to electrophoresis.

Comparing the energy consumption of the experiments, calculated according to Sun et al. [235], Tween 80 has higher energy consumption when compared with saponin (1.6 Wh $g^{-1}$ soil and 4.1 Wh $g^{-1}$ in Exp. D and F, and 1.2 Wh $g^{-1}$ and 0.7 Wh $g^{-1}$ in Exp. A and C, respectively). Added to the low removal percentages, this also contributes to show that Tween 80 is not a suitable surfactant to use with PCB, despite the good results obtained for PAH with this method [207].

Results show that the experiments with direct current have higher removal percentages that the ones without current. The PCB congeners concentrations using saponin with and without current (Exp. A and B) are statistically different at a 0.05 level of significance [one-way ANOVA, $F(1,9) = 5.61$, $p = 0.04$]. This means that electric current also contributes to PCB dechlorination, and this can be done in two different ways. In the experiments without current, the soil suspension with nZVI kept a constant alkaline pH (Figure 5, Section II.8), which promotes the passivation of the iron nanoparticles and prevents PCB dechlorination. Another possibility is the PCB electrocatalytic hydrodechlorination – the production of $H^+$ and the presence of current can promote the Cl removal from PCB generating HCl [236, 237]. The electrocatalytic hydrodechlorination has been demonstrated with specially engineered foam electrodes, in solvent/surfactant-aided solutions and can possibly be also occurring in this two-compartment electrodialytic setup. Further research is needed to evaluate the importance of this dechlorination process.

The pH of the suspended slurry also affects the surfactant behavior, influencing the micelle aggregation and hydrophobicity. At high pH, the net charge on the head groups of saponin molecule will increase, causing electrostatic repulsion between the head groups, which tends to increase the critical micelle concentration (CMC) values, reducing the solubilization capabilities of saponin [238]. Also, the solubilization of heavy metals by the electrodialytic process (like $Cd^{2+}$ and $Zn^{2+}$) and a lower pH (until pH 4) decrease the CMC value of saponin solution and enhance its solubilization properties [238]. With Tween 80, the pH increase had a positive effect on surface tension and the micelles are more stable at higher pH (up to 10) [239].

#### *3.3.3.3 Comparison between two different soils*

Two different soils (Table 3.1), historically contaminated with PCB, were used in experiments using both the three-compartment EK setup and the two-compartment ED setup (Section II.9). Soil 1 was provided by a hazardous waste operator in Portugal and is a mixture of contaminated soils from industrial sites with transformers oils spills. Soil 2 is a surface soil sampled in a decommissioned

school in Hovedstaden (Capital Region of Denmark), and the PCB resulted from the weathering of the windows joint sealants used in 1955-1977 [240].

**Table 3.1.** Physical and chemical characteristics of the soils.

| Parameter | Soil 1 | Soil 2 |
|---|---|---|
| Particles distribution (%) | | |
| Coarse sand (200 < Ø < 2000 µm) | 19.1 | 3.2 |
| Fine sand (20 < Ø < 200 µm) | 67.3 | 69.6 |
| Silt (2 < Ø < 20 µm) | 12.7 | 23.6 |
| Clay (Ø < 2 µm) | 0.9 | 3.6 |
| Textural classification | Loamy sand | Silt loam |
| pH ($H_2O$) | 12.2 | 8.20 |
| Conductivity (mS $cm^{-1}$) | 18.76 | 0.221 |
| Exchangeable cations ($cmol_{(c)}$ $kg^{-1}$) | | |
| $Ca^{2+}$ | 83.75 | 259.14 |
| $Mg^{2+}$ | 3.2 | 9.75 |
| $K^{+}$ | 26.88 | 7.36 |
| $Na^{+}$ | 9.37 | 8.34 |
| Sum of exchangeable cations ($cmol_{(c)}$ $kg^{-1}$) | 123.2 | 284.59 |
| Calcium carbonate (%) | 18.0 | 1.3 |
| Organic matter (%) | 16.46 | 0.57 |
| PCBs[a] (µg $kg^{-1}$) | 258 ± 24 | 156 ± 2 |
| Metals[b] (mg $kg^{-1}$) | | |
| Al | 20980 ± 590 | 4952± 71 |
| As | 9 ± 2 | 0.6 ± 0.97 |
| Cd | 0.7 ± 0.1 | 0.4 ± 0.04 |
| Cr | 52 ± 3 | 2.5 ± 0.04 |
| Cu | 142± 95 | 10 ± 0.3 |
| Fe | 13162 ± 301 | 6773± 97 |
| Ni | 32± 1 | 6 ± 0.3 |
| Pb | 45± 3 | 25 ± 0.9 |
| Zn | 2155 ± 40 | 135 ± 0.1 |

[a] Sum of PCB 52, 65, 101, 138, 153, 180, 204 and 209

[b] Acid digestion with $HNO_3$ according to the Danish Standard DS259.

The results of PCB removal at the end of the experiments using the two-compartment cell are different according to soil type. Soil 1 has the higher PCB removal without saponin, only with direct current, stirring and nZVI (83%). In soil 2, the highest removal was obtained only with nZVI and saponin. No significant differences were found in the ED experiments for soil 2 [one-way ANOVA, $F(3,20) = 0.69$, $p = 0.57$], although the experiment without saponin (Exp. K) showed a lower removal rate. In general, the best results were obtained with soil 1, with an average removal between 21% to 96% for the congeners analyzed, while for soil 2, the average congener removal was between 6% and 68%. The highest removal percentage in Soil 1 can be related to the pH of the soil slurry during the experiments. The initial soil pH and carbonate content allowed to maintain the pH between 6 and 7

for about half the time of the experiment. In the experiments with Soil 2, the pH values turn acidic faster (~30 h after the beginning of the experiment), and this contributes to the corrosion of the iron nanoparticles. This is also consistent with the higher PCB removal obtained in Soil 2 without the direct current, and consequently, without acidification of the soil slurry.

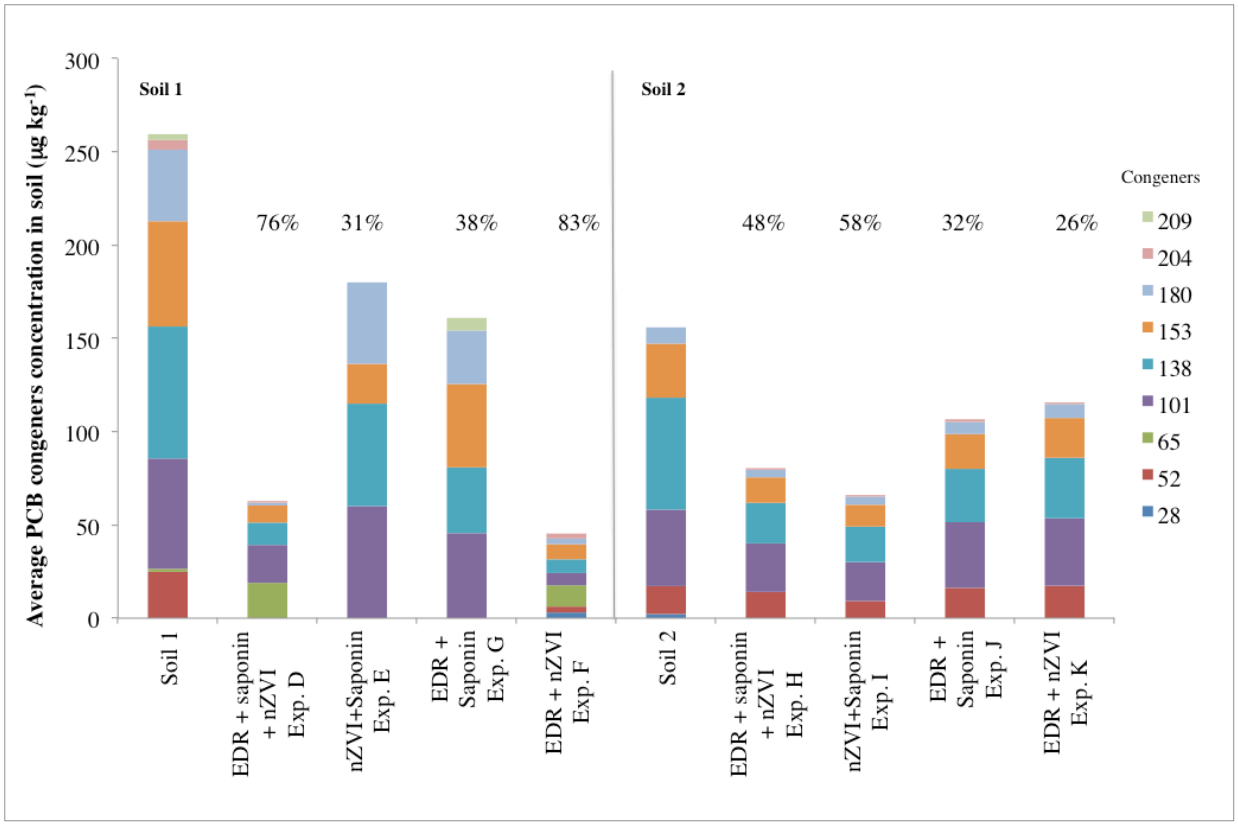


**Figure 3.15.** Average concentration of PCB congeners (PCB28, 52, 65, 101, 138, 153, 180, 204 and 209) in the tested soils before and after the experiments using the two-compartment cell. Percentages on the top of each column represent PCB removal regarding the sum of congeners analyzed in the initial soils.

The removal efficiencies in both soils with the three-compartment electrokinetic setup are much lower (Section II.9), despite the longer duration of the experiments. The highest removal rate was obtained in the experiment with saponin in the anode compartment. The diffusion experiment in soil 1 with the EK setup showed no PCB dechlorination. The highest removal rate in soil 2 corresponds to the experiment without direct current, only the injection of iron nanoparticles. The use of saponin with soil 2 does not show any enhancement compared to the other experiments.

In the ED setup, the soil suspension pH during the experiments had lower values in soil 2 compared with soil 1, which is related with the lower initial pH value and lower carbonates content. The pH

values in soil 2 reached 2.91-3.35, which correspond to less favorable conditions to PCB dechlorination due to the corrosion of zero valent iron. In all the experiments where nZVI was added, higher pH values were measured in the suspension. Also, in the experiments without direct current the pH values showed very little variation.

Figure 3.16 (A and B) shows the comparison between the mass of iron found in each component of the tested cells, respectively, at the end of the experiments. Previous studies showed that in the traditional three-compartment cell, most of the nZVI aggregate and settle in the injection compartment [214, 218, 228, 241], thus not reaching the contaminated soil. The suspended electrodialytic remediation assures that nZVI are mixed with the soil and most of the iron is found there at the end of the experiments.

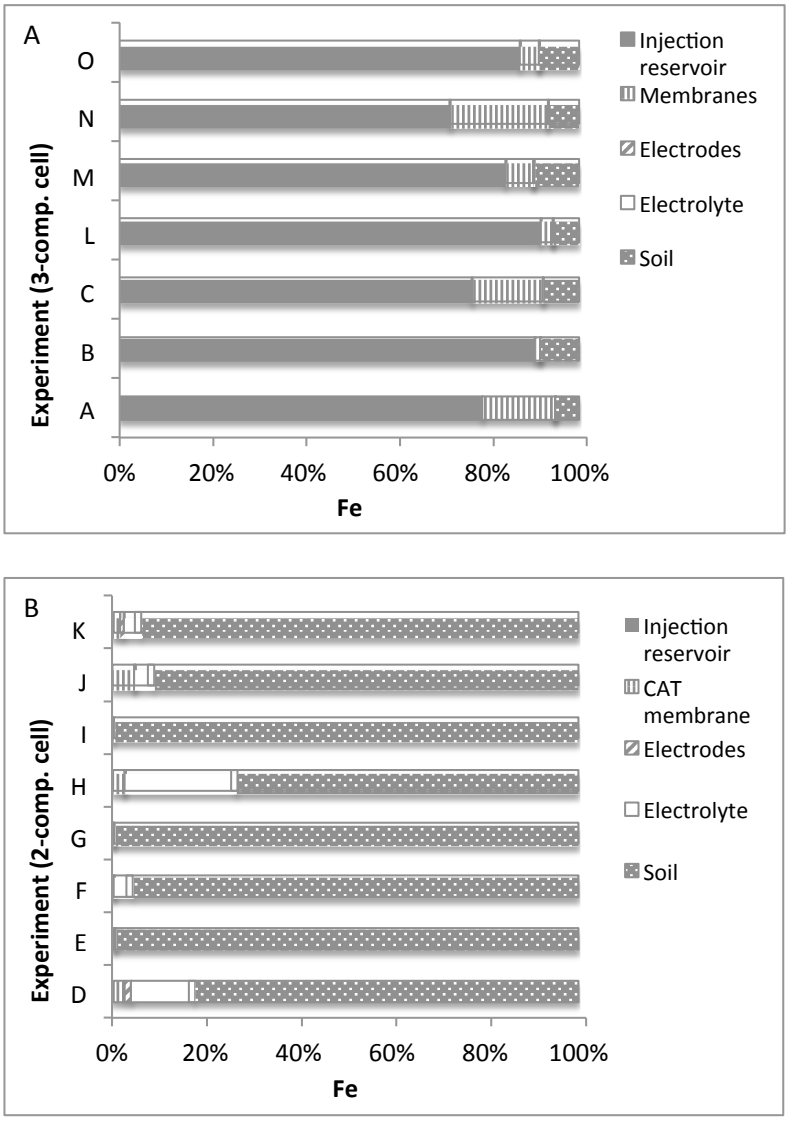


**Figure 3.16.** Comparison of the mass of iron (%) found at the end of the experiments, with the setups tested: A) three-compartment cell, and B) two-compartment cell.

## 3.4 Numerical modeling of nZVI transport

In Section II.10, a generalized physicochemical and numerical model was developed to describe the nZVI transport through different porosity media, under electric fields. The model aims to be sufficiently detailed to describe the main processes, and also a predictive tool for the nZVI transport. The model consists in the Nernst–Planck coupled system of equations, which accounts for the mass balance equation of ionic species in a fluid medium when diffusion and electromigration are considered in the ions transport process. In the case of charged particles of nZVI, diffusion and electrophoretic terms have been taken into account. In both cases, also the electroosmotic flow has included in the equation. Therefore, the flux of any chemical species or charged particles *i* moving from a volume element of the system can be expressed as [242]:

$$N_i = -D_i^* \nabla c_i - U_i^* c_i \nabla \phi - k_e c_i \nabla \phi \tag{3.1}$$

where $c_i$ is the molar concentration, $D_i^*$ is the effective diffusion coefficient, $\phi$ is the electrical potential, $k_e$ is the electroosmotic permeability coefficient and $U_i^*$, is the effective electrophoretic mobility for nZVI charged particles or ionic mobility, estimated by the Einstein–Nernst relation for ions.

Two kinds of reactions, electrochemical and chemical, were also included. The rate of generation term is not included in the continuity equation for the porous medium cells, given the assumption that the only electrochemical reactions, which need to be taken into account in the system, are the reduction and oxidation of water on the electrodes (eq. 1.4 and 1.5, Section 1.1.4).

The results show a good fit between the modeled and experimental results (Figures 3.17 – 3.19), both for the iron masses in the solid matrix and the pH values in the anode and cathode compartment.

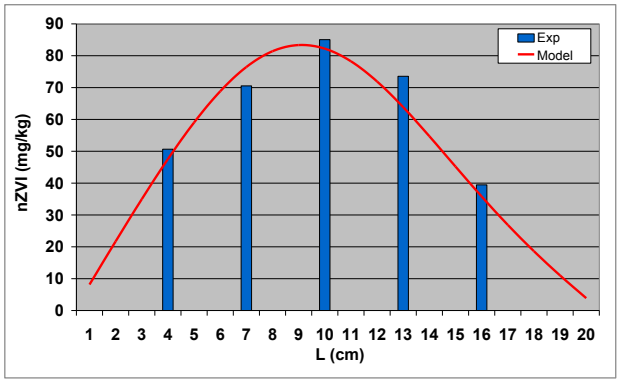


**Figure 3.17.** Comparison between the experimental and model results regarding nZVI diffusive transport in kaolin with 1 mM NaCl.

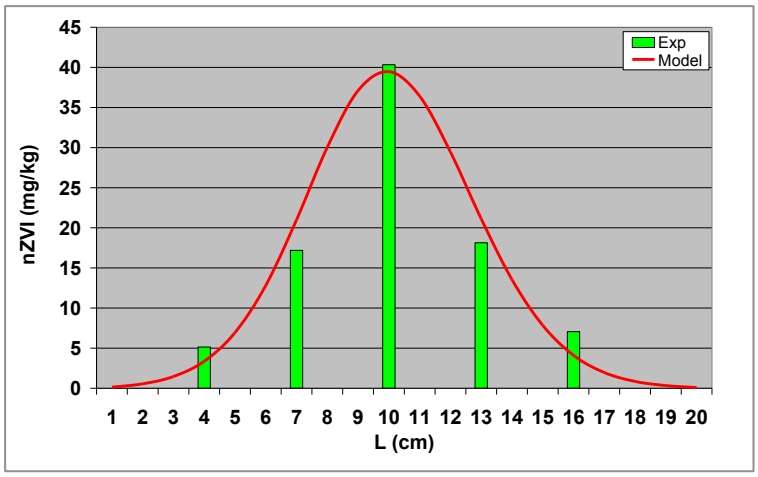


**Figure 3.18.** Comparison between the experimental and model results regarding nZVI assisted transport (under electric fields) in glass beads with 1 mM NaCl.

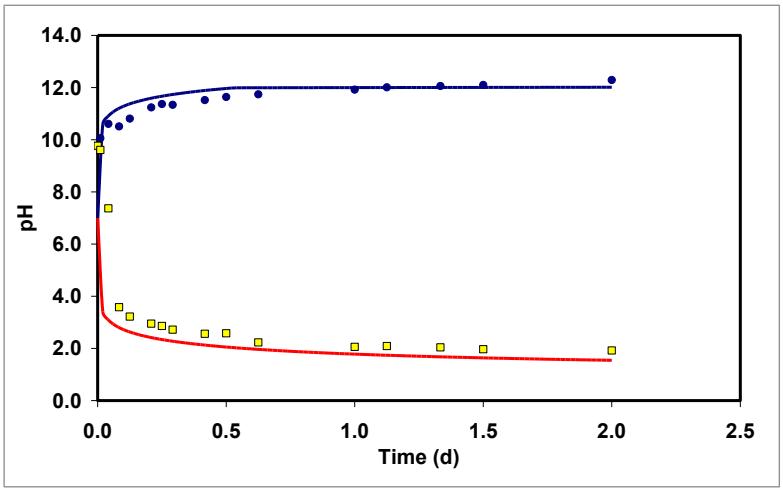


**Figure 3.19.** Comparison between the experimental (dots) and model results (lines) for the pH evolution in the anolyte and the catholyte during the experiments with kaolin and $CaCl_2$ (0.05 M).

The model allowed detecting that, in some cases, an important fraction of the nZVI particles tends to aggregate when their concentration is high relative to the available pore volume, becoming an immobile “iron cake” in the injection spot, but the results also indicate that aggregated mass clearly diminishes in the presence of a direct current.

4

# 4. Discussion and limitations

The experimental work done (Part II, Sections II.3 to II.9) has given some insight on the direct current assisted transport of iron nanoparticles, and also on the simultaneous use of electrokinetics and nZVI on contaminated soils. However, there are some limitations to the experimental setups that need to be discussed.

One of the most important limitations is the fact that currently there is no analytical method for quantification and characterization of nanoparticles in complex matrices, such as soil. So it is impracticable to distinguish between the natural occurring iron in the soil (one of the most common elements in Earth's crust) and the manufactured nanoparticles. Literature reviews on the analytical methods show the limitations of the current techniques [148, 243, 244]. Also, it is complex to isolate and assess the integrity of nanoparticles (and their polymer coatings), their agglomeration and their degree of oxidation or passivation after being mixed in a complex matrix. The iron extraction method used in the experiments (sodium dithionite-citrate-bicarbonate method) was selected as the most suitable after comparison with more aggressive methods, based on acid digestion. Those methods would not have allowed quantifying the small amount of nano iron added when compared with the iron background content in the soil. The Pourbaix diagrams were used as an approximation, but they are relevant only for a system at equilibrium and at low concentrations.

The experiments on assisted direct current were performed in a modified electrophoretic cell that does not allow measuring the electroosmotic flow. As in clays this transport is important, this is a critical limitation of the experiments. Recent works on the nZVI transport in clays (Boom clay) [206] confirmed the transport of nZVI by electro-osmotic advection, with an electro-osmotic conductivity in the range $(0.5\text{-}1.0)\cdot10^{-10}$ $m^2V^{-1}s^{-1}$. However, the presence of nZVI decreased electro-osmotic

conductivities by almost half and affected geochemical conditions of the system, inducing sharper pH profiles and enhancing cation exchange in the clay [206].

In the experimental setup for the transport experiments, the modified electrophoretic cell was closed, but there was a layer of air above the clay, which contributed for the corrosion of iron nanoparticles and could have affected their transport. The intermittent measurement of pH and ORP at fixed times implied that the power had to be turned off for short periods of time, which can cause a disturbance of the applied direct field and this effect was not considered. Other design limitation is related with the effectiveness of the compressed fiberglass wool pads for the passage of current and migrating ions, namely $H^+$ and $OH^-$ from the electrode compartments into the media. The wool pads showed high resistance and low surface area in contact with the matrix. In the other tested setups, there was a larger area of soil in direct contact with the passive membranes or the CAT membrane, and the current values measured were much higher. More accurate information about the iron transport could have been obtained if the injection location was sampled and the iron measured in order to close the mass balance. Another important limitation is the lack of representativeness of thin layers of model soils for further extrapolation for real soils and full-scale applications.

The successful results obtained in kaolin or model soils cannot always be directly transferred to spiked soils or to soils sampled at polluted sites. This is due to the variety of adsorption sites (organic and inorganic) for contaminants present in soils not being present in kaolin, and also to the aging of contamination. So, experiments with real soils and historically contaminated soils, from bench to pilot and full scale are needed to assess the results.

Regarding the molinate experiments, it is important to remark that spiked soils behave differently than historically contaminated soils, and further tests would be needed to confirm if only nZVI would be enough to ensure the soil remediation. The cell design in these experiments favored transport to the anode compartment due to the shorter distance. The testing of different injection locations would have allowed obtaining more information about nZVI transport. The determination of hydrogen peroxide during the experiments would confirm the oxidative degradation pathway of molinate by nZVI in soil. Also, the measurement of soil pH at the end of the molinate experiments could have justified the possible explanation of surface changes in the soil, and the consequent increase in nZVI adsorption.

In the PCB experiments, only some congeners were analyzed and more detail would be required to fully implement the technique. The identification of the congeners using GC/MS would provide some additional information about the dechlorination pathways occurring in all the tested conditions: only

nZVI, nZVI plus EK, nZVI plus ED, with and without the surfactants. Desorption tests and batch degradation tests, with and without surfactant, would allow assessing the best surfactant to enhance PCB desorption, without inhibiting nZVI promoted dechlorination.

The environmental impacts of nanoremediation were not addressed in this dissertation. As mentioned in Section 1.1.3, there are large knowledge gaps concerning the effects of manufactured nanoparticles in ecosystems, their persistence, bioaccumulation, and long-term behavior. Results in the literature are contradictory and inconclusive [142-147] and there is limited information under field conditions [146]. It was also demonstrated that the iron nanoparticles reactivity interferes with assay conditions and interpretation of effects in a microbial community in a natural soil [245]. The ways in which nanomaterials exert toxic effects on the environment have not been conclusively defined yet, with two different hypothesis currently accepted as possible: i) the free ion activity model (the toxicity of nanomaterials is caused by metal ions released from nanoparticles); and ii) the biotic ligand model, which also considers the participation of abiotic and biotic ligands [246].

The current need for sustainable remediation practices is becoming a new imperative, with important implications for regulators, liability owners, consultants, contractors, and technology vendors [247]. The assessment of secondary environmental impacts (e.g., life-cycle greenhouse gas emissions, air pollution, energy consumption, and waste production) from remediation operations can be made using different tools, ranging from simple (qualitative) to more quantitative (multi-criteria and fully monetized cost-benefit analysis) [248]. The use of tools like Life Cycle Assessment (LCA) approach should be considered for comparing the different remediation alternatives, namely the use of combined EK and nZVI with traditional remediation technologies, and even with the “do nothing” alternative.

5

# 5. Main conclusions and further developments

The dimension of the soil contamination problem worldwide is serious and new technologies are needed to tackle with mix contaminations and persistent organic pollutants, usually the most challenging ones. Simultaneously, there is a need to move towards more sustainable solutions and a trend to combine, or use successively, already proven technologies. Nanoremediation is controversial and an exciting research field, opening new possibilities for dealing with complicated contaminants and locations, but also has potential environmental impacts associated.

The characteristics that led to a widespread use of PCB, in various industrial and domestic applications, do present a challenge for the remediation of contaminated soils and sediments. Following PCB entrance into the soil environment, they rapidly adsorb to mineral and organic matter (solid phases). The ability to desorb these contaminants determines, in most cases, the effectiveness of the remediation technologies. Currently, there is no cost-effective alternative to landfilling and incineration of PCB contaminated soils. Also, there is no single, portable technology that is applicable to both *ex situ* and *in situ* remediation of PCB in contaminated soils and sediments. Each case is unique and several factors must be considered. The success of the treatment is dependent on proper selection, design, and adjustment of the remediation technology, based on the congeners present, soils properties and the system performance. The combined use of remediation technologies and the so-called “treatment trains” is a promising approach for persistent contaminants. Although electrokinetic remediation has been used extensively, it was only recently tested to extract PCB from soils, used in conjunction with iron nanoparticles and sodium persulfate, with limited results that did not encourage the scale up of the process.

The main research objective of this Ph.D. study was to find out if coupling electrokinetics and zero valent iron nanoparticles could be an efficient method for treating contaminated soils (with inorganic and organic contaminants), and which enhancement methods could be more useful and cost-effective. The results of the experimental work allow outlining the following conclusions:

- Electrokinetics and nZVI can be used together successfully for soil remediation, but a case-by-case analysis is recommended, as the results depend on the contaminant, type of soil and ionic strength of the aqueous phase.

- It is important to test contaminants degradation with nZVI not only in aqueous solutions, but also in matrices increasingly more complex, such as synthetic groundwaters, real groundwaters, model soils and real soils. The degradation results in soils, like the ones obtained for molinate, are much weaker and more time demanding than in deionized water.

- The aggregation and settling of the iron nanoparticles still remain a problem, although direct current can enhance the transport through different porosity media. The suspended electrodialytic remediation ensures that nZVI are uniformly mixed with the soil, eliminating the problem of the accumulation of the iron in the injection reservoir, as occurred in the three-compartment cell.

- The results show that the soil characteristics are critical and affect the reaction between nZVI and the target contaminant, as well as the iron and the contaminant transport.

- In some cases, it is counterproductive to use both methods simultaneously and better results (higher removal rates) are obtained just with the iron nanoparticles or just with electrokinetics. A case-by-case selection is recommended.

- The use of surfactants as an enhancement method of electrokinetic coupled with nZVI needs to be carefully assessed, to minimize the inhibitory effect of the surfactants on iron nanoparticles reactivity. Combining surfactant and nZVI originated less successful remediation than combining surfactant and electrodialytic remediation. The use of surfactants as enhancements may be a poor choice in many contamination case studies.

- Tween 80 has higher energy consumption when compared with saponin in the two-compartment electrodialytic setup. Associated to the low removal percentages, this also contributes to sustain that Tween 80 is not a suitable surfactant to use with PCB contaminated soils and electrodialytic remediation.

- The two-compartment electrodialytic setup allows PCB dechlorination from contaminated soil *ex situ* at a higher rate, in a shorter time, with lower nZVI consumption, and with the use of half of the voltage gradient when compared with the traditional EK setup. In addition, there is no need to treat and dispose of the anolyte.

- The model allowed detecting that, in some cases, an important fraction of the iron nanoparticles tends to aggregate and to form a large and immobile agglomerate, when their concentration is high relative to the available pore volume. However, the results also indicate that aggregated mass clearly diminishes in the presence of a direct current.

Other important goals were to develop a deeper understanding of the mechanisms of the assisted direct current transport of iron nanoparticles, and the development and testing of a methodological and analytical approach for determining the fate of iron nanoparticles in the soil. The experimental work supported drawing the following conclusions:

- The use of a direct current enhanced the nZVI transport in the kaolin, using high concentrations typical of field applications. However, the iron concentration variability could not be explained by pH, ORP, voltage and electrolyte. In the variation of pH and ORP during the experiments, the electrolyte and its ionic strength proved to be significant, and thus have affected aggregation and fast oxidation of the particles.

- The changes in ORP at low concentrations of nZVI (< 0.1 g $L^{-1}$) may be a viable method to track the relative spatial and temporal distribution of nZVI in controlled experiments.

There are still many knowledge gaps regarding the combined use of electrokinetics and zero valent iron nanoparticles. Some of the most important are:

- The need to develop a method (quick, portable and inexpensive) to identify and quantify iron nanoparticles (and other metals nanoparticles) in soil and other complex matrices.

- The aging of nanoparticles and the polymer coatings in a living environment such as soil is an interesting area of research.

- Further work is necessary for a comprehensive treatise of the behavior of nZVI in clay rich soils under electric field, to assess the electroosmotic advection of iron nanoparticles.

- Scale up of the two-compartment cell and testing with other soils (with higher PCB concentrations) to evaluate the viability of the method to compete with the traditional alternatives for PCB contaminated soils treatment ("dig and dump" and "dig and incinerate").

- Assessment of the possibility of recycling the iron nanoparticles used in the two-compartment ED setup, and transported in the ionic form to the catholyte, through a new step in the process before recirculation, with the addition of a strong reductant such as sodium borohydride.

- Further research on potential side effects during treatment (such as anodic precipitation, oxidation of the conditioning agent, and generation of gases e.g., $Cl_2$) for the scale-up of the ED process.

- Further research is needed to quantify the effect of the electrodechlorination and hydrodechlorination of PCB using the two-compartment cell setup, in order to optimize the combined process as the results showed that the use of a direct current allowed the highest PCB removal rates.

- An important emerging field will also be the assessment of the ecotoxicological and environmental impacts of the application of iron nanoparticles, also considering long-term effects of the use of nanotechnologies.

- The assessment of the sustainability of nanoremediation, through a Life Cycle Assessment, when compared with other current technologies.

# References


[1] B. Singh, R. Naidu, Cleaning contaminated environment: A growing challenge, Biodegradation, 23 (2012) 785-786.

[2] G.P. Marc van Liedekerke, Sabine Rabl-Berger, Mark Kibblewhite, Geertrui Louwagie, Progress in the Management of Contaminated Sites in Europe, Report EUR 26376 EN. Institute for Environment and Sustainability. Joint Research Center. European Commission, Luxembourg, 2014.

[3] USEPA, Superfund - Cleaning up the Nation's Hazardous Wastes Sites, United States Environmental Protection Agency, http://www.epa.gov/superfund/, Accessed the 12th June 2014, 2014.

[4] USEPA, Brownfields and Land Revitalization, United States Environmental Protection Agency, http://www.epa.gov/brownfields/basic_info.htm, Accessed the 12th June 2014, 2014.

[5] Q.Y. Cai, C.H. Mo, Q.T. Wu, A. Katsoyiannis, Q.Y. Zeng, The status of soil contamination by semivolatile organic chemicals (SVOCs) in China: A review, Sci. Total Environ., 389 (2008) 209-224.

[6] S. Khan, Q. Cao, Y.M. Zheng, Y.Z. Huang, Y.G. Zhu, Health risks of heavy metals in contaminated soils and food crops irrigated with wastewater in Beijing, China, Environ. Poll., 152 (2008) 686-692.

[7] L. Niu, F. Yang, C. Xu, H. Yang, W. Liu, Status of metal accumulation in farmland soils across China: From distribution to risk assessment, Environ. Poll., 176 (2013) 55-62.

[8] Z. Li, Z. Ma, T.J. van der Kuijp, Z. Yuan, L. Huang, A review of soil heavy metal pollution from mines in China: Pollution and health risk assessment, Sci. Total Environ., 468–469 (2014) 843-853.

[9] S. Srinivasa Gowd, M. Ramakrishna Reddy, P.K. Govil, Assessment of heavy metal contamination in soils at Jajmau (Kanpur) and Unnao industrial areas of the Ganga Plain, Uttar Pradesh, India, J. Hazard. Mater., 174 (2010) 113-121.

[10] A. Eguchi, T. Isobe, K. Ramu, N.M. Tue, A. Sudaryanto, G. Devanathan, P.H. Viet, R.S. Tana, S. Takahashi, A. Subramanian, S. Tanabe, Soil contamination by brominated flame retardants in open waste dumping sites in Asian developing countries, Chemosphere, 90 (2013) 2365-2371.

[11] A.A. Jennings, Analysis of worldwide regulatory guidance values for the most commonly regulated elemental surface soil contamination, J. Environ.Manag., 118 (2013) 72-95.

[12] S.M. Rodrigues, M.E. Pereira, E.F. da Silva, A.S. Hursthouse, A.C. Duarte, A review of regulatory decisions for environmental protection: Part I — Challenges in the implementation of national soil policies, Environ. Int., 35 (2009) 202-213.

[13] R. Naidu, Recent advances in contaminated site remediation, Water Air Soil Poll., 224 (2013) 1-11.

[14] WHO, Contaminated Sites and Health, R. Pasetto, P. Martin-Olmedo, M. Martuzzi (Eds.), World Health Organization Regional Office for Europe, 2013, 92 pp.

[15] European Comission, Thematic Strategy for Soil Protection. COM(2006)231, Brussels, Belgium, 2006.

[16] European Comission, Proposal for a Directive of the European Parliament and of the Council establishing a framework for the protection of soil and amending Directive 2004/35/EC, COM/2006/0232, 2006.

[17] L. Valentín, A. Nousiainen, A. Mikkonen, Introduction to organic contaminants in soil: Concepts and risks, in: T. Vicent, G. Caminal, E. Eljarrat, D. Barceló (Eds.) Emerging Organic Contaminants in Sludges: Analysis, Fate and Biological Treatment, Springer-Verlag, Berlin Heidelberg, 2013, pp. 1-30.

[18] C. Averill, B.L. Turner, A.C. Finzi, Mycorrhiza-mediated competition between plants and decomposers drives soil carbon storage, Nature, 505 (2014): 543-545.

[19] S.M. Rodrigues, M.E. Pereira, E.F. da Silva, A.S. Hursthouse, A.C. Duarte, A review of regulatory decisions for environmental protection: Part II-The case-study of contaminated land management in Portugal, Environ. Int., 35 (2009) 214-225.

[20] M. Chrysochoou, C.P. Johnston, G. Dahal, A comparative evaluation of hexavalent chromium treatment in contaminated soil by calcium polysulfide and green-tea nanoscale zero-valent iron, J. Hazard. Mater., 201–202 (2012) 33–42.

[21] D. Bagchi, S.J. Stohs, B.W. Downs, M. Bagchi, H.G. Preuss, Cytotoxicity and oxidative mechanisms of different forms of chromium, Toxicol., 180 (2002) 5-22.

[22] R. Singh, V. Misra, R.P. Singh, Synthesis, characterization and role of zero-valent iron nanoparticle in removal of hexavalent chromium from chromium-spiked soil, J. Nanopart. Res., 13 (2011) 4063-4073.

[23] J. Kotaś, Z. Stasicka, Chromium occurrence in the environment and methods of its speciation, Environ. Poll., 107 (2000) 263-283.

[24] UN, Stockholm Convention on Persistent Organic Pollutants, Geneva, 2001, http://chm.pops.int/Convention/tabid/54/language/en-GB/Default.aspx, Accessed 23rd May 2014

[25] M. Castro, A.C. Silva-Ferreira, C.M. Manaia, O.C. Nunes, A case study of molinate application in a Portuguese rice field: herbicide dissipation and proposal of a clean-up methodology, Chemosphere, 59 (2005) 1059-1065.

[26] FAO, Rice Market Monitor, Trade and Markets Division. Food and Agriculture Organization of the United Nations, 2013.

[27] M. Köck-Schulmeyer, M. Villagrasa, M. López de Alda, R. Céspedes-Sánchez, F. Ventura, D. Barceló, Occurrence and behavior of pesticides in wastewater treatment plants and their environmental impact, Sci. Total Environ., 458–460 (2013) 466-476.

[28] M.J. Cerejeira, P. Viana, S. Batista, T. Pereira, E. Silva, M.J. Valério, A. Silva, M. Ferreira, A.M. Silva-Fernandes, Pesticides in Portuguese surface and ground waters, Water Res., 37 (2003) 1055-1063.

[29] A. Hildebrandt, S. Lacorte, D. Barceló, Assessment of priority pesticides, degradation products, and pesticide adjuvants in groundwaters and top soils from agricultural areas of the Ebro river basin, Anal. Bioanal. Chem., 387 (2007) 1459-1468.

[30] M. Koblizkova, P. Ruzicková, P. Cupr, J. Komprda, I. Holoubek, J. Klánová, Soil burdens of persistent organic pollutants: Their levels, fate and risks. Part IV, Quantification of volatilization fluxes of organochlorine pesticides and polychlorinated biphenyls from contaminated soil surfaces, Environ. Sci. Technol., 43 (2009) 3588-3595.

[31] L. Nizzetto, M. Macleod, K. Borgå, A. Cabrerizo, J. Dachs, A.D. Guardo, D. Ghirardello, K.M. Hansen, A. Jarvis, A. Lindroth, B. Ludwig, D. Monteith, J.A. Perlinger, M. Scheringer, L. Schwendenmann, K.T. Semple, L.Y. Wick, G. Zhang, K.C. Jones, Past, present, and future controls on levels of persistent organic pollutants in the global environment, Environ. Sci. Technol., 44 (2010) 6526-6531.

[32] S.G. Donaldson, J.V. Oostdam, C. Tikhonov, M. Feeley, B. Armstrong, P. Ayotte, O. Boucher, W. Bowers, L. Chan, F. Dallaire, R. Dallaire, É. Dewailly, J. Edwards, G.M. Egeland, J. Fontaine, C. Furgal, T. Leech, E. Loring, G. Muckle, T. Nancarrow, D. Pereg, P. Plusquellec, M. Potyrala, O. Receveur, R.G. Sheare, Environmental contaminants and human health in the Canadian Arctic, Sci. Total Environ., 408 (2010) 5165–5234.

[33] I. Holoubek, L. Dušek, M. Sáňka, J. Hofman, P. Čupr, J. Jarkovský, J. Zbíral, J. Klánová, Soil burdens of persistent organic pollutants – Their levels, fate and risk. Part I. Variation of concentration ranges according to different soil uses and locations, Environ. Poll., 157 (2009) 3207-3217.

[34] J. Maervoet, A. Covaci, P. Schepens, C.D. Sandau, R.J. Letcher, A reassessment of the nomenclature of polychlorinated biphenyl (PCB) metabolites, Environ. Health. Perspect., 112 (2003) 291.

[35] H. Fiedler, Polychlorinated biphenyls (PCBs): Uses and environmental releases, United Nations Environmental Programmee. Procedings of the Subregional Awareness Raising Workshop on Persistent Organic Pollutants (POPs), Bangkok, Thailand, 25-28 November 1997. http://www.chem.unep.ch/pops/POPs_Inc/proceedings/bangkok/FIEDLER1.html

[36] H.K. Yak, B.W. Wenclawiak, I.F. Cheng, J.G. Doyle, C.M. Wai, Reductive dechlorination of polychlorinated biphenyls by zerovalent iron in subcritical water, Environ. Sci. Technol., 33 (1999) 1307-1310.

[37] K. Breivik, A. Sweetman, J.M. Pacyna, K.C. Jones, Towards a global historical emission inventory for selected PCB congeners — A mass balance approach 1. Global production and consumption, Sci.Total Environ. 290 (2002) 181-198.

[38] J. Diaz-Ferrero, M.C. Rodriguez-Larena, L. Comellas, B. Jimhnez, Bioanalytical methods applied to endocrine disrupting polychlorinated biphenyls, polychlorinated dibenzo-pdioxins and polychlorinated dibenzofurans. A review, Trend. Anal. Chem., 16 (1997) 563-573.

[39] J. Borja, D.M. Taleon, J. Auresenia, S. Gallardo, Polychlorinated biphenyls and their biodegradation, Process Biochem., 40 (2005) 1999-2013.

[40] M.D. Erickson, R.G. Kaley, Applications of polychlorinated biphenyls, Environ. Sci. Poll. Res., 18 (2011) 135-151.

[41] J. Kas, J. Burkhard, K. Demnerová, J. Kost'ál, T. Macek, M. Macková, J. Pazlarová, Perspectives in biodegradation of alkanes and PCBs, Pure Appl. Chem., 69 (1997) 2357-2369.

[42] UNEP, PCB Transformers and Capacitors From Management to Reclassification and Disposal, UNEP Chemicals, United Nations Environmental Programme, Geneva, Switzerland, 2002.

[43] ATSDR, Toxicological Profile for Polychlorinated Biphenyls (PCBs), in, Agency for Toxic Substances and Disease Registry. U.S. Department of Health and Human Services Atlanta, 2000.

[44] M.L. Diamond, L. Melymuk, S.A. Csiszar, M. Robson, Estimation of PCB stocks, emissions, and urban fate: Will our policies reduce concentrations and exposure?, Environ. Sci. Technol., 44 (2010) 2777-2783.

[45] M. Kohler, J. Tremp, M. Zennegg, C. Seiler, S. Minder-Kohler, M. Beck, P. Lienemann, L. Wegmann, P. Schmid, Joint sealants: An overlooked diffuse source of polychlorinated biphenyls in buildings, Environ. Sci. Technol., 39 (2005) 1967-1973.

[46] E. Priha, S. Hellman, J. Sorvari, PCB contamination from polysulphide sealants in residential areas - Exposure and risk assessment, Chemosphere, 59 (2005) 537-543.

[47] R. Eisler, A.A. Belisle, Planar PCB Hazards to Fish, Wildlife, and Invertebrates: a synoptic review, Patuxent Wildlife Research Center. U.S. National Biological Service, Laurel, 1996.

[48] K. Furukawa, H. Fujihara, Microbial Degradation of Polychlorinated Biphenyls: Biochemical and Molecular Features, J. Biosci. Bioeng., 105 (2008) 433-449.

[49] D. Hu, K.C. Hornbuckle, Inadvertent polychlorinated biphenyls in commercial paint pigments, Environ. Sci. Technol., 44 (2010) 2822-2827.

[50] L.A. Rodenburg, J. Guo, S. Du, G.J. Cavallo, Evidence for unique and ubiquitous environmental sources of 3,3 '-dichlorobiphenyl (PCB 11), Environ. Sci. Technol., 44 (2010) 2816-2821.

[51] A. Mikszewski, Emerging Technologies for the In Situ Remediation of PCB-Contaminated Soils and Sediments: Bioremediation and Nanoscale Zero-Valent Iron, U.S. Environmental Protection Agency, Office of Solid Waste and Emergency Response. Office of Superfund Remediation and Technology Innovation Program, Washington, DC, 2004, pp. 26.

[52] CDC, Fourth National Report on Human Exposure to Environmental Chemicals, Department of Health and Human Services. Centers for Disease Control and Prevention Atlanta, GA, USA, 2009, pp. 519.

[53] ATSDR, Toxicological Profiles, in, Agency for Toxic Substances and Disease Registry. U.S. Department of Health and Human Services, Atlanta, Georgia, 2011.

[54] O.M. Faroon, L.S. Keith, C. Smith, Simon, C.T.D. Rosa, Polychlorinated Biphenyls: Human Health Aspects, World Health Organization, Report published under the joint sponsorship of the United Nations Environment Programme, the International Labour Organization, and the World Health Organization, and produced within the framework of the Inter-Organization Programme for the Sound Management of Chemicals, Geneva, 2003.

[55] G.H. Xing, J.K.Y. Chan, A.O.W. Leung, S.C. Wu, M.H. Wong, Environmental impact and human exposure to PCBs in Guiyu, an electronic waste recycling site in China, Environ. Int., 35 (2009) 76-82.

[56] R. Eisler, Planar PCB Hazards to Fish, Wildlife, and Invertebrates: a synoptic review, Patuxent Wildlife Research Center. U.S. Fish and Wildlife Service, Laurel, 1986.

[57] K. Breivik, A. Sweetman, J.M. Pacyna, K.C. Jones, Towards a global historical emission inventory for selected PCB congeners — A mass balance approach 3. An update, Sci. Total Environ. 377 (2007) 296–307.

[58] K. Breivik, A. Sweetman, J.M. Pacyna, K.C. Jones, Towards a global historical emission inventory for selected PCB congeners — A mass balance approach 2. Emissions, Sci. Total Environ. 290 (2002) 199–224.

[59] W.A. Ockenden, K. Breivik, S.N. Meijer, E. Steinnes, A.J. Sweetman, K.C. Jones, The global re-cycling of persistent organic pollutants is strongly retarded by soils, Environ. Poll., 121 (2003) 75-80.

[60] C. Schmidt, How PCBs are like grasshoppers, Environ. Sci. Technol., 44 (2010) 2752.

[61] A.C. Alder, M.M. Haggblom, S.R. Oppenheimer, L.Y. Young, Reductive dechlorination of polychlorinated biphenyls in anaerobic sediments, Environ. Sci. Technol., 27 (1993) 530-538.

[62] USEPA, Search Superfund Site Information, United States Environmental Protection Agency, http://cumulis.epa.gov/supercpad/cursites/srchsites.cfm, Accessed the 15th June 2014, 2014.

[63] TBS-SCT, Contaminants & Media, Federal Contaminated Sites Inventory. Treasury Board of Canada Secretariat, http://www.tbs-sct.gc.ca/fcsi-rscf/cm-eng.aspx?clear=1, Accessed the 27th February 2014, 2014.

[64] S.N. Meijer, W.A. Ockenden, A. Sweetman, K. Breivik, J.O. Grimalt, K.C. Jones, Global distribution and budget of PCBs and HCB in background surface soils: Implications for sources and environmental processes, Environ. Sci. Technol., 37 (2003) 667-672.

[65] H.I. Gomes, C. Dias-Ferreira, A.B. Ribeiro, Overview of *in situ* and *ex situ* remediation technologies for PCB-contaminated soils and sediments and obstacles for full-scale application, Sci. Total Environ., 445-446 (2013) 237-260.

[66] G. Fan, L. Cang, G. Fang, D. Zhou, Surfactant and oxidant enhanced electrokinetic remediation of a PCBs polluted soil, Sep. Purif. Technol., 123 (2014) 106-113.

[67] Y. Yukselen-Aksoy, K.R. Reddy, Effect of soil composition on electrokinetically enhanced persulfate oxidation of polychlorobiphenyls, Electrochim. Acta, 86 (2012) 164-169.

[68] Y. Li, F. Liang, Y. Zhu, F. Wang, Phytoremediation of a PCB-contaminated soil by alfalfa and tall fescue single and mixed plants cultivation, J. Soil Sediment., 13 (2013) 925-931.

[69] M. Viisimaa, O. Karpenko, V. Novikov, M. Trapido, A. Goi, Influence of biosurfactant on combined chemical-biological treatment of PCB-contaminated soil, Chem. Eng. J., 220 (2013) 352-359.

[70] USEPA, Permeable Reactive Barriers, Permeable Treatment Zones, and Application of Zero-Valent Iron: Overview, Technology Innovation and Field Services Division, Washington, DC, 2011.

[71] C.B. Wang, W. Zhang, Synthesizing nanoscale iron particles for rapid and complete dechlorination of TCE and PCBs, Environ. Sci. Technol., 31 (1997) 2154-2156.

[72] W. Zhang, C.B. Wang, H.L. Lien, Treatment of chlorinated organic contaminants with nanoscale bimetallic particles, Catal. Today, 40 (1998) 387-395.

[73] H. Lin, S. Hou, G. Xie, Z. Yao, Q. Zhou, Degradation of 1-(2-chlorobenzoyl)-3-(4-chlorophenyl) urea by nanoscale zerovalent iron under aerobic and anaerobic conditions, J. Environ. Sci. Health A, 47 (2012) 2270-2276.

[74] A. Ghauch, A. Tuqan, H.A. Assi, Antibiotic removal from water: Elimination of amoxicillin and ampicillin by microscale and nanoscale iron particles, Environ. Poll., 157 (2009) 1626-1635.

[75] S.R. Kanel, B. Manning, L. Charlet, H. Choi, Removal of arsenic (III) from groundwater by nanoscale zero-valent iron, Environ. Sci. Technol., 39 (2005) 1291-1298.

[76] T. Satapanajaru, P. Anurakpongsatorn, P. Pengthamkeerati, H. Boparai, Remediation of atrazine-contaminated soil and water by nano zerovalent iron, Water Air Soil Poll., 192 (2008) 349-359.

[77] H.K. Boparai, M. Joseph, D.M. O'Carroll, Cadmium ($Cd^{2+}$) removal by nano zerovalent iron: surface analysis, effects of solution chemistry and surface complexation modeling, Environ. Sci. Poll. Res., (2013) 1-12.

[78] K. Singh, A. Singh, S. Gupta, P. Rai, Modeling and optimization of reductive degradation of chloramphenicol in aqueous solution by zero-valent bimetallic nanoparticles, Environ. Sci. Poll. Res., 19 (2012) 2063-2078.

[79] H. Song, E.R. Carraway, Reduction of chlorinated ethanes by nanosized zero-valent iron: Kinetics, pathways, and effects of reaction conditions, Environ. Sci. Technol., 39 (2005) 6237-6245.

[80] J. Dries, L. Bastiaens, D. Springael, S.N. Agathos, L. Diels, Combined removal of chlorinated ethenes and heavy metals by zerovalent iron in batch and continuous flow column systems, Environ. Sci. Technol., 39 (2005) 8460-8465.

[81] S.M. Ponder, J.G. Darab, T.E. Mallouk, Remediation of Cr(VI) and Pb(II) aqueous solutions using supported, nanoscale zero-valent iron, Environ. Sci. Technol., 34 (2000) 2564-2569.

[82] S.M. Ponder, J.G. Darab, J. Bucher, D. Caulder, I. Craig, L. Davis, N. Edelstein, W. Lukens, H. Nitsche, L. Rao, D.K. Shuh, T.E. Mallouk, Surface chemistry and electrochemistry of supported zerovalent iron nanoparticles in the remediation of aqueous metal contaminants, Chem. Mater., 13 (2001) 479-486.

[83] R. Singh, V. Misra, M.K.R. Mudiam, L.K.S. Chauhan, R.P. Singh, Degradation of HCH spiked soil using stabilized Pd/$Fe^0$ bimetallic nanoparticles: Pathways, kinetics and effect of reaction conditions, J. Hazard. Mat., 237-238 (2012) 355-364.

[84] Y. Shih, Y. Chen, M. Chen, Y. Tai, C. Tso, Dechlorination of hexachlorobenzene by using nanoscale Fe and nanoscale Pd/Fe bimetallic particles, Colloids Surf. A, 332 (2009) 84-89.

[85] Y. Shih, C. Hsu, Y. Su, Reduction of hexachlorobenzene by nanoscale zero-valent iron: Kinetics, pH effect, and degradation mechanism, Sep. Purif. Technol., 76 (2011) 268-274.

[86] D.W. Elliott, H.L. Lien, W. Zhang, Zerovalent iron nanoparticles for treatment of ground water contaminated by hexachlorocyclohexanes, J. Environ. Qual., 37 (2008) 2192–2201.

[87] G. Naja, A. Halasz, S. Thiboutot, G. Ampleman, J. Hawari, Degradation of hexahydro-1,3,5-trinitro-1,3,5-triazine (RDX) using zerovalent iron nanoparticles, Environ. Sci. Technol., 42 (2008) 4364-4370.

[88] S. Machado, W. Stawiński, P. Slonina, A.R. Pinto, J.P. Grosso, H.P.A. Nouws, J.T. Albergaria, C. Delerue-Matos, Application of green zero-valent iron nanoparticles to the remediation of soils contaminated with ibuprofen, Sci. Total Environ., 461-462 (2013) 323-329.

[89] D.W. Elliott, H.L. Lien, W.X. Zhang, Degradation of lindane by zero-valent iron nanoparticles, J. Environ. Eng., 135 (2009) 317-324.

[90] I. San Román, M.L. Alonso, L. Bartolomé, A. Galdames, E. Goiti, M. Ocejo, M. Moragues, R.M. Alonso, J.L. Vilas, Relevance study of bare and coated zero valent iron nanoparticles for lindane degradation from its by-product monitorization, Chemosphere, 93 (2013) 1324-1332.

[91] R.K. Singhal, B. Gangadhar, H. Basu, V. Manisha, G.R.K. Naidu, A.V.R. Reddy, Remediation of malathion contaminated soil using zero valent iron nano-particles, Am. J. Anal. Chem., 3 (2012) 76-82.

[92] T. Shahwan, S. Abu Sirriah, M. Nairat, E. Boyaci, A.E. Erofülu, T.B. Scott, K.R. Hallam, Green synthesis of iron nanoparticles and their application as a Fenton-like catalyst for the degradation of aqueous cationic and anionic dyes, Chem. Eng. J., 172 (2011) 258-266.

[93] Z. Fang, J. Chen, X. Qiu, X. Qiu, W. Cheng, L. Zhu, Effective removal of antibiotic metronidazole from water by nanoscale zero-valent iron particles, Desalination, 268 (2011) 60-67.

[94] S.H. Joo, A.J. Feitz, T.D. Waite, Oxidative degradation of the carbothioate herbicide, molinate, using nanoscale zero-valent iron, Environ. Sci. Technol., 38 (2004) 2242-2247.

[95] S. Choe, Y.Y. Chang, K.Y. Hwang, J. Khim, Kinetics of reductive denitrification by nanoscale zero-valent iron, Chemosphere, 41 (2000) 1307-1311.

[96] G. Lowry, K. Johnson, Congener-specific dechlorination of dissolved PCBs by microscale and nanoscale zerovalent iron in a water/methanol solution, Environ. Sci. Technol., 38 (2004) 5208-5216.

[97] P. Varanasi, A. Fullana, S. Sidhu, Remediation of PCB contaminated soils using iron nano-particles, Chemosphere, 66 (2007) 1031–1038.

[98] K. Darko-Kagya, A.P. Khodadoust, K.R. Reddy, Reactivity of aluminum lactate-modified nanoscale iron particles with pentachlorophenol in soils, Environ. Eng. Sci., 27 (2010) 861-869.

[99] Y. Shih, Y. Tai, Reaction of decabrominated diphenyl ether by zerovalent iron nanoparticles, Chemosphere, 78 (2010) 1200-1206.

[100] M.C. Chang, H.Y. Kang, Remediation of pyrene-contaminated soil by synthesized nanoscale zero-valent iron particles, J. Environ. Sci. Health A, 44 (2009) 576-582.

[101] J.L. Chen, S.R. Al-Abed, J.A. Ryan, Z. Li, Effects of pH on dechlorination of trichloroethylene by zero-valent iron, J. Hazard. Mater., 83 (2001) 243-254.

[102] F. He, D. Zhao, J. Liu, C.B. Roberts, Stabilization of Fe-Pd nanoparticles with sodium carboxymethyl cellulose for enhanced transport and dechlorination of trichloroethylene in soil and groundwater, Ind. Eng. Chem. Res., 46 (2007) 29-34.

[103] F. He, D. Zhao, Preparation and characterization of a new class of starch-stabilized bimetallic nanoparticles for degradation of chlorinated hydrocarbons in water, Environ. Sci. Technol., 39 (2005) 3314-3320.

[104] D.W. Elliott, W. Zhang, Field assessment of nanoscale bimetallic particles for groundwater treatment, Environ. Sci. Technol., 35 (2001) 4922-4926.

[105] M. Zhang, F. He, D. Zhao, X. Hao, Degradation of soil-sorbed trichloroethylene by stabilized zero valent iron nanoparticles: Effects of sorption, surfactants, and natural organic matter, Water Res. 45 (2011) 2401-2414.

[106] W. Jiamjitrpanich, C. Polprasert, P. Parkpian, R.D. Delaune, A. Jugsujinda, Environmental factors influencing remediation of TNT-contaminated water and soil with nanoscale zero-valent iron particles, J. Environ. Sci. Health A, 45 (2010) 263-274.

[107] M. Dickinson, T.B. Scott, The application of zero-valent iron nanoparticles for the remediation of a uranium-contaminated waste effluent, J. Hazard. Mater., 178 (2010) 171–179.

[108] K.W. Henn, D.W. Waddill, Utilization of nanoscale zero-valent iron for source remediation — A case study, Remediation, 16 (2006) 57-77.

[109] USEPA, Fact sheet on selected sites using or testing nanoparticles for remediation, United States Environmental Protection Agency, http://cluin.org/products/nanozvi/, 2011, Accessed 3 April 2012.

[110] N.C. Mueller, J. Braun, J. Bruns, M. Černík, P. Rissing, D. Rickerby, B. Nowack, Application of nanoscale zero valent iron (NZVI) for groundwater remediation in Europe, Env. Sci. Poll. Res., 19 (2012) 550-558.

[111] D. Rejeski, T. Kuiken, P. Polischuk, E. Pauwels, Nanoremediation Map, Project on Emerging Nanotechnologies, http://www.nanotechproject.org/inventories/remediation_map/, Accessed 5th March 2014, 2014.

[112] R.A. Crane, T.B. Scott, Nanoscale zero-valent iron: Future prospects for an emerging water treatment technology, J. Hazard. Mater., 211-212 (2012) 112-125.

[113] J. Quinn, C. Geiger, C. Clausen, K. Brooks, C. Coon, S. O'Hara, T. Krug, D. Major, W.S. Yoon, A. Gavaskar, T. Holdsworth, Field demonstration of DNAPL dehalogenation using emulsified zero-valent iron, Environ. Sci. Technol., 39 (2005) 1309-1318.

[114] W. Zhang, D.W. Elliott, Applications of iron nanoparticles for groundwater remediation, Remediation, (2006) 7-21.

[115] C. Su, R.W. Puls, T.A. Krug, M.T. Watling, S.K. O'Hara, J.W. Quinn, N.E. Ruiz, A two and half-year-performance evaluation of a field test on treatment of source zone tetrachloroethene and its chlorinated daughter products using emulsified zero valent iron nanoparticles, Water Res., 46 (2012) 5071-5084.

[116] C.M. Kocur, A.I. Chowdhury, N. Sakulchaicharoen, H.K. Boparai, K.P. Weber, P. Sharma, M.M. Krol, L.M. Austrins, C. Peace, B.E. Sleep, D.M. O'Carroll, Characterization of nZVI mobility in a field scale test, Environ. Sci. Technol., 48 (2014) 2862-2869.

[117] T. Phenrat, N. Saleh, K. Sirk, R.D. Tilton, G.V. Lowry, Aggregation and sedimentation of aqueous nanoscale zerovalent iron dispersions, Environ. Sci. Technol., 41 (2007) 284-290.

[118] Y.P. Sun, X.Q. Li, W.X. Zhang, H.P. Wang, A method for the preparation of stable dispersion of zero-valent iron nanoparticles, Colloid Surface A, 308 (2007) 60–66.

[119] A. Tiraferri, K.L. Chen, R. Sethi, M. Elimelech, Reduced aggregation and sedimentation of zero-valent iron nanoparticles in the presence of guar gum, J. Colloid Interface Sci., 324 (2008) 71–79

[120] A. Tiraferri, R. Sethi, Enhanced transport of zerovalent iron nanoparticles in saturated porous media by guar gum, J. Nanopart. Res., 11 (2009) 635-645.

[121] P. Jiemvarangkul, W.X. Zhang, H.L. Lien, Enhanced transport of polyelectrolyte stabilized nanoscale zero-valent iron (nZVI) in porous media, Chem. Eng. J., 170 (2011) 482-491.

[122] Y.H. Lin, H.H. Tseng, M.Y. Wey, M.D. Lin, Characteristics, morphology, and stabilization mechanism of PAA250K-stabilized bimetal nanoparticles, Colloid Surface A, 349 (2009) 137-144.

[123] T. Raychoudhury, G. Naja, S. Ghoshal, Assessment of transport of two polyelectrolyte-stabilized zero-valent iron nanoparticles in porous media, J. Contam. Hydrol., 118 (2010) 143-151.

[124] T. Phenrat, A. Cihan, H.J. Kim, M. Mital, T. Illangasekare, G.V. Lowry, Transport and deposition of polymer-modified $Fe^0$ nanoparticles in 2-D heterogeneous porous media: Effects of particle concentration, $Fe^0$ content, and coatings, Environ. Sci. Technol., 44 (2010) 9086-9083.

[125] T. Phenrat, F. Fagerlund, T. Illangasekare, G.V. Lowry, R.D. Tilton, Polymer-modified $Fe^0$ nanoparticles target entrapped NAPL in two dimensional porous media: Effect of particle

concentration, NAPL saturation, and injection strategy, Environ. Sci. Technol., 45 (2011) 6102-6109.

[126] B.W. Hydutsky, E.J. Mack, B.B. Beckerman, J.M. Skluzacek, T.E. Mallouk, Optimization of nano- and microiron transport through sand columns using polyelectrolyte mixtures, Environ. Sci. Technol., 41 (2007) 6418-6424.

[127] S. Kanel, D. Nepal, B. Manning, H. Choi, Transport of surface-modified iron nanoparticle in porous media and application to arsenic(III) remediation, J. Nanopart. Res., 9 (2007) 725-735.

[128] T. Phenrat, H.J. Kim, F. Fagerlund, T. Illangasekare, R.D. Tilton, G.V. Lowry, Particle size distribution, concentration, and magnetic attraction affect transport of polymer-modified $Fe^0$ nanoparticles in sand columns, Environ. Sci. Technol., 43 (2009) 5079-5085.

[129] N. Saleh, H.J. Kim, T. Phenrat, K. Matyjaszewski, R.D. Tilton, G.V. Lowry, Ionic strength and composition affect the mobility of surface-modified $Fe^0$ nanoparticles in water-saturated sand columns, Environ. Sci. Technol., 42 (2008) 3349-3355.

[130] Y.H. Lin, H.H. Tseng, M.Y. Wey, M.D. Lin, Characteristics of two types of stabilized nano zero-valent iron and transport in porous media, Sci. Total Environ., 408 (2010) 2260-2267.

[131] B. Schrick, B.W. Hydutsky, J.L. Blough, T.E. Mallouk, Delivery vehicles for zerovalent metal nanoparticles in soil and groundwater, Chem. Mater., 16 (2004) 2187–2193.

[132] G.C.C. Yang, H.C. Tu, C.H. Hung, Stability of nanoiron slurries and their transport in the subsurface environment, Sep. Purif. Technol. 58 (2007) 166-172.

[133] T. Phenrat, Y. Liu, R.D. Tilton, G.V. Lowry, Adsorbed polyelectrolyte coatings decrease $Fe^0$ nanoparticle reactivity with TCE in water: conceptual model and mechanisms, Environ. Sci. Technol., 43 (2009) 1507-1514.

[134] T. Tosco, M.P. Papini, C.C. Viggi, R. Sethi, Nanoscale zerovalent iron particles for groundwater remediation: a review, J. Clean. Prod., 77 (2014) 10-21.

[135] C. Noubactep, S. Caré, R. Crane, Nanoscale metallic iron for environmental remediation: Prospects and limitations, Water Air Soil Poll., 223 (2012) 1363-1382.

[136] W. Zhang, Nanoscale iron particles for environmental remediation: an overview, J. Nanopart. Res., 5 (2003) 323-332.

[137] D. O'Carroll, B. Sleep, M. Krol, H. Boparai, C. Kocur, Nanoscale zero valent iron and bimetallic particles for contaminated site remediation, Adv. Water Resour., 51 (2013) 104-122

[138] W. Yan, H.L. Lien, B.E. Koel, W. Zhang, Iron nanoparticles for environmental clean-up: Recent developments and future outlook, Environ. Sci. Process. Impact., 15 (2013) 63-77.

[139] F. He, D. Zhao, C. Paul, Field assessment of carboxymethyl cellulose stabilized iron nanoparticles for in situ destruction of chlorinated solvents in source zones, Water Res., 44 (2010) 2360–2370.

[140] X. Chen, X. Yao, C. Yu, X. Su, C. Shen, C. Chen, R. Huang, X. Xu, Hydrodechlorination of polychlorinated biphenyls in contaminated soil from an e-waste recycling area, using nanoscale zerovalent iron and Pd/Fe bimetallic nanoparticles, Environ. Sci. Poll. Res., 21 (2014) 1-10.

[141] K.D. Grieger, A. Fjordbøge, N.B. Hartmann, E. Eriksson, P.L. Bjerg, A. Baun, Environmental benefits and risks of zero-valent iron nanoparticles (nZVI) for in situ remediation: Risk mitigation or trade-off?, J. Cont. Hydrol., 118 (2010) 165-183.

[142] Y.S. El-Temsah, E.J. Joner, Effects of nano-sized zero-valent iron (nZVI) on DDT degradation in soil and its toxicity to collembola and ostracods, Chemosphere, 92 (2013) 131–137.

[143] C. Fajardo, M.L. Saccà, M. Martinez-Gomariz, G. Costa, M. Nande, M. Martin, Transcriptional and proteomic stress responses of a soil bacterium *Bacillus cereus* to nanosized zero-valent iron (nZVI) particles, Chemosphere, 93 (2013) 1077–1083.

[144] A.A. Keller, K. Garner, R.J. Miller, H.S. Lenihan, Toxicity of nano-zero valent iron to freshwater and marine organisms, PLoS ONE, 7 (2012) e43983.

[145] M. Saccà, C. Fajardo, M. Nande, M. Martín, Effects of nano zero-valent iron on *Klebsiella oxytoca* and stress response, Microb. Ecol., (2013) 1-7.

[146] R. Dinesh, M. Anandaraj, V. Srinivasan, S. Hamza, Engineered nanoparticles in the soil and their potential implications to microbial activity, Geoderma, 173-174 (2012) 19-27.

[147] R.J. Barnes, C.J. van der Gast, O. Riba, L.E. Lehtovirta, J.I. Prosser, P.J. Dobson, I.P. Thompson, The impact of zero-valent iron nanoparticles on a river water bacterial community, J. Hazard. Mater., 184 (2010) 73-80.

[148] K. Tiede, A.B.A. Boxall, S.P. Tear, J. Lewis, H. David, M. Hassellov, Detection and characterization of engineered nanoparticles in food and the environment, Food Addit. Contam., 25 (2008) 795-821.

[149] B. Pan, B. Xing, Applications and implications of manufactured nanoparticles in soils: A review, Eur. J. Soil Sci., 63 (2012) 437-456.

[150] H. Zänker, A. Schierz, Engineered nanoparticles and their identification among natural nanoparticles, Annu. Rev. Anal. Chem., 5 (2012) 107-132.

[151] I.C. Regelink, L. Weng, G.F. Koopmans, W.H. Van Riemsdijk, Asymmetric flow field-flow fractionation as a new approach to analyse iron-(hydr) oxide nanoparticles in soil extracts, Geoderma, 202 (2013) 134-141.

[152] G.Z. Tsogas, D.L. Giokas, A.G. Vlessidis, Ultra-trace determination of silver, gold and iron oxide nanoparticles by micelle mediated preconcentration / selective back-extraction coupled with flow injection chemiluminescence detection, Anal. Chem., 86 (2014) 3484-3492.

[153] R. Lageman, W. Pool, G.A. Seffinga, Electro-Reclamation, Chem.Ind., 18 (1989) 585-590.

[154] S. Pamukcu, J.K. Wittle, Electrokinetic removal of selected heavy metals from soil, Environ. Prog., 11 (1992) 241-250.

[155] Y.B. Acar, A.N. Alshawabkeh, Principles of Electrokinetic Remediation, Environ. Sci. Technol., 27 (1993) 2638-2647.

[156] R.F. Probstein, R.E. Hicks., Removal of contaminants from soil by electric fields, Science, 260 (1993) 498–530.

[157] L.M. Ottosen, H.K. Hansen, S. Laursen, A. Villumsen, Electrodialytic remediation of soil polluted with copper from wood preservation Industry, Environ. Sci. Technol., 31 (1997) 1711-1715.

[158] T. R. Sun, Effect of pulse current on energy consumption and removal of heavy metals during electrodialytic soil remediation, Ph.D Thesis, Technical University of Denmark, 2013.

[159] M.M. Page, C.L. Page, Electroremediation of contaminated soils, J. Environ. Eng., 128 (2002) 208-219.

[160] L.M. Ottosen, H.K. Hansen, S. Laursen, A. Villumsen, Electrodialytic remediation of soil polluted with copper from wood preservation industry, Environ. Sci. Technol., 31 (1997) 1711-1715.

[161] P.E. Jensen, L.M. Ottosen, C. Ferreira, Electrodialytic remediation of soil fines (<63 μm) in suspension—Influence of current strength and L/S, Electrochim. Acta, 52 (2007) 3412-3419.

[162] L.M. Ottosen, P.E. Jensen, H.K. Hansen, A. Ribeiro, B. Allard, Electrodialytic remediation of soil slurry–Removal of Cu, Cr, and As, Sep. Sci. Technol., 44 (2009) 2245-2268.

[163] L. Ottosen, P. Jensen, G. Kirkelund, H. Hansen, Electrodialytic remediation of different heavy metal-polluted soils in suspension, Water Air Soil Poll., 224 (2013) 1-10.

[164] A.B. Ribeiro, E.P. Mateus, L.M. Ottosen, G. Bech-Nielsen, Electrodialytic removal of Cu, Cr and As from chromated copper arsenate-treated timber waste, Environ. Sci. Technol., 34 (2000) 784-788.

[165] H.K. Hansen, A. Rojo, L.M. Ottosen, Electrodialytic remediation of copper mine tailings, J. Hazard. Mater., 117 (2005) 179-183.

[166] L.M. Ottosen, A.T. Lima, A.J. Pedersen, A.B. Ribeiro, Electrodialytic extraction of Cu, Pb and Cl from municipal solid waste incineration fly ash suspended in water, J. Chem. Technol. Biotechnol., 81 (2006) 553-559.

[167] L.M. Ottosen, A.J. Pedersen, H.K. Hansen, A.B. Ribeiro, Screening the possibility for removing cadmium and other heavy metals from wastewater sludge and bio-ashes by an electrodialytic method, Electrochim. Acta, 52 (2007) 3420-3426.

[168] G.M. Kirkelund, L.M. Ottosen, A. Villumsen, Electrodialytic remediation of harbour sediment in suspension—Evaluation of effects induced by changes in stirring velocity and current density on heavy metal removal and pH, J. Hazard. Mater., 169 (2009) 685-690.

[169] P.E. Jensen, C.M.D. Ferreira, H.K. Hansen, J.U. Rype, L.M. Ottosen, A. Villumsen, Electroremediation of air pollution control residues in a continuous reactor, J. App. Electrochem., 40 (2010) 1173–1181

[170] M. Pazos, G.M. Kirkelund, L.M. Ottosen, Electrodialytic treatment for metal removal from sewage sludge ash from fluidized bed combustion, J. Hazard. Mater., 176 (2010) 1073-1078.

[171] L.M. Ottosen, P.E. Jensen, G.M. Kirkelund, B. Ebbers, Electrodialytic separation of heavy metals from particulate material. Patent application EPC 13183278.4-1352, 2013.

[172] J. Virkutyte, M. Sillanpaa, P. Latostenmaa, Electrokinetic soil remediation - Critical overview, Sci. Total Environ., 289 (2002) 97-121.

[173] H.H. Lee, J.W. Yang, A new method to control electrolytes pH by circulation system in electrokinetic soil remediation, J. Hazard. Mater., 77 (2000) 227-240.

[174] R.E. Saichek, K.R. Reddy, Effect of pH control at the anode for the electrokinetic removal of phenanthrene from kaolin soil, Chemosphere, 21 (2003) 273-287.

[175] L.M. Ottosen, A.J. Pedersen, A.B. Ribeiro, H.K. Hansen, Case study on the strategy and application of enhancement solutions to improve remediation of soils contaminated with Cu, Pb and Zn by means of electrodialysis, Eng. Geol., 77 (2005) 317-329.

[176] G.M. Nystroem, A.J. Pedersen, L.M. Ottosen, A. Villumsen, The use of desorbing agents in electrodialytic remediation of harbour sediment, Sci. Total Environ., 357 (2006) 25-37.

[177] R.E. Saichek, K.R. Reddy, Effects of system variables on surfactant enhanced electrokinetic removal of polycyclic aromatic hydrocarbons from clayey soils, Environ. Technol., 24 (2003) 503-515.

[178] H.K. Hansen, A. Rojo, Testing pulsed electric fields in electroremediation of copper mine tailings, Electrochim. Acta, 52 (2007) 3399-3405.

[179] T.R. Sun, L.M. Ottosen, Effects of pulse current on energy consumption and removal of heavy metals during electrodialytic soil remediation, Electrochim. Acta, 86 (2012) 28-35.

[180] A. Rojo, H.K. Hansen, M. Cubillos, Electrokinetic remediation using pulsed sinusoidal electric field, Electrochim. Acta, 86 (2012) 124-129.

[181] R. Lageman, R.L. Clarke, W. Pool, Electro-reclamation, a versatile soil remediation solution, Eng. Geol., 77 (2005) 191-201.

[182] L.M. Ottosen, I.V. Christensen, I. Rörig-Dalgård, P.E. Jensen, H.K. Hansen, Utilization of electromigration in civil and environmental engineering—Processes, transport rates and matrix changes, J. Environ. Sci. Health A, 43 (2008) 795-809.

[183] A.T. Yeung, Milestone developments, myths, and future directions of electrokinetic remediation, Sep. Purif. Technol., 79 (2011) 124–132.

[184] A.N. Alshawabkeh, Electrokinetic soil remediation: Challenges and opportunities, Sep. Sci. Technol., 44 (2009) 2171–2187.

[185] W.S. Kim, G.Y. Park, D.H. Kim, H.B. Jung, S.H. Ko, K. Baek, *In situ* field scale electrokinetic remediation of multi-metals contaminated paddy soil: Influence of electrode configuration, Electrochim. Acta, 86 (2012) 89-95.

[186] H.I. Gomes, C. Dias-Ferreira, A.B. Ribeiro, Electrokinetic remediation of organochlorines in soil: Enhancement techniques and integration with other remediation technologies, Chemosphere, 87 (2012) 1077-1090.

[187] I. Istrate, D. Cocarta, S. Neamtu, T. Cirlioru, The treatment of PCB polluted soil - The approach based on the application of electrochemical treatment, Water Air Soil Poll., 224 (2013) 1-14.

[188] P.S.C. Rao, J.W. Jawitz, C.G. Enfield, R.W. Falta, M.D. Annable, A.L. Wood, Technology integration for contaminated site remediation: Clean-up goals and performance criteria, Groundwater Quality: Natural and Enhanced Restoration of Groundwater Pollutions 2001 Proceedings, Sheffield, UK, 2001, pp. 571-578.

[189] K.R. Reddy, C. Cameselle, P. Ala, Integrated electrokinetic-soil flushing to remove mixed organic and metal contaminants, J. App. Electrochem., 40 (2010) 1269–1279.

[190] X. Mao, J. Wang, A. Ciblak, E.E. Cox, C. Riis, M. Terkelsen, D.B. Gent, A.N. Alshawabkeh, Electrokinetic-enhanced bioaugmentation for remediation of chlorinated solvents contaminated clay, J. Hazard. Mater., 213-214 (2012) 311-317.

[191] J. Huang, W. Liao, S. Lai, R. Yang, Use of hydraulic pressure–improved electrokinetic technique to enhance the efficiencies of the remediation of PCP-contaminated soil, J. Environ. Eng., 139 (2013) 1213-1221.

[192] A. Oonnittan, R.A. Shrestha, M. Sillanpää, Removal of hexachlorobenzene from soil by electrokinetically enhanced chemical oxidation, J. Hazard. Mater., 162 (2009) 989-993.

[193] A. Oonnittan, R.A. Shrestha, M. Sillanpää, Effect of cyclodextrin on the remediation of hexachlorobenzene in soil by electrokinetic Fenton process, Sep. Purif. Technol., 64 (2009) 314-320.

[194] A. Oonnittan, P. Isosaari, M. Sillanpää, Oxidant availability in soil and its effect on HCB removal during electrokinetic Fenton process, Sep. Purif. Technol., 76 (2010) 146-150.

[195] A. Oonnittan, P. Isosaari, M. Sillanpää, Effect of polarity reversal on hexachlorobenzene removal during electrokinetic Fenton process, J. Environ. Eng., 139 (2013) 1228-1232.

[196] P.J. Dugan, R.L. Siegrist, M.L. Crimi, Coupling surfactants/cosolvents with oxidants for enhanced DNAPL removal: A review, Remediation, 20 (2010) 27-49.

[197] S. Pamukcu, L. Hannum, J.K. Wittle, Delivery and activation of nano-iron by DC electric field, J. Environ. Sci. Health A, 43 (2008) 934-944.

[198] G.C.C. Yang, C.H. Hung, H.C. Tu, Electrokinetically enhanced removal and degradation of nitrate in the subsurface using nanosized Pd/Fe slurry, J. Environ. Sci. Health A, 43 (2008) 945-951.

[199] K.R. Reddy, M.R. Karri, Electrokinetic delivery of nanoiron amended with surfactant and cosolvent in contaminated soil, Proceedings of the International Conference on Waste 8 Engineering and Management, May 2008, Hong Kong, 2008.

[200] S.S. Chen, Y.C. Huang, T.Y. Kuo, The remediation of perchloroethylene contaminated groundwater by nanoscale iron reactive barrier integrated with surfactant and electrokinetics, Ground Water Monit. R., 30 (2010) 90–98.

[201] E.H. Jones, D.A. Reynolds, A.L. Wood, D.G. Thomas, Use of electrophoresis for transporting nano-iron in porous media, Ground Water, 49 (2010) 172-183.

[202] G.C.C. Yang, Y.I. Chang, Integration of emulsified nanoiron injection with the electrokinetic process for remediation of trichloroethylene in saturated soil, Sep. Purif. Technol., 79 (2011) 278–284.

[203] A.I.A. Chowdhury, D.M. O'Carroll, Y. Xu, B.E. Sleep, Electrophoresis enhanced transport of nano-scale zero valent iron, Adv. Water Resour., 40 (2012) 71-82.

[204] S. Yuan, H. Long, W. Xie, P. Liao, M. Tong, Electrokinetic transport of CMC-stabilized Pd/Fe nanoparticles for the remediation of PCP-contaminated soil, Geoderma, 185-186 (2012) 18-25.

[205] G. Fan, L. Cang, W. Qin, C. Zhou, H.I. Gomes, D. Zhou, Surfactants-enhanced electrokinetic transport of xanthan gum stabilized nano Pd/Fe for the remediation of PCBs contaminated soils, Sep. Purif. Technol., 114 (2013) 64-72.

[206] E. Rosales, J.P.G. Loch, C. Dias-Ferreira, Electro-osmotic transport of nano zero-valent iron in Boom Clay, Electrochim. Acta, 127 (2014) 27-33.

[207] A.T. Lima, L.M. Ottosen, K. Heister, J.P.G. Loch, Assessing PAH removal from clayey soil by means of electro-osmosis and electrodialysis, Sci. Total Environ., 435–436 (2012) 1-6.

[208] S. Pamukcu, A. Weeks, J.K. Wittle, Enhanced reduction of Cr(VI) by direct electric current in a contaminted clay, Environ. Sci. Technol., 38 (2004) 1236-1241.

[209] A.B. Ribeiro, E.P. Mateus, J.M. Rodríguez-Maroto, Removal of organic contaminants from soils by an electrokinetic process: The case of molinate and bentazone. Experimental and modeling, Sep. Purif. Technol., 79 (2011) 193-203.

[210] Y.T. Wei, S.C. Wu, C.M. Chou, C.H. Che, S.M. Tsai, H.L. Lien, Influence of nanoscale zero-valent iron on geochemical properties of groundwater and vinyl chloride degradation: A field case study, Water Res., 44 (2010) 131-140.

[211] J.B. Michael, V. Ramesh, G. Florin, Status of nZVI technology: Lessons learned from North American and international implementations, C. Geiger, K. Carvalho-Knighton (Eds.) Environmental Applications of Nanoscale and Microscale Reactive Metal Particles, American Chemical Society Symposium Series, 2009, pp. 219-232.

[212] S. O'Hara, T. Krug, J. Quinn, C. Clausen, C. Geiger, Field and laboratory evaluation of the treatment of DNAPL source zones using emulsified zero-valent iron, Remediation, 16 (2006) 35-56.

[213] Z. Shi, J.T. Nurmi, P.G. Tratnyek, Effects of nano zero-valent iron on oxidation-reduction potential, Environ. Sci. Technol., 45 (2011) 1586-1592.

[214] K.R. Reddy, K. Darko-Kagy, C. Cameselle, Electrokinetic-enhanced transport of lactate-modified nanoscale iron particles for degradation of dinitrotoluene in clayey soils, Sep. Purif. Technol., 79 (2011) 230-237.

[215] H.J. Kim, T. Phenrat, R.D. Tilton, G.V. Lowry, Effect of kaolinite, silica fines and pH on transport of polymer-modified zero valent iron nano-particles in heterogeneous porous media, J. Colloid Interface Sci., 370 (2012) 1-10.

[216] J. Busch, T. Meißner, A. Potthoff, S.E. Oswald, Transport of carbon colloid supported nanoscale zero-valent iron in saturated porous media, J. Contam. Hydrol., 164 (2014) 25-34.

[217] C. Su, R.W. Puls, T.A. Krug, M.T. Watling, S.K. O'Hara, J.W. Quinn, N.E. Ruiz, Travel distance and transformation of injected emulsified zerovalent iron nanoparticles in the subsurface during two and half years, Water Res., 47 (2013) 4095-4106.

[218] H.I. Gomes, C. Dias-Ferreira, A.B. Ribeiro, S. Pamukcu, Enhanced transport and transformation of zerovalent nanoiron in clay using direct electric current, Water Air Soil Poll., 224 (2013) 1-12.

[219] D.G. Kim, Y.H. Hwang, H.S. Shin, S.O. Ko, Deactivation of nanoscale zero-valent iron by humic acid and by retention in water, Environ. Technol., 34 (2013) 1-11.

[220] C.M. Kocur, D.M. O'Carroll, B.E. Sleep, Impact of nZVI stability on mobility in porous media, J. Contam. Hydrol., 145 (2013) 17-25.

[221] C.A. Alister, M.A. Araya, M. Kogan, Adsorption and desorption variability of four herbicides used in paddy rice production, J. Environ. Sci. Health B, 46 (2010) 62-68.

[222] J.C.S. Santos, Electrokinetic remediation of rice field soils contaminated by molinate, Master degree in Environmental Engineering, Faculdade de Ciências e Tecnologia, Universidade Nova de Lisboa, 2008, 97 pp.

[223] S. Laumann, V. Micić, G.V. Lowry, T. Hofmann, Carbonate minerals in porous media decrease mobility of polyacrylic acid modified zero-valent iron nanoparticles used for groundwater remediation, Environ. Poll., 179 (2013) 53-60.

[224] Y. Chang, G. Achari, C. Langford, Effect of cocontaminants on the remediation of PCB-impacted soils by hydrogen peroxide, Pract. Period. Hazard. Toxic Radioact. Waste Manag., 14 (2010) 266-268.

[225] B.Z. Wu, H.Y. Chen, S.J. Wang, C.M. Wai, W. Liao, K. Chiu, Reductive dechlorination for remediation of polychlorinated biphenyls, Chemosphere, 88 (2012) 757-768.

[226] G.K. Vasilyeva, E.R. Strijakova, S.N. Nikolaeva, A.T. Lebedev, P.J. Shea, Dynamics of PCB removal and detoxification in historically contaminated soils amended with activated carbon, Environ. Poll., 158 (2010) 770–777.

[227] B. Beckingham, U. Ghosh, Field-scale reduction of PCB bioavailability with activated carbon amendment to river sediments, Environ. Sci. Technol., 45 (2011) 10567-10574.

[228] H.I. Gomes, C. Dias-Ferreira, A.B. Ribeiro, S. Pamukcu, Influence of electrolyte and voltage on the direct current enhanced transport of iron nanoparticles in clay, Chemosphere, 99 (2014) 171-179.

[229] Y. Wang, D. Zhou, Y. Wang, L. Wang, L. Cang, Automatic pH control system enhances the dechlorination of 2,4,4′-trichlorobiphenyl and extracted PCBs from contaminated soil by nanoscale $Fe^0$ and $Pd/Fe^0$, Environ. Sci. Poll. Res., 19 (2012) 448-457.

[230] Q. Zhou, H. Lin, Influence of surfactants on degradation of 1-(2-chlorobenzoyl)-3-(4-chlorophenyl) urea by nanoscale zerovalent iron, CLEAN, 41 (2013) 128-133.

[231] E.J. Weber, Iron-mediated reductive transformations: Investigation of reaction mechanism, Environ. Sci. Technol., 30 (1996) 716-719.

[232] F. He, D. Zhao, Hydrodechlorination of trichloroethene using stabilized Fe-Pd nanoparticles: Reaction mechanism and effects of stabilizers, catalysts and reaction conditions, App. Catal. B, 84 (2008) 533-540.

[233] N.E. Korte, O.R. West, L. Liang, B. Gu, J.L. Zutman, Q. Fernando, The effect of solvent concentration on the use of palladized-iron for the step-wise dechlorination of polychlorinated biphenyls in soil extracts, Waste Manag., 22 (2002) 343-349.

[234] M.D. Erickson, Analytical Chemistry of PCBs, CRC Press, Boca Raton, Florida, 1997, 688 pp.

[235] T.R. Sun, L.M. Ottosen, P.E. Jensen, G.M. Kirkelund, Electrodialytic remediation of suspended soil – Comparison of two different soil fractions, J. Hazard. Mater., 203–204 (2012) 229-235.

[236] B. Yang, G. Yu, J. Huang, Electrocatalytic hydrodechlorination of 2,4,5-trichlorobiphenyl on a palladium-modified nickel foam cathode, Environ. Sci. Technol., 41 (2007) 7503-7508.

[237] B. Yang, G. Yu, D. Shuai, Electrocatalytic hydrodechlorination of 4-chlorobiphenyl in aqueous solution using palladized nickel foam cathode, Chemosphere, 67 (2007) 1361-1367.

[238] W. Zhou, J. Yang, L. Lou, L. Zhu, Solubilization properties of polycyclic aromatic hydrocarbons by saponin, a plant-derived biosurfactant, Environ. Poll., 159 (2011) 1198-1204.

[239] O. Iglesias, M.A. Sanromán, M. Pazos, Surfactant-enhanced solubilization and simultaneous degradation of phenanthrene in marine sediment by electro-Fenton treatment, Ind. Eng. Chem. Res., 53 (2014) 2917-2923.

[240] S.F. Jensen, PCB in Soil. The Contamination of PCB in Selected Locations around Roskilde and Copenhagen, The International Basic Studies in Natural Science, Roskilde University, Denmark, 2009, 29 pp.

[241] H.I. Gomes, G. Fan, E.P. Mateus, C. Dias-Ferreira, A.B. Ribeiro, Assessment of combined electro-nanoremediation of molinate contaminated soil, Sci. Total Environ., 493 (2014) 178-184.

[242] J.M. Paz-García, B. Johannesson, L.M. Ottosen, A.B. Ribeiro, J.M. Rodríguez-Maroto, Computing multi-species chemical equilibrium with an algorithm based on the reaction extents, Comp, Chem. Eng., 58 (2013) 135-143.

[243] M. Farré, J. Sanchís, D. Barceló, Analysis and assessment of the occurrence, the fate and the behavior of nanomaterials in the environment, TrAC Trends Anal. Chem., 30 (2011) 517-527.

[244] B.F. Silva, S. Pérez, P. Gardinalli, R.K. Singhal, A.A. Mozeto, D. Barceló, Analytical chemistry of metallic nanoparticles in natural environments, TrAC Trends Anal. Chem., 30 (2011) 528-540.

[245] L.G. Cullen, E.L. Tilston, G.R. Mitchell, C.D. Collins, L.J. Shaw, Assessing the impact of nano- and micro-scale zerovalent iron particles on soil microbial activities: Particle reactivity interferes with assay conditions and interpretation of genuine microbial effects, Chemosphere, 82 (2011) 1675-1682.

[246] I. Jośko, P. Oleszczuk, Manufactured nanomaterials: The connection between environmental fate and toxicity, Crit. Review. Environ. Sci. Technol., 43 (2013) 2581-2616.

[247] D. Hou, A. Al-Tabbaa, Sustainability: A new imperative in contaminated land remediation, Environ. Sci. Policy, 39 (2014) 25-34.

[248] J.N. Smith, G. Kerrison, Benchmarking of decision-support tools used for tiered sustainable remediation appraisal, Water Air Soil Poll., 224 (2013) 1-11.

# Part II

## II.1. Overview of *in situ* and *ex situ* remediation technologies for PCB-contaminated soils and sediments and obstacles for full-scale application (published in Science of the Total Environment)

Science of the Total Environment 445–446 (2013) 237–260

Contents lists available at SciVerse ScienceDirect

Science of the Total Environment

journal homepage: www.elsevier.com/locate/scitotenv

Review

# Overview of in situ and ex situ remediation technologies for PCB-contaminated soils and sediments and obstacles for full-scale application

Helena I. Gomes [a,b,*], Celia Dias-Ferreira [b], Alexandra B. Ribeiro [a]

[a] CENSE — Center for Environmental and Sustainability Research, Departamento de Ciências e Engenharia do Ambiente, Faculdade de Ciências e Tecnologia, Universidade Nova de Lisboa, 2829-516 Caparica, Portugal
[b] CERNAS — Research Center for Natural Resources, Environment and Society, Campus da Escola Superior Agrária de Coimbra, Bencanta, 3040-316 Coimbra, Portugal

## HIGHLIGHTS

- Remediation technologies for PCB in contaminated soils and sediments
- Review of in situ and ex situ remediation technologies
- Historical overview of full-scale applications for PCB contaminated sites
- Assessment of full-scale applications of emerging technologies

## ARTICLE INFO

*Article history:*
Received 3 October 2012
Received in revised form 28 November 2012
Accepted 28 November 2012
Available online xxxx

*Keywords:*
Polychlorinated biphenyls (PCB)
Remediation technologies
In situ
Ex situ
Contaminated soils and sediments

## ABSTRACT

Polychlorinated biphenyls (PCB) are persistent organic pollutants used worldwide between the 1930s and 1980s. Although their use has been heavily restricted, PCB can be found in contaminated soils and sediments. The most frequent remediation solutions adopted are “dig and dump” and “dig and incinerate”, but there are currently new methods that could be more sustainable alternatives. This paper takes a look into the remediation options available for PCB-contaminated soils and sediments, differentiating between biological, chemical, physical and thermal methods. The use of combined technologies was also reviewed. Most of them are still in an initial development stage and further research in different implementation issues is needed. There is no single technology that is the solution for PCB contamination problem. The successful remediation of a site will depend on proper selection, design and adjustment of the technology or combined technologies to the site characteristics.



**Contents**



* Corresponding author at: CENSE — Center for Environmental and Sustainability Research, Departamento de Ciências e Engenharia do Ambiente, Faculdade de Ciências e Tecnologia, Universidade Nova de Lisboa, 2829-516 Caparica, Portugal. Tel.: +351 212948300; fax: +351 212948554.
*E-mail address:* hrg@campus.fct.unl.pt (H.I. Gomes).

0048-9697/$ – see front matter © 2012 Elsevier B.V. All rights reserved.
http://dx.doi.org/10.1016/j.scitotenv.2012.11.098

## 1. Introduction

Polychlorinated biphenyls (PCB) are a group of anthropogenic chemicals, classified as persistent organic pollutants (POP) by the Stockholm Convention (adopted in 2001). PCB were commercially produced worldwide on a large scale between the 1930s and 1980s. In the late 1960s, some dimension poisonings occurred. In one industrial incident over 14,000 persons became ill in Yusho, Japan, from ingesting PCB-contaminated rice oil and, even today, there are still effects in those populations (Masuda et al., 1998; Todaka et al., 2007). In the 1970s, several countries limited PCB use due to severe concerns on their human toxicity. It was only in 1985 that the European Community heavily restricted the use and marketing of PCB.

The disposal of these xenobiotics is a global problem (Haluska et al., 1995). The uptake of PCB-contaminated sediments by biota at the water-sediment interface can introduce PCB into the food chain (Grittini et al., 1995). PCB move according to the "grasshopper effect", volatilizing from soil to air in warm weather and falling to earth miles away as temperatures cool (Schmidt, 2010). They have been detected in virtually all environmental media (indoor and outdoor air, surface and groundwater, sediments, soil and food) and also in living organisms and in human milk and blood (Donaldson et al., 2010; Hopf et al., 2009; Mikszewski, 2004; Xing et al., 2009).

The extent of PCB contamination worldwide is unknown. In the United States, 350 of the 1290 Superfund Sites are contaminated with PCB (USEPA, 2011a), whereas in Canada there are 148 sites according to the Federal Contaminated Sites Inventory (TBS-SCT, 2011). In European countries, an estimate points towards 242,000 contaminated sites of which 2.4% are contaminated with chlorinated hydrocarbons (EEA, 2007). An inventory on atmospheric deposition in background surface soil, estimates a global soil total PCB burden of 21,000 t (Meijer et al., 2003). In many countries (e.g. UK, Australia, USA), the threshold concentration for contaminated soil varies between 10 and 50 mg $kg^{-1}$, but in some cases it can be as low as 0.5 mg $kg^{-1}$ (CCME, 1999; EPA, 2009; UKEPA, 2004; USEPA, 2012a).

Cleanup of soils contaminated by PCB has been a challenging task for decades. The most frequent soil remediation technologies used are "dig and dump" and also "dig and incinerate". In sediments, dredging followed by dewatering, treatment and/or landfilling are mainly used, but these solutions are disruptive and unsustainable (Agarwal et al., 2007). Cost effective and more sustainable alternatives are needed to safely remove PCB from the environment.

Several reviews were published on the remediation technologies for PCB, such as aerobic and anaerobic biodegradation (Abramowicz, 1995; Tiedje et al., 1993), phytoremediation (Mackova et al., 2006; Van Aken et al., 2010) and thermal, oxidative and reductive methods (Alonso et al., 2002; Gorbunova et al., 2010; Rahuman et al., 2000; Wu et al., 2012; Zanaveskin and Aver'yanov, 1998). These reviews are focused only on a limited number of techniques, and sometimes apply to the destruction of PCB in their pure form, in oils and in different solutions. The current work comprises a comprehensive, up-to-date and integrated review of remediation technologies for in situ and ex situ remediation of PCB-contaminated soils and sediments, including the most recent techniques not yet appearing in other sectorial reviews. It also includes a review on full-scale applications of remediation technologies in PCB contaminated soil and sediments. The main emergent remediation technologies are described and their current status is evaluated, assessing the main factors related with their full-scale application.

## 2. Full-scale applications of PCB remediation technologies in soil and sediments

Table 1 shows full-scale applications of remediation technologies used in historical sites contaminated with PCB for which information is available. A summary is presented mentioning site, media, date, total volume and associated costs, when available. Most of the sites are related with massive industrial contamination, due to decades of activity, discharge of effluents, waste disposal or accidental spills. Some of the remedial processes in important rivers in the USA (Hudson River, Housatonic River, New Bedford Harbor, etc.) are still ongoing, involving enormous costs.

The most common solutions to PCB contaminated soils and sediments are removal for incineration or disposal in an offsite landfill. In the USA, due to regulatory demands (40 CFR 761), incineration is one of the most used remediation technologies since it is mandatory for materials containing over 500 ppm PCB. These solutions are unsustainable and considerable research was made to find new remediation technologies that could be used for these persistent organic pollutants, as presented in the next section. However very limited experience at pilot and field scale application is available.

## 3. Emerging technologies for PCB remediation

In this section, some of the latest developments in technologies for remediation of PCB contaminated soils and sediments are presented, classified by in situ and ex situ methods, differencing biological, physical, chemical and thermal methods, and also natural attenuation and combined technologies. A classification for the technologies described is proposed in Fig. 1.

### 3.1. In situ technologies

#### 3.1.1. Biological treatment

*3.1.1.1. Bioremediation.* Microbial degradation of PCB is known to occur via two main routes: anaerobic and aerobic. Highly chlorinated PCB congeners can be dechlorinated under anaerobic conditions to form lower chlorinated congeners, which are more susceptible to aerobic degradation (Abramowicz, 1995; Furukawa and Fujihara, 2008; Wright et al., 1996), also known as the biphenyl degradation pathway (Magee et al., 2008). This involves $O_2$ insertion at adjacent unsubstituted carbons in the less chlorinated ring of the structure, followed by ring cleavage to form a chlorinated benzoate (Wright et al., 1996).

*3.1.1.1.1. Anaerobic dechlorination.* Anaerobic biodegradation of PCB contaminated sediments (freshwater — pond, lake and river; estuarine and marine) has been studied by several research teams and involves PCB reduction and replacement of chlorine by hydrogen (Alder et al., 1993; Brown et al., 1987; Chen et al., 2001; Natarajan et al., 1997; Quensen et al., 1988, 1990; Ye et al., 1992, 1995; Wu et al., 1998). Bedard and Quensen (1995) postulated that there are at least six separable pathways to dechlorinate PCB: M, Q, H, H′, N and P. Later Wiegel and Wu (2000) identified two more, LP and T (Fig. 2).

**Table 1**
Summary of full-scale applications for remediation of PCB contaminated soils and sediments.

| Site | Medium | Total volume | Technology | Date | Cost | References |
|---|---|---|---|---|---|---|
| Shiawassee River, MI, USA | Soils and sediments | 1341 $m^3$ (soils) 1216 $m^3$ (sediments) | Excavation, dredging and landfilling | 1981–1982, 2004–2005 | 13,558,000 USD | USEPA, 2009; Zarull et al. (1999) |
| LaSalle Electrical Utilities, IL, USA | Soils | 17,782 $m^3$ 51,225 $m^3$ | Excavation and incineration | 1983–1985 1994 | NA | USEPA (2012b) |
| Re-Solve, Inc., MA, USA | Soils | 12,233 $m^3$ 2294 $m^3$ | Excavation and landfilling Excavation and chemical oxidation on site | 1985–1986 1992–1994 | NA | USEPA (2012b) |
| Douglassville Disposal, PA, USA | Soils | NA | Excavation and incineration | 1989 | 13,400,000 USD | USEPA (2012b) |
| New Bedford Harbor, MA, USA | Sediments | 152,911 $m^3$ | Dredging and landfilling Dredging and landfilling, pilot cap | 1994–1995, 2004–2005 ongoing | NA | USEPA (2012b) |
| Florida Steel Corporation, FL, USA | Soil | 28,747 $m^3$ | Excavation, incineration and landfilling | 1987–1988 1995–1996 | NA | Dávila et al. (1993) USEPA (2012b) |
| General Electric Co. (Spokane Shop) WA, USA | Soil | NA | In situ vitrification and asphalt cap | 1991–1999 | NA | GE (2008) |
| Rose Township Dump Superfund Site Holly, MI, USA | Soil | 34,000 t | Excavation and incineration | 1992–1993 | 12,000,000 USD | USEPA (2012b) |
| Hamilton Harbor, Canada | Sediment | 10,000 $m^3$ | Capping | 1992–1995 | 650,000 USD | Zarull et al. (1999) |
| Maumee River, OH, USA | Sediment | 6100 $m^3$ | Dredging and landfilling | 1994–1998 | 5,000,000 USD | Zarull et al. (1999) |
| Manistique River, MI, USA | Sediment | 44,100 $m^3$ | Dredging and landfilling | 1994–2000 | 50,000,000 USD | TEI (2002) |
| Communications manufacturing facility in South West England, UK | Soil | 1200 $m^3$ | Thermal desorption | 1996 | NA | Norris et al. (1999) |
| River Raisin, MI, USA | Sediment | 20,000 $m^3$ | Dredging and landfilling | 1997 | 6,000,000 USD | Zarull et al. (1999) |
| Military radar station, Canadian Arctic | Soil | 20,000 $m^3$ | Excavation, incineration (>50 ppm) and landfilling (<50 ppm) | 1999–2006 | 64,750,000 USD | Kalinovich et al. (2008) |
| Illegal dumping of PCB capacitors in Kobe, Japan | Soil | 68 $m^3$ | Solvent extraction | 2002–2003 | NA | Takigami et al. (2008) |
| North Adams, MA, USA | Soil | 7646 $m^3$ | Excavation and landfilling | na | 850,000 USD | Abscope Environmental (2012) |
| Industrial area, Aviles, Asturias, Spain | Soil | 10,000 $m^3$ | Thermal desorption | 2003 | NA | TPSTEC (2012) |
| GE-Pittsfield/Housatonic River Site, MA, USA | Soils and sediments | 183,875 $m^3$ | Excavation, dredging and landfilling | 2000–2015 | NA | USEPA (2012) |
| Hudson River PCB Superfund Site, NY, USA | Sediments | 2,000,000 $m^3$ | Dredging and landfilling | 2009–2012 | 500,000,000 USD | USEPA (2012b) |

NA — not available.

Microbiologically mediated dechlorination of PCB typically removes *meta* and/or *para* chlorines to generate primarily *ortho*-substituted mono- through tetrachlorobiphenyls (Wiegel and Wu, 2000). The most extensive dechlorination occurs when process M works in combination with process Q. This activity, known as C dechlorination, attacks *meta* and *para* chlorines, resulting in exclusively *ortho* substituted congeners (Zwiernik et al., 1998), non-dioxin-like and that do not readily bioaccumulate.

The first experimental demonstration of a biologically mediated *ortho*-dechlorination of PCB was done with microorganisms eluted from sediments contaminated with hydrocarbon oil and Aroclor from Woods Pond, Massachusetts (Van Dort et al., 1997). Sustained PCB *ortho* dechlorination by bacterial enrichment cultures in the absence of soil or sediments was also demonstrated (Cutter et al., 1998). Rodenburg et al. (2010) showed that anaerobic bacteria in sewers, landfills and contaminated groundwater also dechlorinate PCB — the first convincing evidence occurring outside aquatic sediments. Recently, Fogel et al. (2012) refer that a sediment-free PCB-degrading culture was developed. It contains a strain of *Dehalococcoides* and can grow rapidly in groundwater and artificial media if fed with trichlorobenzene, retaining the ability to degrade PCB (Fogel et al., 2012). This can be an important step in developing PCB bioremediation technologies.

Table 2 summarizes the experiments and the main findings in the literature regarding anaerobic dechlorination and the pathways involved. It also lists experimental conditions, congeners targeted, amount and type of substrate, temperature, pH, incubation time and amendments.

In short, five major factors determine the extent and route of PCB dechlorination: (i) the microbial populations present, (ii) the position (*ortho*, *meta*, or *para*) of the chlorine relative to the opposite phenyl ring, (iii) the surrounding chlorine configuration, (iv) the chlorine configuration on the opposite ring, and (v) the incubation condition (Furukawa and Fujihara, 2008; Wiegel and Wu, 2000). The first of those factors is influenced by environmental conditions such as availability of carbon sources, hydrogen or other electron donors, the presence or absence of electron acceptors other than PCB, temperature and pH (Borja et al., 2005; Wiegel and Wu, 2000).

Although most of the researchers isolated cultures from contaminated sediments (river or estuarine), they have used spiked substrates, which represent more controlled conditions. However, successful results obtained with spiked matrices cannot always be transferred directly to contaminated soils and sediments, both at bench or full-scale, due to the sorption of PCB. The low biodegradability of PCB is due to slow rates of desorption from organic matter in soil and sediments. Both bioavailability and bioactivity limit the rate and extent of PCB degradation and these decrease with increasing chlorination degree (Liu et al., 2007a). However this reduced bioavailability can also be used for remediation purposes, since immobilization of these compounds reduces the potential environmental harm, favoring solutions like monitored natural attenuation.

*3.1.1.1.2. Aerobic biodegradation.* The lightly chlorinated PCB congeners resulting from the dechlorination of higher chlorinated ones can be substrates for aerobic bacteria. Oxidative degradation of PCB consists in the breakdown to chlorobenzoic acid and its further degradation (Borja et al., 2005). PCB can be aerobically degraded also by cometabolism, either by bacteria or by whiterot fungi (e.g. *Phanerochaete chrysosporium*). Earthworms were also used to enhance the dispersal of the bioaugmented PCB-degrading microorganisms (Singer et al., 2001).

Vasilyeva et al. (2010) treated a histosol and an alluvial soil historically contaminated with PCB (4190 and 1585 mg $kg^{-1}$, respectively; primarily tri-, tetra- and pentachlorinated congeners) through bioremediation

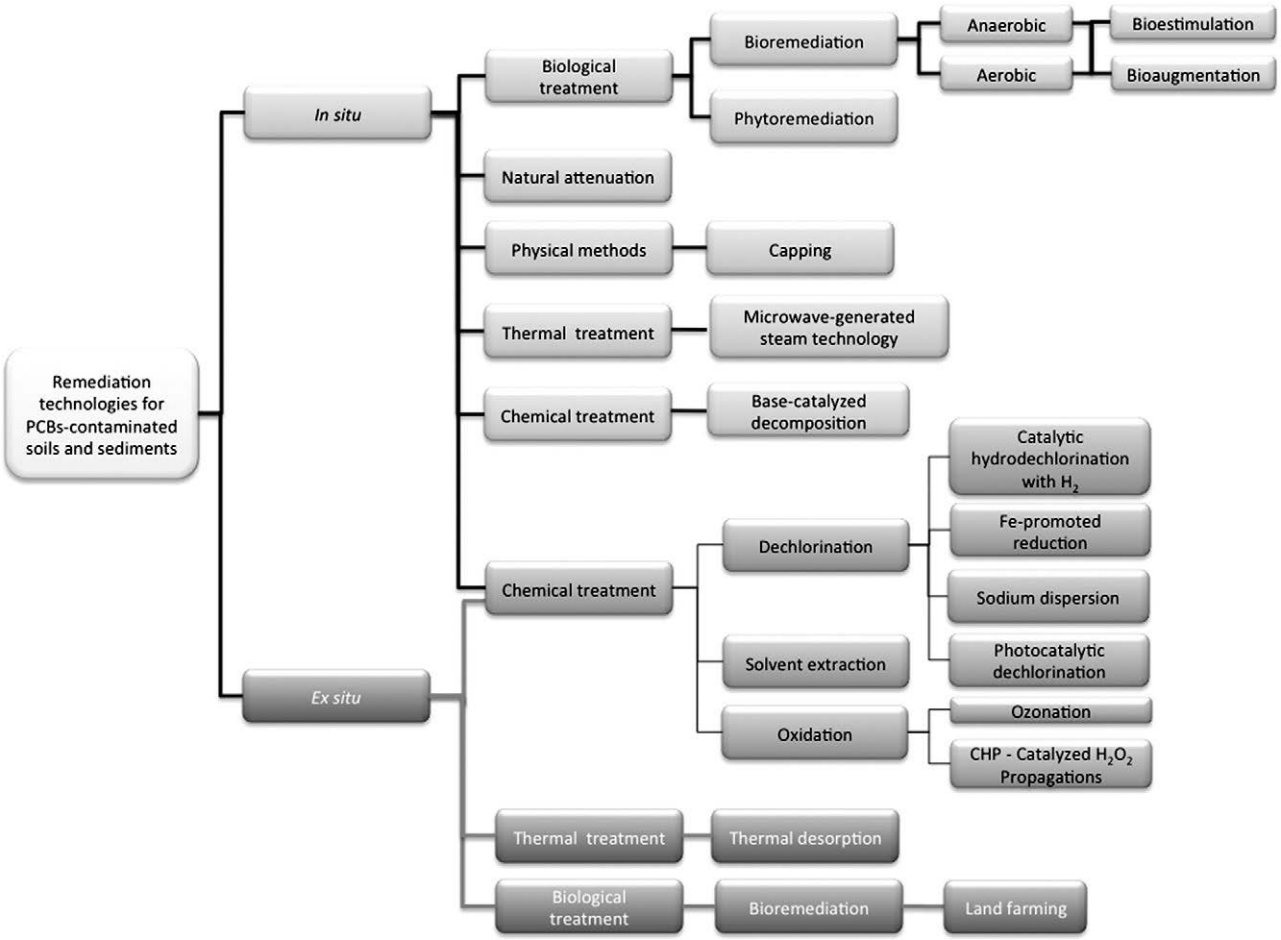


**Fig. 1.** Classification of remediation technologies for remediation of PCB-contaminated soils and sediments.

enhanced with activated carbon, during a 39-month experiment under near natural conditions. The results showed that the tri- and some of the tetrachlorinated congeners were degraded and that the activated carbon reduced PCB bioavailability without slowing degradation (Vasilyeva et al., 2010).

Table 3 summarizes the studies and main findings regarding PCB aerobic degradation, following an identical structure to Table 2 and listing some of the most important conditions tested. The experimental results show that biodegradability is highly dependent on the number of chlorines (decreases with increased number) and their positions, and also highly strain dependent (Furukawa and Fujihara, 2008). PCB congeners with chlorines on only one biphenyl ring are degraded more easily and PCB with chlorine at position 2,6- or 2,2′- (double *ortho*-substituted congeners) are poorly degraded (Furukawa and Fujihara, 2008).

*3.1.1.2. Phytoremediation.* Phytoremediation is based on the use of plants to extract, sequester, and/or detoxify pollutants from contaminated soil (Meagher, 2000; Raskin et al., 1997). In the case of PCB three main mechanisms are involved: i) uptake from soil (phytoextraction) and accumulation in stems and leaves tissues, ii) phytodegradation (enzymatic transformation) and iii) rhizoremediation (plant enhancement of the microbial activity in the root zone, improving bioremediation, by the release of secondary metabolites, such as sugars, amino acids, organic acids, various exsudates and microbial growth factors) (Van Aken et al., 2010).

Table 4 presents a summary on the main studies on phytoremediation of PCB contaminated soils, similar to the previous tables and highlighting the experimental conditions and main conclusions. Some of these studies only focused on PCB's final concentration in the soil neglecting the accumulation of PCB in roots and shoots of the plants. One of the main concerns regarding phytoremediation is crop disposal after phytoextraction and the issues associated with pollution transfer from the biomass disposal.

Although PCB contaminated soils can be phytoremediated, PCB are only taken up and degraded by plants and associated bacteria slowly in field trials, resulting in incomplete treatment and potential release of toxic metabolites into the environment (Van Aken et al., 2010). To improve phytoremediation effectiveness, bacterial genes involved in the metabolism of PCB, such as biphenyl dioxygenases, have been introduced into higher plants, following a strategy similar to the development of transgenic crops, and bacteria have also been genetically modified to improve biodegradation and to maintain stable relationships with plants (Sylvestre, 2012; Van Aken et al., 2010). Transgenic plants for PCB phytoremediation have been produced, but none have reached commercial existence and in some countries (e.g. European Union) cultivation of transgenic plants is still associated to perceived risks for ecosystems (Maestri and Marmiroli, 2011), due to the potential for inserted genetic material to be transferred to indigenous populations (Gerhardt et al., 2009). According to Marmiroli and McCutcheon (2003) the main obstacles to the use of genetically engineered plants in phytoremediation are increased costs for maintenance and monitoring of installations, and also waste disposal in view of strict regulations. The biomass produced during the phytoremediation of contaminated sites could be economically valorized in the form of bioenergy (biogas, biofuels and combustion for energy production and heating), representing an important

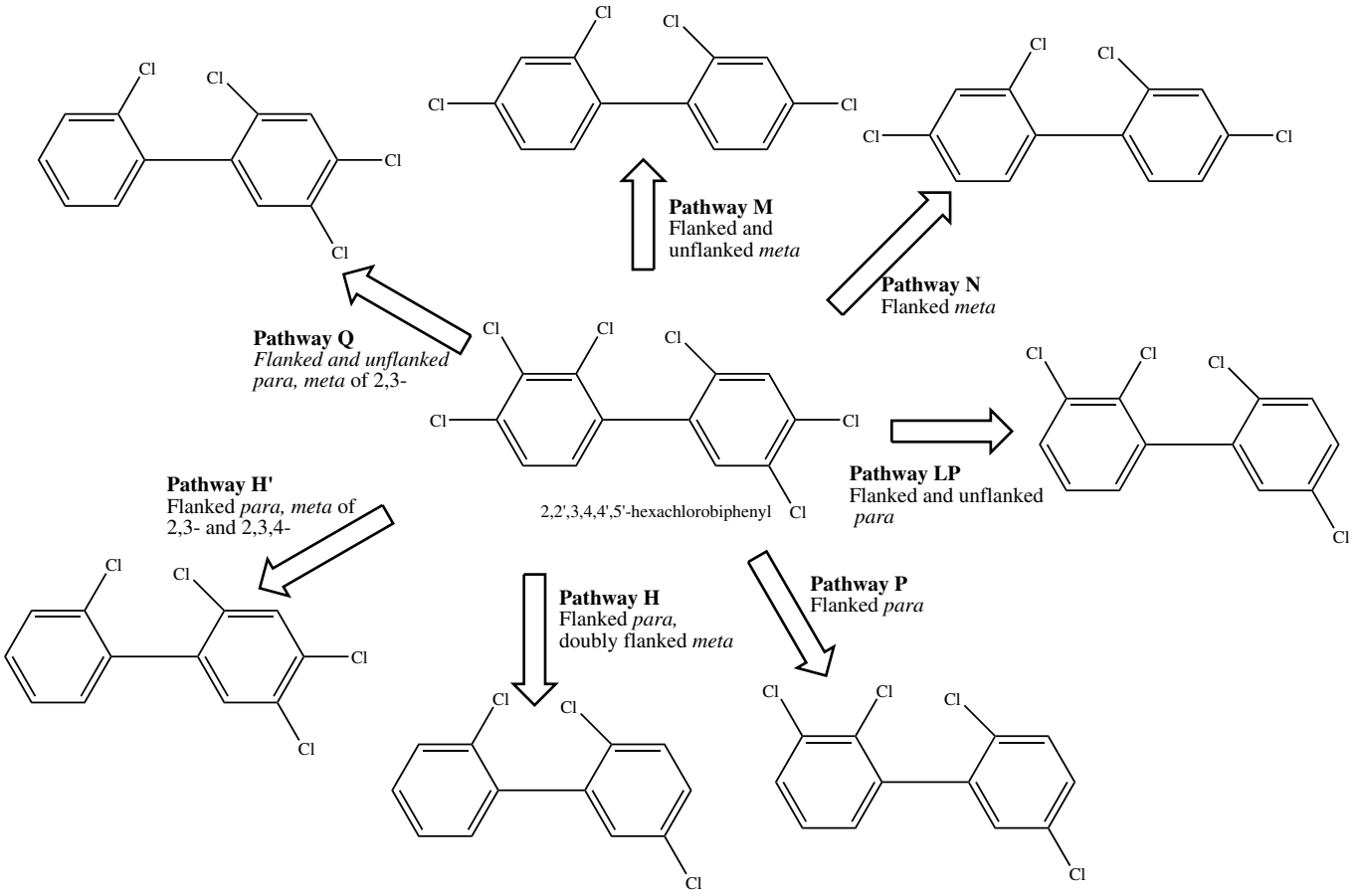


**Fig. 2.** Example of the microbial dechlorination pathways identified by Bedard and Quensen (1995) and Wiegel and Wu (2000) applied to PCB 138 (2,2′,3,4,4′5′-hexachlorobiphenyl). "Flanked" signifies an adjacent chlorine. Beside the pathways presented there is also the T pathway that removes flanked meta chlorine of 2,3,4,5- in hepta- and octachlorobiphenyls.

environmental co-benefit. Gomes (2012) identified the challenges and opportunities associated with the use of phytoremediation for bioenergy production.

*3.1.2. Natural attenuation*

During natural attenuation pollutants are transformed to less harmful forms or immobilized by a wide range of processes that include biodegradation; dispersion; dilution; sorption; volatilization; radioactive decay; and chemical or biological stabilization, transformation, or destruction of contaminants (Brown et al., 2007; Declercq et al., 2012; Megharaj et al., 2011; USEPA, 1999). In sediments, natural attenuation can take place through two primary pathways: burial of contaminated bed by clean sediments (natural capping) and transformation via biodegradation, immobilization, dilution, or volatilization (Agarwal et al., 2007). All these processes reduce bioavailability, thereby reducing the environmental impact.

Monitored natural attenuation (MNA) is a technique used to monitor the progress of natural attenuation processes. It may be used with other remediation technologies as a finishing option or as the only remediation technique if the rate of contaminant degradation is fast enough to protect human health and the environment.

The interest in applying MNA as a treatment approach in contaminated sediments arose after extensive studies on reductive dechlorination of PCB in numerous locations, including the Hudson River (NY, USA), Silver Lake (MA, USA), Sheboygan River (WI, USA), Waukegan Harbor (IL, USA), New Bedford Harbor (MA, USA), and Acushnet Estuary (MA, USA) (Bedard and Quensen, 1995; Pakdeesusuk et al., 2003). In some of these sites, it was decided to dredge the contaminated sediment (Table 1), but in Lake Hartwell MNA was selected as the remedial option, predicting that ongoing deposition of clean sediment would cap the PCB-contaminated material and thereby isolate it from the food chain (Pakdeesusuk et al., 2003). Two decades after, field results show evidence of in situ reductive dechlorination and also that the effectiveness of the natural attenuation is site-specific and is occurring with variable degree of success, being lower in the most contaminated regions (Sivey and Lee, 2007).

Kaštánek et al. (1999) reported the occurrence of PCB natural attenuation in an industrial site contaminated with a PCB mixture with tri- and tetrachlorinated congeners in a soil with a long history of contamination (approx. 20 years). Data showed that under conditions prevailing in the field, only small changes in the composition of PCB congeners had occurred, namely some biodegradation of the lighter congeners occurred in the oxygenated surficial soil layers (Kaštánek et al., 1999).

The lines of evidence that should be considered to support the use of MNA at sediment sites were identified by Magar and Wenning (2006) and Magar et al. (2009), and include assessing chemical transformation, reduction in the contaminant's bioavailability and mobility, physical isolation and dispersion.

*3.1.3. Physical methods — capping*

Capping involves isolating a contaminated sediment bed with a clean layer or "cap" commonly consisting of sand, gravel, silt or crushed rock debris. Passive caps, made of unreactive material, mainly rely on containment rather than treatment. The cap cuts down bioavailability of contaminants by physically separating sediments from the aquatic environment, confining bioturbation to the top clean layer and limiting the possibility of re-suspension of contaminated sediments

**Table 2**
Summary of experimental conditions and main findings of studies on anaerobic dechlorination.

| PCB (commercial name or congeners) | Substrate amount used | Temp. (°C) | pH | Incubation period | Amendments | Observations | Dechlorination pathway | Main findings | Reference |
|---|---|---|---|---|---|---|---|---|---|
| Aroclors 1242, 1248, 1254 and 1260 | 5 μL $g^{-1}$ of sediment | 25 | – | 24 weeks | – | The rate of dechlorination was similar for Aroclors 1242 and 1248, but the extent decreased with increasing degrees of chlorination. | C (occurred in the *meta* and *para* positions) | Two PCB-dechlorinating populations may exist in the Hudson River sediments. | Quensen et al. (1990) |
| Aroclor1242 | 10 g of PCB-free dry sediment and 10 mL of inoculum | 37 | – | 12 w | 10 mL of reduced anaerobic mineral medium, 100 μL of a 10% autoclaved solution of cysteine, and 80 μL of 10% (wt/vol) Aroclor 1242 | Different sterilization techniques were tested: heating at 80 or 85 °C for 15 min, treatment with 50% ethanol for 1 h, and treatment with the combination of heat and ethanol | Pattern C and M | Anaerobic spore formers responsible for the reductive dechlorination of PCB. Microorganisms surviving the heat and ethanol treatments preferentially remove *meta* chlorines, while microorganisms lost from the enrichment mainly contribute to the *para* dechlorination activity. | Ye et al. (1992) |
| Aroclor 1242 and 1260 | 35% (v/v) sediment inoculum in mineral salts medium spiked with 100 ppm Aroclor 1242 in freshwater sediments and 400 ppm Aroclor 1260 for estuarine sediments | – | – | 11 m | A fatty acid mixture with acetate, 0.85 mM; propionate, 1.37 mM, butyrate, 0.57 mM; hexanoic acid, 0.43 mM was added as a carbon source. | Two different reducing conditions were established, methanogenic and sulfidogenic | No *ortho* dechlorination was observed, nor complete PCB dechlorination | Slow degradation process. No activities were detected under sulfate-reducing conditions with any of the sediments. | Alder et al. (1993) |
| 2,3,4- and 2,3,4,2′,4′,5′-chlorobiphenyl | 5 g of sediment in 20 mL of river sediments spiked with different PCB concentrations | Room temp. | – | 7.5 m | Cystine sulfide (0.025%) | – | – | Dechlorination may not be able to occur in areas with low ambient PCB levels because it is concentration-dependent. | Sokol et al. (1995) |
| 2,3,5,6-chlorinated biphenyl (CB), 2,3,5-CB, and 2,3,6-CB | Baltimore Harbor sediments (20% [vol/vol]) | 30 | – | 154 d | Modified basal medium $Na_2CO_3$, 3.0 g $L^{-1}$; $Na_2HPO_4$, 0.6 g $L^{-1}$; $NH_4Cl$, 0.5 g $L^{-1}$; cysteine-HCl•$H_2O$, 0.25 g $L^{-1}$; $Na_2S$ •$9H_2O$, 0.25 g $L^{-1}$; resazurin, 0.001. 1% (vol/vol) each of vitamin and trace element solutions was added. | Estuarine salt medium and marine salt medium were also used in the tests | *Ortho* dechlorination was observed | *Ortho* dechlorination occurred when marine or estuarine conditions were present. In contrast, freshwater sediments incubated under the same conditions exhibited only *meta* and *para* dechlorinations. | Berkaw et al. (1996) |
| Aroclor 1242 and 1248 | 1 kg of contaminated river sediment | Room temp. (20 to 22 °C) and 12 °C | – | 32 w | Addition of wood powder as nutrient source. | A set of 2 L bench-scale glass columns were designed and constructed as microcosms. | Absence of *ortho* and occurrence of *meta* and *para* dechlorination (M pathway). | The rate of dechlorination was slightly higher at ambient temperature. | Natarajan et al. (1997) |
| Aroclor 1242 | 2:3 (vol:vol) sediments and mineral medium 240 mL sediments slurry | Room temp. (23–26 °C) | – | 92 d | A humic acid extract was prepared using upper Hudson River sediment that did not contain PCB and was added to the cultures | Mineral medium reduced with 0.1% L-cysteine hydrochloride. Two bacterial antibiotics, vancomycin and nisin, were added as stock solutions. | M and Q | The additions of 2,3,6-CB and 2,4,6-CB to PCB-contaminated upper Hudson River sediment slurries stimulate the production of reductive dechlorination. | Williams (1997) |

| | | | | | | | | | |
|---|---|---|---|---|---|---|---|---|---|
| Aroclor 1260 | 0.15 g of sediment (dry weight) per mL | 4 to 66 °C | 6.9–7.2 | 1 y | 2346-CB (350 μM of slurry) | The dechlorination was selective and progressed with the incubation time. | Pathways N at 8 to 30 °C, P at 12 to 34 °C, LP at 18 to 30 °C, and T at 50 to 60 °C | The extent and pattern of dechlorination were temperature dependent. Changes in incubation temperature alone (i.e., raising it above ambient temperature) cannot be used to initiate dehalogenation of PCB in these sediments. | Wu et al. (1997b) |
| 2,3,4,6-Tetrachlorobiphenyl | 0.15 g of sediment (dry weight) per mL | 4, 8, 12, 15, 18, 20, 22, 25, 27, 30, 34, 37, 40, 45, 50, 55, 60, and 66 °C | 6.5–6.8 | 1 y | 2346-CB (350 μM of slurry) | Seven discrete dechlorination reactions were observed, four of which occurred in both sediments. These were 2,3,4,6-CB→2,4,6-CB, 2,3,4,6-CB→2,3,6-CB, 2,4,6-CB→2,6-CB, and 2,3,6-CB→2,6-CB. | At most temperatures, *meta* dechlorination of 2,3,4,6-CB to 2,4,6-CB almost completely dominated | Dechlorination was restricted to ~15 to 30 °C and temperature affected lag time. *Para* dechlorination dominated at 20 °C, and *ortho* dechlorination dominated at 15 °C, but at 18 and 22 to 30 °C the relative dominance of *ortho* versus *para* dechlorination varied. Field temperatures play a significant role in dechlorination. | Wu et al. (1997a) |
| Aroclor 1254 | 50 mL river sediments slurry | Room temp. (21–23 °C) | 7.0 | 24 w | Glucose and methanol were added as substrates at 0.1 mg $L^{-1}$ and 0.02 mg $L^{-1}$ | Anaerobic phosphate buffered basal (PBB) medium. | The dechlorination pathway observed is different from the ones reported earlier. | 70% of the PCB were dechlorinated without accumulation of any specific PCB congeners. | Natarajan et al. (1998) |
| Aroclor 1260 | 0.06 g [dry weight] of sediment per mL of estuarine medium without sulfate | 30 | – | 6 m | 800 ppm Aroclor 1260 with and without the addition of 350 μM 2,3,4,5-CB or 2,3,5,6-CB | PCB dechlorination is more stable, when sediments are stored anaerobically at room temperature (20 to 22 °C) than at 4 °C. | Pathway N | The addition of single PCB congeners (2,3,4,5-CB and 2,3,5,6-CB) stimulates *meta* and *ortho* dechlorination of Aroclor 1260. | Wu et al. (1998) |
| Aroclor 1242 | Slurries with 2 g of air-dried clean upstream Hudson River sediment and 3 mL of reduced anaerobic minimal media | 22 | – | 35 w | Unamended control, an autoclaved plus $FeSO_4$ (10 mM) control, and the following treatments: $FeSO_4$ (10 and 20 mM), $Na_2SO_4$ (10 mM), $FeCl_2$ (10 mM), $FeSO_4$ (10 mM) plus $Na_2MoO_4$ (3.7 mM), and $Na_2SO_4$ (10 mM) plus $PbCl_2$ (10 mM). | Only the M dechlorination process occurred in the unamended treatment. | Pathways M, Q, C | $FeSO_4$ provides two mutually beneficial effects: i) sulfate stimulates growth of sulfate reducing organisms responsible for PCB dechlorination, ii) $Fe^{2+}$ reduces sulfide bioavailability by forming the insoluble precipitate FeS. Ferrous sulfate could be used to overcome factors limiting both the extent of in situ dechlorination as well as the implementation of sequential anaerobic/aerobic biotreatment systems. | Zwiernik et al. (1998) |
| Aroclor 1260 | 30 or 15 mL of slurry prepared with wet sediment (2 vol) combined with pond water (3 vol) | Room temp. (22–25 °C) | 7.0 | 240 d | Halobenzoates Brominated Aromatic Compounds | None of the fluorinated or chlorinated benzoates primed PCB dechlorination, but several brominated and iodinated benzoates initiated this activity | Pathways N, P | Halogenated aromatic compounds that are not structural analogs to PCB can prime PCB dechlorination. | Deweerd and Bedard (1999) |

(continued on next page)

**Table 2** (*continued*)

| PCB (commercial name or congeners) | Substrate amount used | Temp. (°C) | pH | Incubation period | Amendments | Observations | Dechlorination pathway | Main findings | Reference |
|---|---|---|---|---|---|---|---|---|---|
| 2 CB; 3 CB, 4 CB, 2-3 CB; 2-4 CB, 3-3 CB, 4-4 CB, 34 CB; 345 CB, 25-3 CB; 25-4 CB; 34-2 CB; 35-4 CB, 25-34 CB; 34-34 CB; 345-4 CB; 345-34 CB; 345-345 CB | Spiked estuarine sediment slurries (30 mL) containing 10% solids (wt./v) | Room temp. (23–25 °C) | 7.2 | 2 y | Surfactant Tween 20 (0.05%, v/v) | Sulfidogenic conditions | *Para* dechlorination of 4-CB, 34-CB and 345-CB and *meta* dechlorination of 25-CB and 35-CB Pathways Q and M | Dechlorination of coplanar and non-planar congeners began with *para* chlorine removal. All *para* chlorines from the mono-, di-, and trichlorobiphenyl groups could be removed by sediment slurries. | Kuo et al. (1999) |
| 2,3,5,6-CB; 2,3,4,5-CB; 2,3,4,5,6-CB | 5 g sediment spiked with PCB in 45 mL mineral medium | 20<br>30<br>40<br>50 | 6.0<br>7.0<br>8.0<br>9.0 | 108 d | 20 mM sodium acetate;<br>20 mM sodium pyruvate;<br>20 mM sodium lactacte;<br>20 mM MnO; 20 mM $FeCl_2$; 20 mM $NaHCO_3$; 20 mM $Na_2SO_4$; 20 mM $NaNO_3$. | Tests were made in sterile control, sediment-free culture sediment; sediment containing culture. | *Meta*, *para* and *ortho* dechlorination | Optimal conditions for dechlorination were 30 °C and pH 7. Methanogen and sulfate-reducing bacteria were involved in the dechlorination. | Chang et al. (2001) |
| Arochlor 1242 | 5 g dry weight of river sediment in 50 mL water, spiked with PCB | Room temp. | – | 8 weeks | – | Synthetic mineral medium. Moisture level of 95%, 70%, 45% and 15%. | – | The maximum level of dechlorination was lower at reduced moisture contents. Dechlorination is closely linked to population growth. | Cho et al. (2001) |
| Arochlor 1248 | 2.5%(w/v) lake sediment — 20 mL slurry spiked with PCB | – | – | 40 weeks | Dried algal powder (2%, w/w) | The addition of supplementary organic carbon did not change the dechlorination pattern. | – | Sediments characteristics or organic carbon content did not play a role in the selection of dechlorinating populations | Kim and Rhee (2001) |
| Aroclor 1248 | PCB-spiked sediments (20 g dry weight) were made into slurries by the addition of 90 mL of reduced St. Lawrence River water in 100-mL serum vials | Room temp. | – | 400 d | Sediments were spiked with Aroclor 1248 at 14 concentrations, ranging from 3.44 to 687 nmol (g of sediment)$^{-1}$ on a dry weight basis. | The time course of dechlorination showed an initial lag period, followed by dechlorination, and then a plateau with no further concentration decrease through the remainder of a 58-week incubation period. | No *ortho* dechlorination was detected | No dechlorination was observed at Aroclor concentrations below 40 ppm. The threshold values and the specific dechlorination rates may not be universally applicable to all contaminated sediments because they may also be a function of physical, chemical, and biological factors (sediment composition, age of contamination, and/or sediment microbial community). | Cho et al. (2003) |
| Aroclor 1016 and 1254 | 50 mL of sediment slurry (containing 5.0–5.5 g of sediment, dry wt) | 22–24 | 7 | 260 d | 500 μg g$^{-1}$ (sediment dry wt). Aroclor 1254 | It was observed formation of methane due to biodegradation f acetone — solvent used for Aroclor 1254. | Pathway M | Lake Hartwell sediments in the vicinity of the highest levels of PCB contamination contain microbial communities capable of mediating *meta* and *para* dechlorination. | Pakdeesusuk et al. (2003) |

| | | | | | | | | | |
|---|---|---|---|---|---|---|---|---|---|
| 2,3,4-CB; 2,2′,3,3′, 4,5,6-CB | 80 mL synthetic wastewater consisting of a basal medium to which a trace element solution with 3 g microbial granules | 34 ± 2 | 7.2 | 150 d | Propionate, butyrate, and methanol were added as the carbon/electron sources. | Anaerobic granules obtained from commercial bioreactors [upflow anaerobic sludge blanket (UASB)]. | Pattern M | Variation of the carbon/electron source had no effect on the dechlorination pathway. The extents and rates of dechlorination were highest for ethanol and formate and lowest for pyruvate. The authors consider that the observed PCB dechlorination is enzymatic. | Nollet et al. (2005) |
| Aroclor 1260 | 50 mL sulfide-free, bicarbonate-buffered mineral medium | 22–24 | 7.0 | 154 d | Selenite, tungstate, vitamins (including vitamin B12), a trace element solution (SL9), and 0.01% yeast extract | The sediment-free JN mixed cultures were established from microcosms of Aroclor 1260-contaminated sediment. | Pattern N | *Dehalococcoides* bacteria may play a major role in the in situ dechlorination of commercial PCB mixtures. | Bedard et al. (2007) |
| PCB 28<br>PCB 53<br>PCB 101<br>PCB 138<br>PCB 153<br>PCB 180 | 3.5 L of waste activated sludge (WAS) spiked with an equivalent amount of 0.5 mg PCB $kg^{-1}$ dw | Termophilic conditions (55 °C) and mesophilic conditions (35 °C) | 6.3 | 26 d | – | Sewage sludge anaerobic digestion | – | Total PCB removal efficiency was 59.4–83.5% under thermophilic conditions and 33.0–58.0% under mesophilic conditions. | El-Hadj et al. (2007) |
| Aroclor 1248 | 2.5% (w/v) sediment with synthetic mineral medium | Room temp. | – | 36 w<br>50 w | 50 μg rhamnolipid biosurfactant $g^{-1}$ sediment | Since the PCB threshold concentration for the inoculum in the first experiment was lower than 40 ppm, another experiment was conducted using sediments with lower PCB concentrations, 10, 20, and 30 ppm. | *Meta* dechlorination was predominant. | There was no significant difference in the extent of dechlorination between surfactant-free and -amended sediments. Surfactant did not change the congener specificity or broaden the congener spectrum for dechlorination at PCB concentrations below 40 ppm. | Kim et al. (2008) |
| 2,3,4,5-CB | 1 g dry sediment and 100 mL of an anaerobic media tap water 0.0021 g $L^{-1}$ $NaNO_3$, 0.014 g $L^{-1}$ cysteine, 0.042 g $L^{-1}$ $NaHCO_3$, and 0.001 g $L^{-1}$ resazurin | 10 and 25 | 6.0–7.1 | 11, 17 and 20 m | 0.024 g cysteine 0.02 g $Fe^0$ per g dry sediment equivalent; 0.06, 0.1, 0.14, 0.4, and 0.4 g $Fe^0$<br>50 mM sodium azide (sterile controls) | Bioaugmentation with 10 mL of culture from Raisin River sediment. | – | Dechlorination was either minimal or absent in the sediments amended with $Fe^0$ and incubated at either 10 or 25 °C, suggesting that $H_2$ was not an appropriate electron donor for the dechlorinating organisms present. Bioaugmentation successfully stimulated PCB dechlorination in all the sediments within 20 d. | Winchell and Novak (2008) |

(continued on next page)

**Table 2** (*continued*)

| PCB (commercial name or congeners) | Substrate amount used | Temp. (°C) | pH | Incubation period | Amendments | Observations | Dechlorination pathway | Main findings | Reference |
|---|---|---|---|---|---|---|---|---|---|
| Aroclors 1248, 1254, and 1260 | 200 mL Anacosia River site sediment | 26 | – | 415 d | A mixture of electron donors; alternate halogenated electron acceptors tetrachlorobenzene (TeCB), pentachloro-nitrobenzene (PCNB), or PCB116; bio-augmentation with a mixed culture containing *D. ethenogenes* strain 195; and PCNB plus bioaugmentation | Analysis of *Chloroflexi* 16S rRNA genes showed that TeCB and PCNB increased native *Dehalococcoides* spp. from the Pinellas subgroup; however this increase was correlated to enhanced dechlorination of low concentration weathered PCB only in PCNB-amended microcosms. | Identification of the exact dechlorination pathway was not the primary objective of the study. | Dechlorination of low concentration weathered PCB were significantly enhanced in Anacostia River sediment microcosms receiving bioaugmentation, PCNB and PCNB plus bioaugmentation, compared to other treatments receiving electron donor only TeCB, or PCB116 | Krumins et al. (2009) |
| 245-2′4′5′ hexachlorobiphenyl | Sediments (10 mL, containing 7 g dry sediment) | 10<br>25<br>40 | – | 250 d | 5 mM $FeSO_4$<br>22.5 mM peptone on a carbon basis<br>2.5 mM each of acetate, propionate, and butyrate | PCB removal was also studied in different sediment layers applying dialysis equilibrators in the field for 4 months. | Dechlorination was not affected by amendments with $FeSO_4$, electron donors, or alternating anaerobic–aerobic conditions in these sediments. | PCB stability in field conditions could be mainly attributed to (a) elevated redox status and (b) low temperature conditions in the sediments. Identified several predominant groups that are involved in the stepwise decomposition of organic matter to acetate and $H_2$, which are substrates for dechlorinators such as *Dehalococcoides*. | D'Angelo and Nunez (2010) |
| 3,4,4′,5-tetrachlorobiphenyl, 3,3′,4,4′,5-pentachlorobiphenyl, and 3,3′,4,4′,5,5′ -hexachlorobiphenyl | Sediment slurries (20% solids, wt/vol) | 25 | 7.6 | 350 d | (i) acetate and lactate, final concentration 5 mM each, and yeast extract (1 g $L^{-1}$) and ferrous sulfate (final concentration 20 mM) and (ii) filtered site water amended with ferrous sulfate (final concentration 20 mM) | No PCB were detected in the site water and original sediment. | *Para* dechlorination occurred prior to *meta* dechlorination during reductive dechlorination of 3,4,4′,5-tetrachlorobiphenyl and 3,3′,4,4′,5-pentachlorobiphenyl. | PCB concentration has effects on biodegradation and the succession of dechlorinating microorganisms. Bacteria or phylotypes with the ability to exclusively dechlorinate flanked and unflanked meta chlorine, and bacteria exclusively dechlorinate double flanked, single flanked, and un- flanked para chlorine were reported. | Ho and Liu (2011) |

**Table 3**
Summary of experimental conditions and main findings of studies on aerobic degradation.

| PCB (commercial name or congeners) | Substrate amount used | Temp. (°C) | pH | Incubation period | Amendments | Observations | Main findings | Reference |
|---|---|---|---|---|---|---|---|---|
| Aroclor 1242 and Aroclor 1260 | 18 g dry wt. spiked soil | 28 | – | 120 d | In order to maintain a high concentration of viable cells and constant soil moisture (20%), soils were reinoculated once a week. | 500 mL of a cultivation medium: glucose, 0.5 g $L^{-1}$; peptone, 0.5 g $L^{-1}$; $KH_2PO_4$, 0.5 g $L^{-1}$ | (i) the survival of the inoculated strain does not correlate with the degradation of PCB congeners; (ii) there are higher differences between degradation of PCB in different soil types than between sterile and nonsterile soils and (iii) efficiency of *Alcaligenes xylosoxidans* is much higher in liquid media than in soils. This indicates that the degradation of PCB is probably related to the soil sorption of the PCB congeners. Degradation is faster in the soils containing an intermediate amount of organic carbon with a high portion of total and aromatic carbon in humic acid | Haluska et al. (1995) |
| Fenclor 42 | Model soil spiked with 1 g $kg^{-1}$ Fenclor 42 87.5 g soil in 0.5 L of distilled water | 20±2 | – | 140 d | 4 g/kg biphenyl, aerobic bacterial co-culture ECO3 ($10^8$ CFU $mL^{-1}$); addition of humic substances 1.5 and 3.0% (w/w) | The authors tested the soil and the biologically active slurry microcosms for ecotoxicity with the plant *Lepidiun sativum* and the animal *Folsomia candida*. | The presence of humic substances influenced significantly the activity of the specialized biomass and the biodegradation of PCB | Fava and Piccolo (2002) |
| Aroclor 1242 | 1 g of PCB-contaminated soil, 10 mL of the phosphate-buffered mineral salts medium | 25±2 | – | 4 m | – | The mixed culture of PCB-degrading bacteria was acquired from New York State Center for Hazardous Wastes Management (Buffalo, NY, USA). | The presence of biphenyl as cosubstrate was the most important factor affecting PCB biodegradation. The biodegradation occurred as a first-order process, and it proved most effective in respect to dichlorinated biphenyls (100% removal), followed by trichlorinated (92%) and tetrachlorinated biphenyls (24%). | Manzano et al. (2003) |
| Delor 103 | 100 mL of SIRAN, 100 mL of mineral medium, trace elements and biphenyl | – | – | 3 w | – | *Pseudomonas* sp. 2 was isolated from PCB-contaminated soil in the Czech Republic | The immobilized cells of *Pseudomonas* sp. 2 were able to degrade all the tested tri- and tetrachlorobiphenyls | Komancová et al. (2003) |
| Aroclors 1242, 1248, and 1260 | 1 kg of contaminated soil was combined with 1500 g of clean soil and 500 g of sterile sand. 200 g of the mixed soil were used. | 28 | – | 6 m | Chicken manure, chicken manure plus 1000 ppm biphenyl, kenaf, and kenaf plus white rot fungus (*Phanerochaete chrysosporium*). | Total Petroleum Hydrocarbons were also analyzed | The chicken manure amended treatments showed faster degradation in the first 45 d compared to the other treatments. Adding biphenyl or white rot fungus to enhance degradation does not seem to enhance degradation of the lower chlorinated PCB. The results suggest that if the soil is provided adequate moisture and mixing, the concentration of lower chlorinated PCB can be readily decreased. | Borazjani et al. (2005) |
| PCB50 and Aroclor 1248 | 10 g of marine sediments was added in SMS medium (100 mL). | 30 | – | 15 d | SMS medium (45 mL) supplemented with biphenyl (0.7 $g^{-1}$) | Seawater mineral salts (SMS) medium, supplemented with biphenyl as the sole carbon source. | All enrichment cultures degraded dichlorobiphenyls, while their capabilities to degrade congeners with three and four substituted chlorines varied greatly. Six isolates belonging to the genus *Rhodococcus* exhibited substantial PCB-degrading activity. | Kolar et al. (2007) |
| PCB congeners present in the soil were mostly tri-, tetra- and penta-chlorinated, plus small amounts of di-, hexa- and hepta- | 1 kg dry weight of historically contaminated soils | Outdoor temperature (Russia) | – | 39 m | 0, 2, or 7% (w/w) Granular (GAC) and 0, 0.5, or 3.5% (w/w) powdered (PAC) activated carbons | Phytotoxicity was determined from germination of clover seeds. | The tri- and some of the tetrachlorinated congeners were degraded during the three-year experiments. Amending the soils with GAC or PAC sharply reduced PCB bioavailability without slowing degradation processes. | Vasilyeva et al. (2010) |
| PCB-Congener-Mix | 200 g of soil (dry weight) were spiked with 400 μg $kg^{-1}$ PCB-Congener-Mix. | 28 | 7.0 | 30 d | 10% or 20% (v:w) of *S. meliloti* suspension culture ($3\times10^8$ cfu $mL^{-1}$) | The authors performed resting cell assay and identification of metabolic intermediates | After 6 d, the percent biodegradation of 2,4,4′-TCB was 77.4% compared with the control. The main intermediate was identified as 2-hydroxy-6-oxo-6-phenylhex-2,4-dienoic acid (HOPDA). Inoculation with *S. meliloti* greatly enhanced the degradation of target PCB mixtures in the soil. | Tu et al. (2011a,b) |

**Table 4**
Summary of experimental conditions and main findings of studies on phytoremediation.

| PCB (commercial name or congeners) | Plants used | Experimental conditions | Duration of the study | Observations | Main findings | Reference |
|---|---|---|---|---|---|---|
| Aroclor 1242, 1248, 1254 and 1260 | *Medicago sativa L.* | Containers packed with 350 g of historically contaminated soil were planted with alfalfa (Medicago *sativa* L.) and augmented with its symbiotic $N_2$-fixing host rhizobium (*Sinorhizobium meliloti*, strain A-025). | 270 days | The plants never reached maturity and some died during the experimental period. Bioaugmentation of the soil had a negative effect on plant growth and health, through the increase of the hardness of the soil. | The depletion, loss or change in PCB levels may be attributed to either direct or indirect biotransformation, biotranslocation and adsorption of PCB due to the presence of alfalfa and/or rhizobial inoculation. Either possibility underscores the possibility of using plant-rhizobacterial associations. | Mehmannavaz et al. (2002) |
| Aroclor 1242 | *Brassica nigra* | Greenhouse study with spiked soil (100 mg $kg^{-1}$) augmented with PCB-degrading bacteria, inducers (carvone and salicylic acid), surfactant (sorbitan trioleate), minimal salts medium in a 20-cm high soil column, or a combination of these elements. | 9 weeks | Results from bioaugmented treatments suggested that plant roots allow increased inoculum penetration, enabling greater subsurface PCB removal. | *Brassica nigra* directly contributed to accelerated PCB removal by increased oxygen diffusion, amendment infiltration, and microbial enrichment. | Singer et al. (2003) |
| Aroclor 1248 | *Medicago sativa* L., *Lathyrus sylvestris* L. *Lespedeza cuneata* Dum.-Cours., *Panicum clandestinum* L. *Phalaris arundinacea* L. *Panicum virgatum* L. *Festuca arundinacea* Schreb. | Spiked soil (100 mg $kg^{-1}$) Growth chamber temperatures were maintained at 25/16 °C, and the light regime was 16/8 h day/night cycle, with photosynthetic photon flux rate of 400–500 μmol $m^{-2}$ $s^{-1}$ from metal halide bulbs. The relative humidity in the chambers was set at 65 ± 5%. | 4 months | Planting with *Phalaris arundinacea* and *Panicum virgatum* resulted in a 70% and 61%, respectively, biodegradation of the initial PCB levels. | Aroclor 1248 biodegradation in soil seems to be positively influenced by the presence of plants and plant–bacteria interactions. | Chekol et al. (2004) |
| Aroclor 1260 | *Festuca arundinacea*, *Glycine max*, *Medicago sativa*, *Phalaris arundinacea*, *Lolium multiflorum*, *Carex normalis*, *Cucurbita pepo ssp. pepo* | Greenhouse experiments with weathered soil controlled for PCB volatilization through the use of a vented enclosure and by isolating the soils with parafilm. | 8 weeks | Concentrations of PCB in plant tissues were greater in the roots than the shoots. Tetra- to hexachlorobiphenyls contribute the most to plant shoots, while hepta- and octa-chlorbiphenyls contributed to roots. | Plants (in particular *C. pepo* varieties) were able to extract PCB from soil and translocate them from their roots to their shoots. | Zeeb et al. (2006) |
| Aroclor 1254/1260 | *Cucurbita pepo ssp pepo cv. Howden*, *Carex normalis*, *Festuca arundinacea* | Pilot-scale field trial at a historically contaminated field site (mean concentration of 46 μg $g^{-1}$; range of 0.6–200 μg $g^{-1}$) total PCB. The soil was amended with fertilizer, an inorganic bulking agent (perlite), and a minimal amount of top soil to achieve suitable growing conditions for the plants without diluting the existing PCB concentrations. | 10 weeks | Sedge (*Carex normalis*) exhibited the highest PCB concentrations in both roots and shoots, followed by pumpkin (*C. pepo*) and then tall fescue (*F. arundinacea*). | This was a successful scale-up of previous greenhouse studies. All three plant species remain viable candidates for possible PCB phytoextraction. Intercropping of the species might provide the best characteristics of all. | Whitfield Äslund et al. (2007) |
| Aroclor 1254/1260 | *Cucurbita pepo ssp pepo cv.* | Pilot-scale field trial at the same site. The soil was amended with fertilizer, a 6-12-12 mixture (C-I-L Tomato Food from Canadian Tire), at the recommended rate of 140 g $m^{-2}$. Following the application of fertilizer, soil plots were thoroughly homogenized by rototilling. | 10 weeks | Plant stem and leaf PCB concentrations were observed to increase significantly from the concentrations reported in the previous year (5.7 and 3.9 μg $g^{-1}$, respectively) while the total biomass produced as well as soil and plant root PCB concentrations did not change. The lower stems of some plants exhibited PCB concentrations as high as 43 μg $g^{-1}$, resulting in bioaccumulation factors (where $BAF_{plant\ part} = [PCB]_{plant\ part}/[PCB]_{soil}$) for parts of the plant shoot as high as 2. | PCB transfer to pumpkin plants was primarily via root uptake and translocation. Increased planting density was observed to significantly decrease both plant biomass and plant stem PCB concentrations (to 7.7 μg $g^{-1}$), but did not change plant root PCB concentrations. | Whitfield Äslund et al. (2008) |
| Crude oil enriched with benzo(a) pyrene, Arochlor 1221, Arochlor 1248 and Arochlor 1262 | *Zostera marina* | Spiked sediment was placed in seawater-supplied outdoor ponds and planted with eelgrass turf consisting of shoots and belowground root- rhizome mats. | 60 weeks | The fraction of PCBs removed was somewhat greater and more statistically significant in the middle layer containing most eelgrass plant roots than in the top or bottom layer. | Total PCBs declined by 60% in the presence of plants while none were removed in the unplanted sediment. PCB are translocated from the roots to the shoots and thus could enter the food chain via aquatic organisms feeding on eelgrass leaves. | Huesemann et al. (2009) |

**Table 4** (*continued*)

| PCB (commercial name or congeners) | Plants used | Experimental conditions | Duration of the study | Observations | Main findings | Reference |
|---|---|---|---|---|---|---|
| PCB congeners 28, 52, 101, 118, 138, 153, 180 | *Brassica napus L.* | Greenhouse experiment with two different spiked soils | 75 days | Plants exhibited several fold higher concentrations of the sum of PCB congeners in roots than in shoots. | Depletion of PCB in the rhizosphere was significantly higher in the soil with lower organic matter content. Plant exsudates and microbial processes involved have a positive effect on reduction of PCB concentration mainly in the rhizosphere. | Javorská et al. (2009) |
| Aroclor 1242 and 1260 | *Nicotiana tabacum*, *Solanum nigrum*, *Salix sp.*, *Medicago sativa*, *Silybum marianum*, *Armoracia rusticana*, *Morus rubra and Zea mays* | Different experimental setups: microcosms (pots and buckets in indoor and outdoor systems), and field plots were established at the site. | 10 years | After the year 1999, thistle (*Silybum marianum*) was no longer used, despite its good growth, as PCB removal results did not differ from those of control soil. | There is a variation in performance of different plant species, changing from year to year as effect of different weather conditions, but obtained PCB conversions were comparable between laboratory and field investigations and in vegetated soil better than in control. | Mackova et al. (2009) |
| Mixed contamination: HCH, DDT and PCB | *Raphanus sativus* | Pilot scale study in a historically contaminated site. Triplicate plots of 1 $m^2$ were prepared. Contaminated soil for the test field was plowed to a depth of 20 cm and treated with commercial NPK fertilizer (11% $NH_4^+$, 7% $K^+$, 11% phosphates, 15% sulfates, 100 g per square meter). | 6 months | Root bioconcentration factor (BCF) values were constant and not correlated to log $K_{OW}$. A negative correlation between BCF and log $K_{OW}$ was found for edible bulbs. | Uptake from air was more significant for shoots than the one from soil. | Mikes et al. (2009) |
| Mixed contamination: PCB and heavy metals (e-waste site) | *Oryza sativa*, *Medicago sativa L.*, *Lolium perenne L. and Festuca arundinacea* | Greenhouse phytoremediation experiment. The soil was fertilized with 1.64 g of $KH_2PO_3$ and 2.28 g of $NH_4NO_3$ per kilogram dry weight of soil. Randomly methylated-$\beta$-cyclodextrins (RAMEB) was supplemented with RAMEB crystals at a final concentration of 3.0% (w/w on air-dried soil basis). | 120 days | Higher PCB removal percentages of 25.6–28.5% in rhizosphere soil were observed compared with those of the non-rhizosphere (10.4–16.9%) and unplanted controls (7.3%). The average PCB removal percentages of four plant species increased from 26.9% to 37.1% in the rhizosphere soil with addition of RAMEB. | All the plant candidates were feasible for phytoremediation of PCB polluted soil. Addition of RAMEB increased the PCB bioavailability and stimulated the microbial communities leading to the enhanced PCB degradation. | Shen et al. (2009) |
| PCB contamination from a former transformer and electronic waste stripping and recycling site | *Medicago sativa L.* | Pilot study with two treatments set up in a randomized block design: (1) soil without planting as a control (CK), and (2) soil planted with alfalfa (P). Each treatment was replicated four times, and each plot was 1.8 m long by 1.8 m wide in size. The soil was pretreated with lime. | 2 years | Alfalfa significantly decreased the initial soil PCB concentrations by 31.4% and 78.4%. | Alfalfa significantly increased soil dehydrogenase and FDA esterase activities and soil bacterial diversity. Some PCB-degrading bacteria such as *Chloroflexi* sp. may have contributed to the rhizoremediation of PCB. | Tu et al. (2011b) |
| PCB contamination from a former transformer and electronic waste stripping and recycling site | *Medicago sativa L.*, *Lolium perenne L.*, *Festuca arundinacea* and *Oryza sativa* | Two sets of greenhouse experiments. Glucose, biphenyl and three surfactants (TritonX-100, randomly methylated- $\beta$ -cyclodextrins and $\beta$-cyclodextrin) were used to enhance the phytoremediation process. | 120 days | All the planted treatments had a significantly higher PCB removal percentage (ranging from 25.6 to 28.5%) compared to the unplanted control pots (7.3%). | *Lolium perenne* enhanced with $\beta$-cyclodextrin showed the best PCB removal. Results suggested that PCB removal was mainly contributed by microbial degradation rather than plant uptake or abiotic dissipation | Chen Y. et al. (2010) |
| Mixture of Aroclors 1254/ 1260 Aroclor 1248 | *Amaranthus retroflexus* *Ambrosia artemisifolia* *Brassica nigra* *Cirsium vulgare* *Daucus carota* *Echinochloa crusgalli* *Lythrum salicaria* *Polygonum persicaria* *Setaria viris* *Solidago canadensis* *Soncus asper* *Symphyotrichum ericoides* *Symphyotrichum novae-angliae* *Vicia cracca* *Chrysanthemum leucanthemum* | 2 industrial sites with historic contamination (31 μg $g^{-1}$ and 4.7 μg $g^{-1}$); pilot plots in situ | 3 years | Minimal soil quality may have affected plant growth. *V. cracca* at the Etobicoke site, and *P. persicaria* at the Lindsay site achieved shoot BAFs $>1$. | All species accumulated PCB in their root and shoot tissues. The plants studied showed potential for the phytoremediation of PCB, considering theoretical density values. Variations in environmental conditions such as precipitation and temperature likely affected plant growth, and thus potentially the plant tissue concentrations. The variation in these results highlights the necessity of conducting field research rather than just controlled experiments. | Ficko et al. (2010) |

(*continued on next page*)

**Table 4** (*continued*)

| PCB (commercial name or congeners) | Plants used | Experimental conditions | Duration of the study | Observations | Main findings | Reference |
|---|---|---|---|---|---|---|
| PCB contamination from a former transformer and electronic waste stripping and recycling site | *Medicago sativa L.* | Pilot plots *in situ* with 20 cement quadrats (1.2 m long × 1.2 m wide × 1.0 m deep). Inoculum of the AM fungus *Glomus caledonium* 90036 and *Rhizobium* cultures were added to the soil. | 180 days | Inoculation with *R. meliloti* had a greater effect than *G. caledonium* on the yield parameters. When alfalfa was inoculated with both, shoot and root dry biomass and root nodule dry weight were significantly greater compared with those inoculated with only *G. caledonium* or uninoculated plants ($p<0.05$). | Planting with alfalfa significantly reduced soil PCB concentrations compared with the control. Soil PCB concentrations were lowest in the dual inoculation treatment. Synergistic interactions between fungi and plants may have great potential to enhance phytoremediation. | Teng et al. (2010) |
| PCB contamination from a former industrial site | *Cucurbita pepo ssp. Pepo*<br>*Bidens cernua*<br>*Chenopodium album*<br>*Daucus carota*<br>*Plantago major*<br>*Rumex crispus* | Greenhouse experiment with a 12-h photoperiod and a set temperature of 25 °C. Soil moisture was monitored on a daily basis, and containers were watered as necessary. | 51 to 171 days | Plants from both the control group and the root exudate group extracted a combined total of ~1.2% PCB from soil. | First report of significant changes in the PCB phytoextraction ability of multiple plant species due to the presence of root exudates. Root exudates of C. *pepo ssp. pepo* can affect the uptake and transport of contaminants within specific plant species. | Ficko et al. (2011) |
| Mixed contamination: PCB, PAH and heavy metals | *Salix miyabeana* | 2 pilot studies in a Canadian former oil refinery | 4 months | High mortality rates were obtained when trying to reach deeper layers through long rooted willow rods, probably due to prolonged submersion periods (i.e. anoxia) or plant sensitivity to certain pollutants or a combination of the two. | PCB concentration decreased deep in the soil. Tissue analysis revealed no traces of organic pollutants in the plants. | Guidi et al. (2011) |
| Mixed contamination: PCB (Delor 106 or Aroclor 1260) and PAH | *Zea mays_L*, *Helianthus annuu*, *Populus nigra x P. maximowiczii Salix x smithiana* | Pilot study in a former waste incinerator site. The plants were treated ordinarily (watering, weeding) and fertilized by addition of 30 g $m^{-1}$ $NH_4NO_3$ for each of the vegetation periods. | 2 years | Maize and sunflower roots accumulated the most considerable amount of congeners No 138, 153 and 180. | *Zea mays_L* and *Helianthus annuu* accumulated hexa- and heptachlorobiphenyl congeners more than tri-, tetra-, and pentachlorobiphenyl congeners. | Kacálková and Tlustoš (2011) |
| Mix of PCB congeners (8, 9, 10, 18, 28, 44, 52, 66, 77, 81, 95, 97, 105, 118, 149, 153 and 169) | *Salix alaxensis* and *Picea glauca* | Microcosm setup: 10 g of PCB spiked soil moistened with 400 μL sterile water. For plant treatments, 1 g crushed fine roots (willow or spruce) was added to individual microcosms. | 180 days | Soils treated with willow root or biphenyl showed significantly greater losses ($p<0.05$) in several PCB congeners beyond what was observed in untreated soils. | *S. alaxensis* may be an effective plant for rhizoremediation by altering microbial community structure, enhancing the loss of some PCB congeners and reducing the toxicity of the soil environment. | Slater et al. (2011) |
| Mix of PCB congeners (15, 28, 47) | *Zea mays* | Hydroponic experiment. The photoperiod was set 14 h $d^{-1}$ at a light intensity of 250 μmol $m^{-2}$ $s^{-1}$ provided by supplementary illumination. The day/night temperature regime was 25 °C/20 °C and the relative humidity was maintained 60–70%. | 216 h | Metabolites were detected, suggesting the existence of in vivo metabolism of PCB. | A significantly positive correlation was found between log RCF (root concentration factor) and log $K_{ow}$, suggesting a control role of their partitioning in plant uptake. | Wang et al. (2011) |
| Mixed contamination: PCB, hydrocarbons and heavy metals | *Populus nigra* | Pilot study. The size of each of the two field plots was approximately 0.25 ha. One of the plots was amended with horse manure (HM). | 1 year | An increase in dehydrogenase activity was observed in the HM + P compared to the HM treatment. Finally, preliminary protein SDS-PAGE results have permitted the identification of proteins that have been recovered in the HM + P soil with respect to the HM. | The decrease of both inorganic (metals) and organic (TPH and PCB) contaminants in the amended soil shows the effectiveness of the phytoremediation system. | Doni et al. (2012) |
| Mix of PCB congeners (total PCB concentration 110 mg $kg^{-1}$). | *Nicotiana tabacum*<br>*Solanum nigrum* | Nine different microcosms were constructed using 300 g of contaminated soil, two different plant species (tobacco and nightshade) and various bacterial strains (strains of *Pseudomonas* spp. and *Ochrobactrum* sp. strain KH-6). | 3 months | Nightshade absorbs higher amount of PCB, but tobacco can transfer PCB to leaves and stem more efficiently. This is important because plants containing PCB are harvested whereas roots can be disrupted during the harvest and can remain in the soil. | The combination of tobacco and *Pseudomonas* sp. KG3 leads to the best biodegradation results | Kurzawova et al. (2012) |

**Table 4** (*continued*)

| PCB (commercial name or congeners) | Plants used | Experimental conditions | Duration of the study | Observations | Main findings | Reference |
|---|---|---|---|---|---|---|
| Mixed contamination: Cd, Cu and PCB | *Sedum plumbizincicola* *Elsholtzia splendens* *Medicago sativa* *Houttuynia cordata* | Real contaminated soil was used in a glasshouse experiment and a field microcosm experiment with different intercropping combinations. In the 2nd year some plots of soil were amended with lime. | 2 years | Adding lime to unplanted soil promoted a decrease in PCB of 25.2%. | *M. sativa* monoculture, *M. sativa* intercropped with *E. splendens*, *M. sativa with E. splendens* and *S. plumbizincicola*, and *M. sativa* with *S. plumbizincicola* (all with lime) showed declines in PCB of 7.6, 20.1, 47.7, and 42.8%, respectively, compared to the control soil with lime. | Wu et al. (2012) |

(Agarwal et al., 2007). Eek et al. (2008) used a laboratory microcosm to demonstrate that the flux of PCB is reduced by 99% when using a 10 cm capping layer. In PCB contaminated soils asphalt caps were used (Table 1).

Caps can also be modified by additives that actively immobilize PCB or destroy them. One example is activated carbon, which according to Cho et al. (2007) may provide enhanced immobilization by strongly partitioning PCB onto its surface. The concept has been tested in a pilot study in Hunters Point Shipyard, in San Francisco, USA (Cho et al., 2009, 2012) in which activated carbon added to the capping layer (3.7% dry wt.) decreased the transfer of PCB from sediments into the aquatic media by up to 73%, during a 5-year span. A more elaborate reactive cap/barrier was proposed by Choi et al. (2009) consisting of pellets of reactive activated carbon (RAC) with zero-valent iron coated with palladium, contained between thin geo-textile membranes. These caps can be installed horizontally at the bottom of estuaries and river banks or alternatively, the RAC can be directly mixed with the PCB-contaminated matrix for sequestration of PCB upon desorption into the aqueous phase, or set-up as a permeable reactive barrier for flow-through groundwater treatment (Choi et al., 2009).

The use of biochar (carbon rich by-product of the thermal decomposition of organic matter under low oxygen concentrations) to reduce PCB bioavailability has been tested in historically contaminated soils, showing a maximum of 89% reduction in PCB root concentration in phytoextractor *Cucurbita pepo ssp.* (Denyes et al., 2012). Other recent study found that biochars had high adsorption affinity for PCB and also that the presence of humic acids and metal cations increased PCB sorption (Wang et al., 2013). Two comprehensive reviews on the biochars' potential for use in contaminated soils (Beesley et al., 2011) and on the carbonaceous materials (activated carbon and biochar) for use in sediments (Rakowska et al., 2012) can be found in the literature.

### 3.1.4. Thermal treatment — microwave energy

Microwave energy can be used for soil remediation, since most soil constituents are transparent to microwave and thus the applied energy is concentrated on contaminants and pore water. Depending on the types of contaminants, soil properties, and the addition of microwave absorbers, the microwave energy may remove or immobilize contaminants through various mechanisms such as thermal desorption, destruction, and vitrification (Wu, 2008).

A series of studies on the decomposition of hexachlorobenzene (HCB), pentachlorophenol (PCP), PCB, and polycyclic aromatic hydrocarbons (PAH) using microwave energy were developed with a modified aluminum bomb that allows the circulation of air around a quartz insert, preventing the hot-spot problem (Abramovitch et al., 1998, 1999a,b). The decomposition of 2,2′,5,5′-tetrachlorobiphenyl in soil was remarkable, ranging from 97.9% (using $Cu_2O$/10 N NaOH) to 87.7% (using Al/10 N NaOH) (Abramovitch et al., 1998). In these experiments very small samples (from 1 to 6 g of soil) were used and the authors mention no aging of the spiking.

Other tests were conducted with graphite and metal rods. The use of graphite powder led to much less decomposition of 2,2′,4,4′,5,5′-hexachlorobiphenyl (47.2%) in soil; however, complete decomposition was achieved for most of the other PCB (Abramovitch et al., 1999b). Based on the determination of the decomposed products, the possible

**Table 5**
Summary of studies on reductive dechlorination of PCB.

| PCB (commercial name or congeners) | Catalyst | Breakdown products | Temperature | Reference |
|---|---|---|---|---|
| Aroclor 1260 and Aroclor 1254 | 0.05% w/w palladium/iron bimetallic system | Biphenyl | Ambient | Grittini et al. (1995) |
| Mix of PCB congeners | Carbon-supported catalysts (Pd/C, Rh/C) | Biphenyl and phenylcyclohexane | <82 °C | Ukisu et al. (1996) |
| Aroclor 1254 | Zero valent iron nanoparticles (nZVI) | Biphenyl | Ambient | Wang and Zhang (1997) |
| Aroclor 1260 | Zero valent iron with sub-critical water | Mix of lower chlorinated congeners | 250 °C | Yak et al. (1999) |
| Aroclor 1254 | Zero valent lead and copper with sub-critical water | Biphenyl | 350 °C | Kubátová et al. (2003) |
| 2,2′-dichlorobiphenyl; 2,4′-dichlorobiphenyl; 2,3,4-trichlorobiphenyl; 2,2′,3,5′-tetrachlorobiphenyl; 2,2′,4,5′-tetrachlorobiphenyl; 3,3′,4,4′-tetrachlorobiphenyl; | Microscale and nanoscale zero valent iron in a water/methanol solution | Mix of lower chlorinated congeners | Ambient | Lowry and Johnson (2004) |
| Mono- and dichlorobiphenyls | Raney Ni–Al alloy in a dilute aqueous alkaline solution | Biphenyl and/or phenylcyclohexane | Ambient | Liu et al. (2009) |
| Transformer oil with PCB | 57.6% wt Ni on $SiO_2$–$Al_2O_3$ | Mix of congeners | 150–300° | Veriansyah et al. (2009) |
| Aroclor 1242 and Concentrated (nondiluted) used PCB from a capacitator | Palladium on carbon (Pd/C) and triethylamine as electron donor | Tri and tetrabiphenyls (average chlorine numbers: 3.42) | Ambient | Monguchi et al. (2010) |
| 2,2′,3,5,5′,6-hexachlorobiphenyl | Mg powder, carboxylic acid and alcohol solvents | Biphenyl | Ambient | Maloney et al. (2011) |
| 2-chlorobiphenyl | Bimetallic Pd/Al particles | Biphenyl | Ambient | Yang et al. (2011) |

**Table 6**
Comparative analysis of remediation technologies for contaminated soils and sediments.

| Technology | Development stage | Field testing | Cost indication | Clean up time | Effectiveness | Social Acceptability | Major advantages | Possible disadvantages |
|---|---|---|---|---|---|---|---|---|
| *In situ* methods | | | | | | | | |
| *Biological treatment* | | | | | | | | |
| Bioremediation | Initial stage | Limited | Low to moderate[a] | Long | Variable | Moderate | Natural process. Improves the overall quality and texture of soils. Different technologies are available and enhancements can be made to improve efficiency: addition of nutrients nitrogen, phosphorus, ammonium chloride, supplementary carbon sources (sugars, organic acids, glutamate and so on), oxygen (peroxide), primers (polybrominated biphenyl), and by analog enrichment (adding biphenyl); by augmentation of the indigenous population with exogenous cultured inoculums (established PCB degraders). | The rate of PCB removal may be orders of magnitude slower in nature than as established in the laboratory because of mass transfer limitations leading to reduced metabolic availability, shortage of one or more crucial nutrients, preferential metabolism of other easy-to-digest substrates, presence of microbial predators and toxins, and other environmental factors that can drastically constrain the microbial metabolism. Very sensitive to temperature, moisture content, the geology/morphology of the site and the congeners to be remediated. Potential for inhibition of biological processes owing to the heavy metals and other toxic compounds found in real contaminated soils and sediments. Inability of introduced microbes to grow to sufficient depths to reach contaminants. |
| Phytoremediation | Practical stage | Substantial | Low to moderate[b] | Long | Variable | High | Natural process. Improves the overall quality and texture of soils. Plants provide groundcover and minimize soil erosion. There is no size restriction for sites. High public acceptance. | Bioaccumulation depends on soils properties, including organic carbon content, soil pH and nutrient levels. Plant stress factors can affect efficiency; high concentrations of contaminants inhibit plant growth. Plant disposal needs to be assessed to prevent pollution transfer. |
| *Natural attenuation* | Practical stage | Substantial | Low | Long | Variable | High | Natural biological, physical and chemical processes. It can be carried out with little or no site disruption. | Intensive and long lasting monitoring process is necessary. It often requires more time to achieve cleanup goals than other conventional remediation methods. It is difficult to predict with high reliability the performance of natural attenuation. |
| *Physical methods* (capping) | Practical stage | Substantial | Moderate to High[c] | No indication possible | No indication possible | High | This technology relies on containment, rather than treatment, of the contaminated media to limit risk. In sediments, it is suitable for sites with low to moderate natural hydrodynamics and navigational traffic and fine-grained cohesive sediments. The use of active/reactive caps can be promising. | There is no guarantee of the destruction of the contaminant. It is necessary to define standards to determine cap deployment, optimal cap thickness, assessing erosion resistance of the cap, and shielding requirements to storm events. |
| *Thermal treatment* | | | | | | | | |
| Microwave energy | Initial stage | None | High | Fast | Moderate | Moderate | Compared to other thermal treatments, it has shorter heating time, selective heating, better process control, and no direct contact of heated materials. | Limited to the length of the conductor rods and the depth of the water layer, which may absorb and dissipate microwave energy. Humus and bacterial colonies should be reintroduced for the restoration of soils. Occurrence of the hotspot phenomenon, which is a type of thermal instability that results in higher-energy exposure and an increased heating rate in some regions. |

**Table 6** (*continued*)

| Technology | Development stage | Field testing | Cost indication | Clean up time | Effectiveness | Social Acceptability | Major advantages | Possible disadvantages |
|---|---|---|---|---|---|---|---|---|
| *Ex situ* methods | | | | | | | | |
| *Biological treatment* | | | | | | | | |
| Landfarming | Practical stage | Limited | Moderate | Fast | Variable | Moderate | Biological process. Amendments can be added to speed the degradation of the contaminants. Can be effective on organic contaminants with slow degradation rates | Need to control soil conditions to optimize the rate of contaminant degradation. Large amount of space is required. High energy consumption during aeration. Dust control is an important factor, especially during tilling and other material handling operations. Runoff collection facilities must be constructed and monitored. |
| *Thermal treatment* | | | | | | | | |
| Thermal desorption | Practical stage | Substantial | High | Fast | High | Moderate | The efficiency of desorption can be greater than 99%. It is insensitive to contaminant concentration levels in the soil. | Special equipment and conditions can be necessary to prevent formation of dioxins and furans. The presence of water reduces its effectiveness. As well, a high clay or silt content hinders the process. |
| Both *in situ* and *ex situ* methods | | | | | | | | |
| *Chemical methods* | | | | | | | | |
| Dechorination | Initial stage | Limited | High | Fast | High | Moderate | Destroy the PCB molecule but do not break down the biphenyl structure of the molecule. Only the chlorine atoms which give the PCB molecule chemical and biological stability are removed. Rapid treatment time. | Cost of metals and catalysts (needs for stoichiometric or an excess amount of transition metal). Dechlorination is limited by desorption of PCB and require a prolonged contact. Complete dechlorination cannot be achieved in some cases. Harsh reaction conditions (elevated temperatures, for instance) are needed. Iron nanoparticles degradation is faster than PCB. nZVI nanoparticles can be passivated. Concerns about ecotoxicologic effects of nanoparticles. |
| Solvent extraction | Initial stage | Limited | High | Fast | Moderate | Moderate | The solvent can be treated to remove and concentrate the contaminants. The treated solvent can then be reused again in the extraction step. | Large volume of effluent, which are not easily detoxified through conventional or advanced biological treatments. |

Capping methods in soils have usually moderate costs (between 25 and 127 USD per $m^3$).
[a] Enhanced bioremediation through bioestimulation and bioaugmentation have higher costs.
[b] Phytoremediation costs depend on the plants used, soil amendments, annual maintenance.
[c] Reactive caps are more expensive than neutral ones.

mechanisms of PCB decomposition using microwave energy seemed to be self-condensation, dechlorination, oxidation, reduction, hydration, and fragmentation (Wu, 2008).

Microwave-generated steam technology showed promising results on laboratory-scale experiments (Di et al., 2002). Evaporation was identified as the dominant mechanism, moreover, increased solubility of PCB into the heated aqueous phase contributed to their removal from the bound phase (Wu, 2008).

The removal of three PCB in contaminated soil (all above 95%) indicates that $MnO_2$ in combination with microwave irradiation can be a promising technology (Huang et al., 2010).

### 3.2. Ex situ technologies

#### 3.2.1. Biological treatment — landfarming

Landfarming is a bioremediation treatment process performed ex situ in biotreatment cells. Contaminated soils, sediments, or sludges are incorporated into the soil surface and periodically turned over to aerate the mixture.

A pilot-scale land biotreatment was tested with 1500 kg (dry weight) of sediment from industrial lagoons containing waste oils and wastewater from industry operations with PCB mixed with 1500 kg of clean sand (medium to fine grade) (Ghosh et al., 2000). Results showed that the noncoplanar PCB congeners, which are more leachable due to their lower hydrophobicity, are less degraded during landfarming. In the presence of an oil phase, reductions in total PCB may not lead to reductions in aqueous PCB availability (Ghosh et al., 2000).

In another multi-year pilot-scale land treatment project for PAH and PCB, ~1 $m^3$ sludge/sediment materials containing industrial waste were placed in a land treatment unit. The results showed that complete biostabilization can be achieved when reversibly sorbed PAH and PCB are biodegraded, while irreversibly sequestrated PAH and PCB remain in soil particles and therefore present no threat to human health and the environment (Liu et al., 2007b).

It was also demonstrated that PCB degradation in land treatment was caused by a combination of photolysis, volatilization and biodegradation mechanisms, rather than by any single process (Tang and Myers, 2002).

#### 3.2.2. Thermal treatment — thermal desorption

Thermal desorption is an environmental remediation technology that utilizes heat to increase the volatility of contaminants for removal

from the solid matrix (typically soil, sludge or filter cake). Low temperature thermal desorption at around 400 °C is used for the treatment of low and middle distillate organic contaminants such as solvents, gasoline, diesel and lubricating oils (Norris et al., 1999). The contaminated material is continuously fed through a rotary kiln where it is heated to temperatures sufficient to evaporate/combust the contaminants, effectively stripping them from the soil. The volatilized contaminants are then either collected or thermally destroyed. A thermal desorption system therefore has two major components: the desorber itself and the off-gas treatment system (USEPA, 1992). The condensed liquid from cooling the off-gas is separated into organic and aqueous fractions. The organic fraction is removed from the site and depending on its composition, either recycled as a supplemental fuel or destroyed in a fixed base incinerator. The water is either disposed of or used to cool the treated solids and prevent dusting.

Low temperature thermal desorption was found to be the most effective and commercially attractive solution for field application in a South West England case study of a 20 ha telecommunications manufacturing facility contaminated with Aroclor 1254 (up to 1300 mg $kg^{-1}$) (Norris et al., 1999). Experiments showed that thermal desorption resulted in 48–70% decomposition of PCB in sediments, but on the other hand lead to unwanted formation of dibenzofurans (PCDFs) (Sato et al., 2010).

*3.2.3. Chemical treatment — base-catalyzed decomposition*

Base-catalyzed decomposition (BCD) is a catalytic hydrogenation process in which atoms of chlorine are removed from molecules and replaced by hydrogen atoms. Contaminated soil is mixed with sodium bicarbonate or sodium hydroxide and a carrier oil, which acts both as suspension medium and hydrogen donor. The mixture is then heated to about 200–400 °C in a rotary reactor, destroying significant fractions of the PCB by promoting the hydrogenation of bonded chlorines with hydrogen split off from the carrier/donor oil (Hu et al., 2011).

After preliminary studies with PCB in oil solutions (Kawahara and Michalakos, 1997; Taniguchi et al., 1996), a two stage pilot plant was developed to use base-catalyzed decomposition in contaminated soils with relatively low (32–72 mg $kg^{-1}$) and intermediate (350–530 mg $kg^{-1}$) PCB concentrations (Taniguchi et al., 1998). High PCB removals were achieved with temperatures >300 °C and reactor retention time of 1 h and it was found that the optimum reaction temperature was 330 °C and optimum $NaHCO_3$ dosage was 3% (Taniguchi et al., 1998). The need for treating exhaust gas was also identified.

In the USA there is an actual remediation case in a technology transfer report: Production Base Catalyzed Decomposition Process Guam, Mariana Islands (NFESC, 1997), where sodium bicarbonate is used to catalyze the process by desorbing and decomposing PCB at 400 °C. Life Cycle Analysis (LCA) showed that environmental impact of BCD was lower than Infrared High Temperature Incineration (Hu et al., 2011).

*3.3. Both in situ and ex situ technologies — chemical methods*

Extensive research has been conducted on chemical treatment of PCB's solutions and oils. This section focuses on soils and sediments chemical remediation technologies and includes three processes: reductive dechlorination, oxidation and solvent extraction.

*3.3.1. Reductive dechlorination*

Reductive dechlorination successively removes chlorine atoms from PCB generating biphenyl, according to the general chemical equation (Wu et al., 2012):

$$C_{12}H_{(10-m)}C1_m + nH_2 \rightarrow C_{12}H_{(10-m+n)}C1_{m-n} + nHC1, \quad m \geqq n. \qquad (1)$$

This dechlorination can be achieved using catalysts, a reducing agent such as zero-valent iron or a base, as detailed in the following sections.

*3.3.1.1. Catalytic hydrodechlorination.* Catalytic hydrodechlorination of PCB is usually performed with transition metals (e.g. Ni or Pd) and $H_2$ as heterogeneous catalysts and reducing agents (Table 5), respectively, in aqueous or organic solvents.

In contaminated soils, PCB were degraded using Samarium II (Sm) iodide, in the presence of hexamethylphosphoramide in tetrahydrofuran (Jackman et al., 1999). Results at bench-scale showed that Sm catalyzed hydrogenolytic dechlorination of highly chlorinated PCB, generating biphenyl, mono- and dichlorinated biphenyls from Aroclor 1242 in a short timescale, under mild conditions (ambient temperature; inert atmosphere) and with low energy requirements. At a hydrogen pressure of 0.69 MPa or a stream of hydrogen at 338–343°K with stirring, Ehsan et al. (2003) used Pd/γ-$Al_2O_3$ for hydrogenolysis (hydrodechlorination and hydrogenation) of PCB in soil/sediment. Dechlorination was virtually complete, provided that excess catalyst was added to samples with higher PCB loadings prior to reaction, otherwise some partial hydrogenation of biphenyl was observed (Ehsan et al., 2003).

Research with Pd/Mg bimetals in clays showed that PCB dechlorination was governed by its desorption, hence the addition of 10–25% ethanol improved the performance (Agarwal et al., 2009). In the same study, the surfactant TritonX-100 effectively desorbed PCB from historically contaminated sediments, but dechlorination was not observed. Investigating possible causes, researchers found that (i) Pd/Mg effectiveness was limited by the complex PCB distribution in historically contaminated sediments and (ii) sulfide concentration (20 mg $L^{-1}$) in sediments was poisoning Pd, compromising its reactivity (Agarwal et al., 2009). These results show that real contaminated matrices are far more complicated to dechlorinate than only PCB solutions.

Korte et al. (2002) tested the application of palladized iron (Pd/Fe) to dechlorinate PCB at ambient temperature in soil extracts and observed the complete conversion to biphenyl. Dechlorination occurred in a step-wise fashion with the *meta*-chlorines being more reactive than *ortho*-chlorines and with no apparent interferences from asphalt and other miscellaneous debris in the soil (Korte et al., 2002).

*3.3.1.2. Fe-based reductive dechlorination.* A different approach is the use of zero-valent iron nanoparticles (nZVI). Zero-valent iron (millimetric particles) has been used in the remediation of contaminated aquifers in permeable reactive barriers (PRB) for about 20 years (USEPA, 2011b). This metal acts as a reducing agent to transform contaminants, being consumed in the process, unlike catalysts (Comba et al., 2011). With the development of nanotechnology, highly reactive nZVI due to their large surface area were tested successfully for the transformation and detoxification of a wide variety of environmental contaminants, such as chlorinated organic solvents, organochlorine pesticides and PCB in groundwater (Wang and Zhang, 1997; Zhang, 2003). Although previous data (Table 5) showed promising results in PCB dechlorination, a field assessment of in situ injection of carboxymethyl cellulose stabilized nZVI, in California, showed that, after two weeks, nZVI had exhausted their reducing power (He et al., 2010). However, the injection of nZVI and the abiotic reductive dechlorination process appeared to have boosted a long-term in situ biological dechlorination thereafter (He et al., 2010). A reduction of 87% of PCB 1242 concentration was evident in one of the monitoring wells.

Other researchers have successfully dechlorinated PCB in contaminated soils using nZVI (Varanasi et al., 2007). However, for achieving the minimum total PCB destruction efficiency of 95% high temperatures (300 °C) were used. Factors like pH can play a very important role in PCB dechlorination by nZVI and it was shown that a weakly acid pH can increase the dechlorination rate (Wang et al., 2012).

Recently, a new approach to combine two different nanomaterials – activated carbon that adsorbs organic pollutants and nZVI that dechlorinate PCB – was made through a low-cost composite using pinewood sawdust and ferric chloride as starting materials in one-step synthesis (Liu and Zhang, 2010). This composite exhibited

an efficient dechlorination of PCB at room temperature, and the dechlorinated products could be completely adsorbed (Liu and Zhang, 2010). However, this porous carbon nZVI was only tested in aqueous solutions and not in real contaminated soils or sediments.

*3.3.1.3. Sodium dispersion.* In the sodium dispersion processes, sodium salts are added to the contaminated media and react with the chlorine atoms in the PCB, to form sodium chloride and biphenyl. A sample of soil from a controlled landfill, after being submitted to a high energy milling technique, was treated with powdered $NaBH_4$, obtaining complete abatement with a starting PCB concentration of about 2600 mg $kg^{-1}$ (Aresta et al., 2003). Results showed that the efficiency of PCB extraction depended on the soil's specific surface and that boron is found as boric acid in the soil and is unrecoverable (Aresta et al., 2003). Although boric acid can occur naturally in soils, boric acid and its sodium borate salts are active ingredients in pesticides used against insects, algae, fungi and weeds and high soil levels of elemental boron are toxic to plants, so attention should be paid to this issue when using this method. The pathways and products of the degradation of PCB by the sodium dispersion method were systematized by Noma et al. (2007) for nine congeners.

Reductions with $Na/NH_3$ were used to dechlorinate PCB at bench-scale with diffusion controlled rates, at room temperature, in both dry $NH_3$ and with the addition of water (Pittman and He, 2002). This method was able to dechlorinate PCB generating sodium chloride, at ambient temperature and at fast rates (Pittman and He, 2002). According to the same authors, other advantages are i) it works in soils (even clay soils), ii) liquid ammonia handling technology is well known and iii) removal, recovery and recycling of $NH_3$ from soils are easy due to its low boiling point (−33 °C) (Pittman and He, 2002). However it is a very aggressive method for soils and in acidic sites results in $NH_4^+$ retention. The amount of retention depends upon the number and strength of acid functions in the soil and the stripping temperature that can regenerate $NH_3$. Soil pH adjustment after treatment may also be employed (Pittman and He, 2002), given that pH increases to 9 or above. The addition of $NH_3$ to soil produces high osmotic potential, affects negatively the populations of soil microorganisms and solubilizes the organic matter in soil. All these environmental impacts should be considered before using this technique both in situ and ex situ.

*3.3.1.4. Photocatalytic dechlorination.* Bench-scale studies have demonstrated that solar radiation can be effectively used to dechlorinate PCB (Aroclor 1254) to biphenyl in 2-propanol in the presence of a trace amount of phenothiazine (Hawari et al., 1992). Other researchers have tested radiolytic (electron beam) and photolytic (ultraviolet, UV) dechlorination of PCB in a marine sediment (Poster et al., 2003). Sediments have been mixed with aqueous alcohol solutions and irradiated with an electron beam or photolyzed. In the electron beam irradiated samples, the concentrations of 29 PCB congeners decreased with irradiation dose. Photolysis leads to about 60% dechlorination, but only after adding triethylamine (Poster et al., 2003).

The results of bench-scale studies on photocatalytic dechlorination under visible light employing methylene blue (MB) and triethylamine in acetonitrile/water, show that PCB-138 can be efficiently dechlorinated (Izadifard et al., 2010). It was also found that the red region of the light is responsible for the reduction of MB and the UVA-blue region for the dechlorination process. If thermal reducing agents were used instead of amines, it would be possible to dechlorinate PCB with light-emitting diode with an output in the ultraviolet A region (Izadifard et al., 2010).

*3.3.2. Oxidation*

According to Hong et al. (2008), an ozonation technique that incorporated rapid, successive cycles of pressurization (690 kPa) and depressurization, was more effective than conventional ozonation treatment. Near complete or complete removal of PCB could be achieved within shorter ozonation time. This efficiency was due to soil aggregate fracturing upon pressure cycles that exposed the contaminants, as well as by the confluence of PCB and $O_3$ at the gas–liquid interface in the presence of microbubbles. According to Hong et al. (2008) the technique is expected to accelerate $O_3$ treatment of a wide range of organic contaminants, and it may provide treatment to dredged and stored contaminated sediment as well as in situ treatment of excavated soil, increasing the medium's utilization or disposal options. This technology was already tested at pilot scale with an in situ sediment ozonator (Hong, 2008).

The use of catalyzed $H_2O_2$ propagations (CHP; modified Fenton's reagent) was also tested for PCB remediation. This process is based on traditional Fenton's reagent, a laboratory procedure where diluted $H_2O_2$ is slowly added to a solution of excess iron (II) to generate hydroxyl radical (OH•), a strong, relatively nonspecific oxidant (Ahmad et al., 2011). Recent studies at bench-scale with two contaminated soils from Superfund Sites showed that PCB-contaminated soils could be effectively treated using aggressive CHP conditions (Ahmad et al., 2011).

The effectiveness of persulfate oxidation for the destruction of tetrachlorobiphenyl as a representative PCB, in spiked subsurface soils was evaluated by Yukselen-Aksoy et al. (2010). Kaolin and glacial till soils were selected as representative soils; spiked with 50 mg PCB per dry kg of soil and dried for 10 d before the experiments. To achieve effective destruction of PCB temperature and high pH were used as activators (Yukselen-Aksoy et al., 2010).

*3.3.3. Solvent extraction*

Solvent extraction uses an organic solvent as an extractant to separate contaminants from soil or sediments. The organic solvent is usually mixed with the contaminated media in an extraction unit, when the technology is used ex situ. The extracted solution is then passed through a separator, where the contaminants and extractant are separated from the soil or sediment. In situ, solvent extraction can also be called soil flushing.

Experiments at bench and semi-pilot scale with binary solvent mixture of alkanes and alcohols yielded 90% extraction efficiencies for PCB (Nam et al., 2001). However this extraction has to be coupled to chemical dehalogenation or radiolytic degradation (γ-ray irradiation) to ensure PCB degradation. The residual organics in the solvent mixture were removed with activated carbon, and the solvent was recycled for subsequent soil extractions (Nam et al., 2001).

Majid et al. (2002) tested a two-stage extraction process, with a series of three wash steps incorporated into the solid–liquid separation operation using a mixture of hexane with 5% acetone. The results showed an efficiency of 95.4% in the removal of Aroclor 1016 (Majid et al., 2002).

Solvent extraction has also proven to be successful in a full case in Kobe, Japan, where an illegal dumping of PCB capacitors was discovered, leaving about 68 $m^3$ (92 t) of soil contaminated with approximately 6.6 kg of PCB (Takigami et al., 2008). Solvent extraction technology, carried out in 2002–2003, using isopropyl alcohol, remedied the soil on site with a removal efficiency of 98.6% (Takigami et al., 2008).

Bench-scale research has also proved that liquefied dimethyl ether (DME) can be effectively used to extract PCB (99%) and water (97%) from contaminated sediment, and DME can be recovered from the extract and easily reused (Oshita et al., 2010). This technology has the advantage of simultaneously dewatering and decontaminating sediments. Experimental results showed that higher chlorinated PCB (hexachlorobiphenyls) could be extracted more easily than lower chlorinated PCB (di to pentachlorobiphenyls) (Oshita et al., 2010).

When using solvent extraction in situ special care should be taken in the delivery, flow control and recovering of the flushing fluid, to avoid the dispersion of the contaminants or the solvents into the environment and the potential environmental impacts associated.

### 3.4. Combined technologies

To enhance the cost effectiveness of a contaminated site remediation, the combination of different technologies is an approach that has been increasingly used lately. This can be done with complementary or separate technologies used sequentially. In the literature, several bench-case studies can be found, such as using surfactant washing of PCB and aerobic biodegradation (Layton et al., 1998), microwave energy and granular activated carbon (Liu and Yu, 2006), thermal desorption technique and catalytic hydrogenation (Aresta et al., 2008), soya lecithin based soil washing process and photocatalytic treatment of resulting effluents (Occulti et al., 2008), polymer beads (thermoplastic polymer Hytrel™) followed by biodegradation of the extracted PCB in a solid–liquid two-phase partitioning bioreactor (Rehmann and Daugulis, 2008), supercritical fluid carbon dioxide extraction with polymer-stabilized palladium nanoparticles (Wang and Chiu, 2009), Pd coated iron and an aerobic bacterium (He et al., 2009), zero-valent metals and hydrogenation catalysts (DeVor et al., 2009), chemical and photodegradation, more specifically $H_2O_2$ in combination with sunlight irradiation (Dasary et al., 2010), electrocatalytic dechlorination with a palladium loaded carbon nanotubes cathode (S. Chen et al., 2010), microwave-irradiated manganese dioxide (Huang et al., 2010), multiwalled carbon nanotubes coupled with $\beta$-cyclodextrin (Shao et al., 2010), microwave irradiation and chemical dechlorination (Liu et al., 2011a), biosurfactants and bioremediation (Liu et al., 2011b); soil washing and $TiO_2$ photocatalytic degradation (Zhu et al., 2012) or persulfate oxidation enhanced with electrokinetics (Yukselen-Aksoy and Reddy, 2012). These studies show promising results, but no pilot scale or field application has been developed so far.

## 4. Assessment for full-scale implementation

The technologies previously described, although aiming to destroy or transform PCB, operate in very different ways and consequently have different clean up times, costs, breakdown products and environmental impacts. Their effectiveness is also site specific, since each technology depends on the contaminants (in most cases, a mix of organic and inorganic pollutants and, even if the contamination is only due to PCB different mixes of congeners), the aging of the contamination, the type of soil and geomorphologic conditions and other environmental factors (like mobility of the contaminants or sorption to soil particles). Generally biological treatments as bioremediation, phytoremediation and natural attenuation, are long-term processes, but have lower costs and environmental impacts than chemical, physical or thermal treatments, as well as higher public acceptance. Their effectiveness is also less predictable. Life Cycle Assessment has shown that bioremediation has less impact than incineration for PCB contaminated soils, with the lowest environmental footprint being for electric aeration, especially in terms of global warming and depletion of abiotic resources (Busset et al., 2012). At equal distances between the polluted sites and the treatment plant, bioremediation had fewer impacts than incineration in eight out of 13 categories. The impact on global warming was nine times greater for incineration producing $6.5\times10^5$ and $7.2\times10^4$ kg eq. $CO_2$, respectively (Busset et al., 2012).

The technologies based in natural degradation processes are more suitable for matrices with low contaminant concentrations, since the survival of the degrading organisms (microorganisms or plants), even the best adapted ones, can be affected by the toxicity associated to highly contaminated sites (Megharaj et al., 2011; Perelo, 2010; Rein et al., 2007). In the case of PCB, the congeners on site and their bioavailability, via desorption, can strongly limit the biological treatment application. PCB with fewer chlorine atoms are more susceptible to complete aerobic mineralization and higher chlorine content corresponds to recalcitrant behavior. However, these highly chlorinated molecules may be partially degraded through the reductive dechlorination, obtaining congeners containing 2 to 3 atoms of chlorine as major metabolites. The successful results on PCB dechlorination obtained at bench-scale cannot be replicated at full-scale, due to mass transfer limitations (that lead to reduced bioavailability), shortage of essential nutrients, presence of microbial predators and toxins and other environmental factors (e.g. temperature, moisture content, pH). A general predictive model applicable to all field conditions is obviously very hard to implement. Important findings were made related to the understanding of the dechlorination patterns and identification of the species and enzymatic processes involved, but more research is needed at pilot and full-scales to optimize their application and select the enhancements that can be made, in terms of bioaugmentation or biostimulation and also about the use of transgenic species.

Biological treatments can be easily combined with other remediation methods. For example, the coupling of phytoextraction with other soil treatments in the so-called "treatment trains" (use of multiple technologies either sequentially or concurrently) is gaining interest; what may be especially useful in cases where mixed contaminants require the use of more than one technique to effectively remediate sites (Marchiol et al., 2004).

Regarding phytoremediation, the ideal plant should possess multiple traits: fast growing, high biomass, deep roots, easy to harvest and should tolerate (and accumulate) contaminants in their aerial and harvestable parts. For organic pollutants like PCB, it is important to use plants that enhance phytodegradation, instead of phytoextraction and accumulation, given the concerns about pollution transfer, regarding crop disposal, and the risk of accumulation in the trophic chain. If the produced biomass from phytoremediation projects could be valorized, for example as bioenergy, then one main drawback (the long required remediation time) becomes less important and slower-working phytoremediation schemes, based on gradual attenuation of the contaminants rather than short-term forced extraction, could be envisaged. Further research is needed on the potential environmental impacts of the use of transgenic plants for PCB phytoremediation.

Natural attenuation, based on biological, physical and chemical processes, is very challenging to predict with a high reliability in its outcome, so it always implies long-term monitoring. To assess this remediation method, the source control must be documented and a statistically significant decline in contaminant concentration, bioavailability, and biological recovery should be demonstrated. The development of a reliable model to predict future soil or sediment quality is also required in most situations. Natural attenuation cannot be used in sites where ecological and human risks are high, due to the long time associated with the natural processes occurring at the site.

Regarding physical methods, in general, reactive caps may be more suitable than passive caps for highly contaminated sites that carry a risk of imminent exposure (Agarwal et al., 2007). The activated carbon surface in reactive caps may act as a substrate on which microbiota grows, increasing biodegradation of PCB in sediments (Agarwal et al., 2007). The high affinity of organics to such material may also cause a capillary effect, leading to possible extraction and sequestration of organics from deeper sediments (Agarwal et al., 2007; Choi et al., 2009). Other authors defend that this high adsorption capacity and capillary effect of activated carbon might facilitate desorption of PCB from a stable sediment matrix into the liquid phase (Choi et al., 2009). This technology might not be an ultimate solution because slight changes in the capping environment can cause the erosion of the capping layer and re-suspension of the sequestered PCB (Choi et al., 2009). Capping is more expensive than bioremediation or natural attenuation, with increasing costs for reactive caps. The re-suspension of contaminated sediments and the temporary increase of contaminants concentration in the water column associated with the capping placement are important factors to be considered.

Chemical treatments are usually faster and can treat contaminants at higher concentrations, but are more expensive and aggressive to the soil (due to the use of high temperatures, strong acid and alkali). PCB desorption and contact with the reactants can also be limiting

factors. The presence of competing substrates, dissolved solids, dissolved oxygen, etc. will also affect PCB dechlorination or oxidation rate. In the case of solvent extraction, a major drawback is the generation of liquid effluent that requires advanced treatment due to the presence of contaminants.

One of the major disadvantages of thermal treatment is that pollution is transferred from one media (soil) to the other (gas) and therefore it is essential to destroy volatilized substances in the gas phase to prevent pollution transfer and the formation of dioxins and furans. The high-energy requirement (that correspond to higher costs) needed to increase the soil temperature from ambient levels to 400 °C is an important disadvantage.

In their current stage of development, photocatalytic dechlorination technologies are limited in their practical application. A combination of excavating/dredging and subsequent treatment by means of such methods, especially with relatively expensive and potentially toxic additives, would be considered only in very special cases. The use of lime for pH adjustment and substitution of benign substances (such as ascorbate) for the alcohol and the amine could make radiation or photochemical processing into a competitive technology (Poster et al., 2003).

Microwave energy for in situ remediation is limited to the length of the conductor rods and the depth of the water layer, which may absorb and dissipate the energy. This treatment is also aggressive to the soil and can lead to hotspot phenomena (higher-energy exposure and an increased heating rate in some regions).

Ultimately, the selection of the technology to use in each site will be based on its cost-effectiveness and social acceptability, as well as to the ecological and health risks associated with the site. Recently, the adoption of combined or sequential remediation technologies has been studied and progress can be made in this area.

Table 6 summarizes the most important advantages and disadvantages of the technologies described in Section 3. Available information from the literature was systematized/grouped into 6 main parameters, considered by the authors as the most relevant: current development stage and field testing, an indication of associated costs, clean-up time, effectiveness and social acceptance. Most applications are still in an initial stage of development, with most studies and research carried out at bench-scale. Some technologies are in practical stage — were tested at pilot or field scale. In the column "field testing" more information is provided about the degree of existent experience in field application, considering three qualitative levels: none, limited (<10 case studies) and substantial (>10 case studies). The column "cost" provides a qualitative indication of the total cost directly associated with the treatment technology application (capital, operation and maintenance), also considering three levels: low (<25 USD per $m^3$), moderate (between 25 and 127 USD per $m^3$) and high (>127 USD per $m^3$). The cost assessment for the remediation technologies was based in compilations of real costs of soil and sediment remediation available in the literature (Khan et al., 2004; McDade et al., 2005; Summersgill, 2006). Also a qualitative indication of remediation time (fast — from months to 2 years, moderate — from 2 to 10 years, long — decades), effectiveness (as a degree of PCB destruction) and social acceptance is presented in Table 6. The main advantages and disadvantages of the technology application are presented in the last two columns. In both, the dominant features are related to technical issues or to environmental concerns.

## 5. Conclusions

The characteristics that led to a widespread use of PCB in different industrial and domestic applications do present a challenge for the remediation of contaminated soils and sediments. Following PCB entrance into the soil environment, they rapidly sorp to mineral and organic matter (solid phases). The ability to desorb these contaminants determines, in most cases, the effectiveness of the remediation technologies. Promising results were obtained in studies at bench-scale, in controlled laboratorial conditions. Most technologies are still in an initial stage of development and further research in several implementation issues is needed. More field data and pilot scale experiments are essential to assess the effectiveness of these technologies. There is no single, portable technology that is applicable to both ex situ and in situ remediation of PCB in contaminated soils and sediments. Each case is unique and several factors must be considered. The successful treatment of a site depends on proper selection, design, and adjustment of the remediation technology, based on the congeners present, soils properties and on the performance of the system. More recently, the combined use of remediation technologies and the so-called treatment trains is a promising approach for persistent contaminants.

## Acknowledgments

This work has been funded by the European Regional Development Fund (ERDF) through COMPETE – Operational Programme for Competitiveness Factors (OPCF), by the Portuguese National funds through "FCT — Fundação para a Ciência e a Tecnologia" under project "PTDC/AGR-AAM/101643/2008 NanoDC", by the research grant SFRH/BD/76070/2011 and by FP7-PEOPLE-IRSES-2010-269289-ELECTROACROSS project.

## References

Abramovitch RA, Huang BZ, Davis M, Peters L. Decomposition of PCB's and other polychlorinated aromatics in soil using microwave energy. Chemosphere 1998;37:1427–36.

Abramovitch RA, Huang BZ, Abramovitch DA, Song JG. In situ decomposition of PCBs in soil using microwave energy. Chemosphere 1999a;38:2227–36.

Abramovitch RA, Huang BZ, Abramovitch DA, Song JG. In situ decomposition of PAHs in soil and desorption of organic solvents using microwave energy. Chemosphere 1999b;39:81–7.

Abramowicz DA. Aerobic and anaerobic PCB biodegradation in the environment. Environ Health Perspect 1995;103:97–9.

Abscope Environmental Inc. North Adams, MA: remediation of PCB soils. http://www.abscope.com/a5108.php, 2012. [Accessed the 12th November 2012].

Agarwal S, Al-Abed SR, Dionysiou DD. In situ technologies for reclamation of PCB-contaminated sediments: current challenges and research thrust areas. J Environ Eng 2007;133:1075–8.

Agarwal S, Al-Abed SR, Dionysiou DD. A feasibility study on Pd/Mg application in historically contaminated sediments and PCB spiked substrates. J Hazard Mater 2009;172:1156–62.

Ahmad M, Simon MA, Sherrin A, Tuccillo ME, Ullman JL, Teel AL, et al. Treatment of polychlorinated biphenyls in two surface soils using catalyzed $H_2O_2$ propagations. Chemosphere 2011;84:855–62.

Alder AC, Haggblom MM, Oppenheimer SR, Young LY. Reductive dechlorination of polychlorinated biphenyls in anaerobic sediments. Environ Sci Technol 1993;27:530–8.

Alonso F, Beletskaya IP, Yus M. Metal-mediated reductive hydrodehalogenation of organic halides. Chem Rev 2002;102:4009–92.

Aresta M, Caramuscio P, De Stefano L, Pastore T. Solid state dehalogenation of PCBs in contaminated soil using $NaBH_4$. Waste Manag 2003;23:315–9.

Aresta M, Dibenedetto A, Fragale C, Giannoccaro P, Pastore C, Zammiello D, et al. Thermal desorption of polychlorobiphenyls from contaminated soils and their hydrodechlorination using Pd- and Rh-supported catalysts. Chemosphere 2008;70:1052–8.

Bedard DL, Quensen JF. Microbial reductive dechlorination of polychlorinated biphenyls. In: Young LY, Cerniglia CE, editors. Microbial transformation and degradation of toxic organic chemicals. New York: Wiley-Liss; 1995. p. 127–216.

Bedard DL, Ritalahti KM, Loffler FE. The *Dehalococcoides* population in sediment-free mixed cultures metabolically dechlorinates the commercial polychlorinated biphenyl mixture Aroclor 1260. Appl Environ Microbiol 2007;73:2513–21.

Beesley L, Moreno-Jiménez E, Gomez-Eyles JL, Harris E, Robinson B, Sizmur T. A review of biochars' potential role in the remediation, revegetation and restoration of contaminated soils. Environ Pollut 2011;159:3269–82.

Berkaw M, Sowers KR, May HD. Anaerobic *ortho* dechlorination of polychlorinated biphenyls by estuarine sediments from Baltimore Harbor. Appl Environ Microbiol 1996;62:2534–9.

Borazjani H, Wiltcher D, Diehl S. Bioremediation of polychlorinated biphenyl and petroleum contaminated soil. In: Lyon WG, Hong JJ, Reddy RK, editors. Proceedings of the International Conference on Environmental Science and Technology. New Orleans, USA: American Science Press; 2005. p. 502–7.

Borja J, Taleon DM, Auresenia J, Gallardo S. Polychlorinated biphenyls and their biodegradation. Process Biochem 2005;40:1999–2013.

Brown JF, Wagner RE, Feng H, Carnahan JC, May RJ. Environmental dechlorination of PCBs. Environ Toxicol Chem 1987;6:579–93.

Brown RA, Wilson JT, Ferrey M. Monitored natural attenuation forum: the case for abiotic MNA. Remediation 2007;17:127–37.

Busset G, Sangely M, Montrejaud-Vignoles M, Thannberger L, Sablayrolles C. Life cycle assessment of polychlorinated biphenyl contaminated soil remediation processes. Int J Life Cycle Assess 2012;17:325–36.

CCME. Canadian soil quality guidelines for the protection of environmental and human health. Total PCBs. Canadian environmental quality guidelines. Canadian Council of Ministers of Environment; 1999.

Chang BV, Liu WG, Yuan SY. Microbial dechlorination of three PCB congeners in river sediment. Chemosphere 2001;45:849–56.

Chekol T, Vough LR, Chaney RL. Phytoremediation of polychlorinated biphenyl-contaminated soils: the rhizosphere effect. Environ Int 2004;30:799–804.

Chen IM, Chang FC, Hsu MF, Wang YS. Comparisons of PCBs dechlorination occurrences in various contaminated sediments. Chemosphere 2001;43:649–54.

Chen S, Qin ZL, Quan X, Zhang YB, Zhao HM. Electrocatalytic dechlorination of 2,4,5-trichlorobiphenyl using an aligned carbon nanotubes electrode deposited with palladium nanoparticles. Chin Sci Bull 2010;55:358–64.

Chen Y, Tang X, Cheema SA, Liu W, Shen C. $\beta$-cyclodextrin enhanced phytoremediation of aged PCBs-contaminated soil from e-waste recycling area. J Environ Monit 2010;12: 1482–9.

Cho YC, Kwo OS, Sokol RC, Bethoney CM, Rhee GY. Microbial PCB dechlorination in dredged sediments and the effect of moisture. Chemosphere 2001;43:1119–26.

Cho YC, Sokol RC, Frohnhoefer RC, Yullrhee G. Reductive dechlorination of polychlorinated biphenyls: threshold concentration and dechlorination kinetics of individual congeners in Aroclor 1248. Environ Sci Technol 2003;37:5651–6.

Cho YM, Smithenry DW, Ghosh U, Kennedy AJ, Millward RN, Bridges TS, et al. Field methods for amending marine sediment with activated carbon and assessing treatment effectiveness. Mar Environ Res 2007;64:541–55.

Cho YM, Ghosh U, Kennedy AJ, Grossman A, Ray G, Tomaszewski JE, et al. Field application of activated carbon amendment for in-situ stabilization of polychlorinated biphenyls in marine sediment. Environ Sci Technol 2009;43:3815–23.

Cho YM, Werner D, Choi Y, Luthy RG. Long-term monitoring and modeling of the mass transfer of polychlorinated biphenyls in sediment following pilot-scale in-situ amendment with activated carbon. J Contam Hydrol 2012;129–130:25–37.

Choi H, Al-Abed SR, Agarwal S. Catalytic role of palladium and relative reactivity of substituted chlorines during adsorption and treatment of PCBs on reactive activated carbon. Environ Sci Technol 2009;43:488–93.

Comba S, Di Molfetta A, Sethi R. A comparison between field applications of nano-, micro-, and millimetric zero-valent iron for the remediation of contaminated aquifers. Water Air Soil Pollut 2011;215:595–607.

Cutter L, Sowers KR, May HD. Microbial dechlorination of 2,3,5,6-tetrachlorobiphenyl under anaerobic conditions in the absence of soil or sediment. Appl Environ Microbiol 1998;64:2966–9.

D'Angelo E, Nunez A. Effect of environmental conditions on polychlorinated biphenyl transformations and bacterial communities in a river sediment. J Soils Sediment 2010;10:1186–99.

Dasary SSR, Saloni J, Fletcher A, Anjaneyulu Y, Yu H. Photodegradation of selected PCBs in the presence of nano-$TiO_2$ as catalyst and $H_2O_2$ as an oxidant. Int J Environ Res Public Health 2010;7:3987–4001.

Dávila B, Whitford KW, Saylor ES. Technology alternatives for the remediation of PCB-contaminated soil and sediment. Office of Research and Development. Office of Solid Waste and Emergency Response. US Environmental Protection Agency; 1993.

Declercq I, Cappuyns V, Duclos Y. Monitored natural attenuation (MNA) of contaminated soils: state of the art in Europe — a critical evaluation. Sci Total Environ 2012;426: 393–405.

Denyes MJ, Langlois VrS, Rutter A, Zeeb BA. The use of biochar to reduce soil PCB bioavailability to *Cucurbita pepo* and *Eisenia fetida*. Sci Total Environ 2012;437:76–82.

DeVor R, Carvalho-Knighton K, Aitken B, Maloney P, Holland E, Talalaj L, et al. Mechanism of the degradation of individual PCB congeners using mechanically alloyed Mg/Pd in methanol. Chemosphere 2009;76:761–6.

Deweerd KA, Bedard DL. Use of halogenated benzoates and other halogenated aromatic compounds to stimulate the microbial dechlorination of PCBs. Environ Sci Technol 1999;33:2057–63.

Di P, Chang DPY, Dwyer HA. Modeling of polychlorinated biphenyl removal from contaminated soil using steam. Environ Sci Technol 2002;36:1845–50.

Donaldson SG, Oostdam JV, Tikhonov C, Feeley M, Armstrong B, Ayotte P, et al. Environmental contaminants and human health in the Canadian Arctic. Sci Total Environ 2010;408:5165–234.

Doni S, Macci C, Peruzzi E, Arenella M, Ceccanti B, Masciandaro G. In situ phytoremediation of a soil historically contaminated by metals, hydrocarbons and polychlorobiphenyls. J Environ Monit 2012;14:1383–90.

EEA. Progress in management of contaminated sites. European Environment Agency, Report CSI 015. Copenhagen, Denmark, 2007.

Eek E, Cornelissen G, Kibsgaard A, Breedveld GD. Diffusion of PAH and PCB from contaminated sediments with and without mineral capping; measurement and modelling. Chemosphere 2008;71:1629–38.

Ehsan S, Prasher SO, Marshall WD. Estimates of total polychlorinated biphenyl (PCB) compounds in soils/sediments by hydrogenolysis to dicyclohexyl. J Environ Monit 2003;5:644–8.

El-Hadj TB, Dosta J, Torres R, Mata-Álvarez J. PCB and AOX removal in mesophilic and thermophilic sewage sludge digestion. Biochem Eng J 2007;36:281–7.

EPA. Industrial waste resource guidelines. Environment protection (industrial waste resource) regulations 2009. Environmental Protection Agency Victoria; 2009 [Publication IWRG643.1. September].

Fava F, Piccolo A. Effects of humic substances on the bioavailability and aerobic biodegradation of polychlorinated biphenyls in a model soil. Biotechnol Bioeng 2002;77: 204–11.

Ficko SA, Rutter A, Zeeb BA. Potential for phytoextraction of PCBs from contaminated soils using weeds. Sci Total Environ 2010;408:3469–76.

Ficko S, Rutter A, Zeeb B. Effect of pumpkin root exudates on ex situ polychlorinated biphenyl (PCB) phytoextraction by pumpkin and weed species. Environ Sci Pollut Res 2011;18:1536–43.

Fogel S, Findlay M, Smoler D. PCB biodegradation by a sediment-dree *Dehalococcoides* culture grown on trichlorobenzenes. Poster. Battelle Conference — Remediation of Chlorinated and Recalcitrant Compounds, Monterey, California, 12-14 May, 2012; 2012.

Furukawa K, Fujihara H. Microbial degradation of polychlorinated biphenyls: biochemical and molecular features. J Biosci Bioeng 2008;105:433–49.

GE. Periodic review available to the public. General Electric Spokane Site, 4323 East Mission Avenue, Spokane, Spokane County, Washington, Facility Site ID 630; 2008.

Gerhardt KE, Huang X-D, Glick BR, Greenberg BM. Phytoremediation and rhizoremediation of organic soil contaminants: potential and challenges. Plant Sci 2009;176:20–30.

Ghosh U, Weber AS, Jensen JN, Smith JR. Relationship between PCB desorption equilibrium, kinetics, and availability during land biotreatment. Environ Sci Technol 2000;34: 2542–8.

Gomes HI. Phytoremediation for bioenergy: challenges and opportunities. Environ Technol Rev 2012:1–8.

Gorbunova TI, Saloutin VI, Chupakhin ON. Chemical methods of transformation of polychlorobiphenyls. Russ Chem Rev 2010;79:511–30.

Grittini C, Malcomson M, Fernando Q, Korte N. Rapid dechlorination of polychorinated biphenyls on the surface of a Pd/Fe bimetallic system. Environ Sci Technol 1995;29:2898–900.

Guidi W, Kadri H, Labrecque M. Establishment techniques to using willow for phytoremediation on a former oil refinery in southern Quebec: achievements and constraints. Chem Ecol 2011;28:49–64.

Haluska L, Baranciková G, Baláz S, Dercová K, Vrana B, Paz-Weisshaar M, et al. Degradation of PCB in different soils by inoculated *Alcaligenes xylosoxidans*. Sci Total Environ 1995;175:275–85.

Hawari J, Demeter A, Samson R. Sensitized photolysis of polychlorobiphenys in alkaline 2-propanol: dechlorination of Aroclor 1254 in soil samples by solar radiation. Environ Sci Technol 1992;26:2022–7.

He N, Li P, Zhou Y, Fan S, Ren W. Degradation of pentachlorobiphenyl by a sequential treatment using Pd coated iron and an aerobic bacterium (*H1*). Chemosphere 2009;76:1491–7.

He F, Zhao D, Paul C. Field assessment of carboxymethyl cellulose stabilized iron nanoparticles for in situ destruction of chlorinated solvents in source zones. Water Res 2010;44:2360–70.

Ho CH, Liu SM. Effect of coplanar PCB concentration on dechlorinating microbial communities and dechlorination in estuarine sediments. Chemosphere 2011;82:48–55.

Hong A. In situ sediment ozonator for remediation of PCB, PAH, DDT and other recalcitrant chemicals. Salt Lake City, UT: NOAA/UNH Cooperative Institute for Coastal and Estuarine Environmental Technology (CICEET); 2008.

Hong PKA, Nakra S, Kao CMJ, Hayes DF. Pressure-assisted ozonation of PCB and PAH contaminated sediments. Chemosphere 2008;72:1757–64.

Hopf NB, Ruder AM, Succop P. Background levels of polychlorinated biphenyls in the U.S. population. Sci Total Environ 2009;407:6109–19.

Hu X, Zhu J, Ding Q. Environmental life-cycle comparisons of two polychlorinated biphenyl remediation technologies: incineration and base catalyzed decomposition. J Hazard Mater 2011;191:258–68.

Huang G, Zhao L, Dong Y, Zhang Q. Remediation of soils contaminated with polychlorinated biphenyls by microwave-irradiated manganese dioxide. J Hazard Mater 2010;186: 128–32.

Huesemann MH, Hausmann TS, Fortman TJ, Thom RM, Cullinan V. In situ phytoremediation of PAH- and PCB-contaminated marine sediments with eelgrass (*Zostera marina*). Ecol Eng 2009;35:1395–404.

Izadifard M, Langford CH, Achari G. Photocatalytic dechlorination of PCB 138 using leuco-methylene blue and visible light; reaction conditions and mechanisms. J Hazard Mater 2010;181:393–8.

Jackman SA, Knowles CJ, Robinson GK. SACRED — a novel catalytic process for the environmental remediation of polychlorinated biphenyls (PCBs). Chemosphere 1999;38:1889–900.

Javorská H, Tlustoš P, Kaliszová R. Degradation of polychlorinated biphenyls in the rhizosphere of rape, *Brassica napus* L. Bull Environ Contam Toxicol 2009;82:727–31.

Kacálková L, Tlustoš P. The uptake of persistent organic pollutants by plants. Cent Eur J Biol 2011;6:223–35.

Kalinovich I, Rutter A, Poland JS, Cairns G, Rowe RK. Remediation of PCB contaminated soils in the Canadian Arctic: excavation and surface PRB technology. Sci Total Environ 2008;407:53–66.

Kaštánek F, Demnerová K, Pazlarová J, Burkhard J, Maléterová Y. Biodegradation of polychlorinated biphenyls and volatile chlorinated hydrocarbons in contaminated soils and ground water in field condition. Int Biodeter Biodegr 1999;44:39–47.

Kawahara FK, Michalakos PM. Base-catalyzed destruction of PCBs — new donors, new transfer agents/catalysts. Ind Eng Chem Res 1997;36:1580–5.

Khan FI, Husain T, Hejazi R. An overview and analysis of site remediation technologies. J Environ Manage 2004;71:95-122.

Kim J, Rhee GY. Reductive dechlorination of polychlorinated biphenyls as affected by sediment characteristics. Chemosphere 2001;44:1413–20.

Kim J, Frohnhoefer RC, Cho YC, Cho W, Rhee GY. Reductive dechlorination of low concentration polychlorinated byphenyls as affected by a rhamnolipid biosurfactant. J Microb Biotechnol 2008;18:1564–71.

Kolar AB, Hrsak D, Fingler S, Cetkovic H, Petric I, Kolic NU. PCB-degrading potential of aerobic bacteria enriched from marine sediments. Int Biodeterior Biodegrad 2007;60:16–24.

Komancová M, Jurcová I, Kochánková L, Burkhard J. Metabolic pathways of polychlorinated biphenyls degradation by *Pseudomonas* sp. 2. Chemosphere 2003;50:537–43.

Korte NE, West OR, Liang L, Gu B, Zutman JL, Fernando Q. The effect of solvent concentration on the use of palladized-iron for the step-wise dechlorination of polychlorinated biphenyls in soil extracts. Waste Manag 2002;22:343–9.

Krumins V, Park JW, Son EK, Rodenburg LA, Kerkhof LJ, Haggblom MM, et al. PCB dechlorination enhancement in Anacostia river sediment microcosms. Water Res 2009;43:4549–58.

Kubátová A, Herman J, Steckler TS, Veil M, Miller DJ, Klunder EB, et al. Subcritical (hot/liquid) water dechlorination of PCBs (Aroclor 1254) with metal additives and in waste paint. Environ Sci Technol 2003;37:5757–62.

Kuo CE, Liu SM, Liu C. Biodegradation of coplanar polychlorinated biphenyls by anaerobic microorganisms from estuarine sediments. Chemosphere 1999;39:1445–58.

Kurzawova V, Stursa P, Uhlik O, Norkova K, Strohalm M, Lipov J, et al. Plant/microorganism interactions in bioremediation of polychlorinated biphenyl-contaminated soil. New Biotechnol 2012;30:15–22.

Layton AC, Lajoie CA, Easter JP, Muccini M, Sayler GS. An integrated surfactant solubilization and PCB bioremediation process for soils. Biorem J 1998;2:43–56.

Liu X, Yu G. Combined effect of microwave and activated carbon on the remediation of polychlorinated biphenyl-contaminated soil. Chemosphere 2006;63:228–35.

Liu Z, Zhang FS. Nano-zerovalent iron contained porous carbons developed from waste biomass for the adsorption and dechlorination of PCBs. Bioresour Technol 2010;101:2562–4.

Liu L, Tindall JA, Friedel MJ. Biodegradation of PAHs and PCBs in soils and sludges. Water Air Soil Pollut 2007a;181:281–96.

Liu Y, Phenrat T, Lowry GV. Effect of TCE concentration and dissolved groundwater solutes on nZVI-promoted TCE dechlorination and $H_2$ evolution. Environ Sci Technol 2007b;41:7881–7.

Liu GB, Tashiro M, Thiemann T. A facile method for the dechlorination of mono- and dichlorobiphenyls using Raney Ni–Al alloy in dilute aqueous solutions of alkali hydroxides or alkali metal carbonates. Tetrahedron 2009;65:2497–505.

Liu X, Zhao W, Sun K, Zhang G, Zhao Y. Dechlorination of PCBs in the simulative transformer oil by microwave-hydrothermal reaction with zero-valent iron involved. Chemosphere 2011a;82:773–7.

Liu Y, Ma M, Shi Z. Application of Rhamnolipid biosurfactant for removing polychlorinated biphenyls from contaminated soil. Adv Mater Res 2011b;233–235:608–13.

Lowry G, Johnson K. Congener-specific dechlorination of dissolved PCBs by microscale and nanoscale zerovalent iron in a water/methanol solution. Environ Sci Technol 2004;38:5208–16.

Mackova M, Barriault D, Francova K, Sylvestre M, Möder M, Vrchotova B, et al. Phytoremediation of polychlorinated biphenyls. In: Mackova M, Downling DN, Macek T, editors. Phytoremediation rhizoremediation. Dordrecht, The Netherlands: Springer; 2006. p. 143–67.

Mackova M, Prouzova P, Stursa P, Ryslava E, Uhlik O, Beranova K, et al. Phyto/rhizoremediation studies using long-term PCB-contaminated soil. Environ Sci Pollut Res 2009;16:817–29.

Maestri E, Marmiroli N. Transgenic plants for phytoremediation. Int J Phytoremediation 2011;13:264–79.

Magar VS, Wenning RJ. The role of monitored natural recovery in sediment remediation. Integr Environ Assess Manag 2006;2:66–74.

Magar VS, Chadwick DB, Bridges TS, Fuchsman PC, Conder JM, Dekker TJ, et al. Monitored natural recovery at contaminated sediment sites. Technical Guide. ENVIRON International Corp, ESTCP Project ER-0622, ADA512822, Arlington, VA, USA; 2009.

Magee KD, Michael A, Ullah H, Dutta SK. Dechlorination of PCB in the presence of plant nitrate reductase. Environ Toxicol Pharmacol 2008;25:144–7.

Majid A, Argue S, Sparks BD. Removal of Aroclor 1016 from contaminated soil by solvent extraction soil agglomeration process. J Environ Eng Sci 2002;1:59–64.

Maloney P, DeVor R, Novaes-Card S, Saitta E, Quinn J, Clausen CA, et al. Dechlorination of polychlorinated biphenyls using magnesium and acidified alcohols. J Hazard Mater 2011;187:235–40.

Manzano MA, Perales JA, Sales D, Quiroga JM. Enhancement of aerobic microbial degradation of polychlorinated biphenyl in soil microcosms. Environ Toxicol Chem 2003;22:699–705.

Marchiol L, Assolari S, Sacco P, Zerbi G. Phytoextraction of heavy metals by canola (*Brassica napus*) and radish (*Raphanus sativus*) grown on multicontaminated soil. Environ Pollut 2004;132:21–7.

Marmiroli N, McCutcheon SC. Making phytoremediation a successful technology. In: Mc-Cutcheon SC, Schnoor JL, editors. Phytoremediation: transformation and control of contaminants. Hoboken (NJ): Wiley-Interscience, Inc.; 2003. p. 75-107.

Masuda Y, Schecter A, Papke O. Concentrations of PCBs, PCDFs and PCDDs in the blood of Yusho patients and their toxic equivalent contribution. Chemosphere 1998;31:1773–80.

McDade JM, McGuire TM, Newell CJ. Analysis of DNAPL source-depletion costs at 36 field sites. Remediation 2005;15:9-18.

Meagher RB. Phytoremediation of toxic elemental and organic pollutants. Curr Opin Plant Biol 2000;3:153–62.

Megharaj M, Ramakrishnan B, Venkateswarlu K, Sethunathan N, Naidu R. Bioremediation approaches for organic pollutants: a critical perspective. Environ Int 2011;37:1362–75.

Mehmannavaz R, Prasher SO, Ahmad D. Rhizospheric effects of alfalfa on biotransformation of polychlorinated biphenyls in a contaminated soil augmented with *Sinorhizobium meliloti*. Process Biochem 2002;37:955–63.

Meijer SN, Ockenden WA, Sweetman A, Breivik K, Grimalt JO, Jones KC. Global distribution and budget of PCBs and HCB in background surface soils: implications for sources and environmental processes. Environ Sci Technol 2003;37:667–72.

Mikes O, Cupr P, Trapp S, Klanova J. Uptake of polychlorinated biphenyls and organochlorine pesticides from soil and air into radishes (*Raphanus sativus*). Environ Pollut 2009;157:488–96.

Mikszewski A. Emerging technologies for the in situ remediation of PCB-contaminated soils and sediments: bioremediation and nanoscale zero-valent iron. Washington, DC: U.S. Environmental Protection Agency, Office of Solid Waste and Emergency Response. Office of Superfund Remediation and Technology Innovation Program; 2004. p. 26.

Monguchi Y, Ishihara S, Ido A, Niikawa M, Kamiya K, Sawama Y, et al. Pilot-plant study of the PCB degradation at ambient temperature and pressure. Org Process Res Dev 2010;14:1140–6.

Nam P, Kapila S, Liu Q, Tumiatti W, Porciani A, Flanigan V. Solvent extraction and tandem dechlorination for decontamination of soil. Chemosphere 2001;43:485–91.

Natarajan MR, Nye J, Wu WM, Wang H, Jain MK. Reductive dechlorination of PCB contaminated Raisin river sediments by anaerobic microbial granules. Biotechnol Bioeng 1997;55:182–90.

Natarajan MR, Wu WM, Wang H, Bhatnagar L, Jain MK. Dechlorination of spiked PCBs in lake sediment by anaerobic microbial granules. Water Res 1998;32:3013–20.

Naval Facilities Engineering Service Center. Technology transfer report: production base catalyzed decomposition process Guam, Mariana Islands. Technical Report TR-2075-ENV; 1997. [October].

Nollet H, Putte IV, Raskin L, Verstraete W. Carbon/electron source dependence of polychlorinated biphenyl dechlorination pathways for anaerobic granules. Chemosphere 2005;58:299–310.

Noma Y, Mitsuhara Y, Matsuyama K, Sakai S-i. Pathways and products of the degradation of PCBs by the sodium dispersion method. Chemosphere 2007;68:871–9.

Norris G, Al-Dhahir Z, Birnstingl J, Plant SJ, Cui S, Mayell P. A case study of the management and remediation of soil contaminated with polychlorinated biphenyls. Eng Geol 1999;53:177–85.

Occulti F, Roda GC, Berselli S, Fava F. Sustainable decontamination of an actual-site aged PCB-polluted soil through a biosurfactant-based washing followed by a photocatalytic treatment. Biotechnol Bioeng 2008;99:1525–34.

Oshita K, Takaoka M, Kitade S, Takeda N, Kanda H, Makino H, et al. Extraction of PCBs and water from river sediment using liquefied dimethyl ether as an extractant. Chemosphere 2010;78:1148–54.

Pakdeesusuk U, Freedman DL, Lee CM, Coates JT. Reductive dechlorination of polychlorinated biphenyls in sediment from the twelve mile creek arm of Lake Hartwell, South Carolina, USA. Environ Toxicol Chem 2003;22:1214–20.

Perelo LW. Review: in situ and bioremediation of organic pollutants in aquatic sediments. J Hazard Mater 2010;177:81–9.

Pittman Jr CU, He J. Dechlorination of PCBs, CAHs, herbicides and pesticides neat and in soils at 25°C using $Na/NH_3$. J Hazard Mater 2002;92:51–62.

Poster DL, Chaychian M, Neta P, Huie RE, Silverman J, Al-Sheikhly M. Degradation of PCBs in a marine sediment treated with ionizing and UV radiation. Environ Sci Technol 2003;37:3808–15.

Quensen JF, Tiedje JM, Boyd SA. Reductive dechlorination of polychlorinated biphenyls by anaerobic microorganisms from sediments. Science 1988;42:752–4.

Quensen JF, Boyd SA, Tiedje JM. Dechlorination of four commercial polychlorinated biphenyls mistures (Aroclors) by anaerobic microorganisms from sediments. Appl Environ Microbiol 1990;56:2360–9.

Rahuman M, Pistone L, Trifiro F, Miertus S. Destruction technologies for polychlorinated biphenyls (PCBs). ICS-UNIDO Publications, Proceedings of Expert Group Meetings on POPs and Pesticides Contamination; 2000.

Rakowska MI, Kupryianchyk D, Harmsen J, Grotenhuis T, Koelmans AA. In situ remediation of contaminated sediments using carbonaceous materials. Environ Toxicol Chem 2012;31:693–704.

Raskin l, Smith RD, Salt DE. Phytoremediation of metals: using plants to remove pollutants from the environment. Curr Opin Biotechnol 1997;8:221–6.

Rehmann L, Daugulis AJ. Biodegradation of PCBs in two-phase partitioning bioreactors following solid extraction from soil. Biotechnol Bioeng 2008;99:1273–80.

Rein A, Fernqvist MM, Mayer P, Trapp S, Bittens M, Karlson UG. Degradation of PCB congeners by bacterial strains. Appl Microbiol Biotechnol 2007;77:469–81.

Rodenburg LA, Du S, Fennell DE, Cavallo GJ. Evidence for unique and ubiquitous environmental sources of 3,3′-dichlorobiphenyl (PCB 11). Environ Sci Technol 2010;44:2816–21.

Sato T, Todoroki T, Shimoda K, Terada A, Hosomi M. Behavior of PCDDs/PCDFs in remediation of PCBs-contaminated sediments by thermal desorption. Chemosphere 2010;80:184–9.

Schmidt C. How PCBs are like grasshoppers. Environ Sci Technol 2010;44:2752.

Shao D, Sheng G, Chen C, Wang X, Nagatsu M. Removal of polychlorinated biphenyls from aqueous solutions using β-cyclodextrin grafted multiwalled carbon nanotubes. Chemosphere 2010;79:679–85.

Shen C, Tang X, Cheema SA, Zhang C, Khan MI, Liang F, et al. Enhanced phytoremediation potential of polychlorinated biphenyl contaminated soil from e-waste recycling area in the presence of randomly methylated-β-cyclodextrins. J Hazard Mater 2009;172:1671–6.

Singer AC, Jury W, Luepromchai E, Yahng CS, Crowley DE. Contribution of earthworms to PCB bioremediation. Soil Biol Biochem 2001;33:765–76.

Singer AC, Smith D, Jury WA, Hathuc K, Crowley DE. Impact of the plant rhizosphere and augmentation on remediation of polychlorinated biphenyl contaminated soil. Environ Toxicol Chem 2003;22:1998–2004.

Sivey JD, Lee CM. Polychlorinated biphenyl contamination trends in Lake Hartwell, South Carolina (USA): sediment recovery profiles spanning two decades. Chemosphere 2007;66:1821–8.

Slater H, Gouin T, Leigh MB. Assessing the potential for rhizoremediation of PCB contaminated soils in northern regions using native tree species. Chemosphere 2011;84:199–206.

Sokol RC, Bethoney CM, Rhee GY. Effect of PCB concentration on reductive dechlorination and dechlorination potential in natural sediments. Water Res 1995;29:45–8.
Summersgill M. Remediation technology costs in the UK & Europe; drivers and changes from 2001 to 2005. In: Telford T, editor. Proceedings of the 5th International GeoEnviro Conference, June 2006, Cardiff; 2006.
Sylvestre M. Prospects for using combined engineered bacterial enzymes and plant systems to rhizoremediate polychlorinated biphenyls. Environ Microbiol 2012. http://dx.doi.org/10.1111/1462-2920.12007.
Takigami H, Etoh T, Nishio T, Sakai S. Chemical and bioassay monitoring of PCB-contaminated soil remediation using solvent extraction technology. J Environ Monitor 2008;10:198–205.
Tang NH, Myers TE. PCB removal from contaminated dredged material. Chemosphere 2002;46:477–84.
Taniguchi S, Hosomi M, Murakami A, Iimura S, Usukura K, Ozawa S. Chemical decomposition of toxic organic chlorine compounds. Chemosphere 1996;32:199–202.
Taniguchi S, Miyamura A, Ebihara A, Hosomi M, Murakami A. Treatment of PCB-contaminated soil in a pilot-scale continuous decomposition system. Chemosphere 1998;37:2315–26.
TBS-SCT. Contaminants & media, federal contaminated sites inventory. Treasury Board of Canada Secretariat; 2011.
TEI. Remedial Action Plan Update Manistique River and Harbor Area of Concern. Project No. W023452Manistique, Michigan: Great Lakes Commission and Department of Environmental Quality, Triade Engineering Inc. and Terrafirma Environmental Inc.; 2002.
Teng Y, Luo Y, Sun X, Tu C, Xu L, Liu W, et al. Influence of arbuscular *Mycorrhiza* and *Rhizobium* on phytoremediation by alfalfa of an agricultural soil contaminated with weathered PCBs: a field study. Int J Phytoremediation 2010;12:516–33.
Tiedje JM, Quensen JF, Chee-Sanford J, Schimel JP, Boyd SA. Microbial reductive dechlorination of PCBs. Biodegradation 1993;4:231–40.
Todaka T, Hirakawa H, Hori T, Tobiishi K, Iida T, Furue M. Concentrations of polychlorinated dibenzo-p-dioxins, polychlorinated dibenzofurans, and non-*ortho* and mono-*ortho* polychlorinated biphenyls in blood of Yusho patients. Chemosphere 2007;66:1983–9.
TPSTEC. PCB's in Spain — Arcelor. http://www.tpstech.com/references/176. [Accessed the 12th November 2012].
Tu C, Teng Y, Luo Y, Li X, Sun X, Li Z, et al. Potential for biodegradation of polychlorinated biphenyls (PCBs) by *Sinorhizobium meliloti*. J Hazard Mater 2011a;186:1438–44.
Tu C, Teng Y, Luo Y, Sun X, Deng S, Li Z, et al. PCB removal, soil enzyme activities, and microbial community structures during the phytoremediation by alfalfa in field soils. J Soils Sediment 2011b;11:649–56.
UKEPA. Framework for the classification of contaminated soils as hazardous waste. United Kingdom Environmental Protection Agency; 2004.
Ukisu Y, Iimura S, Uchida R. Catalytic dechlorination of polychlorinated biphenyls with carbon-supported noble metal catalysts under mild conditions. Chemosphere 1996;33:1523–30.
USEPA. Low-temperature thermal treatment technology: applications analysis report. Cincinnati, OH: U.S. EPA, Office of Research and Development; 1992 [EPA/540/AR-92/019].
USEPA. OSWER Directive 9200.4-17P — use of monitored natural attenuation at superfund, RCRA corrective action, and underground storage tank sites. Washington, DC: Office of Solid Waste and Emergency Response; 1999.
USEPA. Five-year review report for Shiawassee River Site, Howell, Michigan. Region 5, Chicago. Illinois: United States Environmental Protection Agency; 2009.
USEPA. Search Superfund Site Information. http://cumulis.epa.gov/supercpad/cursites/srchsites.cfm, 2011. [Accessed 29 April 2011].
USEPA. Permeable reactive barriers, permeable treatment zones, and application of zero-valent iron: overview. Washington, DC: Technology Innovation and Field Services Division; 2011b [http://www.clu-in.org/techfocus/default.focus/sec/Permeable_Reactive_Barriers%2C_Permeable_Treatment_Zones%2C_and_Application_of_Zero-Valent_Iron/cat/Overview/. Accessed 24 September 2012].
USEPA. PCB regulations at 40 CFR Part 761. United States Environmental Protection Agency. Toxic Substances Control Act; 2012a.
USEPA. Superfund Site Information. http://www.epa.gov/superfund/sites/, 2012. [Accessed 12 November 2012].
Van Aken B, Correa PA, Schnoor JL. Phytoremediation of polychlorinated biphenyls: new trends and promises. Environ Sci Technol 2010;44:2767–76.
Van Dort HM, Smullen LA, May RJ, Bedard DL. Priming microbial meta-dechlorination of polychlorinated biphenyls that have persisted in Housatonic River sediments for decades. Environ Sci Technol 1997;31:3300–7.
Varanasi P, Fullana A, Sidhu S. Remediation of PCB contaminated soils using iron nano-particles. Chemosphere 2007;66:1031–8.
Vasilyeva GK, Strijakova ER, Nikolaeva SN, Lebedev AT, Shea PJ. Dynamics of PCB removal and detoxification in historically contaminated soils amended with activated carbon. Environ Pollut 2010;158:770–7.
Veriansyah B, Choi HM, Lee YW, Kang JW, Kim JD, Kim J. Continuous catalytic hydrodechlorination of polychlorinated biphenyls (PCBs) in transformer oil. J Environ Sci Health A 2009;44:1538–44.
Wang JS, Chiu K. Destruction of pentachlorobiphenyl in soil by supercritical $CO_{(2)}$ extraction coupled with polymer-stabilized palladium nanoparticles. Chemosphere 2009;75:629–33.
Wang CB, Zhang W. Synthesizing nanoscale iron particles for rapid and complete dechlorination of TCE and PCBs. Environ Sci Technol 1997;31:2154–6.
Wang S, Zhang S, Huang H, Zhao M, Lv J. Uptake, translocation and metabolism of polybrominated diphenyl ethers (PBDEs) and polychlorinated biphenyls (PCBs) in maize (*Zea mays* L.). Chemosphere 2011;85:379–85.
Wang Y, Zhou D, Wang Y, Wang L, Cang L. Automatic pH control system enhances the dechlorination of 2,4,4′-trichlorobiphenyl and extracted PCBs from contaminated soil by nanoscale $Fe^0$ and $Pd/Fe^0$. Environ Sci Pollut Res 2012;19:448–57.
Wang Y, Wang L, Fang G, Herath HMSK, Wang Y, Cang L, et al. Enhanced PCBs sorption on biochars as affected by environmental factors: humic acid and metal cations. Environ Pollut 2013;172:86–93.
Whitfield Äslund ML, Zeeb BA, Rutter A, Reimer KJ. In situ phytoextraction of polychlorinated biphenyl — (PCB)contaminated soil. Sci Total Environ 2007;374:1-12.
Whitfield Äslund ML, Rutter A, Reimer KJ, Zeeb BA. The effects of repeated planting, planting density, and specific transfer pathways on PCB uptake by *Cucurbita pepo* grown in field conditions. Sci Total Environ 2008;405:14–25.
Wiegel J, Wu Q. Microbial reductive dehalogenation of polychlorinated biphenyls. FEMS Microbiol Ecol 2000;32:1-15.
Williams WA. Stimulation and enrichment of two microbial polychlorinated biphenyl reductive dechlorination activities. Chemosphere 1997;34:655–69.
Winchell LJ, Novak PJ. Enhancing polychlorinated biphenyl dechlorination in fresh water sediment with biostimulation and bioaugmentation. Chemosphere 2008;71:176–82.
Wright MA, Knowles CJ, Stratford J, Jackman SA, Robinson GK. The dechlorination and degradation of Aroclor 1242. Int Biodeter Biodegr 1996;38:61–7.
Wu TN. Environmental perspectives of microwave applications as remedial alternatives: review. Pract Period Hazard Toxic Radioact Waste Manage 2008;12:102–15.
Wu Q, Bedard DL, Wiegel J. Effect of incubation temperature on the route of microbial reductive dechlorination of 2,3,4,6-tetrachlorobiphenyl in polychlorinated biphenyl (PCB)-contaminated and PCB-free freshwater sediments. Appl Environ Microbiol 1997a;63:2836–43.
Wu Q, Bedard DL, Wiegel J. Temperature determines the pattern of anaerobic microbial dechlorination of Aroclor 1260 primed by 2,3,4,6-tetrachlorobiphenyl in woods pond sediment. Appl Environ Microbiol 1997b;63:4818–25.
Wu Q, Sowers KR, May HD. Microbial reductive dechlorination of Aroclor 1260 in anaerobic slurries of estuarine sediments. Appl Environ Microbiol 1998;64:1052–8.
Wu L, Li Z, Han C, Liu L, Teng Y, Sun X, et al. Phytoremediation of soil contaminated with cadmium, copper and polychlorinated biphenyls. Int J Phytoremediation 2012;14:570–84.
Xing GH, Chan JKY, Leung AOW, Wu SC, Wong MH. Environmental impact and human exposure to PCBs in Guiyu, an electronic waste recycling site in China. Environ Int 2009;35:76–82.
Yak HK, Wenclawiak BW, Cheng IF, Doyle JG, Wai CM. Reductive dechlorination of polychlorinated biphenyls by zerovalent iron in subcritical water. Environ Sci Technol 1999;33:1307–10.
Yang B, Deng S, Yu G, Zhang H, Wu J, Zhuo Q. Bimetallic Pd/Al particles for highly efficient hydrodechlorination of 2-chlorobiphenyl in acidic aqueous solution. J Hazard Mater 2011;189:76–83.
Ye D, Quensen JF, Tiedje JM, Boyd SA. Anaerobic dechlorination of polychlorobiphenyls (Aroclor 1242) by pasteurized and ethanol-treated microorganisms from sediments. Appl Environ Microbiol 1992;58:1110–4.
Ye D, Quensen JF, Tiedje JM, Boyd SA. Evidence for para dechlorination of polychlorobiphenyls by methanogenic bacteria. Appl Environ Microbiol 1995;61:2166–71.
Yukselen-Aksoy Y, Reddy KR. Effect of soil composition on electrokinetically enhanced persulfate oxidation of polychlorobiphenyls. Electrochim Acta 2012. http://dx.doi.org/10.1016/j.electacta.2012.03.049.
Yukselen-Aksoy Y, Khodadoust AP, Reddy KR. Destruction of PCB 44 in spiked subsurface soils using activated persulfate oxidation. Water Air Soil Pollut 2010;209:419–27.
Zanaveskin LN, Aver'yanov VA. Polychlorobiphenyls: problems of the pollution of the environment and technological neutralization methods. Russ Chem Rev 1998;67:713–24.
Zarull M, Hartig J, Maynard L. Ecological benefits of contaminated sediment remediation in the Great Lakes Basin. Sediment Priority Action Committee, Great Lakes Water Quality Board; 1999 [www.ijc.org. Accessed 12 November 2012].
Zeeb BA, Amphlett JS, Rutter A, Reimer KJ. Potential for phytoremediation of polychlorinated biphenyl-(PCB)-contaminated soil. Int J Phytoremediation 2006;8:199–221.
Zhang W. Nanoscale iron particles for environmental remediation: an overview. J Nanopart Res 2003;5:323–32.
Zhu X, Zhou D, Wang Y, Cang L, Fang G, Fan J. Remediation of polychlorinated biphenyl-contaminated soil by soil washing and subsequent $TiO_2$ photocatalytic degradation. J Soils Sediment 2012. http://dx.doi.org/10.1007/s11368-012-0556-3.
Zwiernik MJ, Quensen JF, Boyd SA. $FeSO_4$ amendments stimulate extensive anaerobic PCB dechlorination. Environ Sci Technol 1998;32:3360–5.

## II.2. Electrokinetic remediation of organochlorines in soil: Enhancement techniques and integration with other remediation technologies (published in Chemosphere)

Chemosphere 87 (2012) 1077–1090

Contents lists available at SciVerse ScienceDirect

Chemosphere

journal homepage: www.elsevier.com/locate/chemosphere

Review

# Electrokinetic remediation of organochlorines in soil: Enhancement techniques and integration with other remediation technologies

Helena I. Gomes [a,*], Celia Dias-Ferreira [b], Alexandra B. Ribeiro [a]

[a] CENSE, Departamento de Ciências e Engenharia do Ambiente, Faculdade de Ciências e Tecnologia, Universidade Nova de Lisboa, 2829-516 Caparica, Portugal
[b] CERNAS, Departamento de Ambiente, Escola Superior Agrária de Coimbra, Bencanta, 3040-316 Coimbra, Portugal

ARTICLE INFO

*Article history:*
Received 4 December 2011
Received in revised form 7 February 2012
Accepted 10 February 2012
Available online 3 March 2012

*Keywords:*
Soil remediation
Electroremediation
Enhanced electrokinetics
Coupled technologies
Organochlorines

ABSTRACT

Electrokinetic remediation has been increasingly used in soils and other matrices for numerous contaminants such as inorganic, organic, radionuclides, explosives and their mixtures. Several strategies were tested to improve this technology effectiveness, namely techniques to solubilize contaminants, control soil pH and also couple electrokinetics with other remediation technologies. This review focus in the experimental work carried out in organochlorines soil electroremediation, aiming to systemize useful information to researchers in this field. It is not possible to clearly state what technique is the best, since experimental approaches and targeted contaminants are different. Further research is needed in the application of some of the reviewed techniques. Also a number of technical and environmental issues will require evaluation for full-scale application. Removal efficiencies reported in real contaminated soils are much lower than the ones obtained with spiked kaolinite, showing the influence of other factors like aging of the contamination and adsorption to soil particles, resulting in important challenges when transferring technologies into the field.



**Contents**



* Corresponding author. Tel.: +351 212948300; fax: +351 212948554.
*E-mail address:* hrg@campus.fct.unl.pt (H.I. Gomes).

0045-6535/$ - see front matter © 2012 Elsevier Ltd. All rights reserved.
doi:10.1016/j.chemosphere.2012.02.037

## 1. Introduction

Soil contamination is a major environmental issue worldwide, as a result of mining, agricultural, industrial and urban activities over the past two centuries. In European countries, an estimate points towards 242 000 contaminated sites of which 2.4% are contaminated with organochlorines (EEA, 2007), a group of toxic compounds mostly used as refrigerants, industrial solvents, lubricants, dielectric and dry cleaning fluids, and pesticides.

Electrokinetic (EK) remediation is a technology that already proved its value, especially in contaminated fine-grain soils. The method uses a low-level direct current as the "cleaning agent", several transport mechanisms (electroosmosis, electromigration and electrophoresis) and electrochemical reactions (electrolysis and electrodeposition) are induced (Acar and Alshawabkeh, 1993). Some of its advantages are close control over the direction of movement of water and dissolved contaminants, retention of contaminants within a confined zone, and low power consumption (Page and Page, 2002). A major advantage is the possibility of treating low permeability soils, inaccessible for other remediation techniques. The general principle of the EK process is presented elsewhere and several authors have critically reviewed its historic developments, state of knowledge and future directions (Yeung et al., 1997; Kim et al., 2002, 2011; Page and Page, 2002; Virkutyte et al., 2002; Alshawabkeh et al., 2004; Ribeiro and Rodríguez-Maroto, 2006; Wick et al., 2007; Yeung, 2008, 2011; Alshawabkeh, 2009).

Since the late 1980s, EK remediation has been successfully used to treat different types of soils (Lageman et al., 1989; Pamukcu and Wittle, 1992; Acar and Alshawabkeh, 1993; Probstein and Hicks, 1993; Ottosen et al., 1997; Ribeiro and Mexia, 1997) and waste materials (Ribeiro et al., 2000; Hansen et al., 2001, 2007; Ferreira et al., 2005; Nystroem et al., 2005; Wang et al., 2007; Ottosen et al., 2008; Jensen et al., 2010). Although EK removal of heavy metals from soils is one of the most studied processes (Virkutyte et al., 2002), this method has also been applied to organic contaminants such as phenol (Acar et al., 1995), chlorinated solvents (Rabbi et al., 2000; Rohrs et al., 2002), petroleum hydrocarbons (Park et al., 2005; Murillo-Rivera et al., 2009), herbicides (Ribeiro et al., 2005, 2011), creosote (Mateus et al., 2010), calmagite (Agarwal et al., 2008) and polycyclic aromatic hydrocarbons (PAHs) (Maini et al., 2000; Niqui-Arroyo et al., 2006; Alcántara et al., 2008, 2010; Lima et al., 2011). A review on electroremediation of PAH contaminated soils was made by Pazos et al. (2010), covering the use of solubilizing agents and hybrid technologies and another review on hydrophobic organics can be found in Saichek and Reddy (2005a).

The EK effectiveness may be diminished by sorption of contaminants on soil particle surfaces and several effects induced by the $H_2$ and $OH^-$ generated at the electrodes. Various enhancement techniques have been developed and a review and classification was made by Yeung and Gu (2011). This article will focus on the experimental work done in the organochlorines electroremediation and the enhancement techniques and/or coupled technologies applied, using that classification (Yeung and Gu, 2011). It aims to compile in a systematic way the experimental work available in the literature. After a brief review of chemical properties of organochlorines (Section 2), EK remediation of organochlorine polluted soil is evaluated in Section 3. Section 4 presents several enhancement techniques and a comparative analysis, while Section 5 is dedicated to the coupling of EK with other technologies. Section 6 presents the conclusions.

## 2. Organochlorines

Chlorinated organic compounds (COCs) are originated by the substitution of one or more hydrogen in aliphatic and aromatic hydrocarbons, and their derivatives, by chlorine. This class of compounds has a wide set of applications in industry, agriculture or domestic activities. Many organochlorines are endocrine disruptors; show carcinogenic effects, and have been listed as priority pollutants by the US Environmental Protection Agency (USEPA). When released into the environment, these compounds are chemically stable and difficult to destroy, and can be transported in both air and water. COCs are eventually deposited in soils and sediments due to their hydrophobicity (Hanberg, 1996; Moermond, 2007; ATSDR, 2011) and they become long-term sources of these contaminants, posing threats to human health and ecosystems (Reible and Thibodeaux, 1999; Oostdam et al., 2005; Lu and Yuan, 2009).

Organochlorines can be divided in different families of compounds such as chlorinated aliphatic hydrocarbons (CAHs), chlorophenols (CPs), chlorobenzenes (CBs), polychlorinated biphenyls (PCBs), organochlorine pesticides (OPs), chlorofluorocarbons (CFCs), polychlorinated dibenzodioxins (PCDDs) or dioxins and polychlorinated dibenzofurans (PCDFs) or furans. The last three families were excluded in this review, since they originate primarily atmospheric pollution problems. Table 1 presents a summary of the essential information about the families included in this review.

## 3. Electrokinetic remediation of organochlorine polluted soil

In the literature, EK application on organochlorines was not studied as intensively as other organics, like PAH. In the organochlorines families, CP are the most studied due to their polarity. Bench-scale tests with spiked kaolin showed high removal rate for chlorophenol (85%), after only 140 min of treatment (1200 $V\,m^{-1}$, 10 mA and pH 9) (Cong et al., 2005), which can be explained by the spiking method, since the researchers injected the contaminant and simultaneously the electric field was applied. It was found that pH could significantly affect the migration, being easier to remove CP at higher pH, and that the soil was remediated by both EK and electrochemical degradation (Cong et al., 2005).

In another study with kaolinite and humic acid kaolinite complexes spiked with 2,6-dichlorophenol (DCP) or 3-(3,4-dichlorophenyl)-1,1-dimethylurea (diuron), results showed that DCP was partially oxidized during the treatment, as revealed by the presence of benzoquinone, a product of DCP oxidation, in the catholyte and the clay (Polcaro et al., 2007). In the presence of humic acids, the removal efficiency of diuron decreased from 90% to 35%, while time increased from 50 h to 160 h. Regarding DCP this effect was lower: removal from kaolinite (without organic matter) reached 90% after 110 h, while from kaolinite modified by humic acid it was only 80% after 160 h (Polcaro et al., 2007). These results have important implications for application in real soils, since organochlorines tend to strongly adsorb the soil organic matter and therefore their extraction using non-enhanced EK will probably fail. Therefore it is not surprising that Lu and Yuan (2009) found that the removal of CB from soils was inefficient and that for Karagunduz (2009) the sorption and desorption capabilities of OP limited the success of electro-osmotic transport.

Another study showed pentachlorophenol (PCP) removal efficiencies of 40–95% by electroosmotic flow (EOF) after 500 h in low permeability clayey soil spiked with 100 $mg\,kg^{-1}$ PCP (Reddy

**Table 1**
Essential information on the families of chlorinated hydrocarbons.

| Family | Chemical structure (general formula) | Common uses | Examples | Notes |
|---|---|---|---|---|
| Chlorinated aliphatic hydrocarbons (CAHs) | 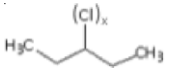 | Organic solvents (degreasing in industries such as: dry cleaning, electronics, industrial manufacturing and equipment maintenance) | – Perchlorethylene (PCE) | – Dense, non-aqueous, phase liquid (DNAPL) contaminants |
| | | | – Trichloroethylene (TCE)<br>– Trichloroethane (TCA) | – Increasingly detected in soil, groundwater and sediments |
| Chlorophenols (CPs) | 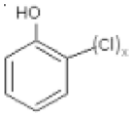 | Preservative agents for wood, paints, vegetable fibers and leather; disinfectants, herbicides, fungicides, insecticides and as intermediates in the production of pharmaceuticals and dyes | – Monochlorophenol | – Phenols with one to five chlorine atoms added on the benzene ring, comprising 19 congeners |
| | | | – 3-Chlorophenol<br>– Pentachlorophenol (PCP) | |
| Chlorobenzenes (CBs) | 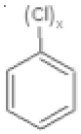 | Mono-CB is used as a solvent for some pesticide formulations, as a degreaser, and a source of other chemicals. Hexachlorobenzene (HCB) has been used directly in the manufacture of pyrotechnics, tracer bullets, and as a fluxing agent in the manufacture of aluminum and also as a funcigide | – Monochorobenzene | – 12 Different congeners |
| | | | – Hexachlorobenzene (HCB) | – Intermediates in the synthesis of pesticides and other chemicals |
| Polychlorinated biphenyls (PCBs) | 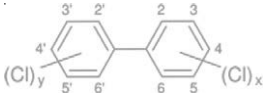 | Components in electrical and hydraulic equipment such as transformers, capacitors, heat transfer systems. PCBs have also been used as pesticide extenders, sealants, carbonless copy paper, lubricants (industrial oils), paints, adhesives, plastics, flame retardants and dedusting agents to control dust on roads. | – 2,4-Dichlorobiphenyl | – Each benzene ring can have up to 5 chlorine substituents in the *ortho*, *meta*, or *para* positions |
| | | | – 2,3,3′,4′-Tetrachlorobiphenyl | – 209 Congeners ranging from mono- to decachlorobiphenyl that are very persistent to degradation and hazardous to the biosphere |
| | | | – Decachlorodiphenyl | |
| Organochlorine pesticides (OPs) | No general structure<br><br>Each pesticide is different | Insecticides, fungicides, biocides | – Aldrin | – The most frequently reported chlorinated pesticides are *p,p′*-DDE, *p,p′*-DDT, dieldrin and mirex |
| | | | – DDT<br>– Dieldrin<br>– Endrin<br>– Heptachlor<br>– Mirex<br>– Taxophene<br>– Lindane<br>– 2,4-D<br>– 2,4,5-T | |

**Table 2**
Use of surfactants in bench-scale electrokinetic remediation of organic contaminants.

| Target contaminant | Matrix | Surfactant | % Removal best results | Reference |
|---|---|---|---|---|
| 1,2,3,4-Tetrachlorobenzene (TeCB), 1,2,4,5-tetrachlorobenzene (i-TeCB), and 1,2,3-trichlorobenzene (TCB) | Spiked kaolin | CDC | 70–80 | Yuan et al. (2007) |
| Benzo[α]pyrene | Spiked kaolin | Brij 35 | 76 | Gómez et al. (2009) |
| Chlorobenzene (CB) and trichloroethylene (TCE) | Spiked soil | Triton X-100, OS-20ALM | 85 | Kolosov et al. (2001) |
| Diesel | Spiked sand | Sodium dodecyl sulfate (SDS) | – | Kim and Lee (1999) |
| DDT | Spiked soil | Tween 80 and SDBS | 13 | Karagunduz et al. (2007) |
| Ethylbenzene | Spiked soil | SDS | 98 | Yuan and Weng (2004) |
| | | PANNOX 110 | | |
| Gasoil | Spiked soil | Citric acid | 87 | Gonzini et al. (2010) |
| Heavy metals and PAHs | Marine contaminated sediments | Tween 80 | 62–84 for metals18 for PAH | Colacicco et al. (2010) |
| Hexachlorobenzene | Spiked kaolin | Tween 80 and β-cyclodextrin | 80 | Yuan et al. (2006) |
| Mixture of benzene, toluene, ethylbenzene, xylenes [BTEX] and three selected polycyclic hydrocarbons [PAHs] | Spiked clay | Cetyltrimethylammonium bromide (CTAB) | 97 | Ranjan et al. (2006) |
| PAH (fluoranthene, pyrene, and benzanthracene) | Spiked kaolin | Tween 80 | 40 | Alcántara et al. (2010) |
| PAH (16 priority PAH) | Contaminated soil (⩾100 years) | Tween 80 | 30 | Lima et al. (2011) |
| Naphthalene and 2,4-dinitrotoluene (2,4-DNT) | Spiked soil | CMCD | 83 and 89 | Jiradecha et al. (2006) |
| Phenanthrene | Spiked kaolin | HPCD | 75 | Ko et al. (2000) |
| Phenanthrene | Spiked kaolinite | APG | 98 | Yang et al. (2005) |
| | | Calfax 16L-35 | | |
| Phenanthrene | Spiked kaolin and sand | Igepal CA-720 | 90 | Saichek and Reddy (2005b) |
| Phenanthrene | Spiked kaolin | APG | 75 | Park et al. (2007) |
| | | Brij 30 | | |
| | | SDS | | |
| Phenanthrene | Spiked soil | Triton X-100 rhamnolipid | 30 | Chang et al. (2009) |
| Phenanthrene and nickel | Spiked kaolin | HPCD | – | Maturi and Reddy (2006) |
| Lubricant oil and zinc | Contaminated soil | Tergitol | 45 | Park et al. (2009) |

et al., 2011b). The direct reductive process at the electrodes was also observed.

In a systematic analysis of the factors affecting electroremediation of CAHs, CPs and CBs made by Lu and Yuan (2009), the sorption/desorption behavior of organochlorines on the interface of soil and pore solution, their aqueous solubilities and soil pH were identified as the most important factors. More hydrophobic compounds tend to adsorb and bind strongly to the soil, so electroremediation efficiencies are lower.

## 4. Enhanced electrokinetics

Enhancement techniques currently used in EK are mainly directed toward maintaining or bringing contaminants into solution by addition of enhancement solutions and controlling pH (Ottosen et al., 2005). This section presents some of the most common techniques.

### *4.1. Techniques to solubilize contaminants*

#### *4.1.1. Surfactants*

For organic contaminants, surfactants are commonly used as flushing solutions to substantially increase desorption and solubilization, through micellisation and surface tension reduction (Saichek and Reddy, 2004). Several reviews on the use of surfactants for soil washing can be found in the literature (Mulligan et al., 2001; Wang and Mulligan, 2004), with more emphasis recently in biosurfactants, due to their biodegradability and low toxicity (Mulligan, 2009). Surfactants adsorb to soils and alter their surface properties affecting EOF and sorption of hydrophobic organics. Depending on the type of surfactants, micelles and the organic contaminants within may be transported toward the anode or cathode (Karagunduz, 2009). Table 2 summarizes some experimental results on the use of surfactants for enhanced EK. It is not possible to directly compare these results, since experimental approaches are different (contaminants, surfactants used and type of soil), but it is clear that both real contaminated soils and sediments have lower efficiencies than spiked kaolin.

Experimental results indicate that anionic surfactants produce negative ζ (zeta) potentials (Kaya and Yukselen, 2005). However, since anionic surfactant micelles have electrophoretic mobility, the electromigration of micelles and, therefore, organochlorines, toward the anode becomes an important driving force. Cationic surfactants have limited applications to EK due to their strong interactions with the soil matrix (Karagunduz, 2009) and can even retard the movement of contaminants (Ranjan et al., 2006).

Regarding organochlorines, only a nonionic surfactant, Tween 80, and an anionic surfactant, SDBS were tested to enhance EK

**Table 3**
Comparison of enhancement methods for organochlorines electroremediation.

| Enhancement method | Current status | Organochlorines tested | Major advantages | Possible disadvantages |
|---|---|---|---|---|
| Surfactants | Tested[a] | DDT (Karagunduz, 2009) | Lower the surface tension of a liquid. Enhance contaminants solubility | Success of surfactants depends on their type and other environmental factors |
| Cyclodextrins | Tested[a] | TeCB, i-TeCB, TCB (Yuan et al., 2007), HCB (Yuan et al., 2006; Li et al., 2009, 2010b) | Chemical stability and reliable electroosmotic flow | Inclusion compounds between complexing agents and organochlorines may be less soluble |
| Sequential use of enhancement solutions | Not tested | – | More effective on mixed contaminations. Can combine the use of chelants, surfactants and complexing agents | Variable – depend on the enhancement solution used. Possible interferences between enhancement solutions |
| Soil pH control | Tested[a] | 2,4-DCP (Luo et al., 2005a), PCE, TCE, carbon tetrachloride and chloroform (Chang et al., 2006), PCP (Reddy et al., 2011b,c) | Maintain anolyte and catholyte pH within appropriate ranges | Variable – depend on the method used to control pH. The addition of some acids may pose environmental issues |

[a] Bench-scale tests.

remediation of DDT (Karagunduz et al., 2007). It was found that both had similar solubilization potentials for that contaminant.

The potential success of surfactants depends on their type, soil properties and other factors (i.e., pH, presence of other cations, etc.). It is recommended that the $\zeta$ potential of soils is determined before using EK in order to maximize the efficiency of the technique (Kaya and Yukselen, 2005). It was also found that the pH control in the cathode maximized EOF and the surfactant enhanced EK (Alcántara et al., 2010).

#### 4.1.2. Cyclodextrins

Cyclodextrins are considered advantageous over regular surfactants due to their nontoxicity, biodegradability and low sorption to the solid phase at a wide range of pH values (Maturi and Reddy, 2006).

The effect of $\beta$-cyclodextrin ($\beta$-CD) on EK removal of multiple CB, including 1,2,3,4-tetrachlorobenzene (TeCB), 1,2,4,5-tetrachlorobenzene (i-TeCB), and 1,2,3-trichlorobenzene (TCB) in contaminated clay soils was studied by Yuan et al. (2007). The addition of $\beta$-CD was not recommended, since the inclusion compounds formed were less soluble than CB and their formation reduced the aqueous solubility of CB and led to the partial immobilization of CB desorbed from soil (Yuan et al., 2007).

Different conclusions were obtained in another study, where two solubilizing agents, ethanol and methyl-$\beta$-cyclodextrin (MCD), were compared in terms of either EK parameters or enhancement of hexachlorobenzene (HCB) movement in real contaminated sediments (Wan et al., 2009). Although the test with 50% ethanol exhibited the highest performance, researchers observed that ethanol had a more negative effect on cumulative EOF than MCD. They concluded that MCD could perform better than ethanol for a long-term field application, given the reliable EOF and chemical stability (Wan et al., 2009). The authors also refer *in situ* degradation of HCB in regions near the cathode and the direct electrochemical degradation of HCB at the electrodes.

In a pilot test with real aged sediments contaminated with HCB and Zn, hydroxypropyl-$\beta$-cyclodextrin (HPCD) was successfully penetrated across sediments by electroosmosis (Li et al., 2009, 2010b). However, the researchers concluded that the simultaneous removal of HOCs and heavy metals was rather difficult in relatively large-scale treatment and other enhancements were needed for metals removal.

#### 4.1.3. Sequential use of enhancement solutions

The sequential use of the extractants is also a way to enhance EK, although no literature was found on organochlorines. Khodadoust et al. (2004) found that 5% Tween 80 followed by 1 M citric acid or 1 M citric acid followed by 5% Igepal CA-720 were effective for the removal of both nickel and phenanthrene from spiked kaolin. Removal of both PAHs and heavy metals in a silty sand soil collected from a polluted former manufactured gas plant was enhanced with 0.2 M EDTA flushing in two stages (without and with voltage gradient, 1 V $cm^{-1}$), followed by 5% Igepal flushing also in two stages (Reddy et al., 2010). Removal efficiencies varied between 20% and 80% and showed that a carefully designed sequential hydraulic flushing scheme, with chelants and surfactants, is needed for the removal of mixed contaminations.

Since in most field applications mixed contaminations are usually found, it is important to study the sequential use of enhancement solutions to improve removal efficiency, minimizing also possible interferences and negative environmental impacts.

### 4.2. Soil pH control

Both theoretical and experimental analysis showed that pH regulation is an effective method for enhancing electroremedia-

**Table 4**
Combination of electrokinetic remediation and other methods for removal of organic contaminants in bench-scale experiments.

| Target contaminant | Matrix | Enhancement method | % Removal | Reference |
|---|---|---|---|---|
| Acid dye (acid blue 25) | Spiked kaolin | Electrokinetics and electrochemical oxidation | 89 | Lee et al. (2009) |
| Benzo[a]pyrene | Spiked kaolin | Electrokinetics and liquid electrochemical oxidation | 76 | Gómez et al. (2009) |
| Chrysene | Spiked kaolin | Ultrasonic electrokinetic (EK-US) and AC-electrokinetic (EK-AC) | 54 | Shrestha et al. (2009) |
| Creosote | Contaminated clay soil | Electrokinetics and chemical (Fenton) oxidation | 35 | Isosaari et al. (2007) |
| Creosote | Two creosote-polluted clay soils and an agricultural soil | Electrokinetic bioremediation | 53 | Niqui-Arroyo and Ortega-Calvo (2007) |
| Dinitrotoluene | Spiked kaolin | Electrokinetics and bare nanoscale iron particles (NIPs) and lactate modified NIP (LM-NIP) | 30–65 | Reddy et al. (2011a) |
| Petroleum hydrocarbons | Spiked soil | Electrokinetic bioremediation | 45 | Li et al. (2010a) |
| Nickel and phenanthrene | Spiked kaolin | Electrokinetics and chemical (Fenton) oxidation | – | Reddy and Karri (2008a) |
| Phenanthrene | Spiked kaolin | Electrokinetically enhanced soil flushing | – | Saichek and Reddy (2003) |
| Phenanthrene | Spiked sandy soil | Electrokinetics and chemical (Fenton) oxidation | 82 | Park et al. (2005) |
| Phenanthrene | Contaminated clay soil | Electrokinetic bioremediation | – | Niqui-Arroyo et al. (2006) |
| Phenanthrene | Spiked kaolin and Hadong clay | Electrokinetics and chemical (Fenton) oxidation | – | Kim et al. (2006) |
| Phenanthrene | Spiked Hadong clay soil | Electrokinetics and chemical (Fenton) oxidation with stabilizers | – | Kim et al. (2007) |
| Phenanthrene | Spiked kaolin | Electrokinetics and chemical oxidation | 95 | Alcántara et al. (2008) |
| Phenanthrene | Spiked Hadong clay | Electrokinetics and chemical (Fenton) oxidation | – | Kim et al. (2009) |
| Phenanthrene | Alginate beads | Electrokinetic bioremediation | – | Shi et al. (2008a) |
| Phenol | Spiked sandy loam | Electrokinetic bioremediation | 58 | Luo et al. (2006) |
| Total petroleum hydrocarbon-diesel (TPH-D) | Contaminated soil | Electrokinetics and Fenton chemical oxidation | 97 | Tsai et al. (2010) |

tion (Mishchuk et al., 2007; Lysenko and Mishchuk, 2009). Different strategies are used to control soil pH, like electrode conditioning (Puppala et al., 1997; Saichek and Reddy, 2003; Baek et al., 2009), electrolyte circulation or circulation-enhanced electrokinetics (Lee and Yang, 2000; Chang and Liao, 2006), non-uniform electrokinetics (Luo et al., 2005a), ion exchange membranes or barriers (Ottosen and Hansen, 1992; Kim et al., 2005; Virkutyte and Sillanpaa, 2007), polarity exchange technique (Pazos et al., 2006) and approaching anodes (Shen et al., 2007).

In experimental tests with tetrachloroethylene (PCE), trichloroethylene (TCE), carbon tetrachloride and chloroform, a buffer solution of $CH_3COONa$ and a working-solution circulation system to neutralize the pH were used (Chang et al., 2006). A removal efficiency ranging from 85% to 98% was obtained after 2 weeks of treatment. This EK process produced a roughly stable EOF rate ($180\ mL\ d^{-1}$), pH (around 6.0), and current density ($0.26–0.27\ mA\ cm^{-2}$). The mobility of chlorinated solvents in soils increased with its water solubility, i.e., chloroform > carbon tetrachloride > TCE > PCE (Chang et al., 2006).

Researchers also showed that non-uniform electrokinetics (generated by tubular electrodes) could accelerate the desorption and movement of phenol and 2,4-DCP in spiked unsaturated soils (Luo et al., 2005a).

In another study, the highest degradation of PCP (78%) was obtained with $2\ V\ cm^{-1}$ voltage gradient and recirculation application (Reddy et al., 2011c). The pH control allowed PCP transport to the cathode where it underwent direct electrochemical reductive dechlorination.

No literature was found in the use of ion exchange membranes for organochlorines electroremediation.

### 4.3. Comparative analysis and discussion

Table 3 presents a comparative analysis of the techniques used to enhance EK, identifying if the technique has already been tested, which were the organochlorines targeted, major advantages and possible disadvantages associated.

Regarding enhancement techniques, CB were the most studied organochlorines, followed by OP and CAH. None of these techniques has been tested on CP or PCB. It is not possible to clearly state what enhancement technique is the best, since experimental approaches differed. Results with real contaminated soils or sediments showed much lower EK efficiency, reflecting the influence of other factors like aging of the contamination and adsorption to soil particles, especially to organic matter.

Some of the techniques have not been tested for organochlorines so more research is needed. Given that EK efficiencies are low with hydrophobic compounds, it is important to develop new methods to improve those efficiencies.

## 5. Coupling with other remediation technologies

The mobilizing potential of EK can be coupled to other technologies in order to maximize contaminant removal in a cost-effectiveness perspective. Several studies at bench-scale have been made on this area. Table 4 summarizes the possibilities of integrating remediation technologies for organic contaminants, whereas Table 5 details on organochlorines. These integrated technologies will be further detailed in the next sections.

### 5.1. Oxidation/reduction

Chemical oxidation typically involves reduction/oxidation reactions that chemically convert hazardous contaminants into nonhazardous or less toxic compounds that are more stable, less mobile or inert. The most common oxidants are ozone, hydrogen peroxide, hypochlorites, chlorine, chlorine dioxide, potassium permanganate and Fenton's reagent (hydrogen peroxide and iron) (USEPA, 2011).

Combining EK with chemical oxidation was tested by several researchers, namely for phenanthrene spiked soil with Fenton's reagent (Kim et al., 2006), phenol spiked kaolin with $KMnO_4$ (Thepsithar and Roberts, 2006) and diesel contaminated soils with $H_2O_2$ (Tsai et al., 2010). Reviews on the coupling of these

**Table 5**
Coupling of electrokinetic remediation and other technologies for removal of organochlorines in bench-scale experiments.

| Target contaminant | Matrix | Combined technologies | Duration of test(s) | Process fluid | | Voltage gradient ($V\ cm^{-1}$) | % Removal best results | Reference |
|---|---|---|---|---|---|---|---|---|
| | | | | Anode | Cathode | | | |
| 2,4-Dichlorophenoxyacetic acid (2,4-D) | Spiked soil | Bioremediation and electrokinetics | 4; 22 d | 0.2 M $Na_2HPO_4$<br>0.5 M $Na_2HPO_4$ | 4 M $CH_3COOH$<br>0.5 M $HNO_3$ | 1.75 | 39 | Jackman et al. (2001) |
| Trichloroethylene (TCE) | Spiked soil | Electrokinetics and Fenton oxidation | 10 d | $H_2O_2$ (<4000 mg $L^{-1}$) | Deionized water | 1.0 | 89 | Yang and Liu (2001) |
| Perchloroethylene | Spiked soil | Electrokinetics and zero-valent metals (iron and zinc) | 10 d | 0.01 M $Na_2CO_3$ | 0.01 M $Na_2CO_3$ | 1.0 | 90 | Chang and Cheng (2006) |
| TCE and Cd | Spiked Kimpo clay | Electrokinetics and permeable reactive barrier | 200 h | Deionized water | Deionized water | 2.0 | 90 and 70 | Chung and Lee (2007) |
| Pentachlorophenol | Spiked kaolin | Electrokinetics and Nanoparticles of zero valent iron (NIP) | 427 h<br>960 h<br>960 h | 5 g $L^{-1}$ NIP, 5 g $L^{-1}$ NIP in,<br>5% Igepal CA720<br>5 g $L^{-1}$ NIP in 5% Ethanol | $H_2O$ | 1.0 | 45–55 | Reddy and Karri (2008b) |
| Pentachlorophenol | Spiked soil | Bioremediation and reverse field electrokinetics | 36; 95 d | $H_2O$ | $H_2O + H_2SO_4$ | 1.0 | – | Harbottle et al. (2009) |
| Hexachlorobenzene (HCB) | Spiked kaolin | Electrokinetics and Fenton chemical oxidation | 15 d | $H_2O_2$ solutions (30%, 15% and 5%)<br>1% (by weight) β-cyclodextrin solutions | – | 0.67 | 76 | Oonnittan et al. (2009a) |
| Hexachlorobenzene (HCB) | Spiked kaolin | Electrokinetics and Fenton chemical oxidation | 15 d | Ferrous sulfate solution with 1% (by weight) β-cyclodextrin solutions<br>After 48 h when current developed, 15% $H_2O_2$ was added | Deionized water | 1.0 | 64 | Oonnittan et al. (2009b) |
| Hexachlorobenzene (HCB), phenanthrene (PHE) and fluoranthene (FLU) | Spiked kaolin | Ultrasonically enhanced electrokinetics | 10; 15 d | 0.01 M NaOH0.01 M $Na_2CO_3$ | $H_2O$ | 1.5 | 70–83<br>82–96<br>82–97 | Pham et al. (2009) |
| 2,4-Dichlorophenoland Cd | Spiked sandy loam | Activated bamboo charcoal (adsorbent) and different periodic polarity-reversals | 10.5 d | 0.01 M $KNO_3$ | 0.01 M $KNO_3$ | 1.0 | 76 of Cd and 55 of 2,4-DCP | Ma et al. (2010) |
| Hexachlorobenzene (HCB) | Spiked kaolin | Electrokinetics and Fenton chemical oxidation | 10; 20 d | 10–12% $H_2O_2H_2O_2 + FeSO_4$ | $H_2O$ | 1.5–2.0 | 57 | Oonnittan et al. (2010) |
| Hexachlorobenzene (HCB) | Spiked soil | Electrokinetics and microscale Pd/Fe PRB enhanced with surfactant | 5; 10 d | TX-100 solution at 10 mM (50 cmc) | 0.025 M $Na_2SO_4$ solution | ≈2 | 64 | Wan et al. (2010) |
| Pentachlorophenol (PCP) | Spiked soil | Electrokinetics and Pd/Fe permeable reactive barrier | 5–15 d | 0.025 M $Na_2CO_3$ | 0.025 M $Na_2SO_4$ | 2.0 | 49 | Li et al. (2011) |
| Trichloroethylene (TCE) | Spiked sandy soil | Electrokinetics and Fenton oxidation with injection of nanoscale $Fe_3O_4$ | 7–14 d | 1.0–10.0 g $L^{-1}$ $Na_2S_2O_8$<br>0.217 g of nanoscale $Fe_3O_4$ | 1.0–10.0 g $L^{-1}$ $Na_2S_2O_8$ | 1.0 | 100 | Yang and Yeh (2011) |

techniques can be found in Yang (2009),Yeung and Gu (2011) and Yap et al. (2011).

Regarding organochlorines, the results of experiments carried out on HCB spiked kaolin, showed 57% contaminant removal (Oonnittan et al., 2010). There was no pH dependence in the range 2.9–5 and the results revealed the importance of efficient oxidant delivery methods in the treatment duration reduction (Oonnittan et al., 2010).

Research made on *in situ* EK-Fenton process for oxidation of TCE showed that graphite electrodes were superior to stainless steel electrodes. It was also found that the soil with a higher organic matter content resulted in a lower treatment efficiency (Yang and Liu, 2001). The cost analysis indicated that the EK-Fenton process is very cost-effective (Yang and Liu, 2001).

A different approach is the use of electrically induced reduction or EIR. It involves feeding an electric current through electrodes and creating favorable conditions for redox reactions to occur in the matrix, without the migration of contaminants (Jin and Fallgren, 2010). The applied electric potential is substantially lower than those used in EK process. This was tested in clay spiked with TCE, using weak electric potentials of 6, 9, and 12 V $m^{-1}$. The results showed that up to 97% of TCE was depleted. Corresponding increases in chloride concentrations were observed indicating a reductive dechlorination pathway (Jin and Fallgren, 2010).

Yang and Yeh (2011) evaluated the effectiveness of EK enhanced persulfate oxidation for destruction of TCE in a spiked sandy clay soil. Experimental results showed that EK greatly enhances the transport of injected persulfate from the anode to the cathode through EOF, aiding *in situ* chemical oxidation of TCE. Such a coupled process was found to be capable of effective destruction of TCE in the soil and electrode compartments (Yang and Yeh, 2011).

### 5.2. Bioremediation

Bioremediation uses microorganisms (e.g. yeast, fungi or bacteria) to degrade organic contaminants in soil, sludge and solids either excavated or *in situ*. The microorganisms break down contaminants by using them as a carbon source or cometabolizing them with a food source.

Combining EK with bioremediation can be done with the purpose of improving biodegradation by promoting transport of nutrients such as nitrogen and phosphorus, and electron acceptors (Elektorowicz and Boeva, 1996; Lee et al., 2006; Wu et al., 2007; Lohner et al., 2008a,b; Ottosen et al., 2008; Schmidt et al., 2008; Xu et al., 2010). EK has also the potential to enhance bioremediation of organic contaminants through control and movement of both contaminant and bacteria (DeFlaun and Condee, 1997; Lahlou et al., 2000; Wick et al., 2004; Olszanowski and Piechowiak, 2006; Shi et al., 2008b,c; Rocha et al., 2009), facilitating greater interaction and hence contaminant bioavailability (Wick et al., 2007). Enhancement techniques like bidirectional operation (Luo et al., 2005b) and an electrode matrix and a rotational operation mode showed increases in the bioremediation rate of phenol (Luo et al., 2006). Reviews on the combination of bioremediation and EK can be found in Wick (2009) and in Lohner et al. (2009).

Regarding organochlorines, it was found that constant electric currents caused large pH and moisture content changes due to water electrolysis and electroosmotic effects, with negative impacts on biodegradation parameters (enzyme activity and contaminant mineralization) of PCP (Harbottle et al., 2009). Regularly reversed electric currents caused little change in pH and moisture content and led to more rapid contaminant mineralization, lower soil contaminant concentration and increased soil enzyme activity (except for soil immediately adjacent to the anode) (Harbottle et al., 2009).

The EK injection of benzoic acid cometabolite to enhance the biodegradation of TCE was tested by Rabbi et al. (2000). Results showed that EK biodegradation of TCE in clays may be practical, in particular for sites where traditional pump and treat technology are ineffective.

There is some controversy about the impact of the electric field in the soils microbial communities. Some authors defend that the electric field, if suitably applied, will not influence the composition and physiology of microbial communities and hence not affect their potential to biodegrade contaminants (Wick et al., 2010). Other authors defend the contrary (Lear et al., 2007; Tiehm et al., 2009). A better awareness of the interactions between EK processes and microbial communities is needed.

### 5.3. Permeable reactive barriers

A permeable reactive barrier (PRB) is an *in situ* remediation method that combines a passive chemical or biological treatment zone with subsurface fluid flow management. Treatment media may include zero-valent iron ($Fe^0$), chelators, sorbents and also bacteria to address a wide variety of ground-water contaminants. The contaminants are either degraded or retained in the barrier material, which may need to be replaced periodically.

A review on coupling EK and permeable reactive barriers can be found in Weng (2009), where the potential for *in situ* application of these remediation technologies and its ability to remove reactive contaminants from low-permeability soil were recognized. The main advantage of this integration is that it does not only remove organochlorines from soil, but also convert these pollutants into less toxic compounds through dechlorination.

#### 5.3.1. Zero valent iron PRB

The mechanisms of TCE degradation in groundwater with electrokinetics coupled with a zero valent iron (ZVI) PRB were investigated by Moon et al. (2005). Their results indicate that the rate of reductive dechlorination of TCE was improved up to six times of that of a ZVI PRB alone. The most effective configuration of electrode and ZVI PRB for TCE removal was with the cathode installed at the hydraulic down-gradient (Moon et al., 2005).

In other research, a bench-scale flow-through $Fe^0$ reactor column with direct current was tested to increase the efficiency in TCE dechlorination (Roh et al., 2000). The tests were made with real contaminated groundwater and the results showed that the combination is highly effective in enhancing the rate of TCE dechlorination, cutting by tenfold the half-life time (Roh et al., 2000).

Chang and Cheng (2006) combined the EK process with zero valent metal (ZVM) to remediate PCE contaminated soils. ZVM installed positions tested were: (i) around 5.0 cm away from the anode, (ii) in middle area and (iii) around 5.0 cm away from the cathode. The removal efficiency reached 99% and 90% in the pore-water and soil, respectively, after 10 d of treatment. The zero-valent zinc performed better the PCE degradation than ZVI (Chang and Cheng, 2006).

A permeable reactive barrier filled with reactive Pd/Fe particles was installed between anode and cathode to test the dechlorination of PCP coupled with electrokinetics (Li et al., 2011). The mechanism for PCP removal was the EK movement of PCP into the PRB compartment, the complete dechlorination of PCP to phenol by Pd/Fe and the subsequent removal of phenol by electroosmosis (Li et al., 2011).

In other bench-scale research, surfactant-enhanced electrokinetics was coupled with a PRB composed of microscale Pd/Fe to treat a HCB spiked soil (Wan et al., 2010). A nonionic surfactant, Triton X-100, was used as the solubility-enhancing agent. Results showed that the HCB removal was generally increased by a factor

**Table 6**
Coupling of electrokinetic remediation and zero valent iron nanoparticles in bench-scale experiments.

| Concentration and type of nZVI | Matrix | Target contaminant | Duration of test(s) | Electrolyte | Voltage gradient ($V\ cm^{-1}$) | % Removal best results | Reference |
|---|---|---|---|---|---|---|---|
| 5.0 mL of the diluted PV3A coated nZVI solution (460 mg $L^{-1}$) | White Georgia kaolinite clay | – | 46 h | 0.2 M NaCl | 0.1 | – | Pamukcu et al. (2008) |
| Daily addition of 20 mL nZVI (1 vol.% of PAA-modified nano iron slurry) with a Fe concentration of 2.5 g $L^{-1}$ to the anode reservoir | Loamy sand | – | 6 d | Simulated groundwater | 1.0 | – | Yang et al. (2007) |
| 20 mL $d^{-1}$ of PAA-modified Pd/Fe bimetallic nanoparticles slurry (4 g $L^{-1}$) | Spiked soil | $KNO_3$ | 6 d | Simulated groundwater | 1.0 | 99 | Yang et al. (2008) |
| 5 g $L^{-1}$ nZVI in 5% Igepal CA720 and 5 g $L^{-1}$ nZVI in 5% ethanol at the anode | Spiked kaolin | PCP | 427; 960 h | Deionized water | 1.0 | 55 | Reddy and Karri (2008b) |
| 44.62 g of bare nZVI and 51,27 g in 120 mg $L^{-1}$ of Tween 80 | Spiked silica sand | PCE | 100 h | 0.01 M of $Na_2CO_3$ | 1.0 | 76 | Chen et al. (2010) |
| 0.5 g $L^{-1}$ nZVI dispersed in 2% or 5% weight PAA | 40/60 or 100/200 sands | – | 10 d | 7 or 20 mM of NaCl | 0.55 and 1.30 | – | Jones et al. (2010) |
| Nano iron dose = 0.75 g $L^{-1}$ into the anode reservoir (in test 1) or cathode reservoir (in test 2). Nano iron with a pulp density of 87 wt.% was added to the mixture of 10 wt.% of soybean oil and 3 wt.% of mixed surfactants (Span 80 and Tween 40) for the preparation of emulsified nano scale zero valent iron | Spiked sandy soil | TCE | 10 d | Simulated groundwater | 1.0 | 70 | Yang and Chang (2011) |

of 4 by EK coupled with PRB compared with EK alone (60% vs. 13%). In the EK–PRB system, HCB was removed from soil through several sequential processes: the movement driven by EOF in the anode, the complete adsorption/degradation by the Pd/Fe particles and the consequent movement by EOF and probable electrochemical reactions in the cathode (Wan et al., 2010).

#### 5.3.2. Lasagna process

A different approach is proposed in an *in situ* electroremediation technology called Lasagna™ (Ho et al., 1995; Ho et al., 1997, 1999a,b) because of the layering of electrodes and treatment zones for sorption, immobilization and/or degradation of contaminants. It was used for cleaning up TCE contaminated low-permeability soils. TCE in the soils was transported into carbon containing treatment zones where it was trapped. Over 98% of TCE was removed from the contaminated soils, with most samples showing a removal of over 99% (Ho et al., 1999a). Field scale applications have shown good results in remediation of TCE contaminated clay soils after 2-year operation (Athmer, 2004). This technology was also applied to 2,4-dichlorophenoxyacetic acid (2,4-D) at bench-scale (Jackman et al., 2001). Under a current density of 0.89 A $m^{-2}$, the contaminant moved towards a microorganism active treatment zone (*Burkholderia* spp. RASC c2), where it was biodegraded. Results showed that it is possible to move an organic contaminant into a biodegradative zone for mineralization *in situ*.

#### 5.3.3. PRBs of different reactive media

In a bench-scale study, TCE and Cd were successfully removed from spiked Kimpo clay, using atomizing slag (composites of CaO, FeO and $Fe_2O_3$) as an inexpensive PRB material coupled with electrokinetics (Chung and Lee, 2007). Experimental results showed the TCE concentrations of effluent solution through the PRB material were much lower than those of EK remediation alone. Some of the TCE passing through the PRB was dechlorinated by the atomizing slag, as shown by the chloride concentrations measured (Chung and Lee, 2007).

A surfactant assisted EK remediation (SAEK) process coupled with carbon nanotubes (CNTs) barrier has been investigated for 1,2-dichlorobenzene (DCB) removal (Yuan et al., 2009). The best result (up to 76%) was achieved with sodium dodecyl sulfate (SDS) as processing fluid. The authors observed that removal of DCB was mainly contributed by surface sorption on CNT rather than by EK (Yuan et al., 2009).

### 5.4. Zero valent iron nanoparticles

Research has shown that zero valent iron nanoparticles (nZVIs) are very effective for the transformation and detoxification of a wide variety of common environmental contaminants such as chlorinated organic solvents, OP and PCBs (Zhang, 2003). Nanoparticles are traditionally injected under pressure and/or by gravity to the contaminated plume where treatment is needed. However, the transport of nZVI is normally limited by their aggregation and settlement (Tiraferri et al., 2008; Reddy and Karri, 2009; Tiraferri and Sethi, 2009; Jiemvarangkul et al., 2011). The mobility of nZVI will be less than a few meters under almost all conditions, so the possibility of enhancing its transport through EK is very interesting. There is also a lot of potential in the application of nZVI to organochlorines, given their high reactivity and the fact that it effectively dechlorinates these compounds into less toxic and more biodegradable ones (He, 2007; Shih et al., 2009; Zhang et al., 2011). Table 6 summarizes the bench-scale experiments made with EK and nZVI.

Reddy and Karri (2009) studied the enhanced delivery of nZVI amended with surfactant or cosolvent under different electric potentials for the remediation of a low permeable kaolin soil spiked with PCP (1000 mg $kg^{-1}$ of dry soil). Results revealed that the iron concentrations in the soil increased with higher voltage gradient (2 V $cm^{-1}$) and operating duration (938 h). The transport of nZVI was limited by their aggregation, settlement and partial oxidation within the anode. PCP was partially reduced (40–50%) in all the experiments (Reddy and Karri, 2009).

**Table 7**
Current status, major advantages and possible disadvantages of coupling electrokinetics with other remediation technologies for organochlorines removal or treatment.

| Remediation technology coupled with EK | Current status | Organochlorines tested | Major advantages | Possible disadvantages |
|---|---|---|---|---|
| Oxidation/ reduction | Tested[a] | HCB (Oonnittan et al., 2010), TCE (Yang and Liu, 2001) | Destruction of organic contaminants by oxidation. Applicability to mixed contaminations | Depend on the oxidant/reductant used. Intermediate anions generated can change the electrical current intensity |
| Bioremediation | Tested[a] | TCE (Rabbi et al., 2000), PCP (Harbottle et al., 2009) | Improve biodegradation with transport of nutrients and electron donnors | Adverse effect on microbial communities in soils |
| Permeable reactive barrier (PRB) | Tested[a],[b] | TCE (Ho et al., 1999a,b; Roh et al., 2000; Moon et al., 2005; Chung and Lee, 2007); PCE (Chang and Cheng, 2006), PCP (Li et al., 2011) | *In situ* application for low permeable soils. Enhanced transport of contaminants towards the PRB | pH gradient generated by EK may affect sorption and degradation in the PRB |
| Zero valent iron nanoparticles (nZVIs) | Tested[a] | TCE (Yang and Yeh, 2011), PCP (Reddy and Karri, 2009), PCE (Chen et al., 2010) | Reduction of chlorinated compounds *in situ*. Enhanced nZVI mobility with electric fields | Need to protect nZVI from oxidation prior to contact with contaminant. Toxicity of intermediate compounds. |
| Phytoremediation | Not tested | – | Enhance bioavailability and transport of contaminants to shoots and roots of plants | EK can affect plant growth (biomass production) |
| Ultrasonication | Tested[a] | HCB (Pham et al., 2009) | Increase the volume flow rate and removal efficiencies | Performance depends on the chemical stability of contaminants |

[a] Bench-scale tests.
[b] Field application.

Chen et al. (2010) used nZVI with surfactant and EK for the remediation of PCE. Experiments were performed in a glass sandbox to simulate the transport and degradation of PCE in the aquifer. The results revealed that the PCE concentrations at the bottom layer were higher than those at the mid and upper layers, and that the surfactant Tween 80 mobilized PCE in the aquifer. The degradation tests showed that nZVI activity could be promoted by EK. Chlorinated byproducts were not detected, so PCE was completely dechlorinated (Chen et al., 2010).

More recently, Reddy et al. (2011a) also studied the transport and reactivity of bare nanoscale iron particles (NIPs) and lactate modified NIP (LM-NIP) in kaolin spiked with dinitrotoluene (DNT) under applied electric potential. The highest DNT degradation was achieved using LM-NIP and attributed to both NIP and EK. Their conclusions indicate that EK can enhance the delivery of nanoscale iron particles in low permeability soils (Reddy et al., 2011a).

Yang and Yeh (2011) also tested the injection of emulsified nanoscale zero valent iron (ENZVI) and EK remediation for treatment of a TCE spiked sandy soil. EK enhanced the transport of ENZVI in the porous media and EOF played a key role in removing TCE from the soil matrix to the cathode reservoir.

### 5.5. Phytoremediation

The coupling of EK and phytoremediation was used mainly for heavy metals: Cd, Cu and As (O'Connor et al., 2003), Pb and As (Lim et al., 2004); Cu and Zn (Zhou et al., 2007); Zn, Pb, Cu and Cd (Aboughalma et al., 2008); Cd, Cu, Pb and Zn (Cang et al., 2011); Cd, Zn and Pb (Bi et al., 2011). An analysis on benefits and constraints of the combination of these two remediation techniques was made by Bedmar et al. (2009) and it is an improved tool for soil remediation under certain conditions such as low quantities of heavy metals and when it is needed to restore soil functions.

Several studies on phytoremediation of organochlorine pesticides (Chuluun et al., 2009), chlorinated solvents (RTDF, 2005) and TCE (Meagher, 2000; Newman and Reynolds, 2004) are available. A review on recent advances in phytoremediation for the treatment of PCBs, including the development of transgenic plants and associated bacteria, was published by Aken et al. (2010). However, no reference was found in the literature on the use of both techniques on organic contaminants and more precisely on organochlorines.

### 5.6. Ultrasonication

High power ultrasound relies on the phenomenon of cavitation to destroy contaminants such as PCBs, PAH and organochlorines which adsorb to the surface of soil particles, because of their inherent hydrophobicity (Collings et al., 2006).

Chung and Kamon (2005) obtained removal efficiencies in EK and ultrasonic process which were increased in 3.4% for Pb and 5.9% for phenanthrene when compared with simple EK process. Similar tests were made to study and to compare the combining effects of these two methods on the removal of the three persistent organic pollutants HCB, phenanthrene and fluoranthene from spiked kaolin (Pham et al., 2009). Two pair tests were conducted into two experiments with different initial low (10 mg $kg^{-1}$) and high (500 mg $kg^{-1}$) concentrations. Results showed that, generally, EK-US have higher EOF, higher current and better performance than EK alone. However, ultrasonic enhancement can increase the removal rate only up to about 10% more. Among the three POPs, HCB was the most difficult to treat because of its very stable structure, while the other two PAHs were easier to remove (Pham et al., 2009). Removal efficiency decreased with increasing initial concentration (Pham et al., 2009).

### 5.7. Full scale applications

Several full scale projects developed by Geokinetics' and HMT's were described by Lageman et al. (2005). Since contaminated sites contain often a mixture of both inorganic and organic components, a combination of techniques was used: (i) EK recovery of inorganic contamination and electroheated recovery of organic contamination in combination with soil vapor extraction and low flow groundwater extraction; (ii) electroheated and EK enhanced biodegradation in combination with addition of nutrients and electron donors or acceptors and (iii) EK containment and remediation of polluted sites and groundwater plumes (Lageman et al., 2005).

In another case study, the site of a former silver factory in the Netherlands, severely polluted with chlorinated solvents, was treated by electro-bioreclamation: heating soil and groundwater in the source areas, combined with soil vapor extraction and low-yield groundwater pumping, and enhancing biodegradation in the groundwater plume area. Two years of heating and 2.5 years of biodegradation resulted in near-complete removal of the contaminants (Lageman and Godschalk, 2007).

### 5.8. Comparative analysis and discussion

A comparative analysis of EK coupled with other remediation technologies is presented in Table 7, identifying the technology, if it has been tested or not, the organochlorines tested, and major advantages and possible disadvantages. Comparing with enhancement techniques, more research has been made on coupling electrokinetics with other technologies, and even full-scale applications were tested. It is not possible to compare directly the different technologies integrated with EK, since different experimental approaches were used and the way these technologies act on contaminants is also different. Further research is needed on technologies like phytoremediation and to expand these applications to other organochlorine families, like PCBs for example, since most of the studies were targeting CAH, CB and CP.

## 6. Conclusions

The main factors influencing the effectiveness of remediation technologies are the chemical properties of organochlorines, specifically their low water solubility and sorption to soil particles. To use EK remediation in these compounds, enhancement techniques and the integration with other technologies are needed, both to remove contaminants and to increase dechlorination.

Most of the research works analyzed are based on spiked kaolinite or model soils and the successful results obtained cannot always be transferred directly to spiked soils or to soils sampled at polluted sites. This is due to the variety of adsorption sites for organochlorines present in homogeneous soils (organic and inorganic) not being present in kaolinite and also to the aging of contamination. The relative rareness of data available for real contaminated soils may reflect the challenges involved in transferring technology into the field.

Further research is needed since technical and environmental issues will require a careful evaluation for further full-scale implementation. These include controlling side effects during treatment (such as anodic precipitation, oxidation of the conditioning agent and generation of toxic gases e.g., $Cl_2$), as well as evaluating the potential ecotoxicological effects of the surfactants, co-solvents, oxidants or reductants used.

Although EK remediation has been used quite extensively, it has never been used to extract PCBs from soils neither enhanced nor coupled EK with other technologies. According to the latest research developments, there is a great potential to use electrokinetics coupled with nZVI to remediate PCBs and other organochlorines contaminated soils and sediments.

## Acknowledgments

This work has been funded by the European Regional Development Fund (ERDF) through COMPETE – Operational Programme for Competitiveness Factors (OPCF), by Portuguese National funds through "FCT – Fundação para a Ciência e a Tecnologia" under Project «PTDC/AGR AAM/101643/2008 NanoDC» and by FP7-PEOPLE-IRSES-2010-269289-ELECTROACROSS.

## References

Aboughalma, H., Bi, R., Schlaak, M., 2008. Electrokinetic enhancement on phytoremediation in Zn, Pb, Cu and Cd contaminated soil using potato plants. J. Environ. Sci. Health, A 43, 926–933.

Acar, Y.B., Alshawabkeh, A.N., 1993. Principles of electrokinetic remediation. Environ. Sci. Technol. 27, 2638–2647.

Acar, Y.B., Gale, R.J., Alshawabkeh, A.N., Marks, R.E., Puppula, S., Bricka, M., Parker, R., 1995. Electrokinetic remediation: basics and technology status. J. Hazard. Mater. 40, 117–137.

Agarwal, S., Cluxton, P., Kemper, M., Dionysiou, D.D., Al-Abed, S.R., 2008. Assessment of the functionality of a pilot-scale reactor and its potential for electrochemical degradation of calmagite, a sulfonated azo-dye. Chemosphere 73, 837–843.

Aken, B.V., Correa, P.A., Schnoor, J.L., 2010. Phytoremediation of polychlorinated biphenyls: new trends and promises. Environ. Sci. Technol. 44, 2767–2776.

Alcántara, T., Pazos, M., Cameselle, C., Sanromán, M.A., 2008. Electrochemical remediation of phenanthrene from contaminated kaolinite. Environ. Geochem. Health 30, 89–94.

Alcántara, M.T., Gómez, J., Pazos, M., Sanromán, M.A., 2010. Electrokinetic remediation of PAH mixtures from kaolin. J. Hazard. Mater. 179, 1156–1160.

Alshawabkeh, A.N., 2009. Electrokinetic soil remediation: challenges and opportunities. Sep. Sci. Technol. 44, 2171–2187.

Alshawabkeh, A.N., Sheahan, T.C., Wu, X., 2004. Coupling of electrochemical and mechanical processes in soils under DC fields. Mech. Mater. 36, 453–465.

Athmer, C., 2004. In-situ remediation of TCE in clayey soils. Soil Sediment Contam. 13, 381–390.

ATSDR, 2011. Toxicological Profiles. Agency for Toxic Substances and Disease Registry. US Department of Health and Human Services, Atlanta, Georgia.

Baek, K., Kim, D.-H., Park, S.-W., Ryu, B.-G., Bajargal, T., Yang, J.-S., 2009. Electrolyte conditioning-enhanced electrokinetic remediation of arsenic-contaminated mine tailing. J. Hazard. Mater. 161, 457–462.

Bedmar, M.C.L., Pérez-Sanz, A., Martínez-Iñigo, M.J., Benito, A.P., 2009. Influence of coupled electrokinetic – phytoremediation on soil remediation. In: Reddy, K.R., Cameselle, C. (Eds.), Electrochemical Remediation Technologies for Polluted Soils, Sediments and Groundwater. John Wiley & Sons, Inc., Hoboken, New Jersey, pp. 417–433.

Bi, R., Schlaak, M., Siefert, E., Lord, R., Connolly, H., 2011. Influence of electrical fields (AC and DC) on phytoremediation of metal polluted soils with rapeseed (*Brassica napus*) and tobacco (*Nicotiana tabacum*). Chemosphere 83, 318–326.

Cang, L., Wang, Q.Y., Zhou, D.M., Xu, H., 2011. Effects of electrokinetic-assisted phytoremediation of a multiple-metal contaminated soil on soil metal bioavailability and uptake by Indian mustard. Sep. Purif. Technol. 79, 246–253.

Chang, J.-H., Cheng, S.-F., 2006. The remediation performance of a specific electrokinetics integrated with zero-valent metals for perchloroethylene contaminated soils. J. Hazard. Mater. B 131, 153–162.

Chang, J.-H., Liao, Y.-C., 2006. The effect of critical operational parameters on the circulation-enhanced electrokinetics. J. Hazard. Mater. B 129, 186–193.

Chang, J.-H., Qiang, Z., Huang, C.-P., 2006. Remediation and stimulation of selected chlorinated organic solvents in unsaturated soil by a specific enhanced electrokinetics. Colloids Surf., A 287, 86–93.

Chang, J.-H., Qiang, Z., Huang, C.-P., Ellis, A.V., 2009. Phenanthrene removal in unsaturated soils treated by electrokinetics with different surfactants—Triton X-100 and rhamnolipid. Colloids Surf., A 348, 157–163.

Chen, S.-S., Huang, Y.-C., Kuo, T.-Y., 2010. The remediation of perchloroethylene contaminated groundwater by nanoscale iron reactive barrier integrated with surfactant and electrokinetics. Ground Water Monit. R 30, 90–98.

Chuluun, B., Iamchaturapatr, J., Rhee, J.S., 2009. Phytoremediation of organophosphorus and organochlorine pesticides by *Acorus gramineus*. Environ. Eng. Res. 14, 226–236.

Chung, H.I., Kamon, M., 2005. Ultrasonically enhanced electrokinetic remediation for removal of Pb and phenanthrene in contaminated soils. Eng. Geol. 77, 233–242.

Chung, H.I., Lee, M., 2007. A new method for remedial treatment of contaminated clayey soils by electrokinetics coupled with permeable reactive barriers. Electrochim. Acta 52, 3427–3431.

Colacicco, A., Gioannis, G.D., Muntoni, A., Pettinao, E., Polettini, A., Pomi, R., 2010. Enhanced electrokinetic treatment of marine sediments contaminated by heavy metals and PAHs. Chemosphere 81, 46–56.

Collings, A.F., Farmer, A.D., Gwan, P.B., Pintos, A.P.S., Leo, C.J., 2006. Processing contaminated soils and sediments by high power ultrasound. Miner. Eng. 19, 450–453.

Cong, Y., Ye, Q., Wu, Z., 2005. Electrokinetic behaviour of chlorinated phenols in soil and their electrochemical degradation. Process Saf. Environ. 83, 178–183.

DeFlaun, M.F., Condee, C.W., 1997. Electrokinetic transport of bacteria. J. Hazard. Mater. 55, 263–277.

EEA, 2007. Progress in Management of Contaminated Sites. European Environment Agency, Report CSI 015. Copenhagen, Denmark.

Elektorowicz, M., Boeva, V., 1996. Electrokinetic supply of nutrients in soil bioremediation. Environ. Technol. 17, 1339–1349.

Ferreira, C., Ribeiro, A., Ottosen, L., 2005. Effect of major constituents of MSW fly ash during electrodialytic remediation of heavy metals. Sep. Sci. Technol. 40, 2007–2019.

Gómez, J., Alcántara, M.T., Pazos, M., Sanromán, M.A., 2009. A two-stage process using electrokinetic remediation and electrochemical degradation for treating benzo[a]pyrene spiked kaolin. Chemosphere 74, 1516–1521.

Gonzini, O., Plaza, A., Palma, L.D., Lobo, M.C., 2010. Electrokinetic remediation of gasoil contaminated soil enhanced by rhamnolipid. J. Appl. Electrochem. 40, 1239–1248.

Hanberg, A., 1996. Toxicology of environmentally persistent chlorinated organic compounds. Pure Appl. Chem. 68, 1791–1799.

Hansen, H.K., Ottosen, L.M., Pedersen, A.J., Villumsen, A., 2001. Speciation and mobility of cadmium in straw and wood combustion fly ash. Chemosphere 45, 123–128.

Hansen, H.K., Ribeiro, A.B., Mateus, E.P., Ottosen, L.M., 2007. Diagnostic analysis of electrodialysis in mine tailing materials. Electrochim. Acta 52, 3406–3411.

Harbottle, M.J., Lear, G., Sills, G.C., Thompson, I.P., 2009. Enhanced biodegradation of pentachlorophenol in unsaturated soil using reversed field electrokinetics. J. Environ. Manage. 90, 1893–1900.

He, F., 2007. Preparation, Characterization, and Applications of Polysaccharide-Stabilized Metal Nanoparticles for Remediation of Chlorinated Solvents in Soils and Groundwater. PhD thesis. Auburn University, Auburn, Alabama, p. 277.

Ho, S.V., Sheridan, P.W., Athmer, C.J., Heitkamp, M.A., Brackin, J.M., Weber, D., Brodsky, P.H., 1995. Integrated in situ soil remediation technology: the Lasagna process. Environ. Sci. Technol. 29, 2528–2534.

Ho, S.V., Athmer, C.J., Sheridan, P.W., Shapiro, A.P., 1997. Scale-up aspects of the "Lasagna" process for in situ soil decontamination. J. Hazard. Mater. 55, 39–60.

Ho, S.V., Athmer, C., Sheridan, P.W., Hughes, B.M., Orth, R., McKenzie, D., Brodsky, P.H., Shapiro, A., Thornton, R., Salvo, J., Schultz, D., Landis, R., Griffith, R., Shoemaker, S., 1999a. The Lasagna technology for in situ soil remediation. 1. Small field test. Environ. Sci. Technol. 33, 1086–1091.

Ho, S.V., Athmer, C., Sheridan, P.W., Hughes, B.M., Orth, R., McKenzie, D., Brodsky, P.H., Shapiro, A., Sivavec, T.M., Salvo, J., Schultz, D., Landis, R., Griffith, R., Shoemaker, S., 1999b. The Lasagna technology for in situ soil remediation. 2. Large field test. Environ. Sci. Technol. 33, 1092–1099.

Isosaari, P., Piskonen, R., Ojala, P., Voipio, S., Eilola, K., Lehmus, E., Itavaara, M., 2007. Integration of electrokinetics and chemical oxidation for the remediation of creosote-contaminated clay. J. Hazard. Mater. 144, 538–548.

Jackman, S.A., Maini, G., Sharman, A.K., Sunderland, G., Knowles, C.J., 2001. Electrokinetic movement and biodegradation of 2,4-dichlorophenoxyacetic acid in silt soil. Biotechnol. Bioeng. 74, 40–48.

Jensen, P.E., Ferreira, C.M.D., Hansen, H.K., Rype, J.-U., Ottosen, L.M., Villumsen, A., 2010. Electroremediation of air pollution control residues in a continuous reactor. J. Appl. Electrochem. 40, 1173–1181.

Jiemvarangkul, P., Zhang, W.X., Lien, H.L., 2011. Enhanced transport of polyelectrolyte stabilized nanoscale zero-valent iron (nZVI) in porous media. Chem. Eng. J. 170, 482–491.

Jin, S., Fallgren, P.H., 2010. Electrically induced reduction of trichloroethene in clay. J. Hazard. Mater. 173, 200–204.

Jiradecha, C., Urgun-Demirtas, M., Pagilla, K., 2006. Enhanced electrokinetic dissolution of naphthalene and 2,4-DNT from contaminated soils. J. Hazard. Mater. 136, 61–67.

Jones, E.H., Reynolds, D.A., Wood, A.L., Thomas, D.G., 2010. Use of electrophoresis for transporting nano-iron in porous media. Ground Water 49, 172–183.

Karagunduz, A., 2009. Electrokinetic transport of chlorinated organic pesticides. In: Reddy, K.R., Cameselle, C. (Eds.), Electrochemical Remediation Technologies for Polluted Soils, Sediments and Groundwater. John Wiley & Sons, Inc., Hoboken, New Jersey, pp. 235–248.

Karagunduz, A., Gezer, A., Karasuloglu, G., 2007. Surfactant enhanced electrokinetic remediation of DDT from soils. Sci. Total Environ. 385, 1–11.

Kaya, A., Yukselen, Y., 2005. Zeta potential of soils with surfactants and its relevance to electrokinetic remediation. J. Hazard. Mater. B 120, 119–126.

Khodadoust, A.P., Reddy, K.R., Maturi, K., 2004. Removal of nickel and phenanthrene from kaolin soil using different extractants. Environ. Eng. Sci. 21, 691–704.

Kim, J., Lee, K., 1999. Effects of electric field directions on surfactant enhanced electrokinetic remediation of diesel-contaminated sand column. J. Environ. Sci. Health, A 34, 863–877.

Kim, S.-S., Han, S.-J., Cho, Y.-S., 2002. Electrokinetic remediation strategy considering ground strata: a review. Geosci. J. 6, 57–75.

Kim, W.-S., Kim, S.-O., Kim, K.-W., 2005. Enhanced electrokinetic extraction of heavy metals from soils assisted by ion exchange membranes. J. Hazard. Mater. B 118, 93–102.

Kim, J.-H., Han, S.-J., Kim, S.-S., Yang, J.-W., 2006. Effect of soil chemical properties on the remediation of phenanthrene-contaminated soil by electrokinetic-Fenton process. Chemosphere 63, 1667–1676.

Kim, J.H., Kim, S.S., Yang, J.W., 2007. Role of stabilizers for treatment of clayey soil contaminated with phenanthrene through electrokinetic-Fenton process—some experimental evidences. Electrochim. Acta 53, 1663–1670.

Kim, J.-H., Kim, J.Y., Kim, S.-S., 2009. Effect of $H_2SO_4$ and HCl in the anode purging solution for the electrokinetic-Fenton remediation of soil contaminated with phenanthrene. J. Environ. Sci. Health, A 44, 1111–1119.

Kim, B.-K., Baek, K., Ko, S.-H., Yang, J.-W., 2011. Research and field experiences on electrokinetic remediation in South Korea. Sep. Purif. Technol. 79, 116–123.

Ko, S.-O., Schlautman, M.A., Carraway, E.R., 2000. Cyclodextrin-enhanced electrokinetic removal of phenanthrene from a model clay soil. Environ. Sci. Technol. 4, 1535–1541.

Kolosov, A.Y., Popov, K.I., Shabanova, N.A., Artem'eva, A.A., Kogut, B.M., Frid, A.S., Zel'venskii, V.Y., Urinovich, E.M., 2001. Electrokinetic removal of hydrophobic organic compounds from soil. Russ. J. Appl. Chem. 74, 631–635.

Lageman, R., Godschalk, M.S., 2007. Electro-bioreclamation: a combination of *in situ* remediation techniques proves successful at a site in Zeist, the Netherlands. Electrochim. Acta 52, 3449–3453.

Lageman, R., Pool, W., Seffinga, G.A., 1989. Electro-reclamation. Chem. Ind. 18, 585–590.

Lageman, R., Clarke, R.L., Pool, W., 2005. Electro-reclamation, a versatile soil remediation solution. Eng. Geol. 77, 191–201.

Lahlou, M., Harms, H., Springael, D., Ortega-Calvo, J.-J., 2000. Influence of soil components on the transport of polycyclic aromatic hydrocarbon-degrading bacteria through saturated porous media. Environ. Sci. Technol. 34, 3649–3656.

Lear, G., Harbottle, M.J., Sills, G., Knowles, C.J., Semple, K.T., Thompson, I.P., 2007. Impact of electrokinetic remediation on microbial communities within PCP contaminated soil. Environ. Pollut. 146, 139–146.

Lee, H.-H., Yang, J.-W., 2000. A new method to control electrolytes pH by circulation system in electrokinetic soil remediation. J. Hazard. Mater. B 77, 227–240.

Lee, G., Ro, H., Lee, S., Lee, S., 2006. Electrokinetically enhanced transport of organic and inorganic phosphorus in a low permeability soil. Geosci. J. 10, 85–89.

Lee, Y.J., Han, H., Kim, S.H., Yang, J.W., 2009. Combination of electrokinetic separation and electrochemical oxidation for acid dye removal from soil. Sep. Sci. Technol. 44, 2455–2469.

Li, T., Yuan, S., Wan, J., Lin, L., Long, H., Wu, X., Lu, X., 2009. Pilot-scale electrokinetic movement of HCB and Zn in real contaminated sediments enhanced with hydroxypropyl-β-cyclodextrin. Chemosphere 76, 1226–1232.

Li, T., Guo, S., Wu, B., Li, F., Niu, Z., 2010a. Effect of electric intensity on the microbial degradation of petroleum pollutants in soil. J. Environ. Sci. 22, 1381–1386.

Li, T., Yuan, S., Wan, J., Lu, X., 2010b. Hydroxypropyl-beta-cyclodextrin enhanced electrokinetic remediation of sediment contaminated with HCB and heavy metals. J. Hazard. Mater. 176, 306–312.

Li, Z., Yuan, S., Wan, J., Long, H., Tong, M., 2011. A combination of electrokinetics and Pd/Fe PRB for the remediation of pentachlorophenol-contaminated soil. J. Contam. Hydrol. 124, 99–107.

Lim, J.-M., Salido, A.L., Butcher, D.J., 2004. Phytoremediation of lead using Indian mustard (*Brassica juncea*) with EDTA and electrodics. Microchem. J. 76, 3–9.

Lima, A.T., Kleingeld, P.J., Heister, K., Loch, J.P.G., 2011. Removal of PAHs from contaminated clayey soil by means of electro-osmosis. Sep. Purif. Technol. 79, 221–229.

Lohner, S.T., Katzoreck, D., Tiehm, A., 2008a. Electromigration of microbial electron acceptors and nutrients: (I) transport in synthetic media. J. Environ. Sci. Health, A 43, 913–921.

Lohner, S.T., Katzoreck, D., Tiehm, A., 2008b. Electromigration of microbial electron acceptors and nutrients: (II) transport in groundwater. J. Environ. Sci. Health, A 43, 922–925.

Lohner, S.T., Tiehm, A., Jackman, S.A., Carter, P., 2009. Coupling electrokinetics to the bioremediation of organic contaminants: applied aspects. In: Reddy, K.R., Cameselle, C. (Eds.), Electrochemical Remediation Technologies for Polluted Soils, Sediments and Groundwater. John Wiley & Sons, Inc., Hoboken, New Jersey, pp. 389–416.

Lu, X., Yuan, S., 2009. Electrokinetic removal of chlorinated organic compounds. In: Reddy, K.R., Cameselle, C. (Eds.), Electrochemical Remediation Technologies for Polluted Soils, Sediments and Groundwater. John Wiley & Sons, Inc., Hoboken, New Jersey, pp. 219–234.

Luo, Q., Zhang, X., Wang, H., Qian, Y., 2005a. Mobilization of phenol and dichlorophenol in unsaturated soils by non-uniform electrokinetics. Chemosphere 59, 1289–1298.

Luo, Q., Zhang, X., Wang, H., Qian, Y., 2005b. The use of non-uniform electrokinetics to enhance in situ bioremediation of phenol-contaminated soil. J. Hazard. Mater. B 121, 187–194.

Luo, Q., Wang, H., Zhang, X., Fan, X., Qian, Y., 2006. In situ bioelectrokinetic remediation of phenol-contaminated soil by use of an electrode matrix and a rotational operation mode. Chemosphere 64, 415–422.

Lysenko, L.L., Mishchuk, N.A., 2009. Electrohydrodynamic method of pH regulation at soil decontamination. Colloids Surf., A 333, 59–66.

Ma, J.W., Wang, F.Y., Huang, Z.H., Wang, H., 2010. Simultaneous removal of 2,4-dichlorophenol and Cd from soils by electrokinetic remediation combined with activated bamboo charcoal. J. Hazard. Mater. 176, 715–720.

Maini, G., Sharman, A.K., Knowles, C.J., Sunderland, G., Jackman, S.A., 2000. Electrokinetic remediation of metals and organics from historically contaminated soil. J. Chem. Technol. Biotechnol. 75, 657–664.

Mateus, E.P., Zrostlíková, J., Silva, M.D.R.G.d., Ribeiro, A.B., Marriott, P.J., 2010. Electrokinetic removal of creosote from treated timber waste: a comprehensive gas chromatographic view. J. Appl. Electrochem. 40 (0), 1183–1193.

Maturi, K., Reddy, K.R., 2006. Simultaneous removal of organic compounds and heavy metals from soils by electrokinetic remediation with a modified cyclodextrin. Chemosphere 63, 1022–1031.

Meagher, R.B., 2000. Phytoremediation of toxic elemental and organic pollutants. Curr. Opin. Plant Biol. 3, 153–162.

Mishchuk, N., Kornilovich, B., Klishchenko, R., 2007. PH regulation as a method of intensification of soil electroremediation. Colloids Surf., A 306, 171–179.

Moermond, C.T.A., 2007. Bioaccumulation of Persistent Organic Pollutants from Floodplain Lake Sediments: Linking Models to Measurements. Wageningen University, Wageningen, The Netherlands.

Moon, J.-W., Moon, H.-S., Kim, H., Roh, Y., 2005. Remediation of TCE-contaminated groundwater using zero valent iron and direct current: experimental results and electron competition model. Environ. Geol. 48, 805–817.

Mulligan, C.N., 2009. Recent advances in the environmental applications of biosurfactants. Curr. Opin. Colloid Int. 14, 372–378.

Mulligan, C.N., Yong, R.N., Gibbs, B.F., 2001. Surfactant-enhanced remediation of contaminated soil: a review. Eng. Geol. 60, 371–380.

Murillo-Rivera, B., Labastida, I., Barron, J., Oropeza-Guzman, M.T., Gonzalez, I., Teutli-Leon, M.M.M., 2009. Influence of anolyte and catholyte composition on TPHs removal from low permeability soil by electrokinetic reclamation. Electrochim. Acta 54, 2119–2124.

Newman, L.A., Reynolds, C.M., 2004. Phytodegradation of organic compounds. Curr. Opin. Biotechnol. 15, 225–230.

Niqui-Arroyo, J.-L., Ortega-Calvo, J.-J., 2007. Integrating biodegradation and electroosmosis for the enhanced removal of polycyclic aromatic hydrocarbons from creosote-polluted soils. J. Environ. Qual. 36, 1444–1451.

Niqui-Arroyo, J.-L., Bueno-Montes, M., Posada-Baquero, R., Ortega-Calvo, J.-J., 2006. Electrokinetic enhancement of phenanthrene biodegradation in creosote-polluted clay soil. Environ. Pollut. 142, 326–332.

Nystroem, G.M., Ottosen, L., Villumsen, A., 2005. Electrodialytic removal of Cu, Zn, Pb and Cd from harbour sediment: influences of changing experimental conditions. Environ. Sci. Technol. 38, 2906–2911.

O'Connor, C.S., Lepp, N.W., Edwards, R., Sunderland, G., 2003. The combined use of electrokinetic remediation and phytoremediation to decontaminate metal-polluted soils: a laboratory-scale feasibility. Environ. Monit. Assess. 84, 141–158.

Olszanowski, A., Piechowiak, K., 2006. The use of an electric field to enhance bacterial movement and hydrocarbon biodegradation in soils. Polish J. Environ. Stud. 15, 303–309.

Oonnittan, A., Shrestha, R.A., Sillanpää, M., 2009a. Effect of cyclodextrin on the remediation of hexachlorobenzene in soil by electrokinetic Fenton process. Sep. Purif. Technol. 64, 314–320.

Oonnittan, A., Shrestha, R.A., Sillanpää, M., 2009b. Removal of hexachlorobenzene from soil by electrokinetically enhanced chemical oxidation. J. Hazard. Mater. 162, 989–993.

Oonnittan, A., Isosaari, P., Sillanpää, M., 2010. Oxidant availability in soil and its effect on HCB removal during electrokinetic Fenton process. Sep. Purif. Technol. 76, 146–150.

Oostdam, J.V., Donaldson, S.G., Feeley, M., Arnold, D., Ayotte, P., Bondy, G., Chan, L., Dewaily, E., Furgal, C.M., Kuhnlein, H., Loring, E., Muckle, G., Myles, E., Receveur, O., Tracy, B., Gill, U., Kalhok, S., 2005. Human health implications of environmental contaminants in Artic Canada: a review. Sci. Total Environ. 351–352, 165–246.

Ottosen, L.M., Hansen, H.K., 1992. Electrokinetic Cleaning of Heavy Metal Polluted Soil. Internal Report. Technical University of Denmark, Denmark. p. 9.

Ottosen, L.M., Hansen, H.K., Laursen, S., Villumsen, A., 1997. Electrodialytic remediation of soil polluted with copper from wood preservation industry. Environ. Sci. Technol. 31, 1711–1715.

Ottosen, L.M., Pedersen, A.J., Ribeiro, A.B., Hansen, H.K., 2005. Case study on the strategy and application of enhancement solutions to improve remediation of soils contaminated with Cu, Pb and Zn by means of electrodialysis. Eng. Geol. 77, 317–329.

Ottosen, L.M., Christensen, I.V., Rörig-Dalgård, I., Jensen, P.E., Hansen, H.K., 2008. Utilization of electromigration in civil and environmental engineering – processes, transport rates and matrix changes. J. Environ. Sci. Health, A 43, 795–809.

Page, M.M., Page, C.L., 2002. Electroremediation of contaminated soils. J. Environ. Eng. – ASCE 128, 208–219.

Pamukcu, S., Wittle, J.K., 1992. Electrokinetic removal of selected heavy metals from soil. Environ. Prog. 11, 241–250.

Pamukcu, S., Hannum, L., Wittle, J.K., 2008. Delivery and activation of nano-iron by DC electric field. J. Environ. Sci. Health, A 43, 934–944.

Park, J.-Y., Kim, S.-J., Lee, Y.-J., Baek, K., Yang, J.-W., 2005. EK-Fenton process for removal of phenanthrene in a two-dimensional soil system. Eng. Geol. 77, 217–224.

Park, J.-Y., Lee, H.-H., Kim, S.-J., Lee, Y.-J., Yang, J.-W., 2007. Surfactant-enhanced electrokinetic removal of phenanthrene from kaolinite. J. Hazard. Mater. 140, 230–236.

Park, S.-W., Lee, J.-Y., Yang, J.-S., Kim, K.-J., Baek, K., 2009. Electrokinetic remediation of contaminated soil with waste-lubricant oils and zinc. J. Hazard. Mater. 169, 1168–1172.

Pazos, M., Sanromán, M.A., Cameselle, C., 2006. Improvement in electrokinetic remediation of heavy metal spiked kaolin with the polarity exchange technique. Chemosphere 62, 817–822.

Pazos, M., Rosales, E., Alcántara, T., Gómez, J., Sanromán, M.A., 2010. Decontamination of soils containing PAHs by electroremediation: a review. J. Hazard. Mater. 177, 1–11.

Pham, T.D., Shrestha, R.A., Virkutyte, J., Sillanpää, M., 2009. Combined ultrasonication and electrokinetic remediation for persistent organic removal from contaminated kaolin. Electrochim. Acta 54, 1403–1407.

Polcaro, A.M., Vacca, A., Mascia, M., Palmas, S., 2007. Electrokinetic removal of 2,6-dichlorophenol and diuron from kaolinite and humic acid–clay system. J. Hazard. Mater. 148, 505–512.

Probstein, R.F., Hicks, R.E., 1993. Removal of contaminants from soil by electric fields. Science 260, 498–530.

Puppala, S.K., Alshawabkeh, A.N., Acar, Y.B., Gale, R.J., Bricka, M., 1997. Enhanced electrokinetic remediation of high sorption capacity soil. J. Hazard. Mater. 55, 203–220.

Rabbi, M.F., Clark, B., Gale, R.J., Ozsu-Acar, E., Pardue, J., Jackson, A., 2000. In situ TCE bioremediation study using electrokinetic cometabolite injection. Waste Manage. (Oxford) 20, 279–286.

Ranjan, R.S., Qian, Y., Krishnapillai, M., 2006. Effects of electrokinetics and cationic surfactant cetyltrimethylammonium bromide [CTAB] on the hydrocarbon removal and retention from contaminated soils. Environ. Technol. 27, 767–776.

Reddy, K., Karri, M.R., 2008a. Effect of oxidant dosage on integrated electrochemical remediation of contaminant mixtures in soils. J. Environ. Sci. Health, A 43, 881–893.

Reddy, K.R., Karri, M.R., 2008b. Electrokinetic delivery of nanoiron amended with surfactant and cosolvent in contaminated soil. In: International Conference on Waste Engineering and Management, Hong Kong.

Reddy, K.R., Karri, M.R., 2009. Effect of electric potential on nanoiron particles delivery for pentachlorophenol remediation in low permeability soil. In: Hamza, M., Shahien, M., El-Mossallamy, Y. (Ed.), Proceedings of the 17th International Conference on Soil Mechanics and Geotechnical Engineering: The Academia and Practice of Geotechnical Engineering, Alexandria, Egypt, pp. 2312–2315.

Reddy, K.R., Cameselle, C., Ala, P., 2010. Integrated electrokinetic-soil flushing to remove mixed organic and metal contaminants. J. Appl. Electrochem. 40, 1269–1279.

Reddy, K.R., Darko-Kagy, K., Cameselle, C., 2011a. Electrokinetic-enhanced transport of lactate-modified nanoscale iron particles for degradation of dinitrotoluene in clayey soils. Sep. Purif. Technol. 79, 230–237.

Reddy, K.R., Darko-Kagya, K., Al-Hamdan, A.Z., 2011b. Electrokinetic remediation of chlorinated aromatic and nitroaromatic organic contaminants in clay soil. Environ. Eng. Sci. 28, 405–413.

Reddy, K.R., Darko-Kagya, K., Al-Hamdan, A.Z., 2011c. Electrokinetic remediation of pentachlorophenol contaminated clay soil. Water, Air, Soil Pollut. 221, 35–44.

Reible, D.D., Thibodeaux, L.J., 1999. Using Natural Processes to Define Exposure From Sediments. Risk Based Approach to the Evaluation and Management of Contaminated Sediments, Sediment Management Work Group Technical Paper.

Ribeiro, A.B., Mexia, J.T., 1997. A dynamic model for the electrokinetic removal of copper from polluted soil. J. Hazard. Mater. 56, 257–271.

Ribeiro, A.B., Rodríguez-Maroto, J.M., 2006. Electroremediation of heavy metal-contaminated soils. Processes and applications. In: Prasad, M.N.V., Sajwan, K.S., Naidu, R. (Eds.), Trace Elements in the Environment: Biogeochemistry, Biotechnology and Bioremediation. Taylor & Francis, CRC Press, Florida, USA, pp. 341–368.

Ribeiro, A.B., Mateus, E.P., Ottosen, L.M., Bech-Nielsen, G., 2000. Electrodialytic removal of Cu, Cr and As from chromated copper arsenate-treated timber waste. Environ. Sci. Technol. 34, 784–788.

Ribeiro, A.B., Rodríguez-Maroto, J.M., Mateus, E.P., Gomes, H., 2005. Removal of organic contaminants from soils by an electrokinetic process: the case of atrazine. Experimental and modeling. Chemosphere 59, 1229–1239.

Ribeiro, A.B., Mateus, E.P., Rodríguez-Maroto, J.-M., 2011. Removal of organic contaminants from soils by an electrokinetic process: the case of molinate and bentazone. Experimental and modeling. Sep. Purif. Technol. 79, 193–203.

Rocha, U.N.D., Tótola, M.R., Pessoa, D.M.M., Júnior, J.T.A., Neves, J.C., Borges, A.C., 2009. Mobilisation of bacteria in a fine-grained residual soil by electrophoresis. J. Hazard. Mater. 161, 485–491.

Roh, Y., Lee, S.Y., Elless, M.P., Moon, H.-S., 2000. Electro-enhanced remediation of trichloroethene-contaminated groundwater using zero-valent iron. J. Environ. Sci. Health, A 35, 1061–1076.

Rohrs, J., Ludwig, G., Rahner, D., 2002. Electrochemically induced reactions in soils – a new approach to the in-situ remediation of contaminated soils? Part 2: remediation experiments with a natural soil containing highly chlorinated hydrocarbons. Electrochim. Acta 47, 1405–1414.

RTDF, 2005. Evaluation of Phytoremediation for Management of Chlorinated Solvents in Soil and Groundwater. The Remediation Technologies Development Forum, Phytoremediation of Organics Action Team, Chlorinated Solvents Workgroup, United States Environmental Protection Agency.

Saichek, R.E., Reddy, K.R., 2003. Effect of pH control at the anode for the electrokinetic removal of phenanthrene from kaolin soil. Chemosphere 21, 273–287.

Saichek, R.E., Reddy, K.R., 2004. Evaluation of surfactants/cosolvents for desorption/solubilization of phenanthrene in clayey soils. Int. J. Environ. Stud. 61, 587–604.

Saichek, R.E., Reddy, K.R., 2005a. Electrokinetically enhanced remediation of hydrophobic organic compounds in soils: a review. Crit. Rev. Environ. Sci. Technol. 35, 115–192.

Saichek, R.E., Reddy, K.R., 2005b. Surfactant-enhanced electrokinetic remediation of polycyclic aromatic hydrocarbons in heterogeneous subsurface environments. J. Environ. Eng. Sci. 4, 327–339.

Schmidt, C.A.B., Barbosa, M.C., Almeida, M.d.S.S.d., 2008. A laboratory feasibility study on electrokinetic injection of nutrients on an organic, tropical, clayey soil. J. Hazard. Mater. 143, 655–661.

Shen, Z., Chen, X., Jia, J., Qu, L., Wang, W., 2007. Comparison of electrokinetic soil remediation methods using one fixed anode and approaching anodes. Environ. Pollut. 150, 193–199.

Shi, L., Harms, H., Wick, L.Y., 2008a. EOF stimulates the release of alginate-bound phenanthrene. Environ. Sci. Technol. 42, 2105–2110.

Shi, L., Muller, S., Harms, H., Wick, L.Y., 2008b. Effect of electrokinetic transport on the vulnerability of PAH-degrading bacteria in a model aquifer. Environ. Geochem. Health 30, 177–182.

Shi, L., Muller, S., Harms, H., Wick, L.Y., 2008c. Factors influencing the electrokinetic dispersion of PAH-degrading bacteria in a laboratory model aquifer. Appl. Microbiol. Biotechnol. 80, 507–515.

Shih, Y.-H., Chen, Y.-C., Chen, M.-Y., Tai, Y.-T., Tso, C.-P., 2009. Dechlorination of hexachlorobenzene by using nanoscale Fe and nanoscale Pd/Fe bimetallic particles. Colloids Surf., A 332, 84–89.
Shrestha, R.A., Pham, T.D., Sillanpää, M., 2009. Remediation of chrysene from contaminated soil by enhanced electrokinetics. Int. J. Electrochem. Sci. 4, 1387–1394.
Thepsithar, P., Roberts, E.P.L., 2006. Removal of phenol from contaminated kaolin using electrokinetically enhanced in situ chemical oxidation. Environ. Sci. Technol. 40, 6098–6103.
Tiehm, A., Lohner, S.T., Augenstein, T., 2009. Effects of direct electric current and electrode reactions on vinyl chloride degrading microorganisms. Electrochim. Acta 54, 3453–3459.
Tiraferri, A., Sethi, R., 2009. Enhanced transport of zerovalent iron nanoparticles in saturated porous media by guar gum. J. Nanopart. Res. 11, 635–645.
Tiraferri, A., Chen, K.L., Sethi, R., Elimelech, M., 2008. Reduced aggregation and sedimentation of zero-valent iron nanoparticles in the presence of guar gum. J. Colloid Interface Sci 324, 71–79.
Tsai, T.-T., Sah, J., Kao, C.-M., 2010. Application of iron electrode corrosion enhanced electrokinetic-Fenton oxidation to remediate diesel contaminated soils: a laboratory feasibility study. J. Hydrol. 380, 4–13.
USEPA, 2011. In Situ Oxidation: Overview. Technology Innovation and Field Services Division, Washington, DC.
Virkutyte, J., Sillanpaa, M., 2007. The hindering effect of experimental strategies on advancement of alkaline front and during electrokinetic lake sediment treatment. J. Hazard. Mater. 143, 673–681.
Virkutyte, J., Sillanpaa, M., Latostenmaa, P., 2002. Electrokinetic soil remediation – critical overview. Sci. Total Environ. 289, 97–121.
Wan, J., Yuan, S., Chen, J., Li, T., Lin, L., Lu, X., 2009. Solubility-enhanced electrokinetic movement of hexachlorobenzene in sediments: a comparison of cosolvent and cyclodextrin. J. Hazard. Mater. 166, 221–226.
Wan, J., Li, Z., Lu, X., Yuan, S., 2010. Remediation of a hexachlorobenzene-contaminated soil by surfactant-enhanced electrokinetics coupled with microscale Pd/Fe PRB. J. Hazard. Mater. 184, 184–190.
Wang, S., Mulligan, C.N., 2004. An evaluation of surfactant foam technology in remediation of contaminated soil. Chemosphere 53, 1079–1089.
Wang, J.-Y., Huang, X.-J., Kao, J.C.M., Stabnikova, O., 2007. Simultaneous removal of organic contaminants and heavy metals from kaolin using an upward electrokinetic soil remediation process. J. Hazard. Mater. 144, 292–299.
Weng, C.-H., 2009. Coupled electrokinetic–permeable reactive barriers. In: Reddy, K.R., Cameselle, C. (Eds.), Electrochemical Remediation Technologies for Polluted Soils, Sediments and Groundwater. John Wiley & Sons, Inc., Hoboken, New Jersey, pp. 483–504.
Wick, L.Y., 2009. Coupling electrokinetics to the bioremediation of organic contaminants: principles and fundamental interactions. In: Reddy, K.R., Cameselle, C. (Eds.), Electrochemical Remediation Technologies for Polluted Soils, Sediments and Groundwater. John Wiley & Sons, Inc., Hoboken, New Jersey, pp. 369–388.
Wick, L.Y., Mattle, P.A., Wattiau, P., Harms, H., 2004. Electrokinetic transport of PAH-degrading bacteria in model aquifers and soil. Environ. Sci. Technol. 38, 4596–4602.
Wick, L.Y., Shi, L., Harms, H., 2007. Electro-bioremediation of hydrophobic organic soil-contaminants: a review of fundamental interactions. Electrochim. Acta 52, 3441–3448.
Wick, L.Y., Buchholz, F., Fetzer, I., Kleinsteuber, S., Härtig, C., Shi, L., Miltner, A., Harms, H., Pucci, G.N., 2010. Responses of soil microbial communities to weak electric fields. Sci. Total Environ. 408, 4886–4893.
Wu, X., Alshawabkeh, A.N., Gent, D.B., Larson, S.L., Davis, J.L., 2007. Lactate transport in soil by DC Fields. J. Geotech. Geoenviron. 133, 1587–1596.
Xu, W., Wang, C., Liu, H., Zhang, Z., Sun, H., 2010. A laboratory feasibility study on a new electrokinetic nutrient injection pattern and bioremediation of phenanthrene in a clayey soil. J. Hazard. Mater. 184, 798–804.
Yang, G.C.C., 2009. Electrokinetic – chemical oxidation/reduction. In: Reddy, K.R., Cameselle, C. (Eds.), Electrochemical Remediation Technologies for Polluted Soils, Sediments and Groundwater. John Wiley & Sons, Inc., Hoboken, New Jersey, pp. 439–462.
Yang, G.C.C., Chang, Y.-I., 2011. Integration of emulsified nanoiron injection with the electrokinetic process for remediation of trichloroethylene in saturated soil. Sep. Purif. Technol. 79, 278–284.
Yang, G.C.C., Liu, C.-Y., 2001. Remediation of TCE contaminated soils by in situ EK-Fenton process. J. Hazard. Mater. B 85, 317–331.
Yang, G.C.C., Yeh, C.-F., 2011. Enhanced nano-$Fe_3O_4/S_2O_8^{2-}$ oxidation of trichloroethylene in a clayey soil by electrokinetic. Sep. Purif. Technol. 79, 264–271.
Yang, J.-W., Lee, Y.-J., Park, J.-Y., Kim, S.-J., Lee, J.-Y., 2005. Application of APG and Calfax 16L–35 on surfactant-enhanced electrokinetic removal of phenanthrene from kaolinite. Eng. Geol. 77, 243–251.
Yang, G.C.C., Tu, H.-C., Hung, C.-H., 2007. Stability of nanoiron slurries and their transport in the subsurface environment. Sep. Purif. Technol. 58, 166–172.
Yang, G.C.C., Hung, C.-H., Tu, H.-C., 2008. Electrokinetically enhanced removal and degradation of nitrate in the subsurface using nanosized Pd/Fe slurry. J. Environ. Sci. Health, A 43, 945–951.
Yap, C.L., Gan, S., Ng, H.K., 2011. Fenton based remediation of polycyclic aromatic hydrocarbons-contaminated soils. Chemosphere 83, 1414–1430.
Yeung, A., 2008. Electrokinetics for soil remediation. In: Yeung, A.T., Lo, I.M.C. (Eds.), Proceedings of the Ninth International Symposium on Environmental Geotechnology and Global Sustainable Development, Hong Kong, 1–4 June 2008, pp. 16–25.
Yeung, A.T., 2011. Milestone developments, myths, and future directions of electrokinetic remediation. Sep. Purif. Technol. 79, 124–132.
Yeung, A.T., Gu, Y.-Y., 2011. A review on techniques to enhance electrochemical remediation of contaminated soils. J. Hazard. Mater. 195, 11–29.
Yeung, A.T., Hsu, C.-N., Menon, R.M., 1997. Physicochemical soil-contaminant interactions during electrokinetic extraction. J. Hazard. Mater. 55, 221–237.
Yuan, C., Weng, C.-H., 2004. Remediating ethylbenzene-contaminated clayey soil by a surfactant-aided electrokinetic (SAEK) process. Chemosphere 57, 225–232.
Yuan, S., Tian, M., Lu, X., 2006. Electrokinetic movement of hexachlorobenzene in clayed soils enhanced by Tween 80 and β-cyclodextrin. J. Hazard. Mater. 137, 1218–1225.
Yuan, S.-H., Wan, J.-Z., Lu, X.-H., 2007. Electrokinetic movement of multiple chlorobenzenes in contaminated soils in the presence of β-cyclodextrin. J. Environ. Sci. 19, 968–976.
Yuan, C., Hung, C.-H., Huang, W.-L., 2009. Enhancement with carbon nanotube barrier on 1,2-dichlorobenzene removal from soil by surfactant-assisted electrokinetic (SAEK) process – the effect of processing fluid. Sep. Sci. Technol. 44, 2284–2303.
Zhang, W.-X., 2003. Nanoscale iron particles for environmental remediation: an overview. J. Nanopart. Res. 5, 323–332.
Zhang, M., He, F., Zhao, D., Hao, X., 2011. Degradation of soil-sorbed trichloroethylene by stabilized zero valent iron nanoparticles: effects of sorption, surfactants, and natural organic matter. Water Res. 45, 2401–2414.
Zhou, D.-M., Chen, H.-F., Cang, L., Wang, Y.-J., 2007. Ryegrass uptake of soil Cu/Zn induced by EDTA/EDDS together with a vertical direct-current electrical field. Chemosphere 67, 1671–1676.

## II.3. Enhanced transport and transformation of zerovalent nanoiron in clay using direct electric current (published in Water, Air and Soil Pollution)

Water Air Soil Pollut (2013) 224:1710
DOI 10.1007/s11270-013-1710-2

# Enhanced Transport and Transformation of Zerovalent Nanoiron in Clay Using Direct Electric Current

**Helena I. Gomes · Celia Dias-Ferreira · Alexandra B. Ribeiro · Sibel Pamukcu**

Received: 16 August 2012 / Accepted: 27 March 2013


**Abstract** One of the major obstacles to zerovalent iron nanoparticles (nZVI) application in soil and groundwater remediation is the limited transport, especially in low-permeability soils. In this study, direct current (constant potential of 5.0 V) was used to enhance polymer-coated nZVI mobility in different porous media, including a bed of glass beads and kaolin clay. The tests were conducted using a modified electrophoretic cell and with nZVI concentrations typical of field applications (4 g $L^{-1}$). Experimental results indicate that the use of direct current can enhance the transport of the polymer-modified nanoparticles when compared with natural diffusion in low permeability or surface neutral porous medium. The applied electric field appeared to enhance the oxidation–reduction potential, creating a synergistic effect of nZVI usage with electrokinetics. Aggregation of the nanoparticles, observed near the injection point, remained unresolved.

**Keywords** Zerovalent iron nanoparticles (nZVI) · Enhanced transport · Direct current · Electrokinetics · Electrochemical treatment

Guest Editors: R Naidu, Euan Smith, MH Wong, Megharaj Mallavarapu, Nanthi Bolan, Albert Juhasz, and Enzo Lombi

This article is part of the Topical Collection on *Remediation of Site Contamination*

H. I. Gomes (✉) · S. Pamukcu
Department of Civil and Environmental Engineering, Fritz Engineering Laboratory, Lehigh University, 13 E. Packer Avenue, Bethlehem, PA 18015-4729, USA
e-mail: hrg@campus.fct.unl.pt

H. I. Gomes · A. B. Ribeiro
CENSE, Departamento de Ciências e Engenharia do Ambiente, Faculdade de Ciências e Tecnologia, Universidade Nova de Lisboa, 2829-516 Caparica, Portugal

H. I. Gomes · C. Dias-Ferreira
Instituto Politécnico de Coimbra, CERNAS – Research Center for Natural Resources, Environment and Society, Campus da Escola Superior Agrária de Coimbra, Bencanta, 3040-316 Coimbra, Portugal

## 1 Introduction

Zerovalent iron nanoparticles (nZVI) are a convenient and emergent remediation technology that could provide cost-effective solutions to soil and groundwater contamination (USEPA 2011). These nanoparticles have large surface areas for rapid uptake and transformation of a large number of environmental contaminants (Masciangioli and Zhang 2003; Li et al. 2006). Nanoparticles provide more flexibility for in situ applications than granular iron and can remain reactive for extended periods of time (>4–8 weeks) (Zhang 2003), showing characteristics of both iron oxides (sorbent) and metallic iron (reductant) (Sun et al. 2006). In field applications, the nanoparticle–water slurry has been injected under pressure and/or by gravity into the contaminated plume where treatment is needed; alternatively, nZVI can be transported by the flow of groundwater. However, in low porosity clay-rich media, it is challenging to achieve a uniform distribution of the slurry for effective remediation. Moreover, due to the relatively high ionic strength of most groundwater, favorable for colloidal

Published online: 20 November 2013

aggregation, bare nZVI has very limited mobility in the subsurface (Phenrat et al. 2007; Yang et al. 2007; Kanel et al. 2008; Bennett et al. 2010; He et al. 2010; Comba et al. 2011).

It is possible to use electric fields to effectively move nanoparticles through the soil. Some work has already been done to test this possibility, such as the one conducted by Pamukcu et al. (2008), in which polymer-coated nanoparticles were transported in kaolin by electrophoresis. Jones et al. (2010) also found that nZVI could be transported through fine-grained sand with rates comparable to those predicted by electrokinetic (EK) theory. More recently, modified or emulsified nZVI have been tested together with EK to treat dinitrotoluene (Reddy et al. 2011), trichloroethylene (Yang and Yeh 2011), and pentachlorophenol (Reddy and Karri 2009; Yuan et al. 2012) in spiked kaolin. Experiments with coarse and fine sand and sodium carboxymethyl cellulose stabilized nZVI showed that the electrophoretic enhancement in transport compared to diffusion was proportional to the applied current (Chowdhury et al. 2012).

The work presented here shows the advantages of direct electric current to overcome nZVI transport limitation while enhancing its activation in low permeability soils. Integrating both technologies, the role of direct electric current would be quite the opposite of the traditional one; instead of aiming at getting the contaminants out, it is used to get nZVI into the soil for in situ transformation and subsequent destruction of the contaminants. Bench-scale EK experiments in a modified electrophoretic cell were performed to investigate if the direct current enhances the transport and transformation of polymer-coated nZVI (Lin et al. 2010; Jiemvarangkul et al. 2011). A methodological and analytical approach including expeditious techniques to measure pH, electrical conductivity, oxidation–reduction potential (ORP), and iron content for determining the fate of nZVI in the soil was also developed and tested.

## 2 Experimental

### 2.1 Chemicals

Deionized (DI) water purged with ultra purified grade nitrogen gas ($N_2$) was used in all experiments. The purging was continued for at least 1 h so that the dissolved oxygen would fall to a level below 20 %. nZVI were prepared though the reduction of $FeSO_4$ $7H_2O$ (Fisher Chemicals) by sodium borohydride (Hydrifin$^{TM}$). The polymer coating of the nanoparticles was done using two different methods. For high concentration suspensions, bare nanoparticles were prepared and coated with polyacrylic acid, sodium salt—PAA Mw ~2,100 (Polysciences, Inc.) at 30 % following Jiemvarangkul et al. (2011). For the transport experiments, the freshly prepared suspension had a concentration of 4 g $L^{-1}$ of nZVI, made using the one-step procedure described by Kanel et al. (2008). The particle size distribution of the nanoparticles had a mean value of particle diameter 62.66±39.6 nm and the median size was 60.2 nm (Jiemvarangkul 2012).

The electrolyte solution of 1 mM NaCl (Sigma Ultra) used in the electrode chambers was deoxygenated with $N_2$ for a minimum of 1 h before use.

### 2.2 Expedite Methods

Suspensions of different concentrations of PAA-nZVI (0, 0.0001, 0.001, 0.01, 0.1, 0.2, 0.5, 1, 2.5, 5, 10, 10, and 50 g $L^{-1}$) were prepared with 0.1 and 0.001 M solutions of NaCl with deionized water. Initially, the ORP, pH, and conductivity of these PAA-nZVI suspensions were measured with OAKTON bench-top meters at time steps of 0, 4, 12, 24, and 48 h. This data was used to generate calibration curves of relative nZVI concentration and reactivity. All the measurement probes (pH, conductivity, and ORP) were recalibrated before each measurement.

### 2.3 Electrophoretic Cell

A commercially available electrophoretic cell (EP) (Econo-Submarine Gel Unit, model SGE-020), originally designed for molecular separation, was modified to undertake these experiments (Fig. 1). The cell is a rectangular translucent box with a square (20 cm×20 cm) sample tray. There are two liquid chambers on each side of the sample tray (to hold the electrolyte reservoirs) and a lid that covers the whole apparatus. The standard cell is equipped with platinum working electrodes. Auxiliary electrodes and a reference electrode were added to the system for this experiment. The modified EP cell allowed direct measurement of the redox potential (ORP) in the test medium by use of 0.25-mm diameter platinum wire electrodes (auxiliary electrodes) fixed in the base plate of

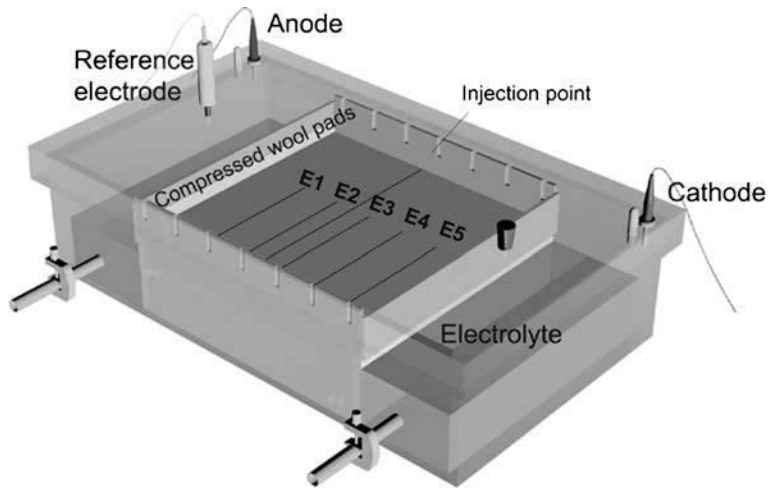


**Fig. 1** Schematic diagram of the modified electrophoretic cell test setup

the sample tray at equal intervals (3 cm) with conductive glue. Redox potential measurements were made in the wire electrodes, using an Ag/AgCl reference electrode (Accumet) with 4.0 M KCl solution (Fig. 1). The auxiliary electrodes were labeled as E1–E5 starting from the anode electrode side of the tray (Fig. 1). An OAKTON pH probe (model WD-35805-18) was used for pH measurements in the test medium. Compressed fiberglass wool pads saturated and immersed in the electrolyte solutions on both sides of the tray were used to help transport the migrating ions from the electrolyte into the test medium and vice versa. The levels of the electrolyte liquids in the anode and cathode chambers were kept slightly below that of the test medium in the sample tray to avoid flooding, hence prevent preferential transport of nZVI through a water pool at the top. The experimental setup also includes a power supply, wiring, and a multimeter (Fluke 179).

## 2.4 Direct Current Enhanced Transport Experiments

Different porosity and surface reactivity test media, ranging from glass beads (with diameter less than 1 mm, previously sieved) to white Georgia kaolinite clay (>2 μm) were used in the enhanced transport experiments. Table 1 shows the various parameters of the experiments conducted in this study. A kaolin clay, previously characterized by Pamukcu et al. (2004), was used in this study. It was prepared to a final water content of 60 %, and the mixture had bulk mass density of 1.63 g $cm^{-3}$ (Pamukcu et al. 2004).

The final pastes with different percentages of kaolin and glass beads were transferred to the tray of the electrophoretic cell and spread uniformly over the wire electrodes to an approximate thickness of 2 mm. PAA-nZVI were delivered using a syringe to inject 2 mL of its homogenized suspension through a tube and spreading it into a precut channel into the clay paste between the electrode ports E2 and E3 (Fig. 1).

A constant potential of 5.0 V was applied across the working electrodes for 48 h. This low potential was selected to remain within the linear range of the power supply used and also to prevent excessive gas generation. The constant potential of 5 V resulted in a current density in the range of 1.12 to $7.24\times10^{-4}$ mA $cm^{-2}$. The cell was kept in a dark location to prevent iron photo-oxidation. Two sets of control experiments were conducted for each mixture under the same conditions, one without direct current application, and another with current but without the injection of PAA-nZVI.

Measurements were taken periodically at the following times: 0.25, 0.50, 0.75, 1, 2, 3, 5, 6, 7, 10, 12, 15, 24, 27, 32, 36, and 48 h. At each measurement, time voltage, current, ORP, and pH were monitored. At the end of each test, aqueous samples were collected from the electrode chambers, and composite solid samples were collected above the auxiliary wire electrodes E1-E5. The nZVI injection point was not sampled. The solid and aqueous samples were analyzed for total iron and ferrous iron concentrations. The iron was extracted from the matrix with the sodium dithionite-citrate-bicarbonate method (Mehra and Jackson 1960). The iron analyses were conducted using a PerkinElmer

**Table 1** Enhanced transport experimental program and conditions

| Test Number | Matrix | Moisture content (%) | PAAnZVI added (mL) | Average voltage (V) | Average current (mA) | Notes |
|---|---|---|---|---|---|---|
| 1 | Kaolin | 60 | 2 | 5.043 | 0.27 | Enhanced transport of nZVI |
| 2 | Kaolin | 60 | 2 | – | – | Diffusion control test |
| 3 | Kaolin | 60 | – | 4.918 | 0.24 | Control test without nZVI |
| 4 | 50 % glass beads and 50 % kaolin | 30 | 2 | 5.022 | 0.13 | Enhanced transport of nZVI |
| 5 | 50 % glass beads and 50 % kaolin | 30 | 2 | – | – | Diffusion control test |
| 6 | 75 % glass beads and 25 % kaolin | 30 | 2 | 5.097 | 0.10 | Enhanced transport of nZVI |
| 7 | 75 % glass beads and 25 % kaolin | 30 | 2 | – | – | Diffusion control test |
| 8 | 100 % glass beads | 20 | 2 | 5.110 | 0.27 | Enhanced transport of nZVI |
| 9 | 100 % glass beads | 20 | 2 | – | – | Diffusion control test |
| 10 | 100 % glass beads | 20 | – | 5.248 0 | 10 | Control test without nZVI |

AAnalyst 200 flame atomic absorption spectroscopy and a Hach DR 2800 spectrophotometer (UV).

## 3 Results and Discussion

### 3.1 Expedited Methods

The PAA-nZVI concentrations in DI water showed good fits to the linear regression analysis for conductivity for all, except for the measurements made at 12 h (Fig. 2). These curves did not change with the concentration of PAA-nZVI for either of the two concentrations of NaCl (0.001 and 0.1 M) in the suspension because the conductivity of NaCl completely masked the nZVI present. Hence, the conductivity could not be used as an expedite method to assess the distribution trends of the iron nanoparticles in the enhanced transport experiments.

There was no clear fit for the pH calibration curves in any of the tested suspensions, as the pH values measured at different concentrations of PAA-nZVI were identical and did not show meaningful changes in time (Fig. 3).

Since ORP measurements have been widely used as an indirect method to assess the results of injection of nZVI for groundwater remediation (Elliott and Zhang 2001; Henn and Waddill 2006; O'Hara et al. 2006), it was expected that these values could be used as a reliable indicator of nZVI concentration in the transport experiments. It was challenging to obtain stable values of the ORP for the suspensions tested, with some readings taking more than 30 min. The results showed that ORP decreased with increasing concentration of nZVI. The relationships between these variables were highly nonlinear, suggesting a complex response function that cannot be used reliably as a calibration curve (Fig. 4).

Examining the ORP variations in Fig. 4, the results for nZVI concentrations lower than 0.1 g $L^{-1}$ suggest an approximately linear relationship (with $R^2$>0.90), consistent with a Nernstian dependence of this parameter on nZVI concentration. However, at higher concentrations, the ORP becomes relatively independent of the nZVI concentration. Both observations are consistent with the results of Shi et al. (2011) that used rotating disk electrodes in nZVI suspensions to assess the effects of nanoparticles on ORP. These researchers found that the response of ORP electrodes to suspensions of nZVI is not a simple function of iron nanoparticles concentration. At high concentrations of nZVI, ORP is dominated by direct interaction between the electrode and the nanoparticles, but this response is nonlinear and saturates with increased coverage of the electrode surface with adsorbed particles (Shi et al. 2011). At low nZVI concentrations, in aqueous suspensions, the measured ORP is a mixture of contributions that includes adsorbed nZVI and the dissolved $H_2$ and the $Fe^{II}$ species that arise from corrosion of nZVI (Shi et al. 2011). Hence, the changes in ORP at low concentrations of nZVI

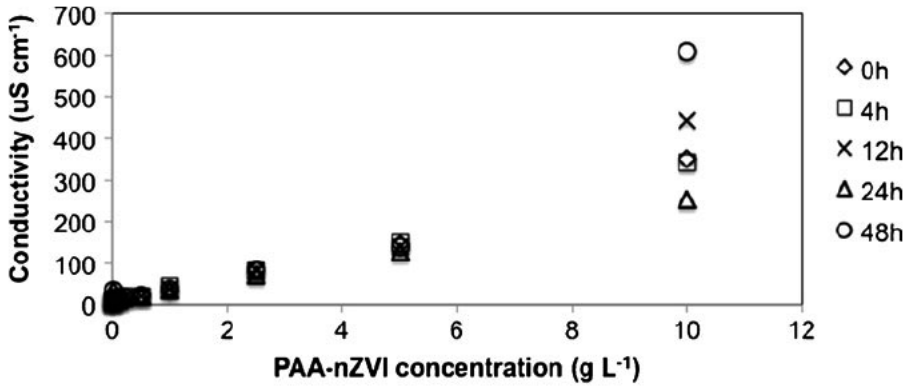


| Time (h) | Linear regression | $R^2$ |
|---|---|---|
| 0 | y = 33.161 x + 5.0706 | 0.9917 |
| 4 | y = 32.471 x + 6.9457 | 0.9938 |
| 12 | y = 26.88 x – 88.461 | 0.4722 |
| 24 | y = 23.331 x + 15.328 | 0.9912 |
| 48 | y = 53.488 x – 2.0660 | 0.9129 |

**Fig. 2** Calibration curves for conductivity in deionized water

(<0.1 g $L^{-1}$) may be a viable method to track the relative spatial and temporal distribution of nZVI in controlled experiments.

## 3.2 Enhanced Transport of PAA-nZVI

### *3.2.1 Oxidation–Reduction Potential*

The redox measurements in the kaolin during the experiments show the trend of oxidizing to reducing conditions from the anode towards the cathode when direct current is applied (Fig. 5). In general, the presence of clay appear to push the ORP up to more oxidizing conditions, while over time, the ORP values decreased, favoring reducing conditions in all samples. In the experiments with more percentage of glass beads, and in particular in the experiment with 100 % glass beads, there is an accentuated drop in the ORP values in the electrodes E1, E2, and E3 due to the injection and fast electrophoretic transport of PAA-nZVI in the absence of clay. The system attains equilibrium with more or less uniform and constant ORP

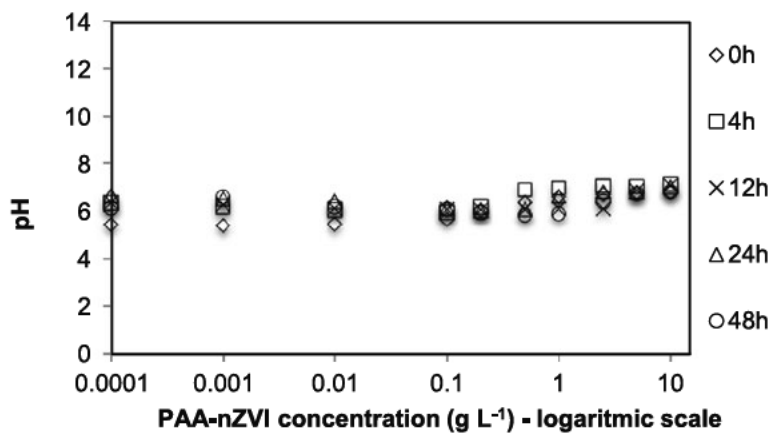


**Fig. 3** pH values measured in the PAA-nZVI solution with 0.001 M NaCl

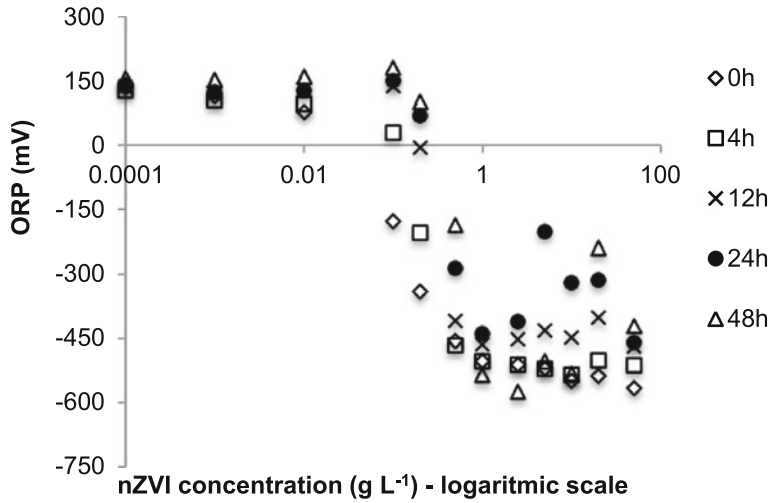


**Fig. 4** ORP values measured in the PAA-nZVI solution with 0.1 M NaCl

after 15 h. In contrast, the presence of clay introduces a delay in ORP reduction possibly due to competing processes with iron reactivity such as sorption and electroosmotic transport of nZVI.

In the diffusion control experiments, the ORP values measured in all the electrodes (E1 to E5) showed little variation and are characteristic of oxidizing conditions (Fig. 6). In the glass beads experiment, the influence of the PAA-nZVI injection in both E2 and E3 is evident with a difference of more than 100 mV when compared to E1 and E4. In the experiments that included kaolin, this drop in ORP was not significant. Compared to the spatial and temporal distribution of ORP in the diffusion tests, the electric field enhance the spending of the nZVI through faster transport and activation, while presence of clay delay both processes.

### *3.2.2 pH*

The initial pH in the different experiments varied from 4.05 to 4.85 when kaolin was present and from 5.40 to

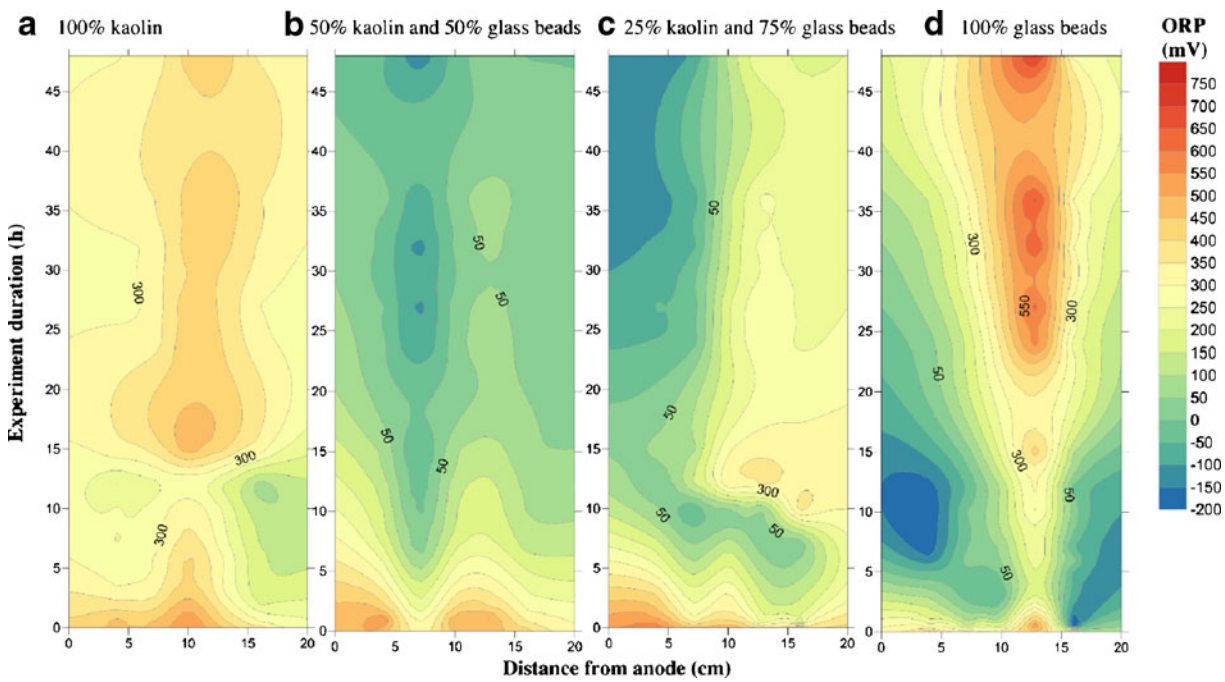


**Fig. 5** ORP values measured at the auxiliary electrodes during the enhanced transport of nZVI tests in the different porous materials

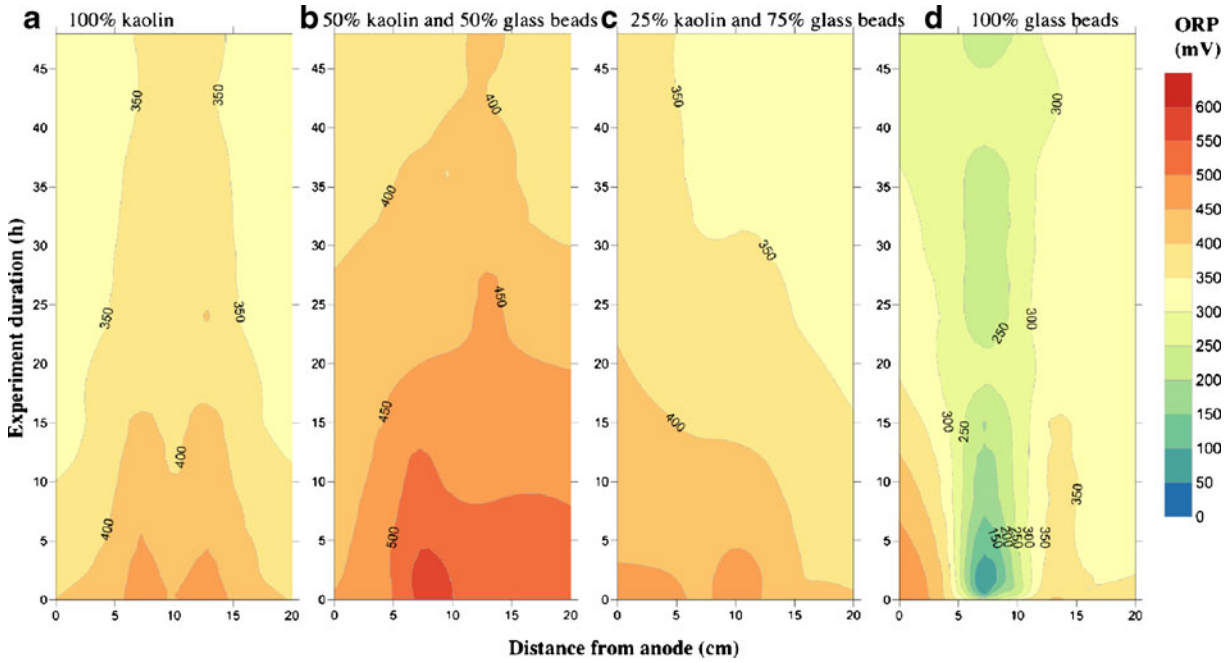


**Fig. 6** ORP values measured in the electrodes during the diffusion tests in the different porous materials

7.19 in the experiments with 100 % glass beads (Fig. 7). This pH is favorable to the nZVI oxidation. Other researchers have observed that low pH increases deposition of nZVI in clay, as well as nZVI aggregation (Kim et al. 2012). Therefore, the initial conditions in the matrix were not advantageous to the mobility of PAA-nZVI. The pH values measured during the experiments showed some fluctuation, with values between 3 and 5.52, when some percentage of kaolin existed in the matrix. The typical profile of a pH front increasing from the anode to the cathode in electrokinetic treatments was not observed in these tests (Fig. 7). This outcome can be attributed to the low values of current density applied, the absence of the physical conditions for fast transport of $H^+$ and $OH^-$ from the electrode compartments into the media, and possibly the presence of iron that kept the pH low at the cathode side. Only in the experimental setups with 100 % glass beads was the effect on pH from the injection of the PAA-nZVI noticed, particularly in E2, E3, and E4, where pH values higher than 8 were measured.

Normally, due to the electrolysis of water in the electrode compartments that produce $H^+$ ions at the anode and $OH^-$ ions at the cathode, the final solution pH values would approach values around 2 and 12, respectively. The values observed in the experiments (Fig. 8) varied between 2.71 and 11.03 and are consistent with those electrochemical reactions of water electrolysis. In the diffusion experiments, a small decrease in the pH in both anode and cathode compartment was observed. A possible explanation is the increase in $H^+$ in solution due to the oxidation of $Fe^0$.

### *3.2.3 Iron-Enhanced Transport*

Since PAA-coated nanoparticles have negative zeta potential and tend to electrophoretically transport towards the anode (Yang et al. 2008), some of the earlier preliminary experiments were conducted with the injection point located near the cathode (results not shown). In those experiments, it was observed that the electroosmotic flow (EOF) was counterbalancing the electrophoretic transport of the nZVI. This is consistent with the predictions of Jones et al. (2010) that the EOF rates will increase, due to the large apparent zeta potentials existent in natural clays, counteracting electrophoresis and reducing the overall migration rate of nZVI when compared with diffusion. Other researchers also tested different injection points in electrokinetic experiments to enhance nZVI transport. Experimental results showed that the cathode reservoir was the most unsuitable injection spot, due to the alkaline environment that promotes the formation of iron oxides at the surface on nZVI (Yang et al. 2008;

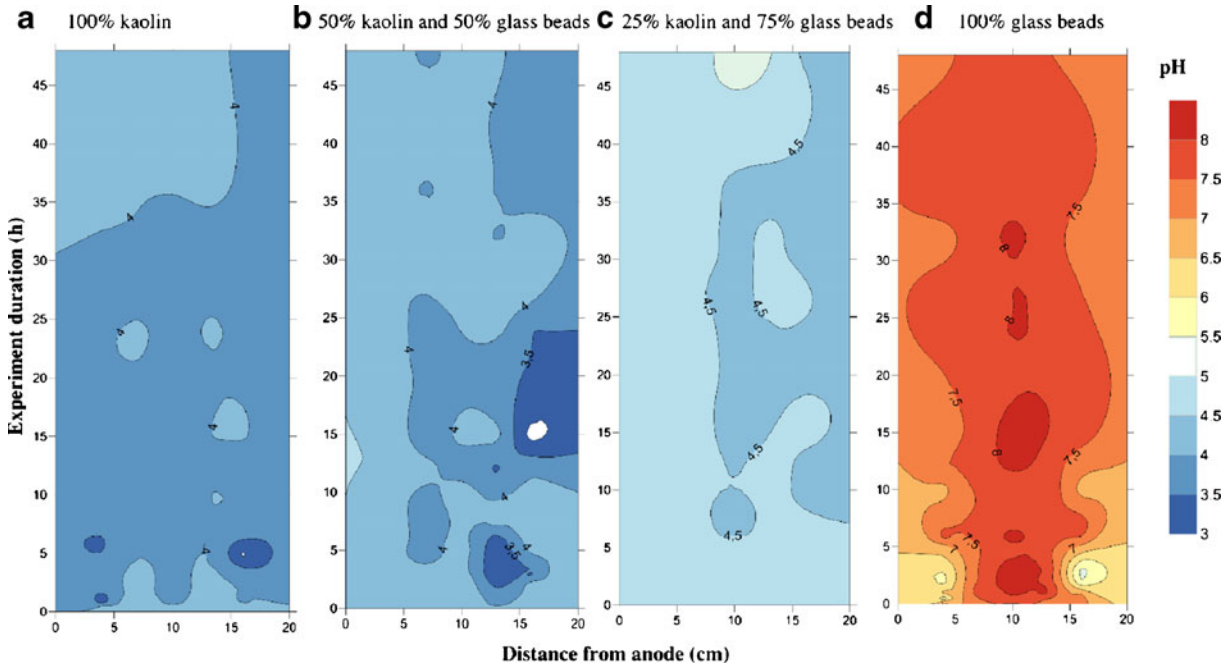


**Fig. 7** Variation of pH in the matrices tested during the experiments

Yang and Yeh 2011). On the other hand, it was also found that corrosion on nZVI was higher when injected in the anode compartment, due to increased dissolved oxygen and lower pH (Chang and Cheng 2006; Chowdhury et al. 2012). Based on the observations of the preliminary tests conducted and the results available in the literature, the injection point used in the experiments was selected in the central area of the EP

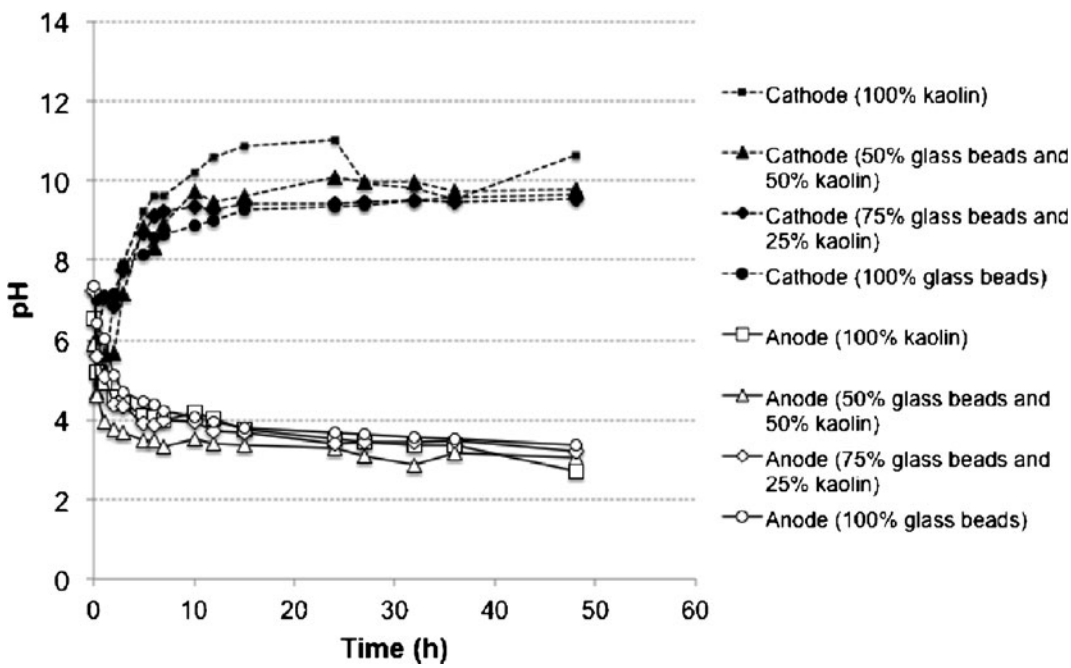


**Fig. 8** Variation of pH in the cathode and anode compartments during the enhanced transport experiments

cell (between E2 and E3), to avoid rapid corrosion of the nZVI by extreme pH conditions and be able to discern the controlling transport mechanism of the nanoparticles (i.e., electrophoresis towards the anode or electroosmosis towards the cathode).

Figure 9 shows the total iron distribution in the electrophoretic cell at the end of the experiments and compares the direct current enhanced transport with diffusion. In general, there are higher concentrations of iron across the test bed when direct current is applied. It is also clear that higher concentrations near the cathode (E5) are only obtained when the matrix has higher percentage of kaolin, reflecting the importance of EOF. In all the experiments with glass beads, there is a very well-defined peak of concentration at E3 (i.e., practically the injection point). This is potentially due to the aggregation or fast corrosion of the iron nanoparticles, or to both phenomena. It has been previously shown that at high particle concentrations (1–6 g $L^{-1}$), there is a higher tendency for agglomeration (Phenrat et al. 2009). When nZVI aggregate and form agglomerations larger than the soil pores, their transport becomes restricted (Reddy et al. 2011). There can also be changes to the mobility of nZVI due to volumetric expansion with corrosion. The volume of corrosion products (Fe hydroxide or oxide) is larger than that of the original metal ($Fe^0$), and these products are likely to contribute to porosity loss and also promote particle agglomeration (Noubactep et al. 2012).

According to Bahranowski et al. (1993), Fe may be present in kaolinite as a part of its structure or as separate Fe-rich phases. Usually, both types of contamination, referred to as "structural" and "nonstructural", or "free" iron, coexist in kaolinite. In the former case, Fe may either substitute for Al in the octahedral gibbsite [$Al(OH)_3$] sheet or Si in the tetrahedral Si-O skeleton. In the latter, it belongs to separate Fe-rich phases such as Fe-bearing micas or iron oxides/oxyhydroxides (Bahranowski et al. 1993). The lower concentrations of Fe in the experiment with 100 % of glass beads when compared to those with kaolin might be explained by Fe impurities present in the kaolin. In fact, the blank samples with the same percentages of kaolin and glass beads showed background iron concentrations directly proportional to the percentage of kaolin present in the matrix.

It was also observed that PAA-nZVI did not move into the water phase in the electrode chambers, except for the cathode chamber in the enhanced transport tests with 100 % kaolin (final concentration of 0.43 mg $L^{-1}$) and 100 % glass beads (0.74 mg $L^{-1}$ in the anode compartment and 0.09 mg $L^{-1}$ in the cathode). This indicates that EOF was dominant in transporting nZVI in pure clay,

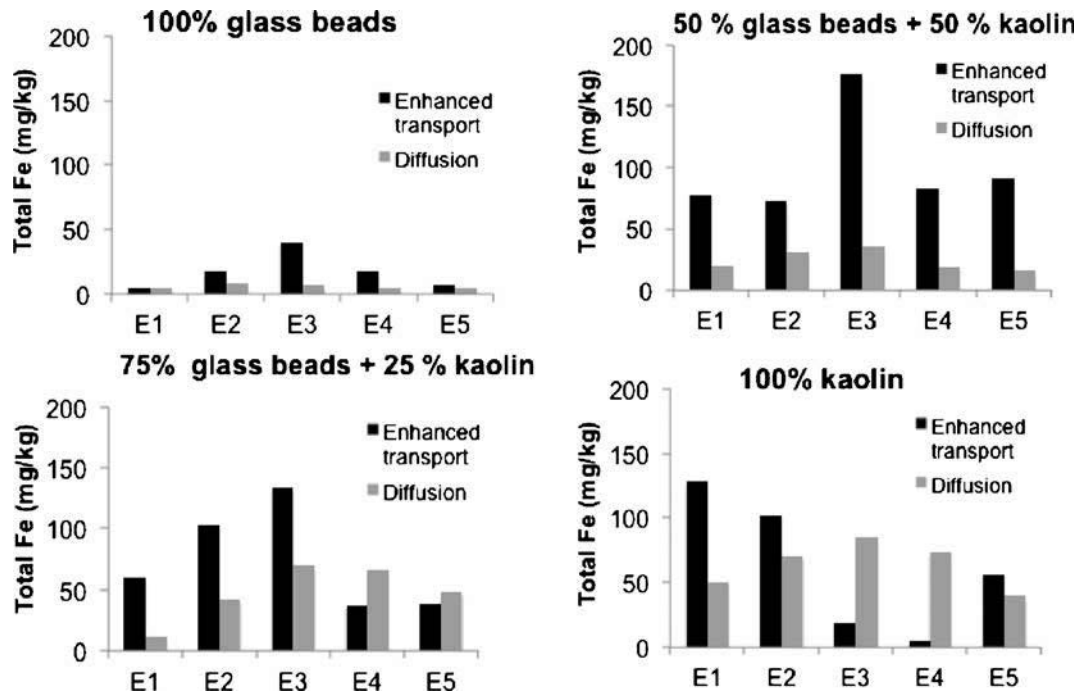


**Fig. 9** Total iron distribution on the electrophoretic cell

while electrophoresis was the only mechanism to transport nZVI in surface neutral glass beads. In mixed samples, it appears that EOF and electrophoresis competes, resulting in prolonged presence of iron in the pores and potential capture on the clay surfaces. Other experimental results showed that there was greater deposition of nZVI onto clay minerals compared to similar sized silica fines due to charge heterogeneity on clay mineral surfaces (Kim et al. 2012).

### *3.2.4 Iron Oxidation State*

All oxidation–reduction potentials measured in the electrodes across the electrophoretic cell were referenced to the normal hydrogen electrode by subtracting the potential of the Ag/AgCl reference electrode. These values combined with pH values allowed the construction of a Pourbaix (Eh–pH) diagram, showing the potential oxidation states of the iron (Fig. 10). Since predictions from stability diagrams are only accurate when the system approaches thermodynamic equilibrium in aqueous solutions, the plot is only intended to give an indication of the dominance of particular Fe species at the recorded Eh and pH measurements. In this diagram, all data from diffusion tests form a cluster that corresponds to the formation of $Fe_2O_3$ under oxidizing conditions (passivity region). Regarding the experiments with direct current enhanced transport of PAA-nZVI, the values measured above E1 and E2 electrodes (i.e., nearest to the anode), during the first 6–7 h of the experiments, match the $Fe^{2+}$ area (corrosion region). There is a very distinct cluster of values measured in the glass beads bed, where pH values were much higher than in other experiments. These results are consistent with the visual observations of the iron injected in the cell, since only after 1 h, it was clearly visible that iron nanoparticles had started to present an orange color, typical of its oxidation.

## 4 Conclusions

In this study, very low current densities were used to enhance the transport of polymer-coated iron nanoparticles in different porous media, using high nZVI concentrations typical of field applications. Because of these conditions, some aggregation of the nanoparticles was observed, particularly near the injection point. Higher currents should be tested with these concentrations to check if the enhancement in transport compared to diffusion is proportional to the applied current as reported by other researchers. The experimental results show that the electrical field applied to clay-rich media enhances the ORP creating a synergistic

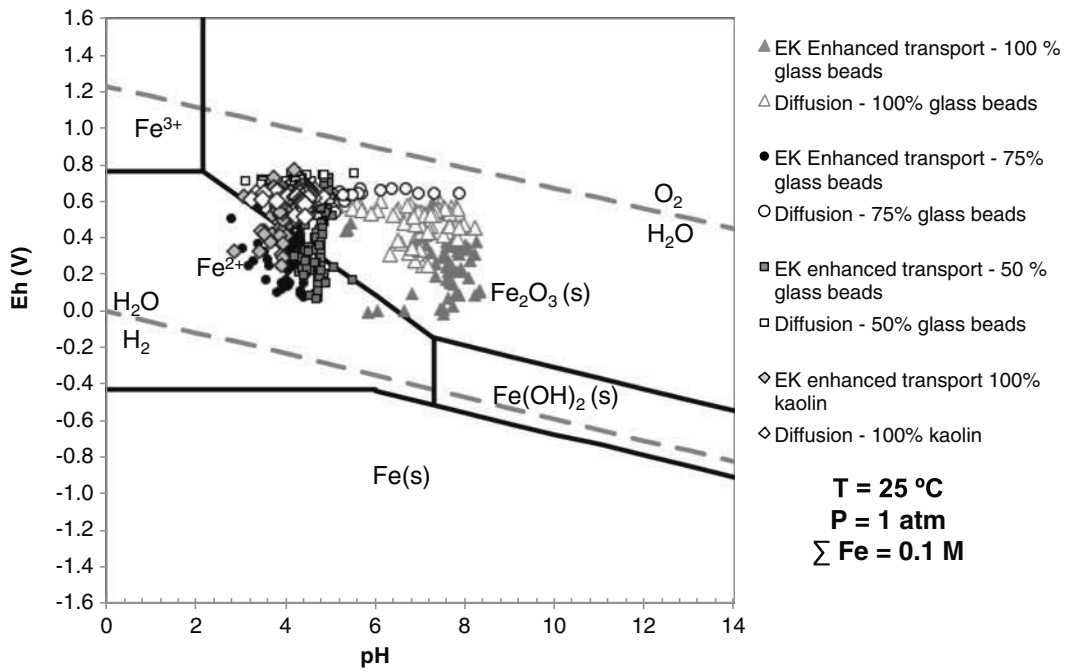


**Fig. 10** Pourbaix diagram with the values measured during 48 h in the electrodes embedded in the electrophoretic cell

effect of nZVI usage with electrokinetics, delaying its corrosion reaction. This effect was also observed in earlier studies, where the ORP enhancement was attributed to the polarization of the diffuse double layer of the clay media.

The transport of polymer-stabilized iron nanoparticles can be enhanced by the direct current, in low permeability clay soils, where EOF can be effective in distributing the particles as well as electrophoretic mobility of the particles themselves. Further work is necessary for comprehensive treatise of the behavior of nZVI in clay-rich soils under direct current applications, namely the measuring of the EOF.

**Acknowledgments** This work has been funded by the European Regional Development Fund (ERDF) through COMPETE—Operational Program for Competitiveness Factors (OPCF), by Portuguese National funds through "FCT—Fundação para a Ciência e a Tecnologia" under project «PTDC/AGR-AAM/101643/2008 NanoDC», by the research grant SFRH/BD/76070/2011, by FP7-PEOPLE-IRSES-2010-269289-ELECTROACROSS and by RIARTAS-Red Iberoamericana de aprovechamiento de residuos industriales para el tratamiento de suelos y aguas contaminadas, Programa Iberoamericano de Ciencia y Tecnología para el Desarrollo (Cyted). The Department of Civil and Environmental Engineering at Lehigh University is acknowledged, where all the equipment development, testing, and analysis for this work were funded. Dan Zeroka is kindly acknowledged for the electrophoretic cell modification.

## References

Bahranowski, K., Serwicka, E. M., Stoch, L., & Srycharski, P. (1993). On the possibility of removal of nonstructural iron from kaolinite-group minerals. *Clay Minerals, 28*, 379–391.

Bennett, P., He, F., Zhao, D., Aiken, B., & Feldman, L. (2010). In situ testing of metallic iron nanoparticle mobility and reactivity in a shallow granular aquifer. *Journal of Contaminant Hydrology, 116*(1–4), 35–46.

Chang, J.-H., & Cheng, S.-F. (2006). The remediation performance of a specific electrokinetics integrated with zerovalent metals for perchloroethylene-contaminated soils. *Journal of Hazardous Materials B, 131*, 153–162.

Chowdhury, A. I. A., O'Carroll, D. M., Xu, Y., & Sleep, B. E. (2012). Electrophoresis enhanced transport of nanoscale zerovalent iron. *Advances in Water Resources, 40*, 71–82.

Comba, S., Di Molfetta, A., & Sethi, R. (2011). A comparison between field applications of nano-, micro-, and millimetric zerovalent iron for the remediation of contaminated aquifers. *Water, Air, & Soil Pollution, 215*(1), 595–607.

Elliott, D. W., & Zhang, W. (2001). Field assessment of nanoscale bimetallic particles for groundwater treatment. *Environmental Science & Technology, 35*, 4922–4926.

He, F., Zhao, D., & Paul, C. (2010). Field assessment of carboxymethyl cellulose stabilized iron nanoparticles for in situ destruction of chlorinated solvents in source zones. *Water Research, 44*, 2360–2370.

Henn, K. W., & Waddill, D. W. (2006). Utilization of nanoscale zerovalent iron for source remediation—A case study. *Remediation, 16*(2), 57–77.

Jiemvarangkul, P. (2012). Nanoparticles for Nonaqueous-phase liquids (NAPLs) Remediation, Dissertation presented to the Graduate and Research Committee of Lehigh University for the Degree of Doctor of Philosophy in Environmental Engineering.

Jiemvarangkul, P., Zhang, W. X., & Lien, H. L. (2011). Enhanced transport of polyelectrolyte stabilized nanoscale zerovalent iron (nZVI) in porous media. *Chemical Engineering Journal, 170*(2–3), 482–491.

Jones, E. H., Reynolds, D. A., Wood, A. L., & Thomas, D. G. (2010). Use of electrophoresis for transporting nano-iron in porous media. *Ground Water, 49*(2), 172–183.

Kanel, S. R., Goswami, R. R., Clement, T. P., Barnett, M. O., & Zhao, D. (2008). Two-dimensional transport characteristics of surface stabilized zerovalent iron nanoparticles in porous media. *Environmental Science & Technology, 42*, 896–900.

Kim, H.-J., Phenrat, T., Tilton, R. D., & Lowry, G. V. (2012). Effect of kaolinite, silica fines, and pH on transport of polymer-modified zerovalent iron nanoparticles in heterogeneous porous media. *Journal of Colloid and Interface Science, 370*(1), 1–10.

Li, X., Elliott, D. W., & Zhang, W. (2006). Zerovalent iron nanoparticles for abatement of environmental pollutants: materials and engineering aspects. *Critical Reviews in Solid State and Materials Sciences, 31*(4), 111–122.

Lin, Y.-H., Tseng, H.-H., Wey, M.-Y., & Lin, M.-D. (2010). Characteristics of two types of stabilized nano zerovalent iron and transport in porous media. *Science of the Total Environment, 408*(10), 2260–2267.

Masciangioli, T., & Zhang, W. (2003). Environmental technologies at the nanoscale. *Environmental Science & Technology, 37*(5), 102A–108A.

Mehra, O. P., & Jackson, M. L. (1960). Iron oxide removal from soils and clays by a dithionite–citrate system buffered with sodium bicarbonate. *Clays and Clay Minerals, 7*, 317–327.

Noubactep, C., Caré, S., & Crane, R. (2012). Nanoscale metallic iron for environmental remediation: prospects and limitations. *Water, Air, & Soil Pollution, 223*(3), 1363–1382.

O'Hara, S., Krug, T., Quinn, J., Clausen, C., & Geiger, C. (2006). Field and laboratory evaluation of the treatment of DNAPL source zones using emulsified zerovalent iron. *Remediation, 16*(2), 35–56.

Pamukcu, S., Weeks, A., & Wittle, J. K. (2004). Enhanced reduction of Cr(VI) by direct electric current in a contaminted clay. *Environmental Science & Technology, 38*, 1236–1241.

Pamukcu, S., Hannum, L., & Wittle, J. K. (2008). Delivery and activation of nano-iron by DC electric field. *Journal of Environmental Science and Health, Part A, 43*(8), 934–944.

Phenrat, T., Saleh, N., Sirk, K., Tilton, R. D., & Lowry, G. V. (2007). Aggregation and sedimentation of aqueous nanoscale zerovalent iron dispersions. *Environmental Science & Technology, 41*, 284–290.

Phenrat, T., Kim, H.-J., Fagerlund, F., Illangasekare, T., Tilton, R. D., & Lowry, G. V. (2009). Particle size distribution, concentration, and magnetic attraction affect transport of polymer-modified $Fe^0$ nanoparticles in sand columns. *Environmental Science & Technology, 43*, 5079–5085.

Reddy, K. R., & Karri, M. R. Effect of electric potential on nanoiron particles delivery for pentachlorophenol remediation in low permeability soil. In M. Hamza et al. (Ed.), Proceedings of the 17th International Conference on Soil Mechanics and Geotechnical Engineering: The Academia and Practice of Geotechnical Engineering, Alexandria, Egypt, 5–9 October 2009, 2312–2315.

Reddy, K. R., Darko-Kagy, K., & Cameselle, C. (2011). Electrokinetic-enhanced transport of lactate-modified nanoscale iron particles for degradation of dinitrotoluene in clayey soils. *Separation and Purification Technology, 79*(2), 230–237.

Shi, Z., Nurmi, J. T., & Tratnyek, P. G. (2011). Effects of nano zerovalent iron on oxidation-reduction potential. *Environmental Science and Technology, 45*, 1586–1592.

Sun, Y.-P., Li, X., Cao, J., Zhang, W., & Wang, H. P. (2006). Characterization of zerovalent iron nanoparticles. *Advances in Colloid and Interface Science, 120*, 47–56.

USEPA (2011). Fact sheet on selected sites using or testing nanoparticles for remediation. United States Environmental Protection Agency. http://cluin.org/products/nanozvi/. Accessed 3 April 2012

Yang, G. C. C., & Yeh, C.-F. (2011). Enhanced nano-$Fe_3O_4/S_2O_8^{2-}$ oxidation of trichloroethylene in a clayey soil by electrokinetic. *Separation and Purification Technology, 79*, 264–271.

Yang, G. C. C., Tu, H.-C., & Hung, C.-H. (2007). Stability of nanoiron slurries and their transport in the subsurface environment. *Separation and Purification Technology, 58*, 166–172.

Yang, G. C. C., Hung, C.-H., & Tu, H.-C. (2008). Electrokinetically enhanced removal and degradation of nitrate in the subsurface using nanosized Pd/Fe slurry. *Journal of Environmental Science and Health, Part A, 43*(8), 945–951.

Yuan, S., Long, H., Xie, W., Liao, P., & Tong, M. (2012). Electrokinetic transport of CMC-stabilized Pd/Fe nanoparticles for the remediation of PCP-contaminated soil. *Geoderma, 185–186*, 18–25.

Zhang, W. (2003). Nanoscale iron particles for environmental remediation: an overview. *Journal of Nanoparticle Research, 5*, 323–332.

## II.4. Influence of electrolyte and voltage on the direct current enhanced transport of iron nanoparticles in clay (published in Chemosphere)

Chemosphere 99 (2014) 171–179

Contents lists available at ScienceDirect

Chemosphere

journal homepage: www.elsevier.com/locate/chemosphere

# Influence of electrolyte and voltage on the direct current enhanced transport of iron nanoparticles in clay

Helena I. Gomes [a,b,c,*], Celia Dias-Ferreira [c], Alexandra B. Ribeiro [b], Sibel Pamukcu [a]

[a] Department of Civil and Environmental Engineering, Fritz Engineering Laboratory, Lehigh University, 13 E. Packer Avenue, Bethlehem, PA 18015-4729, USA
[b] CENSE, Departamento de Ciências e Engenharia do Ambiente, Faculdade de Ciências e Tecnologia, Universidade Nova de Lisboa, 2829-516 Caparica, Portugal
[c] CERNAS – Research Center for Natural Resources, Environment and Society, Escola Superior Agrária de Coimbra, Instituto Politécnico de Coimbra, Bencanta, 3045-601 Coimbra, Portugal

## HIGHLIGHTS

- Direct current can enhance iron nanoparticles transport in clay by 25%.
- Oxidizing conditions and higher ionic strength limit nZVI enhanced transport.
- Ionic strength was significant, promoting nanoparticles aggregation and oxidation.

## ARTICLE INFO

*Article history:*
Received 19 June 2013
Received in revised form 19 October 2013
Accepted 25 October 2013
Available online 16 November 2013

*Keywords:*
Zero valent iron nanoparticles (nZVI)
Oxidation–reduction potential (ORP)
Electrokinetics (EK)
Electrolyte
Voltage

## ABSTRACT

Zero valent iron nanoparticles (nZVI) transport for soil and groundwater remediation is slowed down or halted by aggregation or fast depletion in the soil pores. Direct electric current can enhance the transport of nZVI in low permeability soils. However operational factors, including pH, oxidation–reduction potential (ORP), voltage and ionic strength of the electrolyte can play an important role in the treatment effectiveness. Experiments were conducted to enhance polymer coated nZVI mobility in a model low permeability soil medium (kaolin clay) using low direct current. Different electrolytes of varying ionic strengths and initial pH and high nZVI concentrations were applied. Results showed that the nZVI transport is enhanced by direct current, even considering concentrations typical of field application that favor nanoparticle aggregation. However, the factors considered (pH, ORP, voltage and electrolyte) failed to explain the iron concentration variation. The electrolyte and its ionic strength proved to be significant for pH and ORP measured during the experiments, and therefore will affect aggregation and fast oxidation of the particles.



## 1. Introduction

Zero valent iron nanoparticles (nZVI) are considered an emergent solution for *in situ* soil and groundwater remediation due to their high specific surface area and reactivity and because they target a vast number of contaminants, from organochlorines to heavy metals (Masciangioli and Zhang, 2003; Zhang, 2003; Zhang and Elliott, 2006). The growing use of nZVI in pilot and full-scale applications in the last decade is notable (USEPA, 2011; Mueller et al., 2012; Rejeski et al., 2012). However, one of the major limitations is the effective long distance transport without aggregation and loss of their reactivity – the mobility of nZVI in the subsurface is normally less than a few meters (Bennett et al., 2010; He et al., 2010; Comba et al., 2011; Su et al., 2013). Coated nanoparticles are more mobile than bare nZVI (He et al., 2007; Phenrat et al., 2007; Sun et al., 2007; Kanel et al., 2008; Tiraferri et al., 2008; Lin et al., 2009; Phenrat et al., 2009; Tiraferri and Sethi, 2009; Phenrat et al., 2010; Raychoudhury et al., 2010; Jiemvarangkul et al., 2011; Phenrat et al., 2011), but aggregation remains and can be determined by the particle size distribution and $Fe^0$ content of nZVI, as well as by soil water ionic strength and composition (Saleh et al., 2008; Lin et al., 2010).

Electrokinetic (EK) remediation is a well-known technology with demonstrated results, especially in low permeability fine-grain soils. Direct current can enhance the transport of iron nanoparticles in sands (Jones et al., 2010; Chowdhury et al., 2012) and clay (Pamukcu et al., 2008) and improve the remediation effectiveness for different contaminants (Yang et al., 2008; Reddy et al., 2011; Gomes et al., 2012a,b; Yuan et al., 2012; Fan et al., 2013). The primary mechanisms for the nZVI enhanced transport are: electrophoresis, towards the anode, and electroosmotic advection, towards the cathode. In sands, with lower surface

* Corresponding author at: Department of Civil and Environmental Engineering, Fritz Engineering Laboratory, Lehigh University, 13 E. Packer Avenue, Bethlehem, PA 18015-4729, USA. Tel.: +351 212948300; fax: +351 212948554.
*E-mail address:* hrg@campus.fct.unl.pt (H.I. Gomes).

0045-6535/$ - see front matter © 2013 Elsevier Ltd. All rights reserved.
http://dx.doi.org/10.1016/j.chemosphere.2013.10.065

charge, electrophoresis dominates, while in clays, electroosmosis can be the most important transport mechanism, counteracting electrophoresis. The existing studies tested low nZVI concentrations and overlooked parameters such as ionic strength, pH, oxidation–reduction potential (ORP) and electric field strength that can influence the nZVI transport, given that the external supply of electric energy can enhance favorable oxidation–reduction reactions in clay-electrolyte systems (Pamukcu, 2009).

The main objective of the current study was to assess if low direct current can enhance the transport of high nZVI concentrations, typical of field applications, in clay rich soils varying the electrolyte ionic strength and voltage. We used kaolin clay to represent a low permeability medium, and an experimental setup that allowed us to study the variation in the oxidation–reduction potential and pH values in the kaolin during short-term experiments, and estimate the temporal and spatial distribution of the iron oxidation states and hence the reactivity of the nanoparticles.

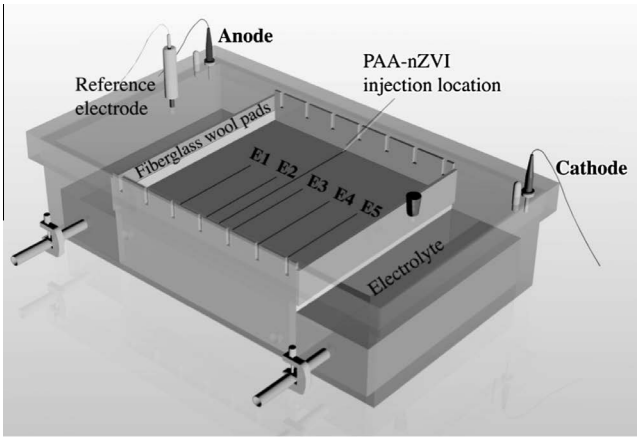


**Fig. 1.** Schematic diagram of the modified electrophoretic cell test setup.

## 2. Material and methods

### 2.1. Chemicals

Before synthesis of the iron nanoparticles, deionized (DI) water was purged with ultra-purified grade nitrogen gas ($N_2$) for 1 h so that dissolved oxygen would fall to a level below 20%. Iron nanoparticles were prepared reducing $FeSO_4{\cdot}7H_2O$ (MP Biomedicals), dissolved in a polyacrylic acid, sodium salt – (PAA) Mw ~2100 (Polysciences, Inc.) solution, by sodium borohydride (Hydrifin™), using the procedure described by Kanel et al. (2008). The PAA–nZVI suspensions were freshly prepared before each experiment and had a concentration of 4 g $L^{-1}$ of nZVI. The particle size distribution of the nanoparticles had a mean value of particle diameter 62.66 ± 39.6 nm and the median size was 60.2 nm, based on a count of 420 particles in TEM images.

All chemicals were reagent grade (NaCl, NaOH, $Na_2SO_3$, sodium citrate dihydrate – $HOC(COONa)(CH_2COONa)_2{\cdot}2H_2O$ from Sigma Aldrich, $CaCl_2$ from Fisher Science Education, $NaHCO_3$ from Research Organics, and $Na_2S_2O_3{\cdot}5H_2O$ from Amresco ProPure). Water was purified from deionized water in a Barnstead NANOpure system (18 MΩ cm). In all the tests, the electrolyte solutions were deoxygenated with ultra-purified grade nitrogen gas ($N_2$) for a minimum of 1 h before each use.

### 2.2. Enhanced transport experiments

#### 2.2.1. Electrophoretic cell

A commercially available electrophoretic cell (EP) (Econo-Submarine Gel Unit, model SGE-020), originally designed for molecular separation, was modified to undertake these experiments (Fig. 1). The cell is a rectangular translucent box 10 cm height, 40 cm long and 23 cm width, with a square (20 cm × 20 cm) sample tray and a lid that covers the whole apparatus. The left and right sides of the sample tray have a liquid chamber (to hold the anolyte and the catholyte, respectively) with platinum working electrodes.

The modified EP cell allowed direct measurement of the redox potential (ORP) in the clay during the experiments, using auxiliary platinum wire electrodes (0.25 mm diameter; 99.9% metals basis, Alfa Aesar) fixed at the base surface of the sample tray at equal intervals (3 cm) with conductive glue. These measurements were made using an Ag/AgCl reference electrode (Accumet) with 4.0 M KCl solution. The auxiliary electrodes were labeled E1 to E5 starting from the anode side (Fig. 1). An OAKTON pH probe (Model WD-35805-18) was used for measuring pH in the kaolin on the electrodes E1–E5.

In all experiments, both anolyte and catholyte compartments were filled with the same electrolyte solutions (volume of 650 mL each), keeping the level slightly below the clay surface and preventing preferential transport of nZVI through a water pool on top of the kaolin. Compressed fiberglass wool pads, saturated and immersed in the electrolyte solution, helped transport the migrating ions from the electrolyte into the clay and vice versa. The experimental set-up included a power supply, wiring and a multi-meter (Fluke 179).

#### 2.2.2. Experimental conditions

Table 1 shows the experimental conditions used in this study. High-purity (china grade, EMD Chemicals) colloidal kaolinite clay with a nominal particle size of 2 μm, pH 4.97 and with 125.24 ± 13 mg $kg^{-1}$ of extractable iron was used to prepare the test medium. The final water content of the test clay was 60% (by dry weight, before placing it the EP cell) with a mass density of 1.63 g $cm^{-3}$. The $pH_{iep}$ of this clay is 2.5 (Brosky and Pamukcu, 2013). A more detailed characterization of the kaolin used can be found in Pamukcu et al. (2004). The kaolin mixture was transferred to the tray of the electrophoretic cell and spread uniformly over the wire electrodes to a thickness of 5 mm (200 $cm^3$).

Two sets of control experiments were conducted for each mixture under the same conditions, one without direct current but with PAA–nZVI, and another with current but without PAA–nZVI. In the experiments with current, a constant potential was applied for 48 h. Table 1 presents the average values of the actual voltage and current measured during the tests. The potentials of 5 V and 10 V resulted in average current densities of $1.12 \times 10^{-4}$ to $7.24 \times 10^{-4}$ mA $cm^{-2}$, respectively. The cell was kept in a dark location to prevent iron photo-oxidation.

The nanoparticle suspension was delivered in the electrophoretic cell using a syringe to inject 2 mL through a tube, which allowed the suspension dispersion into a pre-cut shallow channel in the clay between the auxiliary electrodes E2 and E3 (Fig. 1). The nZVI injection location in the electrophoretic cell was selected in the central area of the clay bed (between E2 and E3) to avoid interference of extreme pH conditions generated in the electrode compartments. Results available in the literature show that the injection of nanoparticles either at the cathode (Yang et al., 2008; Yang and Wu, 2011) or the anode (Chang and Cheng, 2006; Chowdhury et al., 2012) promote the passivation or corrosion of the nZVI, respectively. Recently, a central injection position was used for stabilized nano Pd/Fe for the remediation of pentachlorophenol-contaminated soil (Yuan et al., 2012) with improved results. As such, a central position of nZVI injection was adopted in this study.

Measurements were taken periodically at 0.25 h, 0.50 h, 0.75 h, 1 h, 2 h, 3 h, 5 h, 6 h, 7 h, 10 h, 12 h, 15 h, 24 h, 27 h, 32 h, 36 h and

**Table 1**
Enhanced transport experimental program and conditions.

| Test number | Electrolyte | PAA–nZVI added (mL) | Average voltage (V) | Average current (mA) | Notes |
|---|---|---|---|---|---|
| 1 | 0.001 M NaCl | 2 | 5.04 | 0.27 | Enhanced transport of nZVI |
| 2 | 0.001 M NaCl | 2 | – | – | Diffusion control test |
| 3 | 0.001 M NaCl | – | 4.92 | 0.04 | Control test without nZVI |
| 4 | 0.001 M NaCl | 2 | 10.38 | 0.82 | Enhanced transport of nZVI |
| 5 | 0.001 M NaCl | – | 9.99 | 0.62 | Control test without nZVI |
| 6 | 0.001 M NaOH | 2 | 5.26 | 0.13 | Enhanced transport of nZVI |
| 7 | 0.001 M NaOH | – | 5.35 | 0.24 | Control test without nZVI |
| 8 | 0.001 M NaOH | 2 | – | – | Diffusion control test |
| 9 | 0.1 M $Na_2SO_3$ | 2 | 5.33 | 1.63 | Enhanced transport of nZVI |
| 10 | 0.1 M $Na_2SO_3$ | 2 | – | – | Diffusion control test |
| 11 | 0.1 M $Na_2SO_3$ | – | 5.33 | 1.56 | Control test without nZVI |
| 12 | 0.05 M $CaCl_2$ | 2 | 5.05 | 5.04 | Enhanced transport of nZVI |
| 13 | 0.05 M $CaCl_2$ | 2 | – | – | Diffusion control test |
| 14 | 0.05 M $CaCl_2$ | – | 5.10 | 5.37 | Control test without nZVI |

48 h. At each time the voltage, current, ORP and pH were measured across the working and auxiliary electrodes. At the end of each test, aqueous samples were collected from the electrolyte chambers, and composite soil samples were collected above the auxiliary wire electrodes E1–E5, avoiding the nZVI injection point. The soil and aqueous samples were analyzed for total iron and ferrous iron concentrations. The iron was extracted from the test medium with the sodium dithionite-citrate-bicarbonate (DCB) method (Mehra and Jackson, 1960). The iron analyses were conducted using a Perkin–Elmer AAnalyst 200 flame atomic absorption spectroscopy (AAS) and a Hach DR 2800 spectrophotometer (UV).

## 3. Results and discussion

### 3.1. Enhanced transport of iron nanoparticles

In general, higher iron concentrations were measured when direct current was applied (Fig. 2), indicating an enhancement of nZVI transport over diffusion in kaolin clay. An average concentration increase of 25% was observed when using high concentrations of nZVI, typical of field applications. The Fe concentrations obtained in the enhanced transport tests are statistically different from the diffusion tests at a 0.05 level of significance [one-way ANOVA, $F(1,38) = 5.04$, $p = 0.03$]. Use of statistic models, with variables of pH, ORP, electrode location and voltage to explain this variability, did not return any of these variables to be significant. No differences were found in the diffusion experiments for the tested electrolytes [one-way ANOVA, $F(3,16) = 0.60$, $p = 0.62$].

The enhanced transport with 1 mM NaOH presents higher differences when compared with diffusion, as well as higher iron concentrations near the cathode in relation with the other electrolytes (Fig. 2). The experiments with higher currents, 1.5 and 5.5 mA, using $Na_2SO_3$ and $CaCl_2$ as electrolytes respectively, showed limited enhancement in PAA–nZVI transport when compared with diffusion. The higher ionic strength of these electrolytes may have contributed to lower nanoparticles stability, increasing their agglomeration and limiting the transport. Also, the higher ionic strength and the divalent cation $Ca^{2+}$ will have affected the clay by reducing the diffuse double layer of the clay particles. This will reduce the electroosmotic transport.

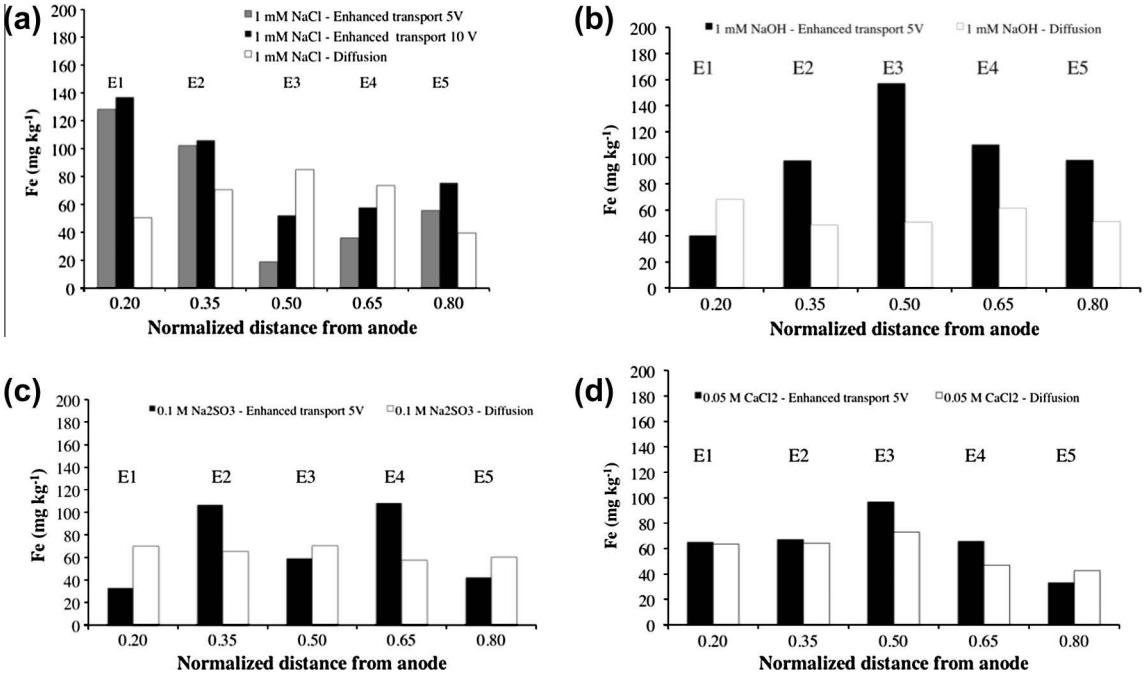


**Fig. 2.** Additional total iron (mg $kg^{-1}$) in soil sections compared with the initial soil concentration using different electrolytes and voltages in the enhanced transport and diffusion experiments: (a) Results using 1 mM NaCl with 0, 5 and 10 V; (b) 1 mM NaOH using 0 and 5 V; (c) 0.1 M $Na_2SO_3$ using 0 and 5 V and (d) 0.05 M $CaCl_2$ using 0 and 5 V.

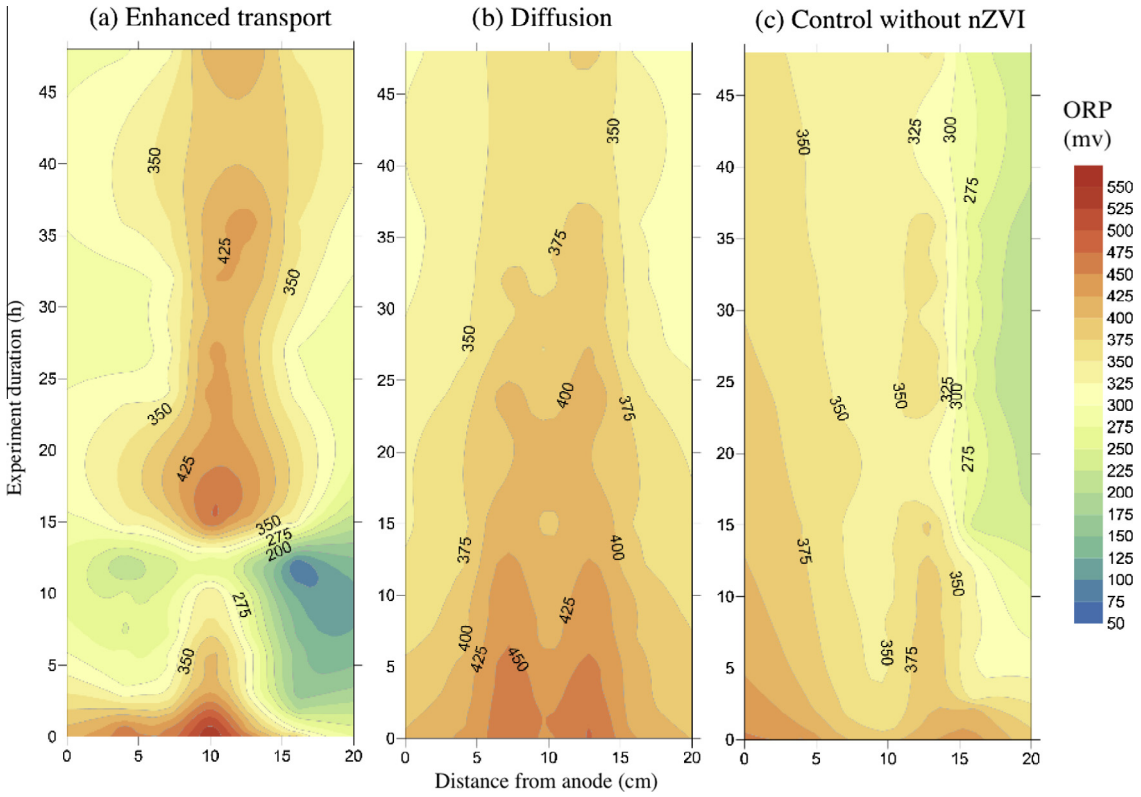


**Fig. 3.** Variation of ORP in the kaolin medium in the (a) enhanced transport (Test 1), (b) diffusion (Test 2) and c) control (Test 3) experiments using 1 mM NaCl as electrolyte and 5 V. The plots were obtained by interpolation (kriging) of the ORP values measured in each electrode (E1–E5) over time.

The increase in the applied voltage resulted in an increase in the transport of nZVI towards the cathode side locations (E4 and E5) for the NaCl electrolyte clay sample, as well as in an even larger increase in transport towards the anode side. This transport towards the anode is mainly due to electrophoresis, due to the negative charge of the nZVI polymer coating, while the movement towards the cathode is due to electroosmosis. The concentrations of total Fe measured in the 10 V test in E4 and E5 are approximately 1.5 times higher than in the 5 V test, possibly due to an increase in the electroosmotic advection with voltage. Yang et al. (2008) considered electroosmosis as the most relevant mechanism for Pd/Fe bimetallic nanoparticles transport under direct electric current. Electroosmotic flow measurements were not made in the experiments reported here, but the results indicate the need for additional research to assess the electroosmotic advection in nZVI enhanced transport in clays.

Other researchers observed that the enhancement in transport of nZVI from the cathode to the anode, compared to diffusion, was proportional to the applied current (Jones et al., 2010; Chowdhury et al., 2012). In those studies, electrophoresis was the predominant transport mechanism, because the test soils were fine-grained sands. In clay systems it appears that electroosmotic advection may be strong enough to counteract electrophoresis, reducing the overall migration rate of nZVI toward the anolyte. However, if the pH is low, the polarity of the surface charge may become inverted and electroosmosis towards the anode will occur. Potentially electroosmosis towards the anode could have happened in the experiments with $CaCl_2$, as we measure pH values close and bellow the $pH_{iep}$ 2.5 for the clay.

Electroosmotic flow (EOF) can be reduced to zero if the pH is kept at the isoelectric point, $pH_{iep}$ for the clay. The specific value of $pH_{iep}$ varies temporally and spatially during electrokinetic treatment as the ionic strength and the ionic species in bulk solution change. Such changes could also alter the nZVI zeta potential making it less stable and leading to lower transportation rates (Hydutsky et al., 2007; Jones et al., 2010).

In the aqueous samples, only in Experiment 4 (1 mM NaCl at 10 V) a noticeable iron was measured in the anolyte (0.09 mg $L^{-1}$). The post-test concentrations of $Fe^{2+}$ measured in the soil and aqueous samples were low in comparison to the total iron hence they were not plotted.

Release of electrons from nZVI to the reaction system might enhance the transmission of electric current. However, contrary to this expectation and to reports in other studies (Yang and Chang, 2011), the experiments with nZVI did not show an increase in the electric current density. There was no statistical difference in the current densities measured in the enhanced transport experiments and the control without nZVI at the $p < 0.05$ level [one-way ANOVA, $F(1,138) = 1.05$, $p = 0.31$].

In all the experiments, PAA–nZVI accumulation was visible around the injection location. First of all, this is due to the generally slow dispersion from an injection point in this kind of porous media. This was also attributed to the aggregation of the iron nanoparticles or to their corrosion, or to both. At high particle concentration (1–6 g $L^{-1}$) there is higher agglomeration (Phenrat et al., 2009). When nZVI particles aggregate they become larger than the soil pores, restricting their transport through soil (Reddy et al., 2011). Mobility changes will also take place due to nZVI volumetric expansion with corrosion. The volume of corrosion products (Fe hydroxide or oxide) is larger than the original metal ($Fe^0$) and these products are likely to contribute to porosity loss and increase particle agglomeration (Noubactep et al., 2012).

### 3.2. Oxidation–reduction potential

When direct current is applied, the ORP values show the general trend of oxidizing to reducing conditions from the anode toward the cathode (E1 to E5), respectively. This trend is due to the oxidation occurring in the anode and the reduction in the cathode, resulting in water electrolysis according to the following equations:

$$2H_2O - 4e^- \rightarrow O_2 \uparrow + 4H^+ \quad E_0 = -1.229 \text{ (anode)} \tag{1}$$

$$2H_2O + 2e^- \rightarrow H_2 \uparrow + 2OH^- \quad E_0 = -0.828 \text{ (cathode)} \tag{2}$$

The temporal and spatial evolution of ORP from the tests with 0.001 M NaCl in the pore fluid is plotted in Fig. 3. As observed, a gradual decrease of ORP takes place in the diffusion specimen as the nZVI diffuses away from the injection location between E2 and E3 and undergoes oxidation from exposure to air and water (Fig. 3b). In the EK tests without nZVI, the ORP dropped faster and further than that in the diffusion test. In these tests, typically the electrode nearest to cathode, E5, registered the largest decrease in ORP within the first 12 h, after which it remained approximately constant (Fig. 3c). This is consistent with evolving ORP in EK treatment of clays, which possess low ionic strength low electrical conductivity of pore water hence expanded electric double layer, initially. Under such circumstances the applied electrical field reduces ORP of the system by collapsing the expanded double layer (Pamukcu et al., 2008; Cirtiu et al., 2011; Brosky and Pamukcu, 2013), as observed by the temporal evolution of ORP from its initial values in Fig. 3c. Diffuse double layer (DDL) processes of clay have been already suggested to be involved in the *in situ* conversion of heavy metal soil contaminants to potentially less toxic forms by application of an external direct current to a clay-electrolyte system (Pamukcu et al., 2008). The applied current flows through the higher conductivity bulk liquid, as well as the lower conductivity DDL of the clay particles. Due to the large difference in the conductivity of these two charge conduits, an electrochemical potential difference develops across the DDL, compressing it (Bard and Faulkner, 2001). The clay DDL essentially becomes a microcapacitor and the charge accumulated in the DDL is passed through it to the electrolyte solution. As the intensity of the electrical charge increases across the DDL, a cathodic current runs outward reducing the oxidation states of the available heavy metal constituents in the electrolyte solution near the DDL, thereby reducing the ORP of the clay-electrolyte system.

The ORP values measured in the clay are well above typical values associated with nZVI in groundwater in field applications (−100 mV) (Elliott and Zhang, 2001; Henn and Waddill, 2006; He et al., 2010; Su et al., 2013), and those needed for reductive dechlorination, but are consistent with other studies on nZVI enhanced transport in clay (Pamukcu et al., 2008; Reddy et al., 2011). The effect of nZVI on clay ORP is smaller than in water. Others works showed also that the interpretation of ORP when using nZVI is complicated, because the platinum wire electrode response, at low nZVI concentrations, is a mixed potential reflecting contributions from dissolved $Fe^{2+}$ and $H_2$, as well as deposited and (possibly) suspended nanoparticulate iron (Shi et al., 2011). At high concentrations of nZVI, ORP is dominated by direct interaction between the electrode and the nanoparticles, but this response is nonlinear and saturates with increased coverage of the electrode surface with adsorbed particles (Shi et al., 2011).

The ORP for the enhanced transport drops more than those of the control cases at all electrode locations, stronger near the cathode than near the anode, for the first 12 h of the test. Soon after the 12 h period, the ORP shifts back up to or slightly above the control values at all electrode locations. These results are consistent with the ones reported by Pamukcu et al. (2008) that observed lowered values of ORP in the first six hours of the experiments, after which the values increased above the average ORP distribution for the control tests. The nZVI life span was estimated as 8.8 h for a nanoparticle with 25 nm diameter (Noubactep et al., 2012). The first 6-h reduction in ORP reported in the previous work (Pamukcu et al., 2008), and the 12-h reduction in ORP reported in here are likely due to the average available life span of the nanoparticles during their transport. The difference in the time of ORP

**Table 2**
ANOVA test for determining the significance difference between levels of a variable in ORP and pH measurements on the auxiliary electrodes (E1–E5).

| | Sum of squares | *df* | Mean square | *F* | *p*-Value |
|---|---|---|---|---|---|
| *ORP* | | | | | |
| Between "Electrode" groups | 0.331 | 4 | 0.083 | 2.494 | **0.041** |
| Within "Electrode" groups | 38.626 | 1165 | 0.033 | | |
| Total | 38.957 | 1169 | | | |
| Between "Voltage" groups | 3.195 | 2 | 1.597 | 52.123 | **<0.001** |
| Within "Voltage" groups | 35.762 | 1167 | 0.031 | | |
| Total | 38.957 | 1169 | | | |
| Between "Electrolyte" groups | 27.959 | 3 | 9.320 | 988.101 | **<0.001** |
| Within "Electrolyte" groups | 10.998 | 1166 | 0.009 | | |
| Total | 38.957 | 1169 | | | |
| Between "nZVI" groups | 0.238 | 1 | 0.238 | 7.170 | **0.008** |
| Within "nZVI" groups | 38.719 | 1168 | 0.033 | | |
| Total | 38.957 | 1169 | | | |
| *pH* | | | | | |
| Between "Electrode" groups | 1,467 | 4 | 0.367 | 0.456 | 0.768 |
| Within "Electrode" groups | 575685 | 715 | 0.805 | | |
| Total | 577152 | 719 | | | |
| Between "Voltage" groups | 24.440 | 2 | 0.771 | 15.852 | **<0.001** |
| Within "Voltage" groups | 552.712 | 717 | 12.220 | | |
| Total | 577.152 | 719 | | | |
| Between "Electrolyte" groups | 372.027 | 3 | 124.009 | 432.862 | **<0.001** |
| Within "Electrolyte" groups | 205.124 | 716 | 0.286 | | |
| Total | 577.152 | 719 | | | |

Bold—significant, *p*-value inferior to 0.05.

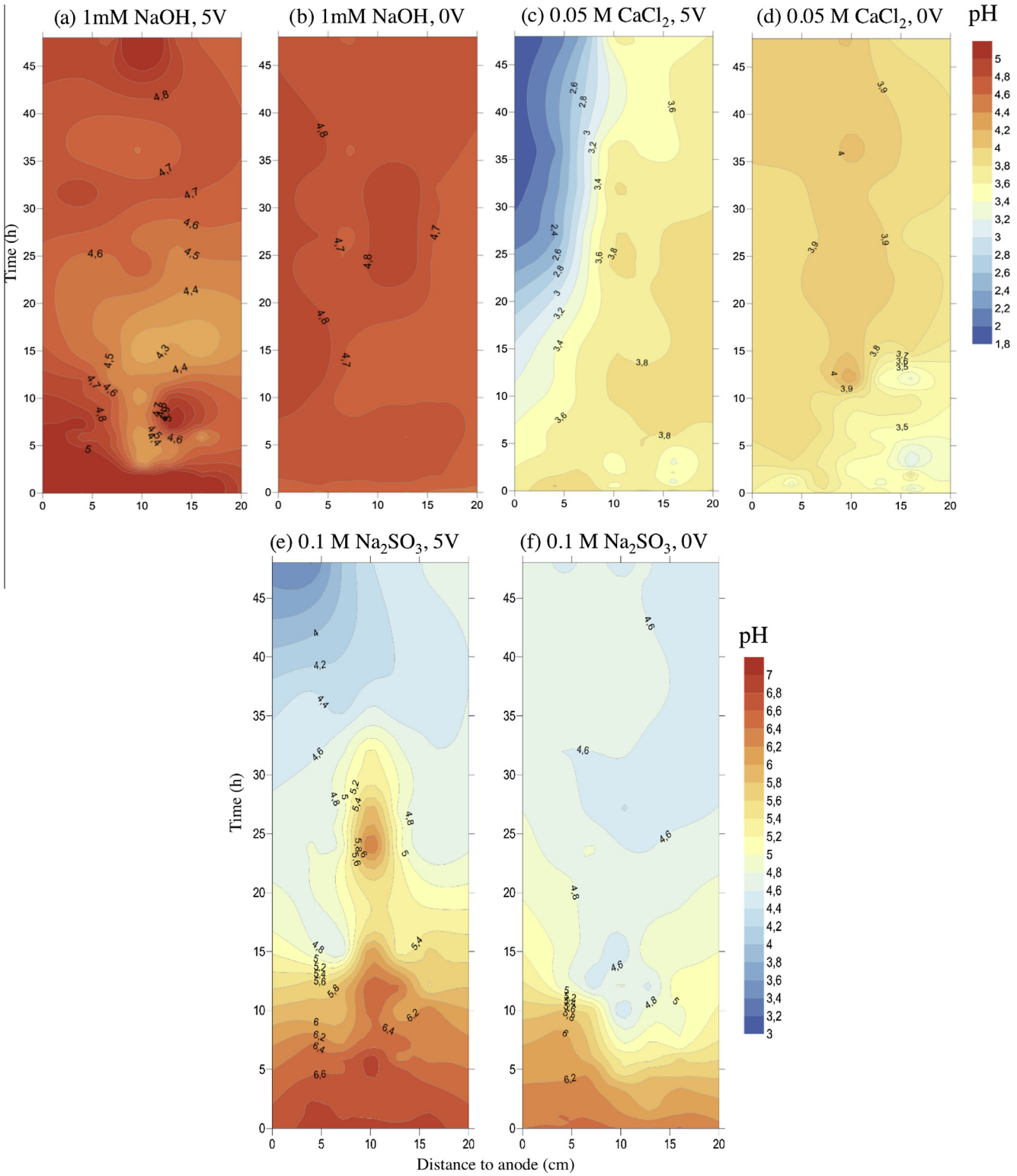


**Fig. 4.** Variation of pH in the kaolin medium in the (a) enhanced transport (Test 6), (b) diffusion (Test 8) using 1 mM NaOH as electrolyte and (c) enhanced transport (Test 12), experiments, (d) diffusion (Test 13) using 0.05 M $CaCl_2$ as electrolyte, (e) enhanced transport (Test 9), experiments and (f) diffusion (Test 10) using 0.1 M $Na_2SO_3$as electrolyte. The plots were obtained by interpolation (kriging) of the pH values measured in each electrode (E1-E5) over time.

reduction period can be attributed to different starting nZVI concentrations, the former being significantly lower, at 5.0 mL of 460 mg $L^{-1}$ nZVI than the latter one, at 2.0 mL of 4000 mg $L^{-1}$.

The ORP values were used to determine which factors had the higher level of significance: "Electrode" – the auxiliary electrodes E1 to E5; "Voltage" – 0 in the diffusion tests, 5 V and 10 V; "Electrolyte" – 1 mM NaCl, 1 mM NaOH, 0.1 M $Na_2SO_3$, 0.05 M $CaCl_2$; "nZVI" – test with and without nZVI. An analysis of variance (ANOVA) was carried out to identify which ordinal or nominal factors presented significant differences between levels (Table 2). This

was followed by Bonferroni multiple comparison method, in order to determine differences between levels of the same significant variable (Supplementary information, Table 1). All tested factors were statistically different (Table 2), but *post hoc* comparisons using the Bonferroni test showed that there was no statistical difference between the electrodes E1 to E5 (Supplementary information, Table 1). A multifactorial ANOVA with only the significant factors "Voltage", "Electrolyte" and "nZVI" showed an interaction between the three factors that could explain most of the ORP variability ($\omega^2 = 0.62$). Independently, the factor more significantly was "Electrolyte" ($\omega^2 = 0.12$). In general, higher voltages corresponded to lower ORP values (with or without nanoparticles), with exception of the experiments with NaOH, where the inverse occurred. Higher ORP values were obtained with $CaCl_2$. Taken together these results show the importance of the electrolyte and the respective ionic strength in the variation of the oxidation–reduction potential and how to interpret it for effectiveness of nZVI transport.

### 3.3. pH

The electrolyte and kaolin mixtures' initial pH varied from 4.23 ± 0.13 to 4.77 ± 0.28, except with the electrolytes $Na_2SO_3$ (6.66 ± 0.28) and $CaCl_2$ (3.73 ± 0.28) that presented the highest and lowest pH values, respectively. The initial acidic pH measured in the clay was favorable for nZVI oxidation. Also, other researchers have observed that low pH increased deposition of nZVI in clay, as well as nZVI aggregation (Kim et al., 2012). Hence the clay initial conditions were unfavorable for PAA–nZVI mobility.

The anolyte and catholyte pH values measured were consistent with the electrochemical reactions of water electrolysis, which produce $H^+$ ions at the anode and $OH^-$ ions in the cathode. The final solution pH values approached 2 in the anolyte and 12 in the catholyte. The lowest pH values were observed with $CaCl_2$ as electrolyte that also displayed the highest current measured (>5 mA). When $Na_2SO_3$ was used as electrolyte, the anolyte pH dropped 3 units between 27 h and 32 h, both in the enhanced transport experiment and in the control without PAA–nZVI, probably due to the exhaustion of the buffer capacity of the electrolyte solution. No statistical difference was found in the anolyte and catholyte pH when comparing the enhanced transport tests with the control without nZVI at the $p < 0.05$ level [one-way ANOVA, $F(1,318) = 0.03$, $p = 0.86$], which is consistent with the iron concentrations bellow the detection limits found in most of the electrolytes samples.

Similar to ORP trends, a higher variation of pH was observed at higher voltage gradients in the first 12 h of the experiments. Acidification of the kaolin at E1 and E2 (near the anode) after 24 h and 30 h, respectively, was noted in all the EK tests. When NaOH was used, both with and without current, the pH values remained nearly neutral initially and stabilized at 5 within the first 12 h (Fig. 4). The electrolyte that showed most variation in the pH values was $Na_2SO_3$, especially near the injection point of PAA–nZVI (E2 and E3), between 6 h and 32 h. A similar trend was observed in the diffusion tests with $Na_2SO_3$ as the electrolyte. This was attributed to the oxidation of $SO_3^{2-}$ to $SO_4^{2-}$ generating acid. The other diffusion tests showed little variation in the pH values.

Table 2 shows the results of the ANOVA for the pH values, considering the variables "Electrode", "Voltage" and "Electrolyte", to identify which variables presented significant differences. Contrary to the ORP values, no statistical difference was found between pH values in the auxiliary electrodes E1-E5, but both "Voltage" and "Electrolyte" show significant difference. *Post hoc* comparisons using the Bonferroni test for the significant variables indicate that the pH values measured with "Voltage" = 10 V were significantly different from the diffusion tests (0 V) and 5 V tests,

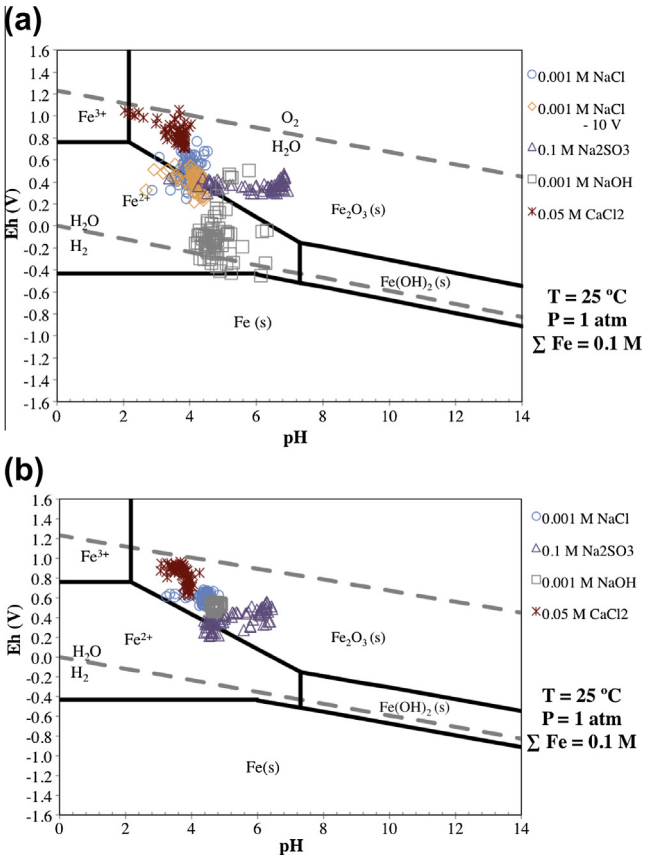


**Fig. 5.** Pourbaix diagram with the values measured at 48 h in the electrodes embedded in the electrophoretic cell: (a) assisted current enhanced transport and (b) diffusion tests.

but no difference was found between 0 and 5 V (Supplementary information, Table 2). Regarding the "Electrolyte" (Supplementary information, Table 2), all the differences between the tested electrolytes were significant. A two-way ANOVA considering the factors "Voltage" and "Electrolyte" showed that the interaction between the two was not significant and that "Electrolyte" could explain most of the pH variability ($\omega^2 = 0.64$). Taken together, these results suggest that the electrolyte and its ionic strength is the most important factor in the pH variation during the experiments.

### 3.4. Iron oxidation state

The oxidation–reduction potentials measured in the electrodes E1 to E5 in the enhanced transport and diffusion experiments were referenced to the normal hydrogen electrode by subtracting the potential of the Ag/AgCl reference electrode (200 mV, at 25 °C, 4 M KCl). These values combined with pH values allowed their introduction into Pourbaix (Eh-pH) diagrams for the Fe oxidation states (Fig. 5). Because predictions from stability diagrams are only accurate when the system approaches thermodynamic equilibrium in aqueous solutions, the plots are intended to give relative approximate dominance of Fe species at the recorded Eh and pH values.

Regarding the experiments with direct current enhanced transport of PAA–nZVI the values are distinct for each electrolyte, with the most oxidizing conditions occurring with $CaCl_2$ and the most reducing conditions with NaOH. This is in agreement with the PAA–nZVI enhanced transport results. Fig. 5b presents the data from the diffusion tests showing a cluster that correspond to the

formation of $Fe_2O_3$ under oxidizing conditions (passivity region), with small differences between the electrolytes tested. From the comparison of the two diagrams, the effect of the direct current in the kaolin pH and redox conditions is discernible in its influence on the distribution of the iron oxidation states. The data shows us the difference between what is likely in each system if equilibrium would be reached.

## 4. Conclusions

The use of direct current enhanced the nZVI transport in the kaolin, using high concentrations, typical of field applications. However, the iron concentration variability could not be explained by pH, ORP, voltage and electrolyte. In the variation of pH and ORP during the experiments, the electrolyte and its ionic strength proved to be significant, and thus will have affected aggregation and fast oxidation of the particles. Clear distinctions were observed in ORP distribution between electrically enhanced transport, diffusion and control tests. The data showed larger variability, both in space and time, in ORP measurements in enhanced transport experiments, which therefore can be explored further as a field index in assessing temporal and spatial efficacy of nZVI nanoparticles transport.

Although real soil contamination cases are complex, the nZVI nanoparticles are often targeted to neutralize specific contaminants of significant concentrations in the subsurface soils. Large changes in certain field parameters, such as ORP, relative to their background values can be an important index to monitor within a treatment area to determine the efficacy of nZVI and the frequency and distribution of soil sampling for laboratory testing. Furthermore, the results of the experiments of electrically enhanced transport of nZVI nanoparticles in a thin layer of pure clay reported here gave us fundamental insights about the critical parameters and governing issues for this enhancement in clay rich soils, which can be used in predictive models.

## Acknowledgments

This work has been funded by FP7-PEOPLE-IRSES-2010-269289-ELECTROACROSS, by Portuguese National funds through "FCT – Fundação para a Ciência e a Tecnologia" under project PTDC/AGR-AAM/101643/2008 NanoDC and by the research grant SFRH/BD/76070/2011. The Department of Civil and Environmental Engineering at Lehigh University is acknowledged where all the equipment development, testing and analysis were funded.

## Appendix A. Supplementary material

Supplementary data associated with this article can be found, in the online version, at http://dx.doi.org/10.1016/j.chemosphere.2013.10.065.

## References

Bard, A.J., Faulkner, L.R., 2001. Electrochemical Methods: Fundamentals and Applications. Wiley, New York.

Bennett, P., He, F., Zhao, D., Aiken, B., Feldman, L., 2010. *In situ* testing of metallic iron nanoparticle mobility and reactivity in a shallow granular aquifer. J. Contam. Hydrol. 116, 35–46.

Brosky, R.T. and Pamukcu, S., 2013. Role of DDL processes during electrolytic reduction of Cu(II) in a low oxygen environment. J. Hazard. Mater. <http://dx.doi.org/10.1016/j.jhazmat.2013.09.032>.

Chang, J.H., Cheng, S.F., 2006. The remediation performance of a specific electrokinetics integrated with zero-valent metals for perchloroethylene contaminated soils. J. Hazard. Mater. B 131, 153–162.

Chowdhury, A.I.A., O'Carroll, D.M., Xu, Y., Sleep, B.E., 2012. Electrophoresis enhanced transport of nano-scale zero valent iron. Adv. Water Resour. 40, 71–82.

Cirtiu, C.M., Raychoudhury, T., Ghoshal, S., Moores, A., 2011. Systematic comparison of the size, surface characteristics and colloidal stability of zero valent iron nanoparticles pre- and post-grafted with common polymers. Colloid Surface A 390, 95–104.

Comba, S., Di Molfetta, A., Sethi, R., 2011. A comparison between field applications of nano-, micro-, and millimetric zero-valent iron for the remediation of contaminated aquifers. Water Air Soil Poll. 215, 595–607.

Elliott, D.W., Zhang, W., 2001. Field assessment of nanoscale bimetallic particles for groundwater treatment. Environ. Sci. Technol. 35, 4922–4926.

Fan, G., Cang, L., Qin, W., Zhou, C., Gomes, H.I., Zhou, D., 2013. Surfactants-enhanced electrokinetic transport of xanthan gum stabilized nano Pd/Fe for the remediation of PCBs contaminated soils. Sep. Purif. Technol. <http://dx.doi.org/10.1016/j.seppur.2013.1004.1030>.

Gomes, H.I., Dias-Ferreira, C., Ribeiro, A.B., 2012a. Electrokinetic remediation of organochlorines in soil: Enhancement techniques and integration with other remediation technologies. Chemosphere 87, 1077–1090.

Gomes, H.I., Dias-Ferreira, C., Ribeiro, A.B., Pamukcu, S., 2012b. Electrokinetic enhanced transport of zero valent iron nanoparticles for chromium (VI) reduction in soils. Chem. Eng. Trans. 28, 139–144.

He, F., Zhao, D., Liu, J., Roberts, C.B., 2007. Stabilization of Fe–Pd nanoparticles with sodium carboxymethyl cellulose for enhanced transport and dechlorination of trichloroethylene in soil and groundwater. Ind. Eng. Chem. Res. 46, 29–34.

He, F., Zhao, D., Paul, C., 2010. Field assessment of carboxymethyl cellulose stabilized iron nanoparticles for *in situ* destruction of chlorinated solvents in source zones. Water Res. 44, 2360–2370.

Henn, K.W., Waddill, D.W., 2006. Utilization of nanoscale zero-valent iron for source remediation—A case study. Remediation 16, 57–77.

Hydutsky, B.W., Mack, E.J., Beckerman, B.B., Skluzacek, J.M., Mallouk, T.E., 2007. Optimization of nano- and microiron transport through sand columns using polyelectrolyte mixtures. Environ. Sci. Technol. 41, 6418–6424.

Jiemvarangkul, P., Zhang, W.X., Lien, H.L., 2011. Enhanced transport of polyelectrolyte stabilized nanoscale zero-valent iron (nZVI) in porous media. Chem. Eng. J. 170, 482–491.

Jones, E.H., Reynolds, D.A., Wood, A.L., Thomas, D.G., 2010. Use of electrophoresis for transporting nano-iron in porous media. Ground Water 49, 172–183.

Kanel, S.R., Goswami, R.R., Clement, T.P., Barnett, M.O., Zhao, D., 2008. Two dimensional transport characteristics of surface stabilized zero-valent iron nanoparticles in porous media. Environ. Sci. Technol. 42, 896–900.

Kim, H.J., Phenrat, T., Tilton, R.D., Lowry, G.V., 2012. Effect of kaolinite, silica fines and pH on transport of polymer-modified zero valent iron nano-particles in heterogeneous porous media. J. Colloid Interface Sci. 370, 1–10.

Lin, Y.H., Tseng, H.H., Wey, M.Y., Lin, M.D., 2009. Characteristics, morphology, and stabilization mechanism of PAA250k-stabilized bimetal nanoparticles. Colloid Surface A 349, 137–144.

Lin, Y.H., Tseng, H.H., Wey, M.Y., Lin, M.D., 2010. Characteristics of two types of stabilized nano zero-valent iron and transport in porous media. Sci. Total Environ. 408, 2260–2267.

Masciangioli, T., Zhang, W., 2003. Environmental technologies at the nanoscale. Environ. Sci. Technol. 37, 102A–108A.

Mehra, O.P., Jackson, M.L., 1960. Iron oxide removal from soils and clays by a dithionite–citrate system buffered with sodium bicarbonate. Clays Clay Miner. 7, 317–327.

Mueller, N.C., Braun, Jr., Bruns, J., Černík, M., Rissing, P., Rickerby, D., Nowack, B., 2012. Application of nanoscale zero valent iron (nZVI) for groundwater remediation in Europe. Environ. Sci. Pollut. R 19, 550–558.

Noubactep, C., Caré, S., Crane, R., 2012. Nanoscale metallic iron for environmental remediation: prospects and limitations. Water Air Soil Poll. 223, 1363–1382.

Pamukcu, S., 2009. Electrochemical transport and transformations. In: Reddy, K.R., Cameselle, C. (Eds.), Electrochemical Remediation Technologies for Polluted Soils, Sediments and Groundwater. John Wiley & Sons, Inc., Hoboken, New Jersey, pp. 29–64.

Pamukcu, S., Hannum, L., Wittle, J.K., 2008. Delivery and activation of nano-iron by DC electric field. J. Environ. Sci. Health A 43, 934–944.

Pamukcu, S., Weeks, A., Wittle, J.K., 2004. Enhanced reduction of Cr(VI) by direct electric current in a contaminated clay. Environ. Sci. Technol. 38, 1236–1241.

Phenrat, T., Cihan, A., Kim, H.-J., Mital, M., Illangasekare, T., Lowry, G.V., 2010. Transport and deposition of polymer-modified $Fe^0$ nanoparticles in 2-D heterogeneous porous media: effects of particle concentration, $Fe^0$ content, and coatings. Environ. Sci. Technol. 44. 9086-9083.

Phenrat, T., Fagerlund, F., Illangasekare, T., Lowry, G.V., Tilton, R.D., 2011. Polymer-modified $Fe^0$ nanoparticles target entrapped NAPL in two dimensional porous media: effect of particle concentration, NAPL saturation, and injection strategy. Environ. Sci. Technol. 45, 6102–6109.

Phenrat, T., Kim, H.J., Fagerlund, F., Illangasekare, T., Tilton, R.D., Lowry, G.V., 2009. Particle size distribution, concentration, and magnetic attraction affect transport of polymer-modified $Fe^0$ nanoparticles in sand columns. Environ. Sci. Technol. 43, 5079–5085.

Phenrat, T., Saleh, N., Sirk, K., Tilton, R.D., Lowry, G.V., 2007. Aggregation and sedimentation of aqueous nanoscale zerovalent iron dispersions. Environ. Sci. Technol. 41, 284–290.

Raychoudhury, T., Naja, G., Ghoshal, S., 2010. Assessment of transport of two polyelectrolyte-stabilized zero-valent iron nanoparticles in porous media. J. Contam. Hydrol. 118, 143–151.

Reddy, K.R., Darko-Kagy, K., Cameselle, C., 2011. Electrokinetic-enhanced transport of lactate-modified nanoscale iron particles for degradation of dinitrotoluene in clayey soils. Separ. Purif. Technol. 79, 230–237.

Rejeski, D., Kuiken, T., Polischuk, P., Pauwels, E., 2012. Nanoremediation map. Project on Emerging Nanotechnologies. <http://www.nanotechproject.org/inventories/remediation_map/>. (3 April 2012).

Saleh, N., Kim, H.-J., Phenrat, T., Matyjaszewski, K., Tilton, R.D., Lowry, G.V., 2008. Ionic strength and composition affect the mobility of surface-modified $Fe^0$ nanoparticles in water-saturated sand columns. Environ. Sci. Technol. 42, 3349–3355.

Shi, Z., Nurmi, J.T., Tratnyek, P.G., 2011. Effects of nano zero-valent iron on oxidation–reduction potential. Environ. Sci. Technol. 45, 1586–1592.

Su, C., Puls, R.W., Krug, T.A., Watling, M.T., O'Hara, S.K., Quinn, J.W., Ruiz, N.E., 2013. Travel distance and transformation of injected emulsified zero valent iron nanoparticles in the subsurface during two and half years. Water Res. <http://dx.doi.org/10.1016/j.watres.2012.1012.1042>.

Sun, Y.P., Li, X.Q., Zhang, W.X., Wang, H.P., 2007. A method for the preparation of stable dispersion of zero-valent iron nanoparticles. Colloid Surface A 308, 60–66.

Tiraferri, A., Chen, K.L., Sethi, R., Elimelech, M., 2008. Reduced aggregation and sedimentation of zero-valent iron nanoparticles in the presence of guar gum. J. Colloid Interface Sci. 324, 71–79.

Tiraferri, A., Sethi, R., 2009. Enhanced transport of zerovalent iron nanoparticles in saturated porous media by guar gum. J. Nanopart. Res. 11, 635–645.

USEPA, 2011. Fact sheet on selected sites using or testing nanoparticles for remediation. United States Environmental Protection Agency. <http://cluin.org/products/nanozvi/>. (accessed 3 April 2012).

Yang, G.C.C., Chang, Y.I., 2011. Integration of emulsified nanoiron injection with the electrokinetic process for remediation of trichloroethylene in saturated soil. Sep. Purif. Technol. 79, 278–284.

Yang, G.C.C., Hung, C.H., Tu, H.C., 2008. Electrokinetically enhanced removal and degradation of nitrate in the subsurface using nanosized Pd/Fe slurry. J. Environ. Sci. Health A 43, 945–951.

Yang, G.C.C., Wu, M.Y., 2011. Injection of nanoscale $Fe_3O_4$ slurry coupled with the electrokinetic process for remediation of $NO_3^-$ in saturated soil: remediation performance and reaction behavior. Separ. Purif. Technol. 79, 272–277.

Yuan, S., Long, H., Xie, W., Liao, P., Tong, M., 2012. Electrokinetic transport of CMC-stabilized Pd/Fe nanoparticles for the remediation of PCP-contaminated soil. Geoderma 185–186, 18–25.

Zhang, W., 2003. Nanoscale iron particles for environmental remediation: an overview. J. Nanopart. Res. 5, 323–332.

Zhang, W., Elliott, D.W., 2006. Applications of iron nanoparticles for groundwater remediation. Remediation, 7–21.

## Supplementary Information

**Table 1.** Multiple comparisons test using Bonferroni method, with ORP as dependent variable, for "Electrode", "Voltage" and "Electrolyte". *Post hoc* tests were not performed for "nZVI" because there are fewer than three groups.

| | (I) | (J) Electrode | Mean Difference (I-J) | Std. Error | Sig. | 95% Confidence Interval | |
|---|---|---|---|---|---|---|---|
| | | | | | | Lower Bound | Upper Bound |
| Electrode | E1 | E2 | 0.031 | 0.017 | 0.657 | -0.016 | 0.078 |
| | | E3 | 0.014 | 0.017 | *1.000* | -0.034 | 0.061 |
| | | E4 | -0.005 | 0.017 | *1.000* | -0.052 | 0.043 |
| | | E5 | 0.038 | 0.017 | 0.233 | -0.009 | 0.086 |
| | E2 | E1 | -0.031 | 0.017 | 0.657 | -0.078 | 0.016 |
| | | E3 | -0.017 | 0.017 | *1.000* | -0.065 | 0.030 |
| | | E4 | -0.036 | 0.017 | 0.336 | -0.083 | 0.012 |
| | | E5 | 0.007 | 0.017 | *1.000* | -0.040 | 0.055 |
| | E3 | E1 | -0.014 | 0.017 | *1.000* | -0.061 | 0.034 |
| | | E2 | 0.017 | 0.017 | *1.000* | -0.030 | 0.065 |
| | | E4 | -0.018 | 0.017 | *1.000* | -0.066 | 0.029 |
| | | E5 | 0.025 | 0.017 | *1.000* | -0.023 | 0.072 |
| | E4 | E1 | 0.005 | 0.017 | *1.000* | -0.043 | 0.052 |
| | | E2 | 0.036 | 0.017 | 0.336 | -0.012 | 0.083 |
| | | E3 | 0.018 | 0.017 | *1.000* | -0.029 | 0.066 |
| | | E5 | 0.043 | 0.017 | 0.107 | -0.004 | 0.090 |
| | E5 | E1 | -0.038 | 0.017 | 0.233 | -0.086 | 0.009 |
| | | E2 | -0.007 | 0.017 | *1.000* | -0.055 | 0.040 |
| | | E3 | -0.025 | 0.017 | *1.000* | -0.072 | 0.023 |
| | | E4 | -0.043 | 0.017 | 0.107 | -0.090 | 0.004 |
| Voltage | 0 | 5 | -0.004 | 0.012 | *1.000* | -0.032 | 0.025 |
| | | 10 | 0.146* | 0.017 | **< 0.001** | 0.106 | 0.185 |
| | 5 | 0 | 0.004 | 0.012 | *1.000* | -0.025 | 0.032 |
| | | 10 | 0.149* | 0.015 | **< 0.001** | 0.113 | 0.185 |
| | 10 | 0 | -0.146* | 0.017 | **< 0.001** | -0.185 | -0.106 |
| | | 5 | -0.149* | 0.011 | **< 0.001** | -0.185 | -0.113 |
| Electrolyte | NaCl | NaOH | -0.081* | 0.008 | **< 0.001** | -0.102 | -0.061 |
| | | $Na_2SO_3$ | 0.134* | 0.008 | **< 0.001** | 0.114 | 0.155 |
| | | $CaCl_2$ | -0.320* | 0.008 | **< 0.001** | -0.341 | -0.300 |
| | NaOH | NaCl | 0.081* | 0.008 | **< 0.001** | 0.061 | 0.102 |
| | | $Na_2SO_3$ | 0.216* | 0.009 | **< 0.001** | 0.193 | 0.239 |
| | | $CaCl_2$ | -0.239* | 0.009 | **< 0.001** | -0.262 | -0.216 |
| | $Na_2SO_3$ | NaCl | -0.134* | 0.008 | **< 0.001** | -0.155 | -0.114 |
| | | NaOH | -0.216* | 0.009 | **< 0.001** | -0.239 | -0.193 |
| | | $CaCl_2$ | -0.454* | 0.009 | **< 0.001** | -0.477 | -0.431 |
| | $CaCl_2$ | NaCl | 0.320* | 0.008 | **< 0.001** | 0.300 | 0.341 |
| | | NaOH | 0.239* | 0.009 | **< 0.001** | 0.216 | 0.262 |
| | | $Na_2SO_3$ | 0.454* | 0.009 | **< 0.001** | 0.431 | 0.477 |

*. The mean difference is significant at the 0.05 level.
Bold—significant, p-value inferior to 0.05. Italic—high similarity, p-value equal to 1.

**Table 2.** Multiple comparisons test using Bonferroni method, with pH as dependent variable, for "Voltage" and "Electrolyte".

| | (I) | (J) | Mean Difference (I-J) | Std. Error | Sig. | 95% Confidence Interval | |
|---|---|---|---|---|---|---|---|
| | | | | | | Lower Bound | Upper Bound |
| Voltage | 0 | 5 | -0.013 | 0.069 | *1.000* | -0.180 | 0.154 |
| | | 10 | 0.579* | 0.110 | **< 0.001** | 0.316 | 0.843 |
| | 5 | 0 | 0.013 | 0.069 | *1.000* | -0.154 | 0.180 |
| | | 10 | 0.592* | 0.110 | **< 0.001** | 0.329 | 0.856 |
| | 10 | 0 | -0.579* | 0.110 | **< 0.001** | -0.843 | -0.316 |
| | | 5 | -0.592* | 0.110 | **< 0.001** | -0.856 | -0.329 |
| Electrolyte | NaCl | NaOH | -0.655* | 0.546 | **< 0.001** | -0.799 | -0.510 |
| | | $Na_2SO_3$ | -1.520* | 0.055 | **< 0.001** | -1.664 | -1.375 |
| | | $CaCl_2$ | 0.477* | 0.055 | **< 0.001** | 0.333 | 0.622 |
| | NaOH | NaCl | 0.655* | 0.055 | **< 0.001** | 0.510 | 0.799 |
| | | $Na_2SO_3$ | -0.865* | 0.060 | **< 0.001** | -1.023 | -0.706 |
| | | $CaCl_2$ | 1.132* | 0.055 | **< 0.001** | 0.974 | 1.290 |
| | $Na_2SO_3$ | NaCl | 1.520* | 0.055 | **< 0.001** | 1.375 | 1.664 |
| | | NaOH | 0.865* | 0.060 | **< 0.001** | 0.706 | 1.023 |
| | | $CaCl_2$ | 1.997* | 0.060 | **< 0.001** | 1.838 | 1.155 |
| | $CaCl_2$ | NaCl | -0.477* | 0.055 | **< 0.001** | -0.622 | -0.333 |
| | | NaOH | -1.132* | 0.060 | **< 0.001** | -1.290 | -0.974 |
| | | $Na_2SO_3$ | -1.997* | 0.060 | **< 0.001** | -2.155 | -1.838 |

*. The mean difference is significant at the 0.05 level.
Bold—significant, p-value inferior to 0.05. Italic—high similarity, p-value equal to 1.

## II.5. Electrokinetic enhanced transport of zero valent iron nanoparticles for chromium(VI) reduction in soils

## (published in Chemical Engineering Transactions)

CHEMICAL ENGINEERING TRANSACTIONS
VOL. 28, 2012
A publication of AIDIC
The Italian Association of Chemical Engineering
Online at: www.aidic.it/cet
Guest Editor: Carlo Merli

**ISBN** 978-88-95608-19-8; **ISSN** 1974-9791

# Electrokinetic Enhanced Transport of Zero Valent Iron Nanoparticles for Chromium(VI) Reduction in Soils

Helena I. Gomes[a,b]*, Celia Dias-Ferreira[c], Alexandra B. Ribeiro[b], Sibel Pamukcu[a]

[a]Department of Civil and Environmental Engineering, Fritz Engineering Laboratory, 13 E. Packer Avenue, Lehigh University, Bethlehem, PA 18015-4729, USA
[b]CENSE, Departamento de Ciências e Engenharia do Ambiente, Faculdade de Ciências e Tecnologia, Universidade Nova de Lisboa, 2829-516 Caparica, Portugal
[c]CERNAS, Departamento de Ambiente, Escola Superior Agrária de Coimbra, Bencanta, 3040-316 Coimbra, Portugal
hig311@lehigh.edu

Zero valent iron nanoparticles (nZVI) are a promising technology that could provide cost-effective solutions to soil and groundwater remediation. However, transport of nZVI is normally limited by their aggregation and settling, and with mobility being normally less than a few meters.The main research objective of this study is to find out if coupling electrokinetics and reactive iron nanoparticles can be an effective method for treating chromium contaminated clay soils. Direct current was used to enhance poly(acrylic acid), sodium salt (PAA) coated iron nanoparticles (PAA-nZVI) mobility in Cr(VI) spiked kaolin.A commercially available electrophoretic cell was modified for these experiments and equipped with internal auxiliary electrodes that allow to measure the redox potential directly in the clay. A constant potential of 5.0 V wasapplied across the test bed. Experimental results show that electrokinetics can enhance the delivery of nanoscale iron particles for the reduction of hexavalent chromium to the less toxic trivalent chromium. Direct current enhanced nZVI transport up to 74 % when compared with diffusion, maximum value found when comparing iron concentrations ratios. Activation of nZVI was also observed with a decrease in the redox potential of 531 mV, in average, after the injection point.

## 1. Introduction

Large quantities of chromium have been discharged into the environment, mainly to soils and groundwater, due to improper disposal and leakagein industrial activities (ore refining, production of steel and alloys, metal plating, tannery, wood preservation and pigmentation). Chromium is one of the most frequent metal soil contaminants and is one of the top 20 contaminants on the Superfund priority list of hazardous substances for the past 15 years(Chrysochoouet al., 2011).
Oxidation states ofCr range from -4 to +6, but only the +3 (III) and +6 (VI) states are stable under most natural environments. These twooxidation states are drasticallydifferent in charge, physicochemical properties as well as chemical and biochemical reactivity (Bagchiet al., 2002). Cr(VI) is extremely mobile in the environment and is toxic to humans, animals, plants, and microorganisms. Because of its significant mobility in the subsurface environment, the potential risk of groundwater contamination is high. Cr(III), on the other hand, is less toxic, immobile, and readily precipitates as $Cr(OH)_3$(Singhet al.,

2011).Cr(III) is also considered to be a trace element essential for the proper functioning of living organisms(Kotaś and Stasicka, 2000).
Several researchers have already demonstrated, at bench-scale, that nZVI could be used to promote reduction of Cr(VI) to Cr(III) in groundwater (Ponderet al., 2000; Melitaset al., 2001; Drieset al., 2005) and also in soils (Xu and Zhao, 2007; Francoet al., 2009; Chrysochoouet al., 2011; Singhet al., 2011, 2012).Experimental results from X-ray photoelectron spectroscopy and X-ray absorption spectroscopy showed that nano $Fe^0$ reduces Cr(VI) and corrodes to form lepidocrocite[a product of Fe(II) oxidation - $\gamma$FeOOH] which then acts as a substrate for precipitation of $Cr(OH)_3$ and/or $Cr_xFe_{1-x}(OH)_3$ (Manningetal., 2007). $Fe^0$ is ultimately oxidized to Fe(III), which precipitates as ferric hydroxides, while Cr(VI) is reduced to Cr(III).The net reactions of Cr(VI) reduction with Fe(0) and coprecipitation of Cr(III) and Fe(III) are as follows(Qianet al., 2008), involving also indirect reduction by Fe(II) according to the reactions (3) and (4)(Chrysochoouet al., 2011):

$$CrO_4^{2-} + Fe^0 + 8H^+ \rightarrow Fe^{3+} + Cr^{3+} + 4H_2O \quad (1)$$

$$_{(1-x)}Fe^{3+} +_{(x)}Cr^{3+} +2H_2O \rightarrow 2Fe_{(1-x)}Cr_xOOH\ (s) + 3H^+ \quad (2)$$

where *x* can vary from 0 to 1.

$$2HCrO_4^- + 3Fe^0 + 14H^+ \rightarrow 3Fe^{2+} + 2Cr^{3+} + 8H_2O \quad (3)$$

$$Fe^0 +2H^+ \rightarrow Fe^{2+} + H_2 \quad (4)$$

$$3Fe^{2+} + CrO_4^{2-} + 16H^+ \rightarrow 3Fe^{3+} + Cr^{3+} + 8H_2O \quad (5)$$

In field applications, nZVI are traditionally injected under pressure and/or by gravity. However, transport of nZVI is normally limited by their aggregation and settling (Phenratet al., 2007), with mobility in the subsurface being normally less than a few meters as several field applications show(Bennettet al., 2010; Combaet al., 2010; Heet al., 2010). Some strategies have been developed to tackle this limitation, such as coating of the nanoparticles with different polymers (Sunet al., 2007; Yanget al., 2007; Phenratet al., 2008; Tiraferriet al., 2008). Electrokinetics can be used to deliver and activate nZVI in low permeability soils (Pamukcuet al., 2008; Reddyet al., 2011; Yang and Chang, 2011). The electrokinetic process can also provide the electrical supply of energy to drive favorable reduction-oxidation reactions. Pamukcu et al.(2004) demonstrated the feasibility of *in situ* reduction of Cr(VI) to Cr(III) by introducing ferrous iron $Fe^{2+}$ to the contaminated soil electrokinetically. This study aims to analyze if coupling electrokinetics and reactive iron nanoparticles can also be an effective method for treating chromium contaminated soils.

## 2. Materials and methods

### 2.1 Electrophoretic cell

A commercially available electrophoretic (EP) (Econo-SubmarineGel Unit, model SGE-020) cell was modified to undertake these experiments (Figure 1). The cell is a rectangular translucent box with a square (20 cm x 20 cm) sample tray. There are two liquid chambers on each side of the sample tray (to hold the electrolyte) and a lid that covers the whole apparatus. The standard cell is equipped with platinum working electrodes and both auxiliary electrodes and a reference electrode were added for this experiment. This modified EP cell allowed direct measurement of the redox potential (ORP) in the soil by use of 0.25 mm diameter platinum wire electrodes fixed in the base plate of the sample tray at equal intervals (3 cm) with conductive glue. ORP measurements were made in the wire electrodes, using a Ag/AgCl reference electrode and a device attached to a low resistance multimeter to facilitate the accurate measurement of soil redox potential (Rabenhorst, 2009) (Figure 1). These electrodes were labeled as E1-E5 starting from the anode end (Figure 1). Compressed fiberglass wool pads were used on both sides to help transport the migrating ions from the electrolyte into the clay and vice versa. The levels of the liquids in the anode and cathode chambers were kept slightly below that of the clay in the sample tray to avoid flooding of the soil cell with excess liquid and any preferential transport of nZVI through water pool at the top.

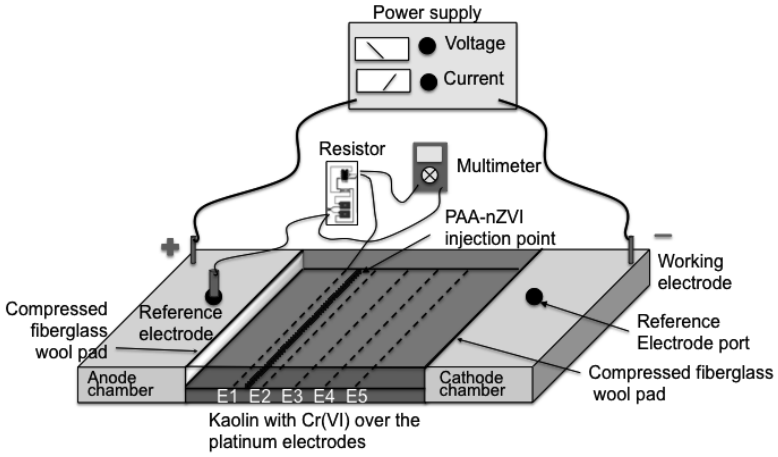


*Figure 1: Schematic diagram of the modified electrophoretic cell test setup.*

**2.2 Chemicals**

Zero valent iron nanoparticles (nZVI) were prepared with the reduction of ferric chloride (Alfa Aesar) by sodium borohydride(Hydrifin$^{TM}$)and after were stabilized by poly(acrylic acid), sodium salt (PAA) (Polysciences, Inc) following the method described inJiemvarangkulet al.(2011). A solution with a concentration of 10 g $L^{-1}$ of nZVI and 30 % (w/w) of PAA was prepared.

All stock solutions were made from ACS reagent grade materials and distilled de-ionized water. The electrolyte solution used in the electrode chambers, 0.001 M NaCl (Sigma Ultra) was deoxygenated with ultra purified grade nitrogen gas ($N_2$) for a minimum of 1 h before use.The molar concentration of the potassium dichromate(Aldrich Chemical) solution was 0.005 M.

**2.3 Enhanced transport experiments**

The chromium spiked clay was prepared by adding $K_2Cr_2O_7$ stock solution to 140 g of white Georgia kaolinite clay, whose properties were described by Pamukcu et al. (2004). The final water content was 60 % by dry weight and the mixture had a density of 1.63 g $cm^{-3}$ (Pamukcuet al., 2004). The paste was transferred into the tray and spread uniformly over the wireelectrodes to a thickness of 2 mm.

PAA-nZVI were delivered using a pipette to add 0.250 mL solution and spreading it into a pre-cut groove into the clay on the anode side, between E1 and E2 (Figure 1). An acrylic cover (2 mm thick) was then placed over to ensure that the clay saturation is maintained under a thin layer of water, butPAA-nZVI transport in the system occurred through the clay layer only.

A constant potential of 5.0 V was applied across the working electrodes for 24 h.This low potential was selected to remainwithin the linear range of the power supply used and alsoprevent excessive gas generation. The24-h duration was selected to allow adequate time for uniformdistribution of iron in the clay based on previously demonstrated results (Pamukcu and Wittle, 1992).The cell was kept in a dark location to prevent iron photo-oxidation. Two control experiments were conducted in the same conditions, without direct current and with current and without nZVI.

Measurements were taken periodically at the following times: 0.25, 0.50, 0.75, 1, 2, 3, 5, 7, 12, 15, 20 and 24 h. At each measurement time voltage, current, ORP, pH and temperature were monitored. At the end of each test, water samples were collected from the electrode chambers, and soil samples were collected in three equidistant locations above the electrodes. The grove where nZVI was injected was not sampled. The soil and water samples were analyzed for total chromium, hexavalent chromium, total iron and ferrous iron concentrations, and pH.All soil and liquid samples were collected, preserved, extracted, and diluted in accordance with the U.S. EPA guidelines (3050B, 3060A,7196A)or standard methods (APHA, 1992). The iron and chromium analysis were conducted using a Perkin-ElmerAAnalyst200flame atomic absorption spectroscopy (AA) and a Hach DR 2800 spectrophotometer (UV).

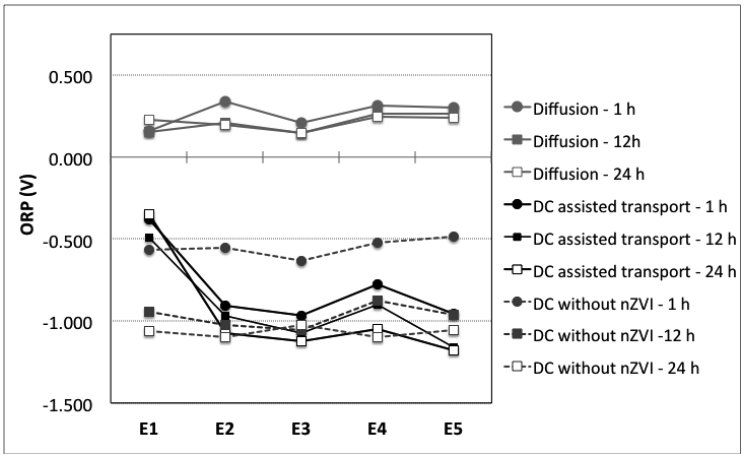


*Figure 2: Distribution of ORPin the clay with and without direct current transport and without nZVI.*

## 3. Results and discussion

### 3.1 Redox potential measurements

The redox measurements in soil show the trend of oxidizing to reducing conditions from the anode toward the cathode when the direct current is applied over time in 24 h (Figure 2). When PAA-nZVI was injected between E1 and E2, it caused decrease in the ORP values of 523 mV within the first hour of transport, showing that there is an activation of the nanoparticles as observed by Pamukcu et al. (2008). In the diffusion test, the ORP values maintained a nearly constant value, around 0.222 V, showing no activation of the nZVI. In the experiments where direct current was applied, thecurrent density was2.7x $10^{-4}$ mA $cm^{-2}$after about 1 h of treatment when no nanoparticles where injected,and1.3 x $10^{-3}$ mA $cm^{-2}$ with PAA-nZVI. This shows the increase in the electrical conductivity when PAA-nZVI are used, causing additional current carriers be introduced into the system with the ensuing reactions.

### 3.2 Chromium and iron distributions

At the end of 24h treatment, no iron or chromium was detected in both the anolyte and the catholyte in all the experiments. The Fe/Cr ratio distribution in soil remained relatively uniform (Figure 3)in the electrodes E1 to E5, throughout the cell as observed by Pamukcu et al. (2004). This is attributed to retarded chromium transport and uniform distribution of the excess iron across the thin cross-section of the kaolin during treatment.

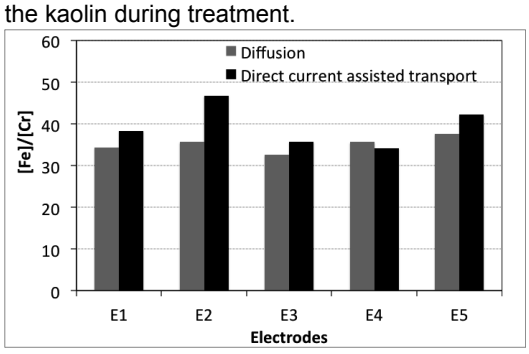


*Figure 3: Post-treatment average distribution of total iron to total chromium ratio in the clay.*

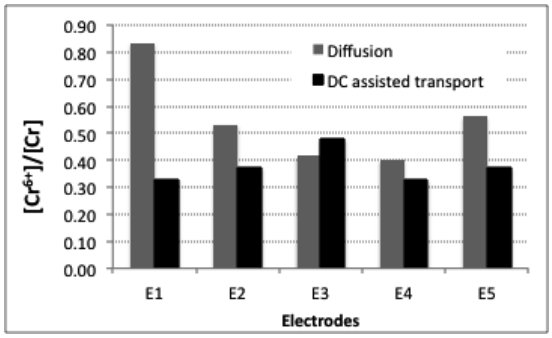


*Figure 4: Average mass fraction distribution of Cr(VI) and total chromium measured for each electrode location.*

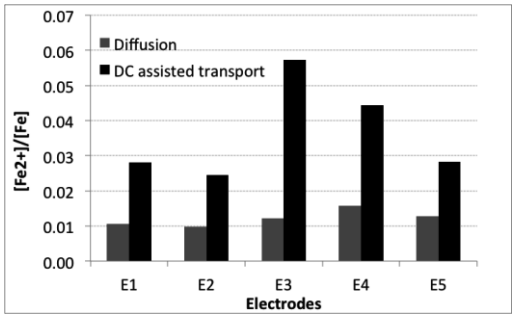


*Figure 5: Average mass fraction distribution of $Fe^{2+}$ and total iron measured for each electrode location.*

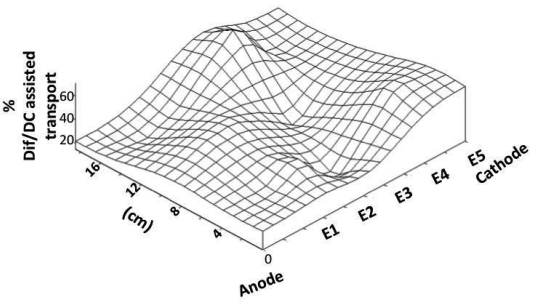


*Figure 6: 2D spatial distribution of the % $[Fe^{2+}]/[Fe]$ observed in the soil comparing the diffusion and DC assisted transport tests of nZVI.*

Comparing the ratio between Cr(VI) and total chromium concentrations along the electrodes (Figure 4), it is apparent that less chromium is on this oxidation state, when direct current is used. In this case, across the soil, at the end of 24 h, an average of 62 % of chromium is transformed into the less toxic and less mobile oxidation state Cr(III). Results also show that PAA-nZVI transport is enhanced with direct current, as more $Fe^{2+}$ was found compared with diffusion (Figure 5).The high value in E3 is consistent with the visual observation of nZVI transport as well. Figure 6 shows the 2-dimensional spatial distribution of the $[Fe^{2+}]/[Fe]$ percentage between the diffusion and enhanced transport. The overall transformation of Fe to Fe(II) is more than doubled in the enhanced transport case (Figure 5), but the spatial distribution of the species achieved at the end of 24 h is not as uniform as that of the diffusion (Figure 6).

## 4. Conclusions

According to the experimental results, it can be concluded that the integration of electrokinetics with nZVI is very promisingin the cleanup of Cr contaminated soil, enhancing the transport of PAA-nZVI and reducing the target contaminant, even with very low current density. ORP distribution and its temporal variation throughout the tests showed that the electrical field enhances the ORP, creating a synergistic effect of nZVI usage with electrokinetics.

The results show that PAA-nZVI can be transported by electric fieldseven in low permeability clay soils, preventing common issues of agglomeration and settlement, while accelerating *in situ* destruction or immobilization of some contaminating compounds. However, further tests should be done, especially with higher amounts of soil and soils with high surface activity. More detailed analysis of the iron speciation; the competition between the different oxidants present in the media and the stoichiometry should also be considered.

## Acknowledgments

This work has been funded by the European Regional Development Fund (ERDF) through COMPETE – Operational Programme for Competitiveness Factors (OPCF), by Portuguese National funds through “FCT - Fundaçãopara a Ciência e a Tecnologia” under project «PTDC/AGR AAM/101643/2008 NanoDC», by the research grant SFRH/BD/76070/2011 and by FP7-PEOPLE-IRSES-2010-269289-ELECTROACROSS. DanZerokais kindly acknowledged for the electrophoretic cell modification and the construction of the device to increase resistance.

## References

APHA, 1992, Standard Methods for the Examination of Water and Wastewater, American Public Health Association, Washington, DC, USA.

Bagchi D., Stohs S.J., Downs B.W., Bagchi M., Preuss H.G., 2002, Cytotoxicity and oxidative mechanisms of different forms of chromium, Toxicology 180, 5-22.

Bennett P., He F., Zhao D., Aiken B., Feldman L., 2010, In situ testing of metallic iron nanoparticle mobility and reactivity in a shallow granular aquifer, J. Contam. Hydrol. 116, 35-46.
Chrysochoou M., Johnston C.P., Dahal G., 2011, A comparative evaluation of hexavalent chromium treatment in contaminated soil by calcium polysulfide and green-tea nanoscale zero-valent iron, J. Hazard. Mater.DOI:10.1016/j.jhazmat.2011.1011.1003.
Comba S., Molfetta A.D., Sethi R., 2010, A comparison between field applications of nano-, micro-, and millimetric zero-valent iron for the remediation of contaminated aquifers, Water Air Soil Pollut., 215, 595-607.
Dries J., Bastiaens L., Springael D., Agathos S.N., Diels L., 2005, Combined removal of chlorinated ethenes and heavy metals by zerovalent iron in batch and continuous flow column systems, Environ. Sci.Technol. 39, 8460-8465.
Franco D.V., Silva L.M., Jardim W.F., 2009,Reduction of hexavalent chromium in soil and ground water using zero-valent iron under batch and semi-batch conditions, Water Air Soil Pollut. 197, 49-60.
He F., Zhao D., Paul C., 2010, Field assessment of carboxymethyl cellulose stabilized iron nanoparticles for in situ destruction of chlorinated solvents in source zones, Water Res. 44, 2360-2370.
Jiemvarangkul P., Zhang W.X., Lien H.L., 2011, Enhanced transport of polyelectrolyte stabilized nanoscale zero-valent iron (nZVI) in porous media, Chem. Eng. J. 170, 482-491.
Kotaś J., Stasicka, Z., 2000. Chromium occurrence in the environment and methods of its speciation, Environ. Pollut. 107, 263-283.
Manning B.A., Kiser J.R., Kwon H., Kanel S.R., 2007, Spectroscopic investigation of Cr(III)- and Cr(VI)-treated nanoscale zerovalent iron, Environ. Sci. Technol. 41, 586-593.
Melitas N., Chuffe-Moscoso O., Farrell J., 2001,Kinetics of soluble chromium removal from contaminated water by zerovalent iron media: Corrosion inhibition and passive oxide effects,Environ. Sci. Technol. 35, 3948-3953.
Pamukcu S., Hannum L., Wittle J.K., 2008, Delivery and activation of nano-iron by DC electric field,J. Environ.Sci. Health A 43, 934-944.
Pamukcu S., Weeks A., Wittle J.K., 2004, Enhanced reduction of Cr(VI) by direct electric current in a contaminted clay,Environ. Sci. Technol.38, 1236-1241.
Pamukcu S., Wittle J.K., 1992, Electrokinetic removal of selected heavy metals from soil, Environ. Prog. 11, 241-250.
Phenrat T., Saleh N., Sirk K., Kim H.-J., Tilton R.D., Lowry G.V., 2008, Stabilization of aqueous nanoscale zerovalent iron dispersions by anionic polyelectrolytes: Adsorbed anionic polyelectrolyte layer properties and their effect on aggregation and sedimentation, J. Nanopart. Res. 10, 795–814.
Phenrat T., Saleh N., Sirk K., Tilton R.D., Lowry G.V., 2007, Aggregation and sedimentation of aqueous nanoscale zerovalent iron dispersions, Environ. Sci. Technol. 41, 284-290.
Ponder S.M., Darab J.G., Mallouk T.E., 2000. Remediation of Cr(VI) and Pb(II) aqueous solutions using supported, nanoscale zero-valent iron,Environ. Sci. Technol. 34, 2564-2569.
Qian H., Wu Y., Liu Y., Xu X., 2008. Kinetics of hexavalent chromium reduction by iron metal, Front. Environ. Sci. Engin. China 2, 51-56.
Rabenhorst M.C., 2009, Making soil oxidation–reduction potential measurements using multimeters, Soil Sci. Soc. Am. J. 73, 2198-2201.
Reddy K.R., Darko-Kagy K., Cameselle C., 2011, Electrokinetic-enhanced transport of lactate-modified nanoscale iron particles for degradation of dinitrotoluene in clayey soils, Sep. Purif. Technol. 79, 230-237.
Singh R., Misra V., Singh R.P., 2011, Synthesis, characterization and role of zero-valent iron nanoparticle in removal of hexavalent chromium from chromium-spiked soil, J. Nanopart. Res. 13, 4063-4073.
Singh R., Misra V., Singh R.P., 2012, Removal of Cr(VI) by nanoscale zero-valent iron (nZVI) from soil contaminated with tannery wastes, Bull. Environ. Contam. Toxicol.88(2), 210-214.
Sun Y.-P., Li X.-Q., Zhang W.-X., Wang H.P., 2007, A method for the preparation of stable dispersion of zero-valent iron nanoparticles, Colloid. Surface. A 308, 60–66.
Tiraferri A., Chen K.L., Sethi R., Elimelech M., 2008, Reduced aggregation and sedimentation of zero-valent iron nanoparticles in the presence of guar gum, J. Colloid Interf. Sci. 324, 71–79.
Xu Y., Zhao D., 2007, Reductive immobilization of chromate in water and soil using stabilized iron nanoparticles, Water Res. 41, 2101-2108.
Yang G.C.C., Chang Y.-I., 2011, Integration of emulsified nanoiron injection with the electrokinetic process for remediation of trichloroethylene in saturated soil, Sep. Purif. Technol. 79, 278–284.
Yang G.C.C., Tu H.-C., Hung C.-H., 2007, Stability of nanoiron slurries and their transport in the subsurface environment, Sep. Purif. Technol. 58 166-172.

## II.6. Assessment of combined electro-nanoremediation of molinate contaminated soil (published in Science of the Total Environment)

Science of the Total Environment 493 (2014) 178–184

Contents lists available at ScienceDirect

Science of the Total Environment

journal homepage: www.elsevier.com/locate/scitotenv

# Assessment of combined electro–nanoremediation of molinate contaminated soil

Helena I. Gomes [a,c,*], Guangping Fan [a,b], Eduardo P. Mateus [a], Celia Dias-Ferreira [c], Alexandra B. Ribeiro [a]

[a] CENSE, Departamento de Ciências e Engenharia do Ambiente, Faculdade de Ciências e Tecnologia, Universidade Nova de Lisboa, 2829-516 Caparica, Portugal
[b] Key Laboratory of Soil Environment and Pollution Remediation, Institute of Soil Science, Chinese Academy of Sciences (ISSCAS), East Beijing Road, Nanjing 210008, China
[c] CERNAS — Research Center for Natural Resources, Environment and Society, Escola Superior Agraria de Coimbra, Instituto Politecnico de Coimbra, Bencanta, 3045-601 Coimbra, Portugal

## HIGHLIGHTS

- Molinate is degraded in soil by zero valent iron nanoparticles (nZVI).
- Higher contact time of nZVI with soil facilitates molinate degradation.
- Soil type was the most significant factor influencing iron and molinate transport.
- When using nZVI and EK molinate is not only transported to catholyte, but also degraded.

## ARTICLE INFO

*Article history:*
Received 21 March 2014
Received in revised form 23 May 2014
Accepted 25 May 2014
Available online xxxx

Editor: Kevin V. Thomas

*Keywords:*
Herbicide
Nanoremediation
Electrokinetics
Contaminated soil
Zero valent iron nanoparticles (nZVI)

## ABSTRACT

Molinate is a pesticide widely used, both in space and time, for weed control in rice paddies. Due to its water solubility and affinity to organic matter, it is a contaminant of concern in ground and surface waters, soils and sediments. Previous works have showed that molinate can be removed from soils through electrokinetic (EK) remediation.

In this work, molinate degradation by zero valent iron nanoparticles (nZVI) was tested in soils for the first time. Soil is a highly complex matrix, and pollutant partitioning between soil and water and its degradation rates in different matrices is quite challenging. A system combining nZVI and EK was also set up in order to study the nanoparticles and molinate transport, as well as molinate degradation.

Results showed that molinate could be degraded by nZVI in soils, even though the process is more time demanding and degradation percentages are lower than in an aqueous solution. This shows the importance of testing contaminant degradation, not only in aqueous solutions, but also in the soil-sorbed fraction. It was also found that soil type was the most significant factor influencing iron and molinate transport. The main advantage of the simultaneous use of both methods is the molinate degradation instead of its accumulation in the catholyte.



## 1. Introduction

The widespread use of pesticides in intensive agriculture leads to soil and groundwater contamination. One of the pesticides that causes environmental concern is molinate (S-ethyl N,N-hexamethylene-1-carbamate), often applied annually to flooded fields during rice seeding to control the overgrowth of weeds (Castro et al., 2005). In 2013, there were 165.5 million hectares of rice paddies worldwide (FAO, 2013). Molinate can be found in natural surface and ground waters and also in wastewaters (Köck-Schulmeyer et al., 2013) due to its high water solubility (Table 1), as well as in soils and sediments near rice paddies (Castro et al., 2005; Cerejeira et al., 2003; Hildebrandt et al., 2007).

Zero valent iron nanoparticles (nZVI) degraded different pesticides in aqueous solutions, such as atrazine (Bezbaruah et al., 2009; Joo and Zhao, 2008; Satapanajaru et al., 2008), lindane (Elliott et al., 2009; Joo and Zhao, 2008), chloroacetanilide (Alachlor) (Bezbaruah et al., 2009) and molinate (Feitz et al., 2005), and remediated soils contaminated with pesticides such as malathion (Singhal et al., 2012), dinoseb (Satapanajaru et al., 2009), and chlorpyrifos (Reddy et al., 2013). Most of the research with iron nanoparticles analyzed the contaminant degradation in aqueous media, showing high degradation rates, including molinate degradation by nZVI through an oxidative process (Feitz et al., 2005; Joo et al., 2004). However, only a limited number of studies have assessed nanoparticle performance for soil-sorbed contaminants

* Corresponding author at: CENSE, Departamento de Ciências e Engenharia do Ambiente, Faculdade de Ciências e Tecnologia, Universidade Nova de Lisboa, 2829-516 Caparica, Portugal. Tel.: +351 212948300; fax: +351 212948554.
*E-mail address:* hrg@campus.fct.unl.pt (H.I. Gomes).

http://dx.doi.org/10.1016/j.scitotenv.2014.05.112
0048-9697/

**Table 1**
Chemical and physical properties of molinate.
Mabury et al., 1996

| Chemical name | Molinate |
|---|---|
| CAS No. | 2212-67-1 |
| Structure | 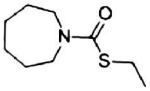 |
| Molecular formula | $C_9H_{17}NOS$ |
| Boiling point | 202 °C (10 mm Hg) |
| Density | 1.06 |
| Water solubility | 800–912 mg $L^{-1}$ |
| Half-life | 21 days |
| $K_{oc}$ | 190 mL $g^{-1}$ OC |
| log $K_{ow}$ | 3.21 |

(Singh et al., 2012; Zhang et al., 2011), and as far as our knowledge concerns, no previous study was done for soil-sorbed molinate.

The combination of electrokinetic remediation (EK) and nZVI allows the enhancement of the transport of iron nanoparticles in low permeability fine-grain soils (Chowdhury et al., 2012; Gomes et al., 2013; Gomes et al., 2014; Jones et al., 2010; Pamukcu et al., 2008; Rosales et al., 2014) and degradation of organic contaminants (Fan et al., 2013; Reddy et al., 2011; Yang and Chang, 2011; Yuan et al., 2012). With the simultaneous use of both remediation techniques (EK and nZVI), the contaminant is not only removed from soil (traditional outcome in EK), but also it is additionally degraded by nZVI, whose transport can also be enhanced by electric direct current. Electrokinetics can successfully remove molinate from soils to the catholyte due to electroosmotic transport as showed by Ribeiro et al. (2011), both by experimental work and modeling.

This work studies for the first time the degradation of molinate in soil using nZVI. It also assesses the integration of nZVI and electrokinetics to enhance the nanoparticles and molinate transport and degradation in two different soils.

## 2. Materials and methods

### 2.1. Soils

We used two different soils: S1 (sandy), sampled near a sanitary landfill at Valadares, Vale de Milhaço, Portugal, and S2 (sandy loam with higher organic matter content), sampled in an industrial park, in central Portugal. Table 2 presents some of their physical and chemical characteristics.

### 2.2. Chemicals and solvents

Molinate standards were of Pestanal grade, obtained from Riedel-de Haën (Seelze, Germany). The technical molinate (95%) used in the experiments was from Herbex (Sintra, Portugal). The solvents used in the present study were from Riedel-de Haën (Seelze, Germany), Panreac (Barcelona, Spain), Carlo Erba (Milan, Italy) and Merck (Darmstadt, Germany). Acetone was of Gradient Grade, hexane was of Pestanal grade, diethyl ether was of ACS grade, methanol was of HPLC grade and dichloromethane was of SupraSolv grade. The water was distilled and purified with a Milli-Q plus system from Millipore (Bedford, MA, USA). The iron nanoparticles were in a slurry-stabilized suspension (NANOFER 25S, NANO IRON, s.r.o., Rajhrad, Czech Republic) negatively charged due to the coating with polyacrylic acid (PAA), with an average particle size of 50 nm, an average surface area of 20–25 $m^2$ $g^{-1}$, a narrow particle size distribution of 20–100 nm and a high iron content in the range of 80–90 wt.%.

**Table 2**
Physical and chemical characteristics of the soils used.

| Parameter | S1 | S2 |
|---|---|---|
| Textural classification | Sandy | Sandy loam |
| Organic matter (g $kg^{-1}$) | 4 | 128.3 |
| pH ($H_2O$) | 5.9 | 6.1 |
| pH (KCl) | 4.5 | 5.4 |
| Exchangeable cations ($cmol_{(c)}$ $kg^{-1}$) | | |
| $Ca^{2+}$ | 0.34 | 16.18 |
| $Mg^{2+}$ | 0.05 | 3.98 |
| $K^+$ | 0.05 | 0.70 |
| $Na^+$ | 0.04 | 0.18 |
| Sum of exchangeable cations ($cmol_{(c)}$ $kg^{-1}$) | 0.48 | 21.04 |
| Cation exchange capacity ($cmol_{(c)}$ $kg^{-1}$) | 1.39 | 23.38 |
| Saturation (%) | 35 | 90 |

### 2.3. Degradation tests

Both soils were spiked with technical molinate to obtain a final concentration of 290 mg $kg^{-1}$. After air-drying, 1 g of soil and 25 mL of deionized water and 200 μL of nZVI slurry (final concentration 1.0 g $L^{-1}$ Fe) were placed in glass vials with a screw cap, in duplicate, under aerobic conditions, as the molinate degradation is an oxidative process (Joo et al., 2004). Blank samples were prepared as control, using the same spiked soil and without nZVI, for all the tested times. These soil suspensions were shaken in an orbital shaker (Bunsen A0 400) at 200 rpm at 25 ± 2 °C. After 24 h, the samples were centrifuged for 10 min at 7500 rpm (Sorvall RC5C Plus centrifuge). The supernatant was then removed and extracted through Solid Phase Extraction (SPE) using Strata X cartridges (200 mg/3 mL; Phenomenex Torrance, CA, USA) on a vacuum rack. The molinate in the soil was extracted by 10 mL hexane after 20 min sonication (Bandelin Sonorex Super RK 102H). The hexane extract was filtered through a 0.45 μm syringe Acrodisc PTFE filter (Pall Gelman Sciences, Ann Arbor, MI, USA) and concentrated under a gentle stream of nitrogen until 1.0 mL before analysis.

### 2.4. Electrokinetic experiments

#### 2.4.1. Electrokinetic cell

The EK experiments were carried out in a laboratorial cell modified at the New University of Lisbon. The cell is divided into three compartments, consisting of two electrode compartments (L = 7.46 cm, internal diameter = 8 cm) and a central one (L = 4 cm, internal diameter = 8 cm), in which the soil, saturated with deionized water, is placed (Fig. 1). This central compartment, made of Plexiglas, was equipped

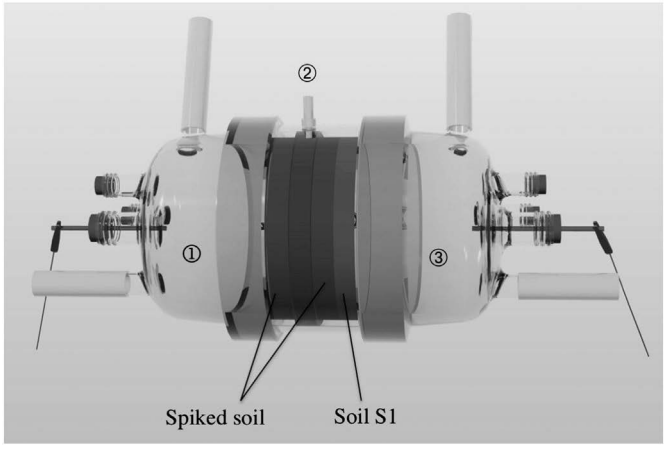


**Fig. 1.** Schematic representation of the laboratory cell. Legend: ① Anode compartment; ② reservoir for the iron nanoparticles injection; ③ cathode compartment. The separation between the soil and the compartments containing liquids was made through passive membranes (filter paper).

with an injection reservoir (L = 1 cm) for the iron nanoparticles, separated with a 1 mm nylon mesh and a low speed filter paper. A set of five cellulose filters, previously tested and known to work as passive membranes (Whatman filter paper), were used to separate the soil from the electrolytes. The soil section near the cathode is a non-spiked S1 soil in order to assess the molinate transport towards the cathode (Fig. 1). A power supply (Hewlett Packard E3612A, Palo Alto, USA) was used to maintain a constant DC and the voltage drop was monitored (Kiotto KT 1000H multimeter). The electrodes were platinized titanium bars, with an L = 5 cm and a diameter of 3 mm (Bergsøe Anti Corrosion A/S, Herfoelge, Denmark). The fresh electrolyte was a $10^{-2}$ M $NaNO_3$ solution, with pH 7.0, and a peristaltic pump (Watson-Marlow 503 U/R, Watson-Marlow Pumps Group, Falmouth, Cornwall, UK) distributed it to the electrode compartments. In all experiments, the electrolytes were collected into flasks and samples were analyzed.

*2.4.2. Experimental conditions*

Five different laboratory experiments (A–E) were carried out, according to the experimental conditions presented in Table 3. The variables considered were: i) the type of soil (two different soils with different textures, cation exchange capacities and organic matter contents), ii) pH control as an EK enhancement method, and iii) the absence of current as control experiments. No pH control experiment was made with soil S1 because its characteristics (sandy texture, low cation exchange capacity and low organic matter content) facilitate both molinate and nZVI transport.

The electrolyte used, in both anode and cathode compartments, was $10^{-2}$ M $NaNO_3$, with a flow rate of 1 mL $min^{-1}$. All experiments lasted 6 days (~145 h). A daily injection of 1 mL nZVI slurry — NANOFER 25S was made at the same time, after 10 min sonication, performing a total of 5 mL injected in each experiment. Electrolyte samples (catholyte and anolyte) were collected daily during the experiments, and their pH and volume were registered. At the end of each experiment, the total soil in the cell was sectioned into three "slices" and the center one was further divided into three (down, center and top) for iron and molinate analyses. Subsamples were collected for humidity measurements. In experiments B and C, pH control was performed in the anolyte, through the manual addition of NaOH 1 M, in order to keep the pH neutral (~7).

*2.5. Iron analysis*

The iron was extracted from soil by the sodium dithionite–citrate–bicarbonate (DCB) method (Mehra and Jackson, 1960) and from the electrokinetic cell and the membranes with concentrated hydrochloric acid. The iron analyses were made using an Inductively Coupled Plasma-Atomic Emission Spectrometer (ICP) on a Horiba Jobin-Yvon equipment.

*2.6. Molinate analysis*

*2.6.1. Aqueous samples: electrolyte solutions*

The extraction of the molinate present in the electrolyte solutions was performed by SPE, using Strata X cartridges (500 mg/6 mL; Phenomenex, Torrance, CA, USA). The SPE cartridges were conditioned by washing with 2 × 3 mL of methanol, followed by 2 × 3 mL of Milli-Q water. The pH of the anolyte and catholyte daily samples was adjusted to values between 5 and 7, adding HCl or NaOH, before extraction. The aqueous samples were passed through the cartridge approximately at a flow-rate of 10 mL $min^{-1}$ by applying a moderate vacuum. After that, the cartridges were washed with water and dried for approximately 1 min by vacuum. The analytes trapped in the cartridges were eluted sequentially with 2 × 2 mL of dichloromethane. The sample extracts were concentrated under a gentle stream of nitrogen to 1 mL. The samples were transferred to a vial and kept at −20 °C until GC analysis.

*2.6.2. Solid samples: soils and passive membranes*

Solid samples were extracted three times by sonication using 50 mL of methanol for 10 min to assure molinate maximum recovery. All the extracts were collected, as one and concentrated to 10 mL using 250 and 50 mL pear-shaped evaporating flasks on a rotary evaporator, Büchi RE 111 (35 °C/moderate vacuum). The concentrated extracts were transferred to a Kuderna Danish concentrator tube and evaporated to approximately 5 mL. In order to remove the particulate matter, the extracts were filtered through 0.5 μm glass microfiber filters (MFV-5, 47 mm; Filter-Lab, Barcelona, Spain), prior to the concentration step, and through 0.2 μm syringe Chromafil PTFE filters (Macherey-Nagel, Duren, Germany) prior to the evaporation step.

*2.6.3. Gas chromatography (GC)*

Molinate analyses were performed by gas chromatography/mass spectrometry (GC/MS) on a HP5890 series II GC coupled to a HP5972 MSD (Hewlett-Packard, Palo Alto, California, USA). The column used was a ZB-5 (5%-phenyl 95%-dimethylpolysiloxane) with 30 m × 0.25 mm i.d. and 0.25 μm film thickness (Phenomenex, Torrance, CA, USA).

The oven temperature was programmed starting at 80 °C for 2 min, increased to 100 °C at a rate of 4 °C $min^{-1}$ and then increased from 8 °C $min^{-1}$ to 250 °C, where it holds for 5 min. Helium was used as carrier gas at a flow rate of 1.0 mL $min^{-1}$. The injector was in a split/splitless mode set at 250 °C. The injections of 1.00 μL were performed at a splitless mode (1 min) using an HP7673 autosampler (Hewlett-Packard, Palo Alto, California, USA).

The mass spectrometer was operated in the electron ionization mode (EI, 70 eV). The interface temperature was set at 280 °C and the EI source was set at 176 °C. Molinate analysis was carried out by full scan for identification (scan range 40–300 amu) and selected ion monitoring (SIM) for quantitative analysis using the base peak of molinate. The HP5972 MSD was tuned before analysis using PFTBA (perfluorotributylamine) as the tuning standard. The data was registered and analyzed using ChemStation software (G1701BA, Version B.01.00).

## 3. Results and discussion

*3.1. Degradation tests*

For both soils, the molinate concentrations in the supernatant are similar with and without iron nanoparticles. We would expect to find also identical concentrations in soils, but that does not occur (Fig. 2), with molinate concentrations in soil being residual when iron

**Table 3**
Summary of experimental conditions. The electrolyte used was $10^{-2}$ M $NaNO_3$ and the duration of the experiments was 6 days.

| Exp. | Soil | Current (mA) | Soil — dry weight (g) | Molinate added to soil (mg) | pH control |
|---|---|---|---|---|---|
| A | S2 | 10 | 321.46 | 51.2 | No |
| B | S1 | 10 | 381.41 | 55.8 | NaOH 1 M added to anolyte |
| C | S2 | 10 | 344.31 | 52.7 | NaOH 1 M added to anolyte |
| D | S2 | 0 | 251.89 | 52.6 | No |
| E | S1 | 0 | 387.42 | 52.6 | No |

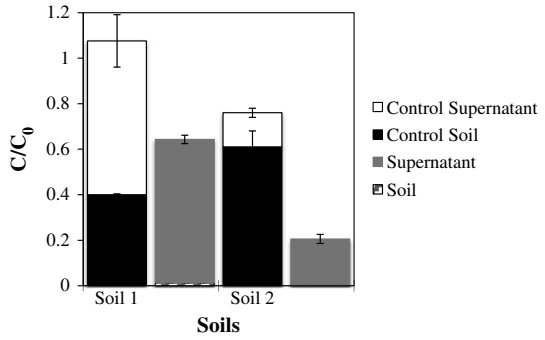


**Fig. 2.** Molinate concentrations in the soil and supernatant after 24 h, with and without nZVI (control) in S1 sandy soil and S2 sandy-loam soil. Initial molinate concentration in soil was 290 mg $kg^{-1}$. Data plotted as mean of duplicates, error bars indicate standard deviation.

nanoparticles are used. Comparing the molinate final amount in the experiments with and without nanoparticles (one-way analysis of variance — ANOVA), we found a significant difference for the concentrations of molinate in soils ($p < 0.01$). This supports the hypothesis that the iron nanoparticles degraded molinate added to the soil.

Molinate degradation occurs via an oxidative pathway that requires oxygen and the formation of hydrogen peroxide and hydroxyl radical (Joo et al., 2004). The degradation in an aqueous solution can shift the molinate equilibrium between water and soil, facilitating molinate desorption from soil, and its subsequent degradation while in solution. We can also hypothesize that part of molinate degradation occurred during the centrifugation and the extraction of the soil samples. Iron nanoparticles were removed from the aqueous solution and were visible in the solid phase — here they remained in contact with the soil for about 30 to 45 min and molinate degradation could occur. Iron nanoparticles, because they are very strong reducing agents, are traditionally used for dechlorination of organochlorines (Elliott et al., 2008; Liu et al., 2005; Lowry and Johnson, 2004; Wang and Zhang, 1997). In reduction, the reaction occurs in the surface of the nanoparticles (Masciangioli and Zhang, 2003; Yan et al., 2013). However, in the oxidative pathway, the reaction is dependent on the formation of hydrogen peroxide and the hydroxyl radical, and only occurs in aerobic media, being consequently favored in the supernatant where molinate can more easily react with the hydroxyl radical.

A lower recovery of molinate was found in soil S2 (55 ± 15%), when compared to recovery in soil S1 (76 ± 17%), what may be related to its higher soluble organic matter content that, probably, overloaded the SPE columns that presented a dark brown color after the extraction. Potential losses due to hydrolysis, biodegradation, photolysis and evaporation processes (Köck-Schulmeyer et al., 2013) can also contribute to this low recovery.

### 3.2. Electrokinetic experiments

#### 3.2.1. Transport of iron nanoparticles

In all experiments, the aqueous solution in the anode compartment presented higher Fe concentrations than the one in the cathode compartment. In the majority of the catholyte samples, the iron concentrations were below the detection limit (100% of the samples in experiment A, 43% in experiment B, 86% in experiment C and 57% in experiment D, Table S2 in the Supplementary materials).

We measured the highest iron concentrations in the aqueous solutions in the diffusion experiments (D and E) and more specifically in the anode compartment, due to the lower distance from the injection reservoir (only 1 cm, Figs. 1 and 3). A strong orange color and nanoparticle sedimentation in the anode compartment were visible in these diffusion experiments, which explain the peaks in the last segment of the cumulative Fe curves (Fig. 3). This sedimentation did not occur in the cathode. Concerning the variable soil, we measured near the double of

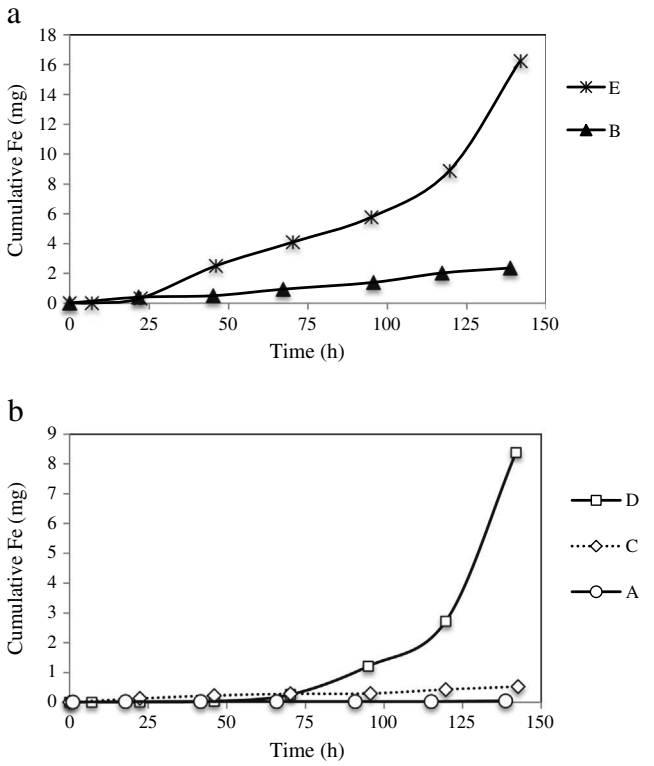


**Fig. 3.** Cumulative amounts of total iron (mg) in the anolyte solutions during the experiments. a) Experiments with soil 1 (sandy soil): B (EK with pH control) and E (diffusion); b) experiments with soil 2 (sandy loam with high organic matter content): A (EK without pH control), C (EK with pH control) and D (diffusion). In the cathode compartment, iron was detected in very low concentrations and in most of the samples was below the detection limit.

iron (16.24 mg vs. 8.38 mg) in the anolyte in experiment E (soil S1, sandy soil) when compared with experiment D (soil S2, loamy soil with high organic matter content). Similarly, more iron was found at the anolyte for experiment B (soil S1) than experiment C (soil S2). The difference in the soils texture contributes to this difference in transport. The sandy soil S1 will allow a faster transport of the iron nanoparticles, due to its higher pore volume (Gomes et al., 2013). Adsorption phenomena (Zhang et al., 2011) in soil particles and humic acid accumulation on the nZVI surface (Kim et al., 2013) most likely hinder iron transport and this can also contribute to the lower iron concentrations in the anolyte

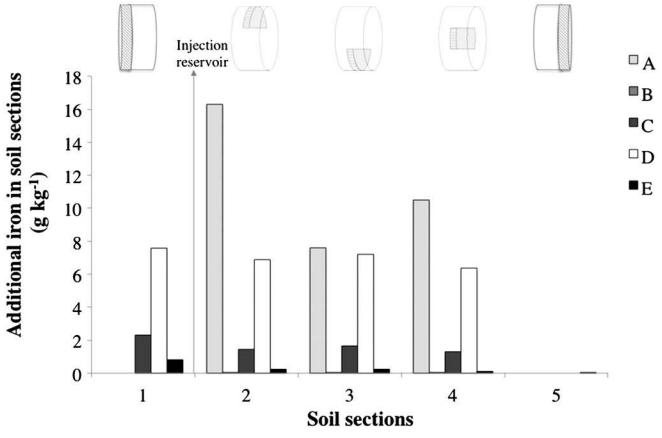


**Fig. 4.** Iron enrichment (g $kg^{-1}$) in soil sections (compared to initial soil concentration: 18.43 g $kg^{-1}$ in soil S1 and 0.85 g $kg^{-1}$ in soil S2) in experiments A–E. Section 1: between the anode compartment and the injection reservoir; Section 2: central soil section after the injection reservoir, top; Section 3: central soil section after the injection reservoir, bottom; Section 4: central soil section after the injection reservoir, center; and Section 5: between the central soil section and the cathode compartment.

in experiments with soil S2, when compared to those with soil S1 under similar operational conditions (Figs. 3 and 4).

In the experiments with direct current (A, B and C), lower amounts of Fe were measured in the anolyte than in the diffusion experiments (D and E). Even though nanoparticles have a negative surface charge due to the polymer (PAA) coating, being expected to be electrophoretically transported towards the anode, electroosmotic flow generally occurs in the opposite direction (towards the cathode), and may hinder transport towards the anode, explaining lower concentrations found in the anolyte when direct current was applied. In the experiment with pH control (Exp. C, soil S2) 10 times more iron was, in average, found in the anolyte than in experiment A without pH control (soil S2), possibly because in this last case the advance of the acid front ($H^+$) oxidizes nanoparticles ($Fe^0 \rightarrow Fe^{2+}$), and the resulting positively charged iron ion is transported towards the cathode. However, only very small amounts of iron were measured in the catholyte in all experiments, probably because there was not enough time to reach the cathode compartment.

Comparing the amount of iron added and the remaining iron in the injection reservoir by the end of the experiments, the higher mobilization rate ($1 - C_f / C_0 \times 100$) was obtained for experiment B (72%), followed by C (70%), E (62%), D (47%) and A (29%). The experiments with pH control (B and C) show an identical mobilization rate.

An analysis of variance (ANOVA) with the iron concentrations in the aqueous phase showed that the observed variance can be explained, at a 0.05 level, by the type of soil (S1 and S2) and the electric current (0 and 10 mA) (Table S1, Supplementary materials). The pH control was not significant to explain this variance.

In addition to iron in the electrolyte, its presence in the soil was also analyzed and compared to the initial content. Iron enrichment in the different soil slices is shown in Fig. 4. Experiment A had more additional iron in the soil (Fig. 4), followed by experiments D, C, B and E. This higher iron concentration in the soil in experiment A may be explained by the change of the soil charge with the advance of the acid front from the anode end due to the absence of pH control. In these conditions, ions of $H^+$ may adsorb to soil particles and increase the zeta-potential resulting in an increased adsorption of the PAA-coated iron nanoparticles. In all experiments, most of the iron was in the sections immediately after the injection reservoir. The section near the cathode (Section 5) presented the lowest amounts of additional iron (Fig. 4), what is consistent with the concentrations found in the catholyte. This means that the iron accumulates in the nearest sections to the injection point. Nevertheless, no major differences existed in the three samples in the middle section (top, central and bottom) in experiments B, C and D, with a relative standard deviation (RSD) of 9%, 6% and 5%, respectively; while in experiments A and E the relative standard deviation was higher (22% and 37%). There was no iron accumulation or deposition in the bottom part of this section (Section 3), when compared to the central and top samples.

The mass balance of the iron shows that most of it stays in the injection reservoir of the cell, followed by the sum found in the soil and the passive membranes (Fig. 5). This balance indicates a low mobility of the iron nanoparticles inside the experimental electrokinetic cell, most likely due to aggregation and sedimentation as also showed in other experimental setups with columns (Kocur et al., 2013; Phenrat et al., 2009; Saleh et al., 2008).

*3.2.2. Transport and degradation of molinate*

Our results confirm the transport of molinate towards the cathode with EK (Fig. 6), as the experimental data and modeling by Ribeiro et al. (2011) showed. In the diffusion experiments (D and E) more molinate is found in the anode than in the cathode due to direct contact between molinate-spiked soil and the anode compartment, while at the cathode side a non-contaminated soil layer is placed adjacent to the cathode compartment (Figs. 1 and 6), hindering the appearance of molinate in the catholyte. Table 4 presents the electroosmotic transport of molinate towards the cathode, the diffusion towards the anode, the final content in the soils and its removal rate. Removal rate includes molinate transport from the soil and molinate degradation, calculated as the percentage of the quotient between the difference of the initial and final concentrations, and the initial concentration.

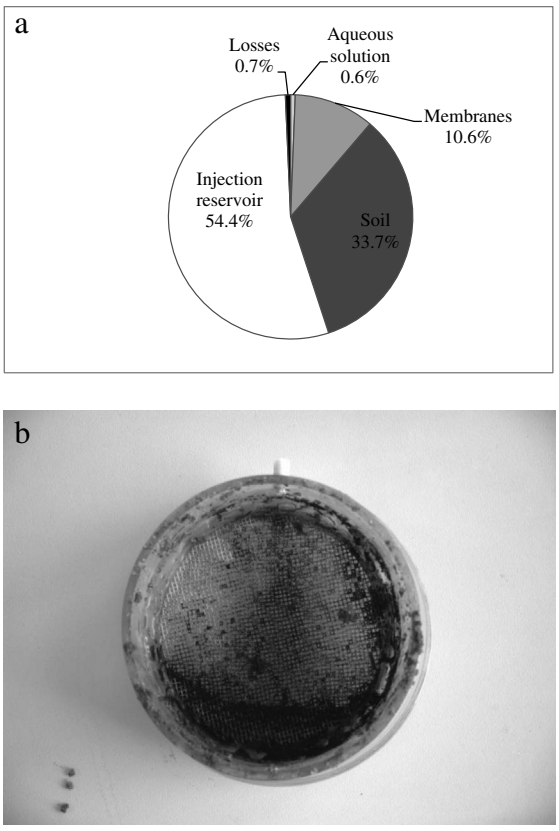


**Fig. 5.** a) Average mass balance of iron after the experiments. Average recovery of iron was 86%. b) Photo of the experimental cell showing the iron accumulation in the injection reservoir.

Previous studies have showed the strong adsorption of molinate in soils with high organic matter content (Alister et al., 2010) and this explains the 10-fold decrease in molinate in the anolyte of experiment D (soil S2, sandy-loam, 12.8% organic matter) when compared to experiment E (soil S1, sandy, 0.4% organic matter) (Fig. 7).

The soil type is statistically significant to explain the molinate variance in the electrolyte (Table S1, Supplementary materials). Comparing the data of all experiments, the direct current and pH control are not statistically significant ($p = 0.05$) to explain molinate concentrations in the aqueous phase.

When an electric current is applied (experiments A, B, and C) the amount of molinate in the anolyte decreases and molinate appears in soil section 5 (initially clean) near the cathode (Fig. 7). This shows the electrokinetic transport of molinate towards the cathode. Once again, the higher amount of molinate in soil S2 (experiment C) compared to soil S1 (experiment B) can be explained by adsorption to soil organic matter, resulting in lower molinate removal efficiencies in these experiments (around 70% in B versus almost 90% in C).

The cumulative amounts of molinate found in the electrolyte (anolyte and catholyte) are less than 6% the initial amount in the soil (Table 4). In previous studies with EK but without nanoparticles (Santos, 2008), approximately 60% of the molinate was found in the catholyte, less than 2% was found in the anolyte and a maximum of 9% was found in soil. These differences support the hypothesis that there was molinate degradation by nZVI in our experiments as, in identical conditions, fewer molinate was found in the electrolytes (catholyte).

The results now obtained show no enhancement in molinate degradation when both EK and nZVI are used, contrary to what was found for

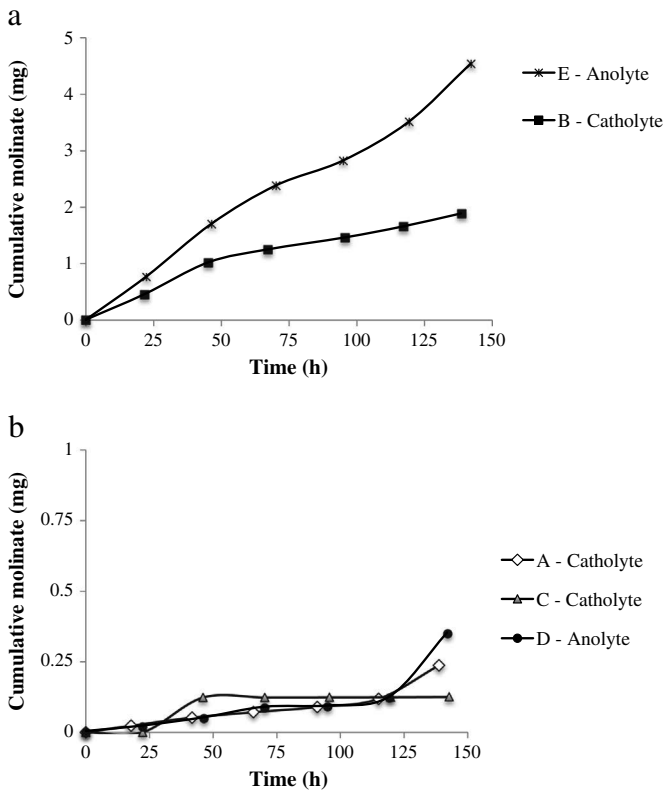


**Fig. 6.** Cumulative amounts of molinate (mg) in the anolyte and catholyte solutions during the experiments. a) Experiments with soil 1 (sandy soil): B (EK with pH control) and E (diffusion); b) experiments with soil 2 (sandy loam with high organic matter content): A (EK without pH control), C (EK with pH control) and D (diffusion). In the diffusion experiments (D and E) higher molinate content was found in the anolyte due to the direct contact with the spiked soil.

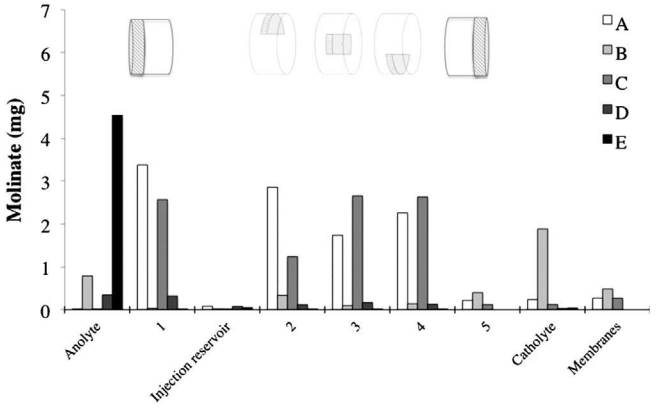


**Fig. 7.** Mass of molinate in different compartments by the end of the experiments.

nitrates (Yang et al., 2008), dinitrotoluene (Reddy et al., 2011) and pentachlorophenol (Yuan et al., 2012). Although in those studies no diffusion tests were made, we must remark that the degradation rates are dependent on reduction reactions and molinate is degraded by nano-$Fe^0$ via an oxidative pathway with hydroxyl radicals (Joo et al., 2004), not via the most common reductive pathway. This requires desorption of molinate and higher contact times than the reductive pathway. In our experiments, the diffusion tests were more effective for soil S2, most likely because EK, by transporting the molinate out of the system faster, reduced the contact times with iron nanoparticles. For soil S1 with lower resistance for molinate mobility, the applied direct current is not significant for its removal.

## 4. Conclusions

Results show that molinate degradation by zero valent iron nanoparticles via an oxidative pathway can also occur in soils. The soil-sorbed molinate degradation results show the importance of testing contaminant degradation with nZVI not only in aqueous solutions, but also in matrices increasingly more complex, such as synthetic groundwaters, real groundwaters, model soils and real soils. The degradation results in soils now obtained are much lower and more time demanding than in deionized water.

Soil type was the most significant variable for iron and molinate transport. In the tested conditions, iron moves preferentially to anode and molinate to cathode. Diffusion was the transport mechanism that yielded higher Fe concentrations in the anolyte. In the EK experiments, electrophoretic transport of iron nanoparticles was counteracted by electroosmosis (higher in soil S2). For these experimental conditions, direct current was a significant variable to explain iron concentrations in the aqueous solutions, but it was not significant for molinate. In the tested conditions, there was no advantage in using the electric current to enhance the iron nanoparticle transport. We also observed limited mobility of the iron nanoparticles, with an average of 54% of the nanoparticles remaining in the injection reservoir.

$Fe^0$ nanoparticles and electrokinetics can degrade and remove molinate from soils, respectively. With electrokinetics, molinate can be removed from soil to an aqueous solution, and with nZVI molinate can be degraded in situ. The major advantage of the simultaneous use of both methods is the molinate degradation instead of its accumulation in the catholyte.

## Acknowledgments

This work has been funded by FP7-PEOPLE-IRSES-2010-269289-ELECTROACROSS, by the Portuguese National funds through "Fundação para a Ciência e a Tecnologia" under projects PTDC/ECM/111860/2009 and PTDC/AGR-AAM/101643/2008 and by the research grant SFRH/BD/76070/2011. Carla Rodrigues from REQUIMTE is acknowledged for the ICP analysis, and NANO IRON, s.r.o. is acknowledged for kindly providing the NANOFER 25S samples.

## Appendix A. Supplementary data

Supplementary data to this article can be found online at http://dx.doi.org/10.1016/j.scitotenv.2014.05.112.

**Table 4**
Molinate removal rate.

| Experiment | Soil | Initial content in soils (mg) | Transported to the anode (mg) | Transported to the cathode (mg) | Final content in soils (mg) | Removal rate (%) |
|---|---|---|---|---|---|---|
| A | S2 | 51.2 | 0.004 | 0.237 | 10.46 | 72.3 |
| B | S1 | 55.8 | 1.323 | 1.886 | 1.01 | 89.9 |
| C | S2 | 52.7 | 0.003 | 0.125 | 9.22 | 71.2 |
| D | S2 | 52.6 | 0.349 | 0.003 | 0.74 | 97.5 |
| E | S1 | 52.6 | 4.540 | 0.044 | 0.00 | 91.3 |

## References


Alister CA, Araya MA, Kogan M. Adsorption and desorption variability of four herbicides used in paddy rice production. J Environ Sci Health B 2010;46:62–8.

Bezbaruah AN, Thompson JM, Chisholm BJ. Remediation of alachlor and atrazine contaminated water with zero-valent iron nanoparticles. J Environ Sci Health B 2009;44: 518–24.

Castro M, AnC Silva-Ferreira, ClM Manaia, Nunes OC. A case study of molinate application in a Portuguese rice field: herbicide dissipation and proposal of a clean-up methodology. Chemosphere 2005;59:1059–65.

Cerejeira MJ, Viana P, Batista S, Pereira T, Silva E, Valério MJ, et al. Pesticides in Portuguese surface and ground waters. Water Res 2003;37:1055–63.

Chowdhury AIA, O'Carroll DM, Xu Y, Sleep BE. Electrophoresis enhanced transport of nano-scale zero valent iron. Adv Water Res 2012;40:71–82.

Elliott DW, Lien H-L, Zhang W. Zerovalent iron nanoparticles for treatment of ground water contaminated by hexachlorocyclohexanes. J Environ Qual 2008;37:2192–201.

Elliott DW, Lien HL, Zhang WX. Degradation of lindane by zero-valent iron nanoparticles. J Environ Eng 2009;135:317–24.

Fan G, Cang L, Qin W, Zhou C, Gomes HI, Zhou D. Surfactants-enhanced electrokinetic transport of xanthan gum stabilized nano Pd/Fe for the remediation of PCBs contaminated soils. Sep Purif Technol 2013;114:64–72.

FAO. Rice market monitor. XVI (3), XVI (3)Trade and Markets Division. Food and Agriculture Organization of the United Nations; 2013.

Feitz AJ, Joo SH, Guan J, Sun Q, Sedlak DL, David Waite T. Oxidative transformation of contaminants using colloidal zero-valent iron. Colloid Surf A 2005;265:88–94.

Gomes H, Dias-Ferreira C, Ribeiro A, Pamukcu S. Enhanced transport and transformation of zerovalent nanoiron in clay using direct electric current. Water Air Soil Pollut 2013; 224:1–12.

Gomes HI, Dias-Ferreira C, Ribeiro AB, Pamukcu S. Influence of electrolyte and voltage on the direct current enhanced transport of iron nanoparticles in clay. Chemosphere 2014;99:171–9.

Hildebrandt A, Lacorte S, Barceló D. Assessment of priority pesticides, degradation products, and pesticide adjuvants in groundwaters and top soils from agricultural areas of the Ebro river basin. Anal Bioanal Chem 2007;387:1459–68.

Jones EH, Reynolds DA, Wood AL, Thomas DG. Use of electrophoresis for transporting nano-iron in porous media. Ground Water 2010;49:172–83.

Joo SH, Zhao D. Destruction of lindane and atrazine using stabilized iron nanoparticles under aerobic and anaerobic conditions: effects of catalyst and stabilizer. Chemosphere 2008;70:418–25.

Joo SH, Feitz AJ, Waite TD. Oxidative degradation of the carbothioate herbicide, molinate, using nanoscale zero-valent iron. Environ Sci Technol 2004;38:2242–7.

Kim D-G, Hwang Y-H, Shin H-S, Ko S-O. Deactivation of nanoscale zero-valent iron by humic acid and by retention in water. Environ Technol 2013;34:1–11.

Köck-Schulmeyer M, Villagrasa M, López de Alda M, Céspedes-Sánchez R, Ventura F, Barceló D. Occurrence and behavior of pesticides in wastewater treatment plants and their environmental impact. Sci Total Environ 2013;458–460:466–76.

Kocur CM, O'Carroll DM, Sleep BE. Impact of nZVI stability on mobility in porous media. J Contam Hydrol 2013;145:17–25.

Liu Y, Majetich SA, Tilton RD, Sholl DS, Lowry GV. TCE dechlorination rates, pathways, and efficiency of nanoscale iron particles with different properties. Environ Sci Technol 2005;39:1338–45.

Lowry G, Johnson K. Congener-specific dechlorination of dissolved PCBs by microscale and nanoscale zerovalent iron in a water/methanol solution. Environ Sci Technol 2004;38:5208–16.

Mabury SA, Cox JS, Crosby DG. Environmental fate of rice pesticides in California. In: Ware G, editor. Reviews of environmental contamination and toxicology, 147. New York: Springer; 1996. p. 71–117.

Masciangioli T, Zhang W. Environmental technologies at the nanoscale. Environ Sci Technol 2003;37:102A–8A.

Mehra OP, Jackson ML. Iron oxide removal from soils and clays by a dithionite–citrate system buffered with sodium bicarbonate. Clays Clay Minerals 1960;7:317–27.

Pamukcu S, Hannum L, Wittle JK. Delivery and activation of nano-iron by DC electric field. J Environ Sci Health A 2008;43:934–44.

Phenrat T, Kim H-J, Fagerlund F, Illangasekare T, Tilton RD, Lowry GV. Particle size distribution, concentration, and magnetic attraction affect transport of polymer-modified $Fe^0$ nanoparticles in sand columns. Environ Sci Technol 2009;43:5079–85.

Reddy KR, Darko-Kagy K, Cameselle C. Electrokinetic-enhanced transport of lactate-modified nanoscale iron particles for degradation of dinitrotoluene in clayey soils. Sep Purif Technol 2011;79:230–7.

Reddy AVB, Madhavi V, Reddy KG, Madhavi G. Remediation of chlorpyrifos-contaminated soils by laboratory-synthesized zero-valent nano iron particles: effect of pH and aluminium salts. J Chem 2013;2013:1–7.

Ribeiro AB, Mateus EP, Rodríguez-Maroto J-M. Removal of organic contaminants from soils by an electrokinetic process: the case of molinate and bentazone. Exp model Sep Purif Technol 2011;79:193–203.

Rosales E, Loch JPG, Dias-Ferreira C. Electro-osmotic transport of nano zero-valent iron in Boom Clay. Electrochim Acta 2014;127:27–33.

Saleh N, Kim H-J, Phenrat T, Matyjaszewski K, Tilton RD, Lowry GV. Ionic strength and composition affect the mobility of surface-modified $Fe^0$ nanoparticles in water-saturated sand columns. Environ Sci Technol 2008;42:3349–55.

Santos JCS. Electrokinetic remediation of rice field soils contaminated by molinate. Dissertação de Mestrado Faculdade de Ciências e Tecnologia da Universidade Nova de Lisboa; 2008 [97 pp.].

Satapanajaru T, Anurakpongsatorn P, Pengthamkeerati P, Boparai H. Remediation of atrazine-contaminated soil and water by nano zerovalent iron. Water Air Soil Pollut 2008;192:349–59.

Satapanajaru T, Onanong S, Comfort SD, Snow DD, Cassada DA, Harris C. Remediating dinoseb-contaminated soil with zerovalent iron. J Hazard Mater 2009;168:930–7.

Singh R, Misra V, Mudiam MKR, Chauhan LKS, Singh RP. Degradation of HCH spiked soil using stabilized $Pd/Fe^0$ bimetallic nanoparticles: pathways, kinetics and effect of reaction conditions. J Hazard Mater 2012;237–238:355–64.

Singhal RK, Gangadhar B, Basu H, Manisha V, Naidu GRK, Reddy AVR. Remediation of malathion contaminated soil using zero valent iron nano-particles. Am J Anal Chem 2012;3:76–82.

Wang C-B, Zhang W. Synthesizing nanoscale iron particles for rapid and complete dechlorination of TCE and PCBs. Environ Sci Technol 1997;31:2154–6.

Yan W, Lien H-L, Koel BE, Zhang W-x. Iron nanoparticles for environmental clean-up: recent developments and future outlook. Environ Sci Process Impacts 2013;15:63–77.

Yang GCC, Chang Y-I. Integration of emulsified nanoiron injection with the electrokinetic process for remediation of trichloroethylene in saturated soil. Sep Purif Technol 2011; 79:278–84.

Yang GCC, Hung C-H, Tu H-C. Electrokinetically enhanced removal and degradation of nitrate in the subsurface using nanosized Pd/Fe slurry. J Environ Sci Health A 2008;43: 945–51.

Yuan S, Long H, Xie W, Liao P, Tong M. Electrokinetic transport of CMC-stabilized Pd/Fe nanoparticles for the remediation of PCP-contaminated soil. Geoderma 2012; 185–186:18–25.

Zhang M, He F, Zhao D, Hao X. Degradation of soil-sorbed trichloroethylene by stabilized zero valent iron nanoparticles: effects of sorption, surfactants, and natural organic matter. Water Res 2011;45:2401–14.

# Assessment of combined electro-nano remediation of molinate contaminated soil

Helena I. Gomes[1,3], Guangping Fan[1,2], Eduardo P. Mateus[1], Celia Dias-Ferreira[3], Alexandra B. Ribeiro[1]

[1]CENSE, Departamento de Ciências e Engenharia do Ambiente, Faculdade de Ciências e Tecnologia, Universidade Nova de Lisboa, 2829-516 Caparica, Portugal

[2]Key Laboratory of Soil Environment and Pollution Remediation, Institute of Soil Science, Chinese Academy of Sciences (ISSCAS), East Beijing Road, Nanjing 210008, China

[3] CERNAS – Research Center for Natural Resources, Environment and Society, Escola Superior Agraria de Coimbra, Instituto Politecnico de Coimbra, Bencanta, 3045-601 Coimbra, Portugal

* Corresponding author. Tel. +351 212948300, Fax. +351 212948554. E-mail address: hrg@campus.fct.unl.pt (Helena I. Gomes)

**Table S1. Analysis of variance (ANOVA) test for determining the significance difference between levels of a variable in the electrolyte concentration for iron and molinate. Variable "Soil" represents the two different soils tested, "Current" represents the EK and diffusion tests and "pH Control" the addition (or not) of NaOH in the anode compartment.**

| | Sum of squares | df | Mean square | F | *p*-value |
|---|---|---|---|---|---|
| **Total iron concentration** | | | | | |
| Between "Soil" groups | 3.487 | 1 | 3.487 | 14.491 | **0.001** |
| Within "Soil" groups | 6.978 | 29 | 0.241 | | |
| Total | 10.465 | 30 | | | |
| Between "Current" groups | 3.849 | 1 | 3.849 | 16.867 | **< 0.001** |
| Within "Current" groups | 6.617 | 29 | 0.228 | | |
| Total | 10.465 | 30 | | | |
| Between "pH control" groups | 0.753 | 1 | 0.753 | 2.247 | 0.145 |
| Within "pH control" groups | 9.713 | 29 | 0.335 | | |
| Total | 10.465 | 30 | | | |
| **Molinate concentration** | | | | | |
| Between "Soil" groups | 60417.964 | 1 | 60417.964 | 68.283 | **< 0.001** |
| Within "Soil" groups | 24774.974 | 28 | 884.820 | | |
| Total | 85192.937 | 29 | | | |
| Between "Current" groups | 60417.964 | 1 | 5148.731 | 1.801 | 0.190 |
| Within "Current" groups | 24774.974 | 28 | 2858.722 | | |
| Total | 85192.937 | 29 | | | |
| Between "pH control" groups | 363.603 | 1 | 363.603 | 0.120 | 0.732 |
| Within "pH control" groups | 84829.334 | 28 | 3029.619 | | |
| Total | 85192.937 | 29 | | | |

Bold—significant, p-value inferior to 0.05
*Post hoc* tests were not performed because there are fewer than three groups.

**Table S2. Cumulative amounts of total iron (mg) in the catholyte solutions in the experiments.**

| Experiment | Soil | Iron found in the catholyte (mg) |
|---|---|---|
| A | S2 | Bellow detection limit (<0.003) |
| B | S1 | 1.17 |
| C | S2 | 0.004 |
| D | S2 | 0.03 |
| E | S1 | 0.04 |

## II.7. Electroremediation of PCB contaminated soil with iron nanoparticles: Performance of a new electrodialytic setup (submitted)

# Electroremediation of PCB contaminated soil with iron nanoparticles: performance of a new electrodialytic setup

Helena I. Gomes[1,2,3], Celia Dias-Ferreira[2], Lisbeth M. Ottosen[3], Alexandra B. Ribeiro[1]

[1]CENSE, Departamento de Ciências e Engenharia do Ambiente, Faculdade de Ciências e Tecnologia, Universidade Nova de Lisboa, 2829-516 Caparica, Portugal

[2] CERNAS – Research Center for Natural Resources, Environment and Society, Escola Superior Agraria de Coimbra, Instituto Politecnico de Coimbra, Bencanta, 3045-601 Coimbra, Portugal

[3] Department of Civil Engineering, Technical University of Denmark, Brovej, Building 118, DK 2800 Kgs. Lyngby, Denmark

* Corresponding author. Tel. +351 212948300, Fax. +351 212948554. E-mail address: hrg@campus.fct.unl.pt (Helena I. Gomes)

**Abstract**

Contaminated soils and sediments with polychlorinated biphenyls (PCB) are an important environmental problem due to the persistence of these synthetic aromatic compounds and to the lack of a cost-effective and sustainable remediation technology. In this work we compared an electrodialytic setup developed at the Technical University of Denmark (DTU), in which the soil is suspended and stirred simultaneously with the addition of zero valent iron nanoparticles (nZVI), with the conventional electrokinetic (EK) setup. The electrodialytic setup showed several advantages, such as a higher PCB dechlorination in contaminated soil, in a shorter time, with lower nZVI consumption, and with the use of half of the voltage gradient when compared with the traditional EK setup.

**Highlights**

- Suspended electrodialytic remediation with nZVI was tested for PCB for the 1st time
- Higher PCB removal (83%) was achieved with suspended EDR in comparison to EK
- Shorter times and less nanoparticles were needed using the electrodialytic setup
- Higher chlorinated congeners were also degraded
- Direct current enhanced dechlorination in the EK setup through pH conditions
- The EDR setup with nZVI is competitive compared with incineration and landfilling

**Keywords**

Electrokinetics, electrodialytic remediation, nZVI, polychlorinated biphenyls, PCB

## 1. **Introduction**

Polychlorinated biphenyls (PCB) are a family of 209 congeners, classified as persistent organic pollutants (POP), carcinogenic and recalcitrant, which strongly adsorb to soils and sediments. Despite the environmental concern regarding PCB ecotoxicity and accumulation in the food chain, there is no quantification of the total volumes of PCB contaminated soils and sediments worldwide. Recently, Gomes et al. (2013a) reviewed *in situ* and *ex situ* remediation technologies available for PCB-contaminated soils and sediments, and identified the urgent need to find cost effective and more sustainable alternatives than the commonly adopted "dig and dump" and "dig and incinerate".

Electroremediation of contaminated soils is a group of technologies that has evolved over the last decades with the incorporation of enhancement techniques and the combination with other remediation technologies (Gomes et al., 2012), targeting a wide range of contaminants. Electrodialytic remediation (EDR) – a method based on the combination of the electrokinetic movement of ions in soil with the principle of electrodialysis (Ottosen et al., 1997) – was used successfully in different matrices such as mine tailings (Hansen et al., 2007; Rojo et al., 2006), soils (Hansen et al., 1997; Ottosen et al., 2009), different types of fly ashes (Ferreira et al., 2005; Ferreira et al., 2002; Jensen et al., 2010), sewage sludge (Pazos et al., 2010), freshwater sediments and harbor sediments (Kirkelund et al., 2009; Nystroem et al., 2005). Electrodialytic remediation of suspended soil has proven to be a faster process to be used *ex situ* for the removal of heavy metals (Jensen et al., 2007; Ottosen et al., 2013a; Ottosen et al., 2009; Sun et al., 2012), but it was never tested for PCB, only for polycyclic aromatic hydrocarbons (PAH) (Lima et al., 2012).

Zero valent iron nanoparticles (nZVI) were considered a promising alternative for PCB dechlorination in aqueous solutions (He et al., 2010; Lowry and Johnson, 2004; Wang and Zhang, 1997; Zhuang et al., 2011). In general, the dechlorination can be expressed by the following reaction (Zhang et al., 1998):

$$C_xH_yCl_z + zH^+ + zFe^0 \rightarrow C_xH_{y+z} + zFe^{2+} + zCl^-$$

(1)

in which iron acts as a reductant (electron donor) for the removal of chlorine. This reaction is similar to the process occurring during iron corrosion, with the beneficial effects of transforming chlorinated pollutants. Still a 95% PCB dechlorination in soils was just achieved at high temperatures (300ºC) (Varanasi et al., 2007). In field applications, nZVI can be injected in the aquifers through injection wells, or incorporated to topsoil to adsorb or degrade pollutants (Crane and Scott, 2012). Results in aquifers show that nZVI have limited mobility, ranging from 1 m (Kocur et al., 2014) to 6-10 m (Zhang and Elliott, 2006). One of the methods tested to enhance nZVI mobility was the use of direct current (DC) (Gomes et al., 2013b; Jones et al., 2010; Pamukcu et al., 2008; Yang et al., 2007), using the same principles of electrokinetic remediation (EK). Electroremediation and nZVI were combined by Fan et al. (2013) and they obtained a PCB removal rate from soils of only 20% using Fe/Pd bimetallic nanoparticles in conjunction with EK after 14 d. Another study reported 82 and 53% PCB removal from soils in batch tests with 12 d duration, using the Pd/Fe bimetallic nanoparticles, compared with 67 and 48% using nZVI (Chen et al., 2014). In this work, we tested the two-compartment electrodialytic setup developed at the Technical University of Denmark (DTU) (Ottosen et al., 2013b), in which the soil is suspended and stirred simultaneously in combination with the addition of nZVI. The main objectives were to: i) assess the effectiveness for the dechlorination of PCB by nZVI of the new two-

compartment electrodialytic setup in comparison with the traditional three-compartment electrokinetic setup; ii) test if longer EK experiments with nZVI could result in an increased PCB dechlorination; and to iii) evaluate the need of using direct electric current in the reactor with suspended soil and nZVI.

## 2. Materials and Methods

### *2.1. Chemicals and solvents*

PCB standards were analytical grade, obtained from Fluka, Sigma-Aldrich (PCB 28, 52, 101, 138, 153, 180 and 209) and Ultrascientific (PCB 30; PCB 65 and PCB 204). The solvents hexane and acetone were Pestinorm (VWR BDH Prolabo). Hydrochloric (37.6%), nitric (65%) and sulfuric (95-07%) acids were tracemetal. Anhydrous $Na_2SO_4$, $KMnO_4$, NaCl, and silica gel (silicic acid) were lab grade. Silica gel was cleaned up before use according to the USEPA method 3630C. The water was deionized with a Milli-Q plus system from Millipore (Bedford, MA, USA). A slurry-stabilized suspension of zero valent iron nanoparticles (NANOFER 25S, NANO IRON, s.r.o., Rajhrad, Czech Republic) was used in the experiments, with 50 nm average particles size, an average surface area of 20-25 $m^2 g^{-1}$, a particle size distribution of 20-100 nm and iron content in the range of 80-90 wt. %.

### *2.2 Soil characterization*

The contaminated soil used in the experiments was provided by a hazardous waste operator in Portugal and is a mixture of contaminated soils from industrial sites with transformers oils spills. The soil characterization methods used were described in Jensen et al. (Jensen et al., 2007). The elemental analysis were made using Inductively Coupled Plasma-Atomic Emission Spectrometer (ICP) on an Agilent ICP-OES Varian 720-ES equipment. Table 1 presents the physical and chemical characteristics of the soil used in the experiments. The soil

was homogenized, air dried and sieved, and only the particles with size < 2 mm were used in the electroremediation experiments.

*2.3 PCB analysis*

The soil samples were extracted according to the USEPA method 3550C, and the extracts were then cleaned following the USEPA methods 3665A and 3630C. The PCB congeners were analyzed by gas chromatography (GC) on an HP with ECD detector, HP 6890 Series (Hewlett-Packard, Palo Alto, California, USA). The column used was a TRB–5–MS with 30 m × 0.25 mm i.d. and 0.25 μm film thickness (Phenomenex, Torrance, CA, USA). The oven temperature was programmed starting at 70ºC for 2 min, increased to 150ºC at a rate of 25ºC $min^{-1}$ and then increased 4ºC $min^{-1}$ to 200ºC, 8ºC $min^{-1}$ to 280ºC where it holds for 4 min and finally 10ºC $min^{-1}$ to 300ºC, where it holds for 2 min. Pure nitrogen was used as the carrier gas. The injector was splitless set at 260°C. The injections of 1.00 μl were performed manually.

*2.4 Electroremediation experiments*

The electroremediation experiments were carried out in two different laboratorial cylindrical Plexiglas-cells developed at DTU. The electrokinetic cell (EK) is divided into three compartments, consisting of two electrode compartments (L = 5 cm, internal diameter Ø = 4 cm) and a central one subdivided in three (L = 1.5 cm each, total of 4.5 cm, Ø = 4 cm), in which the saturated soil (deionized water) is placed, as well as the zero valent iron nanoparticles [Figure 1 a)]. Cellulose filters (passive membranes) were used to assure the separation between the soil and electrolytes, and the soil and the iron nanoparticles.

In the electrodialytic cell (ED), there is one compartment (L = 10 cm, Ø = 8 cm) where the anode, the soil slurry (with a liquid solid ratio of 5) and the plastic-flaps attached to a glass-stick stirrer (Lab-egg Bie&Bernsten, Denmark, ~350 rpm) are placed. A cation exchange

membrane (CAT, GE Water & Process Technologies Bvba - ED, Cation, CR67, MKIII, Blank) separates this compartment from the one (L = 5 cm, Ø = 8 cm) where the cathode is placed [Figure 1 b)]. In this setup, catholytes were recirculated by mechanical pumps (Plastomec magnet pump, model P05) between the chamber and glass bottle.

In both setups, a power supply (Hewlett Packard E3612A, Palo Alto, USA) was used to maintain a constant voltage and the current was monitored (Fluke 179 multimeter). The working electrodes were platinized titanium bars, with a diameter of 3 mm and a length of 5 cm in the 3 compartments setup and 10 cm in the 2 compartments setup (Permascand®).

Six different laboratory experiments (A–F) were carried out, according to the experimental conditions presented in Table 2. The iron nanoparticles were placed in the center of both cells. In the electrokinetic set-up (experiments A, B, C and D), the central reservoir was filled at the beginning of the experiments with nZVI. In C more nZVI was added (2 mL) in days 7 and 9. In the electrodialytic setup (experiments E and F), two injections of 5 mL nZVI were made at 24 and 48 h. The electrolyte used in all experiments was $10^{-2}$ M NaCl. In the electrodialytic setup, the catholyte pH was manually maintained around 2 by the periodic addition of HCl 5M.

The current between working electrodes, the pH in the soil suspension and in the electrolytes were measured every 24 h. In the ED setup, at the end of the experiment the suspension from the central compartment was filtered though qualitative filter paper overnight. In the EK setup, samples from the anode and the cathode side were considered separately. Subsamples were collected for humidity measurements. For both setups, the soil was air-dried and crushed lightly in a mortar before the PCB extraction and pH measurements.

## 3. Results and Discussion

*3.1 Comparison between the two experimental setups*

The two-compartment electrodialytic setup shows PCB removal percentages of 83% with and 29% without direct current, as shown in Figure 2. These results are higher than in previous studies with EK (Fan et al., 2013) and batch tests without current (Chen et al., 2014). The suspension and stirring of the soil can enhance the PCB dechlorination by nZVI, due to an increase in desorption from soil and/or to a higher contact and reaction between nZVI and PCB. In the traditional three-compartment electrokinetic setup, the iron has to be transported across the compacted saturated soil to reach the contaminants. Even a low proportion of carbonate minerals may cause an increase in the deposition of PAA-nZVI particles and aggregates, due to a weaker negative surface charge (Laumann et al., 2013). As the soil used in the experiments has high carbonate content (18%), the limited dechlorination observed (12-58%) (Figure 2) can be due to this soil characteristic.

In both setups, there are chemical reactions that deplete the $Fe^0$ reductant power:

$$2Fe^0_{(s)} + 4H^+_{(aq)} + O_{2\,(aq)} \rightarrow 2Fe^{2+}_{(aq)} + 2H_2O_{(l)} \quad (2)$$

$$Fe^0_{(s)} + 2H_2O_{(l)} \rightarrow Fe^{2+}_{(aq)} + H_{2(g)} + 2OH^-_{(aq)} \quad (3)$$

$$Fe^{2+}_{(aq)} + CO_3^{2-}{}_{(aq)} \rightarrow FeCO_{3(s)} \quad (4)$$

Also, the presence of transformer oil was found to adversely affect the PCB degradation (Chang et al., 2010). Despite the introduction of $H^+$ (resultant of hydrolysis in the anode) and the atmospheric $O_2$ dissolved by the slurry stirring that oxidize $Fe^0$, a higher PCB removal is obtained in the ED setup compared with the traditional electrokinetic setup.

In other remediation techniques (Beckingham and Ghosh, 2011; Li et al., 2013; Vasilyeva et al., 2010; Wu et al., 2012) lower chlorinated congeners (tri and

tetrachlorobiphenyls) were the ones with highest removal rates. In this study lower chlorinated congeners were degraded, namely PCB28, PCB52 and PCB65 (particularly in the EK setup), but higher chlorinated congeners were also degraded (Experiment F). In some experiments PCB65 increased due to dechlorination of higher chlorinated congeners, such as PCB204. In the EK setup removal rates for each congener are lower than in the ED setup.

*3.2 Different duration experiments*

The experiments with the electrokinetic setup had different durations to assess if longer times would increase the PCB dechlorination. Comparing the 10 d experiment (A) with the 45 d experiment (D), the PCB removal has a small increase (27% vs. 36%) (Figure 2). Although the removal percentages are higher than in previous studies with 14 d experiments (Fan et al., 2013), their values are not encouraging for a scale up of the process (pilot and full scale) for the remediation of PCB contaminated soils and sediments. The higher dechlorination rate in experiment C is related with the additional nZVI injected at days 7 and 9, not with the exposure duration. The congeners concentrations obtained in the soil are not statistically different in the three experiments (A, C and D) at a 0.05 level of significance [one-way ANOVA, $F(2,20) = 2.14$, $p = 0.14$].

*3.3 Experiments without direct current*

Direct current can be used to enhance nZVI transport in different porous matrices or model soils (Gomes et al., 2013b; Gomes et al., 2014), but, in the electrodialytic setup, the contact between the nanoparticles and the contaminated soil is ensured by the stirring so the current may not be needed for the PCB dechlorination. However, results show that the experiment with direct current (exp. F) had a much higher PCB removal rate (83%) than the experiment just with the iron nanoparticles (exp. E) (29%), due to the high pH and buffer

capacity of the soil tested (Table 1 and Figure 3). In the experiment without current (exp. E), the soil suspension with nZVI kept a constant alkaline pH, which promotes the passivation of the iron nanoparticles. In the experiment with current (exp. F) water electrolysis produces $H^+$ in the anode, thus lowering the pH. A slightly acidic pH (4.90–5.10) increases the dechlorination rate of PCB by nZVI and nZVI/Pd (Wang et al., 2012).

The sum of energy and nZVI costs (operation costs for a full-scale reactor) for the remediation of a cubic meter of PCB contaminated soil using the two compartments cell electrodialytic setup is about 72 €, considering the average cost of energy in the European Union (EUROSTAT 2011). If we are only dealing with organic contaminants that can be completely degraded, there is no need to treat and dispose the anolyte after separation from the solids. Even adding the excavation and transport costs, this solution is competitive when compared with the off-site incineration average costs (885 €/$m^3$) and off-site landfilling costs (231 €/$m^3$) (Summersgill, 2006).

**4. Conclusions**

The two-compartment electrodialytic setup tested in this work allows PCB dechlorination from contaminated soil *ex situ* at a higher rate, in a shorter time, with lower nZVI consumption, and with the use of half of the voltage gradient when compared with the traditional EK setup. In addition, there is no need to treat and dispose of the anolyte.

The results show that the soil characteristics are important and affect the reaction between nZVI and the target contaminant, especially pH and carbonate content. Direct current can enhance dechlorination in the two compartments electrodialytic setup.

**Acknowledgments**

This work has been funded by the European Regional Development Fund (ERDF) through COMPETE – Operational Programme for Competitiveness Factors (OPCF), by Portuguese National funds through "FCT - Fundação para a Ciência e a Tecnologia" under project «PTDC/AGR-AAM/101643/2008 NanoDC», by FP7-PEOPLE-IRSES-2010-269289-ELECTROACROSS and by the research grant SFRH/BD/76070/2011. Prof. Jorge Varejão and Helena Silva are acknowledged for GC analysis and Sabrina Madsen for ICP analysis. NANO IRON, s.r.o. kindly provided NANOFER 25S samples.

**References**

Beckingham B, Ghosh U. Field-scale reduction of PCB bioavailability with activated carbon amendment to river sediments. Environ. Sci. Technol. 2011; 45: 10567-10574.

Chang Y, Achari G, Langford C. Effect of cocontaminants on the remediation of PCB-impacted soils by hydrogen peroxide. Pract. Period. Hazard. Toxic Radioact. Waste Manag. 2010; 14: 266-268.

Chen X, Yao X, Yu C, Su X, Shen C, Chen C, et al. Hydrodechlorination of polychlorinated biphenyls in contaminated soil from an e-waste recycling area, using nanoscale zerovalent iron and Pd/Fe bimetallic nanoparticles. Environ. Sci. Poll. Res. 2014: 1-10.

Crane RA, Scott TB. Nanoscale zero-valent iron: Future prospects for an emerging water treatment technology. J. Hazard. Mat. 2012; 211-212: 112-125.

Fan G, Cang L, Qin W, Zhou C, Gomes HI, Zhou D. Surfactants-enhanced electrokinetic transport of xanthan gum stabilized nano Pd/Fe for the remediation of PCBs contaminated soils. Sep. Purif. Technol. 2013; 114: 64-72.

Ferreira C, Ribeiro A, Ottosen L. Effect of major constituents of MSW fly ash during electrodialytic remediation of heavy metals. Sep. Sci. Technol. 2005; 40: 2007-2019.

Ferreira C, Ribeiro AB, Ottosen LM. Study of different assisting agents for the removal of heavy metals from MSW fly ashes. In: Almorza D, Brebbia CA, Sales D, Popov V, editors. Waste Management and the Environment. WIT Press, UK, 2002, pp. 171-179.

Gomes HI, Dias-Ferreira C, Ribeiro AB. Electrokinetic remediation of organochlorines in soil: Enhancement techniques and integration with other remediation technologies. Chemosphere 2012; 87: 1077-1090.

Gomes HI, Dias-Ferreira C, Ribeiro AB. Overview of *in situ* and *ex situ* remediation technologies for PCB-contaminated soils and sediments and obstacles for full-scale application. Sci. Total Environ. 2013a; 445-446: 237-260.

Gomes HI, Dias-Ferreira C, Ribeiro AB, Pamukcu S. Enhanced transport and transformation of zerovalent nanoiron in clay using direct electric current. Water Air Soil Poll. 2013b; 224: 1-12.

Gomes HI, Dias-Ferreira C, Ribeiro AB, Pamukcu S. Influence of electrolyte and voltage on the direct current enhanced transport of iron nanoparticles in clay. Chemosphere 2014; 99: 171-179.

Hansen HK, Ottosen LM, Kliem BK, Villumsen A. Electrodialytic remediation of soils polluted with Cu, Cr, Hg, Pb and Zn. J. Chem.Technol. Biotechnol. 1997; 70: 67-73.

Hansen HK, Ribeiro AB, Mateus EP, Ottosen LM. Diagnostic analysis of electrodialysis in mine tailing materials. Electrochim. Acta 2007; 52: 3406-3411.

He F, Zhao D, Paul C. Field assessment of carboxymethyl cellulose stabilized iron nanoparticles for *in situ* destruction of chlorinated solvents in source zones. Water Res. 2010; 44: 2360–2370.

Jensen PE, Ferreira CMD, Hansen HK, Rype JU, Ottosen LM, Villumsen A. Electroremediation of air pollution control residues in a continuous reactor. J. App. Electrochem. 2010; 40: 1173–1181

Jensen PE, Ottosen LM, Ferreira C. Electrodialytic remediation of soil fines (<63 $\mu$ m) in suspension−Influence of current strength and L/S. Electrochim. Acta 2007; 52: 3412-3419.

Jones EH, Reynolds DA, Wood AL, Thomas DG. Use of Electrophoresis for transporting nano-iron in porous media. Ground Water 2010; 49: 172-183.

Kirkelund GM, Ottosen LM, Villumsen A. Electrodialytic remediation of harbour sediment in suspension—Evaluation of effects induced by changes in stirring velocity and current density on heavy metal removal and pH. J. Hazard. Mater. 2009; 169: 685-690.

Kocur CM, Chowdhury AI, Sakulchaicharoen N, Boparai HK, Weber KP, Sharma P, et al. Characterization of nZVI mobility in a field scale test. Environ. Sci. Technol. 2014: DOI: 10.1021/es4044209.

Laumann S, Micić V, Lowry GV, Hofmann T. Carbonate minerals in porous media decrease mobility of polyacrylic acid modified zero-valent iron nanoparticles used for groundwater remediation. Environ. Poll. 2013; 179: 53-60.

Li Y, Liang F, Zhu Y, Wang F. Phytoremediation of a PCB-contaminated soil by alfalfa and tall fescue single and mixed plants cultivation. J. Soil Sedim. 2013; 13: 925-931.

Lima AT, Ottosen LM, Heister K, Loch JPG. Assessing PAH removal from clayey soil by means of electro-osmosis and electrodialysis. Sci. Total Environ. 2012; 435–436: 1-6.

Lowry G, Johnson K. Congener-specific dechlorination of dissolved PCBs by microscale and nanoscale zerovalent iron in a water/methanol solution. Environ. Sci. Technol. 2004; 38: 5208-5216.

Nystroem GM, Ottosen L, Villumsen A. Electrodyalitic removal of Cu, Zn, Pb and Cd from harbour sediment: Influences of changing experimental conditions. Environ. Sci. Technol. 2005; 38: 2906-2911.

Ottosen L, Jensen P, Kirkelund G, Hansen H. Electrodialytic remediation of different heavy metal-polluted soils in suspension. Water Air Soil Poll. 2013a; 224: 1-10.

Ottosen LM, Hansen HK, Laursen S, Villumsen A. Electrodialytic remediation of soil polluted with copper from wood preservation industry. Environ. Sci. Technol. 1997; 31: 1711-1715.

Ottosen LM, Jensen PE, Hansen HK, Ribeiro A, Allard B. Electrodialytic remediation of soil slurry–removal of Cu, Cr, and As. Sep. Sci. Technol. 2009; 44: 2245-2268.

Ottosen LM, Jensen PE, Kirkelund GM, Ebbers B. Electrodialytic separation of heavy metals from particulate material. Patent application EPC 13183278.4-1352, 2013b.

Pamukcu S, Hannum L, Wittle JK. Delivery and activation of nano-iron by DC electric field. J. Environ. Sci. Health A 2008; 43: 934-944.

Pazos M, Kirkelund GM, Ottosen LM. Electrodialytic treatment for metal removal from sewage sludge ash from fluidized bed combustion. J. Hazard. Mater. 2010; 176: 1073-1078.

Rojo A, Hansen HK, Ottosen LM. Electrodialytic remediation of copper mine tailings: Comparing different operational conditions. Miner. Eng. 2006; 19: 500-504.

Summersgill M. Remediation technology costs in the UK & Europe; Drivers and changes from 2001 to 2005. In: Telford T, editor. Proceedings of the 5th International GeoEnviro Conference, June 2006, Cardiff, 2006.

Sun TR, Ottosen LM, Jensen PE, Kirkelund GM. Electrodialytic remediation of suspended soil – Comparison of two different soil fractions. J. Hazard. Mater. 2012; 203–204: 229-235.

Varanasi P, Fullana A, Sidhu S. Remediation of PCB contaminated soils using iron nano-particles. Chemosphere 2007; 66: 1031–1038.

Vasilyeva GK, Strijakova ER, Nikolaeva SN, Lebedev AT, Shea PJ. Dynamics of PCB removal and detoxification in historically contaminated soils amended with activated carbon. Environ. Poll. 2010; 158: 770–777.

Wang CB, Zhang W. Synthesizing nanoscale iron particles for rapid and complete dechlorination of TCE and PCBs. Environ. Sci. Technol. 1997; 31: 2154-2156.

Wang Y, Zhou D, Wang Y, Wang L, Cang L. Automatic pH control system enhances the dechlorination of 2,4,4'-trichlorobiphenyl and extracted PCBs from contaminated soil by nanoscale $Fe^0$ and $Pd/Fe^0$. Environ. Sci. Poll. Res. 2012; 19: 448-457.

Wu BZ, Chen HY, Wang SJ, Wai CM, Liao W, Chiu K. Reductive dechlorination for remediation of polychlorinated biphenyls. Chemosphere 2012; 88: 757-768.

Yang GCC, Tu HC, Hung CH. Stability of nanoiron slurries and their transport in the subsurface environment. Sep. Purif. Technol. 2007; 58 166-172.

Zhang W, Elliott DW. Applications of iron nanoparticles for groundwater remediation. Remediation 2006: 7-21.

Zhang W, Wang CB, Lien HL. Treatment of chlorinated organic contaminants with nanoscale bimetallic particles. Catal. Today 1998; 40: 387-395.

Zhuang Y, Ahn S, Seyfferth AL, Masue-Slowey Y, Fendorf S, Luthy RG. Dehalogenation of polybrominated diphenyl ethers and polychlorinated biphenyl by bimetallic, impregnated, and nanoscale zerovalent iron. Environ. Sci. Technol. 2011; 45: 4896-4903.

Table 1. Physical and chemical characteristics of the soil.

| **Parameter** | |
|---|---|
| Soil particles (%) | |
| Coarse sand (200 < Ø < 2000 µm) | 19.1 |
| Fine sand (20 < Ø < 200 µm) | 67.3 |
| Silt (2 < Ø < 20 µm) | 12.7 |
| Clay (Ø < 2 µm) | 0.9 |
| Textural classification | Loamy sand |
| pH ($H_2O$) | 12.2 |
| Conductivity (mS $cm^{-1}$) | 18.76 |
| Exchangeable cations ($cmol_{(c)}$ $kg^{-1}$) | |
| $Ca^{2+}$ | 83.75 |
| $Mg^{2+}$ | 3.2 |
| $K^{+}$ | 26.88 |
| $Na^{+}$ | 9.37 |
| Sum of exchangeable cations ($cmol_{(c)}$ $kg^{-1}$) | 123.2 |
| Calcium carbonate (%) | 18.0 |
| Organic matter (%) | 16.46 |
| Total PCB[a] (µg $kg^{-1}$) | 258 ± 24 |
| Metals[b] (mg $kg^{-1}$) | |
| Al | 20980 ± 590 |
| As | 8.6 ± 2.0 |
| Cd | 0.68 ± 0.14 |
| Cr | 51.66 ± 2.69 |
| Cu | 141.73 ± 94.62 |
| Fe | 13162 ± 301 |
| Ni | 31.98 ± 1.26 |
| Pb | 45.43 ± 3.31 |
| Zn | 2155 ± 40 |

[a] Sum of PCB 28, 30, 52, 65, 101, 138, 153, 180, 204 and 209
[b] Acid digestion with $HNO_3$ according to the Danish Standard DS259.

Table 2. Summary of experimental conditions.

| Exp. | nZVI (mL) | Type of injection | Voltage ($V\ cm^{-1}$) | Soil (g, dry weight) | Duration (d) |
|---|---|---|---|---|---|
| A | 13 | Unique (in the beginning of experiment) | 2 | 65.30 | 10 |
| B | 13 | Unique (in the beginning of experiment) | 0 | 49.84 | 10 |
| C | 20 | Repeated (additional iron in days 7 and 9) | 2 | 67.50 | 20 |
| D | 13 | Unique (in the beginning of experiment) | 2 | 69.94 | 45 |
| E | 10 | 2 injections of 5 mL at 24 and 48 h | 0 | 50.01 | 5 |
| F | 10 | 2 injections of 5 mL at 24 and 48 h | 1 | 50.05 | 5 |

**Figure**
**Click here to download Figure: Figures.pdf**

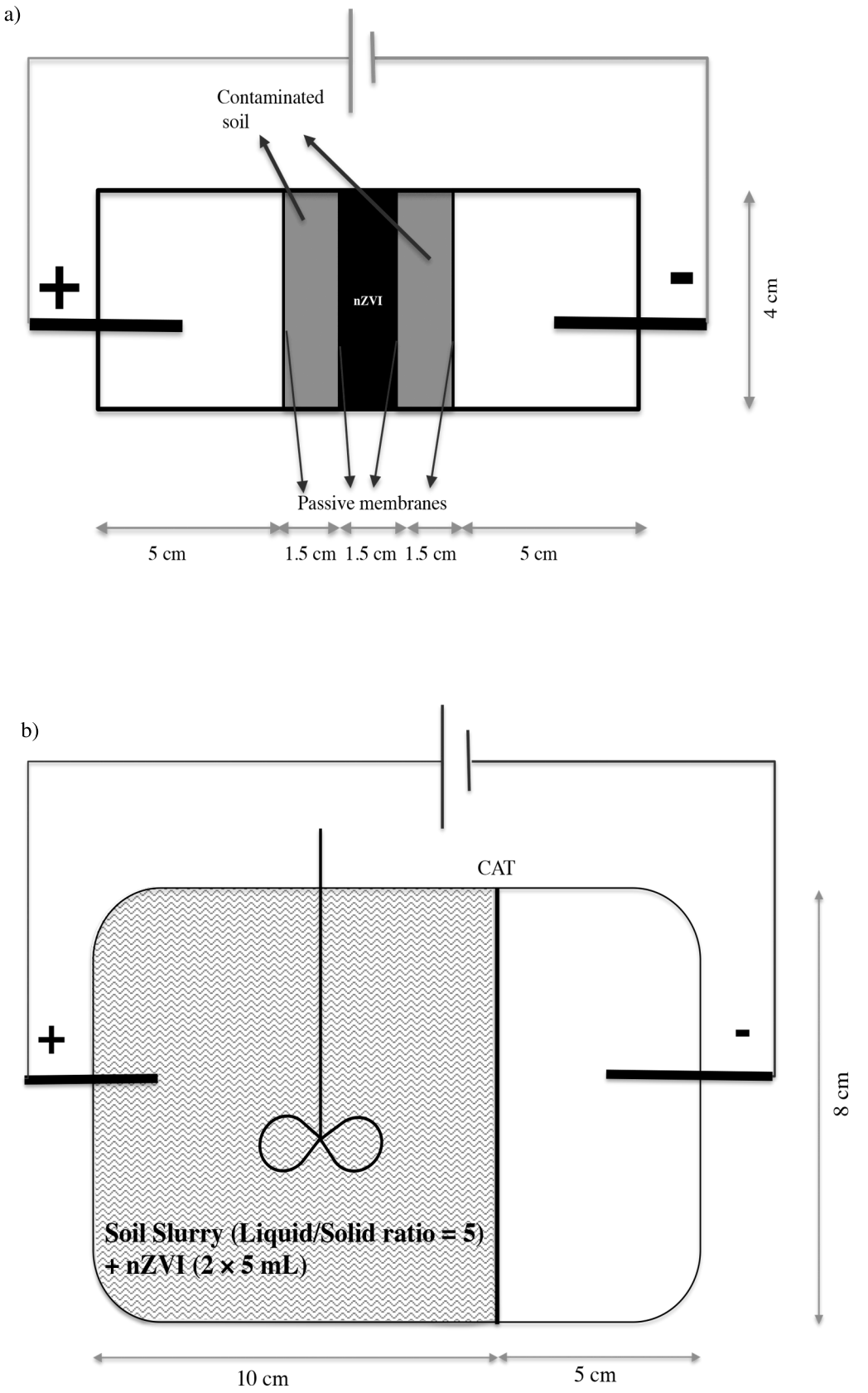


Figure 1. Schematic representation of the experimental setups used in the experiments: a) three compartment electrokinetic cell and b) two compartment electrodialytic cell (CAT – cation exchange membrane).

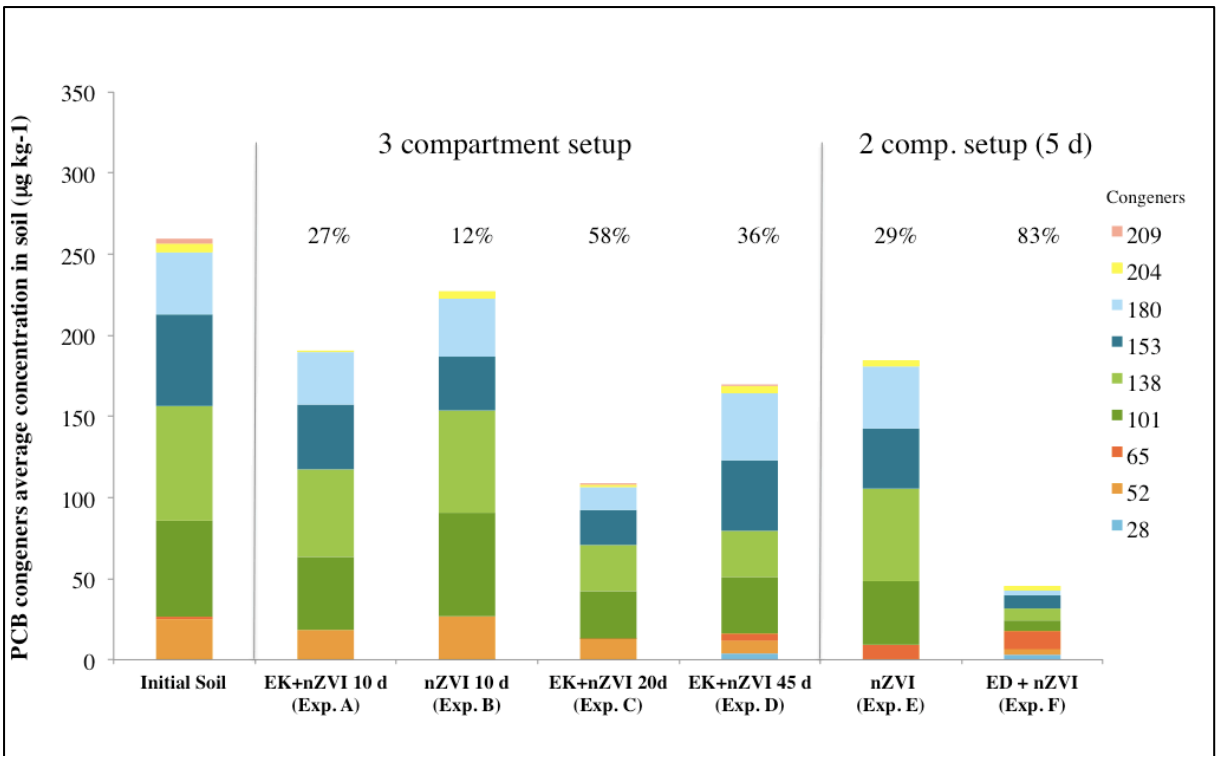


Figure 2. Average concentration of PCB congeners (PCB28, 52, 65, 101, 138, 153, 180, 204 and 209) in soil before and after the experiments using the 3-compartment electrokinetic setup and the 2-compartment electrodialytic setup. Percentages on the top of each column represent PCB removal regarding the sum of congeners analyzed in the initial soil.

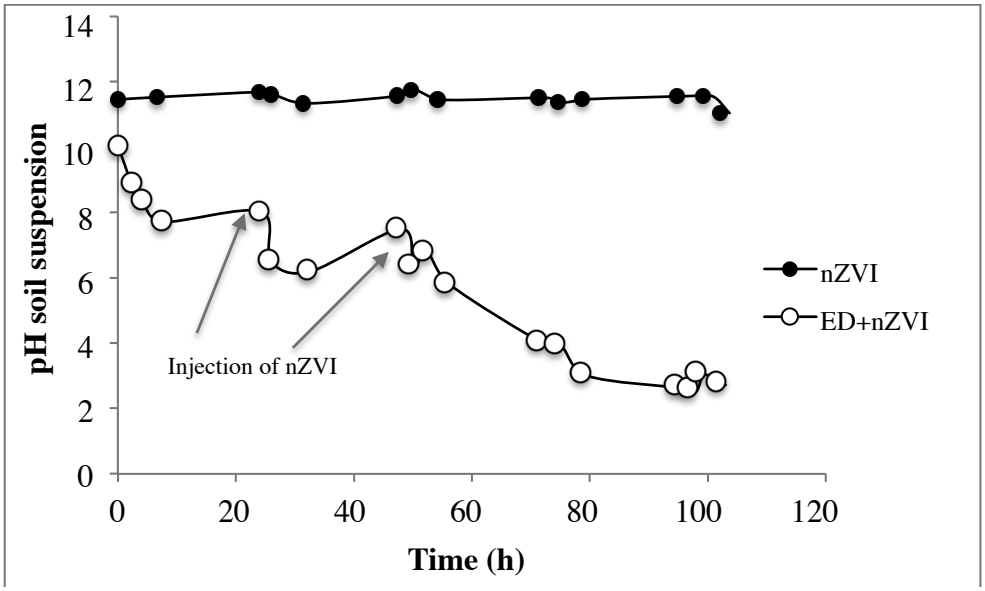

Figure 3. Evolution of pH in the soil suspension during the experiments using the two-compartment ED setup.

## II.8 Electrodialytic suspended remediation of PCB contaminated soil with iron nanoparticles and two different surfactants (published in the Journal of Colloid and Interface Science)

Journal of Colloid and Interface Science 433 (2014) 189–195

Contents lists available at ScienceDirect

Journal of Colloid and Interface Science

www.elsevier.com/locate/jcis

# Electrodialytic remediation of polychlorinated biphenyls contaminated soil with iron nanoparticles and two different surfactants

Helena I. Gomes [a,b,c,*], Celia Dias-Ferreira [b], Lisbeth M. Ottosen [c], Alexandra B. Ribeiro [a]

[a] CENSE – Center for Environmental and Sustainability Research, Departamento de Ciências e Engenharia do Ambiente, Faculdade de Ciências e Tecnologia, Universidade Nova de Lisboa, 2829-516 Caparica, Portugal
[b] CERNAS – Research Center for Natural Resources, Environment and Society, Escola Superior Agraria de Coimbra, Instituto Politecnico de Coimbra, Bencanta, 3045-601 Coimbra, Portugal
[c] Department of Civil Engineering, Technical University of Denmark, Brovej, Building 118, DK 2800 Kgs. Lyngby, Denmark

ARTICLE INFO

*Article history:*
Received 16 May 2014
Accepted 17 July 2014
Available online 1 August 2014

*Keywords:*
Electrodialytic remediation
nZVI
Surfactants
Saponin
Tween 80
PCB

ABSTRACT

Polychlorinated biphenyls (PCB) are persistent organic pollutants (POP) that strongly adsorb in soils and sediments. There is a need to develop new and cost-effective solutions for the remediation of PCB contaminated soils. The suspended electrodialytic remediation combined with zero valent iron nanoparticles (nZVI) could be a competitive alternative to the commonly adapted solutions of incineration or landfilling. Surfactants can enhance the PCB desorption, dechlorination, and the contaminated soil cleanup.

In this work, two different surfactants (saponin and Tween 80) were tested to enhance PCB desorption and removal from a soil sampled at a polluted site, in a two-compartment cell where the soil was stirred in a slurry with 1% surfactant, 10 mL of nZVI commercial suspension, and a voltage gradient of 1 V $cm^{-1}$.

The highest PCB removal was obtained with saponin. Higher chlorinated PCB congeners (penta, hexa, hepta and octachlorobiphenyl) showed removal percentages between 9% and 96%, and the congeners with highest removal were PCB138, PCB153 and PCB180. The use of low level direct current enhanced PCB removal, especially with saponin. Electrodechlorination of PCB with surfactants and nZVI showed encouraging tendencies and a base is thus formed for further optimization towards a new method for remediation of PCB polluted soils.



## 1. Introduction

Soil contamination with persistent organic pollutants, such as polychlorinated biphenyls (PCB), is an important environmental problem, due to their persistence, chemical stability and strong adsorption to soils that inhibits their extraction and degradation, and also to the risks associated with human health and ecosystems [1,2]. An inclusive state of the art review on the technologies available for PCB contaminated soils and sediments showed the advantages and disadvantages of the existing methods, and highlighted the need to find cost-effective and sustainable alternatives [3]. One possible solution to cope with recalcitrant contaminants such as PCB can be the integration of remediation technologies that, when coupled together (simultaneously or in succession, in the so called "treatment trains"), work in a synergistic manner, minimizing the remediation costs for achieving risk-based endpoints, in a quicker and more efficient way than employing single technologies [4].

Zero valent iron nanoparticles (nZVI) are strong reductants that can dechlorinate PCB in aqueous solutions [5–7], but revealed limited results in soils so far [8,9]. Pd/Fe bimetallic nanoparticles, when combined with electrokinetic remediation (EK), resulted in only 20% PCB removal after 14 days with historically contaminated soil [10]. The electrodialytic remediation of suspended soil in conjunction with nZVI enabled a 83% PCB removal in just 5 days [11].

Electroremediation is a group of evolving technologies that started in the 1990s, now targeting a wide range of contaminants, and have lately incorporated enhancement techniques and the combination with other technologies [12]. The use of surfactants for enhancing electrokinetic remediation of contaminated soil with organochlorines and mixed contaminations was reviewed by Gomes et al. [12] and Cameselle et al. [13]. Surfactants improve solubilization and desorption behavior of hydrophobic organic compounds, increasing their availability in contaminated environments [14,15], which can boost the remediation technologies efficacy. Different surfactants have already been tested, but beyond their desorption properties, they should also be environmental

* Corresponding author at: CENSE – Center for Environmental and Sustainability Research, Departamento de Ciências e Engenharia do Ambiente, Faculdade de Ciências e Tecnologia, Universidade Nova de Lisboa, 2829-516 Caparica, Portugal. Fax: +351 212948554.
*E-mail address:* hrg@campus.fct.unl.pt (H.I. Gomes).

http://dx.doi.org/10.1016/j.jcis.2014.07.022
0021-9797/

**Table 1**
Properties of the nonionic surfactants used in the experiments.

| Trade name | Molecular weight | Molecular structure | CMC – Critical micelle concentration (mg $L^{-1}$) |
|---|---|---|---|
| Saponin | 1650 | 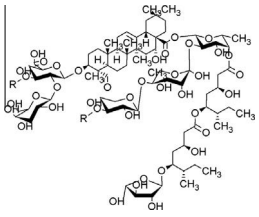 | 42.6 [18] |
| Tween 80 | 1310 | 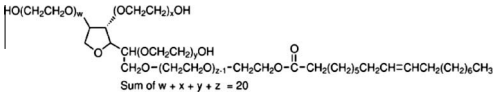  | 40 [28] |

friendly substances [16] and minimize the inhibitory effect of the surfactants on iron nanoparticles reactivity [10,17]. Saponin is a representative non-ionic plant-derived biosurfactant that can efficiently increase desorption and degradation of PCB in contaminated soils [18,19]. Tween 80, a nonionic surfactant used in the food industry, was tested for enhanced EK remediation of dichlorodiphenyltrichloroethane (DDT) [20], hexachlorobenzene [21], perchloroethylene [22], and polycyclic aromatic hydrocarbons (PAH) [23,24]. Both surfactants were also tested simultaneously and individually for the electro-Fenton degradation of phenanthrene in marine sediment [25]. The electrodialytic remediation of PAH with Tween 80 in spiked and contaminated soils was also tested by Lima et al. [26].

In this work, we tested two different surfactants (saponin and Tween 80) to enhance the electroremediation of PCB contaminated soil in the two-compartment electrodialytic (ED) setup developed at the Technical University of Denmark (DTU) [27], in which the soil is suspended and stirred simultaneously in combination with the addition of nZVI. The main objectives were to: (i) compare the effectiveness of the two surfactants for increasing PCB desorption and the subsequent dechlorination; (ii) evaluate the need of using direct electric current in the reactor with suspended soil and nZVI; (iii) assess the potential inhibitory effect of the surfactant in the nZVI reactivity.

## 2. Materials and methods

### 2.1. Chemicals and solvents

PCB standards were analytical grade, obtained from Fluka, Sigma–Aldrich (PCB 28, 52, 101, 138, 153, 180 and 209) and Ultrascientific (PCB 30; PCB 65 and PCB 204). The solvents hexane and acetone were Pestinorm (VWR BDH Prolabo). The surfactants Tween 80 (Sigma Aldrich) and saponin (GPR Rectapur) were lab grade (Table 1). Hydrochloric (37.6%), nitric (65%) and sulfuric (95–97%) acids were trace metal grade. Anhydrous $Na_2SO_4$, $KMnO_4$, NaCl, and silica gel (silicic acid) were lab grade. Silica gel was cleaned up before use according to the USEPA method 3630C. The water was deionized with a Milli-Q plus system from Millipore (Bedford, MA, USA). A nZVI slurry-stabilized suspension (NANOFER 25S, NANO IRON, s.r.o., Rajhrad, Czeck Republic) was used in the experiments (Table 2).

**Table 2**
Characterization of the zero valent iron nanoparticles used in the experiments, according to the supplier information.

| Product Name | NANOFER 25S (NANO IRON, s.r.o.) |
|---|---|
| Stabilizer | Polyacrylic acid (PAA) |
| pH | 11–12 |
| Suspension density | 1.15–1.25 g $cm^{-3}$ (20 °C) |
| Average particles size | 50 nm |
| Particle size distribution | 20–100 nm |
| Average surface area | 20–25 $m^2$ $g^{-1}$ |
| Iron content | 80–90 wt.% |

### 2.2. Soil characterization

The contaminated soil used in the experiments was provided by a hazardous waste operator in Portugal and is a mixture of contaminated soils from industrial sites with transformers oils spills. Table 3 presents the physical and chemical characteristics of the soil used in the experiments. The soil was homogenized, air dried and sieved, and only the particles with size <2 mm were used in the experiments.

**Table 3**
Physical and chemical characteristics of the soil.

| Parameter | |
|---|---|
| Particle size distribution (%) | |
| Coarse sand (200 < Ø < 2000 μm) | 19.1 |
| Fine sand (20 < Ø < 200 μm) | 67.3 |
| Silt (2 < Ø < 20 μm) | 12.7 |
| Clay (Ø < 2 μm) | 0.9 |
| Textural classification | Loamy sand |
| pH ($H_2O$) | 12.2 |
| Conductivity (mS $cm^{-1}$) | 18.76 |
| Exchangeable cations ($cmol_{(c)}$ $kg^{-1}$) | |
| $Ca^{2+}$ | 83.75 |
| $Mg^{2+}$ | 3.2 |
| $K^+$ | 26.88 |
| $Na^+$ | 9.37 |
| Sum of exchangeable cations ($cmol_{(c)}$ $kg^{-1}$) | 123.2 |
| Calcium carbonate (%) | 18.0 |
| Organic matter (%) | 16.46 |
| Total PCB[a] (μg $kg^{-1}$) | 258 ± 24 |
| Metals[b] (mg $kg^{-1}$) | |
| Al | 20,980 ± 590 |
| As | 9 ± 2 |
| Cd | 0.7 ± 0.1 |
| Cr | 52 ± 3 |
| Cu | 142 ± 95 |
| Fe | 13,162 ± 301 |
| Ni | 32 ± 1 |
| Pb | 45 ± 3 |
| Zn | 2155 ± 40 |

[a] Sum of PCB28, 30, 52, 65, 101, 138, 153, 180, 204 and 209.
[b] Acid digestion with $HNO_3$ according to the Danish Standard DS259.

### 2.3. PCB analysis

The soil samples extraction followed the USEPA method 3550C, in which 10 g of soil was extracted with 3 × 30 mL of acetone–hexane (1:1) in a glass vial by ultrasonication (20 kHz) for 60 min. After vacuum filtration and concentration, the extracts were then cleaned following the USEPA methods 3665A and 3630C. Aqueous samples (soil filtrate and catholyte) were extracted according to the method used by Lowry and Johnson [5], after adjusting the pH of the acid samples to pH 7 by NaOH addition.

The PCB congeners were analyzed by gas chromatography (GC) on a HP with ECD detector, HP 6890 Series (Hewlett–Packard, Palo Alto, California, USA). The column used was a TRB–5–MS with 30 m × 0.25 mm i.d. and 0.25 μm film thickness (Phenomenex, Torrance, CA, USA). The oven temperature was programmed starting at 70 °C for 2 min, increased to 150 °C at a rate of 25 °C $min^{-1}$ and then increased 4 °C $min^{-1}$ to 200 °C, 8 °C $min^{-1}$ to 280 °C where it holds for 4 min and finally 10 °C $min^{-1}$ to 300 °C, where it holds for 2 min. Pure nitrogen was used as the carrier gas. The injector was splitless set at 260 °C. The injections of 1.00 μl were made manually.

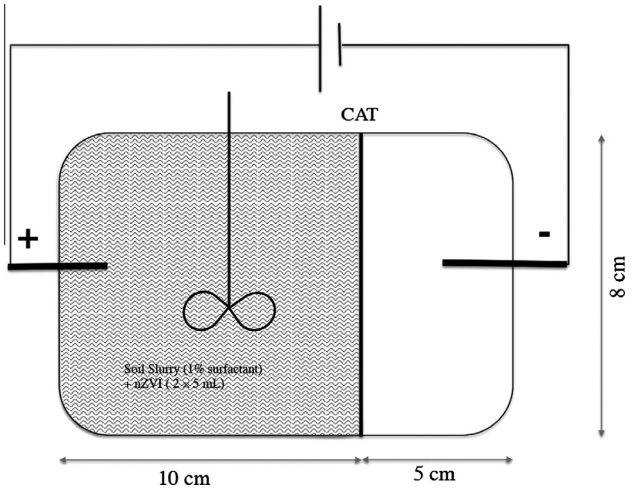


**Fig. 1.** Schematic representation of the experimental electrodialytic (ED) setup. The soil slurry had a liquid solid ratio of 5 and was made with 1% solution of the tested surfactant (saponin and Tween 80). CAT = cation exchange membrane. In the cell, the electrodes are not aligned, but parallel.

**Table 4**
Summary of experimental conditions.

| Exp. | Voltage (V $cm^{-1}$) | Surfactant | nZVI (mL) | Soil (g, dry weight) |
|---|---|---|---|---|
| A | 1 | 1% saponin | 5 + 5 | 50.00 |
| B | 0 | 1% saponin | 5 + 5 | 50.03 |
| C | 1 | 1% saponin | 0 | 50.01 |
| D | 1 | 1% Tween 80 | 5 + 5 | 50.04 |
| E | 0 | 1% Tween 80 | 5 + 5 | 50.01 |
| F | 1 | 1% Tween 80 | 0 | 50.01 |

### 2.4. Electroremediation experiments

The electroremediation experiments were carried out in an electrodialytic cell (ED) developed at DTU. The ED laboratorial cylindrical Plexiglas-cell has one compartment ($L$ = 10 cm, Ø = 8 cm) where the anode, the soil slurry (with a liquid solid ratio of 5; 1% of surfactant solution added) and the plastic-flaps attached to a glass-stick stirrer (Lab-egg Bie&Bernsten, Denmark, ~350 rpm) are placed. A cation exchange membrane (CAT, GE Water & Process Technologies Bvba – ED, Cation, CR67, MKIII, Blank) separates this compartment from the one ($L$ = 5 cm, Ø = 8 cm) where the cathode is placed (Fig. 1). Catholytes were recirculated by mechanical pumps (Plastomec magnet pump, model P05) between the chamber and glass bottle. A power supply (Hewlett Packard E3612A, Palo Alto, USA) was used to maintain a constant voltage and the current was monitored (Fluke 179 multimeter). The working electrodes were platinized titanium bars, with a 3 mm diameter and a length of 10 cm (Permascand®).

Six different experiments (A–F) were carried out during 5 days. Experimental conditions are presented in Table 4. The iron nanoparticles (5 mL) were injected at 24 and 48 h, totalizing 10 mL of NANOFER 25S slurry. The electrolyte used in the cathode compartment was $10^{-2}$ M NaCl. The catholyte pH was manually maintained around 2 by the periodic addition of 5 M HCl to prevent excessive pH rise in the catholyte, except in experiments B and E.

The current between working electrodes (presented in the Supplementary Materials), the pH in the soil suspension and the electrolytes were measured every 24 h. At the end of the experiments,

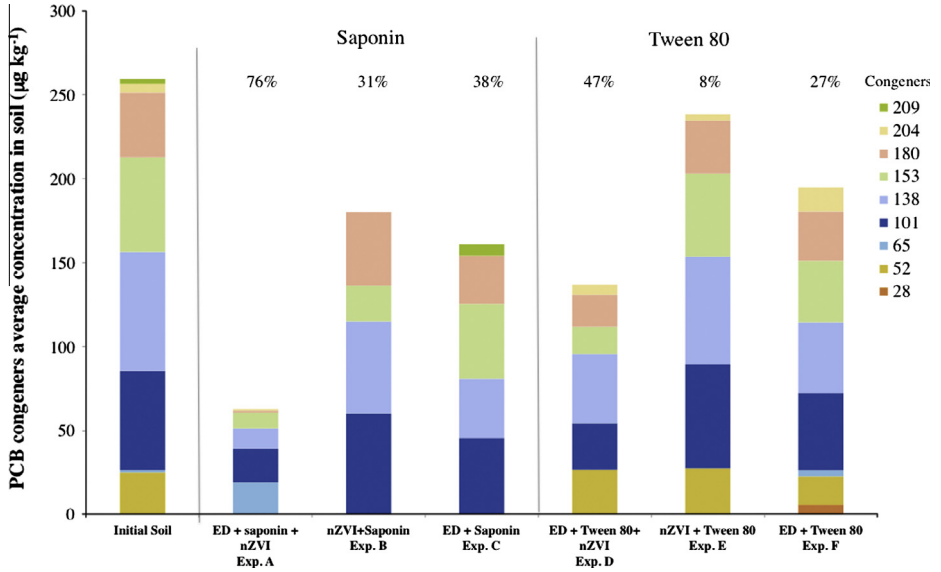


**Fig. 2.** Average concentration of PCB congeners (PCB28, 52, 65, 101, 138, 153, 180, 204 and 209) in soil before and after the electrodialytic experiments using saponin and Tween 80. Percentages on the top of each column represent PCB removal regarding the sum of congeners analyzed in the initial soil.

the contents of Fe in the different parts of the cell (membranes, soil, solutions, and electrodes) were determined. The contents of Fe in the CAT membranes and at the electrodes were measured after extraction in 1 M $HNO_3$ and 5 M $HNO_3$, respectively. The suspension from the central compartment was filtered through filter paper overnight. The soil was dried and slightly crushed in a mortar before the PCB extraction and pH were measured. The iron was extracted from soil by the sodium dithionite–citrate–bicarbonate (DCB) method [29]. The iron analyses were made using Inductively Coupled Plasma-Atomic Emission Spectrometer (ICP) on an Agilent ICP-OES Varian 720-ES equipment.

## 3. Results and discussion

### 3.1. Comparison of the two surfactants

The results show that, in the tested conditions, saponin allowed to obtain higher PCB removal from soil (Fig. 2) when compared with Tween 80. The most efficient removal (76%) was obtained with 1% saponin, 10 mL nZVI and a voltage gradient of 1 V $cm^{-1}$ (Exp. A). The lowest removal was obtained with 1% Tween 80 and nZVI (8% removal), without application of direct current. This removal is consistent with previous studies that showed that Tween 80 was one of the surfactants with the least efficient degradation of 1-(2-chloro-benzoyl)-3-(4-chlorophenyl) urea by nZVI, when compared with Triton X-100, Tween 20, sodium dodecyl sulfonate (SDS), and cetyltrimethylammonium bromide (CTAB), probably due to the effect of the hydrophobic chain length [30].

Surfactants increase the rates of desorption of hydrophobic compounds from soil and transfer the target contaminants into aqueous micelles through solubilization. However, these surfactants have also affinity for PCB and nZVI surface sites and can influence their interactions. Thus, surfactants can affect the degradation of PCB through various mechanisms, such as enhanced solubilization, enhanced sorption, competitive sorption, and electron transfer mediation [30]. PCB dechlorination by nZVI, like other reductive reactions, is a surface-mediated reaction [31], heterogeneous in nature, involving adsorption of the contaminants at the iron surface prior to breaking of carbon–chlorine bonds [32]. It was shown that the adsorbed polyelectrolyte used to stabilize nZVI suspensions decreased dechlorination activity of nZVI, by either blocking available reactive surface sites or else by a combination of site blocking and inhibited mass transfer of chlorinated organic compounds in bulk solution to the nanoparticle surface [33,34]. Cationic and non-ionic surfactants were also found to inhibit the trichloroethylene degradation by carboxymethyl cellulose stabilized nZVI [17]. The possibility of using non-stabilized micro zero valent iron in this setup should be further investigated as it avoids these inhibition problems.

Usually lower chlorinated congeners (tri and tetrachlorobiphenyls) are the ones with highest removal rates from contaminated soils [35–38]. In this work, beside lower chlorinated congeners, also higher chlorinated congeners (penta, hexa, hepta and octachlorobiphenyl) showed removal percentages between 9% and 96% (average value 44%). We also observed an increase in the concentration of PCB52 (4% in Exp. D and 11% in Exp. E), PCB65 (ten times more in Exp. A and 128% in Exp. F) and PCB101 (2% in Exp.

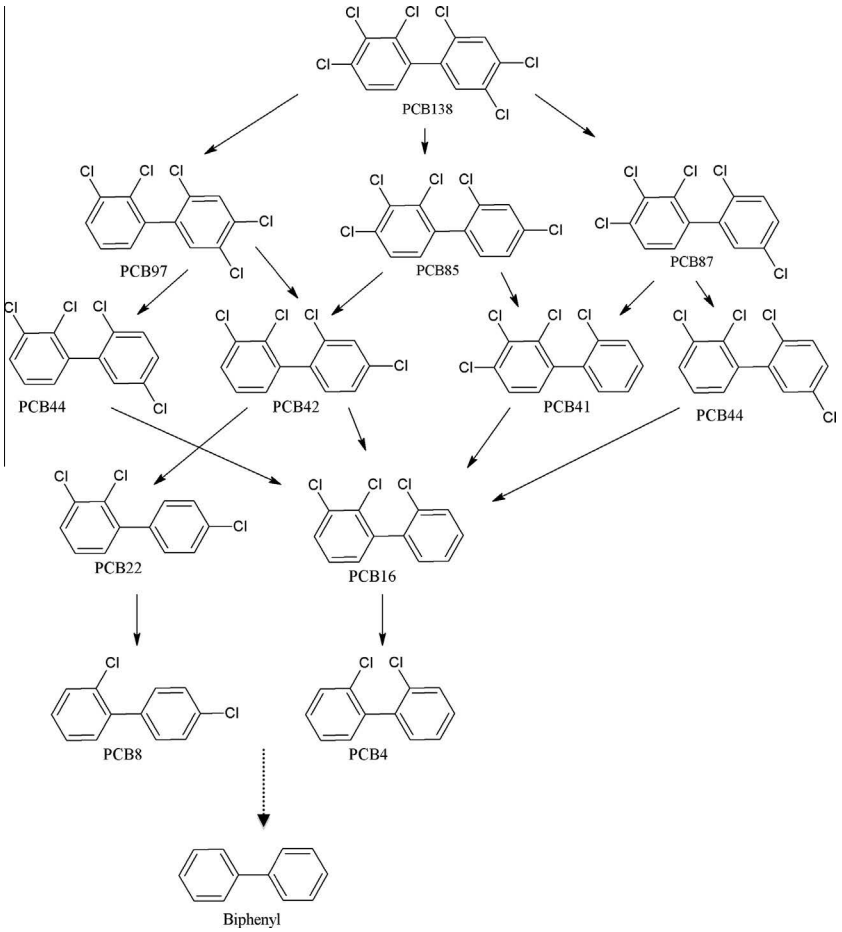


**Fig. 3.** Possible dechlorination pathways proposed for PCB138.

B and 4% in Exp. E), due to dechlorination of higher chlorinated congeners. The congeners with higher removal rates were PCB138 (Exp. C and F), PCB153 (Exp. A, B and D), and PCB180 (Exp. A). Chen et al. [9] identified the PCB153 dechlorination pathways by nZVI. Figs. 3 and 4 show the proposed dechlorination pathways for PCB138 and PCB180, considering that nZVI reactivity decreases according to the chlorine position in the following order: *ortho* < *para* < *meta* [36,39].

In the aqueous samples (soil filtrate and catholyte), most of the PCB congeners were below the detection limit. PCB have very low water solubility (0.0027–0.42 ng $L^{-1}$) and are very hydrophobic [40]. In the soil filtrate, we could measure PCB only in two samples. Experiment B had 0.08 ng $L^{-1}$ of PCB153 and Experiment D presented 3.81 ng $L^{-1}$ of PCB101. These concentrations, higher than the typical solubility range, are due to the surfactants. In the catholyte samples (Table S1, Supplementary Material), some congeners were also found, mostly lower chlorinated congeners (PCB28), but also penta, hexa and heptachlorobiphenyls. These congeners are identified only in the experiments with applied current, probably due to the electrophoresis.

Although in the suspended electrodialytic setup, there are chemical reactions that deplete the $Fe^0$ reductant power:

$$2Fe^0_{(s)} + 4H^+_{(aq)} + O_{2(aq)} \rightarrow 2Fe^{2+}_{(aq)} + 2H_2O_{(l)} \quad (1)$$

$$Fe^0_{(s)} + 2H_2O_{(l)} \rightarrow Fe^{2+}_{(aq)} + H_{2(g)} + 2OH^-_{(aq)} \quad (2)$$

there is also water electrolysis occurring in the electrodes, and secondary reactions with metals $M_e$ [41]:

$$2H_2O - 4e^- \rightarrow O_{2(g)} + 4H^{+}\cdot \quad E_0 = -1.229\ \text{V (anode)} \quad (3)$$

$$2H_2O + 2e^- \rightarrow H_{2(g)} + 2OH^{-}\cdot \quad E_0 = -0.828\ \text{V (cathode)} \quad (4)$$

$$M^{n+}_e + ne^- \rightarrow M_e \quad (5)$$

$$Me(OH)_{n(s)} + ne^- \rightarrow \cdot M_e + nOH^- \quad (6)$$

The water electrolysis reactions (3) and (4) are responsible for the generation of an acid front from the anode and an alkaline front from the cathode, due to the pH values obtained (2 at the anolyte and 12 at the catholyte). The $H^+$ generated at the anode can solubilize transition metals such as Fe and Ni from soil, that can degrade PCB via catalytic hydrodechlorination with $H_2$ successively removing chlorine atoms from PCB generating biphenyl, according to the general chemical equation [36]:

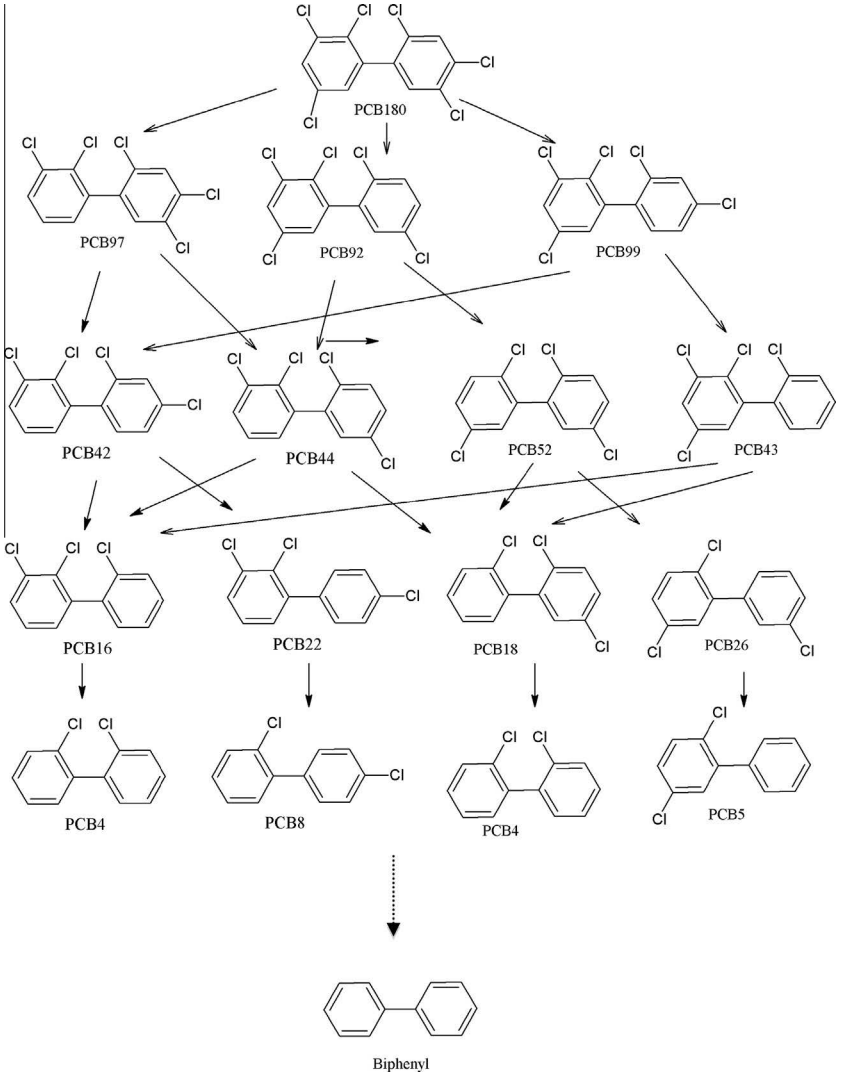


**Fig. 4.** Possible dechlorination pathways proposed for PCB180.

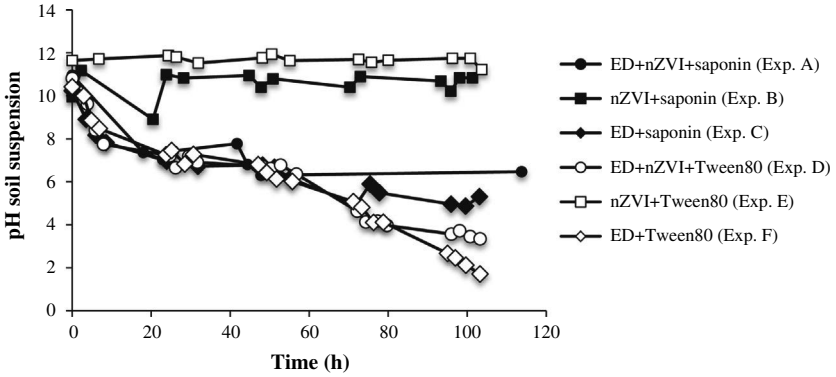


**Fig. 5.** Soil suspension pH evolution during the experiments.

**Table 6**
Mass of iron (mg) in each cell component after the end of the experiments.

| Exp. | Injection reservoir | Cation exchange membrane | Electrodes | Electrolyte (filtrate + catholyte) | Soil |
|---|---|---|---|---|---|
| A | 7.3 | 37.3 | 23.7 | 215 | 1307 |
| B | 4.1 | 6.6 | – | 0.5 | 1181 |
| C | 0.6 | 1.0 | 0.4 | 1.2 | 353 |
| D | 6.1 | 19.4 | 64.7 | 127 | 2299 |
| E | 2.5 | 2.4 | – | 0.2 | 1121 |
| F | 1.1 | 8.4 | 0.3 | 99.2 | 417 |

$$C_{12}H_{(10-m)}Cl_m + nH_2 \rightarrow C_{12}H_{(10-m+n)}Cl_{m-n} + nHCl, \quad m \geqq n \qquad (7)$$

Although this hydrodechlorination was studied in aqueous or organic solvents, in the tested setup, there are all the needed conditions for it to occur.

Comparing the energy consumption of the experiments, calculated according to Sun et al. [42], we note that Tween 80 has higher energy consumption when compared with saponin (1.6 W h $g^{-1}$ soil and 4.1 W h $g^{-1}$ in Exp. D and F, and 1.2 W h $g^{-1}$ soil and 0.7 W h $g^{-1}$ in Exp. A and C, respectively). Added to the low removal percentages, this also contributes to show that Tween 80 is not a suitable surfactant to use with PCB, despite the good results obtained for PAH with this method [26].

### 3.2. Experiments without current

Results show that the experiments with direct current have higher removal percentages than the ones without current. The PCB congeners concentrations using saponin with and without current (Exp. A and B) are statistically different at a 0.05 level of significance [one-way ANOVA, $F(1,9) = 5.61$, $p = 0.04$]. Theoretically, only the mixture of the nanoparticles with the soil slurry should be enough to promote PCB dechlorination, but there are much better results when a direct current is applied. This means that electric current also contributes to PCB dechlorination, and this can be done in two different ways. The first is by lowering the pH due to water electrolysis at the anode: a slightly acidic pH (4.90–5.10) increases the dechlorination rate of PCB by nZVI [43], while an alkaline pH (as occurs in the experiments without current – Fig. 5) promotes the passivation of the iron nanoparticles and prevents PCB dechlorination. The fact that the electric current was able to lower pH (Fig. 5), despite the high buffering capacity of this soil, shows the potential of the technique and the tested setup. The second way is related with the PCB electrocatalytic hydrodechlorination – the production of $H^+$ and the presence of current can promote the Cl removal from PCB, generating HCl [44,45]. The electrocatalytic hydrodechlorination has been demonstrated with specially engineered foam electrodes, in solvent/surfactant-aided solutions and can possibly be also occurring in this two-compartment electrodialytic setup. Further research is needed to evaluate the importance of this dechlorination process, to assess how iron (natural and manufactured) and other metals act as catalysts.

The pH of the suspended slurry also affects the surfactant behavior, influencing the micelle aggregation and hydrophobicity. At high pH, the net charge on the head groups of saponin molecule will increase, causing electrostatic repulsion between the head groups, which tends to increase the critical micelle concentration (CMC) values, reducing the solubilization capabilities of saponin [46]. Also, the solubilization of heavy metals by the electrodialytic process (like $Cd^{2+}$ and $Zn^{2+}$) and a lower pH (until pH 4) decrease the CMC value of saponin solution and enhance its solubilization properties [46]. With Tween 80, the pH increase had a positive effect on surface tension and the micelles are more stable at higher pH (up to 10) [25].

Table 6 shows the mass of iron found in each component of the cell at the end of the experiments. Previous studies showed that in the traditional electrokinetic setups most of the nZVI aggregate and settle in the injection compartment [47–49], thus not reaching the contaminated soil. The suspended electrodialytic remediation assures that nZVI are mixed with the soil and most of the iron is found there at the end of the experiments.

## 4. Conclusions

The work combined three different remediation components for PCB contaminated soil: Surfactant, nZVI and electrodialysis. Two surfactants were tested (saponin and Tween 80). Saponin showed the best results, but both surfactants presented a similar behavior (higher PCB removal rates with direct current and iron nanoparticles). Combining surfactant and nZVI gave less successful remediation than combining surfactant and ED. The best result was though obtained when all three components were combined. With saponin, 76% PCB was removed in 5 days. Further research is needed to quantify the effect of the electrodechlorination and hydrodechlorination of PCB using this two-compartment electrodia-

lytic setup in order to optimize the combined process, as the results showed that the use of direct current allowed the highest PCB removal rates.

## Acknowledgments

This work was funded by the European Regional Development Fund (ERDF) through COMPETE – Operational Programme for Competitiveness Factors (OPCF), by Portuguese National funds through "FCT – Fundação para a Ciência e a Tecnologia" under Project «PTDC/AGR-AAM/101643/2008 NanoDC», by FP7-PEOPLE-IRSES-2010-269289-ELECTROACROSS and by the research Grant SFRH/BD/76070/2011. Prof. Jorge Varejão and Helena Silva are acknowledged for GC analysis and Sabrina Madsen for ICP analysis. NANO IRON, s.r.o. kindly provided NANOFER 25S samples.

## Appendix A. Supplementary material

Supplementary data associated with this article can be found, in the online version, at http://dx.doi.org/10.1016/j.jcis.2014.07.022.

## References

[1] L. Nizzetto, M. Macleod, K. Borgå, A. Cabrerizo, J. Dachs, A.D. Guardo, D. Ghirardello, K.M. Hansen, A. Jarvis, A. Lindroth, B. Ludwig, D. Monteith, J.A. Perlinger, M. Scheringer, L. Schwendenmann, K.T. Semple, L.Y. Wick, G. Zhang, K.C. Jones, Environ. Sci. Technol. 44 (2010) 6526–6531.
[2] B. Wang, J. Huang, S. Deng, X. Yang, G. Yu, Front. Environ. Sci. Eng. 6 (2012) 2–16.
[3] H.I. Gomes, C. Dias-Ferreira, A.B. Ribeiro, Sci. Total Environ. 445–446 (2013) 237–260.
[4] P.S.C. Rao, J.W. Jawitz, C.G. Enfield, R.W. Falta, M.D. Annable, A.L. Wood, Technology integration for contaminated site remediation: clean-up goals and performance criteria, in: Groundwater Quality: Natural and Enhanced Restoration of Groundwater Pollutions 2001 Proceedings, Sheffield, UK, 2001, pp. 571–578.
[5] G. Lowry, K. Johnson, Environ. Sci. Technol. 38 (2004) 5208–5216.
[6] C.B. Wang, W. Zhang, Environ. Sci. Technol. 31 (1997) 2154–2156.
[7] F. He, D. Zhao, C. Paul, Water Res. 44 (2010) 2360–2370.
[8] P. Varanasi, A. Fullana, S. Sidhu, Chemosphere 66 (2007) 1031–1038.
[9] X. Chen, X. Yao, C. Yu, X. Su, C. Shen, C. Chen, R. Huang, X. Xu, Environ. Sci. Pollut. Res. (2014) 1–10.
[10] G. Fan, L. Cang, W. Qin, C. Zhou, H.I. Gomes, D. Zhou, Sep. Purif. Technol. 114 (2013) 64–72.
[11] H.I. Gomes, C. Dias-Ferreira, L.M. Ottosen, A.B. Ribeiro, Electroremediation of PCB contaminated soil with iron nanoparticles: performance of a new electrodialytic setup (submitted for publication).
[12] H.I. Gomes, C. Dias-Ferreira, A.B. Ribeiro, Chemosphere 87 (2012) 1077–1090.
[13] C. Cameselle, S. Gouveia, D.E. Akretche, B. Belhadj, Advances in electrokinetic remediation for the removal of organic contaminants in soils, in: M.N. Rashed (Ed.), Soils, Organic Pollutants – Monitoring, Risk and Treatment, 2013. <http://www.intechopen.com/books/organic-pollutants-monitoring-risk-and-treatment/advances-in-electrokinetic-remediation-for-the-removal-of-organic-contaminants-in-soils>.
[14] M. Viisimaa, O. Karpenko, V. Novikov, M. Trapido, A. Goi, Chem. Eng. J. 220 (2013) 352–359.
[15] C.N. Mulligan, R.N. Yong, B.F. Gibbs, Eng. Geol. 60 (2001) 371–380.
[16] C.N. Mulligan, Curr. Opin. Colloid Interface Sci. 14 (2009) 372–378.
[17] M. Zhang, F. He, D. Zhao, X. Hao, Water Res. 45 (2011) 2401–2414.
[18] M. Cao, Y. Hu, Q. Sun, L. Wang, J. Chen, X. Lu, Environ. Pollut. 174 (2013) 93–99.
[19] H. Xia, X. Chi, Z. Yan, W. Cheng, Bioresour. Technol. 100 (2009) 4649–4653.
[20] A. Karagunduz, A. Gezer, G. Karasuloglu, Sci. Total Environ. 385 (2007) 1–11.
[21] S. Yuan, M. Tian, X. Lu, J. Hazard. Mater. 137 (2006) 1218–1225.
[22] S.S. Chen, Y.C. Huang, T.Y. Kuo, Ground Water Monitor. Remed. 30 (2010) 90–98.
[23] A.T. Lima, P.J. Kleingeld, K. Heister, J.P.G. Loch, Sep. Purif. Technol. 79 (2011) 221–229.
[24] M.T. Alcántara, J. Gómez, M. Pazos, M.A. Sanromán, J. Hazard. Mater. 179 (2010) 1156–1160.
[25] O. Iglesias, M.A. Sanromán, M. Pazos, Ind. Eng. Chem. Res. 53 (2014) 2917–2923.
[26] A.T. Lima, L.M. Ottosen, K. Heister, J.P.G. Loch, Sci. Total Environ. 435–436 (2012) 1–6.
[27] L.M. Ottosen, P.E. Jensen, G.M. Kirkelund, B. Ebbers, Electrodialytic Separation of Heavy Metals from Particulate Material, Patent Application EPC 13183278.4-1352, 2013.
[28] W. Zhou, X. Wang, C. Chen, L. Zhu, Colloids Surf., A 425 (2013) 122–128.
[29] O.P. Mehra, M.L. Jackson, Clays Clay Miner. 7 (1960) 317–327.
[30] Q. Zhou, H. Lin, CLEAN 41 (2013) 128–133.
[31] E.J. Weber, Environ. Sci. Technol. 30 (1996) 716–719.
[32] W. Yan, H.L. Lien, B.E. Koel, W. Zhang, Environ. Sci. Process. Impacts 15 (2013) 63–77.
[33] F. He, D. Zhao, Appl. Catal., B 84 (2008) 533–540.
[34] T. Phenrat, Y. Liu, R.D. Tilton, G.V. Lowry, Environ. Sci. Technol. 43 (2009) 1507–1514.
[35] Y. Li, F. Liang, Y. Zhu, F. Wang, J. Soils Sed. 13 (2013) 925–931.
[36] B.Z. Wu, H.Y. Chen, S.J. Wang, C.M. Wai, W. Liao, K. Chiu, Chemosphere 88 (2012) 757–768.
[37] G.K. Vasilyeva, E.R. Strijakova, S.N. Nikolaeva, A.T. Lebedev, P.J. Shea, Environ. Pollut. 158 (2010) 770–777.
[38] B. Beckingham, U. Ghosh, Environ. Sci. Technol. 45 (2011) 10567–10574.
[39] N.E. Korte, O.R. West, L. Liang, B. Gu, J.L. Zutman, Q. Fernando, Waste Manage. 22 (2002) 343–349.
[40] M.D. Erickson, Analytical Chemistry of PCBs, CRC Press, Boca Raton, Florida, 1997.
[41] Y.B. Acar, A.N. Alshawabkeh, Environ. Sci. Technol. 27 (1993) 2638–2647.
[42] T.R. Sun, L.M. Ottosen, P.E. Jensen, G.M. Kirkelund, J. Hazard. Mater. 203–204 (2012) 229–235.
[43] Y. Wang, D. Zhou, Y. Wang, L. Wang, L. Cang, Environ. Sci. Pollut. Res. 19 (2012) 448–457.
[44] B. Yang, G. Yu, J. Huang, Environ. Sci. Technol. 41 (2007) 7503–7508.
[45] B. Yang, G. Yu, D. Shuai, Chemosphere 67 (2007) 1361–1367.
[46] W. Zhou, J. Yang, L. Lou, L. Zhu, Environ. Pollut. 159 (2011) 1198–1204.
[47] H.I. Gomes, C. Dias-Ferreira, A.B. Ribeiro, S. Pamukcu, Chemosphere 99 (2014) 171–179.
[48] H.I. Gomes, C. Dias-Ferreira, A.B. Ribeiro, S. Pamukcu, Water, Air, Soil Pollut. 224 (2013) 1–12.
[49] K.R. Reddy, K. Darko-Kagy, C. Cameselle, Sep. Purif. Technol. 79 (2011) 230–237.

## II.9 Enhanced electrokinetic techniques for remediation of different PCB polluted soils (submitted)

# Enhanced electrokinetic techniques for remediation of different PCB polluted soils

Helena I. Gomes[1,2,3], Celia Dias-Ferreira[2], Lisbeth M. Ottosen[3], Alexandra B. Ribeiro[1]

[1]CENSE - Center for Environmental and Sustainability Research, Departamento de Ciências e Engenharia do Ambiente, Faculdade de Ciências e Tecnologia, Universidade Nova de Lisboa, 2829-516 Caparica, Portugal

[2]CERNAS – Research Center for Natural Resources, Environment and Society, Escola Superior Agraria de Coimbra, Instituto Politecnico de Coimbra, Bencanta, 3045-601 Coimbra, Portugal

[3]Department of Civil Engineering, Technical University of Denmark, Brovej, Building 118, DK 2800 Kgs. Lyngby, Denmark

* Corresponding author. Tel. +351 212948300, Fax. +351 212948554. E-mail address: hrg@campus.fct.unl.pt (Helena I. Gomes)

**Abstract**

Polychlorinated biphenyls (PCB) are carcinogenic and persistent organic pollutants that accumulate in soils and sediments. Currently, there is no cost-effective and sustainable remediation technology for these contaminants. In this work, a new combination of electrodialytic remediation and zero valent iron particles in a two-compartment cell is tested and compared to a more conventional combination of electrokinetic remediation and nZVI in a three-compartment cell. In the new two-compartment cell, the soil is suspended and stirred simultaneously with the addition of zero valent iron nanoparticles. Remediation experiments are made with two different historically PCB contaminated soils, which differ in both soil composition and contamination source. Soil 1 is a mix of soils with spills of transformer oils, while Soil 2 is a superficial soil from a decommissioned school where PCB were used as windows sealants. Remediation of Soil 1 (with highest pH, carbonate content, organic matter and PCB concentrations) obtained the maximum 83% and 60% PCB removal with the two-compartment and the three-compartment cell, respectively. The highest removal with Soil 2 were 58% and 45%, in the two-compartment and the three-compartment cell, respectively, in the experiments without direct current. The pH of the soil suspension in the two-compartment treatment appears to be a determining factor for the PCB dechlorination, and this cell allowed a uniform distribution of the nanoparticles in the soil, while there was iron accumulation in the injection reservoir in the three-compartment cell.

## 1. Introduction

Electrokinetic (EKR) and electrodialytic (EDR) remediation are reliable technologies, successfully used, both at laboratorial and pilot scale, for the removal of organic and inorganic contaminants from different matrices, like soils, sediments, mine tailings, wastes and ashes [1-8]. In both methods, a low level direct current is responsible for the transport of contaminants through different mechanisms (electroosmosis, electromigration and electrophoresis), and additionally induces electrochemical reactions (electrolysis and electrodeposition) [9]. The use of electrokinetics in soil has evolved to include distinct enhancement techniques and the combination with other technologies [10]. Common problems in EKR remediation, such as the nonlinear and transient geochemical changes in the soil, were coped by treating a suspension of soils with uniform stirring in electrodialytic remediation, which allowed increasing the remediation rate [11-13]. A two-compartment electrodialytic setup recently developed at the Technical University of Denmark [14] is a step forward, showing additional advantages like a direct acidification of the matrix without strong acids, and it is not necessary to dispose the anolyte.

Polychlorinated biphenyls (PCB) were classified as persistent organic pollutants (POP) by the United Nations Stockholm Convention. There is a need to find cost effective and more sustainable remediation alternatives for PCB-contaminated soils and sediments [15]. Zero valent iron nanoparticles (nZVI) were used with success for PCB dechlorination in aqueous solutions [16-18], but revealed limited results in soils so far [19, 20]. Pd/Fe bimetallic nanoparticles, when combined with EKR, resulted in only 20% PCB removal after 14 days with historically contaminated soil [21]. Very recently, the new two-compartment cell was successfully used for POP in conjunction with nZVI. This combination enabled a 83% PCB removal in just 5 days, which is much higher than the reported 27% removal in 10 days as the best result so far with EKR/nZVI [22].

The effects of soil composition on electroremediation are described in several studies. Especially the soil buffer capacity and the carbonate content, which can neutralize the acid front generated at the anode, is an important soil parameter, as the acidification aids many of the remediation processes [23-29]. Soil texture is also relevant for electroremediation [12, 27] and nZVI transport in EKR/nZVI [30, 31], as the soil particles distribution and their charge affect the transport mechanisms. The soil cation exchange capacity is also important, as it allows the soil to immobilize significant quantities of heavy metal ions [32]. The organic matter content can strongly influence the sorption/desorption of contaminants and it was also shown to affect the electroosmotic properties and ionic modification of soils [33]. In the present work, two electroremediation techniques, EKR and EDR, are compared experimentally for remediation of two different historically PCB contaminated soils. The differences between the techniques other than the design of the reactor are the use of ion-selective membranes for EDR while EKR uses passive membranes. In both setups the remediation was enhanced with a surfactant (saponin) and nZVI, as suggested beneficial in Gomes et al. [22]. The main objective was to assess the influence of soil composition on these enhanced electroremediation techniques.

## 2. Materials and Methods

### *2.1. Chemicals and solvents*

PCB standards were analytical grade, obtained from Fluka, Sigma-Aldrich (PCB28, 52, 101, 138, 153, 180 and 209) and Ultrascientific (PCB30; PCB65 and PCB204). The solvents hexane and acetone were Pestinorm (VWR BDH Prolabo). Saponin (GPR Rectapur) was the lab grade surfactant used to enhance PCB desorption. Hydrochloric (37.6%), nitric (65%) and sulfuric (95-07%) acids were tracemetal. Anhydrous $Na_2SO_4$, $KMnO_4$, NaCl, and silica gel (silicic acid) were lab grade. Silica gel was cleaned up before use according to the USEPA method 3630C. The water was deionized with a Milli-Q plus system from Millipore

89 (Bedford, MA, USA). A nZVI slurry-stabilized suspension (NANOFER 25S, NANO IRON,
90 s.r.o., Rajhrad, Czeck Republic) was used in the experiments (Table S1, Suplementary
91 Information).

92 *2.2 Soil characterization*

93 Two different soils, historically contaminated with PCB, were used for the
94 experiments. Soil 1 was provided by a hazardous waste operator in Portugal and is a mixture
95 of contaminated soils from industrial sites with transformers oils spills. Soil 2 is a surface soil
96 sampled in a decommissioned school in Hovedstaden (Capital Region of Denmark), and the
97 PCB resulted from the weathering of the windows joint sealants used in 1955-1977 [34].

98 The soil characterization methods used were described in Jensen et al. [11]. The initial
99 soils were analyzed for Al, As, Cd, Cr, Cu, Fe, Ni, Pb, Zn using Inductively Coupled Plasma-
100 Atomic Emission Spectrometer (ICP) on an Agilent ICP-OES Varian 720-ES equipment. Soil
101 texture was determined by laser diffraction with a Malvern Mastersizer 2000. The soil was
102 homogenized, air dried and sieved, and only the particles with size < 2 mm were used in the
103 experiments.

104 For PCB analysis, the soil extraction method used was the USEPA method 3550C, in
105 which 10 g of soil was extracted with 3 × 30 mL of acetone-hexane (1:1) in a glass vial by
106 ultrasonication (20 kHz) for 60 min. After vacuum filtration and concentration, the extracts
107 were cleaned following the USEPA methods 3665A and 3630C. Aqueous samples (soil
108 filtrate and catholyte) were extracted according to the method used by Lowry and Johnson
109 [16], after adjusting the pH of the acid samples to pH 7 by NaOH addition. The PCB
110 congeners were analyzed by gas chromatography (GC) on a HP with ECD detector, HP 6890
111 Series (Hewlett-Packard, Palo Alto, California, USA). The column used was a TRB–5–MS
112 with 30 m × 0.25 mm i.d. and 0.25 μm film thickness (Phenomenex, Torrance, CA, USA).
113 The oven temperature was programmed starting at 70ºC for 2 min, increased to 150ºC at a

114 rate of 25ºC $min^{-1}$ and then increased 4ºC $min^{-1}$ to 200ºC, 8ºC $min^{-1}$ to 280ºC where it holds
115 for 4 min and finally 10ºC $min^{-1}$ to 300ºC, where it holds for 2 min. Pure nitrogen was used
116 as the carrier gas. The injector was splitless set at 260°C. The injections of 1.00 µl were
117 performed manually.

118 *2.3 Electroremediation experiments*

119 The electroremediation experiments were carried out in two different laboratorial
120 cylindrical Plexiglas-cells. The EKR cell was divided into three compartments: of two
121 electrode compartments (L = 5 cm, internal diameter Ø = 4 cm) and a central compartment.
122 The central compartment subdivided in three parts (L = 1.5 cm each, total of 4.5 cm, Ø = 4
123 cm). The nZVI was placed in the middle part and the soil in the other two [Figure 1 a)]. The
124 soil was saturated with deionized water before the experiments. Cellulose filters (passive
125 membranes) were used to assure the separation between the soil and electrolytes, and the soil
126 and the nZVI.

127 The EDR cell had two compartments [Figure 1 b)]. In one compartment (L = 10 cm,
128 Ø = 8 cm) the anode was placed directly into the soil slurry and a plastic-flaps attached to a
129 glass-stick overhead stirrer (Lab-egg Bie&Bernsten, Denmark, ~350 rpm) maintained the soil
130 in suspension during the treatment. The soil slurry was made with 1% saponin solution (with
131 a liquid solid ratio of 5). Saponin is a representative plant-derived biosurfactant that can
132 efficiently increase desorption and degradation of PCB in contaminated soils [35, 36]. A
133 cation-exchange membrane (CAT, GE Water & Process Technologies Bvba - ED, Cation,
134 CR67, MKIII, Blank) separates this compartment from the cathode compartment (L = 5 cm,
135 Ø = 8 cm) [Figure 1 b)]. The catholyte was recirculated by mechanical pumps (Plastomec
136 magnet pump, model P05) between the chamber and a glass bottle.

137

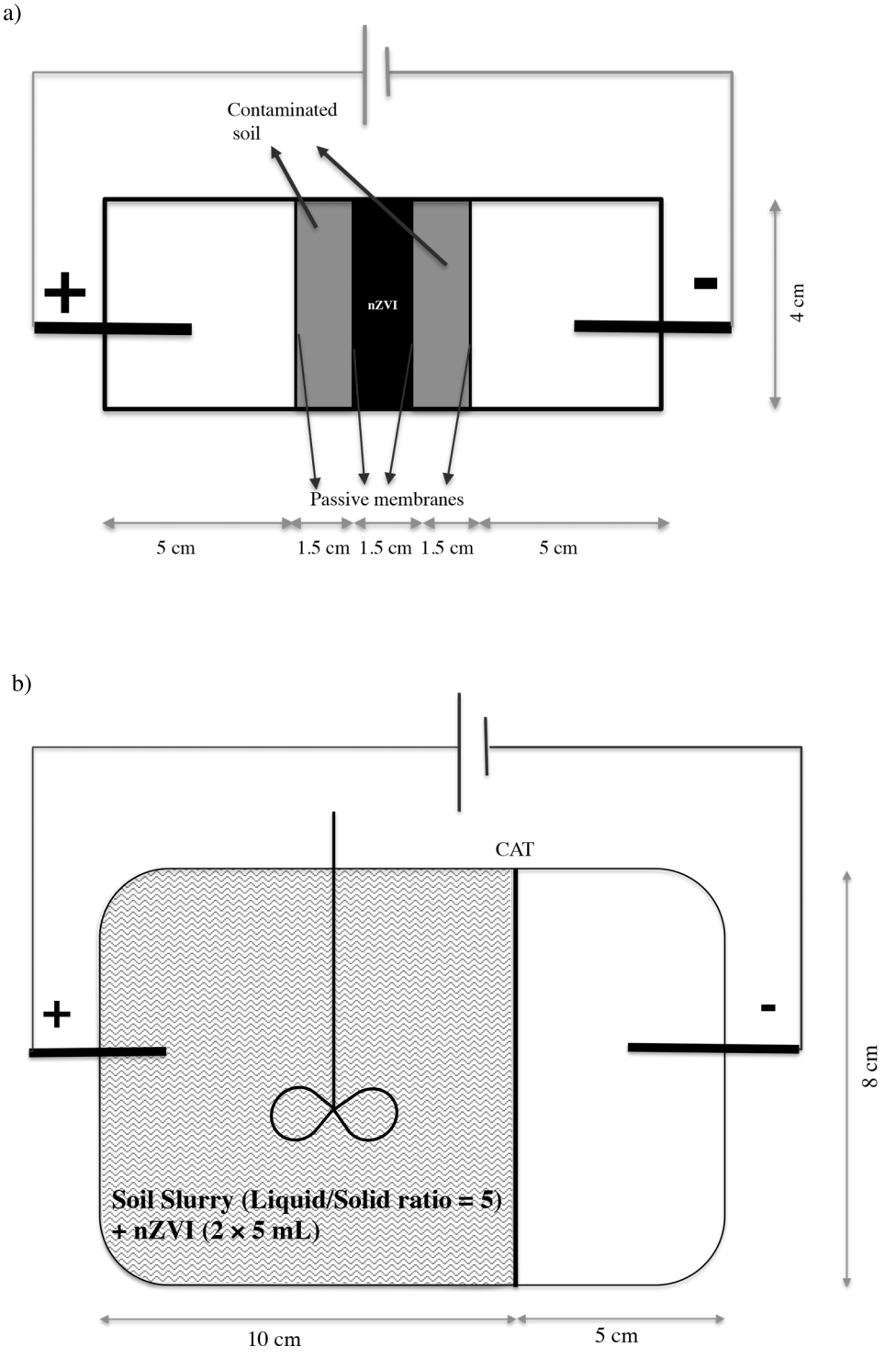


141 Figure 1 – Schematic representation of the experimental setups used in the experiments: a) three-compartment
142 electrokinetic cell and b) two-compartment electrodialytic cell (CAT = cation exchange membrane).
143

144 In both setups, a power supply (Hewlett Packard E3612A, Palo Alto, USA) was used
145 to maintain a constant voltage and the current was monitored (Fluke 179 multimeter). The
146 working electrodes were platinized titanium bars, with a diameter of 3 mm and a length of
147 5 cm in the three compartments cell and 10 cm in the two compartments cell (Permascand®).
148 Results from 10 new laboratory experiments are given in the present paper. For
149 completeness of the investigation, results from five previously reported experiments are
150 included. The experimental conditions are given in Table 1. As seen, experiments were made
151 with different combinations of (i) applied electric field, (ii) surfactant and (iii) nZVI. To
152 study the combined effect, experiments were made with all combinations with two techniques
153 and one experiment where all three techniques are combined. The experiments with
154 enhancement methods for the EKR include the use of saponin in the anode compartment
155 (Exp. B and O ), and also the pH control in the catholyte (Exp. M).
156 The electrolyte used was $10^{-2}$ M NaCl. In the two-chamber setup, the catholyte pH
157 was manually maintained around 2 by the addition of HCl 5M. The nZVI were placed in the
158 center of both cells, consisting of two injections of 5 mL at 24 and 48 h in the two-
159 compartment cell, and different injections in the three-compartment cell (Table 1).
160 The electric current between working electrodes, the pH in the soil suspension and in
161 the electrolytes were measured every 24 h. In the two-compartment cell, at the end of the
162 experiments, the suspension from the central compartment was filtered by gravity through
163 filter paper. In the three-compartment cell, samples from the anode and the cathode side were
164 collected separately. Subsamples were collected for humidity measurements. For both setups,
165 the soil was air-dried and crushed slightly in a mortar before the PCB extraction and pH
166 measurements. At the end of the experiments, the Fe contents in the different parts of the cell
167 (membranes, soil, solutions, and electrodes) were determined. The contents of Fe in the CAT
168 membranes and at the electrodes were measured after extraction in 1 M $HNO_3$ and 5 M

169 $HNO_3$, respectively. The Fe was extracted from soil by the sodium dithionite-citrate-
170 bicarbonate method [37] and from the passive membranes with concentrated HCl.

171

172 Table 1 – Summary of experimental conditions. In the two-compartment cell, the soil slurry had a liquid solid
173 ratio of 5.

| Exp. | nZVI (mL) | Type of injection | Exp. Setup | Voltage (V $cm^{-1}$) | Soil (g, dry weight) | Soil | Duration (d) | Observations |
|---|---|---|---|---|---|---|---|---|
| A | 13 | Unique (in the beginning of experiment) | 3 comp. cell | 2 | 65.30 | 1 | 10 | (1) |
| B | 13 | Unique (in the beginning of experiment) | 3 comp. cell. | 2 | 46.69 | 1 | 10 | 1% saponin solution in the anode compartment |
| C | 13 | Unique (in the beginning of experiment) | 3 comp. cell | 0 | 49.84 | 1 | 10 | No current |
| D | 10 | 2 injections of 5 mL at 24 and 48 h | 2 comp. cell | 1 | 69.94 | 1 | 45 | 1% saponin solution (2) |
| E | 10 | 2 injections of 5 mL at 24 and 48 h | 2 comp. cell | 0 | 50.01 | 1 | 5 | 1% saponin solution (2) |
| F | 10 | 2 injections of 5 mL at 24 and 48 h | 2 comp. cell | 1 | 50.05 | 1 | 5 | No surfactant (1) |
| G | 0 | 2 injections of 5 mL at 24 and 48 h | 2 comp. cell | 1 | 50.01 | 1 | 5 | 1% saponin solution, no nZVI (2) |
| H | 10 | 2 injections of 5 mL at 24 and 48 h | 2 comp. cell | 1 | 50.02 | 2 | 5 | 1% saponin solution |
| I | 10 | 2 injections of 5 mL at 24 and 48 h | 2 comp. cell | 0 | 50.02 | 2 | 5 | 1% saponin solution, no current |
| J | 0 | 2 injections of 5 mL at 24 and 48 h | 2 comp. cell | 1 | 50.05 | 2 | 5 | |
| K | 10 | 2 injections of 5 mL at 24 and 48 h | 2 comp. cell | 1 | 50.00 | 2 | 5 | No surfactant |
| L | 13 | Unique (in the beginning of experiment) | 3 comp. cell | 2 | 53.89 | 2 | 10 | |
| M | 13 | Unique (in the beginning of experiment) | 3 comp. cell | 2 | 55.20 | 2 | 10 | pH control in the cathode |
| N | 13 | Unique (in the beginning of experiment) | 3 comp. cell | 0 | 52.62 | 2 | 10 | No current |
| O | 13 | Unique (in the beginning of experiment) | 3 comp. cell | 2 | 56.59 | 2 | 10 | 1% saponin solution in the anode compartment |

174 (1) Data reported in [22]; (2) Data reported in [38]

175

176

177 **3. Results and Discussion**

178 *3.1 Soils characterization*

179 Table 2 presents the results from the soil characterization. Both soils are alkaline, but
180 Soil 1 has the highest pH value. As a carbonate rich soil has a pH around 7-8 [39], this
181 alkaline pH can be due to the presence of strong basis of industrial origin. Soil 1 is a mixture
182 of industrial contaminated soils, so it is also possible to have ashes from coal fired boilers or
183 power plants, rich in calcium oxide (CaO), which readily dissolves in water to form $Ca(OH)_2$
184 [40]. Comparing the soils, Soil 1 has a higher conductivity, higher organic matter content and
185 higher metal concentrations. The high organic matter content in Soil 1 is probably related to
186 the presence of transformer oils, as the soil origin and intense smell corroborate. Soil 2, on
187 the other hand, has a higher sum of exchangeable cations. The PCB congeners concentrations
188 are also different – Soil 1 has the highest PCB concentrations (sum of congeners PCB52, 65,
189 101, 138, 153, 180, 204 and 209) and also the highest concentrations of metals. The PCB
190 concentrations measured in the soils are above the guidance values for total PCB in Denmark,
191 although only some congeners were measured. In Denmark, the limit for soil quality is
192 0.02 mg $kg^{-1}$ total PCB and if the concentration exceeds 50 mg $kg^{-1,}$ the soil is classified as
193 hazardous waste [34]. In other countries (e.g. UK, Australia, USA), the threshold
194 concentration for the total PCB concentration in contaminated soil varies between
195 10-50 mg $kg^{-1}$ [41-43].
196
197

198 Table 2 – Physical and chemical characteristics of the soils.

| Parameter | Soil 1 | Soil 2 |
|---|---|---|
| Particles distribution (%) | | |
| Coarse sand (200 < Ø < 2000 μm) | 19.1 | 3.2 |
| Fine sand (20 < Ø < 200 μm) | 67.3 | 69.6 |
| Silt (2 < Ø < 20 μm) | 12.7 | 23.6 |
| Clay (Ø < 2 μm) | 0.9 | 3.6 |
| Textural classification | Loamy sand | Silty loam |
| pH ($H_2O$) | 12.2 | 8.20 |
| Conductivity (mS $cm^{-1}$) | 18.76 | 0.221 |
| Exchangeable cations ($cmol_{(c)}$ $kg^{-1}$) | | |
| $Ca^{2+}$ | 83.75 | 259.14 |
| $Mg^{2+}$ | 3.2 | 9.75 |
| $K^{+}$ | 26.88 | 7.36 |
| $Na^{+}$ | 9.37 | 8.34 |
| Sum of exchangeable cations ($cmol_{(c)}$ $kg^{-1}$) | 123.2 | 284.59 |
| Calcium carbonate (%) | 18.0 | 1.3 |
| Organic matter (%) | 16.46 | 0.57 |
| PCBs[a] (μg $kg^{-1}$) | 258 ± 24 | 156 ± 2 |
| Metals[b] (mg $kg^{-1}$) | | |
| Al | 20980 ± 590 | 4952± 71 |
| As | 9 ± 2 | 0.6 ± 0.97 |
| Cd | 0.7 ± 0.1 | 0.4 ± 0.04 |
| Cr | 52 ± 3 | 2.5 ± 0.04 |
| Cu | 142± 95 | 10 ± 0.3 |
| Fe | 13162 ± 301 | 6773± 97 |
| Ni | 32± 1 | 6 ± 0.3 |
| Pb | 45± 3 | 25 ± 0.9 |
| Zn | 2155 ± 40 | 135 ± 0.1 |

199 [a] Sum of PCB 52, 65, 101, 138, 153, 180, 204 and 209
200 [b] Acid digestion with $HNO_3$ according to the Danish Standard DS259.
201

202 *3.2 PCB dechlorination*

203 Figure 2 shows the total PCB removal at the end of the experiments using the two-
204 compartment cell. The results are different according to soil type. In general, the best results
205 were obtained with Soil 1. The highest removal percentage in Soil 1 can be related to the pH
206 of the soil slurry during the experiments (Figure 4). The initial soil pH and carbonate content
207 allowed to maintain the pH between 6 and 7 for about half the time of the experiment. In the
208 experiments with Soil 2, the pH values turn acidic faster (~30 h after the beginning of the
209 experiment), and this contributes to the nZVI corrosion. This is also consistent with the
210 higher PCB removal obtained in Soil 2 without the direct current, and consequently, without
211 acidification of the soil slurry.

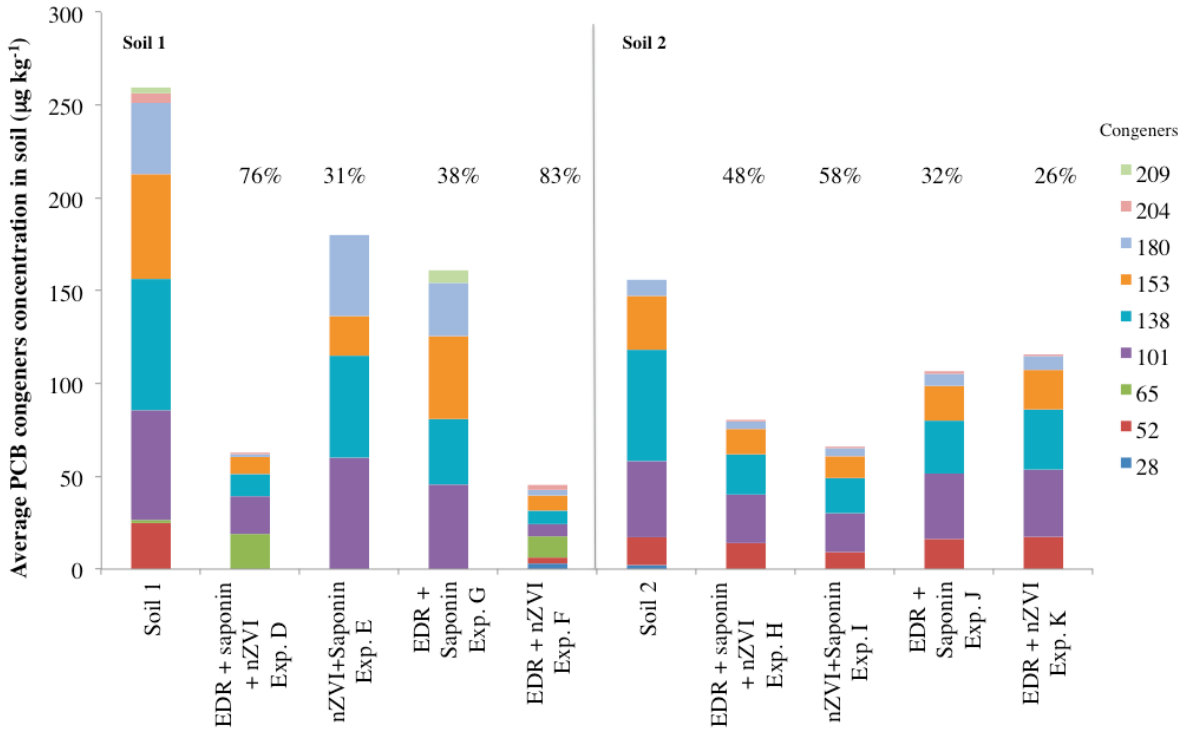


Figure 2 – Average concentration of PCB congeners (PCB28, 52, 65, 101, 138, 153, 180, 204 and 209) in Soils 1 and 2 before and after the experiments using the two-compartment cell. Percentages on the top of each column represent PCB removal regarding the sum of congeners analyzed in the initial soils.

Soil 1 has the higher PCB removal without the saponin, only with direct current, stirring and nZVI (83%). In Soil 2, the highest removal was obtained in the experiment I, only with nZVI and saponin. No significant differences were found in the EDR experiments for Soil 2 [one-way ANOVA, $F(3,20) = 0.69$, $p = 0.57$], although the experiment without the saponin (Exp. K) showed a lower removal percentage. Saponin, as a surfactant, should increase PCB desorption from soil, probably some interference with the nZVI dechlorination occurred. The dechlorination activity of nZVI decrease due to the polyelectrolyte coating, due to blocking of the available reactive surface sites, or by a combination of site blocking and inhibited mass transfer of chlorinated organic compounds in bulk solution to the nanoparticle surface [44, 45]. The pH of the suspended slurry also affects the surfactant behavior, influencing the micelle aggregation and their hydrophobicity. At high pH, the net

charge on the head groups of saponin molecule will increase, causing electrostatic repulsion between the head groups, which tends to increase the critical micelle concentration (CMC) values, reducing the solubilization capabilities of saponin [46].

The removal efficiencies in both soils with the three-compartment cell are much lower (Figure 3) than with the 2-compartment cell despite the longer duration of the experiments (Table 1). In Soil 1, the average PCB removal percentages were 26%, 60% and -34% for experiments A, B and C, respectively. The highest removal rate was obtained in the experiment with saponin in the anode compartment. The diffusion experiment in Soil 1 with the two compartments cell showed no PCB dechlorination. In Soil 2 (Figure 3B), the average removal percentages were 33%, 30%, 45% and 28% for experiments L, M, N and O, respectively. The highest removal percentage in Soil 2 corresponds to the experiment without direct current, only the nZVI injection. The use of saponin with Soil 2 (Exp. O) does not show any enhancement compared to the other experiments with that soil. Regarding the aqueous samples, only in experiments A, D, E and G some congeners were detected, due to the high PCB hydrophobicity and strong adsorption to soils.

Comparing the soil samples in the three-compartment cell (Figure 3), from the anode and cathode sides, in Soil 2, lower PCB concentrations are found in the cathode side, which can be related with the electroosmotic flow. While in Soil 1 no electroosmotic flow was observed, in experiments L, M and O it was 84, 36 and 78 mL (total of the 10 d), respectively. The experiment with pH control in the catholyte did not show any enhancement in PCB dechlorination when compared with the others, for Soil 2.

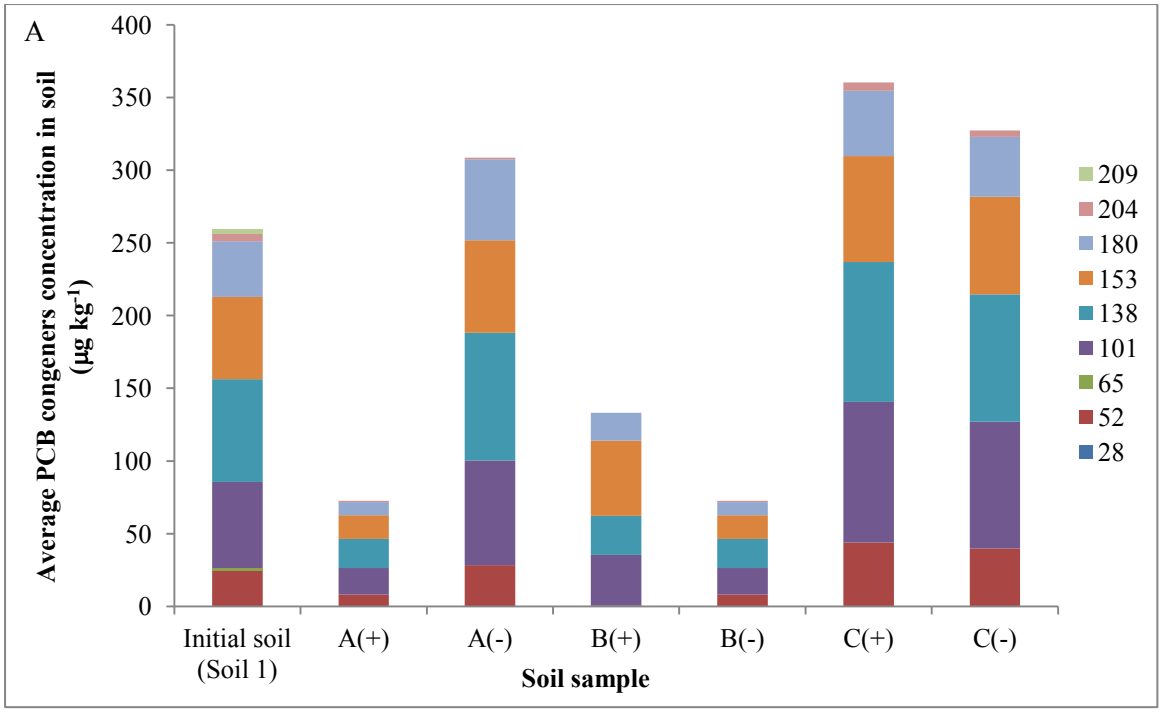


249

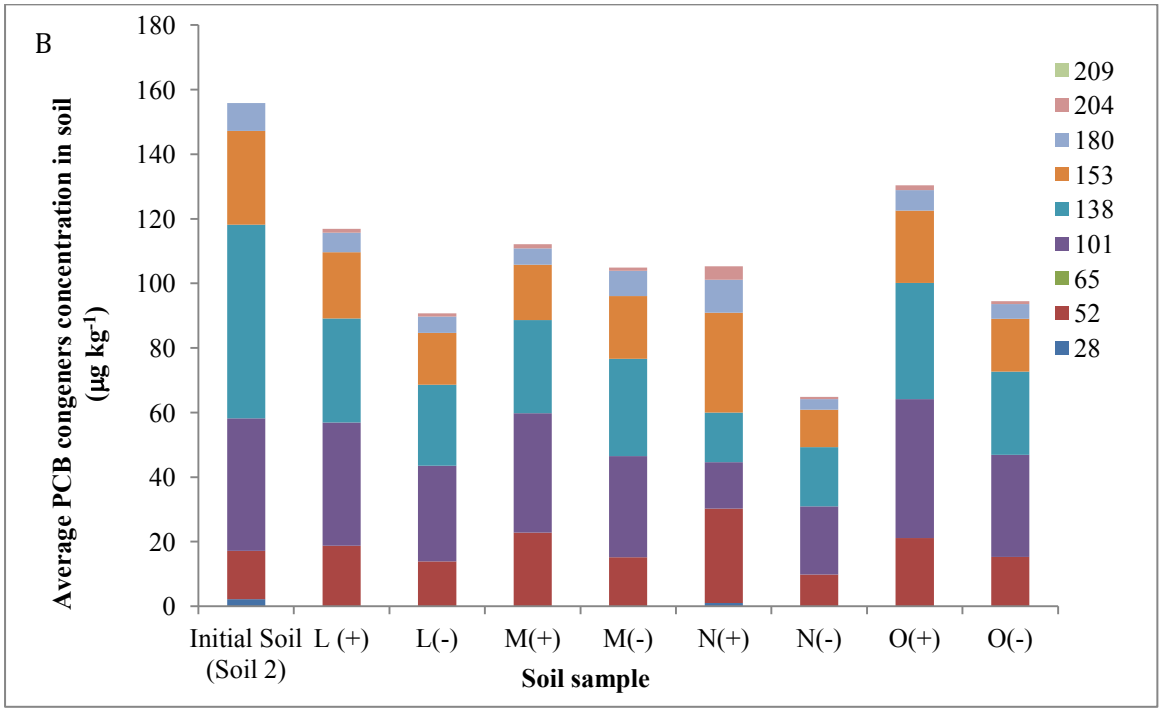


250

251 Figure 3 – Average concentration of PCB congeners (PCB28, 52, 65, 101, 138, 153, 180, 204 and 209) in the
252 soils before and after the experiments using the three-compartment cell in soil 1 (plot A) and soil 2 (plot B).
253 Each letter represents one the experiment. The symbol (+) indicates the soil sample of the anode side while (-)
254 indicates the soil sample from the cathode side. In the experiments without current (Exp. C and N), (+) indicates
255 the soil sample of the left side of the cell while (-) indicates the soil sample from the right side.

256

Soil is an heterogeneous medium and its spatial variability is not confined to field conditions, there is also variability among the samples and the intrinsic variability of the sample [47]. This variability can help explain some of the results, like the differences in the PCB removal between experiments D and E, for example, as well as the negative removal percentages obtained with the three compartments cell.

*3.3 pH variation*

In the two-compartment cell, the soil suspension pH during the experiments had lower values in Soil 2 compared to Soil 1, which is related to the lower initial pH and lower carbonates content (Figure 4). Although a slightly acidic pH (4.90–5.10) increases the PCB removal by nZVI and nZVI/Pd in aqueous solutions [48], the pH values in Soil 2 reached 2.91-3.35, which correspond to less favorable conditions to PCB dechlorination due to the nZVI corrosion. In all the experiments with nZVI, we observed higher pH values in the suspension. Without direct current the pH values showed very little variation.

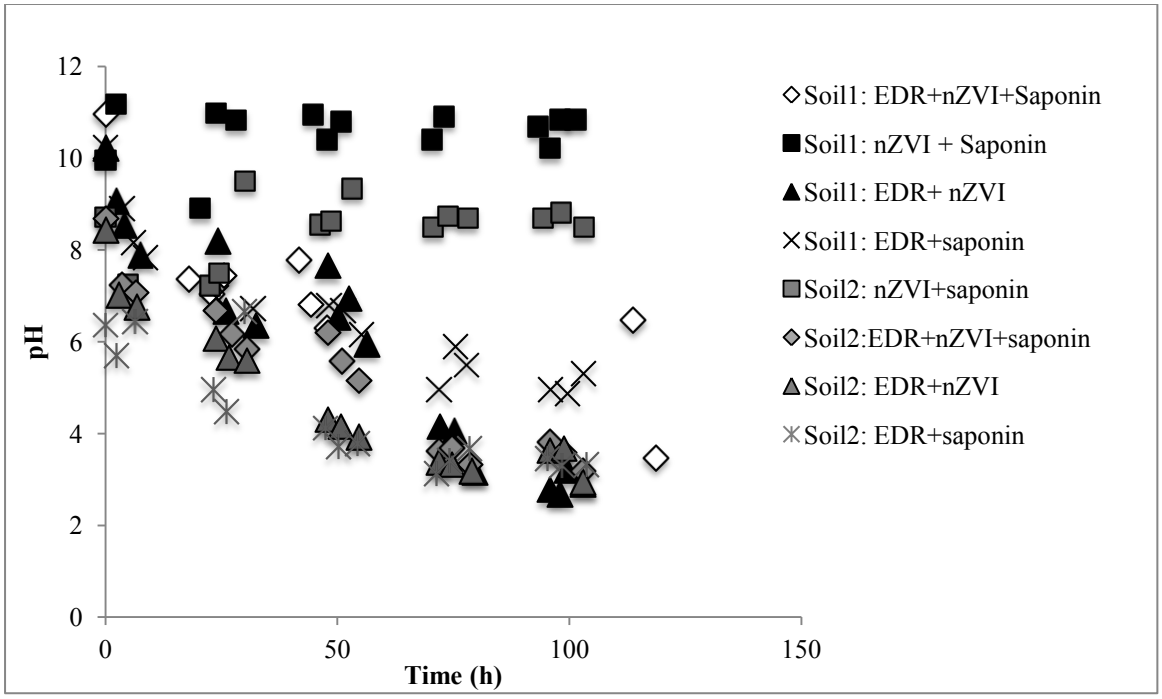


Figure 4 – Comparison of the pH evolution in the soil suspension in the two-compartment cell during the experiments.

274 Soil 1, with high buffer capacity, presents higher pH values in the soils at the end of
275 the experiments than Soil 2 in both cells (Table S2, Supplementary information), with
276 minimal changes in the three-compartment cell (Exp. A, B and C). Soil 2, in the three-
277 compartment cell, shows the traditional profile of the migration of the acid and alkaline
278 fronts, from the anode and the cathode, respectively. Experiment M, with pH control at the
279 catholyte, shows a neutral pH in the soil near that compartment. Experiment C and N show
280 the effect of the nZVI in the soil pH, without direct current, but only diffusive transport. In
281 the two-compartment cell, pH values are also higher for Soil 1 compared with Soil 2, due to
282 the higher initial pH. The lower pH value obtained for soil 1 was 5.70, much higher than 3.27
283 in Soil 2 (Exp. K).
284
285 *3.4 Iron content*
286 Figure 5 (A and B) shows the comparison between the mass of iron found in each
287 component of the three- and two-compartment cells, respectively, at the end of the
288 experiments. Previous studies showed that in the traditional three-compartment cell, most of
289 the nZVI aggregate and settle in the injection compartment [31, 49-51], thus not reaching the
290 contaminated soil. The suspended electrodialytic remediation assures that nZVI are mixed
291 with the soil, and most of the iron is found there at the end of the experiments.

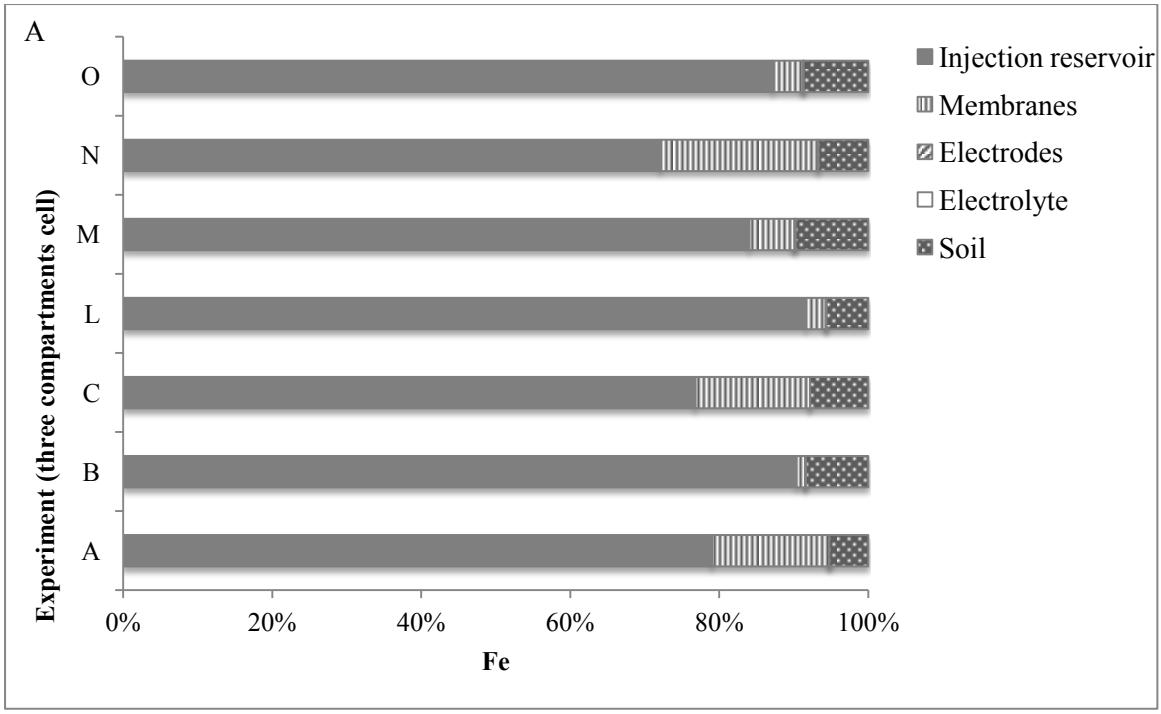


292

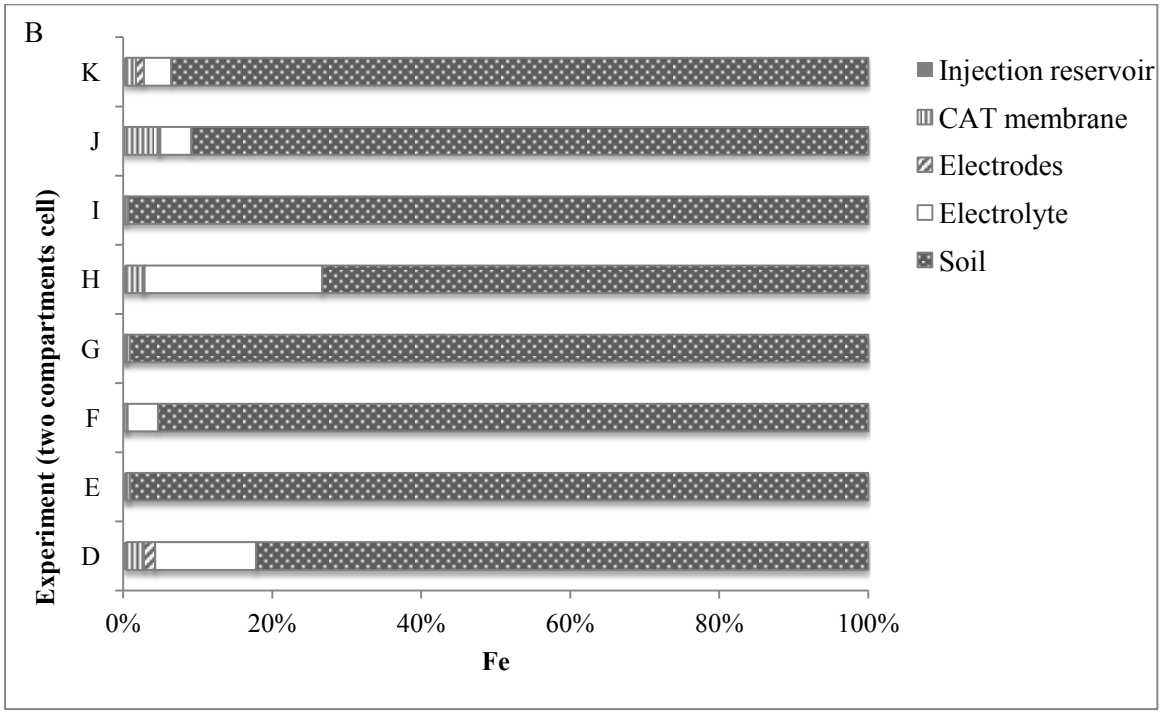


293

294 Figure 5 – Comparison of the mass of iron (%) found at the end of the experiments, with the setups tested: A)
295 three compartments cell, and B) two compartments cell.

296

297

## 4. Conclusions

The work compared two different historically contaminated soils and two different cells with different enhancements. Higher PCB removal percentages were obtained for Soil 1 (loamy sand with highest pH, carbonate content, organic matter and PCB concentrations) with the electrodialytic two-compartment cell, while for Soil 2 (silty loam with highest sum of exchangeable cations) only the nZVI addition in the three compartments cell allowed to obtain the highest removal percentage. The use of enhancement techniques such as surfactants (saponin) and pH control did not improve the PCB removal.

The use of the two-compartment cell allowed a uniform distribution of iron nanoparticles through the soil, while in the three-compartments cell, there was accumulation in the injection reservoir.

The results show that the soil characteristics, like pH and buffer capacity, are important and affect the reaction between nZVI and the target contaminant.

## Acknowledgments

This work was funded by the European Regional Development Fund (ERDF) through COMPETE – Operational Programme for Competitiveness Factors (OPCF), by Portuguese National funds through "FCT - Fundação para a Ciência e a Tecnologia" under project «PTDC/AGR-AAM/101643/2008 NanoDC», by FP7-PEOPLE-IRSES-2010-269289-ELECTROACROSS and by the research grant SFRH/BD/76070/2011. Prof. Jorge Varejão and Helena Silva are acknowledged for GC analysis and Sabrina Madsen for ICP analysis. NANO IRON, s.r.o. kindly provided NANOFER 25S samples.

## References


[1] A.B. Ribeiro, E.P. Mateus, L.M. Ottosen, G. Bech-Nielsen, Electrodialytic removal of Cu, Cr and As from chromated copper arsenate-treated timber waste, Environ. Sci. Technol., 34 (2000) 784-788.

[2] A.B. Ribeiro, J.M. Rodríguez-Maroto, Electroremediation of heavy metal-contaminated soils. Processes and applications, in: M.N.V. Prasad, K.S. Sajwan, R. Naidu (Eds.) Trace Elements in the Environment: Biogeochemistry, Biotechnology and Bioremediation, Taylor & Francis, CRC Press, Florida, USA, 2006, pp. 341-368.

[3] L.M. Ottosen, A.T. Lima, A.J. Pedersen, A.B. Ribeiro, Electrodialytic extraction of Cu, Pb and Cl from municipal solid waste incineration fly ash suspended in water, J. Chem. Technol. Biotechnol., 81 (2006) 553-559.

[4] L.M. Ottosen, P.E. Jensen, H.K. Hansen, A. Ribeiro, B. Allard, Electrodialytic remediation of soil slurry – Removal of Cu, Cr, and As, Sep. Sci. Technol., 44 (2009) 2245-2268.

[5] L.M. Ottosen, I.V. Christensen, I. Rörig-Dalgård, P.E. Jensen, H.K. Hansen, Utilization of electromigration in civil and environmental engineering—Processes, transport rates and matrix changes, J. Environ. Sci. Health A, 43 (2008) 795-809.

[6] A.B. Ribeiro, J.M. Rodríguez-Maroto, E.P. Mateus, H. Gomes, Removal of organic contaminants from soils by an electrokinetic process: The case of atrazine. Experimental and modeling, Chemosphere, 59 (2005) 1229–1239.

[7] A.B. Ribeiro, E.P. Mateus, J.-M. Rodríguez-Maroto, Removal of organic contaminants from soils by an electrokinetic process: The case of molinate and bentazone. Experimental and modeling, Sep. Purif .Technol., 79 (2011) 193-203.

[8] C. Ferreira, A. Ribeiro, L. Ottosen, Effect of major constituents of MSW fly ash during electrodialytic remediation of heavy metals, Sep. Sci. Technol., 40 (2005) 2007-2019.

346 [9] Y.B. Acar, A.N. Alshawabkeh, Principles of electrokinetic remediation, Environ. Sci.
347 Technol., 27 (1993) 2638-2647.
348 [10] H.I. Gomes, C. Dias-Ferreira, A.B. Ribeiro, Electrokinetic remediation of
349 organochlorines in soil: Enhancement techniques and integration with other remediation
350 technologies, Chemosphere, 87 (2012) 1077-1090.
351 [11] P.E. Jensen, L.M. Ottosen, C. Ferreira, Electrodialytic remediation of soil fines
352 (<63 μm) in suspension—Influence of current strength and L/S, Electrochim. Acta, 52
353 (2007) 3412-3419.
354 [12] T.R. Sun, L.M. Ottosen, P.E. Jensen, G.M. Kirkelund, Electrodialytic remediation of
355 suspended soil – Comparison of two different soil fractions, J. Hazard. Mater., 203–204
356 (2012) 229-235.
357 [13] L. Ottosen, P. Jensen, G. Kirkelund, H. Hansen, Electrodialytic remediation of different
358 heavy metal-polluted soils in suspension, Water Air Soil Poll., 224 (2013) 1-10.
359 [14] L.M. Ottosen, P.E. Jensen, G.M. Kirkelund, B. Ebbers, Electrodialytic separation of
360 heavy metals from particulate material. Patent application EPC 13183278.4-1352, 2013.
361 [15] H.I. Gomes, C. Dias-Ferreira, A.B. Ribeiro, Overview of *in situ* and *ex situ* remediation
362 technologies for PCB-contaminated soils and sediments and obstacles for full-scale
363 application, Sci. Total Environ., 445-446 (2013) 237-260.
364 [16] G. Lowry, K. Johnson, Congener-specific dechlorination of dissolved PCBs by
365 microscale and nanoscale zerovalent iron in a water/methanol solution, Environ. Sci.
366 Technol., 38 (2004) 5208-5216.
367 [17] C.B. Wang, W. Zhang, Synthesizing nanoscale iron particles for rapid and complete
368 dechlorination of TCE and PCBs, Environ. Sci. Technol., 31 (1997) 2154-2156.

369 [18] F. He, D. Zhao, C. Paul, Field assessment of carboxymethyl cellulose stabilized iron
370 nanoparticles for *in situ* destruction of chlorinated solvents in source zones, Water Res.,
371 44 (2010) 2360–2370.
372 [19] P. Varanasi, A. Fullana, S. Sidhu, Remediation of PCB contaminated soils using iron
373 nano-particles, Chemosphere, 66 (2007) 1031–1038.
374 [20] X. Chen, X. Yao, C. Yu, X. Su, C. Shen, C. Chen, R. Huang, X. Xu,
375 Hydrodechlorination of polychlorinated biphenyls in contaminated soil from an e-waste
376 recycling area, using nanoscale zerovalent iron and Pd/Fe bimetallic nanoparticles,
377 Environ. Sci. Poll. Res., (2014) 1-10.
378 [21] G. Fan, L. Cang, W. Qin, C. Zhou, H.I. Gomes, D. Zhou, Surfactants-enhanced
379 electrokinetic transport of xanthan gum stabilized nano Pd/Fe for the remediation of
380 PCBs contaminated soils, Sep. Purif. Technol., 114 (2013) 64-72.
381 [22] H.I. Gomes, C. Dias-Ferreira, L.M. Ottosen, A.B. Ribeiro, Electroremediation of PCB
382 contaminated soil with iron nanoparticles: Performance of a new electrodialytic setup.
383 Submitted.
384 [23] K.R. Reddy, U.S. Parupudi, S.N. Devulapalli, C.Y. Xu, Effects of soil composition on
385 the removal of chromium by electrokinetics, J. Hazard. Mater., 55 (1997) 135-158.
386 [24] J.H. Kim, S.J. Han, S.S. Kim, J.W. Yang, Effect of soil chemical properties on the
387 remediation of phenanthrene-contaminated soil by electrokinetic-Fenton process,
388 Chemosphere, 63 (2006) 1667-1676.
389 [25] V.R. Ouhadi, R.N. Yong, N. Shariatmadari, S. Saeidijam, A.R. Goodarzi, M. Safari-
390 Zanjani, Impact of carbonate on the efficiency of heavy metal removal from kaolinite
391 soil by the electrokinetic soil remediation method, J. Hazard. Mater., 173 (2010) 87-94.
392 [26] K. Reddy, R. Saichek, Effect of soil type on electrokinetic removal of phenanthrene
393 using surfactants and cosolvents, J. Environ. Eng., 129 (2003) 336-346.

394 [27] E. Mena, J. Villaseñor, P. Cañizares, M.A. Rodrigo, Influence of soil texture on the
395 electrokinetic transport of diesel-degrading microorganisms, J. Environ. Sci. Health A,
396 46 (2011) 914-919.
397 [28] C. Cameselle, K.R. Reddy, Development and enhancement of electro-osmotic flow for
398 the removal of contaminants from soils, Electrochim. Acta, 86 (2012) 10-22.
399 [29] L.M. Ottosen, H.K. Hansen, A.B. Ribeiro, A. Villumsen, Removal of Cu, Pb and Zn in
400 an applied electric field in calcareous and non-calcareous soils, J. Hazard. Mater., 85
401 (2001) 291-299.
402 [30] G.C.C. Yang, Y.I. Chang, Integration of emulsified nanoiron injection with the
403 electrokinetic process for remediation of trichloroethylene in saturated soil, Sep. Purif.
404 Technol., 79 (2011) 278–284.
405 [31] H.I. Gomes, C. Dias-Ferreira, A.B. Ribeiro, S. Pamukcu, Enhanced transport and
406 transformation of zerovalent nanoiron in clay using direct electric current, Water Air Soil
407 Poll., 224 (2013) 1-12.
408 [32] R. Lageman, W. Pool, Experiences with field applications of electrokinetic remediation,
409 in: K.R. Reddy, C. Cameselle (Eds.) Electrochemical Remediation Technologies for
410 Polluted soils, Sediments and Groundwater, John Wiley & Sons, Inc., Hoboken, New
411 Jersey, 2009, pp. 697-717.
412 [33] A. Asadi, B.K. Huat, M. Hanafi, T. Mohamed, N. Shariatmadari, Role of organic matter
413 on electroosmotic properties and ionic modification of organic soils, Geosciences J., 13
414 (2009) 175-181.
415 [34] S.F. Jensen, PCB in Soil. The Contamination of PCB in Selected Locations around
416 Roskilde and Copenhagen, Report, Roskilde University, Denmark, 2009.

417 [35] M. Cao, Y. Hu, Q. Sun, L. Wang, J. Chen, X. Lu, Enhanced desorption of PCB and trace
418 metal elements (Pb and Cu) from contaminated soils by saponin and EDDS mixed
419 solution, Environ. Poll., 174 (2013) 93-99.
420 [36] H. Xia, X. Chi, Z. Yan, W. Cheng, Enhancing plant uptake of polychlorinated biphenyls
421 and cadmium using tea saponin, Biores. Technol., 100 (2009) 4649-4653.
422 [37] O.P. Mehra, M.L. Jackson, Iron oxide removal from soils and clays by a dithionite-
423 citrate system buffered with sodium bicarbonate, Clays Clay Miner., 7 (1960) 317-327.
424 [38] H.I. Gomes, C. Dias-Ferreira, L.M. Ottosen, A.B. Ribeiro, Electrodialytic remediation of
425 PCB contaminated soil with iron nanoparticles and two different surfactants. Submitted
426 [39] L. Ottosen, H. Hansen, P. Jensen, Relation between pH and desorption of Cu, Cr, Zn,
427 and Pb from industrially polluted soils, Water Air Soil Poll., 201 (2009) 295-304.
428 [40] A. Lopareva-Pohu, B. Pourrut, C. Waterlot, G. Garçon, G. Bidar, C. Pruvot, P. Shirali,
429 F. Douay, Assessment of fly ash-aided phytostabilisation of highly contaminated soils
430 after an 8-year field trial: Part 1. Influence on soil parameters and metal extractability,
431 Sci. Total Environ., 409 (2011) 647-654.
432 [41] CCME, Canadian Soil Quality Guidelines for the Protection of Environmental and
433 Human Health. Total PCBs. Canadian Environmental Quality Guidelines. Canadian
434 Council of Ministers of Environment, 1999.
435 [42] EPA, Industrial Waste Resource Guidelines. Environment Protection (Industrial Waste
436 Resource) Regulations 2009. Publication IWRG643.1. Environmental Protection Agency
437 Victoria, Australia, 2009.
438 [43] USEPA, PCB regulations at 40 CFR Part 761. United States Environmental Protection
439 Agency. Toxic Substances Control Act, 2012.

[44] F. He, D. Zhao, Hydrodechlorination of trichloroethene using stabilized Fe-Pd nanoparticles: Reaction mechanism and effects of stabilizers, catalysts and reaction conditions, App. Catal. B, 84 (2008) 533-540.

[45] T. Phenrat, Y. Liu, R.D. Tilton, G.V. Lowry, Adsorbed polyelectrolyte coatings decrease $Fe^0$ nanoparticle reactivity with TCE in water: Conceptual model and mechanisms, Environ. Sci. Technol., 43 (2009) 1507-1514.

[46] W. Zhou, J. Yang, L. Lou, L. Zhu, Solubilization properties of polycyclic aromatic hydrocarbons by saponin, a plant-derived biosurfactant, Environ. Pollut., 159 (2011) 1198-1204.

[47] B. Yaron, R. Prost, R. Calvet, Soil Pollution Processes and Dynamics. New York Springer-Verlag Berlin Heidelberg, 1996.

[48] Y. Wang, D. Zhou, Y. Wang, L. Wang, L. Cang, Automatic pH control system enhances the dechlorination of 2,4,4'-trichlorobiphenyl and extracted PCBs from contaminated soil by nanoscale $Fe^0$ and Pd/$Fe^0$, Environ. Sci. Pollut. Res., 19 (2012) 448-457.

[49] H.I. Gomes, C. Dias-Ferreira, A.B. Ribeiro, S. Pamukcu, Influence of electrolyte and voltage on the direct current enhanced transport of iron nanoparticles in clay, Chemosphere, 99 (2014) 171-179.

[50] K.R. Reddy, K. Darko-Kagy, C. Cameselle, Electrokinetic-enhanced transport of lactate-modified nanoscale iron particles for degradation of dinitrotoluene in clayey soils, Sep. Purif. Technol., 79 (2011) 230-237.

[51] H.I. Gomes, G. Fan, E.P. Mateus, C. Dias-Ferreira, A.B. Ribeiro, Assessment of combined electro–nanoremediation of molinate contaminated soil, Sci. Total Environ., 493 (2014) 178-184.

# Enhanced electrokinetic techniques for remediation of different PCB polluted soils

## Supplementary information

Helena I. Gomes[1,2,3], Celia Dias-Ferreira[2], Lisbeth M. Ottosen[3], Alexandra B. Ribeiro[1]

[1]CENSE - Center for Environmental and Sustainability Research, Departamento de Ciências e Engenharia do Ambiente, Faculdade de Ciências e Tecnologia, Universidade Nova de Lisboa, 2829-516 Caparica, Portugal
[2]CERNAS – Research Center for Natural Resources, Environment and Society, Escola Superior Agraria de Coimbra, Instituto Politecnico de Coimbra, Bencanta, 3045-601 Coimbra, Portugal
[3]Department of Civil Engineering, Technical University of Denmark, Brovej, Building 118, DK 2800 Kgs. Lyngby, Denmark
* Corresponding author. Tel. +351 212948300, Fax. +351 212948554. E-mail address: hrg@campus.fct.unl.pt (Helena I. Gomes)

Table S1 – Characterization of the zero valent iron nanoparticles used in the experiments, according to the supplier information.

| | |
|---|---|
| **Product Name** | NANOFER 25S (NANO IRON, s.r.o.) |
| **Stabilizer** | Polyacrylic acid (PAA) |
| **pH** | 11-12 |
| **Density** | 1.15 – 1.25 g $cm^{-3}$ (20°C) |
| **Average particles size** | 50 nm |
| **Particle size distribution** | 20-100 nm |
| **Average surface area** | 20-25 $m^2 g^{-1}$ |
| **Iron content** | 80-90 wt. % |

Table S2 – Soil pH at the end of the experiments. Initial soil pH is 12.2 for Soil 1 and 8.20 for Soil 2.

| **Three-compartment cell** | | | **Two-compartment cell** | |
|---|---|---|---|---|
| Exp. | Anode side | Cathode side | Exp. | Soil pH |
| A | 11.28 | 12.18 | D | 8.49 |
| B | 11.37 | 12.06 | E | 9.72 |
| C | 12.25 | 12.07 | F | 5.70 |
| L | 5.23 | 11.57 | G | 7.69 |
| M | 3.61 | 7.58 | H | 3.05 |
| N | 9.63 | 9.54 | I | 8.01 |
| O | 5.55 | 11.72 | J | 2.96 |
| | | | K | 2.37 |

# II.10 Numerical prediction of diffusion and electric field-induced iron nanoparticle transport (submitted)

# Numerical prediction of diffusion and electric field-induced iron nanoparticle transport

Helena I. Gomes[a,d], José Miguel Rodríguez-Maroto[b,1], Alexandra B. Ribeiro[a], Sibel Pamukcu[c,1], Celia Dias-Ferreira[d]

[a] CENSE, Departamento de Ciências e Engenharia do Ambiente, Faculdade de Ciências e Tecnologia, Universidade Nova de Lisboa, 2829-516 Caparica, Portugal

[b] Department of Chemical Engineering, University of Málaga, Campus de Teatinos, 29071-Málaga, Spain

[c] Department of Civil and Environmental Engineering, Fritz Engineering Laboratory, 13 E. Packer Avenue, Lehigh University, Bethlehem, PA 18015-4729, USA

[d] CERNAS – Research Center for Natural Resources, Environment and Society, Escola Superior Agraria de Coimbra, Instituto Politecnico de Coimbra, Bencanta, 3045-601 Coimbra, Portugal

* Corresponding author. Tel. +351 212948300, Fax. +351 212948554. E-mail address: hrg@campus.fct.unl.pt (Helena I. Gomes)

[1] ISE member

**Abstract**

Zero valent iron nanoparticles (nZVI) are considered very promising for the remediation of contaminated soils and groundwaters. However, an important issue related to their limited mobility remains unsolved. Direct current can be used to enhance the nanoparticles transport, based on the same principles of electrokinetic remediation. In this work, a generalized physicochemical model was developed and solved numerically to describe the nZVI transport through porous media under electric field, and with different electrolytes (with different ionic strengths). The model consists of the Nernst–Planck coupled system of equations, which accounts for the mass balance of ionic species in a fluid medium, when both the diffusion and electromigration of the ions are considered. The diffusion and electrophoretic transport of the negatively charged nZVI particles were also considered in the system. The contribution of electroosmotic flow to the overall mass transport was included in the model for all cases. The nZVI effective mobility values in the porous medium are very low ($10^{-7}$-$10^{-4}$ $cm^2$ $V^{-1}$ $s^{-1}$), due to the counterbalance between the positive electroosmotic flow and the electrophoretic transport of the negatively charged nanoparticles. The higher the nZVI concentration is in the matrix, the higher the aggregation; therefore, low concentration of nZVI suspensions must be used for successful field application.

## Highlights

- Numerical model describes the nZVI transport by diffusion and under electric fields
- Data from different porosity media and electrolytes were used to validate the model
- Diffusion, electromigration, electrophoresis and electroosmosis were considered
- Aggregation of nZVI particles due to high suspension concentrations
- Electrophoretic transport of the nZVI is counteracted by electroosmosis

## Keywords

Electrokinetics; nZVI; porous media; electrolytes; Nernst–Planck equations

## 1. Introduction

Zero valent iron was used successfully for soil and groundwater remediation in permeable reactive barriers for more than two decades [1-3]. With the development of advanced nanotechnologies since late nineties, due to their size and reactivity that allowed an easy injection, zero valent iron nanoparticles (nZVI) were considered a promising step forward in soil and groundwater clean-up, particularly targeting organochlorines [4-8]. The nZVI transport in porous media was studied in column tests with sand [9-16], glass beads [17-19] and model soils [20, 21]. These studies showed that nZVI has a tendency to aggregate quickly and settle in the pores, primarily due to magnetic attractive forces [22]. Results from field scale applications [23-27] confirm this limited mobility, ranging from 1 m [28] to 6-10 m [26], depending on soil characteristics, test operations, and injection velocities [29].

One of the methods tested to overcome poor nZVI mobility was the use of direct current (DC) [16, 30-34], using the same principles of electrokinetic remediation (EKR). In this method, low-level direct current is the "cleaning agent", inducing different transport mechanisms (electroosmosis, electromigration and electrophoresis) and electrochemical reactions (electrolysis and electrodeposition) in contaminated soils [35]. Direct comparison of the results provided in previous studies on nZVI enhanced transport with direct current is limited due to the differences in experimental setups, soils or other solid media used, types of iron nanoparticles, injection places (i.e., directly in the soil, anode or cathode compartments), magnitude and duration of the voltage gradients applied. In general electrophoretic transport of the particles was shown to be predominant in sandy soil [33, 36, 37], while electro-osmotic transport appeared more important in kaolin clay and loamy sand soil [16, 32]. The available analytical models of the nanoparticle transport in literature include only the electrophoretic effect that mostly takes place in sands [33, 37].

In this work, a generalized physicochemical model has been developed to describe the electrically induced transport of nZVI particles through different types of porous media of varying porosity and surface reactivity. The model is sufficiently detailed, including the fundamental processes, and its numerical solution offers a reliable prediction of the nZVI transport. Experimental data using different porosity media and different pore fluid electrolytes were used to validate the model [30, 31].

## 2. Model Description

The analytical model operates in two steps: first the kinetic process is simulated by integrating forward in time the one-dimensional transport equations, including the electrochemical reactions at the electrodes; then the chemical equilibriums are reestablished before the next step of integration. This is done because chemical equilibriums are considered instantaneous when compared with the transport time.

### *2.1. General description of experiments used to validate model*

The experimental data used for the validation of the model have been published previously by Gomes et al [30, 31], where the experimental conditions are described in detail. The experiments were designed so that the transport of nZVI took place in the domain of a layer of porous solid (kaolin and/or glass beads) saturated with an electrolyte.

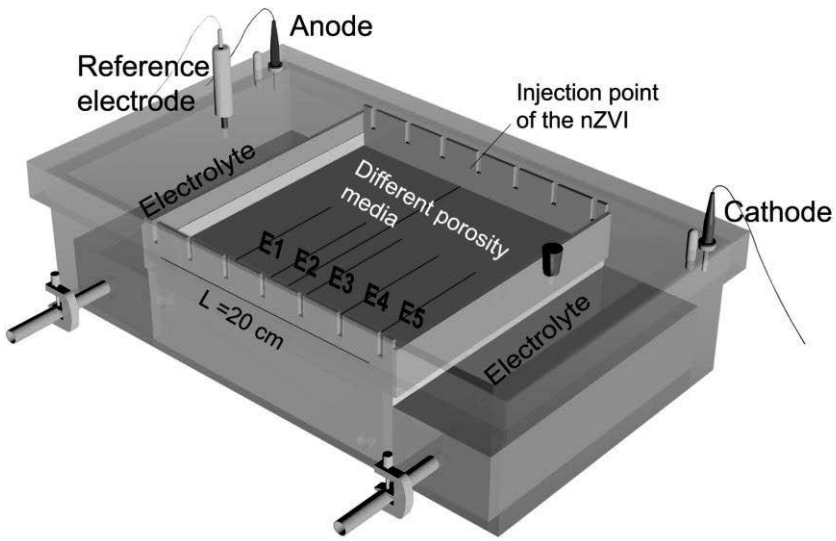


Figure 1. Modified electrophoretic cell used in the experiments [30, 31]. E1 to E5 are auxiliary platinum electrodes and represent the locations of the solid samples for iron quantification.

The experiments were conducted in a modified electrophoretic cell (Econo-Submarine Gel Unit, model SGE-020) as shown in Figure 1. The cell is a rectangular translucent box 10 cm height, 40 cm long and 23 cm width, with a square (20 cm x 20 cm) sample tray and a lid that covers the whole apparatus. Two liquid chambers hold the anolyte and the catholyte and platinum working electrodes on either side of the sample tray (Figure 1). In all experiments, both the anolyte and catholyte compartments were filled with the same electrolyte solution (volume of 650 mL each, Table 1) as that used to saturate the porous specimen. The level of the solutions in the side compartments was kept slightly below the specimen surface, thus preventing preferential transport of nZVI through a liquid pool over the specimen. Compressed fiberglass wool pads, saturated and immersed in the electrolyte solution, helped transport the migrating ions from the solution into the specimen and vice versa. Different porosity and surface reactivity test media, ranging from glass beads (with

particle diameter less than 1 mm, previously sieved) to white Georgia kaolinite clay (> 2 μm) were used in the transport experiments (Table 1). The PAA-nZVI suspensions were freshly prepared before each experiment and had a concentration of 4 g $L^{-1}$ of nZVI. The particle size distribution of the nanoparticles had a mean particle diameter value of 62.66±39.6 nm and the median size was 60.2 nm, based on a count of 420 particles in TEM images [30, 31]. Two sets of control experiments were conducted for each mixture under the same conditions, one without direct current but with PAA-nZVI, and another with current but without PAA-nZVI. In the experiments with current, a constant potential was applied for 48 h. The cell was kept in a dark location to prevent iron photo-oxidation. The nanoparticle suspension was delivered in the electrophoretic cell using a syringe to inject 2 mL through a tube, which allowed the suspension disperse into a pre-cut shallow channel in the porous specimen between the auxiliary electrodes E2 and E3.

*2.2. Governing equations*

The mass conservation equation for $i^{th}$ species in a $j^{th}$ volume element, including electrochemical reactions, is described by:

$$V_j\left(\frac{dc_{ij}}{dt}\right) = \left(N_{i,j-1} + N_{i,j}\right)A + R_i V_j \qquad (1)$$

where $V_j$ is volume of water in $j^{th}$ cell ($cm^3$), $c_{ij}$ is the concentration of $i^{th}$ species (ions and nZVI) in the aqueous phase of the $j^{th}$ volume element (mol $cm^{-3}$), $t$ is the time, $N_{i,j-1}$ and $N_{i,j}$ the mass flux of $i^{th}$ species from $(j-1)^{th}$ into $j^{th}$ element volume and from $j^{th}$ into $(j+1)_{th}$ volume element (mol $cm^2$ $s^{-1}$), $A$ cross-sectional area of the domain ($cm^2$), and $R_i$ the reaction rate for $i$ species. With respect to the chemical reactions, only the chemical equilibria and the electrochemical reactions at the electrodes are considered.

The model consists of a coupled system of Nernst–Planck equations, which accounts for the mass balance of the ionic species in a fluid medium, when diffusion and electromigration are considered in the transport process. In the case of charged nZVI (i.e., the nanoparticles are stabilized with polyacrylic acid – PAA, which gives them the negative charge), diffusion and electrophoretic terms have to be taken into account. The electroosmotic flow is included in all cases.

Therefore, the flux of any chemical species or charged particles $i$ from a $j^{th}$ volume element of the system can be expressed as:

$$N_i = -D_i^* \nabla c_i - U_i^* c_i \nabla \phi - k_e c_i \nabla \phi \quad (2)$$

where (sub index $j$ is omitted), $c_i$ is the molar concentration, $D_i^*$ is the effective diffusion coefficient, and $\nabla\phi$ is the electrical potential, $k_e$ is the electroosmotic permeability coefficient and $U_i^*$, is the effective electrophoretic mobility for nZVI charged particles or effective ionic mobility, estimated by the Einstein–Nernst relation for ions [38]:

$$U_i^* = \frac{D_i^* z_i F}{RT} \quad (3)$$

where $R$ is the ideal gas constant, $F$ is the Faraday constant, $z_i$ is the ionic charge of the species and $T$ is the temperature (K), assuming a constant room temperature of 25 ºC. The value of the electroosmotic permeability usually is in a very tight range of $10^{-5}$ to $10^{-4}$ cm$^2$ s$^{-1}$ V$^{-1}$ [39]. Electroosmotic permeability and mobility can be combined into a new effective mobility in the porous medium, $U_i^{**}$:

$$U_i^{**} = U_i^* + k_e \quad (4)$$

The mass balance equations for nZVI and the ionic species are integrated over the one-dimensional region limited by the electrodes compartments in order to obtain the concentration profile for a given set of experimental conditions. Due to the negative charge of

polyacrylic acid coated nZVI, the sign of electrophoretic term is negative, whereas the electroosmotic term is positive, resulting in a low value for the effective mobility.

Table 1 shows the experimental conditions and parameters used in solution of the model to simulate the experimental tests. The nZVI effective diffusion coefficient values in Table 1 were obtained from fitting the experimental results, that varied between $0.5 \times 10^{-5}$ and $5.9 \times 10^{-5}$ $cm^2 s^{-1}$. The electrophoretic mobility (EPM) of PAA-nZVI was obtained from experimental measures for the different particle suspensions using Laser Doppler Velocimetry in a ZetaSizer Nano ZS, Malvern (Southborough, MA). Stock suspensions of PAA-nZVI were diluted to 2 g $L^{-1}$ to obtain measurements for the electrolytes used in the transport tests.

Table 1. Parameters used in modeling to simulate the experimental tests

**Solid layer length, $L$**: 20 cm
**Solid layer Area, $A$**: 10 $cm^2$ or 4 $cm^2$
**Number of volume elements used to represented solid column, $N$**: 20
**Electrode compartment volume, $V_0$ and $V_{N+1}$**: 650 $cm^3$
$\eta = 1$
$\Delta t$: 5 seconds
**Initial mass of nZVI injected in the system**: 0.008 g (2 mL of 4 g $L^{-1}$ solution)
**Electric Potential**: 5 V (Experiments 5 to 11) and 10 V (Experiment 12)

| **Diffusion control tests** | | | | | | |
|---|---|---|---|---|---|---|
| **Test number** | **Layer thickness (mm)** | **Matrix** | **Porosity** | **Electrolyte** | $D^*_{nZVI}\left(cm^2 s^{-1}\right)$ | $U^*_{nZVI}\left(cm^2 V^{-1} s^{-1}\right)$ |
| 1 | 5 | 100% Kaolin | 0.65 | NaCl (0.001M) | $5.9\ 10^{-5}$ | $-\ 1.7\ 10^{-4}$ |
| 2 | 2 | 50% glass beads and 50% kaolin | 0.57 | NaCl (0.001M) | $4.6\ 10^{-5}$ | $-\ 1.5\ 10^{-4}$ |
| 3 | 2 | 75% glass beads and 25% kaolin | 0.35 | NaCl (0.001M) | $3.9\ 10^{-5}$ | $-\ 0.9\ 10^{-4}$ |
| 4 | 2 | 100% glass beads | 0.20 | NaCl (0.001M) | $1.8\ 10^{-5}$ | $-\ 0.5\ 10^{-4}$ |
| **Enhanced transport tests** | | | | | | |
| **Test number** | **Layer thickness (mm)** | **Matrix** | **Porosity** | **Electrolyte** | $D^*_{nZVI}\left(cm^2 s^{-1}\right)$ | $U^*_{nZVI}\left(cm^2 V^{-1} s^{-1}\right)$ |
| 5 | 5 | 100% Kaolin | 0.65 | NaCl (0.001M) | $1.6\ 10^{-5}$ | $-\ 1.1\ 10^{-4}$ |
| 6 | 2 | 50% glass beads and 50 % kaolin | 0.57 | NaCl (0.001M) | $2.8\ 10^{-5}$ | $2.4\ 10^{-5}$ |
| 7 | 2 | 75% glass beads and 25% kaolin | 0.35 | NaCl (0.001M) | $1.4\ 10^{-5}$ | $2.1\ 10^{-6}$ |
| 8 | 2 | 100% glass beads | 0.20 | NaCl (0.001M) | $4.6\ 10^{-6}$ | $8\ 10^{-6}$ |
| 9 | 5 | 100% Kaolin | 0.65 | NaOH (0.001M) | $1.7\ 10^{-5}$ | $4.7\ 10^{-5}$ |
| 10 | 5 | 100% Kaolin | 0.65 | $CaCl_2$ (0.05M) | $4.8\ 10^{-5}$ | $-9.7\ 10^{-7}$ |
| 11 | 5 | 100% Kaolin | 0.65 | $Na_2SO_3$ (0.1M) | $3.3\ 10^{-5}$ | $1.8\ 10^{-4}$ |
| 12 | 5 | 100% Kaolin | 0.65 | NaCl (0.001M) | $2.3\ 10^{-5}$ | $-\ 5.7\ 10^{-5}$ |

*2.3. Electrochemical reactions*

The rate of generation term is not included in the continuity equation for the porous specimen because we assume that the main chemical reactions that need to be considered are the electrochemical reduction and oxidation of water at the electrodes. The other electrochemical reactions had to be taken into account only in experiments 10 and 11, as explained in the following paragraphs. Nernst equation is used to calculate the redox potential for each electrochemical half reaction, as:

$$E = E^0 - \frac{RT}{\upsilon F} ln\, Q \tag{5}$$

where $Q$ is the reaction quotient, defined as the product of the activities of the chemical species to the power of their stoichiometric coefficients, for non-equilibrium conditions. In the special case that the reaction is at equilibrium, the reaction quotient is equal to the equilibrium constant. $\upsilon$ in this case is the stoichiometric coefficient of the electrons in the redox equation, i.e. the number of electrons exchanged during the oxidation or reaction process. $E$ (V) is the redox potential in the reduction sense and $E^0$ (V) is the standard redox potential, which is measured under standard conditions which are 25 ºC, 1 M concentration for each ion participating in the reaction, a partial pressure of 1 atm is assigned for each gas that is part of the reaction and metals in their pure state [40].

At the cathode, cations $Na^+$ and $Ca^{2+}$ are attracted, but the redox potential of alkali and alkaline earth metals is too high to be competitive to that of water in aqueous media. Consequently, it seems reasonable to assume that only water reduction is taking place at the cathode. Thus, the only electrochemical half-reaction at the cathode is:

$$2H_2O + 2e^- \rightarrow 2OH^-(aq) + H_2(gas) \qquad E^0 = -0.828 \text{ V} \tag{6}$$

On the other hand, anions are attracted to the anode, where oxidation reactions occur. In the most of experiments (5 to 9 and 12) only water oxidation is expected. In contrast, the

oxidation of ions $Cl^-$ (0.1 M) in experiment 10 and of ions $SO_3^=$ (0.1 M) in experiment 11 could compete with the water oxidation at the anode. Therefore, the possible half-reactions at the anode is given by equation (7) for experiments 5 to 9 and 12; by equations (7) and (8) for experiment 10; and by equations (7) and (9) for experiment 11:

$$2H_2O \rightarrow 4H^+(aq) + O_2(gas) + 4e^- \qquad E^0 = -1.229 \text{ V} \qquad (7)$$

$$2Cl^- \rightleftarrows Cl_2 + 2e^- \qquad E^0 = -1.360 \text{ V} \qquad (8)$$

$$SO_3^= + 2OH^- \rightleftarrows SO_4^= + 2e^- + H_2O \qquad E^0 = 0.936 \text{ V} \qquad (9)$$

Although a slight smell to chlorine was detected in experiment 10, the calculations revealed that even in the most favourable conditions (pH < 1) the fraction of current used for chloride oxidation is negligible. On the contrary, the sulphite oxidation predominates at the anode in the experiment 11.

The electrochemical reactions were included in the mass balance equations of anode and cathode compartments as given in equations (10) and (11) for all the experiments, with the exception of experiment 11 which also included the equations (12) and (13):

$$V_0\left(\frac{dc_{10}}{dt}\right)_{ER} = \frac{I}{F}\eta \qquad (10)$$

$$V_{N+1}\left(\frac{dc_{2N+1}}{dt}\right)_{ER} = \frac{I}{F}\eta \qquad (11)$$

$$V_0\left(\frac{dc_{40}}{dt}\right)_{ER} = -\frac{I}{zF}\eta \qquad (12)$$

$$V_0\left(\frac{dc_{120}}{dt}\right)_{ER} = \frac{I}{zF}\eta \qquad (13)$$

where $V_0$ and $V_{N+1}$ are the volumes of electrolyte in the anodic and cathodic compartments, $c_{10}$ and $c_{2N+1}$, $H^+$ and $OH^-$ concentrations generated there by electrochemical reactions, $c_{40}$ and $c_{120}$, $SO_3^=$ and $SO_4^=$ concentrations at the anodic compartment corresponding to the mass

of sulfite and sulfate consumed and generated by oxidation respectively, $I$ is the current intensity, $F$, the Faraday's constant and $\eta$ the Faradic efficiency.

*2.4. Chemical equilibria*

Once the transport calculations are completed at each time step, the value of concentration corresponding to the chemical equilibrium of every species is calculated from the last value obtained from the transport. Therefore, in every volume element a system of non-linear equations given by the mass balances, the electrical neutrality condition, and the equilibrium mass action equations were solved.

The extremely rapid reactions between protons and hydroxyls to form water and reverse must be taken into account in all the experiments. The chemical equilibrium of water is:

$$H^+ + OH^- \rightleftarrows H_2O \qquad K_w = \left[H^+\right]\left[OH^-\right] = 10^{-14} \tag{14}$$

In the experiments using NaCl (0.001 M) as electrolyte, as no equilibrium process affects $Cl^-$ and $Na^+$, the conservation equations for them are trivial. In contrast, additional equilibrium equations are necessary for the experiments 9, 10 and 11, using NaOH (0.001 M), $CaCl_2$ (0.05 M) and $Na_2SO_3$ (0.1 M) as electrolytes, respectively. The exchanges between the atmospheric $CO_2$ and the electrolyte were also considered in the simulations:

$$CO_3^{=} + H^+ \rightleftarrows HCO_3^- \Rightarrow K_1 = \frac{\left[HCO_3^-\right]}{\left[CO_3^{=}\right]\left[H^+\right]} = 2.13 \cdot 10^{10} \tag{15}$$

$$CO_3^{=} + 2H^+ \rightleftarrows H_2CO_3 \Rightarrow K_2 = \frac{\left[H_2CO_3\right]}{\left[CO_3^{=}\right]\left[H^+\right]^2} = 4.8 \cdot 10^{16} \tag{16}$$

$$Na^+ + H_2O - H^+ \rightleftarrows NaOH \Rightarrow K_3 = \frac{\left[NaOH\right]\left[H^+\right]}{\left[Na^+\right]} = 1.27 \cdot 10^{-14} \tag{17}$$

$$CO_3^{=} + Na^+ \rightleftarrows NaCO_3^- \Rightarrow K_4 = \frac{\left[NaCO_3^-\right]}{\left[CO_3^{=}\right]\left[Na^+\right]} = 18.6 \tag{18}$$

The only effect expected of $Ca^{2+}$ ion is its precipitation as $Ca(OH)_2$ due to the high pH present in the cathodic zone.

$$Ca^{2+} + 2OH^- \rightleftarrows Ca(OH)_2 \qquad K_0 = \left[Ca^{2+}\right]\left[OH^-\right]^2 = 5.02\cdot10^{-6} \tag{19}$$

In fact, in this experiment, a white precipitate was observed at the cathode compartment as predicted by the model calculations.

In the case of sulfite, several equilibrium equations were taken into account:

$$SO_3^{=} + H^+ \rightleftarrows HSO_3^- \Rightarrow K_1 = \frac{\left[HSO_3^-\right]}{\left[SO_3^{=}\right]\ \left[H^+\right]} = 1.55\cdot10^{-7} \tag{20}$$

$$SO_3^{=} + 2H^+ \rightleftarrows H_2SO_3 \Rightarrow K_2 = \frac{\left[H_2SO_3\right]}{\left[SO_3^{=}\right]\ \left[H^+\right]^2} = 1.1\cdot10^{9} \tag{21}$$

$$Na^+ + H_2O - H^+ \rightleftarrows NaOH \Rightarrow K_3 = \frac{\left[NaOH\right]\left[H^+\right]}{\left[Na^+\right]} = 1.27\cdot10^{-14} \tag{22}$$

$$SO_3^{=} + Na^+ \rightleftarrows NaSO_3^- \Rightarrow K_4 = \frac{\left[NaSO_3^-\right]}{\left[SO_3^{=}\right]\ \left[Na^+\right]} = 6.76 \tag{23}$$

$$2SO_3^{=} + 2H^+ - H_2O \rightleftarrows S_2O_5^{2-} \Rightarrow K_5 = \frac{\left[S_2O_5^{2-}\right]}{\left[SO_3^{=}\right]^2\ \left[H^+\right]^2} = 7.41\cdot10^{-15} \tag{24}$$

$$SO_4^{=} + H^+ \rightleftarrows H\ SO_4^- \Rightarrow K_6 = \frac{\left[HSO_4^-\right]}{\left[SO_4^{=}\right]\ \left[H^+\right]} = 97.72 \tag{25}$$

## 3. Results and Discussion

The model reproduces satisfactorily the nZVI concentration profiles in the porous media, as well as the anodic and cathodic pH values over time.

Model and experimental results for nZVI concentrations profiles in the various porous specimens at the end of the 48 h diffusion control tests are presented in Figure 2. It was detected that, in some cases, an important fraction of the nZVI tends to aggregate when the

concentration is high relative to the available pore volume, becoming immobile. In fact, in experiments 2 and 4 only about 19% and 8% of the injected nZVI remained mobile over the experiment, respectively. At high iron nanoparticle concentration (1-6 g $L^{-1}$) there is higher agglomeration [11]. Also, when iron nanoparticles aggregate they become larger than the pores, restricting their transport through the matrix [41].

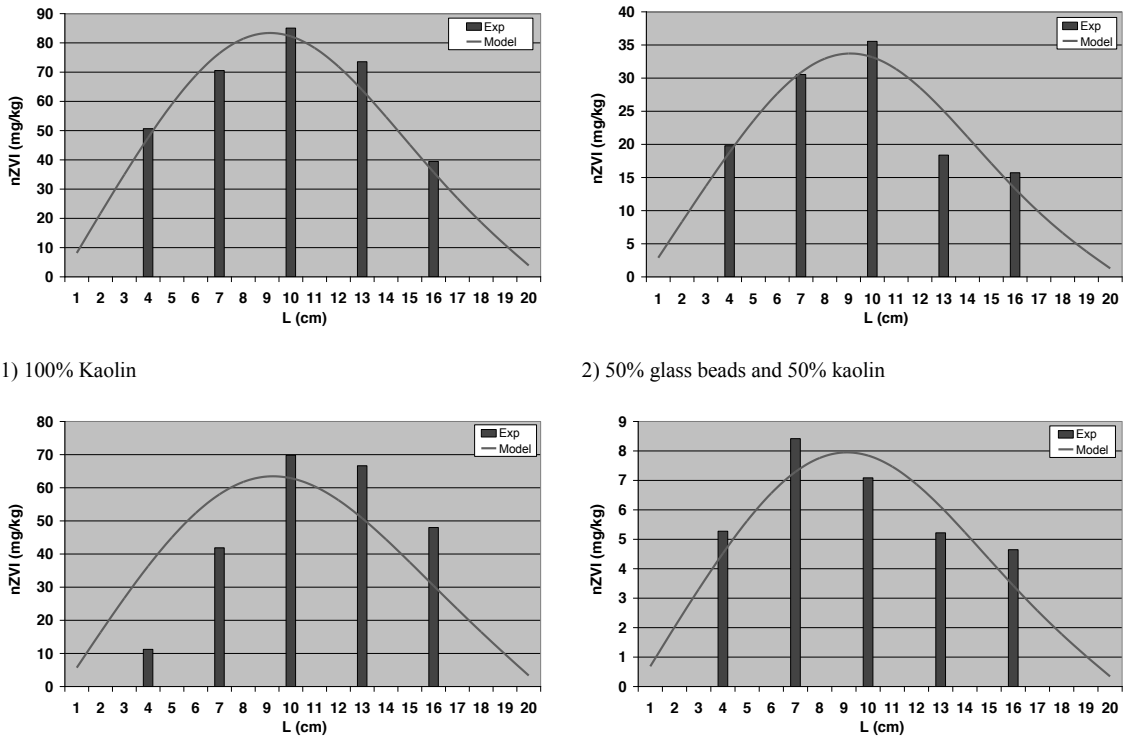


1) 100% Kaolin

2) 50% glass beads and 50% kaolin

3) 75% glass beads and 25% kaolin

4) 100% glass beads

Figure 2. Iron concentrations across the electrophoretic cell in the diffusion control tests for the porous media tested (Experiments 1 to 4).

Model and experimental results for nZVI concentrations profiles and pH at the anode and cathode over time in enhanced transport tests are presented in Figures 3 and 4. As can be seen, the concentration of nZVI away from the injection point is higher than in the experiments without current, in all the cases. This result shows that the current enhances nZVI transport by preventing or hindering the nZVI aggregation at the injection location. In

Figure 5, the mobile mass of nZVI *vs*. pore volume is shown for the nZVI transport without and with current. In all cases, the mobile mass is higher in the experiments with current.

The model predicts very low effective mobility values in the porous medium ($U_i^{**}$) as showed in Table 1 as a consequence of the opposing transport directions between the electroosmotic advection and the electrophoretic migration of the negatively charged nanoparticles. This effect manifests itself as higher concentrations close to the injection point in most of experiments. Thus, if the nanoparticles could be stabilized with a surface modifier to give them a positive charge, the nZVI effective mobility could potentially be increased. Nevertheless the probability of the positively charged particles be attracted onto the soil particle surfaces, particularly clays, could increase. Also the use of stabilizers without charge could enhance the electroosmotic transport of the iron nanoparticles.

The ionic strength of the electrolyte was also determinant in the transport of the nanoparticles – the higher the ionic strength of the electrolyte the lower the transport, what should also be considered for field applications with contaminated groundwaters with high concentrations of salts and metals. The distance covered by iron nanoparticles when using 0.001 M NaCl as the electrolyte is approximately the double when compared with 0.05 M $CaCl_2$ and 0.1 M $Na_2SO_3$.

Figure 6 shows the model predictions of the transport distance covered by the iron nanoparticles using different electrolytes and porous media, with and without current. It is clearly distinct the enhancement of the nZVI transport when current in applied, especially in the kaolin clay. When using only kaolin clay and direct current the distance covered by iron nanoparticles is almost the double of diffusion only.

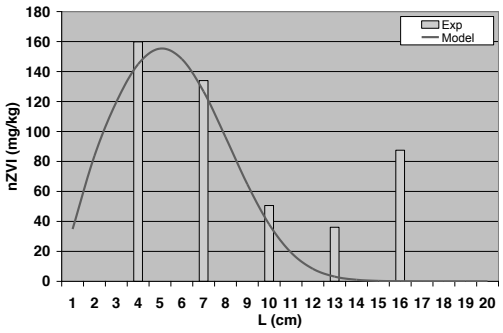


Exp. 5 a)

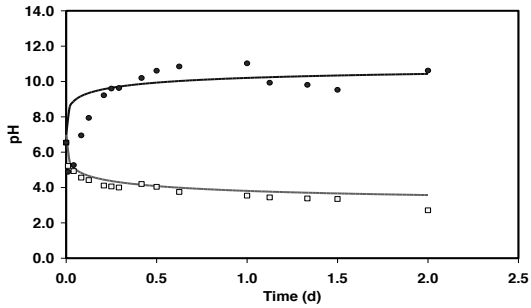


Exp. 5 b)

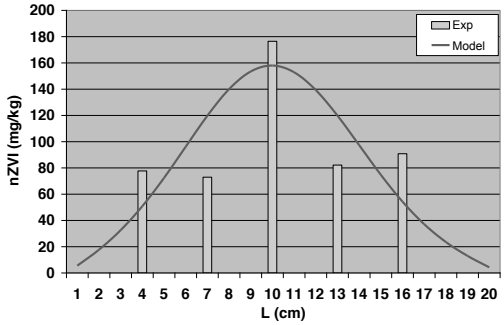


Exp. 6 a)

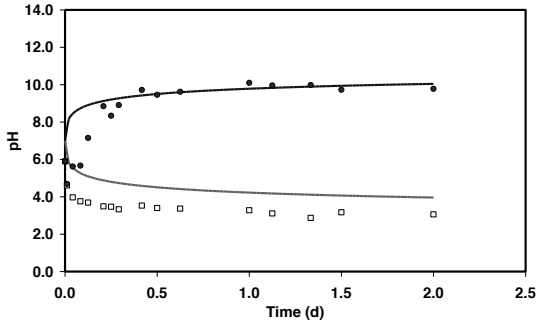


Exp. 6 b)

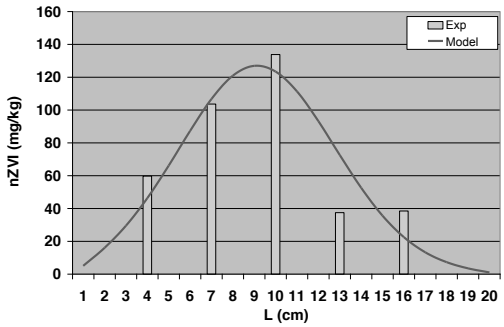


Exp. 7 a)

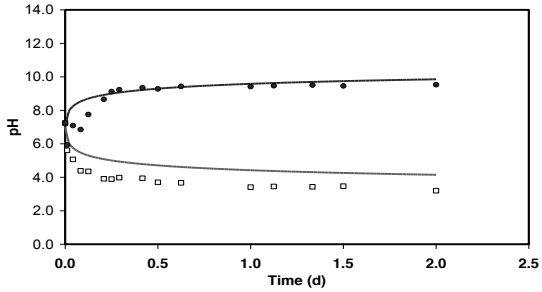


Exp. 7 b)

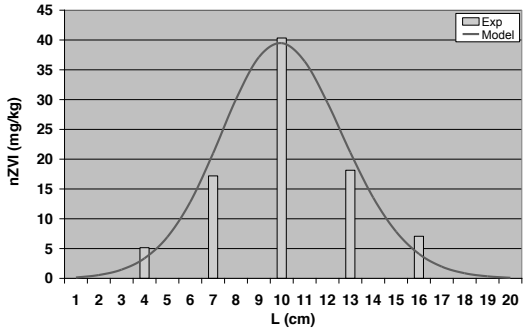


Exp. 8 a)

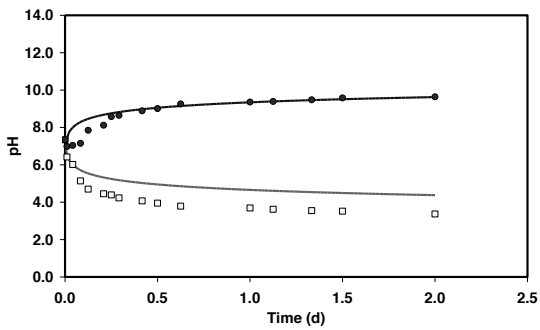


Exp. 8 b)

Figure 3. Enhanced transport tests: a) iron concentrations in the solid matrix and b) pH variation in the anolyte (yellow squares and red line) and catholyte (blue circles and line).

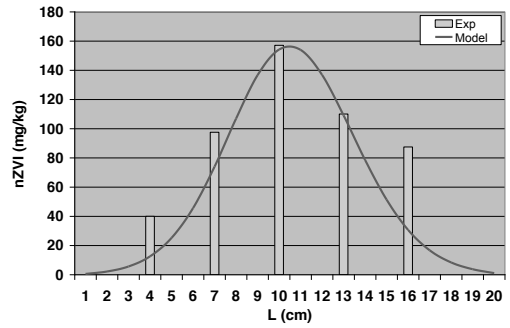


Exp. 9 a)

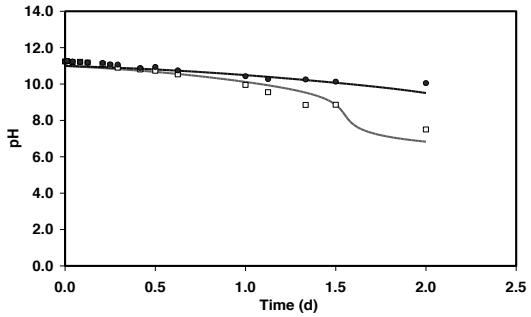


Exp. 9 b)

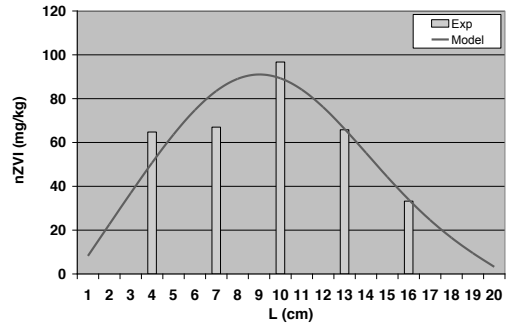


Exp. 10 a)

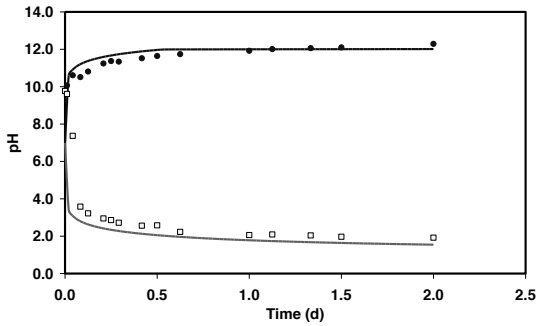


Exp. 10 b)

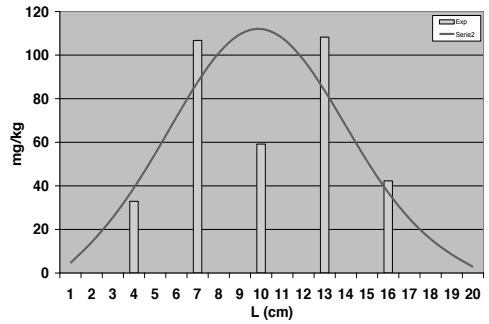


Exp. 11 a)

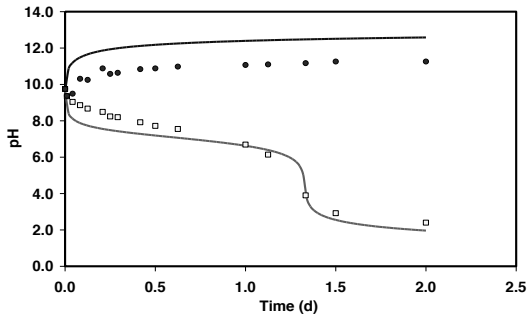


Exp. 11 b)

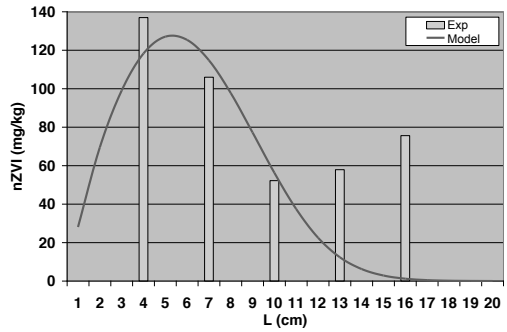


Exp. 12 a)

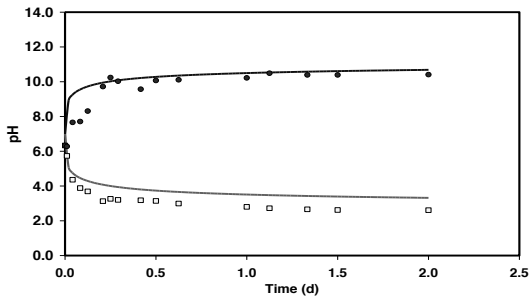


Exp. 12 b)

Figure 4. Enhanced transport tests: a) iron concentrations in the solid matrix and b) pH variation in the anolyte (yellow squares and red line) and catholyte (blue circles and line).

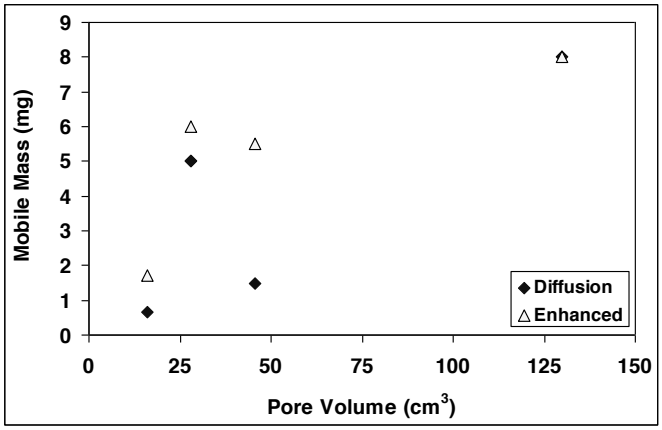


Figure 5. Mobile mass of nZVI in the diffusion and enhanced transport experiments.

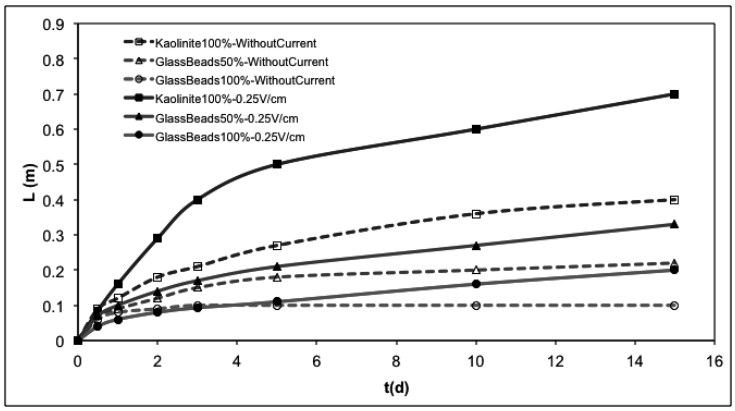


Figure 6. Prediction of the distances covered by nanoparticles in the different porosity media with and without current.

## 4. Conclusions

The use of polymers which increase the repulsion between nanoparticles (inhibiting aggregation) and between nanoparticles and surfaces (inhibiting attachment) aims at enhancing the dispersibility and transport of nZVI through the porous medium. However, despite the use of polyacrylic acid to modify the surface, an important aggregation of nZVI is observed in the experiments when the particles are allowed to diffuse into porous medium from an injection point. The higher the nZVI concentration is in the matrix, the higher the aggregation; therefore, low concentrations suspensions must be used for successful field application.

The use of electrical current to transport the nanoparticles prevents or hinders the nZVI particle aggregation, increasing their mobility. However, opposing directions of electrophoretic transport of negatively charged particles and the electroosmotic advection still produces low nZVI transport that could be improved by reversing the charge of the iron nanoparticle surface or by using neutrally charged nanoparticles that could be transported by electroosmotic advection. A detailed physicochemical model which included advective, diffusive and electrophoretic transport, electrolyte specific electrochemical reactions, as well as mass balances, was developed and solved. The model predictions agreed well with the experimental findings of the nZVI distribution in various porous systems, as well as the pH evolution in the anolyte and catholyte in the enhanced transport and diffusion tests.

**Acknowledgments**

This work has been funded by the research grant SFRH/BD/76070/2011, by project PTDC/AGR-AAM/101643/2008 NanoDC under Portuguese National funds through "Fundação para a Ciência e a Tecnologia" and by FP7-PEOPLE-IRSES-2010-269289-ELECTROACROSS. The Department of Civil and Environmental Engineering at Lehigh University is acknowledged for the funding of equipment development, testing and analysis of the nZVI transport experiments.

**References**

[1] USEPA, Permeable Reactive Barrier Technologies for Contaminant Remediation, Technical Innovation Office. Office of Solid Waste and Emergency Response U. S. Environmental Protection Agency Washington DC, National Risk Management Research Laboratory Office of Research and Development, U. S. Environmental Protection Agency Cincinnati, Ohio 1998.

[2] S. Comba, A. Di Molfetta, R. Sethi, Water Air Soil Poll., 215 (2011) 595-607.

[3] J.M. Rodríguez-Maroto, F. García-Herruzo, A. García-Rubio, C. Gómez-Lahoz, C. Vereda-Alonso, Chemosphere, 74 (2009) 804-809.

[4] C.B. Wang, W. Zhang, Environ. Sci. Technol., 31 (1997) 2154-2156.

[5] W. Zhang, C. B. Wang, H.L. Lien, Catal. Today, 40 (1998) 387-395.

[6] J. Dries, L. Bastiaens, D. Springael, S.N. Agathos, L. Diels, Environ. Sci. Technol., 39 (2005) 8460-8465.

[7] Y. Liu, H. Choi, D. Dionysiou, G.V. Lowry, Chem. Mat., 17 (2005) 5315-5322.

[8] H. Song, E.R. Carraway, Environ. Sci. Technol., 39 (2005) 6237-6245.

[9] B.W. Hydutsky, E.J. Mack, B.B. Beckerman, J.M. Skluzacek, T.E. Mallouk, Environ. Sci. Technol., 41 (2007) 6418-6424.

[10] S. Kanel, D. Nepal, B. Manning, H. Choi, J. Nanopart. Res., 9 (2007) 725-735.

[11] T. Phenrat, H.J. Kim, F. Fagerlund, T. Illangasekare, R.D. Tilton, G.V. Lowry, Environ. Sci. Technol., 43 (2009) 5079-5085.

[12] T. Raychoudhury, G. Naja, S. Ghoshal, J. Contam. Hydrol., 118 (2010) 143-151.

[13] T. Raychoudhury, N. Tufenkji, S. Ghoshal, Water Res., 46 (2012) 1735-1744.

[14] T. Raychoudhury, N. Tufenkji, S. Ghoshal, Water Res., 50 (2014) 80-89.

[15] N. Saleh, H. Kim, T. Phenrat, K. Matyjaszewski, R.D. Tilton, G.V. Lowry, Environ. Sci. Technol., 42 (2008) 3349-3355.

[16] G.C.C. Yang, H.C. Tu, C.H. Hung, Sep. Purif. Technol. 58 (2007) 166-172.

[17] P. Jiemvarangkul, W.X. Zhang, H.L. Lien, Chem. Eng. J., 170 (2011) 482-491.

[18] S.R. Kanel, R.R. Goswami, T.P. Clement, M.O. Barnett, D. Zhao, Environ. Sci. Technol., 42 (2008) 896-900.

[19] Y.H. Lin, H.H. Tseng, M.Y. Wey, M.D. Lin, Sci. Total Environ., 408 (2010) 2260-2267.

[20] F. He, D. Zhao, J. Liu, C.B. Roberts, Ind. Eng. Chem. Res., 46 (2007) 29-34.

[21] B. Schrick, B.W. Hydutsky, J.L. Blough, T.E. Mallouk, Chem. Mater., 16 (2004) 2187–2193.

[22] T. Phenrat, N. Saleh, K. Sirk, R.D. Tilton, G.V. Lowry, Environ. Sci. Technol., 41 (2007) 284-290.

[23] D.W. Elliott, W. Zhang, Environ. Sci. Technol., 35 (2001) 4922-4926.

[24] J. Quinn, C. Geiger, C. Clausen, K. Brooks, C. Coon, S. O'Hara, T. Krug, D. Major, W.-S. Yoon, A. Gavaskar, T. Holdsworth, Environ. Sci. Technol., 39 (2005) 1309-1318.

[25] K.W. Henn, D.W. Waddill, Remediation, 16 (2006) 57-77.

[26] W. Zhang, D.W. Elliott, Remediation, (2006) 7-21.

[27] C. Su, R.W. Puls, T.A. Krug, M.T. Watling, S.K. O'Hara, J.W. Quinn, N.E. Ruiz, Water Res., 46 (2012) 5071-5084.

[28] C.M. Kocur, A.I. Chowdhury, N. Sakulchaicharoen, H.K. Boparai, K.P. Weber, P. Sharma, M.M. Krol, L.M. Austrins, C. Peace, B.E. Sleep, D.M. O'Carroll, Environ. Sci. Technol., (2014) DOI: 10.1021/es4044209.

[29] M.M. Krol, A.J. Oleniuk, C.M. Kocur, B.E. Sleep, P. Bennett, X. Zhong, D.M. O'Carroll, Environ. Sci. Technol., 47 (2013) 7332-7340.

[30] H.I. Gomes, C. Dias-Ferreira, A.B. Ribeiro, S. Pamukcu, Water Air Soil Poll., 224 (2013) 1-12.

[31] H.I. Gomes, C. Dias-Ferreira, A.B. Ribeiro, S. Pamukcu, Chemosphere, 99 (2014) 171-179.

[32] S. Pamukcu, L. Hannum, J.K. Wittle, J. Environ. Sci. Health A, 43 (2008) 934-944.

[33] E.H. Jones, D.A. Reynolds, A.L. Wood, D.G. Thomas, Ground Water, 49 (2010) 172-183.

[34] E. Rosales, J.P.G. Loch, C. Dias-Ferreira, Electrochim. Acta, 127 (2014) 27-33.

[35] Y.B. Acar, A.N. Alshawabkeh, Environ. Sci. Technol., 27 (1993) 2638-2647.

[36] G.C.C. Yang, C.-H. Hung, H.-C. Tu, J. Environ. Sci. Health A, 43 (2008) 945-951.

[37] A.I.A. Chowdhury, D.M. O'Carroll, Y. Xu, B.E. Sleep, Adv. Water Resour., 40 (2012) 71-82.

[38] J. Newman, Electrochemical Systems, Prentice Hall, Englewood Cliffs, 1991.

[39] J.K. Mitchell, Fundamentals of Soil Behavior, 2nd ed. ed., John Wiley & Sons, New York, 1993.

[40] R. Chang, J. Overby, General Chemistry – The Essential Concepts, McGraw-Hill, New York, 2011.

[41] K.R. Reddy, K. Darko-Kagy, C. Cameselle, Sep. Purif. Technol., 79 (2011) 230-237.

## Appendix A. Nomenclature

| | |
|---|---|
| A | cross-sectional area ($cm^2$) |
| $c$ | concentration (mol $cm^{-3}$) |
| $D$* | effective diffusion coefficient |
| E | redox potential (V) |
| $E^0$ | standard redox potential (V) |
| $F$ | Faraday constant |
| $I$ | current intensity |
| $k_e$ | electroosmotic permeability coefficient |
| $N$ | mass flux (mol $cm^2$ $s^{-1}$) |
| Q | reaction quotient |
| $R$ | ideal gas constant |
| $R$ | reaction rate |
| $T$ | temperature (K), assuming a constant room temperature of 25ºC |
| $t$ | time |
| U* | effective electrophoretic mobility |
| $V$ | volume ($cm^3$) |
| $z$ | ionic charge |

### Greek letters

| | |
|---|---|
| $\phi$ | electrical potential |
| $\eta$ | Faradaic efficiency |

### Subscripts

| | |
|---|---|
| i | species |
| j | cell |